Polish Academy of Sciences Branch in Lublin
The Volodymyr Dahl East-Ukrainian National University in Lugansk

TEKA

COMMISSION OF MOTORIZATION AND ENERGETICS IN AGRICULTURE

AN INTERNATIONAL JOURNAL ON MOTORIZATION, VEHICLE OPERATION, ENERGY EFFICIENCY AND MECHANICAL ENGINEERING

Vol. 12. No 1

LUBLIN – LUGANSK 2012

Commission of Motorization and Energetics in Agriculture
Wielkopolska Str. 62, 20-725 Lublin, Poland
e-mail: eugeniusz.krasowski@up.lublin.pl

ISSN 1641-7739

Edition 200+16 vol.

TEKA. COMMISSION OF MOTORIZATION AND ENERGETICS IN AGRICULTURE – 2012, Vol. 12, No. 1, 03–08

Effect of thermal conditioning of silica-sodium glass on the kinetics of zeta potential changes during soluble sodium silicate gelation

*Andrzej Baliński**

Foundry Research Institute, Krakow, Poland
Zakopiańska str. 73, 30–418 Kraków

Summary. The article describes the results of Zeta potential changes in the system „soluble sodium silicate - ester" according to the time of gelation. It was found out that the time of thermal conditioning of silica-sodium glass is important in terms of nanostructure elements stability of the soluble sodium silicate. Stability characteristics of these elements can affect the binding characteristics of silicate binder-quartz system, and thus their strength properties at ambient temperature.

Key words: soluble sodium silicate, silica-sodium glass, Zeta potential, thermal conditioning.

INTRODUCTION

Soluble sodium silicate, or an aqueous solution of sodium silicate, is one of the oldest inorganic binders used in various industries. In the foundry it is a binder used in the production of the molding sands. The advantage of molding sands with the soluble sodium silicate is a good heat resistance of moulds and cores, which is especially important for medium and heavy cast iron alloy, and no emission of toxic gases in the preparation of the moulding sands, pouring forms and removing casting [4-10,11-17,19-23]. In addition to these environmental and technological considerations, economic considerations are also important. Molding sands with soluble sodium silicate are much cheaper than the moulding sands with the binder resin. Apart from the obvious advantages of moulding sands with the soluble sodium silicate, however, have several disadvantages such as too much residual strength, lower primary strength and tendency to formation of sinters. The sintering process can be reduced by reducing the amount of binder in the moulding sands, but this reduction is possible only if the improvement of its binding properties occurs.

Soluble sodium silicates usually form stable aqueous solutions, but from a chemical point of view, generally do not have a clear composition. They form durable composite structures, which are defined complexes of sodium silicate and silicic acid. Their composition varies and ranges from 4 moles of SiO_2 per 1 mol of Na_2O and 1 mol of SiO_2 to 4 moles of Na_2O. Thus, the general formula of sodium silicate can be written as $xNa_2O \cdot ySiO_2$, and values for x and y vary from 1 to 4 [18].

The main parameter that allows to distinguish between the different sodium silicates is the silica module, which is the molar ratio of silicon dioxide contribution to sodium oxide in the considered system. There are known also sodium silicate crystal structure. They derive from a hypothetical silicic acid of the formula H_4SiO_4:

$$NaH_2SiO_4 \rightarrow Na_2Si_2O_5. \quad \text{bisilicate}$$

$$Na_2H_2SiO_4 \rightarrow Na_2SiO_3. \quad \text{metasilicate}$$

$$Na_3HSiO_4 \rightarrow Na_6Si_2O_7. \quad \text{pirosilicate}$$

$$Na_4SiO_4 \rightarrow Na_4SiO_4. \quad \text{orthosilicate}$$

Some of them are in the form of readily soluble hydrates [3]. It may be noted that while the upper limit of module for soluble sodium silicate is 4, a sodium silicate for the defined limit value is the module 2. Understood is accepted hypothesis that sodium silicates, especially in aqueous solution, represent complex of silica sodium oxide, formed from simple silicates of module to 2 and silicic acid. The structural design of sodium silicate in aqueous solution is very complex due to the presence of hydroxyl ions and the adoption by the tetravalent silicon in the silicate ions sixth coordination number. Change in coordination number from 4 to 6 is facilitated by the presence of free silicon 3d orbitals, able to accept electron pairs. This gives the connections of silicon (in particular with oxygen), specific properties. Investigation of properties of aqueous solutions of sodium silicate, such as

conductivity, refractive index, boiling point and freezing point, confirmed their colloidal nature. The presence and frequency of polisilicate ions (colloidal particles) emerges clearly from the module silicate equal 2. In the sodium silicate solutions with module 2 there are monosilica ions $[H_3SiO_4]^{1-}$ - and bisilica ions $[H_4Si_2O_7]^{2-}$, and in solutions with higher modules there are a mixture of polisilicate ions with higher degrees polycondensation. Especially at higher concentrations of SiO_2 and the modules M>2 identified the polymeric units containing from 4 to 8 or even 12 Si atoms [1,3].

In the solutions of sodium silicate, there is a progressive aggregation of silica from the molecular silicate to the colloidal and eventually solidified gels covering the entire solution. The possibility of interference with the rate of establishment of equilibrium in the aggregate, is used on an industrial scale to manufacture all kinds of binders and adhesives [1].

Examination of concentrated solutions of sodium silicate with module 2 to 4 by ^{29}Si-NMR method [3] showed, that the number of groups Q^o, Q^1, Q^2 decreases with increasing module, where Q is the number of siloxane bonds Si-O-Si, but increasing the number of groups Q^3 and Q^4. For M >1.5 starts polymerization leading to the branched groups (Q^3) of an average nuclearity 6 to 8, and with M>3.5 are formed three-dimensionally cross-linked units (Q^4) with the surface units (Q^3). Q^4 units was observed only at M>2.4. Assumed, however, that colloidal particles are formed at the module about 2 and at high concentrations [3].

PURPOSE AND METHODS

To make sodium silicate glass with the assumed value of the module M = 3.3 was used sand class 1A with the chemical composition: SiO_2 = 99.63%, Al_2O_3 = 0.19%, CaO = 0.09%, MgO = 0.035%, Fe_2O_3 = 0.016%, TiO_2 = 0.039% and light soda with Na_2CO_3 content = 99.30%. Assumed volatility of Na_2O equal 0,59%, which represents 2.48% Na_2O loss in the melting process of glass. Oxide composition of the silica-sodium was: SiO2 = 76.19%, Na_2O = 23.81% + 0.59% (for volatility) = 24.40%.

Melts of glass were performed in a gas furnace (oxidizing atmosphere), in the porcelain crucibles not glazed, with a capacity 3 dm^3. For temperature measurement, thermocouples and optical pyrometers were used. Sets of sand and soda were dosed three times, every 40 minutes. After the last dosage alloys were kept in the crucibles at 1350^{0}C for 60 minutes (sodium silicate glass from which the soluble sodium silicate SW-60 was made), 90 minutes (sodium silicate glass from which the soluble sodium silicate SW-90 was made) and 120 minutes (sodium silicate glass from which the soluble sodium silicate SW-120 was made).

For the dissolution of the silica-sodium glass autoclave type *VAIO-EWG 50 TR* was used. Autoclavisation performed at a temperature of about 160^{0}C and the corresponding pressure approximately 6MPa. For correction of the module of the soluble sodium silicate, sodium hydroxide was used.

Changes in the electrokinetic potential as a function of gel time was determined for samples of the soluble sodium silicate (*SW-60*, *SW-90*, *SW-120*) mixed with the ester (ethylene glycol diacetate). A sample of formed gel was collected after 20, 30, 40, 60, 80 and 100 minutes from the time of connection ester and a soluble sodium silicate, subjected to dispersion in NaCl solution (previously filtered through a membrane filter with a pore diameter of 220 nm in order to remove insoluble impurities) and sonicated. *Zeta* potential was examined using the *ZetaSizer 3000* apparatus.

On the basis of measurements, determined the optimal composition of the electrolyte gel dispersion at which the recorded signal was the most favorable for scattered light and the measured values of *Zeta* potential were the same as when using larger dilution. After determining the *pH* value of the resulting solution, *Zeta* potential measurements were carried out. In order to characterize the sample, average potential distribution was calculated averaging the individual distributions (the sum of the individual channels and calculate the average). Two types of measurements were used in identifying changes in *Zeta* potential: as a function of gel time and after the gels, in order to characterize the surface properties of the resulting gel.

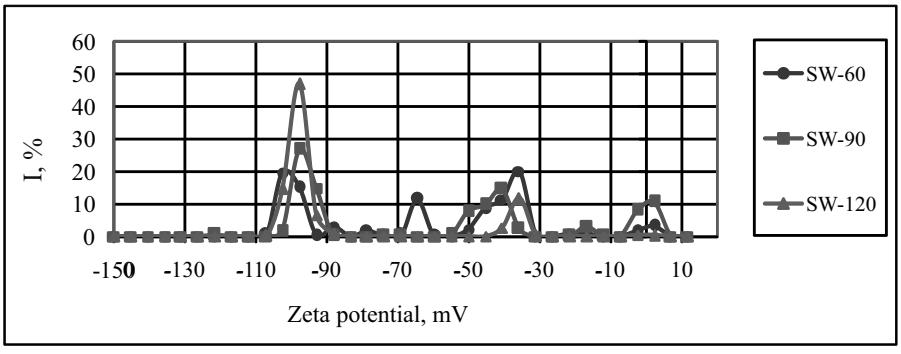

Fig. 1. Changes of the *Zeta* potential and the corresponding signal intensity *I* a laser light scattering on the surface elements of the structure formed after 20 minutes gelation process of the system „soluble sodium silicate (*SW-60*, *SW-90*, *SW-120*) - ethylene glycol diacetate"

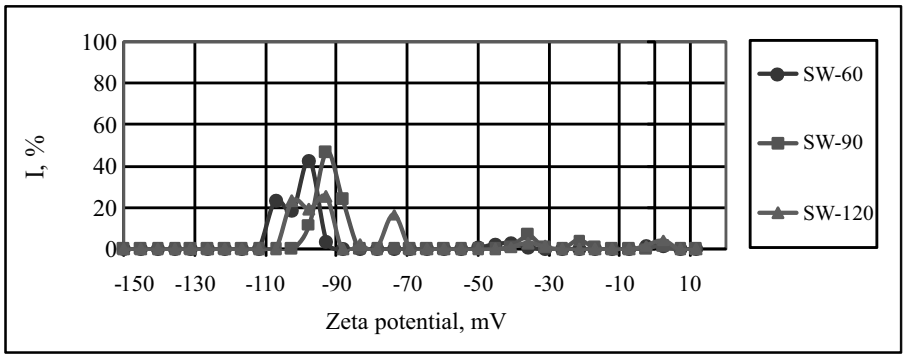

Fig. 2. Changes of the *Zeta* potential and the corresponding signal intensity *I* a laser light scattering on the surface elements of the structure formed after 30 minutes gelation process of the system „soluble sodium silicate (*SW-60*, *SW-90*, *SW-120*) - ethylene glycol diacetate"

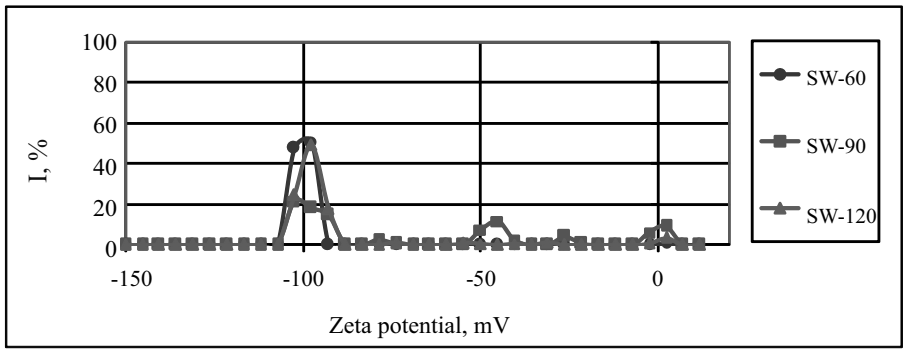

Fig. 3. Changes of the *Zeta* potential and the corresponding signal intensity *I* a laser light scattering on the surface elements of the structure formed after 40 minutes gelation process of the system „soluble sodium silicate (*SW-60*, *SW-90*, *SW-120*) - ethylene glycol diacetate"

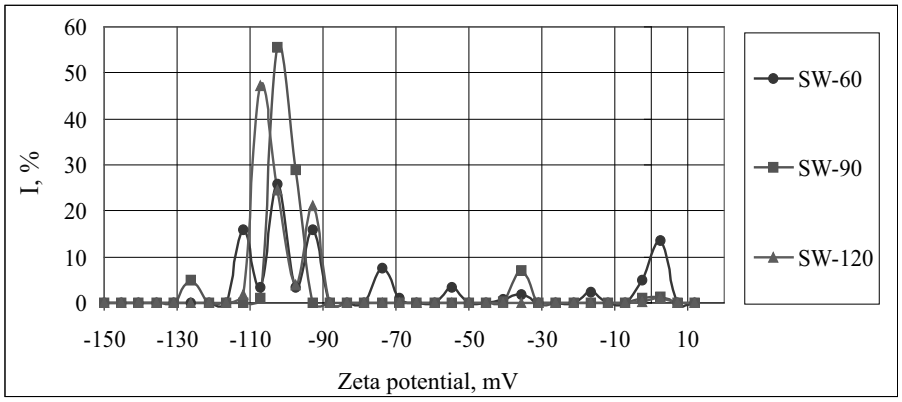

Fig. 4. Changes of the *Zeta* potential and the corresponding signal intensity *I* a laser light scattering on the surface elements of the structure formed after 60 minutes gelation process of the system „soluble sodium silicate (*SW-60*, *SW-90*, *SW-120*) - ethylene glycol diacetate"

RESULTS AND DISCUSION

The results of studies described above are shown in Figures 1 to 6. They illustrate the changes on the *Zeta* potential and the corresponding signal intensity *I* laser light scattering on the surface elements of the structure formed after a certain time of the process of gelation of soluble sodium silicate *SW-60*, *SW-90*, *SW-120*) under the influence of the ester.

The *pH* of the dispersion obtained from the gel varied from $pH \cong 11.0$ for the shortest time of gelation, to the $pH \cong 10.3$ for gel time of 100 minutes. The *pH* values for individual samples little differed and had no significant effect on the *Zeta* potential value. As shown in the placed figures, the initial stage of gelation gives rise of the structural elements with a relatively high value *Zeta* potential ≅ -100 mV. The signal intensity *I* of laser light scattering on the surface of these elements is high for

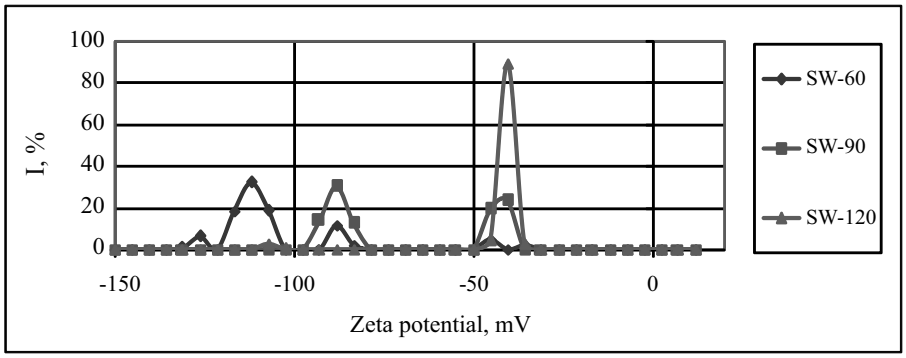

Fig. 5. Changes of the *Zeta* potential and the corresponding signal intensity *I* a laser light scattering on the surface elements of the structure formed after 80 minutes gelation process of the system „soluble sodium silicate (*SW-60*, *SW-90*, *SW-120*) - ethylene glycol diacetate"

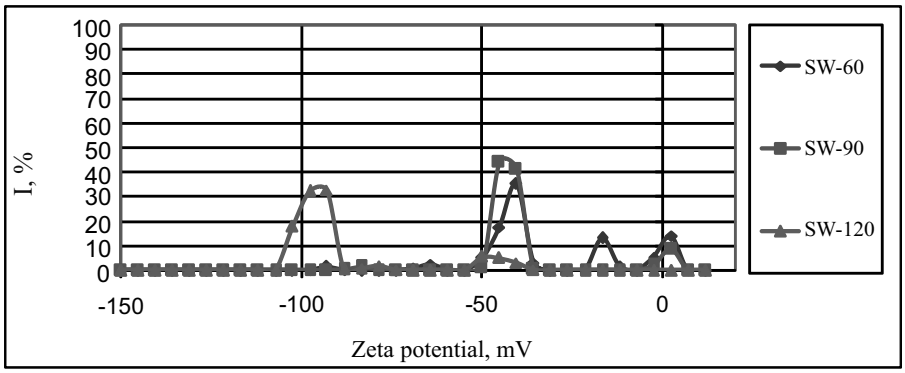

Fig. 6. Changes of the *Zeta* potential and the corresponding signal intensity *I* a laser light scattering on the surface elements of the structure formed after 100 minutes gelation process of the system „soluble sodium silicate (*SW-60*, *SW-90*, *SW-120*) - ethylene glycol diacetate"

a longer gel time, then disappears for particles with the potential ≅ -40 mV. In the case of the gel obtained by the reaction of soluble sodium silicate *SW-60* and *SW-90* with the ester by the time 80 minutes, the signal intensity of laser light scattering on the surface of structural elements with a high *Zeta* potential is less than 10%. In the case of the gel obtained by the reaction of soluble sodium silicate *SW-120* and ester, the signal intensity *I* of laser light scattering on the surface of structural elements with a high potential *Zeta* is significant after 80 minutes of the gelation process. As mentioned above, the signal intensity *I* of laser light scattering elements formed on the surface structure, can be a source of both the abundance of these elements, as well as their size and geometry of the surface (signal intensity *I* laser light scattering is proportional to the radius of the particles in the sixth power). It is also possible to notice the appearing and disappearing signal intensity of laser light scattering on the surface of particles contained in the reactants (soluble sodium silicate and ester). This effect is smallest in the case of gel obtained by the reaction of the ester and soluble sodium silicate *SW-120*, and the most visible in the gel obtained by the reaction of the ester and soluble sodium silicate *SW-60*. This may indicate the not full reaction of the gel reagent and a much slower reaction of soluble sodium silicate gel *SW-60* in comparison to the soluble sodium silicate *SW-120*. The change was deteribed in the value of the *Zeta* potential versus *pH* for soluble sodium silicate gels *SW-60*, *SW-90* and *SW-120*. In the spectra signals were observed from particles of pollution of the reactants, and of the particles created in the process of nucleation. After analysis of the electrokinetic properties in the function of *pH*, *Zeta* potential values were selected for which the signal intensity *I* of laser light scattering on the surface elements of the structure was the biggest. The investigated electrokinetic properties of the systems resemble the properties of the "SiO_2 - electrolyte solutions" [18]. At the same time you can see some significant differences depending on the *Zeta* potential values of ionic strength. The increase in ionic strength of the carrier electrolyte causes the decrease in the absolute value of the *Zeta* potential, but does not move isoelectric point. These relationships are complex, which may indicate that the surface structure of the formed elements may have properties similar to the surface of a „*hair*", occurring on some systems with the organic phase. Some impact on the *Zeta* potential dependence on *pH* can also increase the ionic strength of the electrolyte, due to the presence of electrolyte in the sample gel. As a result, the ionic strength of the electrolyte with the lowest carrier concentration is in fact higher than expected. Comparing the *Zeta* potential values for the gel samples, we can conclude

that the elements of the structure of the gel obtained by the reaction of the ester and soluble sodium silicate *SW-90* showed the highest values potential at *pH*> 8, while elements of gel structure obtained by the reaction of the ester and soluble sodium silicate *SW-60* has the smallest value *Zeta* potential.

CONCLUSIONS

1. *Zeta* potential distribution after 20 minutes of gelation.

All the tested types of soluble sodium silicate have similar distribution *Zeta* potential range from about -110 mV to about -90 mV, but in the case of the soluble sodium silicate *SW-120* the corresponding signal intensity laser light scattering is the greatest. This may be attributable to a large number of particles, their large volume or the more developed surface compared to other types of soluble sodium silicate, particularly *SW-60*. The largest slenderness ratio of the peak intensity of laser light scattering in this range of values of the *Zeta* potential indicates the greatest homogeneity of elements in its structure. The second distinct peak intensity of laser light scattering on the elements of the structure of soluble sodium silicate *SW-120* corresponds to the value *Zeta* potential from about -50 mV to about -30 mV and is the smallest, compared to the peaks of soluble sodium silicate *SW-60* and *SW-90*. It seems that the potential *Zeta* distribution in this period of gelation indicates the greatest stability of soluble sodium silicate *SW-120*.

2. *Zeta* potential distribution after 30 minutes of gelation.

For all the investigated types of soluble sodium silicate the heterogeneity is increased of the structure elements formed in this gelation period, with the *Zeta* potential from about -110 mV to about -90 mV. In the case of soluble sodium silicate *SW-120*, elements of the structure are disappearing of the potential from about -50 mV to about -30 mV, for the benefit of structural elements with a potential from about -80 mV to about -70 mV. In the soluble sodium silicate *SW-60* practically disappearing are elements of the structure of the potential below -90 mV, while in soluble sodium silicate *SW-90* is an insignificant number of elements of the structure with the *Zeta* potential below -90 mV . The distribution of the *Zeta* potential after 30 minutes of gelation, suggests similar stability elements of the structure in all the tested types of soluble sodium silicate.

3. *Zeta* potential distribution after 40 minutes of gelation.

Distribution of the values of *Zeta* potential show increased stability of elements of the structure in the soluble sodium silicate *SW-120* and *SW-60* and a slight decrease in the stability of these elements in soluble sodium silicate *SW-90*, for which again there are elements of structures with *Zeta* potential from about -10 mV to about +10 mV.

4. *Zeta* potential distribution after 60 minutes of gelation.

Clearly increased heterogeneity can be observed of elements of the structure arising from the gelation process of soluble sodium silicate *SW-60*, with the *Zeta* potential from about -120 mV to about -90 mV. For this type of soluble sodium silicate, there are also elements of the structure with the potential from about -80 mV to about -70 mV, from about -60 mV to about -50 mV and from about -10 mV to about +10 mV. This suggests an increasing instability of the elements of the structure of the soluble sodium silicate *SW-60*.

5. *Zeta* potential distribution after 80 minutes of gelation.

In the case of soluble sodium silicate *SW-120*, after the high stability of elements of the structure, there are mainly structural components of the *Zeta* potential from about -50 mV to about -40 mV, indicating a significant decrease in the stability of formed structure. Also the stability is decreased of the system in case of soluble sodium silicate *SW-90*, in which there are elements of the structure of the *Zeta* potential from about -50 mV to about -40 mV, in addition to elements of the structure of the *Zeta* potential from about -100 mV to about -80 mV . The most stable arrangement of the structure of soluble sodium silicate *SW-60*, with the *Zeta* potential from about -130 mV to about -100 mV and from about -100 mV to about -80 mV. Distribution of the potential in the studied types of soluble sodium silicate indicates the highest growth of gelation speed in the soluble sodium silicate *SW-120*, a smaller increase in the speed of gelation in the soluble sodium silicate *SW-90* and the lowest speed of gelation in the soluble sodium silicate *SW-60*.

6. *Zeta* potential distribution after 100 minutes of gelation.

There has been a clear increase in the stability of elements of the structure in the soluble sodium silicate *SW-120*. In this silicate, elements of the structure disappeared with the *Zeta* potential lesser than about -90 mV, while there are elements of the structure of the *Zeta* potential from about -110 mV to about - 90 mV. In the case of soluble sodium silicate *SW-60* and *SW-90* there is a reduction in stability of the system owing to elements of the structure of *Zeta* potential from about -50 mV to about -40 mV and from about -10 mV to about +10 mV.

ACKNOWLEDGEMENTS

The Author would like to express thanks to Professor Wladyslaw Janusz from the University of Maria Curie Sklodowska in Lublin for cooperation in research.

REFERENCES

1. **Baliński A. 2002:** Wytrzymałość resztkowa mas z uwodnionym krzemianem sodu w świetle przemian fazowych powstałego żelu, Archiwum Technologii Maszyn i Automatyzacji PAN, nr 2, p. 24.

2. **Baliński A. 2002:** Pomiar potencjału ζ w aspekcie własności uwodnionego krzemianu sodu. Biuletyn Instytutu Odlewnictwa, nr 2, p. 3.
3. **Baliński A. 2000:** Wybrane zagadnienia technologii mas formierskich ze spoiwami nieorganicznymi. Struktura uwodnionego krzemianu sodu i jej wpływ na wiązanie mas formierskich. Wyd. Instytut Odlewnictwa, Kraków.
4. **Cannon F.S., Voight R.C., Furness J.C. 2002:** Non-Incineration Treatment to Reduce Benzene and VOC Emissions from Greensand System, Final Report U.S. Department of Energy, DE-FC 0799 ID13719.
5. **Glowacki C.R. (et al.), 2003:** Emission Studies At a Test Foundry using an Advanced Oxidation-Clear Water System. AFS Transactions, vol.111, p. 579-598.
6. **Izdebska-Szanda I., Maniowski Z., Pezarski F., Smoluchowska E. 2006:** Nowe spoiwo nieorganiczne do wykonywania mas formierskich. Materials engineering, nr 3, vol. XIII, p. 51-54.
7. **Izdebska-Szanda I., Pezarski F., Smoluchowska E. 2006.:** Investigating the kinetics of the binding process in moulding sands using new, environment-friendly, inorganic binders. Achieves of Foundry Engineering, vol.8, issue 2, p. 61-66.
8. **Izdebska-Szanda I. 2008:** Investigations of a correlation between the type and amount of modifier, high-temperature transformations and residual strength of sands with modified sodium silicates. Transaction of Foundry Research Institute, no 1, p. 49-64.
9. **Izdebska-Szanda I., Stefański Z., Pezarski F., Szolc M. 2009:** Effect of additives promoting the formation of lustrous carbon on the knocking out properties of foundry sands with new inorganic binders. Achieves of Foundry Engineering, vol.9, issue 1, p. 17-20.
10. **Izdebska-Szanda I., Baliński A. 2010:** Zmiany potencjału zeta układu wiążącego „uwodniony krzemian sodu – dioctan glikolu etylenowego. Polska Metalurgia w latach 2006-2010. Wyd. „Akapit", p. 418-425.
11. **Izdebska-Szanda I., Szanda M., Matuszewski S. 2011:** Technological and ecological studies of moulding sands with new inorganic binders for casting of non-ferrous metal alloys. Archives of foundry Engineering, vol.11, issue 1, p. 43-48.
12. **Izdebska-Szanda I. , Baliński A. 2011:** New generation of ecological silicate binders. Imprint: ELSEVIER, vol. 10, p. 887-893.
13. **Jankowski W., Żółkiewicz Z. 2003:** A method to evaluate the permeability and strength of ceramic protective coatings applied on lost foam patterns. Archives of Metalurgy, vol. 48, no 3, p. 277-283.
14. **James R.O., Parks G.A. 1982:** Characterization of aqueous colloids by their electrical double-layer and intrinsic surface chemical proprieties. Surface and Colloid Sci., vol.12, p. 119-129.
15. **Karwiński A., Żółkiewicz Z. 2011:** Application of modern ecological technology lost foam for the implementation of machinery. Teka, v.. XIC, p. 91-99.
16. **Karwiński A., Haratym R., Żółkiewicz Z. 2009:** Określenie możliwości zastosowania modeli zgazowywanych do wykonania odlewów precyzyjnych. Motrol, t. 11, p. 97-103.
17. **Pezarski F., Izdebska-Szanda I., Smoluchowska E., Świder R., Pysz A. 2011:** Zastosowanie mas formierskich ze spoiwem geopolimerowym do produkcji odlewów ze stopów Al. Prace Instytutu Odlewnictwa, t. LI, nr 3, p. 23-34.
18. Projekt badawczy nr 7 T08B 052 20. 2001: Badania wpływu kondycjonowania szkliwa krzemianowo-sodowego na strukturę, potencjał zeta i właściwości kohezyjne uwodnionego krzemianu sodu jako spoiwa wieloskładnikowego układu mas formierskich utwardzanych chemicznie.
19. **Pytel A., Stefański Z. 2011:** An Inovative and Environmentally Safe Method to Manufacture High-Quality Iron Castings for Possible Use as Elements of Agriculture Machines. TEKA, vol. XIC, p. 256-263.
20. **Różycka D., Stechman M., Wilkosz B., Baliński A. 2000:** Szkło wodne jako spoiwo w odlewnictwie. Cz. II. Struktura, Chemik, t.53, nr 8, p. 21.
21. **Smoluchowska E., Pezarski F., Izdebska-Szanda I., Stefański Z. 2007:** Przegląd nowych technologii z zakresu wytwarzania mas formierskich i rdzeniowych. Odlewnictwo – Nauka i Praktyka, nr 1-2, p. 78.
22. **Żółkiewicz Z., Żółkiewicz M. 2009:** Lost foam process – the chance for industry. TEKA. v. IX, p.431-436.
23. **Żółkiewicz Z., Żółkiewicz M. 2010:** Characteristic properties of materials for evaporative patterns. Archives of Foundry Engineering, vol. 10, special issue, p. 289-292.

WPŁYW KONDYCJONOWANIA TERMICZNEGO SZKLIWA KRZEMIANOWO-SODOWEGO NA KINETYKĘ ZMIAN POTENCJAŁU ZETA W PROCESIE ŻELOWANIA UWODNIONEGO KRZEMIANU SODU

S t r e s z c z e n i e . Opisano wyniki badań zmian potencjału Zeta układu „uwodniony krzemian sodu – ester" w zależności od czasu jego żelowania. Stwierdzono, że czas kondycjonowania termicznego szkliwa krzemianowo-sodowego ma istotne znaczenie w aspekcie stabilności elementów nanostruktury uwodnionego krzemianu sodu. Charakterystyka stabilności tych elementów może wpływać na charakterystykę wiązań układu spoiwo krzemianowe-kwarc, a tym samym na ich właściwości wytrzymałościowe w temperaturze otoczenia.

S ł o w a k l u c z o w e : uwodniony krzemian sodu, szkliwo krzemianowo-sodowe, potencjał Zeta, kondycjonowanie termiczne.

TEKA. COMMISSION OF MOTORIZATION AND ENERGETICS IN AGRICULTURE – 2012, Vol. 12, No. 1, 09–12

The wireless notification systems used in car alarm systems

Artur Boguta

Lublin University of Technology
Faculty of Electrical Engineering and Computer ScienceDepartment of Computer and Electrical Engineering,
Nadbystrzycka 38A, 20-618 Lublin,Poland
tel.: (+48 81) 53-84-301, fax: (+48 81) 525-46-01; e-mail: a.boguta@pollub.pl

Summary. More than ten thousand cars disappeared in Poland last year. This situation was caused by relatively quick profit on sale of such cars and their components after disassembling. It happens increasingly often that the driver is stopped and the car is taken by force by thieves. The only one method to protect the car consists in its monitoring associated with the use of modern methods of stolen vehicle tracking. The car alarms systems are provided with several functions and protections sometimes efficiently preventing the car theft or making the car harder to steal. The systems become more and more perfect every day but nobody pays any attention to car alarms owing to their common use and particularly frequent false alarms originating from the cars parked in the streets and parking areas. 24 hour security monitoring is the best method to protect a car. There are companies offering *specialized security services in this scope of property, but their services are rather expensive.* The monitoring system using the car positioning on the basis of GPS satellite signal is a good way to protect the car and to find it thereafter. The signal informing about occurred burglary and the present position of the car is transmitted by means of SMS text message via GSM mobile telephony system. Using bidirectional data transmission path in GSM system it is possible to control, to turn ON/OFF any connected device, to download the readings from any sensors in remote mode. GSM system, except of the reading of geographical location of the receiver, makes it also possible to directly read the altitude above sea level, current time and date. It is also possible to read the current velocity of the object after a little processing of data received from satellite. The full monitoring of our vehicle is possible as a result of the combination of GPS and GSM technology. The possibilities offered by the system depend exclusively on the ingenuity and imagination of its designer.

Key words: car alarm, GPS, GSM.

ALARM SYSTEM STRUCTURE AND CONFIGURATION

The following design inputs are required in order to build a system performing the functions of an alarm control panel and transmitting the current alarm status data:
- informing the local area about occurred burglary;
- transferring the data on the occurrence of an event, its place and time;
- hiding the system in a manner enabling further transmission of messages to inform about the current position of vehicles even after disconnection of signalling devices;
- emergency power supply for communication module to enable its further operation even after power supply shutoff,
- inertial tilt sensor protecting against car towing,
- opening sensor for the door, engine hood, trunk lid etc.;
- SMS message about occurred alarm, about the time of its occurrence and geographical position of the car;
- controlling the alarm control panel (enabling / disabling) using the attempt to connect from an authorized phone number (lack of additional pilot) only;
- co-operation with maps e.g. Google.

CONSTRUCTION OF THE ALARM CONTROL PANEL

The alarm control panel consists of three blocks performing the following functions:
- GPS receiver segment determining the current position of the car;
- GSM modem segment to be used as a communication link;

– micro-controller segment ensuring the system operations management in accordance with elaborated program.

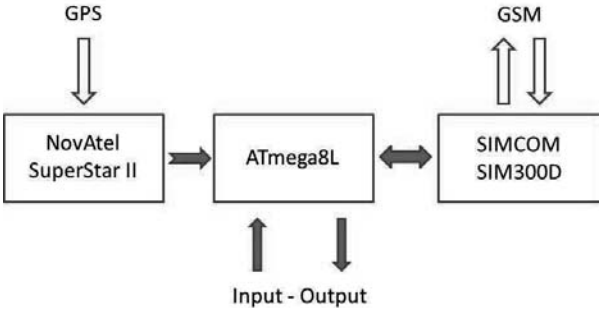

Fig. 1. Block diagram of the alarm control panel

SuperStar II module supplied by NovAtel company has been applied in the system as GPS signal receiver. The module operating in NAVSTAR GPS standard has been designed in the form of 12 channel receiver (receiving the data from maximum 12 satellites simultaneously) and provided with configurable RS-232 interface. StarView software is made available free of charge by the manufacturer in order to enable its configuration, to preview all possible transmission parameters as well as incoming frames in NMEA or binary standard. The receiver position update rate is adjustable between 1Hz and 5 Hz.

After the voltage is applied, available satellites are automatically searched by the receiver and successive frames containing position data are displayed on Tx line of built-in serial interface. The task of the microcontroller is to search the frames and then "to catch" interesting information from $GPGGA frame about GPS coordinates, time and altitude of the location of an object being monitored above sea level. GSM/GPRS SIM300D modem supplied by SIMCOM has been installed in order to enable the data transmitting and receiving. The modem operating in GSM 900MHz, DCS 1800 MHz and GSM 1900MHz bandwidth has been built as a "cellular phone" without unnecessary elements i.e. keyboard, display, loudspeaker, microphone. AVR Atmega8 microcontroller has been used to ensure GPS receiver and GSM modem operation and RLC passive elements in order to ensure the correct collaboration of the systems. The communication is carried out by means of corresponding AT commands transmitted by a serial interface.

AVR Atmega8 microcontroller has been designed as "a bridge" connecting GPS system with GSM system and enabling the management of GPS receiver and GSM module operation. The commands transmitted by the microcontroller trigger an alarm and send the information about occurred event, its time and location. Its program has been elaborated in Basic language in FastAVR environment and downloaded from the computer by means of STK500 interface and AVR studio 4 program.

The purpose of built – in EEPROM in the system is to save the current status of alarm control panel in case of power supply failure.

WORKING PRINCIPLE OF THE ALARM CONTROL PANEL

Before the commencement of the system use, determine the number of mobile phone of the person authorized to control the alarm control panel and to receive SMSs with alarm messages. Therefore, in SIM card (by means of mobile phone) cancel all items in the telephone book of the card including those programmed in the factory by operator . ONLY one entry shall be contained in the telephone book of SIM card on the position No 1 in the following form: name of contact: SIM1, number: +48xxxxxxxxx, where xxxxxxxxx stands for 9 digits of authorized phone number. PIN of the card shall be disabled.

After the card prepared in a manner described above is placed in a basket, the system shall be turned ON by means of a switch installed on the battery. The setting of this switch should be modified until yellow LED3 diode starts to blink. At this time, the main power supply (temporary power pack or target battery of motor vehicle) can be connected.

During the period of about 2 minutes after the system is turned ON, the modem is in course of initialization and registration in mobile telephony operator network. This status is displayed by means of continuously lighting green LED2 diode and LED1 diode blinking with the frequency of about 0.3Hz.

After the correct initialization two short sounds are transmitted by the buzzer to confirm this fact and the normal operation mode of the alarm control panel is commenced. The data on the last operation status are read by the system from EEPROM memory. LED3 diode lights up only if the alarm control panel is enabled or turned off when the alarm control panel is in enabled or alarm status.

The first synchronization of GPS module with satellite by the receiver may take 2 up to even 15 minutes. It depends on whether the alarm control panel was situated in a geographical position other than before prior to turning off and whether the antenna of GPS receiver is "seen" from satellites without any obstacles.

The enabling / disabling and alarm cancelling for the alarm control panel consists in the attempt to communicate with the number represented by installed SIM card. If the attempt to communicate has been made by an authorized person, the incoming connection is rejected by the modem simultaneously changing the status the alarm control panel into opposite one. If the calling number is not conforming with SIM1 item recorded on SIM card of the alarm control panel, the following SMS message is received by the owner of the number saved in SIM1 item:

„Number +48xxxxxxxxx attempted to communicate with the alarm control panel!", where xxxxxxxxx stands for the number of person not authorized to control the alarm control panel. The system does not change its operation status. The same happens in case of an ex-directory (private) number calling to the alarm control panel. Then the following information

message is received by an authorized person indicated in SIM1 item on SIM card of the alarm control panel:

"Ex-directory number attempted to communicate with the alarm control panel!".

In case of an alarm status, the following SMS message is sent to an authorized user:

„Attention, ALARM! GPS data: Time: hh:mm:ss Latitude: xx*yyyyyyy'y Longitude: aaa*bbbbbbb'b Altitude above sea level: ccc,d m" where:

hh:mm:ss– current time downloaded from GPS satellite: hh hour, mm minute, ss second,

xx*yyyyyyy'Y– Latitude: xx – degrees, yyyyyyy minutes, y – E or W,

aaa*bbbbbbb'B- Longitude: aaa – degrees, bbbbbbb minutes, b – N or S,

ccc,d – altitude above sea level: ccc – value in meters, d – tens of meters.

The receiving of the current GPS data frame is carried out with frequency of 1Hz. The data from the part of frame beginning with $GPGGA marker are processed and transmitted to the user.

In case of the lack of GPS receiver synchronization with satellite, incorrect data are contained in SMS messages.

The data received in SMS can be displayed by means of a computer program with a map e.g. Google Maps. Therefore the user is able to display the visualization of the current position of the receiver and consequently, the position of monitored object.

The frequency of transmitted SMSs with GPS coordinates is adjustable as a result of changes of a constant value in the program; its standard setting is equal to 30 seconds.

The alarm control panel is equipped with two inputs generating alarms after triggering. One of inputs has been designed as NC type and another collaborates with the tilt sensor triggered after the change of the car tilt or the change of its acceleration. NC input can be used to connect the opening sensors for the door, engine hood, trunk lid or to the output of car alarm system installed in the factory.

The tilt sensor consists of a miniaturized metal cylinder and a metal ball placed therein. The ball closes or opens the circuit connected thereto depending on the tilt angle of the sensor. At the time of alarm enabling, the sensor status before the enabling is saved by the alarm control panel. An alarm is triggered as a result of the sensor status change simultaneously provided that the pulse duration is larger than 200 ms. This function is intended to reduce false alarms, for instance caused by the vibration generated by a heavy motor vehicle passing by or by strong gust of wind.

The buzzer has been applied in the model as an actuator. In fact it is possible to apply among others a loud alarm siren or ignition / fuel pump cut-off relay for this purpose.

CONCLUSIONS

The purpose of the construction of described system was to present the opportunities offered by the coupling of GPS and GSM technology in practice. The alarm control panel described in the present paper has been built as a model system. Therefore the adaptation of the enclosure to intended working environment would be required in case of practical use of the alarm control panel. The use of a mobile phone as a controlling and notifying medium makes it possible to eliminate a frequently occurring problem in case of typical alarm control panel i.e. the loss or destruction of the control pilot. In case of the mobile phone destruction, SIM card can be moved to another phone and in case of theft a duplicate of SIM card is issued for a small fee, but it is more expensive to duplicate the pilot.

REFERENCES

1. **Buczaj M.:** Wykorzystanie telefonii mobilnej i Internetu w procesie przekazywania informacji w systemach nadzorujących stan chronionego obiektu. Zabezpieczenia nr 1/2010, p. 56-61. [The use of mobile telephony and Internet in the information transfer process in the systems supervising the state of protected objects].
2. **Gavrysh V., Morneva M.:** OF THE WIRELESS DATA TRANSMISSION SYSTEMS, p. 133 Teka -2010 Commission of Motorization and Power Industry in Agriculture 2010.
3. **Bogusz J.:** Moduły GSM w systemach mikroprocesorowych, Wydawnictwo BTC 2007 [GSM modules in microprocessor systems].
4. **Kaniewski P.:** System nawigacji satelitarnej GPS, część 6, Pozycja, prędkość i czas, Elektronika Praktyczna, 7/2006, s 104-106. [GPS satellite navigation system, part 6, Position, velocity and time, Practical Electronics].
5. **Kaniewski P.:** System nawigacji satelitarnej GPS, część 7, Pozycja, prędkość i czas, Elektronika Praktyczna, 8/2006, p. 97-99. [GPS satellite navigation system, part 7, Position, velocity and time, Practical Electronics].
6. **Kaniewski P.:** System nawigacji satelitarnej GPS, część 8, Komunikacja z odbiornikiem GPS, Elektronika Praktyczna, 9/2006, s 108-110. [GPS satellite navigation system, part 8, Communication with GPS receiver, Practical Electronics].
7. **Wierzbicki S.:** Diagnosing microprocessor-controlled systems, s. 182, Teka -2006, Commission of Motorization and Power Industry in Agriculture.
8. **Cupiał K., Grzelka J., Duszyński A., Grzelka P.:** The traction survey and monitoring of a vehicle using a satellite navigation system, Teka -2005, Commission of Motorization and Power Industry in Agriculture.

SYSTEMY POWIADAMIANIA RADIOWEGO STOSOWANE W SYSTEMACH ALARMOWYCH SAMOCHODÓW

Streszczenie. Minionego roku w Polsce zginęło kilkanaście tysięcy aut. Spowodowane to jest dość szybkim zyskiem wynikającym ze sprzedaży takich aut oraz ze sprzedaży

zdemontowanych części. Coraz popularniejsze stają się sytuacje uprowadzeń, kiedy to złodzieje zatrzymują kierowcę i siłą odbierają mu pojazd. Jedynym sposobem na ochronę własnego samochodu jest jego monitoring z wykorzystaniem nowoczesnych metod namierzania skradzionego pojazdu. Systemy alarmowe posiadają szereg funkcji i zabezpieczeń, które potrafią niekiedy skutecznie uniemożliwić lub utrudnić kradzież pojazdu. Alarmy samochodowe z każdym dniem staja się coraz bardziej doskonalsze, lecz ich duża popularność a w szczególności częste fałszywe alarmy dobiegające z aut zaparkowanych na ulicach i parkingach powodują, że nikt na nie, nie zwraca uwagi. Najlepszym sposobem zabezpieczenia pozostawionego auta jest całodobowy monitoring. Istnieją firmy specjalizujące się w takim nadzorze naszego dobytku, ale ich usługi te nie należą do najtańszych.

S ł o w a k l u c z o w e: auto alarm, GPS, GSM.

TEKA. COMMISSION OF MOTORIZATION AND ENERGETICS IN AGRICULTURE – 2012, Vol. 12, No. 1, 13–20

Perspectives of renewable energy sources use in enhancement of environmental and energy security of belarus

*Eugene G. Busko, Sergey S. Pazniak, Sergey B. Kostukevich, Lillia A. Dudkina**

International Sakharov Environmental University, 23,
Dolgobrodskaya St., Minsk 220070, Belarus, e-mail: S.Kostukevich@gmail.com

Summary. Interest in renewable energy sources (RESs) has been growing all over the world in recent years. The market for alternative energy resources is quickly growing in Western Europe and Asia. The development of renewable energy is caused by two major factors, one of which is the environmental policy requirements. Its importance increases from the legislative point of view and from the conditions accepted by the Convention on Climate in December 1997. The main concern is energy production capacity. The preference is given to production forms which can be created and developed quickly. The development of RESs in many cases is closely connected with the maintenance of energy safety of the country, influencing its sovereignty and independence.

Key words: renewable energy sources, alternative energy.

INTRODUCTION

Energy safety problems in Belarus are mainly characterized by the fact that the Republic must buy up to 85% of energy resources. The basic domestic direction for maintaining energy safety includes a number of fundamental ways to prevent threats, thereby reducing the probability of their occurrence and easing the consequences. On the one hand, there are energy wasteful industrial and household sectors in the country; on the other hand, there are essential energy-saving reserves (including RES use), both in the energy and in other sectors of the national economy [4,6,12,15,19,11]. Nowadays, satisfaction of needs in fuel and energy resources (FERs) of Belarusian consumers, maintenance of efficient fuel-energy balance structure of the country, and the quest for additional energy sources have become the three main problems posed for the fuel and energy complex in the Republic (see "The program of increase in the use of local fuel types and alternative energy sources for 2003-2005 and up to 2010"). The involvement of RESs in the economic turnover serves as an energy-saving component which is directed to realization of legal, organizational, scientific, industrial, technical, and economic measures of effective utilization of energy resources.

The Republic of Belarus does not have sufficient amount of its own FERs to maintain national economy needs. National resources of available fossil fuels are few and they are depleted practically up to 80-90%. The country imports about 84% of the consumed FERs. Obsolete capital assets in energy, industry, agriculture and habitation are used up to 70-90% [13]. Therefore, as a result of low supply with its own energy sources (at the level of 15-18% from the general need) the problems of energy safety are the major components of the national and economic security for the country. The necessity for increasing energy safety is mainly caused by the need to quickly solve this problem, because, if the delivery of energy resources is restricted, the Republic can suffer a loss from gross domestic product (GDP) underproduction to the sum of $400-450 with the expectation of 1 ton of standard coal (TSC). It repeatedly exceeds the cost of FER import from any existing or new suppliers according to world prices. In case of emergency conditions in fuel systems or in the event of switching-off the heat supply systems during the winter period, the size of damage can be increased many times [10,19].

The most important branch of the economy in any developed country is power engineering. The moving forces and trends of its development reflect the processes of economical state and development of the country, geopolitical situations, and historical prospects. Realization of the measures taken by the government during 1995-2000 allowed a suspension in the decrease in production in the Republic. By the end of 1996, positive dynamics of main macroeconomic processes were achieved, year-to-year increases of GDP and consumer and industrial goods production were provided. Investment activity grew. We

succeeded in stabilizing the situation in the domestic consumer market as well as financial enterprises. From 2001 to 2005 GDP grew by more than 43%. In Europe, from 2000 to 2004 GDP increased on the average 1.7% a year, in the USA 2.8%, in Japan 1.9%, in Belarus this parameter reached 9.2% in 2005.

In 1990, the total FER gross consumption came to 54,965 million TSC, in 2000 it was only 34.5 million TSC, in 2005 (according to evaluation data) it was 36.8 million TSC (Fig. 1). The main reasons for the sharp decrease in energy resource consumption in Belarus during 1990-2000 was the decrease in industrial production, structural, changes in the energy sector of the national economy, as well as tough governmental policy on every possible economy of energy resources. At the same time, the composition of used fuel was changing. The consumption of heavy oil fuel (black fuel, mazut) was decreasing and the consumption of imported Russian gas was increasing. The average price of Russian gas reached about $50 per 1000 m^3 (2009) and it has constantly been increasing, approaching the world level.

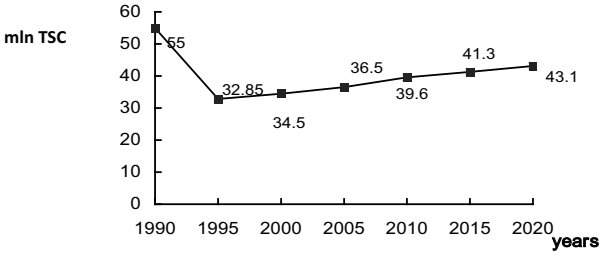

Fig. I. Time history of fuel and energy resources (FER) in Belarus (according to the data given by the Ministry of Statistics of Belarus and national energy development programs)

In the long-term outlook, the total FER gross consumption will grow. According to the formal forecast, by the year 2020, the size of total consumption will reach 43.1 million TSC, which is only 65- 70% of the consumption level that existed in 1990. In the future, the development of the national economy of the Republic should be followed by an increase of energy use efficiency, related to its consumption, development, and transportation. During 2001-2005, the GDP power consumption in the Republic decreased at a rate of 4.7-5.4% per year. In 2006-2010, average annual rates of energy consumption decrease were expected to be higher - 5.1-5.9% per year, and by 2020 they will decrease to 2.2-3.0% per year.

Nowadays, the problems facing power engineering specialists can be divided into two parts: application of new technologies using fossil fuel and development of alternative energy sources (wind and seasonal solar energy, biomass and waste).

ANALYSIS AND PROSPECTS OF THE USE OF ALTERNATIVE AND RENEWABLE ENERGY SOURCES

GENERAL CHARACTERISTIC OF THE PROBLEM

According to natural, geographic, and meteorological conditions in Belarus, alternative and renewable energy sources (RESs) can be the following: firewood and wood waste products, water resources, wind-driven potential, biogas from cattle-breeding waste, solar energy, phytomass, solid domestic waste, plant growing waste, and geothermal resources. There are several reasons why these energy sources should be widely used in the Republic. First of all, the work on the use of RESs will promote the development of our own technologies and equipment which can be exported in the future. Secondly, these sources, as a rule, are pollution free. This contributes to environmental security of Belarus. Thirdly,

Table 1. Economically expedient potential of the use of fire wood and wood waste products for heat and electric energy production

Year	Firewood		Wood waste products (million TSC)	Total (million TSC)
	million cubic meter	million TSC		
2003	4.18	1.11	0.28	1.39
2004	4.51	1.20	0.29	1.49
2005	5.36	1.43	0.31	1.74
2006	6.30	1.68	0.32	2.00
2007	7.29	0.33	2.27	2.27
2008	8.08	2.15	0.35	2.50
2009	8.95	2.38	0.36	2.74
2010	9.40	2.50	0.37	2.87
2011	9.88	2.63	0.39	3.02
2012	10.15	2.70	0.40	3.10

the development of such sources will raise energy safety of the state.

In order to cover the costs for the alternative energy sources, special attention should be paid to technical approaches using equipment produced in the Republic and with maximal use of local materials.

FIREWOOD AND WOOD WASTE PRODUCTS

The Republic of Belarus has huge forest resources. The total area of the forest resources on 1 January 2001 was 9,248,000 ha, forest timber inventory - 1340 million cubic meters. Annual basic increase is 32.37 million cubic meters. A systematical and stable growth of forest resources can be predicted (up to 1.8 times in 2020) if a simultaneous improvement of age and stock forest structure takes place [18].

The centralized logging and firewood preparation in Belarus is carried out by enterprises of the Ministry of Forestry and by the Belarussian concern of wood-paper Industry. In 2003, the annual volume of firewood, sawing, and woodworking waste utilization as boiler stove fuel was 1.4 million TSC [Table 1] [19]. At present firewood fuel consumption for production of electric and heat energy by energy generative settings does not exceed 600,000 TSC per year.

The potential of the Republic to use wood as a fuel is estimated to be 3.5-3.7 million TSC per year, which is 2.5 times higher than in 2003. It should be pointed out that all the regions of Belarus own firewood recourses. On the whole in the Republic, the annual volume of firewood, sawing, and woodworking utilization was about 1.0-1.1 million TSC. Part of the firewood goes to population via self-stocking which is estimated at 0.3-0.4 million ISC.

Limited opportunities for Belarus to use wood as a fuel can be defined from the natural annual firewood increase. It is estimated at 25 million cubic meters or 6.6 million TSC per year including that for the contaminated areas of the Gomel region - 20,000 m^3 or 5300 TSC.

In order to use wood as a fuel in these regions it is necessary to work out and to apply new technologies and equipment for gasification and parallel decontamination. According to the planned double growth of firewood storage by 2015 and taking into account volume increases of wood waste products, sawing wastes and firewood processing, in 2005 the annual volume of firewood increased up to 1.6 million TSC.

International Sakharov Environmental University (ISEU) together with Austrian firm KOB developed a project on installation on the territory of Educational and Research Station Volma, Dzerzhinsk region, in 2006 of two modern heat-and-power engineering stations which will use raw wood bio-material. Heat-and-power engineering station PYROT with the capacity 250 kW (ground firewood) is shown in Fig. 2 (on the left side) [4,10].

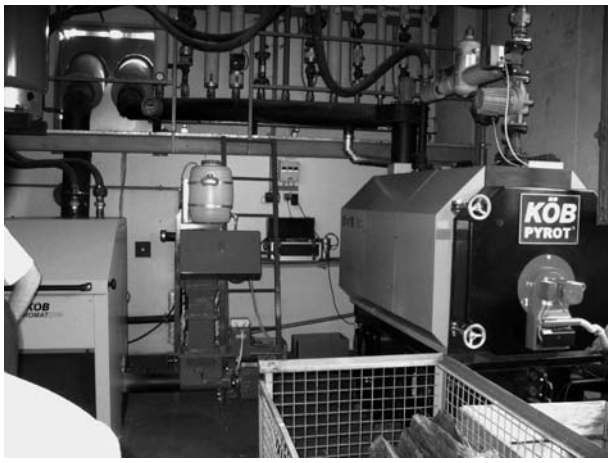

Fig. 2. Overview of heat -and-power engineering stations, KOB firm

Along with the use of wood waste products for heating purposes, it is worthwhile to provide economically grounded involvement of wood waste products of hydrolytic factories (lignine) into the fuel balance of the Republic. In the city of Rechitsa, Gomel region, a new industrial station using lignine has been put into operation. Lignine resources are about 1 million TSC per year, and an expedient volume of use is estimated to be 50,000 TSC per year. To solve the problem we need investment support, an application of the system of fixed prices, and a normative legal base modernization specified on tax preferences for enterprises producing electric and thermal energy from firewood.

WATER POWER RESOURCES

The installed capacity of 20 hydroelectric power stations (HPSs) in Belarus was 10.9 MW on 1 January 2004. Due to water power resources about 28 million kWh of energy is produced annually. It is equivalent to the replacement of imported fuel at the rate of 7900 TSC. The potential capacity of all water channels in Belarus is 850 MW including technically accessible (520 MW) and economically expedient (250 MW) capacities [19].

The main directions of the development of small hydropower engineering in Belarus are the following: construction of new HPS, reconstruction, and restoration of existing UPS. The unit capacity of each hydropower unit will be in the range of 50- 5000 kW (Table 2), and the preference in that case will be given to quick mounted hydropower units of the capsular type.

Having the capacity of hydropower units from 50 to 150 kW it is possible to use asynchronous generators as the simplest and most reliable units in operation. As a rule, all the restored and newly constructed HPSs should work in parallel with power supply systems that will allow, in future, the simplification of circuit and constructive decisions.

Special attention in Belarus should be paid to the problems of cascade HPS construction on the rivers Sozh, Dnepr, and Pripyat because the possible scales of water flooding of the adjacent territories are limited by the zone contaminated with radionuclides.

WIND-DRIVEN POTENTIAL

On the territory of Belarus there are 1840 sites for the installation of wind energy stations with a theoretical energy potential of 1600 MW and annual power generation of 6.5 billion kWh [19]. On 1 January 2005 the total capacity of installed wind energy stations was 1.1 MW and the replacement volume was 0400 TSC (Table 3). In fact, in 2005 in Belarus there were only three wing stations («Ecodom», Naroch-2, «Areola» Minsk-l) with the total capacity of 850 kW, and one rotor wind energy Station (Fig. 3) with the total capacity of 250 kW situated on the territory Educational and Research Station Volma, ISEU.

The development allowing the transformation of wind power into electric power by means of traditional wing wind energy stations used so far, in conditions of Belarus were economically unjustified. This fact was one of the reasons of the development of the rotor wind energy station (Fig. 3). However, modem technical development allows the creation of similar wing wind energy stations with a starting wind speed from 3 m/s and with rated operation speeds of 7-8 m/s. The cost of such stations is varying from $800 to $1200 for 1 kW of the established capacity. This makes such stations more attractive for use [20].

The Republic of Belarus is characterized by weak continental winds with the average speed of 4-6 m/s. Therefore, choosing the sites for the wind energy stations special tests and careful studies of FER on their application are required. In order to get an objective estimation about the reserve opportunity of full wind-driven potential, it is also required to complete a cycle of experimental research. The necessity of parallel work of wind energy stations with power supply system brings some complications into the general scheme and, thus, expenses for creation and operation of wind energy stations will increase considerably. At the same time, while calculating the expenses also the necessity of creation and maintenance of power reserve on other types of power stations should be taken into account. According to expert predictions, no more than 5% of the general potential

Table 2. Real and predicted volumes of the use of water and power resources for the electric energy production

Year	Input capacity (MW)	Total installed HPS capacity	Increase of replacement volume (,000 TSC per year)	Power generation (million kWh_per year)	Total replacement volume (‘000 TSC)
2005	0.76	11.94	0.97	34.9	9.77
2006	0.55	12.49	0.70	37.4	10.47
2007	18.37	30.86	23.50	121.3	33.97
2008	23.30	54.16	29.80	227.8	63.77
2009	20.80	74.96	26.60	322.8	90.37
2010	15.00	89.96	19.20	391.3	109.57
2011	0.29	90.25	0.40	392.8	109.97
2012	5.50	95.75	7.00	417.8	116.97

Table 3. Real and predicted volumes of the use of wind-driven potential for electric energy production

Year	Total installed capacity of wind energy settings (MW)	Power generation (million kWh_per year) (TSC)	Total replacement volume (000 TSC)
2005*	1.2	2.15	0.60
2006	1.7	3.04	0.85
2007	2.2	3.94	1.10
2008	3.7	6.62	1.85
2009	3.7	6.62	1.85
2010	3.7	6.62	1.85
2011	5.2	9.31	2.61
2012	5.2	9.31	2.61

*Actual power for today

will be developed by the year 2005, i.e., 45 million kWh which is equivalent to 12,000 TSC.

Fig. 3. Overview of a rotor wind energy station, ISEU

One of the main directions of wind energy stations application will be their application for pump drive stations with low capacity (5-8 kW) and for water heating in the farming industry. These areas of application arc characterized by minimal requirements for electric energy quality that allows a simplification and sharp reduction in the price of wind energy stations.

BIOGAS FROM LIVESTOCK WASTE

Tests results on biogas production from wastes of cattle-breeding complexes have proved that they are not economically competitive for only biogas production. The main reason is that it is possible to receive pollution-free and high-quality organic fertilizer without additional power expenses and as a result to reduce the power-consuming industry of mineral fertilizer production proportionally. The application of biogas allows us to improve environmental situation near the large-scale farms and cattle-breeding complexes, as well as on the areas under crops where livestock wastes arc spread nowadays, and in addition to receive high-quality biohumus fertilizers. Potential production of commodity biogas from cattle-breeding complexes is estimated to be 160 000 TSC per year, and by 2005 it will be no more than 15,000 TSC [19,2].

GEOTHERMAL RESOURCES

In the Republic of Belarus, geothermal resources with the density of more than 2 TSC/m^2 and the temperature of 50°C at the depth of 1.4-1.8 km, and 90-100°C at the depth of 3.8-4.2 km are found in the Gomel and Brest regions [19]. However, high mineralization, low productivity of available wells, small number of wells and, on the whole, our poor knowledge of this resource will not allow the development of this RES for the next 10-15 years.

SOLAR ENERGY

According to meteorological data, on average in Belarus there are 250 overcast, 85 rainy, and 30 clear days in a year. To satisfy electric power needs of Belarus in the volume of 45 billion kWh, 450 km^2 of heliostats are required. The price of heliostats is $450 per m^2, which is equal to $202.5 billion without the expenses for the exploitation of the synchronizers, building and construction works, cables, control systems, technical services, infrastructure, etc. The listed components will double the given sum.

Taking into account foreign experience and the experience gained from the building of a solar power station in the Crimea, specific capital investments and energy production costs are ten times higher using solar energy than using other sources. Technical progress in this area will promote the reduction of costs; however, in the case of Belarus, electric power production using solar energy will not be practical in the near future.

The main directions of solar energy utilization will be heliowater heaters and various heliostations for intensification and enhancement of drying processes as well as water heating in the farming industry [1,14].

In Belarus heliowater heaters with welded plastic collectors are worked out and prepared for large-scale manufacture. Therefore, the expensive heavy-metal pipes are not required for solar collectors, which makes their production more economical. Provided favorable conditions of economic and manufacturing facilities, the widest application of heliowater heaters in southern regions of the Republic can be expected.

At the same time it is expedient to develop in Belarus the following resources:

– Self-contained power supply with capacity starting from some watts up to 3-5 kW (home equipment, lightening, power supply of residential houses, lines of communication, etc.)
– Modular photoelectric stations for rural consumers with the capacity from 0.5 to 1 kW based on the elements modern generation

The development of such sources and stations needs a number of research efforts to create modern materials, to improve the quality of the existing materials (based on silicium), to reduce its price and, consequently, the price of the finished products.

In the favorable conditions of economic and manufacturing facilities a replacement of about 25,000 TSC per year of organic fuel with solar energy can be expected by 2020.

In the ISEU the solar water heating station («Doma», Austria) with the capacity of 1.0 kW and the photoelectric station («Fotovoltaik», Austria) have been used successfully for more than 5 years. They arc used for emergent lighting of the ground floor and as a training and visual appliance in the educational process (Fig. 4). In the near future it is planned to install also a photoelectric station with a capacity of 1.5 kW («Stromaufwaerts» Austrian firm) in the educational-hotel building of the University in Volma.

DOMESTIC WASTE

The percentage of organic substances in domestic waste is about 40-75%. Domestic waste consists of 35-40% carbon, 50-88% combustible components, and 40-70% ash. The caloric value of domestic waste is 800-2000 kcal/g [19,8].

In world practice, power production from domestic waste can be realized in several ways such as burning, active and passive gasification. Gasification has the greatest potential in contrast to direct burning as the latter causes environmental problems. To solve these problems, an investment twice exceeding the cost of the burning stations would be needed.

In Belarus about 2.4 million tons of solid domestic waste is collected annually. They are dumped or directed to two waste reprocessing plants (in Minsk and Mogilev). Annually, the following amount of solid domestic waste is collected there (in thousand tons):

– Paper - 648.6.
– Food wastes-548.6.
– Glass-117.9.
– Metals - 82.5.
– Textile-70.8.
– Wood-54.2.
– Leather and rubber - 47.2.
– Plastic - 70.8 [19].

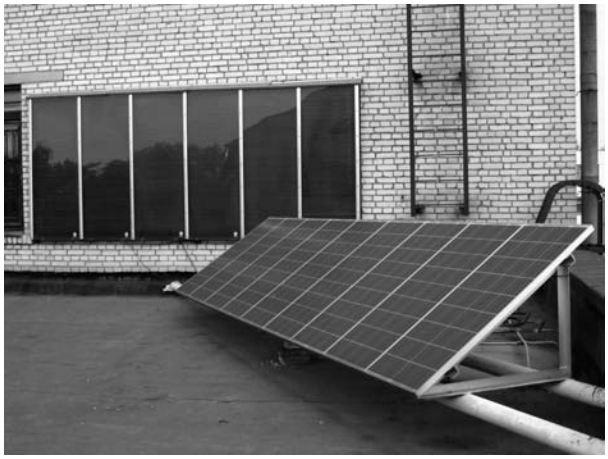

Fig. 4. Overview of solar water heating and photoelectric stations, ISEU

Potential energy of solid domestic waste collected in Belarus equals 470,000 TSC. In the case of biotreatment of these wastes with the purpose of gas production, the efficiency will not exceed 20-25%, which is equal to 100,000-120,000 TSC. Long-term stocks of solid domestic waste from all large cities should be taken into consideration due to the problems of its storage. It could be possible to get about 50,000 TSC from the processing of solid domestic waste into gas in the regional cities of Belarus, while in Minsk this number could be equal to 30,000 TSC. The efficiency of that direction should be estimated not only from the direct output of biogas, but also from the ecological component which is the basis in this problem. Certain characteristics of the effectiveness can be received on the basis of detailed design studies, creation, and operation of experimental-industrial area. By 2005, it can be possible to get up to 10,000 TSC.

PHYTOMASS

As a raw material for liquid and gas fuel production, a periodically RES -phytomass of fast-growing plants and trees - can be used. In the climatic conditions of the Republic, a great number of plants in the amount of 10 t of dry substance which is equal to 5000 TSC are collected from 1 ha of power plantations. Using some additional agricultural methods the productivity of a hectare can be doubled. From this quality of phytomass it could be possible to get 5-7 t of liquid products equivalent to mineral oil. For raw material production the most appropriate would be the use of worked out peat deposits where no conditions for agricultural crops can be found. The area of such deposits in the Republic is about 180,000 ha, which can become a stable, pollution-free source of energy raw material in a volume up to 1.3 million TSC per year [4,16,11].

The use of rapeseed oil as an energy resource has great potential for the Republic of Belarus. The Republic has experience in rape cultivation; there are also some rapeseed-processing plants there. Taking into account the fact that rape does not accumulate radionuclides, its cultivation on the areas contaminated after the Chernobyl accident becomes particularly important. There is some experience gained in that direction. Thus, for example, in 2005 a diesel power station with the capacity of 300 kW (electric energy) and 400 kW (thermal energy) running on rapeseed oil was installed and put into operation by the Institute of Radiology, Otto Hugo Munich University together with ISEU. This station was put into operation in the milk-processing plant in Khoiniki within the framework of a humanitarian project – Fig. 5.

Fig. 5. Overview of diesel power station, working on rapeseed oil in Khoiniki

The lack of experience in the wide use of phytomass for energy production does not allow the estimation

of the expenses and future prices of the fuel. Special techniques, road infrastructure, reprocessing enterprises, etc, should be developed for this purpose. However, according to the integrated calculation the price adds up to $35 per TSC. According to the expert estimations by the year 2012, about 70,000-80,000 TSC can be received due to the use of phytomass for energy production [3,17,5].

PLANT GROWING WASTE

The use of plant growing waste for energy production is considered to be a fundamentally new direction in energy savings. Practical experience of plant growing waste application as the energy earner has been acquired in Belgium and the Scandinavian countries, but not yet in Belarus. The total potential of plant growing waste is estimated to be about 1.46 million TSC per year (Table 4) [19]. The decisions on expedient volumes of burning plant growing waste for fuel production should be made by comparing certain economic needs. By the end of the predicted period this value is estimated at the level of 40,000-50,000 TSC.

Table 4. Real and predicted volumes of the biogas production, domestic waste, phytomass for electric and thermal energy production

Energy resource (,000 TSC)	2007	2008	2009	2010	2011	2012
Biogas	6.6	13.2	19.8	26.4	32.9	39.5
Domestic wastes	4.9	9.9	14.8	19.8	24.7	29.6
Phytomass	12.4	24.7	37.1	49.4	61.8	74.1
Total	23.9	47.8	70.7	95.6	119.4	143.2

From Table 4 it can be seen that due to all renewable and alternative energy sources, as well as thermal secondary power resources, mineral oil, oil gas and peat, the volume of local energy carriers is estimated as 6.75 million TSC per year.

CONCLUSIONS

A working system on the development of the potential including educational programs for decision-making people and users of technologies should be carried out for the further development and application of alternative energy sources in Belarus. In spite of great efforts undertaken by the State Committee of Energy Efficiency and other authorities, alternative power is introduced in Belarus by a small number of pilot projects and technologies. The most successful projects are those using wood waste products for gasification with the subsequent burning and generating of thermal energy; also some small HPSs, four powerful industrial wind energy stations belonging to «Ecodom», «Areola», and ISEU; and one biogas station. Still, that is not enough. One of the low-cost ways to improve the present situation in wind-power engineering in modern economic conditions is to import second-hand wind energy stations with the capacity exceeding 100 kW. It is connected with the fact that in Europe wind energy stations with the capacity of 100-200 kW in the near future will be replaced by more powerful stations with the capacity from 600 kW up to 2.5 MW. The diagram given in Figure 6 describes the prospects of RESs and local fuel type development. A percentage of total consumption of FERs is given by nongovernmental organizations and State Committee of Energy Efficiency.

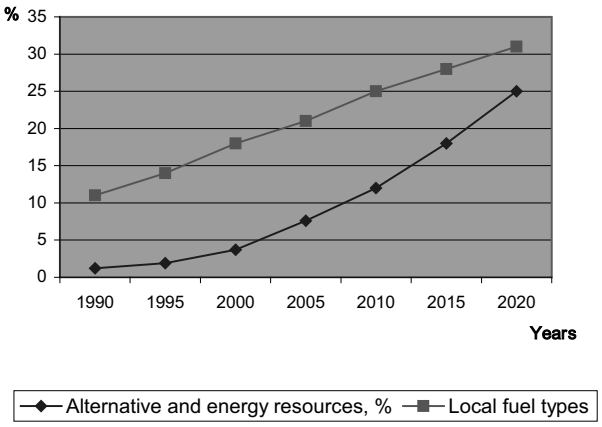

Fig. 6. Prospects of the development of alternative energy sources and local fuel types up to 2020 (ratio of total consumption FER, %)

On the whole, the described tendencies of the alternative and RESs development in the Republic of Belarus meet the same tendencies in Europe. The application of new technologies of biogas production from a renewable biomass - rapeseed oil for diesel engines and ethanol for carburetor engines - shows considerable promise for Belarus. Experience of some agricultural productions in the Grodno and Gomel regions has shown ecological expediency of the application of these technologies. It is very important to complete and update these technologies to the industrial level for local conditions and to introduce them into production by 2020. During this period the drastic cost increase for liquid mineral fuel is predicted with significant reduction of its natural resources.

The application of new technologies of biomass utilization (fast-growing wood, wood waste products) as boiler-stove fuel is also a very important question during the mentioned period. In Belarus production facilities for wide introduction of biomass gasification technologies already exist; also pilot projects on the development of these technologies have been carried out there with the support of UNDP and other international organizations. The development of these technologies will be especially important for cities and towns with wood-processing power and an advanced agrarian sector.

REFERENCES

1. Biofuels barometer. 2011 Eurobserv'er.: Systemes solaires le journal des energies renouvelables. 204 (7). 68-93.
2. Biogas barometer. 2010. Eurobserv'er. 200 (11). 104-119.
3. Building bridges to a more sustainable future. 2011. Ethanol Industry Outlook. Renewable fuels association. 2, p. 36.
4. Ground-sourse heat pump barometer. 2011. Eurobserv'er. Heat pump barometer. 205 (9). 82-101.
5. The global wind energy outlook scenarios. 2010. Global wind energy outlook. 10. 60.
6. IPCC Special Report on Renewable Energy Sources and Climate Change Mitigation. 2011. Final release. Intergovernmental panel on climate change. Working Group III – Mitigation of Climate Change. p. 1544.
7. **Lukanin A.** Disposal of municipal solid waste management. 2011. Ecological Bulletin of Russia. 10. p. 18-25.
8. **Parmuhina E.** Strategy for the Treatment of Solid Waste in Russia. 2011. Ecological Bulletin of Russia. 10. p. 26-27.
9. Photovoltaic barometer. 2011. Eurobserv'er. 5. p. 144-171.
10. The Program of increase in the use of local fuel types and alternative energy sources for 2003-2005 and up to 2010, approved by the decision of Council of Ministers of the Republic of Belarus. 2002. № 1820, amendment 2003. № 1699.
11. Renewable Energy Policy Network for the 21st Centure. 2011. Report Citation REN21. Renewables. Global Status Report. Paris. REN21 Secretariat. p. 116.
12. Renewable municipal waste pump barometer. 2010. Eurobserv'er. 2000 (11). p. 91-103.
13. **Rusan V., 2005.** Energy safety in villages. How to provide it? Power engineering and TEC. 7. p. 31-37.
14. Solar thermal and concentrated solar power barometer. 2011. Eurobserv'er. 203 (5). p. 66-92.
15. **Sidorenko G., Elzova E., Uzhegova Resources E.,** energy effeciency and development ways of Karelia region energy. 2011. Ecological Bulletin. 2(16). p. 87-94.
16. Solid biomass barometer. Electronic Resource. http://www.eurobserv-er.org/pdf/baro200c.asp.
17. Solid biomass barometer. Eurobserv'er. 2010. Barometre biomasse solide. 200 (11). p. 122-139.
18. **Tarasenko V. 2005.** The use of renewable energy sources in Belarus, Sakharov Readings 2005. Environmental problems of the XXI century. Materials of the 5th international conference, 20-21 May 2005, Minsk, Belarus, edited by Kundas, S., Okeanov. A., Shevchuk, V., P.1. Institute of Radiology, Gomel, 2005.
19. **Tarasenko V., Poznyak S. 2005.** Prospects of renewable energy sources in the Republic of Belarus, Seibit. Journal on modern agrarian production. 2. 31-33.
20. World Energy Outlook 2010. International Energy Agency. –2010. – p. 738.

ПЕРСПЕКТИВЫ ИСПОЛЬЗОВАНИЯ ВОЗОБНОВЛЯЕМЫХ ИСТОЧНИКОВ ЭНЕРГИИ В ПОВЫШЕНИЯ ЭКОЛОГИЧЕСКОЙ И ЭНЕРГЕТИЧЕСКОЙ БЕЗОПАСНОСТИ БЕЛАРУСИ

Р е з ю м е . В последние годы интерес к возобновляемым источникам энергии (ВИЭ) растет во всем мире. Рынок альтернативных источников энергии быстро растет в Западной Европе и в Азии. Развитие возобновляемой энергии обусловлено двумя основными факторами, одним из которых являются экологические требования. Ее значение возрастает с законодательной точки зрения и в связи с этими условиями принята Конвенция по изменению климата в декабре 1997 года. Второе требование касается наращивания производства энергии. В соответствии с этим требованием предпочтение отдается производству форм энергии, которые могут быть созданы и быстро развивались. Развитие возобновляемых источников энергии во многих случаях тесно связана с энергетической безопасностью страны, влияющие на ее суверенитет и независимость.

К л ю ч е в ы е с л о в а : возобновляемые источники энергии; альтернативные источники энергии, Беларусь.

TEKA. COMMISSION OF MOTORIZATION AND ENERGETICS IN AGRICULTURE – 2012, Vol. 12, No. 1, 21–23

Biodegradability of thermoplastic starch (TPS)

Maciej Combrzyński

Department of Food Process Engineering, Faculty of Production Engineering, University of Life Sciences in Lublin, Doświadczalna 44, 20-280 Lublin, Poland maciejcombrzynski@gmail.com

Summary. Thermoplastic starch (TPS) can play an important role in the processing of packaging materials. For years the Department of Food Processing has been carrying out investigations in this field. Biodegradability test results of TPS moulding enriched with functional additives are presented in the paper.

Key words: biodegradability, thermoplastic starch, TPS, extrusion, mouldings.

INTRODUCTION

Packaging wastes are now one of the greatest threats to civilization. A big hope for a reduction and perhaps the solution to this problem can be seen in the use of thermoplastic starch (in short TPS).

TPS can be used as a stand-alone packaging material or as an additive which improves the degradation of plastics [1, 3, 4, 5, 7, 9, 10, 11]. Starch is biodegradable in a short time to CO_2 and water. It is a polymer of 6-carbon sugar D-glucose, regardless of the botanical origin. Packaging materials made from thermoplastic starch can be produced by many different methods.

The single-stage method consists in applying low temperature synthetic polymers and starch mixture directly to the machine producing packaging material, e.g. to the plastic extruder. In the second stage the granules, as a half product, are processed with conventional equipment using film blowing or high pressure injecting moulding techniques [9, 10].

In order to obtain thermoplastic starch, the crystalline nature of starch granules must be destroyed, which can be done by thermal and mechanical processing [5, 9, 16]. Because the melting point of pure starch is much higher than its decomposition, during processing a plasticizer, like water, is added. Under the influence of temperature and shear forces natural crystalline structure of starch granules is crushed. In this way polysaccharides make a continuous polymer phase. To increase the flexibility of the material and improve the processing other plasticisers are used, for example: glycerol, propylene glycol, glucose or sorbitol [1, 9, 18, 19, 20]. Glycerol is the best and most common plasticizer. To improve the mechanical properties of rigid TPS packaging forms, different functional additives such as emulsifiers, cellulose, plant fibers, bark, kaolin and pectin are used [12, 13, 14, 15, 17, 21].

For years researches on TPS application in the production of fully biodegradable packaging materials based on potato starch and cereal starch have been conducted at the Department of Food Process Engineering (DFPE), University of Life Sciences in Lublin [3, 5, 12, 13, 14, 15]. The physical properties of the obtained TPS films are very promising (Fig. 1), as well as the mouldings produced in cooperation with Dutch colleagues from the

Fig. 1. The blowing of biodegradable TPS film in DFPE laboratory [5]

Royal University of Groningen. The biodegradability of these products is also analyzed during investigation [11].

BIODEGRADABILITY TESTS OF TPS MOULDINGS

Samples of mouldings (moisture content 4%) were placed in special baskets with the soil of following parameters: moisture content 70%, pH 6.5, and kept for 2, 4, 8 and 12 weeks in an unheated room at the temperature 10 – 15 °C (Fig. 2). Twice in a week water was supplemented to provide constant conditions. In order to widen scope of observation a number of samples were stored individually in the cooling room at the temperature of +3 °C and -36 °C [11].

The mouldings were produced from potato TPS granules containing different amount of glycerol and functional substances (flax and cellulose). After two weeks of storage the mouldings were taken out, weighed and dried to 4% m.c. then again weighed to determine weight loss. The last part of the test was the texture measurement, which was done using Zwick apparatus type BDO-FB0.5TH to determine range of changes in mechanical properties of the samples during the storage [12].

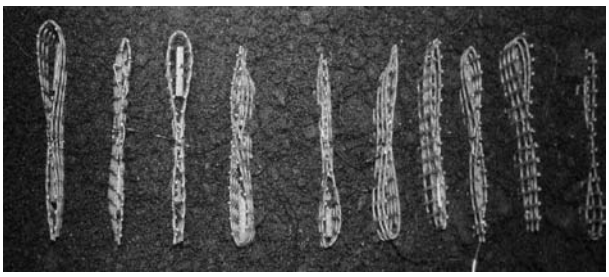

Fig. 2. Mouldings placed in the baskets with soil [11]

Fig. 3. A sample of moulding after 2 weeks of storage [11]

MEASUREMENT RESULTS

During measurements a substantial but varied weight loss of mouldings was observed during storage time. After the first two weeks of storage all samples lost weight rapidly (from 13% - samples containing 20% glycerol to about 23% - samples containing 25% glycerol). The highest change in weight was observed after 12 weeks. The inner moulding's layers (the core) decomposed slower on contact with soil than moulding's topcoat. It was observed that with increasing content of glycerol in the moulding's recipe, changes in weight (loss) were increased.

Increase in flax fiber content of flax limited the rate of destruction of the samples stored during 2 weeks [11]. In subsequent periods of storage (4 to 12 weeks) the weight loss was slower (2 - 6% for all samples). In the initial period of storage many changes on the surface of moulded parts were created because of the biodegradation process (cracks & fissures seen in Fig. 3). Samples produced without the addition of fibers and mouldings containing cellulose fiber crumbled and cracked easily during endurance tests (Fig. 4). After 12 weeks only samples containing added flax fibers had enough consistency to be able to undergo measurements of strength.

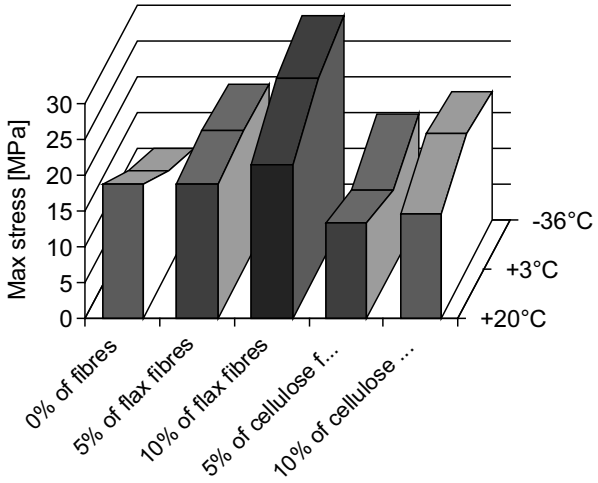

Fig. 4. Influence of storage temperature and the quantity and type of natural fibers in mouldings on the magnitude of maximum stress of mouldings during tension test (glycerol 22%, storage time 24h) [11]

CONCLUSIONS

1. Enrichment of TPS mouldings with functional components gives a very positive effect on their mechanical properties without lowering biodegradability suppleness, which has a practical value for the producers.
2. Results obtained by DFPE researchers confirm the possibility of the production of fully biodegradable packaging material based on TPS.
3. The present study demonstrates the usefulness of further work to improve the application of TPS in the production of packaging materials.
4. At the present time, we are looking for the best use of natural materials; starch seems to be a good alternative in this case. What is important – packaging material made from TPS can be produced using conventional machinery and equipment, typical for synthetic polymers sector.

REFERENCES

1. **Averous L., Fringant C., Moro L. 2001.** *Starch – based biodegradable materials suitable for thermoforming packaging.* "Starch", vol. 53, p. 368.
2. **Borowy T., Kubiak M. S. 2008.** *Opakowania biodegradowalne alternatywą dla opakowań z tworzyw sztucznych*(in Polish). „Gospodarka Mięsna", vol. 5, p. 18–20.
3. **Combrzyński M. 2011.** *Kierunki rozwoju produkcji opakowań biodegradowalnych* (in Polish). Msc Thesis, University of Life Science in Lublin, Poland.
4. **Fritz J., Link U., Braun R. 2001.** *Environmental impacts of biobased/biodegradable packaging*, "Starch", vol. 53, p. 105.
5. **Janssen L.P.B.M., Moscicki L. 2006.** *Thermoplastic starch as packaging material*. "Acta Sci. Pol., Technica Agraria", vol. 5(1).
6. **Kikolski P., Dłuska-Smolik E., Bolińska A. 2005.** *Metodyka oceny biodegradowalności polimerów opakowaniowych w badaniu ich przydatności do odzysku organicznego w wyniku kompostowania* (in Polish). „Polimey", vol. 3.
7. **Leszczynski W. 1999.** *Biodegradowalne materiały opakowaniowe* (in Polish). „Biotechnologia", vol. 2, p. 50.
8. **Łabuzek S., Pająk J., Nowak B. 2005.** *Biodegradacja modyfikowanego polietylenu w warunkach laboratoryjnych* (in Polish). „Polimery", vol. 9, p. 675.
9. **Mościcki L., Mitrus M., Wójtowicz A. 2008.** *Biodegradable Polymers and Their Practical Utility.* Janssen L.P.B.M., Moscicki L. (Eds.) „Thermoplastic Starch", Wiley-VCH Verlag GmbH & Co. KGaA, Weinheim.
10. **Mościcki L. 2008.** *Opakowania biodegradowalne* (in Polish). „Przegląd Zbożowo-Młynarski", vol. 1.
11. **Mościcki L., Oniszczuk T. 2008.** *Storage and Biodegradabality of TPS Moldings*. Janssen L.P.B.M., Moscicki L. (Eds.) „Thermoplastic Starch", Wiley-VCH Verlag GmbH & Co. KGaA, Weinheim.
12. **Oniszczuk T. 2006.** *Effect of parameters of injection moulding process on the structural properties of thermoplastic starch packaging materials*. PhD Thesis, Lublin Agricultural University, Poland.
13. **Oniszczuk T., Mitrus M., Mościcki L. 2008.** *Influence of Natural Fibres Addiction on Mechanical Properties of Biodegradable Packaging Materials*. "Polish Journal of Environmental Studies", vol. 17, 1B, p.257–262.
14. **Oniszczuk T., Janssen L.P.B.M., Moscicki L. 2006.** *Wpływ dodatku włókien naturalnych na wybrane właściwości mechanicznych wyprasek biopolimerowych* (in Polish). "Inżynieria Rolnicza", vol. 6(81), p. 101–107.
15. **Oniszczuk T. 2008.** *Zastosowanie włókien naturalnych w produkcji biodegradowalnych materiałów opakowaniowych* (in Polish). B. Dobrzański Jr., S. Grundas, R. Rybczyński (Eds.): "Metody Fizyczne Diagnostyki Surowców Roślinnych i Produktów Spożywczych". Wyd. Nauk. FRNA, Lublin.
16. **Shogren R.L. 1993.** *Effects of moisture and various plasticizers on the mechanical properties of extruded starch*. Ching Ch., Kaplan D.L., Thomas E.L.: "Biodegradable polymers and packaging", Technomic Publishing Company Inc., Lancaster-Basel, USA-Switzeland.
17. **Sinha Ray S., Bousmina M. 2005.** *Biodegradable polymers and their layered silicate nanocomposites.* "In Greening the 21st Century Materials World, Progress in Materials Science", vol. 50, p. 962.
18. **Van Soest J.J.G., Borger D.B. 1997.** *Structure and properties of compression-molded thermoplastic starch materials from normal and high-amylose maize starches.* "Journal of applied polimer science", vol. 64, p. 631.
19. **Van Soest J.J.G., Hulleman S.H.D., de Wit D., Vliegenthart J.F.G. 1996.** *Changes in the mechanical properties of thermoplastic potato starch in relation with changes in B-type crystallinity.* "Carbohydrate Polymers", vol. 29, p. 225.
20. **Van Soest J.J.G., Vliegenthart J.F.G. 1997.** *Crystallinity in starch plastics: consequences for material properties.* "Trends in Biotechnology", vol. 15, p. 208.
21. **Wollerdorfer M., Bader H. 1998.** *Influence of natural fibres on the mechanical properties of biodegradable polymers.* "Industrial Crops and Products", vol. 8, p. 105.

Streszczenie. Skrobia termoplastyczna (TPS) może odgrywać istotną rolę w produkcji opakowań. Katedra Technologii Żywności od lat prowadzi badania na ten temat. W niniejszym artykule przedstawiono wyniki testów biodegradowalności form z TPS wzbogaconych dodatkami funkcjonalnymi.

Słowa kluczowe: biodegradowalność, skrobia termoplastyczna, TPS, ekstruzja, formy.

TEKA. COMMISSION OF MOTORIZATION AND ENERGETICS IN AGRICULTURE – 2012, Vol. 12, No. 1, 25–28

Selected aspects of thermoplastic starch production

Maciej Combrzyński, Marcin Mitrus, Leszek Mościcki, Tomasz Oniszczuk, Agnieszka Wójtowicz

Department of Food Process Engineering, Faculty of Production Engineering, University of Life Sciences, Doświadczalna 44, 20-280 Lublin

Summary. This paper presents results of process efficiency and specific mechanical energy consumption (SME) during the extrusion-cooking of thermoplastic starch (TPS). The tests proved that the process efficiency of TPS extrusion-cooking largely depends on the amount of plasticizer. With the increase of plasticizer in the mixture reduction in process efficiency was observed. Higher moistening of raw materials resulted in increased TPS efficiency. SME values ranged from 0.060 to 0.076 kWh·kg^{-1} and were dependent on the extruder-cooker screw speed, the mixture recipe and multiplicity of extrusion repetitions for thermoplastic starch processing.

Key words: thermoplastic starch, extrusion-cooking, process efficiency, SME.

INTRODUCTION

Potatoes, corn, rice, tapioca, wheat, rye are only some of plants which are widely used to extract the starch. Starch can be added in varying amounts to plastics to get more environmentally friendly materials [5, 22, 23]. Due to the amount of starch in the mixture for the production of biodegradable plastic materials there should be mentioned plastic-modified starch (from 5 to 15% starch) and plastics based on starch with (40-60) % starch content.

Scientists constantly aim at complete replacement of plastics by natural materials. Thermoplastic starch (TPS) can be one of those materials [3, 9, 12]. In biopolymers starch added to the mixture occurs in two forms: native and extruded form. Extruded starch is different than the native starch as to rheological and physical properties, including the structure. Extruded starch also has a much higher solubility in water [2, 18].

TPS can be obtained by destroying the crystalline nature of starch granules by thermal and mechanical processing [1, 8]. The process needs addition of plasticizers (e.g. water), because the melting point of pure dry starch is much higher than its temperature of decomposition. Shear forces and temperature cause a break of natural crystalline structure of starch granules. The continuous polymer phase is creating.

During the extrusion-cooking process other plasticizers, like glycerin, propylene glycol, glucose or sorbitol, can be used to increase flexibility and improve material properties, but glycerol is most commonly used. Addition of sorbitol induces water and oxygen vaporization through the produced TPS film. Fat added to starch reduces the water vapor permeability. Various functional additives, such as emulsifiers, vegetable fibers, bark or cellulose are also used during the manufacturing process to change mechanical properties of rigid forms of TPS packaging.

Thermoplastic starch can be used as a standalone packaging material or as a component which improves degradation of plastics. Application of TPS is possible due to the relatively short time of degradation to CO_2 and water. Biocomposites which are enriched with starch are used for films, containers, and in the production of foams used in packaging sector [11, 13].

MATERIALS AND METHODS

In the experiments potato and cereal starches were used, additives were: glycerol and water. Moisture of prepared mixtures was from 15 to 28% using the method described by Szymanek and Sobczak [17]. Glycerol content was from 15 to 30% of dry starch mass. The extrusion-cooking process was carried out with a modified single screw extrusion-cooker type TS-45 (Polish design) equipped with elongated plastic-forming section and additional barrel-cooling section before the die [10, 20, 21]. Technical parameters of the equipment were as follow: L/D=16/1, screw rotation speed regulation from 50 to 130 rpm, forming die with 3 openings 1.5 mm each.

Prepared mixtures were processed at the temperature ranged from 80 to 100°C with screw speed 80 and 100 rpm. The process efficiency was measured by products collection after 10 minutes of regular production for each sample at different conditions. The measurements were registered six-times.

Power consumption was measured using standard register connected to extruder's motor for each recipe and screw speed used [16, 19]. After the consideration of motor load and process efficiency, the SME (specific mechanical energy) values were calculated according to the method described by Ryu and Ng [15]:

$$SME = \frac{rpm[test]}{rpm[rated]} \times \frac{\%\ motor\ load}{100} \times \frac{motor\ power[rated]}{feed\ rate} \left[\frac{kWh}{kg}\right]$$

RESULTS

Efficiency of TPS processed by extrusion-cooking depended on glycerol content in prepared mixtures [6]. Process efficiency decreased with increasing glycerol content in the mixture. Increase of glycerol content in the prepared mixture caused almost twice lower efficiency at extreme contents of glycerol at 80 rpm screw speed. With higher screw speed process efficiency increased. It has been observed that during processing highest glycerol content the efficiency of the samples with extrusion-cooking at 100 rpm screw speed was almost 50% smaller.

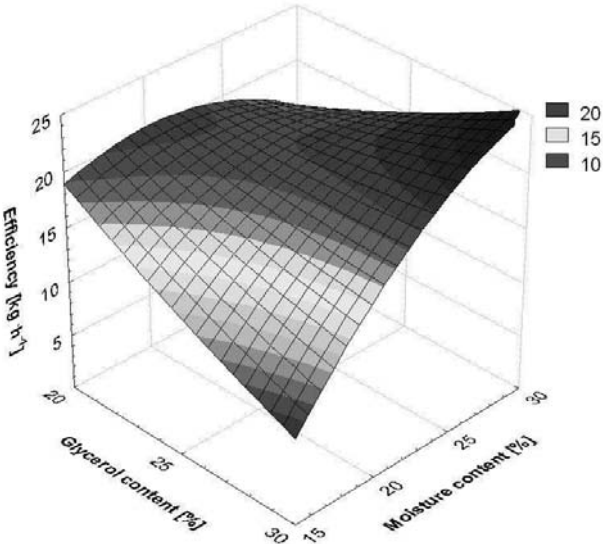

Fig. 1. Efficiency of potato TPS extrusion-cooking depend on glycerol content and mixture moisture

Mitrus [6] has found that also an important role is played by moisture content of processed material. Analyses have shown that extrusion-cooking efficiency increased with higher moisture of potato starch prepared mixture (Fig. 1). If higher glycerol content in the mixture was used, the increase in efficiency was more intense. TPS extrusion efficiency was almost the same for samples with moisture content of 25%. With increase of moisture content of raw materials over 20% the efficiency has been reduced. There was only one exception – a mixture with 30% content of glycerol. In this case TPS extrusion-cooking efficiency was increased with higher moisture.

Using different types of starches, differences in TPS efficiency were observed (Fig. 2). For all the tested starches, it was observed that the higher content of glycerol in prepared mixtures reduced process efficiency [6]. The highest efficiency was recorded using potato starch. The smallest values, twice as low as for potato, were reported in the case of wheat starch.

Efficiency of TPS extrusion-cooking process depends on the number of extrusion repetitions for the same material (Fig. 3). It was observed that the efficiency of the extrusion-cooking of thermoplastic potato starch decreased at multiple extrusions, regardless of glycerol content in the prepared mixture [6].

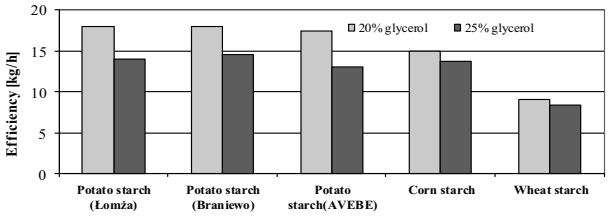

Fig. 2. Effect of starch type and glycerol content on efficiency of TPS extrusion-cooking

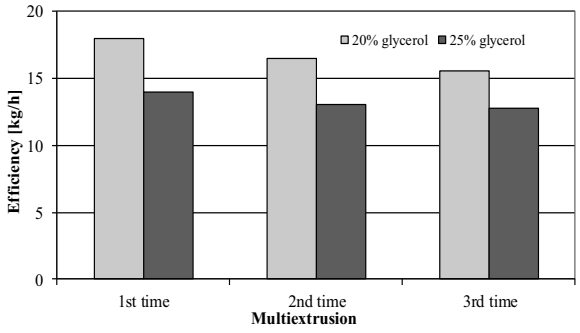

Fig. 3. Efficiency of potato TPS extrusion-cooking dependent on the number of extrusion repetitions

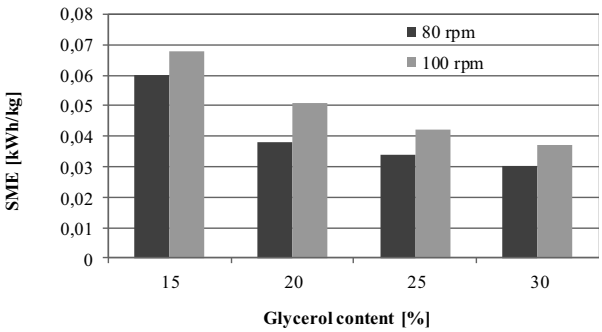

Fig. 4. The SME changes during the extrusion-cooking of thermoplastic potato starch in relation to glycerol content in mixture

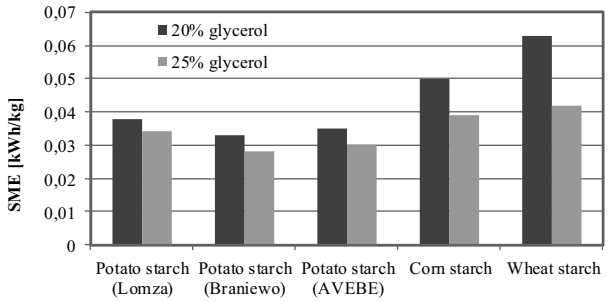

Fig. 5. Effect of starch type and glycerol content on SME

In industrial starch processing with application of extrusion-cooking technology determination of specific mechanical energy consumption (SME) is an important parameter to obtain the product unit costs [4].

It was observed that changes in SME during TPS production are mostly dependent on prepared mixture recipe and extrusion-cooker screw speed [6, 7]. The SME values decreased with higher glycerol content in the mixture (Fig. 4). Furthermore, it was noted, that with increasing the extrusion-cooker screw speed the specific mechanical energy consumption also has been increased. For mixtures with 15% of glycerol content processed at 100 rpm the SME values were 0.068 $kWh \cdot kg^{-1}$. For the same mixtures processed at 80 rpm recorded values were 0.06 $kWh \cdot kg^{-1}$. The lowest values of specific mechanical energy consumption were obtained for mixtures with 30% glycerol content. Studies have shown that during TPS production SME values depend on moisture of prepared mixture [6, 7, 14].

If moisture was higher, SME values were also higher. During the extrusion-cooking of potato starch with 20% of glycerol content and at 20% of moisture content the highest specific mechanical energy consumption was noted (0.076 $kWh \cdot kg^{-1}$).The results for all starches showed that the values of the SME decreased with increased glycerol content in mixture (Fig. 5).

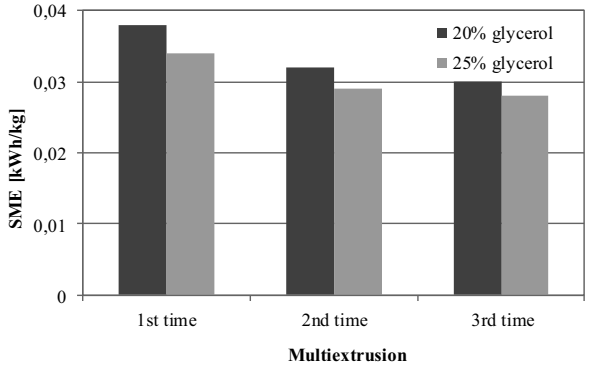

Fig. 6. Values of SME depending on extrusion-cooking repetitions of potato starch

During the potato TPS extrusion-cooking the lowest values of the specific mechanical energy consumption were recorded. The highest SME values were obtained during the extrusion-cooking of wheat starch.

During higher number of extrusion-cooking repetition of potato starch the various values of SME was observed (Fig. 6). If the extrusion-cooking was multiple repeated for the same material, specific mechanical energy consumption was lower [6, 7].

CONCLUSIONS

The obtained results demonstrated that the process efficiency of thermoplastic starch extrusion-cooking decreased with increase of glycerol content in mixture and with higher number of extrusion repetition for the same material. The process efficiency increased with increased of moisture content of potato starch.

The extrusion-cooking of TPS is related with comparatively low energy requirements (0.07 $kWh \cdot kg^{-1}$ on average). During the study it was observed that power consumption during extrusion-cooking depended on the composition of prepared mixtures. The increase of glycerol content in the mixture decreased the specific mechanical energy consumption. SME values were also depending on the screw speed applied during the extrusion-cooking and with multiple repetition of extrusion. The studies indicate the possibility of obtaining optimal values of specific mechanical energy consumption and efficiency of TPS extrusion-cooking.

The obtained results allow for the conclusion that processing of TPS by extrusion-cooking is promising and has to be continued in order to improve production of biodegradable starch packaging materials.

REFERENCES

1. **Borowy T., Kubiak M. S. 2008.** Opakowania biodegradowalne alternatywą dla opakowań z tworzyw sztucznych, Gospodarka Mięsna, 5, p. 18-20.
2. **Camire M.E., Camire A., Krumhar K. 1990.** Chemical and nutritional changes in foods during extrusion, Food Science and Nutrition, Volume 29, p. 35-56.
3. **Janssen L.P.B.M., Mościcki L. (red.) 2008.** Thermoplastic Starch, Wiley-VCH Verlag GmbH & Co. KGaA, Weinheim, p. 1-29.
4. **Janseen L.P.B.M, Mościcki L., Mitrus M. 2002.** Energy aspects in the extrusion-cooking, Int. Agrophysics, 16, p. 191-198.
5. **Kowalczuk M.M. 2009.** Prace badawcze nad polimerami biodegradowalnymi. Opakowanie, 9, p. 46-48.
6. **Mitrus M. 2004.** Wpływ obróbki barotermicznej na zmiany właściwości fizycznych biodegradowalnych biopolimerów skrobiowych, Rozprawa doktorska, UP Lublin.
7. **Mitrus M. 2005.** Changes of specific mechanical energy during extrusion cooking of thermoplastic starch, TEKA Commision of Motorization and Power Industry in Agriculture PAN, Volume V, p. 152-157.
8. **Mitrus M. 2005.** Glass transition temperature of thermoplastic starches, Int. Agrophysics, 19, p. 237-242.
9. **Mitrus M. 2006.** Investigations of thermoplastic starch extrusion cooking process stability, TEKA Commision of Motorization and Power Industry in Agriculture PAN, Volume VIa, s. 138-144.

10. **Mitrus M. 2007.** Badania właściwości mechanicznych skrobi termoplastycznej, Acta Agrophysica PAN, Vol 9(2), p. 423-430.
11. **Mitrus M., Oniszczuk T. 2007.** Wpływ obróbki ciśnieniowo – termicznej na właściwości mechaniczne skrobi termoplastycznej, Właściwości geometryczne, mechaniczne i strukturalne surowców i produktów spożywczych, Wyd. Nauk. FRNA, Lublin, p. 149-150.
12. **Mitrus M., Mościcki L. 2009.** Physical properties of thermoplastic starches, Int. Agrophysics, 23, p. 305-308.
13. **Mościcki L., Mitrus M., Wójtowicz A. 2007.** Technika ekstruzji w przemyśle rolno – spożywczym, PWRiL, Warszawa.
14. **Panasiewicz M. 2009.** An influence of kernel conditioning method on energy consumption during flaming process, TEKA Commision of Motorization and Power Industry in Agriculture PAN, Volume IX, p. 211-216.
15. **Ryu G. H., Ng P.K. 2001.** Effect of selected process parameters on expansion and mechanical properties of wheat flour and whole cornmeal extrudates, Starch/ Starke 53, p. 147-154.
16. **Singh N., Smith C.A. 1997.** A comparison of wheat starch, whole wheat meal and oat flour in the extrusion cooking process, Journal of Food Engineering, 34, p. 15-32.
17. **Szymanek M., Sobczak P. 2009.** Some physical properties of spelt wheat seed, TEKA Commision of Motorization and Power Industry in Agriculture PAN, Volume IX, p. 310-320.
18. **Thomas D.J., Atwell W.A. 1997.** Starch Analysis Methods. Thomas D.J., Atwell W.A.: Starches. Eagan Press, St. Paul, Minnesota, p. 13-18.
19. **Valle G.D., Boche Y., Colonna P., Vergnes B. 1995.** The extrusion behavior of potato starch, Carbohydrate Polymers, 28, p. 255-264.
20. **Wójtowicz A. 2008.** Influence of legumes addition on proceeding of extrusion-cooking process of precooked pasta, TEKA Commision of Motorization and Power Industry in Agriculture PAN, Volume VIIIa, p. 209-216.
21. **Wójtowicz A., Mościcki L. 2008.** Energy consumption during extrusion-cooking of precooked pasta, TEKA Commision of Motorization and Power Industry in Agriculture PAN, Volume VIII, p. 311-318.
22. **Żakowska H. 2005.** Recykling odpadów opakowaniwych, Wyd. COBRO, Warszawa.
23. **Żakowska H. 2006.** Światowy postęp w produkcji opakowań przydatnych do kompostowania. Opakowanie, 2, p. 15-17.

WYBRANE ASPEKTY PRODUKCJI SKROBI TERMOPLASTYCZNEJ

S t r e s z c z e n i e. W niniejszym artykule przedstawiono wyniki pomiarów wydajności i energochłonności procesu ekstruzji skrobi termoplastycznej (TPS). W trakcie badań stwierdzono, że wydajność procesu ekstruzji TPS zależy w dużym stopniu od ilości plastyfikatora. Wraz ze wzrostem udziału procentowego plastyfikatora w mieszance surowcowej zaobserwowano obniżenie wydajności procesu. Wyższa wilgotność mieszanki surowcowej skutkowała wzrostem wydajności TPS. Wartości SME wynosiły od 0,06 do 0,076 kWh.kg^{-1} i uzależnione były od prędkości obrotowej ślimaków ekstrudera, składu surowcowego oraz krotności ekstruzji skrobi termoplastycznej.

S ł o w a k l u c z o w e: skrobia termoplastyczna, ekstruzja, energochłonność, wydajność.

TEKA. COMMISSION OF MOTORIZATION AND ENERGETICS IN AGRICULTURE – 2012, Vol. 12, No. 1, 29–33

The grinding energy as an indicator of wheat milling value

Dariusz Dziki[a], Grażyna Cacak-Pietrzak[b], Beata Biernacka[c], Krzysztof Jończyk[d], Renata Różyło[e], Bożena Gładyszewska[f]*

[a]Department of Thermal Technology, University of Life Sciences, Doświadczalna 44, 20-280 Lublin, Poland; [b]Division of Cereal Technology, Faculty of Food Sciences, Warsaw University of Life Science, Nowoursynowska 159C, 02-786 Warsaw, Poland; [d]Department of Systems and Economics of Crop Production, Institute of Soil Science and Plant Cultivation, Czartoryskich 8, 24-100 Puławy, Poland; [e]Department of Equipment Operation and Maintenance in the Food Industry, Doświadczalna 44, 20-280 Lublin, Poland; [f] Department of Physics, University of Life Sciences, Akademicka 13, 20-950 Lublin, Poland

Summary. The aim of the work was to evaluate the relationships between the specific grinding energy and the milling results. The investigations were carried out on nineteen European wheat cultivars (*Triticum aestivum,* ssp. *vulgare*). The grain came from the field experiment conducted in 2010 at Osiny Experimental Station belonging to the Institute of Soil Science and Plant Cultivation located in Puławy. The conditioned kernels were then milled using a Buhler MLU 202 laboratory mill (Bühler AG, Uzwil, Switzerland) and SK labolatory mill. The specific grinding energy ranged from 17.0 kJkg^{-1} (Kobra Plus and Legenda) to 29,9 kJkg^{-1} (cv. Parabola). The results showed statistically significant and negative correlation between the specific grinding energy and break flour yield (r = -0,761). Also the negative correlation was shown between the grinding energy and the total flour yield (r=-0,625). Furthermore, the positive and significant correlation was found between the reduction bran yield and the specific grinding energy (r=0,641). The results showed that specific grinding energy is a useful tool for milling results prediction.

Key words: wheat, milling, grinding energy, flour.

INTRODUCTION

Wheat has become one of the most important crops mainly due to its wheat grain used to flour production. Wheat milling is the most important unit process in wheat processing. The milling methods and milling parameters depend on the direction of wheat use. The most common way of wheat kernel size reduction is a gradual reduction process during the wheat flour milling. This breaks down the tempered wheat grain in a series of grinding stages. Each grinding stage produces a blend of coarse, medium and fine fractions including flour. These mixtures are then sieved and purified to allow for a good separation of bran and endosperm. Adding moisture to wheat prior to milling facilitates breakage of endosperm while making bran more resistant to breakage [7]. The flour obtained in this way consists mainly of the starchy endosperm, whereas bran with the aleurone layer and germs are by-products [18]. While almost any wheat can be milled, millers produce a wide range of flours with can be used to produce variety of products that have good sensory properties. The different types of grinding mills can be used to this end. However, the most commonly applied in practice are the roller mills [19].

The grinding performance depends on the size reduction method and the properties of raw materials. Several studies have addressed the prediction of wheat milling value on the basis of physical properties of wheat grain. Among all the properties of wheat kernel, its hardness has the most significant influence on the milling process [5]. Grain hardness is a key variety trait for milling. Hard and soft wheat has different processing requirements and end-uses. Wheat hardness results mainly from the degree of adhesion between starch granules and the surrounding protein matrix [10]. This property affects the tempering requirements, flour particle size, flour density, starch damage, water absorption, and milling yield [12,21]. Also other properties of wheat are commonly determined, including: test weight, vitreousness, true density, kernel size and weight, and protein content [15,3,8].

The grinding energy depends mainly on wheat mechanical properties. Thus the grinding energy can be an indirect indicator of wheat mechanical properties and correlated strongly with grain hardness [6,4]. The objective of this study was to investigate the relationships between specific grinding energy and wheat milling results.

MATERIALS AND METHODS

MATERIAL

Investigations were carried out on nineteen European wheat cultivars (*Triticum aestivum, ssp. vulgare*):

Bogatka, Bombona, Bryza, Cytra, Figura, Kobra Plus, Legenda, Nawra, Ostka Strzelecka, Parabola, Raweta, Rywalka, Smuga, Tonacja, Tybalt, Vinjet, Wydma, Zadra, Żura. The grain came from the organic field experiment conducted in 2010 at Osiny Experimental Station belonging to the Institute of Soil Science and Plant Cultivation (State Research Institute) located in Puławy. The grain initial moisture content of kernel ranged form 8.5 to 9.8% (w.b.). The samples of wheat were prepared by adding water to adjust moisture content to 14% (w.b.) and storing for 48 h.

THE GRINDING ENERGY EVALUATION

The samples (50 g) were milled using SK laboratory roller mill. Four grinding stages were applied. The roll gap was 0.85 mm for the first stage, 0.4 mm for the second stage, 0.25 mm for the third stage and 0.15 mm for the fourth stage.

The changes in the power consumption of the electric current during the grinding process were recorded using laboratory equipment including a grinding machine, transducer of power and a special data acquisition card connected to a PC computer and operated with special computer software. The detailed description of the laboratory mill has been provided by Dziki et al [3].

The total grinding energy (E_c) was calculated according to the equation:

$$E_c = \int_0^t P dt, \tag{1}$$

where:

P – the power consumption during grinding process (W),

t – the time of grinding (s).

It was assumed that the power consumption during the kernel grinding process is the difference between the total grinding power and the power of transmission system during the idle running. The idle running energy lose was calculated as follow:

$$E_s = \int_0^t P_j dt, \tag{2}$$

where:

P_j – the power consumption during idle running (W).

The specific grinding energy was calculated according to the formula:

$$E_r = \frac{E_c - E_s}{m}, \tag{3}$$

where:

m – the mass of the grinding sample (kg).

The specific grinding energy was carried out in ten repetitions.

THE MILLING PROCESS

Three kilograms of cleaned wheat kernel from each cultivar were conditioned in two steps. First, water was added to increase the moisture content of wheat kernel to 13.5% (w.b.) moisture level 24 h before milling. Then, kernel moisture was increased to 14% (w.b.) followed by 30 min tempering. The conditioned kernels were then milled using a Buhler MLU 202 Laboratory Mill (Bühler AG, Uzwil, Switzerland). The gap settings and the size of screens used in the mill are presented in Table 1. The break flour and the reduction flour were obtained by blending the flours from the breaking and reduction stages, respectively. The total flour was obtained by blending break flour with the reduction flour. The individual flour yields were expressed as the percentage in weight of ground grains. The content of total ash was determined [13] and the index of milling efficiency was calculated as a ratio of the total flour yield to flour ash content [1,2]. The milling process and the determination of the total ash content were carried out in triplicate.

Table 1. The roll gaps settings and size of screens used in the mill.

Stage	Roll gap (mm)	Size of screen (mm)
S_I^*	0.52	0.244
S_{II}	0.10	0.180
S_{III}	0.07	0.150
W_1	0.05	0.225
W_2	0.01	0.180
W_3	0.01	0.150

*S_I, S_{II}, S_{III} – the first, the second and the third breaking stage, respectively,

W_1, W_2, W_3 – the first, the second and the third reduction stage, respectively

STATISTICAL ANALYSIS

Statistical analysis of the data collected in this study were conducted with Statistica 6.0 software (StatSoft Inc., Tulsa, USA). Variance analysis (using Tukey's test) was used to determine statistical differences between treatment groups. Correlation analysis was also carried out on the data. All the statistical tests were carried out at a significance level of $\alpha = 0.05$.

RESULTS AND DISCUSSION

The results showed that the specific grinding energy ranged form 17.0 kJkg^{-1} (Kobra Plus and Legenda) to 29,9 kJkg^{-1} (cv. Parabola) (Fig. 1). The specific grinding energy is one of the most frequently determined parameters characterizing the grinding process [9,20,14] found that the total specific milling energy ranged from 46 kJ·kg^{-1} for soft wheat cultivars to 124 kJ·kg^{-1} for durum wheat.

The results of wheat milling process were given in tables 2 and 3. The yield of break flour ranged from

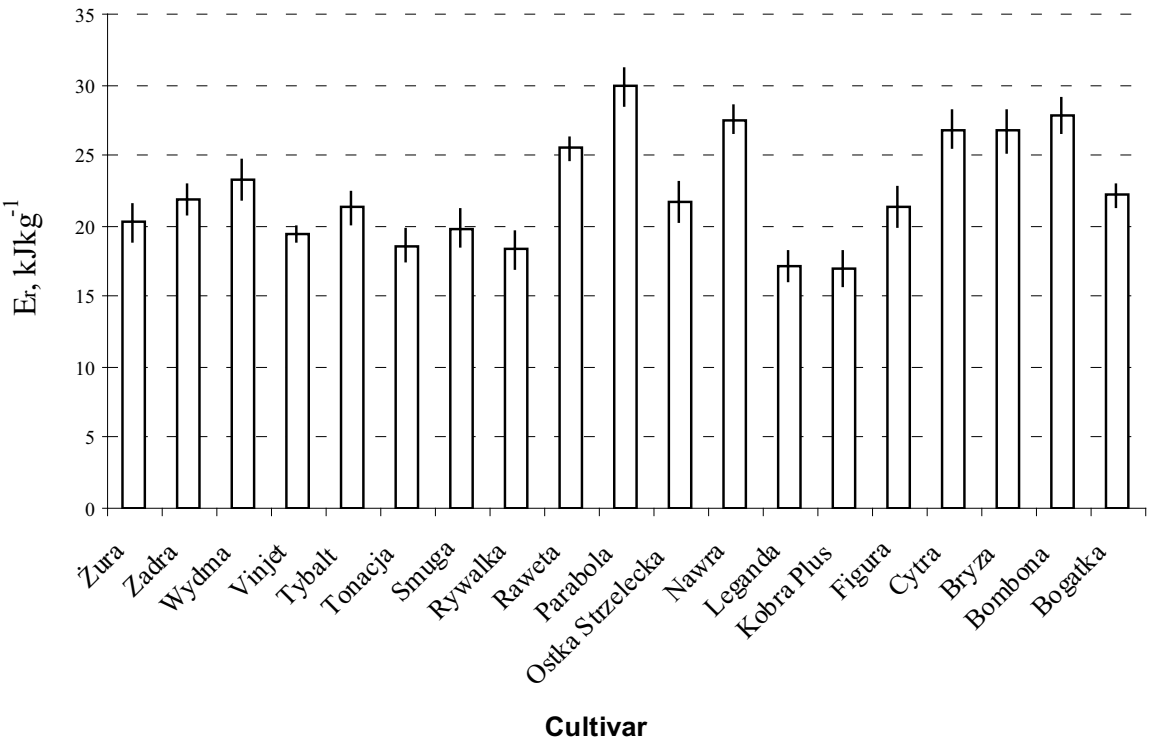

Fig. 1. The results of specific grinding energy of individual wheat cultivars

15.5% (cv. Bombona) to 22.2% (cv. Rywalka). The lowest yield of reduction flour was obtained for Nawra and Żura (53.1% and 53.4%, respectively), and the highest for Bombona (59.1%).

Table 2. The milling results

Cultivar	*BFY** (%)	*RFY* (%)	*BBY* (%)	*RBY* (%)
Bogatka	20.7^{hij**}	55.4^{fg}	12.7^{cd}	11.2^{bcd}
Bombona	$15,5^{a}$	59.1^{j}	13.2^{cde}	12.2^{defg}
Bryza	19^{cde}	$55.7f^{g}$	14.8^{ij}	10.5^{b}
Cytra	17.9^{b}	56.0^{gh}	15.1^{j}	11.0^{bc}
Figura	21.2^{j}	54.4^{cde}	11.9^{ab}	12.5^{efg}
Kobra Plus	20.8^{ijk}	58.3^{i}	12.5^{bc}	8.4^{a}
Legenda	20.5^{hij}	55.4^{fg}	12^{ab}	12.1^{cdef}
Nawra	19.3^{def}	53.1^{a}	13.8^{fgh}	13.8^{h}
Ostka Strzelecka	19.5^{efg}	54.3^{cde}	12.7^{cd}	13.5^{gh}
Parabola	17.9^{bc}	55.7^{fg}	14^{gh}	12.4^{cdef}
Raweta	18.3^{bc}	54.3^{cd}	14.4^{hi}	13^{fgh}
Rywalka	22.2^{k}	53.6^{ab}	12^{ab}	12.2^{cdef}
Smuga	19.7^{efgh}	55^{def}	13.2^{def}	12.1^{cde}
Tonacja	20.2^{ghi}	56.5^{h}	11.8^{a}	11.5^{bcde}
Tybalt	18.4^{bcd}	55.1^{ef}	13.9^{gh}	12.6^{efg}
Vinjet	20.8^{ij}	54.1^{bc}	14^{gh}	11.1^{bc}
Wydma	19.8^{fghi}	54.6^{cde}	12.9^{cd}	12.7^{efg}
Zadra	19.9^{fghi}	54.4^{cde}	13.6^{efg}	12.1^{cdef}
Żura	20.4^{hij}	53.4^{ab}	14^{gh}	12.2^{cdef}

**BFY* – break flour yield, *RFY* – reduction flour yield, *BBY* – break bran yield, *RBY* – reduction bran yield, **the values designated by the different letters in the columns of the table are significantly different ($\alpha = 0.05$);

The total flour extraction ranged from 72.4% to 79.1% for Navra and Kobra Plus, respectively (Table 3). Flour extraction depends mainly on both the kernel properties and the manner of milling. However, during production of white flour apart from yield also the flour ash content has a significance for milling results. Since ash is primarily concentrated in the bran, ash content of flour is

an indicator of the yield and purity of the flour. In many countries wheat flour is classified according to the ash content. One of the best indicators of wheat milling value is a milling efficiency index (*MEI*), which is defined as a ratio of total flour yield to flour ash content, the higher value of this index the better the milling value of wheat [1]. The results showed that the *MEI* ranged from 100.3 (cv. Bryza) to 118.5 (cv. Tybalt).

Table 3. Total flour yield, flour ash content and milling index for the investigated wheat cultivars

Cultivar	*TFY** (%)	*FAC* (%)	*MEI*
Bogatka	76.1^{ef**}	0.681^{efg}	111.1^{cdef}
Bombona	74.6^{cde}	0.639^{bcd}	116.6^{ef}
Bryza	74.7^{cde}	0.745^{i}	100.3^{a}
Cytra	73.9^{bc}	0.721^{hi}	102.6^{ab}
Figura	75.6^{def}	0.695^{fgh}	108.8^{bcd}
Kobra Plus	79.1^{g}	0.702^{fgh}	113.0^{cdef}
Legenda	75.9^{ef}	0.660^{cde}	115.0^{def}
Nawra	72.4^{a}	0.635^{bc}	114.0^{cdef}
Ostka Strzelecka	73.8^{abc}	0.632^{abc}	117.1^{ef}
Parabola	73.6^{bc}	0.671^{def}	109.9^{cde}
Raweta	72.6^{ab}	0.705^{gh}	103.0^{ab}
Rywalka	75.8^{def}	0.655^{cde}	115.7^{def}
Smuga	74.7^{cde}	0.601^{a}	124.5^{g}
Tonacja	76.7^{f}	0.675^{efg}	113.6^{cdef}
Tybalt	73.5^{abc}	0.621^{ab}	118.5^{fg}
Vinjet	74.9^{cde}	0.695^{fgh}	107.8^{bc}
Wydma	74.4^{cde}	0.672^{def}	111.0^{cde}
Zadra	74.3^{cd}	0.670^{def}	110.9^{cde}
Żura	73.8^{abc}	0.671^{def}	113.5^{cde}

**TFY* – total flour yield, *FAC* –flour ash content, *MEI* – milling efficiency index, **the values designated by the different letters in the columns of the table are significantly different (α = 0.05);

The results showed significant correlation between the specific grinding energy and break flour yield (Fig. 2). As the grinding energy increased the break flour yield decreased (r = 0,761). Also, the negative correlation was found between specific grinding energy and total flour yield (r= -0,625) (Fig. 3). Literature data showed that during milling, the wheat hardness significantly affected the break flour yield and the total flour yield [16,10,17]. The soft wheat kernels are characterized by a higher break flour, because degree of adhesion between starch granules and protein matrix is week and thus the higher mass fraction of fine particles is produced [11,21].

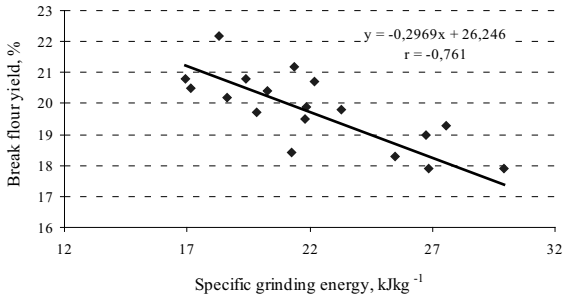

Fig. 2. The relationship between specific grinding energy and break flour yield

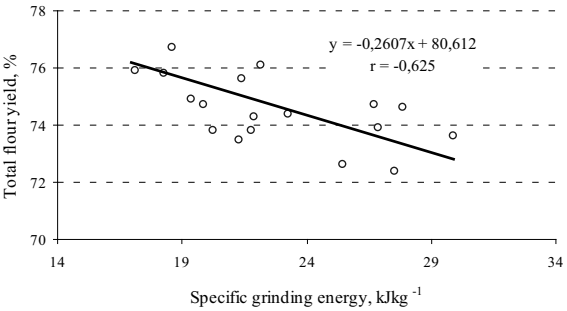

Fig. 3. Relationship between specific grinding energy and the total flour yield

The positive and significant correlation was also found between the reduction bran flour yield and the specific grinding energy (Fig. 4). The coefficient of correlation was significant, but relatively low (r= 0,641).

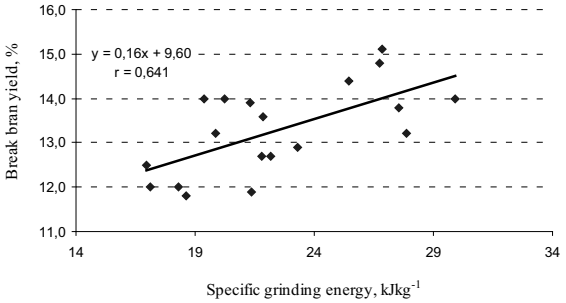

Fig. 4. The relationship between specific grinding energy and bran yield reduction

CONCLUSIONS

On the basis of the obtained investigation results the following conclusions were formulated:

1. The specific grinding energy ranged from 17.0 kJkg^{-1} (Kobra Plus and Legenda) to 29,9 kJkg^{-1} (cv. Parabola).

2. The results showed statistically significant and negative correlation between the specific grinding energy and: break flour yield (r = -0,761), and total flour yield (r = -0,625).

3. The positive correlation was found between grinding energy and reduction bran yield (r= -0,641).

4. The results showed that specific grinding energy is a useful tool for predicting flour yield.

REFERENCES

1. **Cacak-Pietrzak G., Ceglińska A., Gondek E., Jakubczyk E. 2009.** Influence of wheat grain structure on grinding process. Post Tech Przetw Spoż 19/35: p. 53-56 (in Polish).
2. **Cacak-Pietrzak G., Gondek E. 2010.** Milling value of spelt wheat and wheat. Acta Agrophysica, 182, 16(2), p. 263-273. (in Polish).
3. **Dziki D., Laskowski J., Łysiak G. 1997.** Układ pomiarowy do maszyn rozdrabniających z komputerową rejestracją danych. IV Krajowa Konf. „Komputerowe wspomaganie badań naukowych". Świeradów Zdrój. Materiały konferencyjne, p. 59-60 (in Polisch).
4. **Dziki D., Laskowski J. 2004.** Influence of kernel size on grinding process of wheat at respective grinding stages. Polish Journal of Food and Nutritional Sciences, 1(54), p. 29-33.
5. **Dziki D. 2005.** Wheat kernel physical properties and milling process. Acta Agrophysica 6(1), p. 59-71.
6. **Dziki D., Przypek-Ochab D. 2009.** Ocena energochłonności rozdrabniania ziarna pszenicy zróżnicowanego pod względem twardości. Inżynieria Rolnicza. Nr 5 (114), p. 61-67.
7. **Fang Ch., Campbell G.M. 2003.** On Predicting Roller Milling Performance V: Effect of moisture content on the particle size distribution from first break milling of wheat. Journal of Cereal Sciences, 37(1), p. 31-41.
8. **Gaines C.S., Finney P.L., Andrews C. 1997.** Influence of kernel size and shriveling on soft wheat milling and baking quality. Cereal Chemistry, 74(6), p. 700-704.
9. **Grochowicz J., Andrejko D. 2006.** Effect of the moisture content on energy consumption at grinding of lupine seeds. TEKA Kom. Mot. Energ. Roln., 6, p. 22-28.
10. **Greffeuille V., Abecassis J., Barouh N., Villeneuve P., Mabille F., Bar L'Helgouac C., Lullien Pellerin V., Benet J.C. 2007.** Analysis of the milling reduction of bread wheat farina: Physical and biochemical characterization. Journal of Cereal Science 45(1), p. 97-105.
11. **Haddad Y., Mabille F., Mermet A., Abecassis J. & Benet J.C. 1999.** Rheological properties of wheat endosperm with a view on grinding behaviour. Powder Technology, 105(1-3), p. 89-94.
12. **Hrušková M., & Švec I. 2009.** Wheat hardness in relation to other quality factors. Czech Journal of Food Sciences, 27(4), p. 240-248.
13. ICC. 1990. ICC-Standard No 104/1, ICC-Standard No 155. International Association for Cereal Chemistry, Vienna, Austria.
14. **Kilborn R.H., Black H.C., Dexter J.E., Martin D.G. 1982.** Energy consumption during flour milling. Description of two measuring systems and influence of wheat hardness on the energy requirements. Cereal Chemistry 59.
15. **Lin, P.Y., Czuchajowska, Z. 1997.** General characteristic and milling performance of Club Wheat vs. Soft White Winter Wheat. Cereal Foods World, 42 (11), p. 861-866.
16. **Muhamad I.I., Campbell G.M. 2004.** Effects of kernel hardness and moisture content on wheat breakage in the single kernel characterization system. Innovative Food Science and Emerging Technologies, 5(1), p. 119-125.
17. **Ownes G. 2000.** Cereals processing technology (pp. 345-364). Published in North and South America by CRC Press LLC, Corporate Blvd, NW.
18. **Posner E.S., Hibbs A.N. 1997.** Wheat flour milling. American Association of Cereal Chemists (pp. 82-120) St. Paul, USA.
19. **Prabhasankar P., Rao P.H. 2004.** Effect of different milling methods on chemical composition of whole wheat flour. European Food Research and Technology, 213(6), p. 465-469.
20. **Rydzak L., Andrejko D. 2011.** Effect of vacuum impregnation and infrared radiation treatment on energy requirements in wheat grain milling. TEKA Kom. Mot. i Energ. Roln. 11c: p. 291-299.
21. **Turnbull K.M., Rahman S. 2002.** Endosperm texture in wheat. Journal of Cereal Science, 36(3), p. 327-337.

ENERGOCHŁONNOŚĆ ROZDRABNIANIA JAKO WSKAŹNIK WARTOŚCI PRZEMIAŁOWEJ ZIARNA PSZENICY

S t r e s z c z e n i e . Celem pracy było określenie zależności między energochłonnością jednostkową rozdrabniania a wynikiem procesu przemiału ziarna pszenicy. Materiał badawczy stanowiło 19 europejskich odmian pszenicy zwyczajnej (*Triticum aestivum,* ssp. *vulgare*). Ziarno pochodziło ze zbiorów z 2010 roku, ze Stacji Eksperymentalnej w Osinach, należącej do Instytutu Uprawy, Nawożenia i Gleboznastwa w Puławach. Ziarno kondycjonowano do 14% wilgotności i poddawano przemiałowi laboratoryjnemu, wykorzystując młyn Buhler MLU 202 oraz mlewnik walcowy typu SK. Stwierdzono, że energochłonność jednostkowa rozdrabniania kształtowała się od 17.0 $kJkg^{-1}$ (odmiany Kobra Plus i Legenda) do 29,9 $kJkg^{-1}$ (odmiana Parabola). Parametr ten istotnie i ujemnie korelował z wyciągiem mąki śrutowej (r=-0,761) oraz z całkowitym wyciągiem mąki (r=-0,625). Ponadto wykazano występowanie dodatniej korelacji między energochłonnością jednostkową rozdrabniania a wydajnością odtrąb śrutowych (r=0,641). Przeprowadzone badania wykazały, że energochłonność jednostkowa rozdrabniania może być użytecznym narzędziem w prognozowaniu wartości przemiałowej pszenicy.

S ł o w a k l u c z o w e : pszenica, przemiał, energia rozdrabniania, mąka.

TEKA. COMMISSION OF MOTORIZATION AND ENERGETICS IN AGRICULTURE – 2012, Vol. 12, No. 1, 35–40

The change of protein and fat content in the beans seed covers during germination process

Bożena Gładyszewska[1], Dariusz Dziki[2]

[1]Department of Physics, University of Life Sciences, ul. Akademicka 13, 20-950 Lublin, Poland
[2]Department of Thermal Technology, University of Life Sciences, ul. Doświadczalna 44, 20-280 Lublin, Poland
e-mail: bozena.gladyszewska@up.lublin.pl

Summary. The paper presents the results of studies on the percentage variation in protein and fat content in bean seed covers *Phaseolus vulgaris L.* of *Piękny Jaś* variety, during the germination process at a temperature of 20 °C ± 1 °C. The first samples were collected for analysis the next day from the start of the experiment while the others were taken every 24 hours during 5 consecutive days. The experiment showed an increase in fat content in seed covers (0.94 $g \cdot 100g^{-1}$ dm –1.35 $g \cdot 100g^{-1}$ dm) and simultaneous reduction in the protein content from 4.5 $g \cdot 100g^{-1}$ dm to 3.8 $g \cdot 100g^{-1}$ dm along with the increase in germination intensity. The analytical tests were terminated after 144 hours when the majority of seeds had germinated.

Key words: bean seeds, germination, crude protein, fat.

INTRODUCTION

Leguminous plants are considered as a source of protein with very high nutritional value. Peas, beans, broad beans and lentils contain more than 20% of proteins, while soybeans even 35-40%. Apart from the protein, legumes are the source of carbohydrates and fat rich in unsaturated fatty acids. Their presence makes beans recommended in the low cholesterol diet. Pulses are also rich in vitamins from the B group, particularly thiamine and niacin. In the fresh form, legumes are also considered as a good source of vitamin C and carotene. Both, dry and fresh pulses, provide significant amounts of such minerals as iron, copper, magnesium, calcium, potassium and sulfur [20]. Bean seed flour is also used as an additive to wheat flour in the production of instant noodles [24].

From a chemical point of view, fats are the natural organic compounds with varied structure, built from a carbon, oxygen and hydrogen. Fat content in leguminous seeds depends on their variety while it presence ensures the highest nutritional value [26]. Plant after drying (dry mass – dm) contains up to 98% of organic compounds. From the thousands of different substances, some are present in significant quantities in all tissues and cells, but most could be detected only by sensitive analytical methods. The variability of the individual substances is due to the metabolic processes testifying a given tissue vitality [5, 22].

Recent years require that plants resistant to drought should be grown, due to the fact that the effects of climate change are beginning to be felt around the world and drought starts to become a rising problem in a number of countries. Study on proteins commonly found in living organisms that belong to the large family of membrane integral proteins (MIP) and take part in the collection of water, demonstrated that three of them appeared in the germinating seeds after 60 hours since the process starts, i.e. after the main phase of water intake called the physical stage. What is more, a very high level of protein in the cell membrane, which could lead to gain an actual knowledge of the mechanism regulating water intake in the seeds growth and germination processes, was observed [6, 21].

Bean (*Phaselous vulgaris L.)* belongs to the species that in Poland plays an important role for nutritional and commercial reasons in crop production [13, 16]. Beans are consumed in various forms (canned, cooked, dried, frozen) being an important source of vitamins and minerals in the human diet.

The seeds quality and the possibility of a detailed assessment of the germination process are of great importance for agriculture, and for those industries that are closely related to it. The seeds are used for both, ground and greenhouse, production and require considerable financial and labour resources. Under these conditions, seed germination control is essential due to the fact that too low germination rate may lead to significant financial losses [10]. Studies have shown that germinating seeds are very rich in vitamins, thanks to the active enzymes that additionally resolve proteins, carbohydrates and fats on the simple compounds easily assimilated by the body.

Therefore, sprouts are not only healthy, but also easily digestible. It was also found that the sprouts are large reserves of minerals, mineral salts and other nutrients which make them far less caloric than the same seed [19, 23] and what is more are also an element of nutritional products for animals [25].

It is believed that the germination process, especially the first phase of water intake and seeds swelling as well as the biochemical processes during the seeds respiration are the source of energy that appears just after swelling process starts. Respiratory substrates are substances accumulated in them, among other things, fats and proteins [3]. Seed cover is the tissue covering the seed and protecting it that is why its structure and chemical composition play an important physiological role in germination process due to the different water and gas permeability [2, 3].

The aim of this study was to examine changes in the crude protein and fat content in bean seed covers, formed from the seedbud cover which genetic material is only of the stem origin, during *Phaseolus vulgaris L.* of *Piękny Jaś* variety germination.

GERMINATION PROCESS

Biological issues of seeds growth, development and germination in define environmental conditions are closely linked and controlled at the molecular, subcellular and cellular level as well as on the level of whole seed. Gradual reduction in the intensity of physiological processes during seed maturation could be observed while throughout the rest period latent life is maintained. Seeds are also able to resume rapidly the physiological processes during swelling and germination. Preserving vitality viable seeds might remain at latent stage for a long period of time. The standstill period (anabiosis) depends both on the genetic properties and environmental conditions. Dry seeds at latent stage are usually resistant to external factors, despite the biological preparation for further development, which is possible at any time, if only the access to water, proper temperature, oxygen and, for some species to light, are provided [11].

Germination is therefore perceived as a complex process built with partial phases that result in anatomical and morphological changes, observable without the use of a microscope [2]. It is assumed that germination process contains: water uptake, the cells elongation resumption, increase in the number of enzymes and reserve substances decomposition and mixing, increase in respiratory rate and in the intensity of cell division for different tissues [12].

The presence of proteins that are involved in regulating, among other things seed covers elasticity was detected in the seeds cell walls. Their modification is possible by deposition on their surfaces various types of organic compounds that include fats. Polymerized fatty acids coat the cell surfaces, leading to changes in the water conductivity during germination [3, 4].

MATERIAL PREPARATION FOR THE EXAMINATION, ACQUISITION OF THE EXPERIMENTAL DATA

For the tests bean seeds (*Phaselous vulgaris L.*) of *Piękny Jaś* cultivars were selected. In the experiment 1000 seeds were subjected to observation. Seeds were sown in trays on several layers of filter paper to ensure proper germination conditions by continuous supply of deionized water [17]. Before the experiment seeds, along with the tissue paper, were sterilized for 30 min at 70 °C and then cooled to the room temperature. Bean seeds germinated in a dark thermostatic chamber maintaining the temperature at a level of 20 °C ± 1 °C. On the basis of 300 seeds fundamental parameters characterizing their vitality were calculated: germination capacity Z_k and one seed germination time, so called Pieper time t_p. Remained seeds were used for analytical tests on protein and fat content. The use of deionized water prevented providing the seeds with macro- and microelements that could affect or change the content of the analyzed variables [7].

It is believed that the germination process, especially the first phase of water uptake and seed swelling as well as the biochemical processes during the respiration are the source of energy that appears early after the seeds swelling initiation. Respiratory substrates are accumulated backup substances, among other things, fats and proteins found in various parts of the seed, including the shell [3].

The germination capacity of seeds is usually determined by physiological methods which are used to observe the germination process under laboratory conditions. Germination capacity Z_k can be expressed as the percentage of seeds which germinate normally under given conditions over a sufficient period of time:

$$Z_k = \frac{n}{n_c} \cdot 100\%, \tag{1}$$

where: n is the number of sprouted seeds, n_c is the total number of seeds. Germination rate E_k, i.e. the percentage of seeds which germinated normally under the set conditions and in a given period of time, usually the moment of the first recalculation of germinating seeds, is described by the following equation:

$$E_k = \frac{n(t_1)}{n_c} \cdot 100\%, \tag{2}$$

where: $n(t_1)$ is the number of sprouted seeds during the first recalculation; n_c is the total number of sown seeds. Seed viability may also be expressed by Pieper's coefficient t_p [11], i.e. the average time required for one seed to germinate:

$$t_p = \frac{\sum_{i=1}^{n} n_i \cdot t_i}{\sum_{i=1}^{n} n_i}, \tag{3}$$

where: n_i is the number of seeds germinating within a given time interval: i=1,2,3,…,n; t_i is the seed germination time.

Figure 1 shows the experimental and calculated curve drawn for the bean seeds germination process, along with the marked time of seed cover collection for the analysis. Pieper time t_p [11, 15, 18] calculated on the basis of the obtained germs accounted for 212.8 hours. Germination curve is characterized by typical shape with a well-defined saturation after about 340 hours. The calculated germination capacity Z_k reached 87.8%.

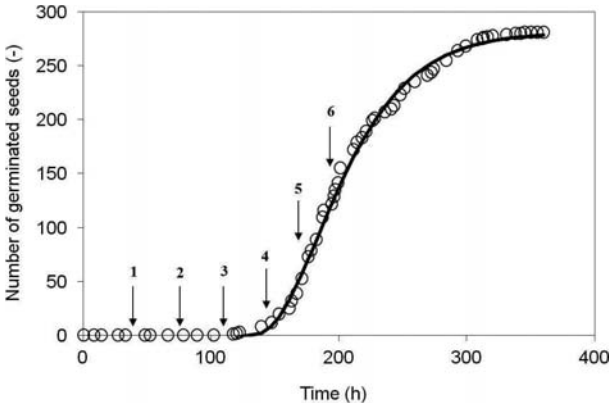

Fig. 1. Experimental (○) and calculated (solid line) germination curves for bean seeds at the temperature of 20°C.

Black arrows indicate the time when seed covers were collected for the analysis:

$$n(t) = n_k \cdot \left(1 - \frac{\alpha \cdot e^{-\lambda_1 (t-t_0)} + \beta \cdot e^{-\lambda_2 (t-t_0)} + \gamma \cdot e^{-\lambda_3 (t-t_0)}}{\alpha + \beta + \gamma}\right). \quad (4)$$

The germination process can be described mathematically with the use of a simulation model [8,9] based on the assumption that germination has three distinctive stages: physical, biochemical and physiological. It has been assumed that the germination process involves gradual evolution through the successive stages at a given level of probability. In its analytical form, the model can be expressed [9] by the equation (4), where:

$$\alpha = \lambda_2 \cdot \lambda_3 \cdot (\lambda_2 - \lambda_3), \quad (5)$$

$$\beta = \lambda_3 \cdot \lambda_1 \cdot (\lambda_3 - \lambda_1), \quad (6)$$

$$\gamma = \lambda_1 \cdot \lambda_2 \cdot (\lambda_1 - \lambda_2). \quad (7)$$

Parameters λ_1, λ_2, λ_3 indicate the probability of the seed's transition from one stage to another; *n(t)* is the number of seeds sprouted at a given time; n_k is the final number of sprouted seeds; t – is the germination time; t_0 – is the time required for the seed to emerge from the latent development stage and to enter the sprout formation stage. For the analyzed germination curve the best fit has been obtained with the following parameters: $\lambda_1 = \lambda_2 = \lambda_3 = 10^{-4}$ s^{-1}, t_0=130 h, n_k =281. The fact that probability parameters are equal indicates that each stage of the seeds evolution is also equally present in the germination process.

CRUDE PROTEIN AND FAT CONTENT DETERMINATION

Protein content was determined with the Kjeldahl method application in the Kjel-Foss Automatic (A / S Foss Electric, Denmark) device according to AOAC 976.05 while the fat content determined by extraction- gravimetric method with the Soxtec HT-6 use in the Central Analytical Laboratory of the University of Life Sciences in Lublin.

The analytical investigation was carried out in parallel with studies on germination in the subsequent days of the experiment which were marked with black arrows in Figure 1. Examined seeds were randomly selected and its cover was removed and next dried for 3 h in thermostatic oven until dry mass was obtained. Then dried material was placed in a mortar, covered with liquid nitrogen at about -186 °C and grinded to a fine dust. Then three dust samples of 0,5g were weighed with an accuracy of ± 0.01 g on the analytical balance WAS 160/C/2. Prepared samples were then poured into a specially-marked 1.5 ml eppendorfs. Each sample was subjected to3 measurements.

Table 1. Fat (a) and protein (b) content in bean seeds during germination in 20°C, marked in three tests

a)

Time (hours)	Fat content (g·100 g^{-1} dm)			
	I test	II test	III test	Average
24	0.89	0.82	0.85	0.85
48	1.05	0.87	0.88	0.93
72	0.80	0.89	0.89	0.86
96	0.89	0.84	0.87	0.87
120	1.12	1.01	1.06	1.06
144	1.89	1.82	1.88	1.86

b)

Time (hours)	Protein content (g·100 g^{-1} dm)			
	I test	II test	III test	Average
24	7.10	7.40	7.44	7.31
48	6.94	6.83	7.00	6.93
72	6.64	6.81	7.20	6.88
96	6.45	6.16	6.35	6.32
120	5.86	5.67	5.58	5.70
144	5.64	5.78	5.69	5.70

RESULTS AND DISSCUSSION

The protein content in whole seeds dry mass for dwarf varieties of common bean: Toffi, Tip Top, Nigeria and Augusta marked by many researchers ranged from 23.96 to 29.85 g·100g^{-1} dm. The fat content in seeds of these varieties was lower and changed from 1.54 to 1.78 g·100g^{-1} dm [1, 4, 10, 14].

Whereas protein content in seed covers is usually much lower. Bean seeds are characterized by protein content values in the range of 5 g·100g^{-1} dm [23], which was confirmed in the presented work.

Table 1 shows numerical values of measured variables for consecutive days of experiment as well as their average value. In table 1 mean difference between the maximum and minimum values at three tests for fat (a) and protein (b) in germinated bean seed covers subjected to germination at the 20 ° C are presented. The fat content in beans covers during germination in deionized water was twice lower than in the whole seeds (0.85 to 1.86 g·100g^{-1} dm), while protein content was considerably lower (7.31- 5.70 g·100g^{-1} dm).

Figure 2 shows the fat content determined by extraction- gravimetric method for dry bean seed covers naturally moistened during the germination process and the maximum deviation from the average values. First marking for seed samples was performed after 24 hours of the beans were sowed in trays on the constantly humidified filter paper. Average fat content determined in three repetitions reached 0.85 g·100g^{-1} dm. Successive days of the research indicated a systematic increase in the fat content. The highest increase occurred between 5th and 6th germination day, when the fat content raised from 1.06 g·100g^{-1} dm to 1.86 g·100g^{-1} dm.

Average protein content value in samples taken from seeds at the same time intervals determined by the Kjeldahl method decreased steadily from 7.31 g·100g^{-1} dm on the first day to 5.7 g·100g^{-1} dm on the last day of analysis (see Fig.3). Recent determination of the protein in experiment 144th hour indicated the same value as in the previous day (120 hrs.).

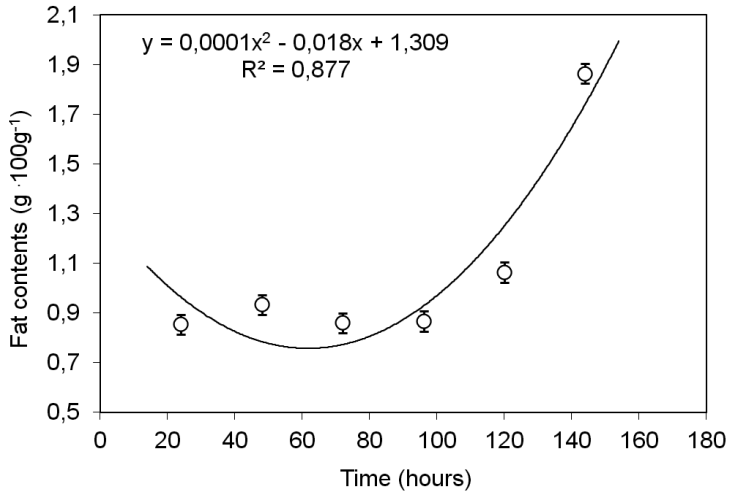

Fig. 2. Fat contents in bean seed cover during germination process. Error bars indicate the average difference between results and the average calculated for three samples

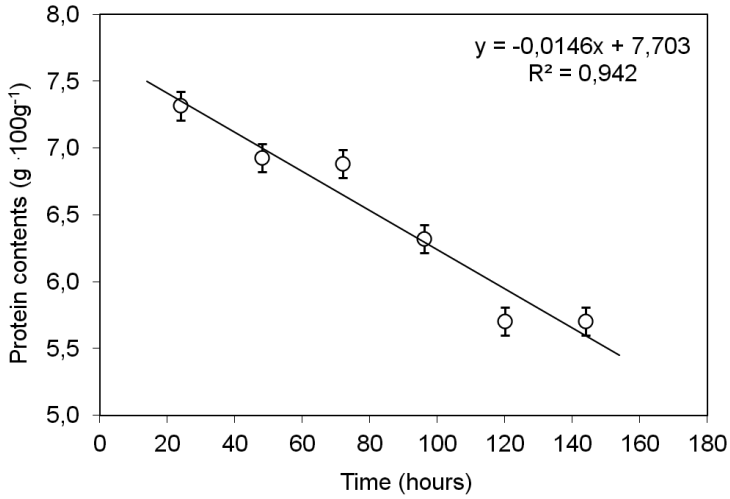

Fig. 3. The protein content in bean seed cover during germination process. Error bars indicate the average difference between results and the average calculated for three samples

In the 72th germination hour, when almost all seeds had completed the swelling stage, protein content in the cover decreased steadily from 6.88 g·100g^{-1} dm (72th hour) to 6.32 g·100g^{-1} dm in the 120th hour An identical value was obtained for seed cover samples on the last day of measurement (144th germination hour). Observed decrease in the protein content was consistent with the highest intensity of germination (Pieper time t_p= 140.8 hours).

Although the germination process took more than 300 hours, chemical analyzes were completed in 144 hours, as most seeds sprout achieving the final effect of the germination process.

CONCLUSIONS

1. The fat content determined with the use of extraction-gravimetric method in seed cover remained steady during first 96 hours at the level of 0.9 g·100g^{-1} dm -1.14 g·100g^{-1} dm. In the next two days (48 hours) fat content increase up to 1.86 g·100g^{-1} dm was observed. The fat content in seeds with visible sprout was doubled in relation to the value determined on the first day of germination.
2. Crude protein content, set with the use of the Kjeldahl method, decreased from 7.31 g·100g^{-1} dm in 24th hour of germination to 5.70 g·100g^{-1} dm – the value defined in 120th experiment hour. This value was maintained for another day which was proved by the protein content measurement in 144th germination hour.
3. Starting from 72th hour of germination a significant increase in fat content could be observed while the protein content strongly decreased (6.88 g·100g^{-1} dm - 5.70 g·100g^{-1} dm). It may indicate that the backup substances causing the seed embryo's growth, cover breakdown and seedling emergence were depleted.

REFERENCES

1. **Berrios J.J., Swanson B.G., Cheong W.A. 1999:** Physico-chemical characterization of stored black beans (Phaseolus vulgaris L.). Food Res. Int., 32, p. 669-676.
2. **Berlyn G.P. 1972:** Seed germination and morphogenesis. In: Kozłowski, Seed biology, Acad. Press, N.Y. London, vol. 1, p. 223-312.
3. **Bewley J.D., Black M. 1972:** Physiology and biochemistry of seed in relation togermination. Vol. 1,2. Springer Verlag, Berlin-Heidelberg-New York.
4. **Candela M., Astiasaran I., Bello J. 1997:** Cooking and warm-holding: effect on general composition and amino acids of kidney beans (Phaseolus vulgaris), chickpeas (Cicer arietinum), and lentils (Lens culinaris). J. Agric. Food Chem., 45, p. 4763-4767.
5. **Cone W.J. 1982:** The Escape From Photocontrol of Seed Germination of Arabidopsis Thaliana. Arabid. Inf. Serv.(19) p. 35.
6. **Gattolin S., Sorieul M., Frigerio L. 2011:** Mapping of tonoplast intrinsic proteins in maturing and germinating arabidopsis seeds reveals dual localization of embryonic tips to the tonoplast and plasma membrane. Molecular Plant 4, p. 180-189.
7. **Gładyszewska B. 2007:** Method of testing of selected mechanical properties of thin biological materials (in Polish), habilitation thesis AU in Lublin, p. 325.
8. **Gładyszewska B. 1998:** Ocena wpływu przedsiewnej laserowej biostymulacji nasion pomidorów na proces ich kiełkowania. Rozprawa doktorska. Lublin.
9. **Gładyszewska B., Koper R.:** Symulacyjny model procesu kiełkowania nasion w ujęciu analitycznym. Inżynieria Rolnicza, 7, p. 59-63
10. **Granito M., Frias J., Doblado R., Guerra A., Champ M. 1960:** Nutritional improvement of beans Phaseolus vulgaris) by natural fermentation. Eur. Food Res. Technol., 2002, 214, p. 226-23.
11. **Grzesiuk S. Kulka S. 1981:** Fizjologia i biochemia nasion. PWRiL., Warszawa.
12. **Kramer P.J., Kozłowski T.T. 1980:** Physiology of trees. MC Graf-Hill N.Y. Toronto, London.
13. **Jasińska Z., Kotecki A. 1993:** Rośliny strączkowe. PWN. Warszawa.
14. **Martín-Cabrejas M.A., Sanfiz B., Vidal A., Mollá E., Esteban R., López-Andréu F.J. 2004:** Effect of fermentation and autoclaving on dietary fiber fractions and antinutritional factors of beans (Phaseolus vulgaris L.). J. Agric. Food Chem., 52, p. 261-266.
15. **Noogle G.R., Fritz G.L. 1976:** Introductory plant physiology. Prentice-Hall, New Jersey, p. 264-265.
16. **Podleśny J. 2005:** Rośliny strączkowe w Polsce- perspektywy uprawy i wykorzystanie nasion. Acta Agrophys. 6 (1), p. 213-224.
17. Polska Norma PN-96/R-65950. Materiał siewny. Metody badania nasion.
18. **Pieper G., Eggebrecht H. 1995:** Das Saatgut. Wydanie II, Berlin.
19. **Shimelis E.A., Rakshit S.K. 2005:** Proximate composition and physico-chemical properties of improved dry bean (Phaseolus vulgaris L.) varieties grown in Ethiopia. Libens Wiss Technol. 38, p. 331-338.
20. **Szczygieł A., Bułhak–Jachymczak B. 1975:** Podstawy fizjologii żywienia. PZWL, Warszawa.
21. **Taormina P.J., Beuchat L.R., Slutsker L. 1999:** Infections Associated with Eating Seed Sprouts: An International Concern. Emerging Infectious Diseases 5, p. 626.
22. **Vargas-Torres A., Osorio-Díaz P., Tovar J., Paredes-López O., Ruales J., Bello-Pérez L.A. 2004:** Chemical composition, starch bioavailability and indigestible fraction of common beans (Phaseolusvulgaris L.). Starch/ Stärke, 56, p. 74-78.
23. **Wu X. 2002:** Correlation of physic-chemical characteristics in the seed covers and canning quality in different dark red kidney bean (Phaseolus Vulgaris L.) cultivars. MSC thesis University of Wisconsin-Stout, Research paper.
24. **Wojtowicz A. 2008:** Influence of legumes addition on proceeding of extrusion-cooking process of precooked pasta. Teka Kom. Mot. Energ. Roln. – OL.PAN, 8a, p. 209-216.
25. **Young A.W., Grummer R.H., Hirschinger C.W. 1977:** Using cullkidney beans in swine protein supplement. Research Report No. 2892, University of Wisconsin-Madison, College of Agricultural and Life Sciences.

26. **Ziemlański Ś., Budzyńska-Topolowska J. 1991:** Tłuszcze pożywienia i lipidy ustrojowe. Wydawnictwo Naukowe PWN. Warszawa.

ZMIANA ZAWARTOŚCI BIAŁKA I TŁUSZCZU
W OKRYWIE NASIENNEJ FASOLI
PODCZAS KIEŁKOWANIA

S t r e s z c z e n i e . W pracy przedstawiono wyniki badań procentowej zmienności zawartości białka ogółem i tłuszczu w okrywach nasion fasoli Phaseolus vulgaris L. odmiany Piękny Jaś, w trakcie procesu kiełkowania przebiegającego w temperaturze 20^{o}C ±1^{o}C. Pierwsze próbki do analizy pobrano następnego dnia od chwili rozpoczęcia eksperymentu, następne pobierano co 24 godziny przez 5 kolejnych dni. Badania wykazały zwiększenie zawartości tłuszczu (0,89 g·100g^{-1} s.m. – 1,86 g·100g^{-1} s.m.) oraz zmniejszenie zawartości białka w okrywach z 7,31 g·100g^{-1} s.m. do 5,70 g·100g^{-1} s.m. wraz ze wzrostem intensywności kiełkowania. Badania analityczne zakończono po 144 godzinach, gdy większość nasion zakończyła już kiełkowanie.

S ł o w a k l u c z o w e : nasiona fasoli, kiełkowanie, białko surowe, tłuszcz.

TEKA. COMMISSION OF MOTORIZATION AND ENERGETICS IN AGRICULTURE – 2012, Vol. 12, No. 1, 41–46

Effect of high-speed traction gearbox ratio on vehicle fuel consumption

Wawrzyniec Gołębiewski, Tomasz Stoeck**

* Department of Automotive Vehicles Operation, West Pomeranian University of Technology in Szczecin

Summary. This paper presents the effect of high-speed traction gearbox ratio on vehicle mileage fuel consumption. Relation was determined for constant linear velocities of a motor vehicle being reached on more than one gearbox ratio. The characteristic curve was prepared based on an engine's torque-speed relationship for respective mileage fuel consumption being obtained when using given gears. Experiments were carried out based on engine standards, according to which the points of external and partial characteristic curves for an engine's torque and its fuel consumption were established by measurement.

It was demonstrated in conclusions that fuel consumption of a motor vehicle increases together with an increase in the value of high-speed traction gearbox ratio.

Key words: high-speed traction gearbox ratio, mileage fuel consumption, energy consumption of vehicle motion.

INTRODUCTION

Mileage fuel consumption is an important parameter characterising a motor vehicle in terms of economy and ecology. It is the clearest characteristic for a potential user, the value of which has been constantly reduced over the years. It can be described by the following relation [2,7]:

$$Q = \frac{G_e \cdot 100}{\gamma \cdot v} \tag{1}$$

where:
Q - mileage fuel consumption [dm^3/100 km],
G_e - hourly fuel consumption [kg/h],
γ - fuel specific gravity [kg/dm^3],
v - vehicle's linear velocity [km/h].

Gearbox ratios are important for fuel consumption. The larger value has the ratio, the accordingly higher is fuel consumption curve located. Engine has to make a larger number of work cycles so that a motor vehicle could cover a specific road section. Then, the most important parameter affecting mileage fuel consumption when moving with a constant speed is high-speed traction gearbox ratio (ratio of engine crankshaft angular velocity ω_S to vehicle linear velocity v or a ratio of power transmission system's overall gear ratio i_C to dynamic wheel radius r_d) [10]:

$$i_S = \frac{\omega_S}{v} = \frac{i_C}{r_d}. \tag{2}$$

Then, the relationship (1) assumes the following form:

$$Q = \frac{G_e \cdot 100 \cdot i_S}{\gamma \cdot \omega_S}. \tag{3}$$

The foregoing considerations being referred to have determined that 5-speed mechanical gearboxes are frequently used in motor vehicles, of which the last gear is an economic one (lowest fuel consumption) but also an overdrive gear (gearbox ratio is less than one) [10].

High-speed traction gearbox ratio is thus an effective indicator of the impact of engine elements' motion mechanics (engine crankshaft speed) on the energy consumption of vehicle motion expressed as fuel consumption.

RESEARCH OBJECTIVE AND METHODS

The objective of this research project was to determine the effect of high-speed traction gearbox ratio on vehicle fuel consumption.

The methods of carried out research are in conformity with standards [15,16,17]. Experiments were conducted according to the requirements specified in them, using an engine test bench. Test points were prepared for feeding an engine with a full fuel dose (external characteristics) and partial fuel doses (25%, 50 % and 75%), i.e. partial power characteristics for Fiat 1.3 JTD Multijet engine. Based on the presented graphs, a full load characteristics was prepared. The final stage was to establish a relation-

ship between mileage fuel consumption and high-speed traction gearbox ratio.

TEST BED

The test bed consisted of the following components:

a) eddy current brake EMX 100 manufactured by Elektromex (Poland);
b) Fiat 1.3 JTD Multijet engine, i.e. a compression-ignition, four-stroke, turbo-supercharged, direct fuel injection engine with fuel feed system of the Common Rail type. Fuel injection was controlled electronically with air supercharging by turbo-supercharger and air cooler. The engine was controlled by means of electronic high pressure injection system designed by Magneti Marelli [14].

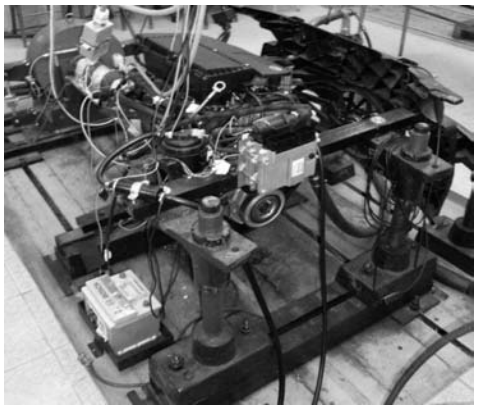

Fig. 1. The view of Fiat 1.3 JTD 16 V Multijet engine connected with eddy current brake EMX 100 by means of drive shaft

Engine details are given in Table 1 below according to manufacturer's data.

Table 1. Engine details according to manufacturer's data [14]

Make: FIAT		Type: 1.3 JTD 16 V Multijet
Work cycle		4-stroke
Cylinder diameter	[mm]	69.6
Piston travel	[mm]	82
Compression ratio		18.1
Number of cylinders		4
Arrangement of cylinders		in-line
Injection sequence		1-3-2-4
Engine capacity	[cm^3]	1248
Maximum power	[KM/kW]	70/51
Rotational speed at maximum power	[min^{-1}]	4000
Maximum torque	[Nm]	145
Rotational speed at maximum torque	[min^{-1}]	1750

VEHICLE INFORMATION

In order to be able to draw a relationship of fuel consumption-high-speed traction gearbox ratio, certain information were necessary, such as – for instance – power transmission system efficiency, kinematic wheel radius and gearbox and final drive ratios. These data are presented in Tables 2 and 3.

Table 2. Basic vehicle and motion resistance data

Element	Value	Unit	where (comment):
η_{UN}	0.9	-	power transmission system efficiency (for passenger cars)
r_k	0.27	[m]	kinematic wheel radius

In Table 3 below, vehicle gearbox and final drive ratios are being considered.

Table 3. Basic C514R gearbox and final drive ratios [14]

I gear	3.909
II gear	2.158
III gear	1.345
IV gear	0.974
V gear	0.766
Final drive	3.438

COURSE OF TESTS AND RESULTS

The graphs made on the basis of measurements were the full power characteristics (external characteristic curve) as well as partial power characteristics (characteristic curves for feeding the engine with 25%, 50 % and 75 % fuel dose). The most important parameters were engine torque and fuel consumption. The collected measurement results are presented in Tab. 4 and Figs 2 and 3:

where: *n* – engine speed, *Ttq25%* – corrected engine torque (fuel feed with 25% nominal dose), *Ttq50%* – corrected engine torque (fuel feed with 50% nominal dose), *Ttq75%* – corrected engine torque (fuel feed with 75% nominal dose), *Ttq100%* – corrected engine torque (fuel feed with 100% nominal dose), *B25 %* – engine fuel consumption (fuel feed with 25 % nominal dose), *B50 %* – engine fuel consumption (fuel feed with 50 % nominal dose), *B75 %* – engine fuel consumption (fuel feed with 75 % nominal dose), *B100 %* – engine fuel consumption (fuel feed with 100 % nominal dose)

Table 4. Measurement results for engine parameters

	n	Ttq25%	Ttq50%	Ttq75%	Ttq100%	B25%	B50%	B75%	B100%
Item	[rpm]	[Nm]	[Nm]	[Nm]	[Nm]	[g/s]	[g/s]	[g/s]	[g/s]
1	1000	12.0	13.1	35.7	71.4	0.23	0.25	0.35	0.59
2	1500	18.4	20.1	62.2	124.4	0.50	0.60	0.84	1.39
3	1700	18.0	19.9	69.8	139.6	0.50	0.55	1.01	1.65
4	1900	19.5	24.2	71.2	140.1	0.57	0.70	1.08	1.78
5	2000	20.2	24.3	70.1	138.1	0.63	0.86	1.12	1.85
6	2200	19.1	25.1	68.9	137.7	0.59	0.91	1.23	2.01
7	2400	18.4	24.3	67.6	135.2	0.72	0.85	1.25	2.08
8	2500	17.1	24.6	67.2	134.4	0.64	0.93	1.33	2.20
9	3000	18.8	26.8	67.3	134.6	0.74	0.99	1.66	2.75
10	3500	18.5	32.9	68.1	124.2	0.95	1.23	1.87	3.08
11	4000	25.0	44.4	70.2	115.1	1.16	1.34	2.09	3.38
12	4500	14.4	43.3	60.3	94.6	1.25	1.50	1.95	3.25

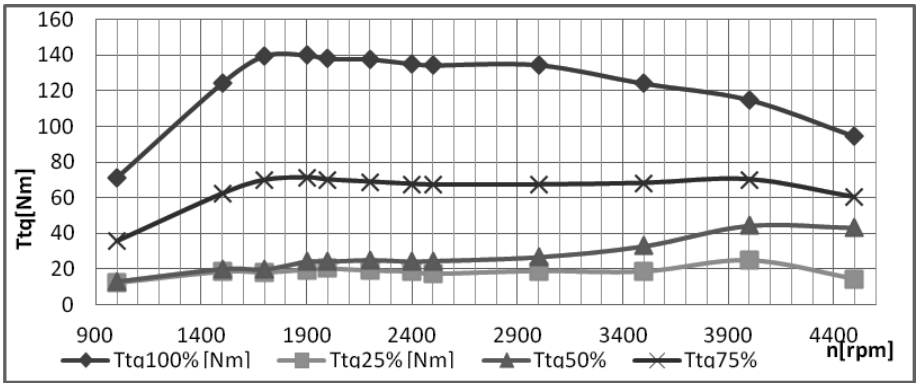

Fig. 2. Partial characteristic curves for engine torque

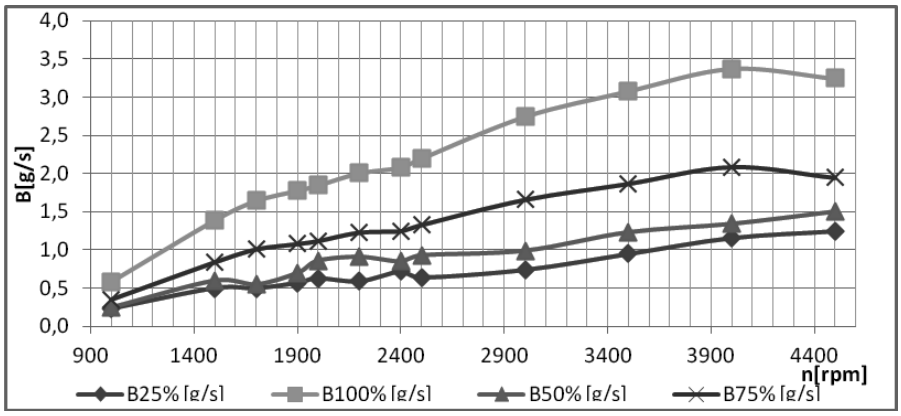

Fig. 3. Partial characteristic curves for fuel consumption

The presented graphic relations allowed for the establishment of the full load characteristics as a fuel consumption-engine torque relationship and transposition of the axes of that characteristics together with the replacement and conversion of hourly fuel consumption into mileage fuel consumption according to relation (1)

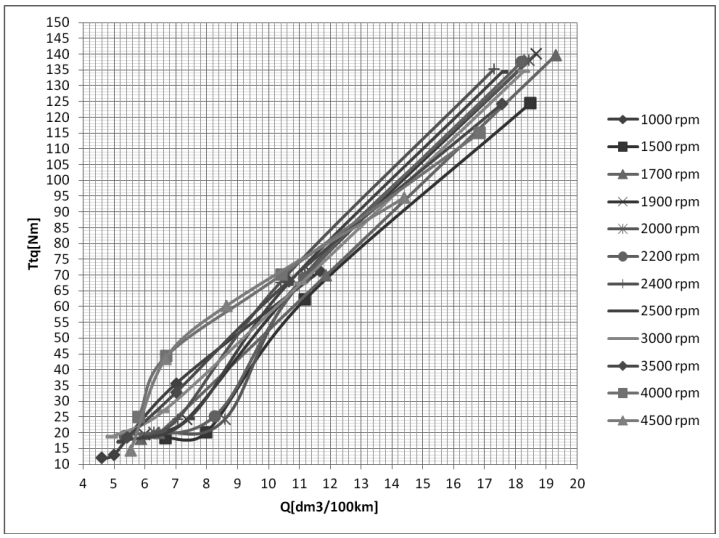

Fig. 4. Engine torque-mileage fuel consumption relationship for the third gear

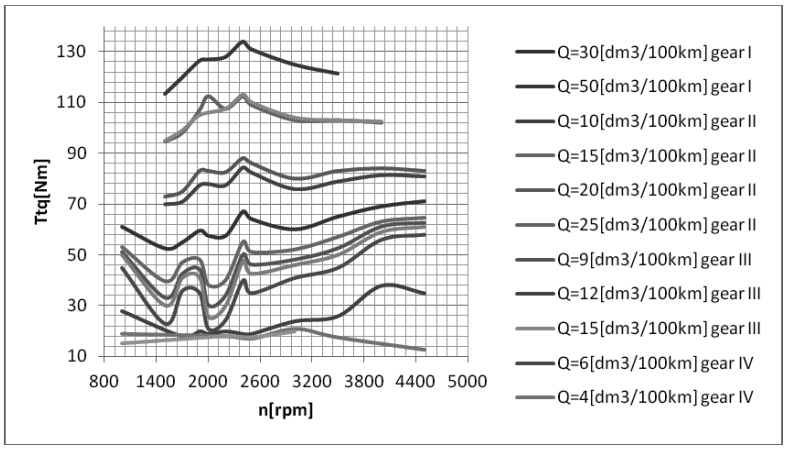

Fig. 5. Relation between engine torque and its speed allowing for sample mileage fuel consumption curves for individual gears

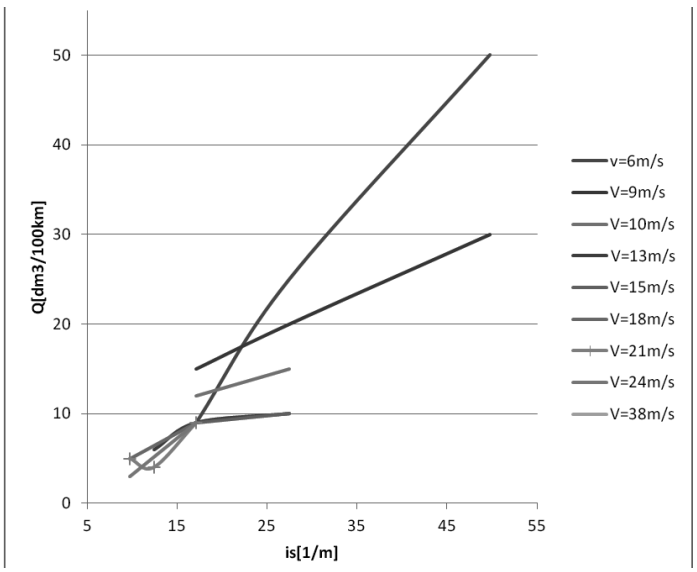

Fig. 6. Effect of high-speed traction gearbox ratio on mileage fuel consumption

Table 5. Constant value of high-speed traction gearbox ratio for first gear

n	n	ω	v	v	i_S
[rpm]	[rps]	[rad/s]	[km/h]	[m/s]	[1/m]
1000	17	104.67	7.570	2	49.77
1500	25	157.00	11.355	3	49.77
1700	28	177.93	12.869	4	49.77
1900	32	198.87	14.383	4	49.77
2000	33	209.33	15.140	4	49.77
2200	37	230.27	16.654	5	49.77
2400	40	251.20	18.168	5	49.77
2500	42	261.67	18.925	5	49.77
3000	50	314.00	22.710	6	49.77
3500	58	366.33	26.495	7	49,77
4000	67	418.67	30.281	8	49,77
4500	75	471.00	34.066	9	49,77

Table 6. Sample fuel consumption for specific high-speed traction gearbox ratios (constant vehicle linear velocities)

	i_S	Q	[dm^3/100km]							
	[1/m]	v=6m/s	v=9 m/s	v=10 m/s	v=13 m/s	v=15 m/s	v=18 m/s	v=21m/s	v=24 m/s	v=38 m/s
i_{sI}	49.77	50	30							
i_{sII}	27.48	25	20	15	10	10				
i_{sIII}	17.13	9	15	12	9	9	9	9	9	4
i_{sIV}	12.40				6			4		
i_{sV}	9.75						5	5	3	5

for each engine speed and for linear velocity ranges for each total ratio (being a product of selectable gearbox ratio and constant final drive ratio) (Fig. 4).

From the graph presented above, sample mileage fuel consumption values were selected (for each gear) and engine torque values corresponding to them were read. This allowed attainment of fuel consumption curves for individual engine speeds (which allowed further replacement into vehicle linear velocities for specific total ratios of power transmission system).

The converted values of high-speed traction gearbox ratio were identical within the whole range of rotational speeds for individual gear ratios (see an example in Tab. 5).

For successive gears, the following values of high-speed traction gearbox ratio were obtained together with specific values of mileage fuel consumption for constant vehicle linear velocities (Tab. 6 and Fig. 6).

CONCLUSIONS

High-speed traction gearbox ratio is an important parameter characterising the ratio of engine angular speed to linear velocity of vehicle wheels. It has a greater value for lower gears, whereas a smaller one for higher gears. Mileage fuel consumption for specific linear vehicle velocities increases with increasing values of high-speed traction gearbox ratio but also decreases for smaller values of high-speed traction gearbox ratio.

The reported arguments allow for the conclusion that the most economical driving (and at the same time the most ecological one) is that one where vehicle speed values are high (over 18 m/s in Fig. 6) and high-speed traction gearbox ratio values are low. Then the mileage fuel consumption is the lowest.

REFERENCES

1. **Arczyński S. 1994:** Mechanika ruchu samochodu. Warszawa, WNT. p. 45-64, 92-104.
2. **Dębicki M.:** Teoria samochodu. Teoria napędu. WNT. Warszawa 1976.p.19-27, 45-60, 106-120, 161-172.
3. **Kropiwnicki J. 2010:** Ocena eksploatacyjnego zużycia paliwa samochodów. Silniki spalinowe nr 3/2010. Wydawnictwo PTNSS. Bielsko–Biała.
4. **Kropiwnicki J. 2011:** Prognozowanie emisji CO_2 samochodu z użyciem dyskretnej mapy warunków eksp-

loatacji. Archiwum Motoryzacji nr 1/2011. Wydawnictwo PTNM i PIMOT. Warszawa.
5. **Lisowski M. 1999:** Ocena własności trakcyjnych samochodu Jelcz 317 wyposażonego w silnik SW – 680 z różnymi systemami doładowania. MOTROL. Lublin.
6. **Lisowski M. 2003:** Teoria ruchu samochodu. Teoria napędu. Politechnika Szczecińska. Szczecin. p. 8-13, 17-19, 43-47, 64-67.
7. **Lisowski M. 2008:** An analysis of fuel consumption by a lorry with the compression ignition dynamic charged engine. TEKA Komisji Motoryzacji i Energetyki Rolnictwa. PAN. Lublin.
8. **Prajwowski K., Gołębiewski W. 2011:** Simulative comparison of the traction properties of Daewoo Lublin 3 Mi van with particular types of gearbox. Journal of Kones Powertrain and Transport Vol.18/No.1. European Science Society of Powertrain and Transport Publication. Warsaw.
9. **Prochowski L. 2007:** Mechanika ruchu. WKiŁ. Warszawa.
10. **Siłka W. 1997:** Energochłonność ruchu samochodu. WKŁ. Warszawa. p. 28-36,
11. **Siłka W. 2011:** Sprawność napędu samochodu przy zmiennej prędkości. Silniki spalinowe nr 1/2011. Wydawnictwo PTNSS. Bielsko–Biała.
12. **Siłka W. 2002:** Teoria ruchu samochodu. WNT. Warszawa. p. 53-144.
13. **Taryma S., Woźniak R. 2010:** Energetyczne aspekty toczenia koła ogumionego o dużej odkształcalności. Archiwum Motoryzacji nr 4/2010. Wydawnictwo Naukowe PTNM. Radom.
14. **Zembowicz J. 2005:** Fiat Panda. WKiŁ. Warszawa. p. 12, 50-51, 136-138.
15. Norma PN-ISO 15550: Silniki spalinowe tłokowe. Określenie i metoda pomiaru mocy silnika. Wymagania ogólne. PKN. Warszawa 2009.
16. Norma PN-ISO 3046-1:2009 Silniki spalinowe tłokowe. Osiągi. Część 1: Deklaracja mocy, zużycia paliwa i oleju smarującego oraz metody badań. Dodatkowe wymagania dotyczące silników ogólnego zastosowania. PKN. Warszawa.
17. Norma PN-ISO 3046-3:2009 Silniki spalinowe tłokowe. Osiągi. Część 3: Pomiary podczas prób. PKN. Warszawa.
18. Instrukcja obsługi paliwomierza AMX 212F. Automex. Gdańsk 2004.
19. Instrukcja obsługi panelu mocy. Automex. Gdańsk 2007.
20. Instrukcja obsługi modułu pomiarowego PM0 AMX 212 PMO. Automex. Gdańsk 2007.
21. Instrukcja obsługi modułu pomiarowego temperatur i ciśnień AMX 212PT. Automex. Gdańsk 2007.

WPŁYW PRZEŁOŻENIA SZYBKOBIEŻNOŚCI NA ZUŻYCIE PALIWA POJAZDU

S t r e s z c z e n i e . Publikacja prezentuje wpływ przełożenia szybkobieżności na przebiegowe zużycie pojazdu. Relację określono dla stałych prędkości liniowych samochodu osiąganych na więcej niż jednym przełożeniu skrzyni biegów. Charakterystykę wykonano na podstawie zależności momentu obrotowego silnika od jego prędkości obrotowej dla poszczególnych przebiegowych zużyć paliwa uzyskanych przy wykorzystaniu danych biegów. Eksperymenty zostały wykonane na podstawie norm silnikowych, według których przez pomiar utworzono punkty charakterystyk zewnętrznych oraz częściowych momentu obrotowego silnika oraz jego zużycia paliwa.

We wnioskach wykazano, że wraz ze wzrostem wartości przełożenia szybkobieżności rośnie konsumpcja paliwa pojazdu samochodowego.

S ł o w a k l u c z o w e : przełożenie szybkobieżności, przebiegowe zużycie paliwa, energochłonność ruchu pojazdu.

TEKA. COMMISSION OF MOTORIZATION AND ENERGETICS IN AGRICULTURE – 2012, Vol. 12, No. 1, 47–52

Determination of specific fuel consumption of IC engine in transient conditions

Janusz Grzelka

Czestochowa University of Technology, 42-201 Czestochowa, A. Krajowej 21
Institute of Thermal Machinery, grzelka@imc.pcz.czest.pl

Summary. This paper presents the results of motor vehicle traction research obtained with the use of satellite navigation techniques as an alternative test method of determination the external characteristics of the engine. The characteristics take into consideration the weather and the vertical profile of the route with simultaneous determination of specific fuel consumption based on measurement of the fuel injector opening time.

Key words: combustion engine, specific fuel consumption, transient conditions.

INTRODUCTION

The paper presents the results of measuring the light fuel injector flow characteristics and the results of calculating the specific fuel consumption of spark ignited engine obtained with the use of above mentioned characteristics at the time of vehicle acceleration:

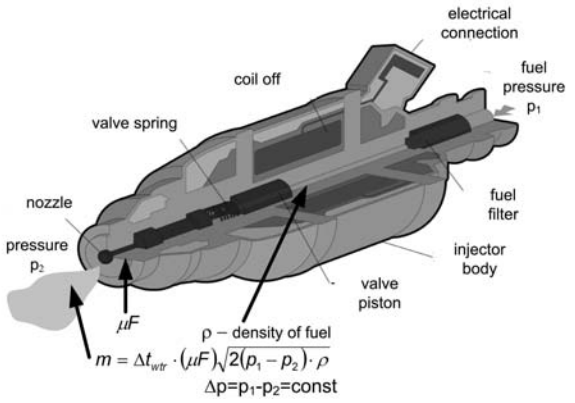

Fig. 1. Fuel flow diagram (description in text) [authors' own, http://commons.wikimedia.org, 2011]

The fuel dose flowing through the injector (fig. 1) can be controlled by variation of the effective area of the minimal section μF, the difference between the fuel pressure p_1 and the injector ambient pressure p_2 or by injector opening time Δt_{wtr}. The mass m flowing uniformly out of the nozzle at the Δt_{wtr} time can be determined by the following equation (1):

$$m = \Delta t_{wtr} \cdot (\mu F)\sqrt{2(p_1 - p_2)\cdot\rho}\,. \tag{1}$$

The fuel dose can be easily controlled as the injector opening time depends on the value of electrical signal. The total amount of fuel delivered to the cylinder is determined by both the duration of single pulse and the number of injections in time. The basic injector characteristics is the dependence between the fuel dose and the injector opening time at constant rotational speed or constant injection frequency.

PURPOSE AND METHODS

Assuming the condition of constant pressure difference p_1 and p_2 and constant fuel temperature (fig. 1), the jet of fuel from the injector is dependent on the diameter and geometry of nozzle as well as the shape and lift of nozzle needle. In order to simplify the measuring results interpretation method, the inertia of injector's moving elements has been neglected in the calculations and it has been assumed that the nozzle needle lift course is inversely proportional to the current curve in the injector coil. The instantaneous fuel consumption of engine operating in transient conditions on the vehicle test house or during the traction research can be determined at known injector characteristics by measuring – recording the opening time and recording or controlling the fuel pressure and temperature independently from the selected injector opening time control system (controlling by the single pulse, controlling with the current bound

or multi-pulse controlling). The engine rotational speed can be recorded with the use of rotational speed sensors installed in the combustion engine control system or it can be determined on the basis of vehicle velocity during acceleration on specific gear measured with the use of e.g. satellite navigation techniques. The research verifying the usefulness of measuring method of the instantaneous fuel consumption in transient conditions were carried out with the use of combustion engine with sequential multipoint injection controlled by single rectangular signal. It is a spark ignited engine of cubic capacity equal 1199 cm^3 and power of 55 kW at 5600 rpm. The maximal torque of above mentioned engine is 110 Nm at 4000 rpm. Using the measurement of injector opening time to determine the specific fuel consumption entails the necessity of determination the characteristics of injector installed in the given combustion engine [10, 11]. Such characteristics are difficult to obtain and therefore the measurement of fuel flow capacity (constant fuel pressure and temperature) in relation with opening time of injector controlled by single pulse at constant opening frequency [20] was carried out. The variation window of injector opening time was determined on the basis of measurements during vehicle acceleration at the conditions of real vehicle exploitation.

The volumetric method was used in order to determine the injector characteristics given by (2):

$$d_w \left[\frac{mm^3}{ms} \right] = f(\Delta t_{wtr}[ms]), \tag{2}$$

where :
d_w - injector fuel flow, mm^3/ms,
Δt_{wtr} - injector opening time, ms.

In the above mentioned method the microprocessor counts the number of pulses in the specific time at the injector opening time controlled by the microprocessor and recorded by the multichannel A/D converter. In the method of determination the injector characteristics, the specific dose of fuel from the injector can be described by the following equation (3):

$$d_w = \frac{V_p}{i_c \cdot \Delta t_{wtr}} \quad \left[\frac{mm^3}{ms} \right], \tag{3}$$

where:
V_p - the volume of injected fuel, mm^3;
i_c - the number of cycles/injections, *cycle*;
Δt_{wtr} - duration of the single cycle, *ms.*

The error of the injector characteristic determination was set as the average square error described by the following equation (4):

$$\Delta d_w = \sqrt{\left(\frac{\delta d_w}{\delta V_p}\right)^2 \cdot \left(\Delta V_p\right)^2 + \left(\frac{\delta d_w}{\delta i_c}\right)^2 \cdot \left(\Delta i_c\right)^2 + \left(\frac{\delta d_w}{\delta \Delta t_{wtr}}\right)^2 \cdot \left(\Delta\left(\Delta t_{wtr}\right)\right)^2}. \tag{4}$$

For the injection time between 11 and 18 ms (corresponding with values at the vehicle acceleration at the throttle fully opened, fuel pressure before the injector equal p_1=0.38 MPa and temperature approximately 42°C), the real flow characteristics at constant injection frequency is not linear and the non-linearity error [21] is at the level of 5% in the range of short opening times as well as for the maximal opening time.

DETERMINATION OF THE ENGINE'S EXTERNAL CHARACTERISTIC IN UNSTEADY CONDITIONS

The application of method using telecommunication techniques [4, 13, 16] to automotive vehicle traction research is fully justified [7], but it requires the knowledge concerning the characteristics of injector in which the vehicle's engine is equipped as well as the correlation between the injector opening times recording units and the software recording the basic physical quantities of vehicle movement in transient conditions obtained with the use of satellite navigation (UTC time, dislocation components P-X, P-Y, P-Z and velocity components V-X, V-Y i V-Z in WGS-84 system) [6, 12, 18]. In order to verify the above mentioned method the research concerning vehicle acceleration [1] with simultaneous recording of its movement parameters using the satellite navigation were carried out. The measuring system was equipped with the set dedicated to registering the injectors opening times, fuel pressure and temperature and the inlet system pressure. The fuel system was equipped with the PLU -116H [3] flow meter with pulse output of resolution equal 6.15 mm^3 per one generated electrical pulse. The flow meter measured the total fuel consumption. The schematic diagram of the measuring system is depicted in figure 2. The analysis of technical data [3, 17] of the applied flow meter reveals that the determination of the fuel consumption is performed with the accuracy of approximately 5 to 7% (at the average injector opening time during tests at the level of 15 to 20 ms).

The following quantities were registered during research:
- Vehicle location components P-X, P-Y i P-Z in WGS-84 system;
- Vehicle velocity components V-X, V-Y i V-Z in WGS-84 system;
- UTC time;
- Wind speed and direction;
- Ambient pressure and temperature;
- Injector opening times (fig. 3) with frequency of 40 kHz;
- Instantaneous fuel consumption (recording of pulses generated by the PLU 116H flow meter with the frequency of 40 kHz);
- Fuel pressure in the fuel rail using the Kistler piezoresistive probe with the frequency of 40 kHz;

Inlet system pressure using the Motorola MPX 5500DP absolute pressure piezoresistive probe with the frequency of 40 kHz;

Fuel temperature in the fuel rail and in the PLU 166 H flow meter (NiCr-NiAl thermocouple).

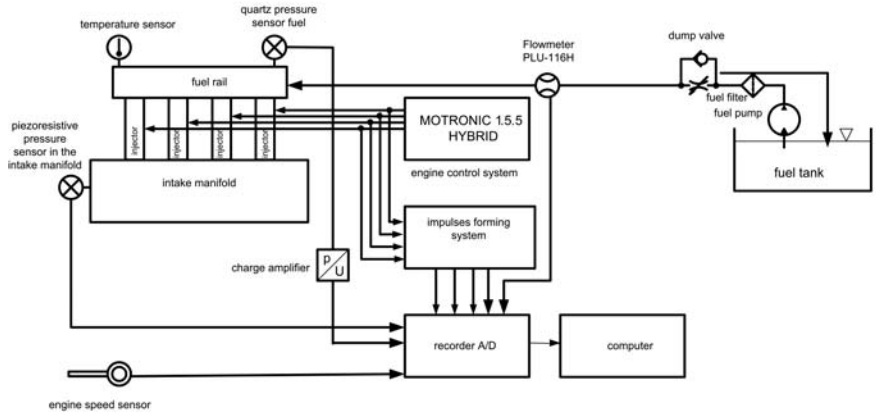

Fig. 2. The schematic diagram of the fuel consumption recording system during the acceleration of vehicle with 1.2 16V Z12XE engine

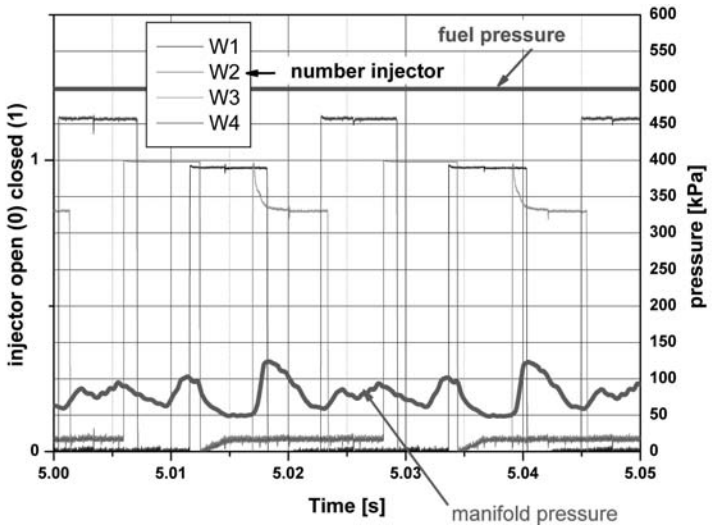

Fig. 3. Injector opening times (W1 ... W4), in relation to changes of pressure in the intake manifold and fuel pressure during acceleration of a vehicle with 1.2 16V Z12XE engine

The exemplary curves depicting injector state (low state – „0"- is the opened injector), variation of fuel pressure in the fuel rail and intake manifold pressure – the pressure sensor located in the vicinity of the injector no. 1 (W1) are depicted in figure 3.

The external characteristics of power and torque as well as specific fuel consumption were obtained from the measurements and analysis of vehicle acceleration on the third gear using the satellite navigation technique. The calculations were carried out taking into consideration the vertical rout profile – the average change in the altitude (5 m) on a test track (596 m) results in the average inclination of 0.84% (the allowable value 0.5% [14, 15]). The calculation results were corrected using the DIN 70020-5 [2] standard to the normal conditions: ambient pressure 1013.25 hPa, ambient temperature 293K. The results depicted in table 1 do not differ significantly from the catalogue data [8].

The analysis of obtained results of injector opening times [5] and the attempt to estimate the specific (taking into consideration the conditions, in which the individual injectors were calibrated – injection to the environment $p_2=b_0$) and hourly fuel consumption revealed rather large differences between the results obtained by measuring

Table 1. The measured maximal values of torque and effective power

Measured values according to [DIN70200-5, 1987]		Catalogue values [http://carfolio.com, 2012]	
Maximal power	Maximal torque	Maximal power	Maximal torque
56.7±1.47(kW) 56.7(kW)± 2.59%	107.1±4.57(Nm) 107.1(Nm)± 4.26%	55.9	110
Difference in relation to catalogue data		1.4%	2.6%

the instantaneous fuel consumption using PLU 116H flow meter. The correlation factor B has been introduced. The factor takes into account both the fact that the injection occurs into the intake manifold, in which the pressure is different than the ambient pressure (the recorded value is marked as p_2 in fig. 1), and the recorded fuel pressure in the fuel rail. The correlation factor was prepared in the form of spatial map $B=f(WT, n)$ – WT – injection time, n – engine rotational speed. The approximating function was the smoothing of least squares weight by distance [21]. The correlation factor was set by equation 5 as relative error of injector outflow in relation to injection to the intake manifold of pressure p_2 assuming the constant product (μF) and fuel density reduced to normal conditions:

$$B\,[\%] = \left[\frac{\sqrt{p_1} - \sqrt{(p_1 - p_2)}}{\sqrt{(p_1 - p_2)}}\right] \cdot 100, \qquad (5)$$

where:
p_1 - absolute pressure of fuel in the fuel rail,
p_2 - absolute pressure in the intake manifold.

The exemplary spatial map of error of estimating the amount of injected fuel in relation to injector opening time and rotational speed taking into consideration the pressure difference $\Delta p=p_1-p_2$ for injector no. 1 is depicted in fig. 4. The range of injector opening times during the vehicle acceleration on a selected gear at the throttle fully opened is marked in fig. 4. The values of correlation factors for each injector were calculated taking into account the phase shift resulting from the four stroke engine cycle.

The maximal relative error of measurement using the selected method was set assuming the normal distribution of instantaneous fuel consumption results for 16 measuring series based on the PLU 116H flow meter results as well as based on the injector opening time

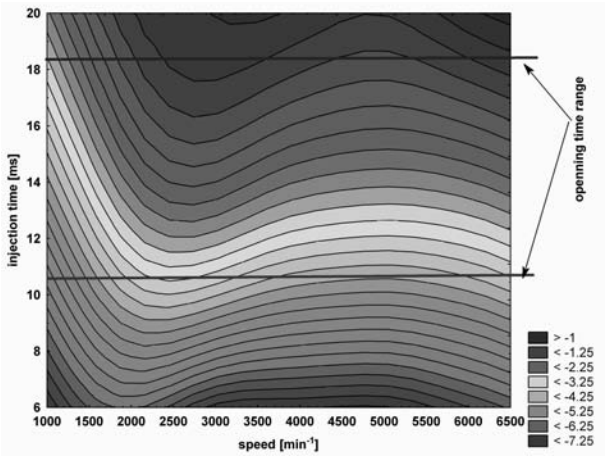

Fig. 4. Percentage relative error of injector 1 outflow in relation with the opening time (WT1) and the engine rotational speed taking into account the inlet manifold pressure and fuel pressure before the injector

(taking into account pressure before and after the injector and fuel temperature) at the confidence level of 0,95. In case of PLU 116H flow meter the relative error for steady measures was taken into consideration. According to the calibration certificate [17] the above mentioned error does not exceed 1% and the relative error resulting from the measuring device resolution is 6.15ml per pulse [3, 17] which in accordance to the measured values gives the average relative error at the level of approximately 6.04±0.14% and the maximal error of measures using the flow meter is at the level of 7%. The instantaneous and average values (approximately 7.2%) are illustrated in fig. 5. In case of PLU 116H flow meter the relatively high time constant of approximately 500 ms [3] must be taken into consideration. It radically overestimates the results concerning the fuel consumption and makes questionable the applicability of this type of flow meter to

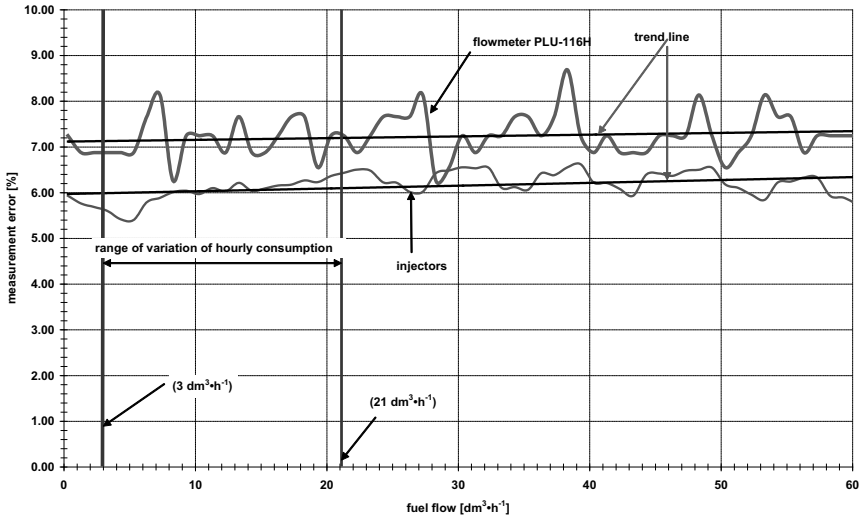

Fig. 5. Maximum errors of fuel consumption measurement using the PLU 116H flow meter and using the injector opening time as a function of fuel flow - the black lines depict the exponential ($y=a\cdot e^{b\cdot x}$) trend line, blue line is the range of changes in hourly fuel consumption during vehicle acceleration

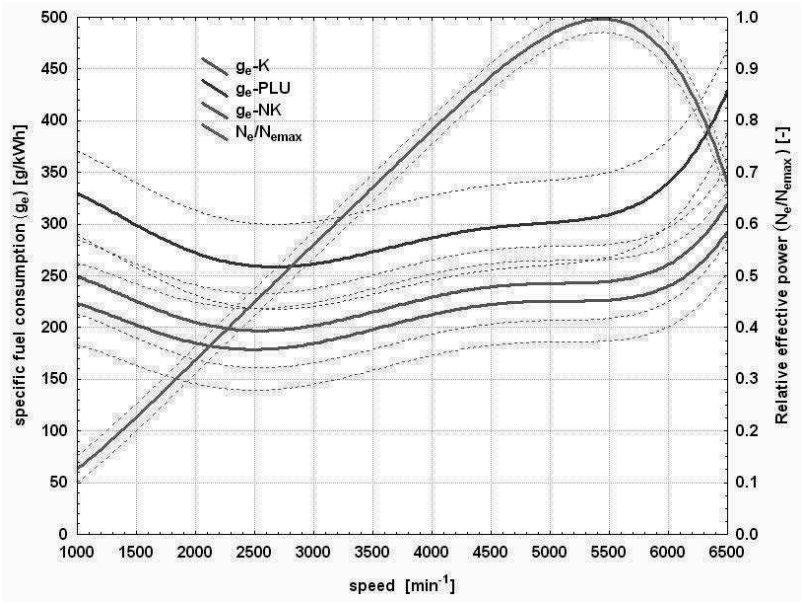

Fig. 6. External characteristic of specific fuel consumption and relative effective power with marked confidence intervals (95%) - (data for 16 measurement series) - the description in the text

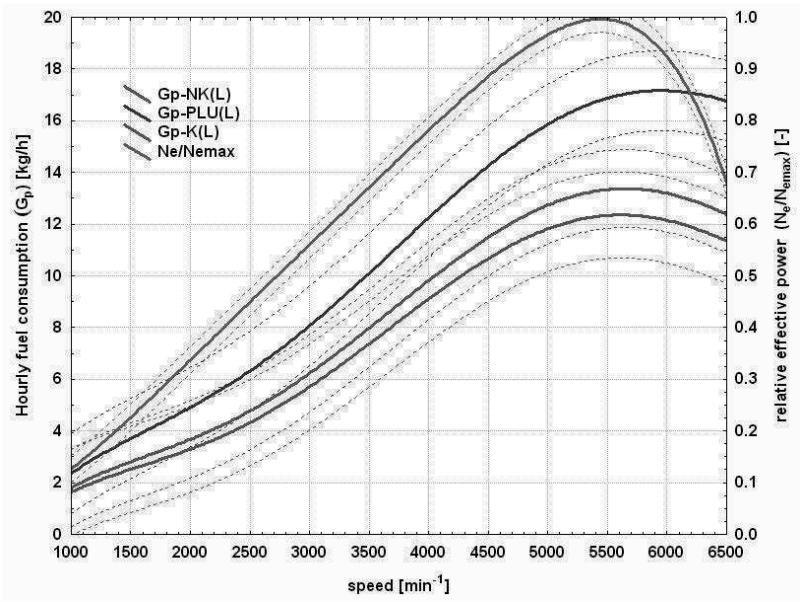

Fig. 7. External characteristics of hourly fuel consumption and relative effective power with marked confidence intervals (95%) - (data for 16 measurement series) - description in text

measurements concerning fuel consumption of combustion engine operating under fast changing unsteady states.

Setting the maximal relative error of instantaneous fuel consumption measurement based on injector opening time generates the relative error of instantaneous liquid fuel consumption (mm^3) equal 5.75±0.3%. The injector's average calibration error is at the level of 4.56% (in relation to fuel dose corresponding with single injector opening window in milliseconds). The instantaneous and mean values taking into account the above mentioned normal distribution give the method relative error (approximately 6.0%), which has been illustrated in fig. 5. Fig 6 and 7 depict the measurement results taking into consideration the above mentioned calculus of errors and after correcting the obtained results to normal conditions according to DIN70020-5 standard [2]. The results are shown in the form of external characteristics, specific fuel consumption and hourly fuel consumption (g_e*-K,* G_p*-K(L))* taking into consideration the pressure before and after the injector and fuel temperature, (g_e*-NK,* G_p*-NK(L)* without fuel pressure after the injector, (g_e*-PLU,* G_p*-PLU*) – measurement using the PLU 116H flow meter) and course of relative effective power (N_e/N_{emax}) determined using the satellite navigation system.

CONCLUSIONS

The application of the described method to traction research of car vehicles using the telecommunication

techniques requires knowledge concerning the characteristics of injector in which the vehicle's engine is equipped as well as the correlation between the injector opening times recording units and the software recording the basic physical quantities of vehicle movement in transient conditions obtained with the use of satellite navigation (UTC time, dislocation components P-X, P-Y, P-Z and velocity components V-X, V-Y i V-Z in WGS-84 system) or other recorders of fast changing parameters of vehicle movement. The errors of estimating the instantaneous fuel consumption during the car vehicle unsteady movement based on measurement of injector opening times with simultaneous measurement of pressure before and after the injector are connected with error resulting mainly from nonlinearity of injector characteristic. The above mentioned errors do not exceed 6%. Using the flow meter of too high time constant (500ms) is not recommended because of the overstating its indications. The voltage decay on the coil at the time of initiating the injectors opening as a result of inertia of its moving elements leads to delay in injector opening. Moreover it is not compensated by delay in the injector closing caused by decreasing force in the needle spring during closing.

REFERENCES

AGREMMENT. CONCERINING THE ADOPTION OF UNIFORM CONDITIONS OF APPROVAL AND RECIPROCAL RECOLGNITION OF APPROVAL FOR MOTORS VEHICLE EQIPMENT AND PARTS. Addendum 67: Regulation No. 68. Rev. 1/Add. 67. Geneva, 1 May 1987

1. **Barth R., 1966:** Luftkräfte Am Kraftfarzeug. DKF, 184
2. DIN 70020-5. Automotive engineering; tyres and wheels; concepts and measuring conditions. Deutsches Institut Fur Normung E.V. (German National Standard) / 01-Dec-1986 /
3. PLU 166H. VL _ PD_ PLU_ 116H_ Flow_ Meter_ENG. doc. AVL List GmbH Hans-List-Platz 1, A-8020 Graz, Austria. Date: 03/04/2009.
4. **Гришкевич А. И., 1986:** Автомобили, Теория, Издательство Вышэищая Школа.
5. **Gruca M., 2010:** Program komputerowy „czas-wtr". Częstochowa.
6. **Grzelka J., Cupiał K., Dużyński A., Grzelka P., 2005:** The traction survey and monitoring of vehicle using a satellite navigation system (in Polish). TEKA Komisji Motoryzacji i Energetyki Rolnictwa. Polska Akademia Nauk Oddział w Lublinie. Volume V. Lublin 2005. ISSN 1641-7739. p. 37…47, rys. 10, lit. 8.
7. **Grzelka J., Cupiał K., Dużyński A., Gruca M., Sosnowski M., 2006:** Satellite navigation in vehicle traction research (in Polish). 10th International Conference „Komputer systems aided science, industry and transport" TRANSCOMP 2006, Zakopane 4…7 December 2006. Vol. 1, p. 173…180, fig 7, tabl. 1, ISSN 1230-7823, ISBN 83-7351-212-8.
8. http://carfolio.com/, 2004-2012.
9. http://commons.wikimedia.org/wiki/File:Wtryskiwacz.gif, I.2011.
10. **Kasedorf J., Woisetschlager E., 2004:** Układy wtryskowe benzyny. WKŁ. Warszawa.
11. **Knebla Zb., Makowski Sł., 2004:** Zasilanie i sterowanie silników. WKŁ. Warszawa.
12. OEM4 Family Manual Vol 2 - Command and Log Reference Rev 12, NovAtel OM-20000047 Rev 12, 2003.
13. **Mitschke M., 1987:** Dynamika samochodu. Napęd i hamowanie. T. I. WKiŁ. Warszawa.
14. PN-87/S-02201: Drogi samochodowe. Nawierzchnie drogowe. Podział, nazwy, określenia. 1987.
15. PN-92/S-77500: Badania samochodów. Pomiar prędkości i intensywności rozpędzania. 1992.
16. **Prochowski L., 2008:** Mechanika ruchu. Pojazdy samochodowe. WKŁ. Warszawa.
17. BD/029/10. Świadectwo wzorcowania. Miernik zużycia paliwa typ: PLU 166H, OBR-SM "BOSMAL", Bielsko Biała, 30.04.2010.
18. **Rintanen K., Mäkelä H., Koskinen K., Puputti J., Sampo M., Ojala M. 1996:** Development of an autonomous navigation system for an outdoor vehicle, Elsevier Science Inc.
19. StatSoft, Inc. (2011). STATISTICA (data analysis software system), version 10. www.statsoft.com.
20. **Wendeker M., 1999:** Sterowanie wtryskiem benzyny w silniku samochodowym. Lubelskie Towarzystwo Naukowe. Politechnika Lubelska. Lublin.
21. **Volk W., 1973:** Statystyka stosowana dla Inżynierów. WNT Warszawa.

WYZNACZANIE JEDNOSTKOWEGO ZUŻYCIA PALIWA SILNIKA SPALINOWEGO W WARUNKACH NIEUSTALONYCH

S t r e s z c z e n i e. W pracy przedstawiono wyniki badań trakcyjnych pojazdu samochodowego uzyskane z wykorzystaniem technik nawigacji satelitarnej, jako alternatywnej metody badawczej, mających na celu wyznaczenie charakterystyki zewnętrznej jego silnika z uwzględnieniem warunków atmosferycznych i profilu pionowego trasy z jednoczesnym wyznaczeniem jednostkowego zużycia paliwa w oparciu o pomiar czasu otwarcia wtryskiwacza paliwa.

S ł o w a k l u c z o w e: silnik spalinowy, jednostkowe zużycie paliwa, warunki nieustalone.

TEKA. COMMISSION OF MOTORIZATION AND ENERGETICS IN AGRICULTURE – 2012, Vol. 12, No. 1, 53–59

Geometric characteristics of triticale grain stored under silo pressure

Tomasz Guz, Zbigniew Kobus, Elżbieta Kusińska, Rafał Nadulski

Department of Food Engineering and Machinery, University of Life Sciences in Lublin
Doświadczalna 44, 20-236 Lublin, Poland, e-mail: tomek.guz@up.lublin.pl

Summary. The aim of this work was to present methodology and results of research on triticale grain (cv Pawo) subjected to storage under silo pressure. The pressure was simulated by the strain of spring-assisted device, which developed 35, 52 and 70 kPa of stress. The aim of this experiment was to detect geometric changes after storing the commodity at heightened moisture (14, 16, 18, 20, 22, 24%) while the temperature of storage was 6 and 20° C. The measurements were taken after stress relaxation by the use of Svistmet computer vision system. The results showed that geometric changes of grain characteristics were detected after storage in high-moisture and high-pressure conditions (20-24% and 52-70 kPa). The most responsible factor of these changes was moisture content of the grain.

Key words: triticale, silo, storage, geometric characteristics, image analysis.

INTRODUCTION

The raise of air flow resistance through the silo is strictly connected with deformations of grain mass and decrease of its porosity [18]. The airflow resistance should be known due to choosing the best solution of air conditioning of the silo [8]. The most important factors that are responsible for airflow resistance are: moisture content, density, porosity, grain shape and friction coefficient [9, 10]. The shape and grain size are dependent on climate conditions, agriculture, variety factors and growth conditions [16]. The volume-to-area ratio is one of the most important factors that influences on airflow resistance of shaken grain layers [11, 12]. Deformations that occurs after silo stress change airflow conditions [3, 8], as well as biological activity and market value of grain [4, 7]. The judgment of external changes in commodity as well as its injuries in an objective way is extremely difficult [13, 14]. The use of up-to-date computer systems is convenient in the judgment of complex processing expressed by colour changes [1, 20]. Sorting of tomatoes [6] or superficial alterations of citrus fruits [2] are an examples of using modern thermo-vision systems. The new measurement systems (computer image analyzers), allows to calculate more complicated biological object parameters such as area, perimeter or colour dispersion [5, 15]. The next example of research with the use of computer vision is assessment of technological value of grain [17], evaluating ingredients quantities [21] or comparison grains of many varieties to specific production applications [19]. The basic application of computer visual systems by means of grain is its morphometric description [22]. This is very important aid to judge of commodity as quality criterion in industrial applications or characterize of various grain varieties [23].

MATERIALS AND METHODS

Triticale grains (cv. Pawo) at initial moisture content of 14% were moistened to 16, 18, 20, 22 and 24% of moisture. The grain then was placed to cylindrical shaped vessels of 2l capacity. Vessels have a specially designed stress-developing mechanism (Fig. 1).

The stress values were 35, 52 and 70 kPa accordingly to the stress simulation in silo conditions. Such a tension is equal to the thrust of over ten meters high bed of grain, which is commonly met in the industry plants. The grain was placed also to non-stressed vessels as reference material. The storage of commodity lased to the stoppage of relaxation in the stressed layer. After storage 3 parts of volume of 30 ml were randomly taken from the vessel and mixed together. Every measurement was taken out with the participation of 100 grains taken from the mixture. Objects of the study were placed on specimen table that was illuminated with backlight to emboss the grain silhouette. Every measurement was taken 10 times with 10 grains which were placed on limited area to improve the measurement precision. Images taken digitally were

stored for further analysis. After storage the images were digitally filtered to dual-color (binary image) (Fig. 2) which was the basis of measurements (SVISTMET).

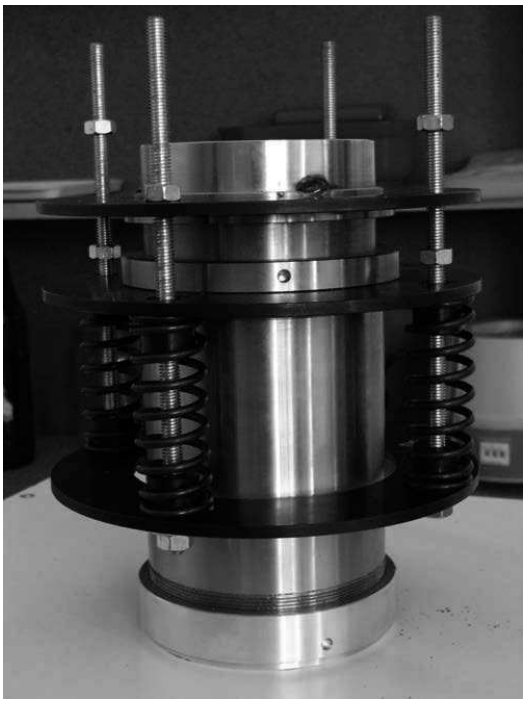

Fig. 1. Specially designed silo-stress simulator vessel

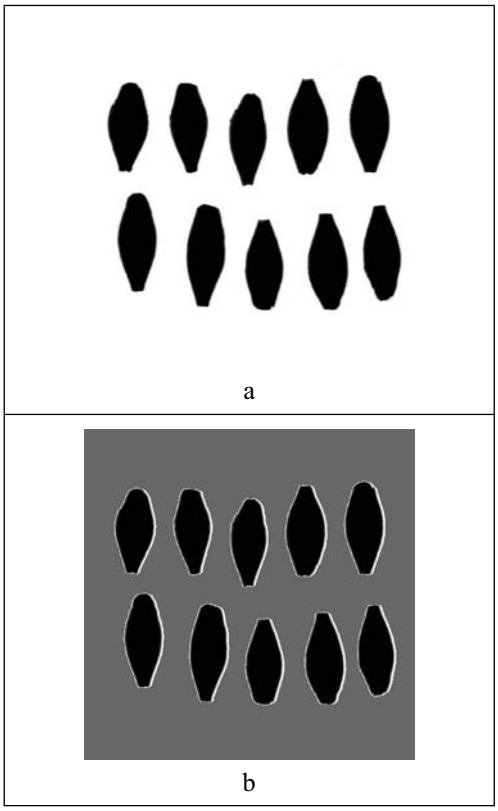

Fig. 2. Triticale grain measurement images: a- digital primary image, b – binary digital image with edge line

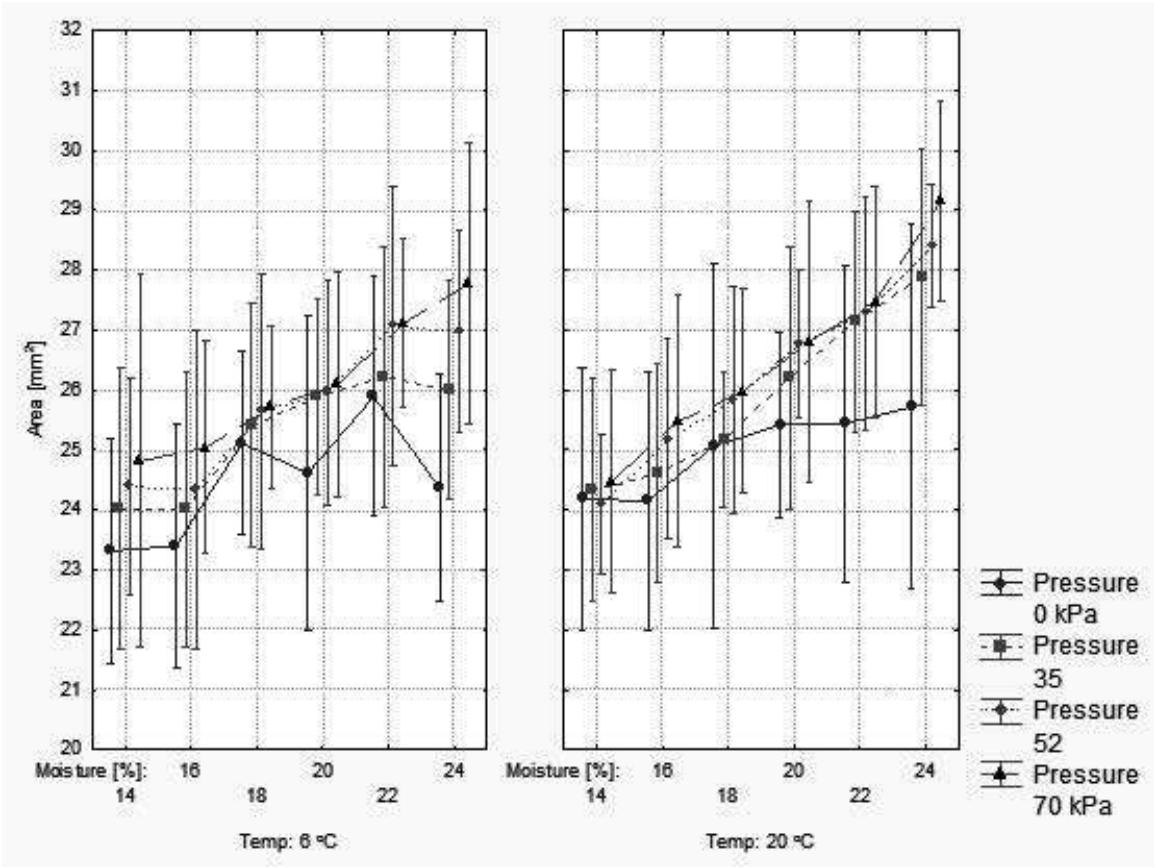

Fig. 3. Area of horizontal projection in dependence of silo pressure

The following were measured: length, width, area of horizontal projection and shape coefficients:

$$K1 = \frac{L}{S}, \quad (1)$$

$$K2 = \frac{4A}{PR}, \quad (2)$$

where:
L – length of grain,
S- width of grain,
A – area of horizontal projection,
P – perimeter of grain,
R – radius of equivalent area.

RESULTS

Triticale grains were analyzed by the detection of its geometric alterations caused by tension formed in the experiment. Moisture content, temperature of storage and stress were taken into account during data analyzing. This procedure is common in this kind of research. The measurements of projected area and accompanying shape coefficients K1 and K2 were taken on 100 grain samples from stress cylinders. Grain extension, expressed by K1 coefficient and K2 coefficient, which defines perimeter to area ratio was presented in Figures 5-8, whereas changes of projected area were explained in Figures 3-4.

The curve shape of projected area changes were similar in accordance to all pressure values applied in cylinders. Slight increase of projected area caused by moisture changes was observed. Neither the value of external load nor temperature of storage influenced significantly the projected area changes (Fig. 3 and 4). Analysis by comparison of the pair of values corresponding to 22% of moisture only 70 kPa of external pressure caused significant extension of grain. This phenomenon was observed for grain stored at 6 °C as well as at 20 °C.

The K1 coefficient for triticale (this is description for grain extension) was stable. Mean values during experiments, taking into account all the experimental factors were at 2,45 to 2, 72 values level, which is standard for non-loaded grain. Temperature and moisture content changes did not influence K1 values for particular value of load (Fig. 5

This is probably associated with strong influence of stress caused by silo as opposed to other factors (i. e. moisture and temperature). The grain subjected to extreme load (70 kPa of stress) keeps constant length-to-width ratio. Slight decrease for higher grain moisture values was observed (Fig. 6).

The values of K2 coefficient stayed resist for non-loaded grain during experiment (Fig. 7). There were no evident changes of this parameter. Higher values of K2 coefficient were obtained at loads over 35 kPa and 20 deg. C storage temperature. This is explained by higher plasticity of grain that occurs in these storage conditions.

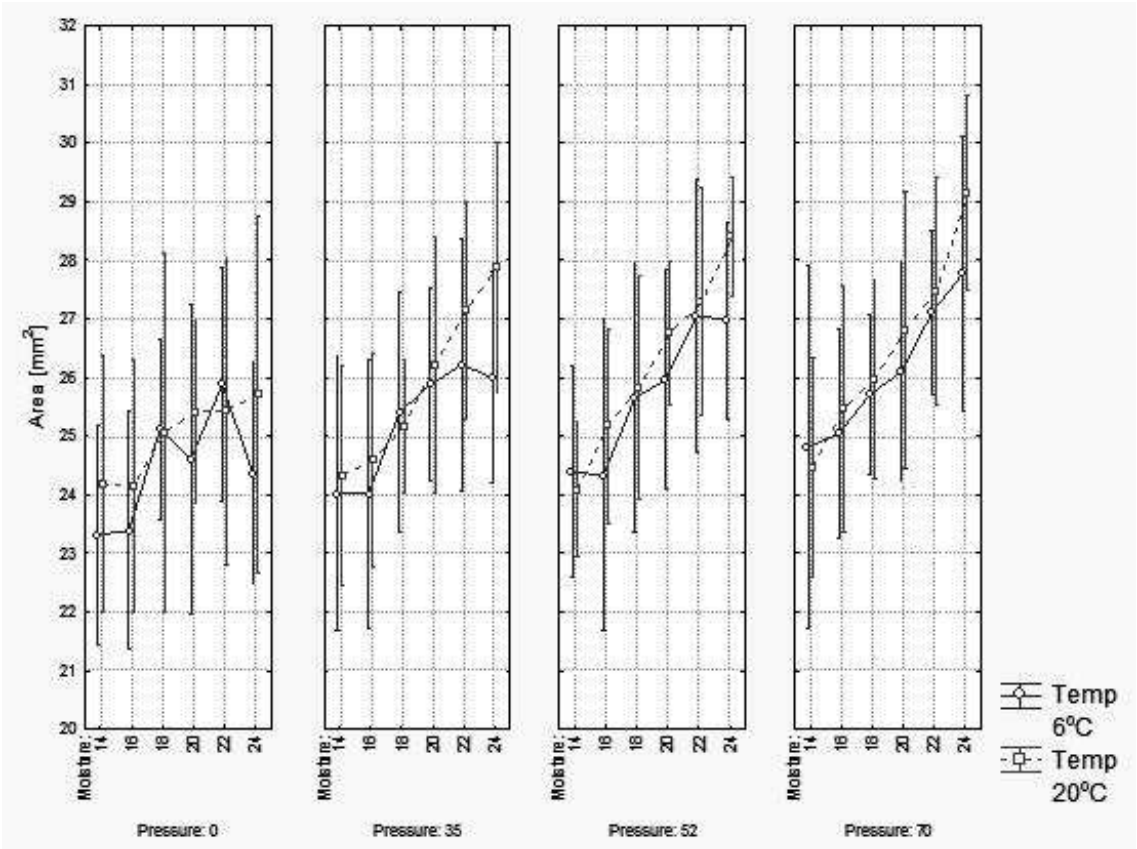

Fig. 4. Area of horizontal projection in dependence of storage temperature

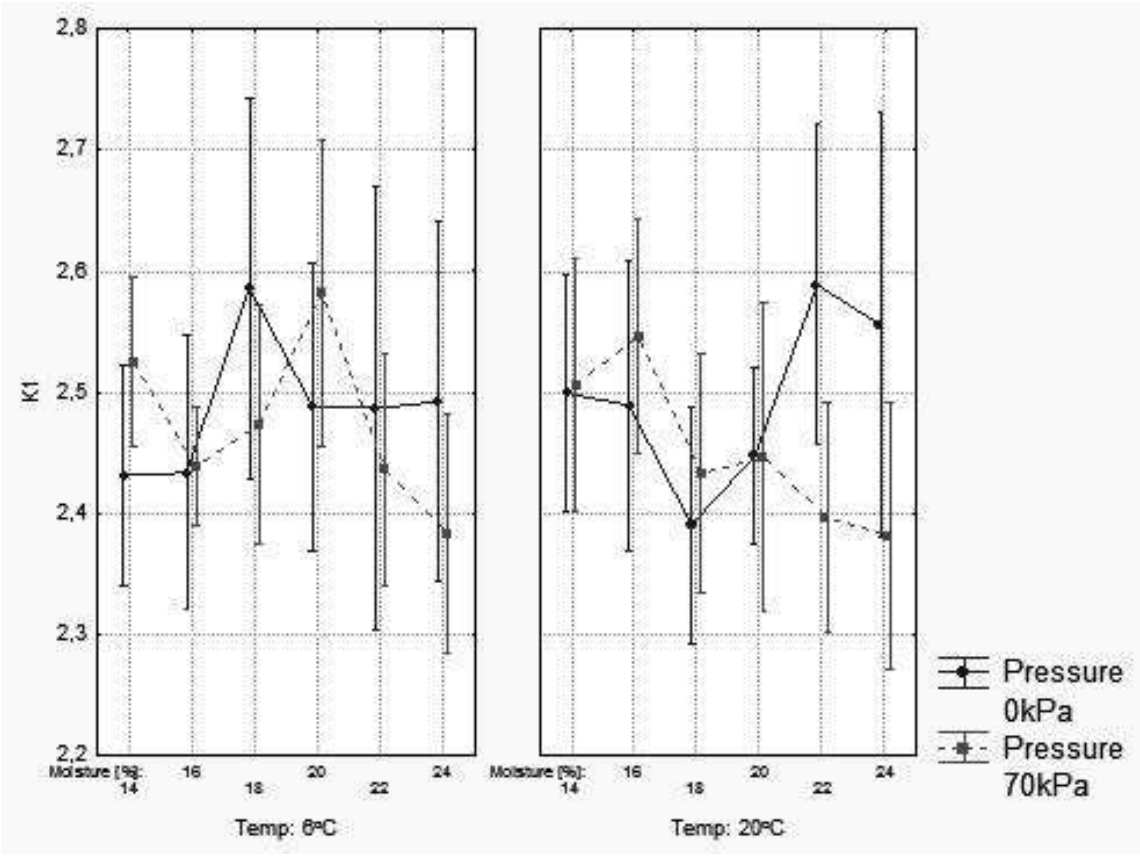

Fig. 5. The comparison of K1 changes caused by storage pressure

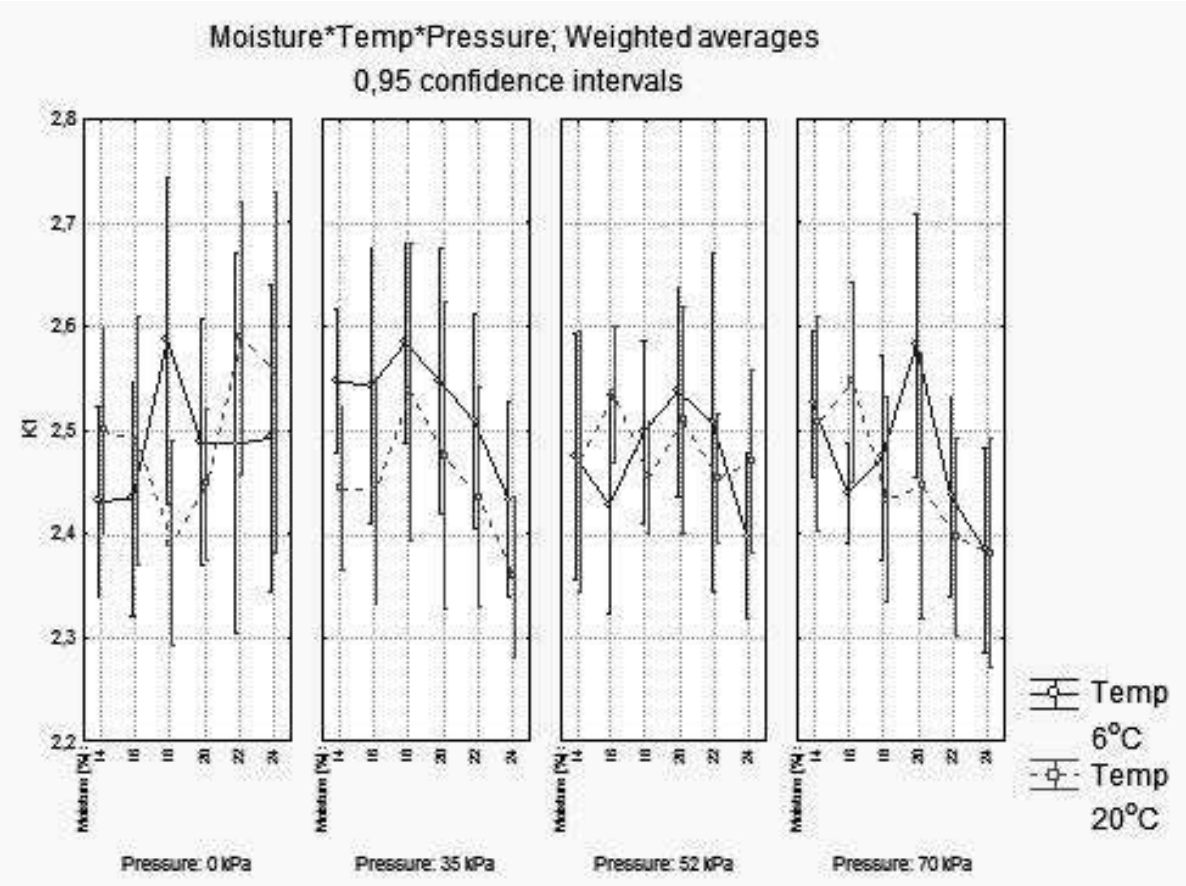

Fig. 6. The temperature course of K1 coefficient

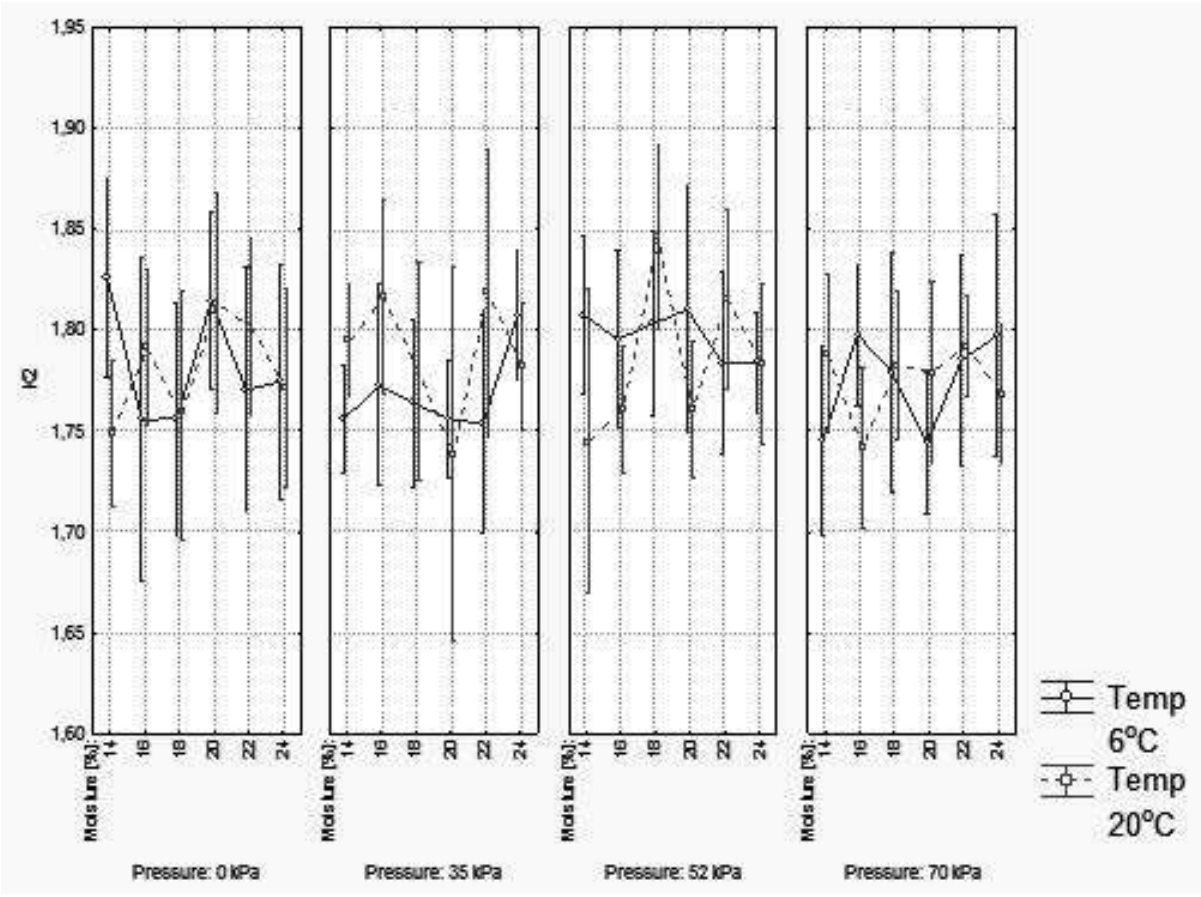

Fig. 7. The temperature course of K2 coefficient

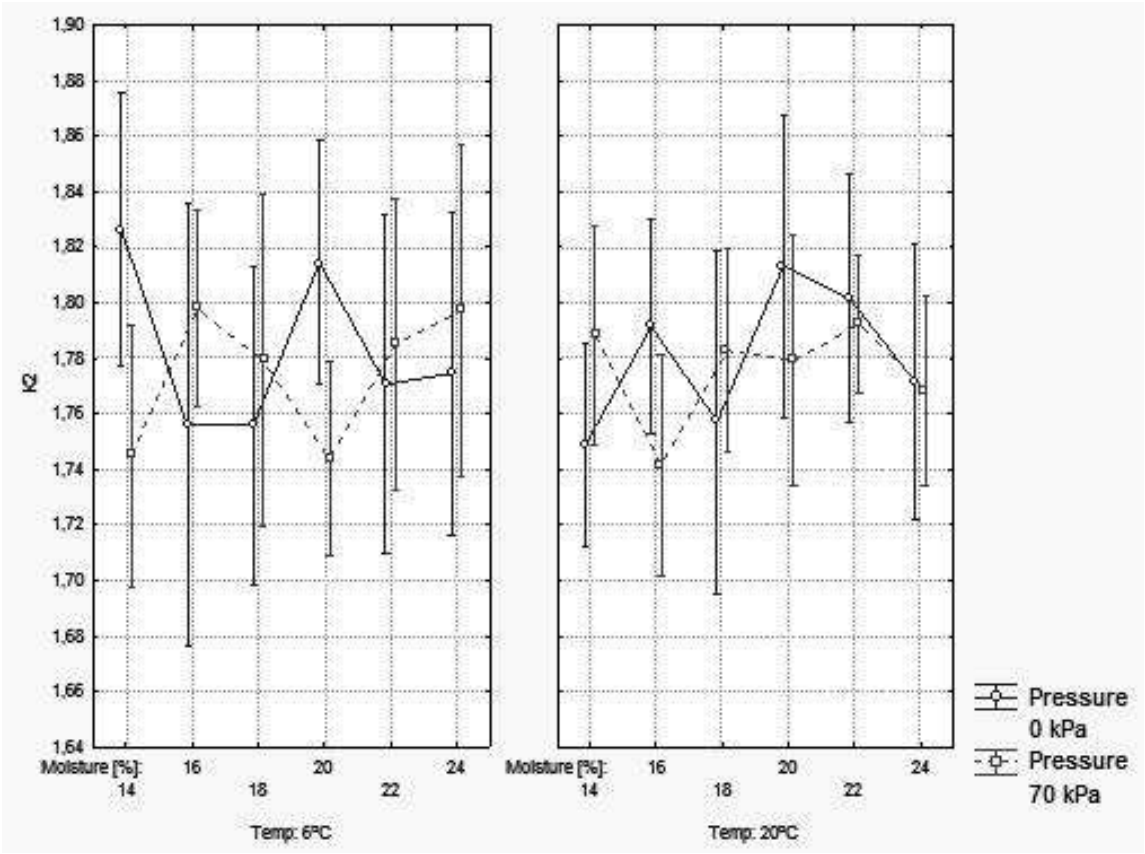

Fig. 8. The pressure course of K2 coefficient

Commodity is less susceptible to damage, which is referred to boundary line changes. Additionally, at higher pressure values the K2 course is disordered doing difficult or impossible to interpret. There was no evidence of pressure control on K2 values curves after storage in the range of 6 to 20 deg. C (Fig. 8).

CONCLUSIONS

1. Temperature of storage had no influence to area changes values during experiment.
2. All shape changes that occurred after storage were constant, being performed without stable damages or breaks, which was proved by K1 and K2 calculations.
3. Slight K2 changes were observed only after high-pressure and high-moisture storage of grain at 20 deg. C.
4. The results of the experiment proved that all grain geometric changes may occur at extreme storage conditions (20 deg. C, 52, and 70 kPa) for grain being moistened at least to 20%. Higher moisture values were the main factor responsible for these variations.

ACKNOWLEDGEMENTS

This research was funded by the State Committee for Scientific Research (KBN) of Poland and is part of the project N° N N313 013336.

REFERENCES

1. **Fernandez L., Castillero C., AguileraJ.M. 2005:** An application of image analysis to dehydration of apple discs. Journal of Food Engineering 67, p. 185-193.
2. **Fito P.J., Ortol, M.D, De los Reyes R., Fito P., De los Reyes E. 2004:** Control of citrus surface drying by image analysis of infrared thermography. Journal of Food Engineering 61, p. 287-290.
3. **Grundas S., Szot B., Woźniak W. 1978:** Variability of the porosity of cereal grain layer under the influence of static loading. Zeszyty Problemowe Postępów Nauk Rolniczych, z. 203, p. 33-39.
4. **Grzesiuk S., Kulka K. 1988:** Biologia ziarniaków zbóż. PWN Warszawa, ISBN 83-01068647.
5. **Guz T. 2009:** The use of image analysis to estimate harvest ripeness of apples. TEKA Kom. Mot. i Energ. Roln. 9, p. 61-68.
6. **Jahns G., Møller Nielsen H., Paul W. 2001:** Measuring image analysis attributes and modelling fuzzy consumer aspects for tomato quality grading. Computers and Electronics in Agriculture 31, p. 17-29.
7. **Kostecki Z. 2003:** Zapewnianie jakości ziarna w okresie jego przechowywania. Przegląd Zbożowo-Młynarski 7, p. 28-29.
8. **Kusińska E. 2006:** Horizontal pressure on the wall of a model silo in relation to the moisture content of oats. TEKA Kom. Mot. i Energ. Roln. 6A, p. 115-122.
9. **Kusińska E. 2008:** Hydraulic resistance of air flow through wheat grain in bulk. *TEKA Kom. Mot. i Energ. Roln. 8*, p. 121-127.
10. **Laskowski J., Skonecki S. 2001:** Pomiar współczynnika tarcia wewnętrznego pszenicy o różnej wilgotności i stopniu rozdrobnienia. Acta Agrophysica 46, p. 95-104.
11. **Łukaszuk J., Stasiak M., Rusinek R., Horabik J. 2001:** Wpływ wilgotności na kąt tarcia wewnętrznego ziarna zbóż. Acta Agrophysica 46, p. 105-113.
12. **Molenda M., Łukaszuk J., Horabik J. 2005:** Airflow resistance of wheat as affected by grain density and moisture content. Electronic Journal of Polish Agricultural Universities, Vol 8, Issue 4, p. 67-77.
13. **Paulus I., De Busscher R.,Schrevens E. 1997:** Use of image analysis to investigate human quality classification of apples. Journal of Agricultural Engineering Research 68, p. 341-353.
14. **Paulus I., Schrevens E. 1999:** Evaluating and modelling the size classification of apples. Journal of Agricultural Engineering Research 74, p. 411-419.
15. **Puchalski C., Gorzelany J.*, Zaguła G., Brusewitz G. 2008:** Image analysis for apple defect detection. TEKA Kom. Mot. i Energ. Roln. 8, p. 197-205.
16. **Szot B. 1983:** Czynniki kształtujące odporność ziarna pszenicy na obciążenia. Zeszyty problemowe Postępów Nauk Rolniczych 258, p. 437-447.
17. **Szulc M., Kahl J., Busscher N., Mergardt G., Doesburg P., Ploeger A. 2010:** Discrimination between organically and conventionally grown winter wheat farm pair samples using the copper chloride crystallisation method in combination with computerised image analysis. Computers and Electronics in Agriculture 74, p. 218-222.
18. **Szwed G., Łukaszuk J. 2003:** Ocena oporu przepływu powietrza przez warstwę nasion rzepaku. Acta Agrophysica 2, p. 645-650.
19. **Venora G., Grillo O., Saccone R. 2009:** Quality assessment of durum wheat storage centres in Sicily: Evaluation of vitreous, starchy and shrunken kernels using an image analysis system Journal of Cereal Science 49, p. 429-440.
20. **Zaguła G., Gorzelany J., Sosnowski S., Puchalski C., Brusewitz G. 2010:** Colour inspection of apple with machine vision. TEKA Kom. Mot. i Energ. Roln. 10, p. 527-537.
21. **Zaguła G., Gorzelany J., Sosnowski S., Puchalski C., Brusewitz G. 2010:** Sugar content determination using computer vision system. TEKA Kom. Mot. i Energ. Roln. 10, p. 538-547.
22. **Zapotoczny P., Zielinska M., Nita Z. 2008:** Application of image analysis for the varietal classification of barley: Morphological features. Journal of Cereal Science 48, p. 104-110.
23. **Zapotoczny P. 2011:** Discrimination of wheat grain varieties using image analysis and neural networks. Part I. Single kernel texture. Journal of Cereal Science 54, p. 60-68.

WPŁYW NACISKÓW W SILOSIE NA ZMIANY CECH GEOMETRYCZNYCH PSZENŻYTA

S t r e s z c z e n i e. Praca przedstawia metodykę i wyniki oceny zmian cech geometrycznych ziarna pszenżyta odmiany Pawo po przechowywaniu w warunkach symulowanego laboratoryjnie obciążenia. Naprężenia o wartościach 35, 52 oraz 70 kPa były wywoływane w specjalnych cylindrach symulujących warunki przechowywania w silosie. Celem pracy było ustale-

nie przebiegu zmian cech geometrycznych nasion w zmiennych (wilg. 14, 16, 18 20, 22 i 24%; temp. 6°C oraz 20°C) warunkach ich przechowywania. Pomiary cech geometrycznych przeprowadzono z użyciem systemu SVISTMET. Wyniki badań wskazują, że zmiany cech geometrycznych ziaren (statystycznie nieistotne) występują tylko w skrajnych warunkach przechowywania (20°C, 52 i 70 kPa) w warunkach wysokiej wilgotności, która była głównym czynnikiem tych zmian.

S ł o w a k l u c z o w e: pszenżyto, silos, przechowywanie, cechy geometryczne, analiza obrazu.

TEKA. COMMISSION OF MOTORIZATION AND ENERGETICS IN AGRICULTURE – 2012, Vol. 12, No. 1, 61–67

Energy efficient control of lighting in an intelligent building

Marek Horyński

Lublin University of Technology, 38 D Nadbystrzycka Str., 20-618 Lublin, Poland

Summary. The present paper refers to the issues associated with energy efficient management in the scope of electric energy. The analysis of the energy balance indicates that the energy consumption for lighting purposes plays an important part in this balance. The introduction of the new energy efficient elements into the lighting control solutions refers not only to fully automatic so called intelligent buildings but is extremely important for the users of the systems based on conventional electrical installations.

Key words: lighting, control, energy efficient, designing, installation.

INTRODUCTION

The amendments in Energy *Performance* Buildings Directive (EPBD) have been adopted by the European Parliament on 18th May 2010. In accordance with these amendments, new buildings since the year 2021 in the territory of European Union will be erected exclusively as the objects with ultra low energy demand and with power supply, at least partially, from renewable energy sources. Thanks to new regulations, it will be easier to overcome the economic, energy and climatic crisis as well as to improve energy safety and security in Europe.

In accordance with adopted amendments, all new buildings built from 2021 onwards in the territory of European Union there will have to be nearly zero-energy buildings. This requirement must be met from 2019 onwards in case of new public buildings. The scope of amendments in Energy *Performance* Buildings Directive (EPBD) encompasses also the old, poorly insulated buildings causing the highest energy losses. The Community decided that, in case of modernization of such objects, each element to be overhauled shall meet the requirements in the scope of energy efficiency at least at minimum level.

It has been observed that electricity consumption by households increased by about 40% over the last decade as a result of growing affluence of the society. Therefore it is possible to use the household appliances which were at first considered luxuries or their potential users became aware of such possibility. The introduction of energy saving procedures into building systems is also imposed by EU and Polish legislation. Due to the fact that 14% of electric energy consumption in European Union and about 19% of electric energy consumption worldwide is used for lighting, the introduction of energy efficient solutions in this area is particularly important. As much as 75% technical solutions in the scope of systems in Europe is obsolete and non – energy – efficient. The bulbs commonly used in Poland as the light sources are characterized by the lowest efficiency and convert less than 5% of the electric energy into light and the rest into heat.

Apart from HVAC system in the building, the lighting system is an area which may be really and appreciably affected by the user via advanced control systems. [1, 4, 7, 9, 14]

The lighting control is needed owing to necessity to save electric energy and owing to the fact that high energy consumption is generated by lighting. The creation of comfortable work and rest environment is also important.

The use of high class lighting fittings (effective reflector, energy efficient light source, electronic stabilizer etc.) is the step required to reduce the energy consumption by the system.

The next decision should concern the application of lighting control systems. It is possible to use KNX or DALI based systems offering, except of remote turn ON and OFF functionality, the comfort improved through integrated control for lighting scenes with blinds or screens in conference rooms or office rooms [1].

Today a modern building is mainly an energy – efficient building i.e. an object with energy consumption

lower than in the buildings erected in conventional technologies, environment friendly and built using state – of – the - art technologies.

Accordingly, the steps should be taken in order to optimize the energy performance in the buildings.

The design of the objects should be the first step in the descriptions of the solutions increasing the energy effectiveness in the buildings. A correctly designed object, selection of proper materials, thermal insulation or selection of windows with satisfactory thermal characteristics and method of their assembling are the basic steps to be completed in order to build an object classified in energy – efficient buildings category.

Another important aspect represents the selection of technological solutions i.e. heat and cool sources or power supply and lighting method. Furthermore the analysis should be carried out in order to check if it is possible to use state – of – the – art solutions i.e. heat pumps or wind or solar energy sources. The importance attached to the use of highly efficient equipment in the scope of refrigeration and heating engineering, ventilation, lighting or electric system is essential.

The essence of changes in an electric system consists in the energy consumption in justified cases only, in adaptation of energy amounts to factual requirements and in use of the equipment in highest possible energy efficiency class.

THE REQUIREMENTS FOR ELECTRICAL INSTALLATIONS.

The electrical installations shall meet three basic requirements:
- To ensure continuous supply of electric energy with the parameters corresponding to user's needs
- To protect the users and the system against electric shock, explosion, fire, switching overvoltages and lightning surges;
- To protect the environment and humans against the emission of magnetic field, noise, vibration with parameters exceeding permissible levels and against contamination [5].

In order to meet these requirements, the installations shall be designed and completed in a manner using determined technical solutions, among others the following:
- Neutral N conductors and protective PE conductors shall be applied as separate conductors,
- Copper wires shall contain the conductors with cross – section up to10 mm^2,
- Receiving circuits shall be protected by means of circuit – breakers and differential current switches;
- Equipotential bondings shall be completed;
- Conductors shall be laid along straight lines parallel to edges of the walls and ceilings [5, 6, 8].

Separate circuits shall be applied in the apartments for:
- Ceiling (main) lighting,
- General purpose plug – in sockets,
- Permanently installed appliances plug – in sockets (washing machine, dish washer etc.) [6].

INTERIOR LIGHTING DESIGN

In order to select the lighting in a correct manner, the choice shall correspond to individual needs. The lighting design is an important element of the building systems because it is crucial for future installation and operation costs.

INTERIOR LIGHTING PRINCIPLES

The designer of interior lighting shall consider several aspects in order to meet the complex human needs associated with lighting. The task to be performed by correctly designed and completed lighting is to meet the following human needs:
- Visual performance,
- Visual comfort,
- Safety [14].

It is necessary to meet the basic lighting requirements included in the lighting standards in order to satisfy these needs. Therefore the work performed by the occupants in a room will be carried out in an accurate manner in comfort conditions in proper time and without excessive tiredness with maintained safety. The essential requirement is to create a correct lighting environment consisting of the following components:
- Illumination
- Glare,
- Luminance distribution,
- Colour rendering,
- Colour temperature,
- Light ripple (pulsation),
- Directionality of light,
- Day light.

The illumination and its distribution in the work field and in its direct vicinity are the principal factors decisive for the execution of visual work and affecting the general evaluation of an interior. Glare occurs when there are excessively glaring objects occurring in the field of view of an occupant and may lead to the feeling of discomfort and may deteriorate the visual comfort. The luminance distribution i.e. the impression received by human eye from a luminous surface is also important. The luminance distribution affects the retinal adaptation status and is crucial for efficient performance of visual work and its impact on human behaviour and perceptions. In order to create a correct lighting environment, it is necessary to ensure a proper colour temperature and light direction. The parameters specified herein will be referred to the rooms in the office and presented below in a detailed manner [14].

In order to ensure the correct choice of lighting, a methodology should be followed. This methodology recommends to firstly determine the role of lighting i.e. if it will perform the role of general or local lighting. After the lighting role is determined precisely, it will be possible

to obtain the information about required illumination and the number of lighting fittings resulting therefrom.

The following parameters shall be also determined:
- Anticipated annual operation time of the lighting.
- Required height of lighting fittings suspension (not always the lighting fittings shall be installed on significant height; the height of lighting fittings suspension can be reduced in the shop floors without travelling cranes. Therefore reduced number of lamps will be sufficient to achieve required illumination level).
- Work areas – this solution makes it possible to turn off unnecessary part of lighting.
- The areas with sufficient lighting by means of day light.

ENERGY-EFFICIENT LIGHTING IN THE BUILDING

The replacement of conventional bulbs by integrated compact fluorescent lamps, halogen lamps or LEDs is the basic and most simple method to achieve an energy-efficient lighting.

The integrated compact fluorescent lamps ("energy-efficient bulbs") introduced more than ten years ago generate much more light from lower power in relation to conventional bulbs. 20% up to 25% of electric energy supplied to the compact fluorescent lamp is converted into the light. Approximated power values for the equivalents of conventional bulbs to energy-efficient bulbs are presented in the table below.

Table 1. Approximated power values for the equivalents of conventional bulbs to energy-efficient bulbs

Power of a conventional bulb; [W]	Approximated power of an equivalent in the form of a compact fluorescent lamp [W]
100	20-23
75	15-16
60	11-12
40	8-9
25	5-6

The replacement of a conventional bulb by an integrated compact fluorescent lamp makes it possible to achieve the electric energy savings of 80%. This saving is very high. However, the use of these light sources is not possible everywhere. Owing to their design solution, the fluorescent lamps are characterized by large luminous surface. Their use is not recommended in the crystal chandeliers with bulbs generating „sparkling" light and various light reflections, because this effect would be eliminated in case of fluorescent lamps. The halogen bulbs can be applied in such situation. They make it possible to achieve the electric energy savings of 50%. This value is lower than in case of fluorescent lamps but an attractive lighting is ensured. The halogen bulbs can be used in the circuits with dimmers or motion sensors.

The significant electric energy savings are possible thanks to the application of LED technology. LED sources can be used to replace E27, E14 conventional lower power bulbs and 12 and 230 V halogen bulbs. The scope of their applications will be and already is significantly wider that in case of the compact fluorescent lamps, because the energy saving of several dozen percent is possible in this case. However further development of this technology is continued and better results may be expected in the years to come. In case of LED sources, particular attention should be paid to their parameters, for instance the colour temperature of generated light and *Colour* Rendering Index. They may significantly differ from each other, depending on the type of applied diodes and their manufacturer.

In case of the description of energy – efficient lighting in the building, mainly the replacement of conventional bulbs by more efficient equivalents is discussed. It should be emphasized that the whole scope of actions intended to achieve the energy – efficient lighting is not limited to the replacement of bulbs.

ENERGY-EFFICIENT LIGHTING CONTROL

The lighting control is performed:
- In manual mode, directly by the users by means of devices constituting the components of an electric installation, pushbuttons, dimmers or IR pilots.

Table 2. Parameters of the light sources which are most popular actually

Parameter	Conventional bulb	Halogen bulb	Integrated compact fluorescent lamp	LED
Durability	1000 h	2000-5000 h	6000-15000 h	30000-50000 h
Colour temperature	2856 K	3000-4000 K	2800-4000 K	Various temperatures and colours of light
Colour Rendering Index	100	100	>80	Various values, even more than 80
Available Power values	From less than ten up to several hundred W	From less than ten up to several hundred W	From less than ten up to several dozen W	
Savings in comparison with conventional bulb	-	For most modern solutions up to 50 %	About 80 %	About 80 %

– In automatic mode, via the system of sensors changing the lighting functions depending on changes of parameters settings.
– In semi-automatic mode, constituting a combination of manual and automatic mode.
– By means of clocks used for the setting of lighting installation operation schedules.

Energy-efficient lighting control in the building is based on the parameters of the applied lighting management system.

The purpose of another important functionality, except of turning ON/ OFF, is to make it possible to change the lighting level by the users for various light sources, from the conventional bulbs being slowly phased out, throughout fluorescent lamps, halogen lamps, HIDs or LEDs. More and more important is the setting of so called lighting scenes consisting in the controlling of various types of light sources in order to create the designed lighting system.

Its essential feature is to apply the proper level of day light in an flexible manner in order to ensure the environmental comfort for the inhabitants / users occupying a room e.g. in course of presentation by means of the projector in course of conference or lecture. The occupants should be also protected against negative effects of the impact of day light i.e. glare / dazzling, reflexes.

The lighting management system in the building should be parametrized in order to define the maximum/ minimum lighting levels for specified areas and lighting scenes to ensure the optimum lighting level as well as the use of lighting energy in an effective and productive manner.

Considering the comfort of users, the designer shall make it possible to individualize the lighting level i.e. the adaptation of the lighting levels in each zone or scene to their individual needs. The adjustment shall be possible in the scope of maximum and minimum lighting levels parametrized vs. existing standards for the user, norms and characteristics of the tasks being completed.

The management of lighting scenes and zones shall enable the programming (predefining) of lighting arrangement in individual zones.

The lighting management system should be also provided with lighting management possibility in central and local mode. Thanks to central management, the users are capable to quickly implement and change the lighting policy and its principles in order to ensure the possibility to change the lighting in individual zones in local mode by means of dimmers, wall – mounted switches, IR pilots.

Zone occupancy and presence control is another important element of the lighting management systems. The lighting management in this case is based on the use of motion, heat and IR sensors.

Further important element of the lighting management systems is an intelligent compensation i.e. the possibility to ensure required lighting level using the compensation of artificial light sources and adaptability i.e. quick adaptation of lighting levels to changes in the rooms' reconfiguration.

A correctly designed lighting management system shall also make it possible to forecast the load of lighting installation as well as to plan the actions intended to reduce the system load in peak pricing hours.

The comprehensive metering system is an extremely important aspect of the energy – efficient building. The metering systems shall be provided for all supplied utilities. Therefore it is possible to gain the knowledge on the amount of energy consumption and its type. Without an advanced monitoring system, the users and administrators of the objects are not able to indicate the locations with the highest energy consumption and the purpose of such consumption as well are not able to detect abnormal conditions. The lack of such systems prevents the improvement of energy balance in the building. A positive symptom consists in increasingly often extension of BMS systems functionalities in the form of electric energy monitoring.

ENERGY SAVING ACTIVITIES

Low saturation of intelligent lighting market creates a very high potential in the scope of energy efficiency – comparable to the replacement of magnetic stabilizers by electronic stabilizers. Owing to introduction of EPBD directive the following energy saving activities should be performed:

– To replace the conventional light sources (incandescent bulbs, fluorescent lamps) by energy efficient ones (compact fluorescent lamps, sodium lamps).
– To choose the appropriate light sources to be applied.
– To install the appropriate lighting fittings.
– To maintain the cleanness of lighting fittings.
– To install the illumination adjustment equipment.
– To install the equipment for lighting turn ON/ OFF in automatic mode.
– To replace the general lighting by general localised lighting
– To use day light properly.

DESIGN OF RESEARCH LABORATORY FOR ENERGY EFFICIENT INSTALLATIONS IN THE BUILDING

The adaptation design has been elaborated for the rooms in the Department of Computer and Electrical Engineering in Lublin University of Technology in line with the intelligent building standards in order to enable the testing of energy efficient lighting installations.

A particularly important aspect of this project concerns the fact that these rooms are situated in an object protected by the conservator of historical monuments. The control tasks in the laboratory have been designed in KNX system enabling the integration of building systems and the realization of established assumptions (Fig. 1).

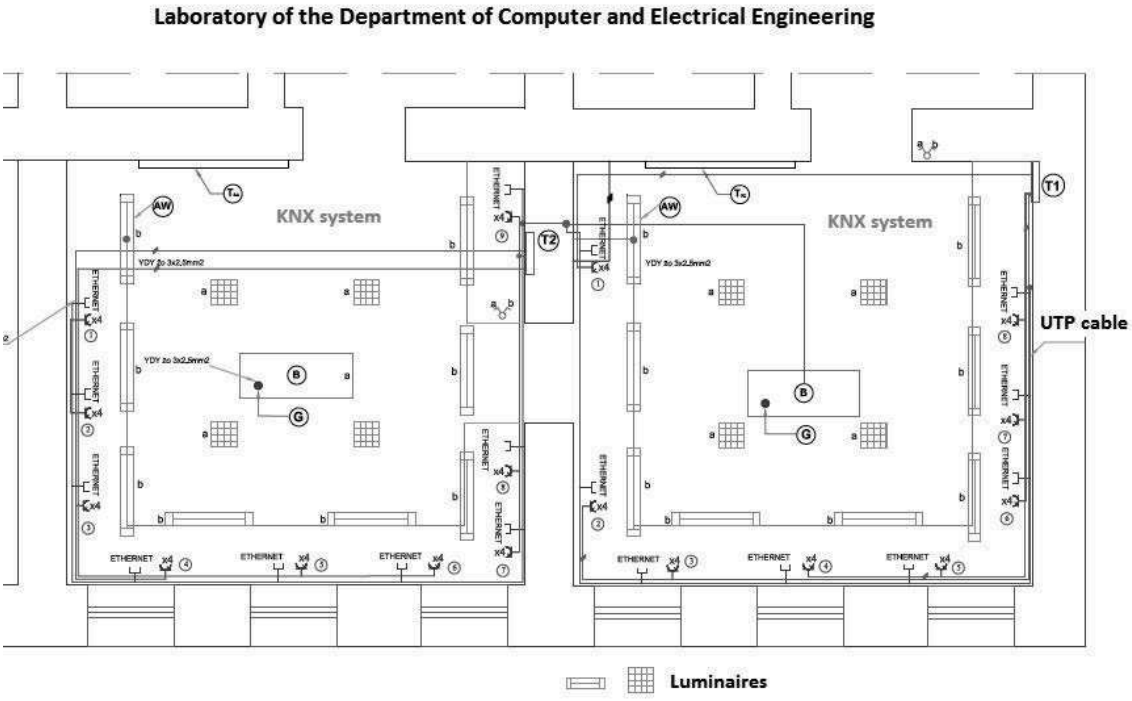

Fig. 1. Electric installations in the research laboratory

In order to achieve the established goal, the following assumptions have been made for KNX installation:
– Lighting control depending on illumination in individual rooms;
– Possibility to turn the lighting ON and OFF.

Fig. 2. Equipment and appearance of a sample room generated in DiaLux program

In order to fulfil the assumptions presented above, KNX devices have been selected and the installation point has been established. The devices will be installed in:
– Switchboard:
  ◦ Power supply unit with coil to provide KNX bus supply,
  ◦ USB communication interface to send created application,
  ◦ Dual channel binary input,
  ◦ Dual channel switching actuator turning ON the lighting in corridor,
  ◦ DALI KNX gate turning ON and controlling the lighting fittings; with DALI interface.
– Assistant Lecturers' room:
  ◦ Single channel switch used to turn ON the lighting via DALI gate,
  ◦ Illumination and motion sensor fastened on the ceiling.
– Laboratory I:
  ◦ Single channel switch used to turn ON the lighting via DALI gate,
  ◦ Illumination and motion sensor fastened on the ceiling.
– Laboratory II:
  ◦ Single channel switch used to turn ON the lighting via DALI gate,
  ◦ Illumination and motion sensor fastened on the ceiling.
– Laboratory III:
  ◦ Single channel switch used to turn ON the lighting via DALI gate,
  ◦ Illumination and motion sensor fastened on the ceiling.
– Corridor:
  ◦ Single channel switch used to turn ON the lighting in corridor.

DALI Light Controller DLR/S 8.16.1M gate is the principal device responsible for the installation control. The gate is able to support up to 64 individually addressed stabilizers operating in 16 independent lighting groups. The stabilizers of the lighting fittings are connected by means of NYM conductor 2x1,5- 2,5 mm^2. Among other things, DALI device makes it possible to determine the rate of illumination change for the sources, to set the values of illumination and to set the emergency lighting turning ON. LF/U 2.1 illumination sensors continuously monitoring the lighting in the rooms, send corresponding signals to DALI gate operating as an actuator control-

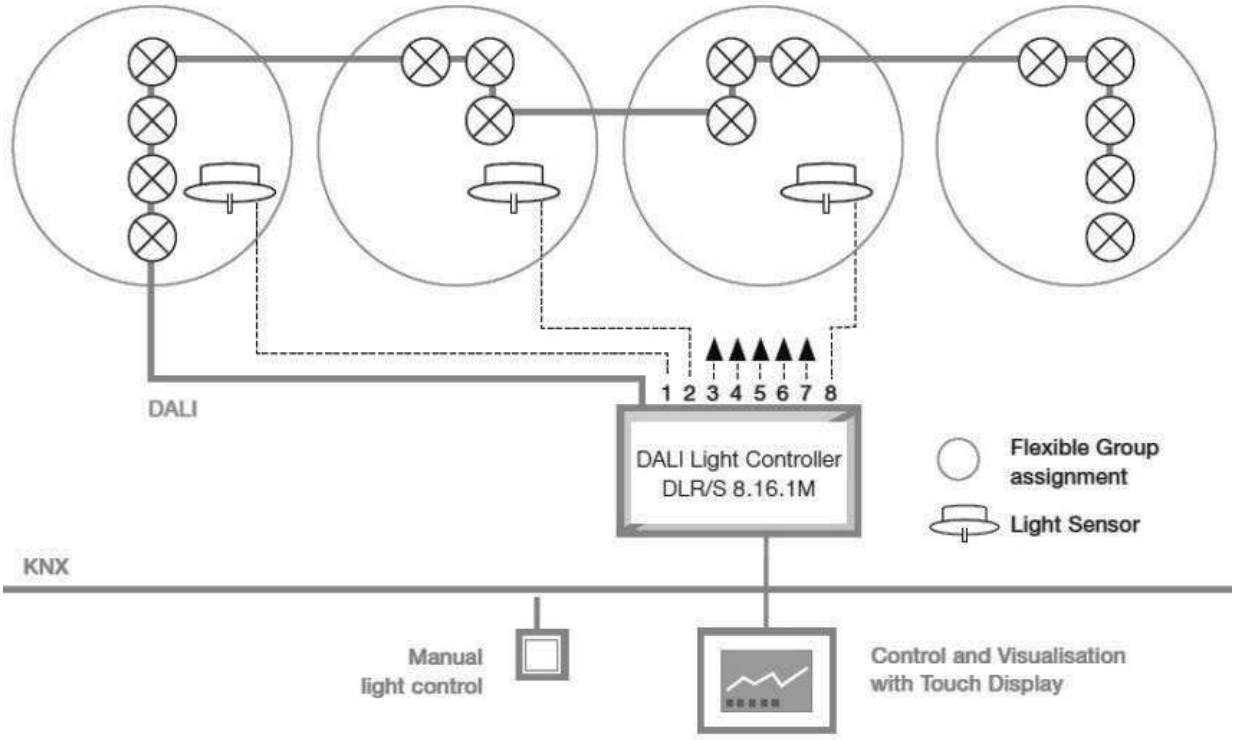

Fig. 3. Pictorial diagram of the connection and operating principles of DALI gate – DALI Light Controller DLR/S 8.16.1M [1,2]

ling the light sources i.e. brightening them or dimming to expected level

CONCLUSIONS

The electric energy consumption for lighting purposes constitutes one of the largest parts of global energy consumption among all types of energy receivers.

There are many technical solutions and types of lighting but still the majority of light sources being installed is characterized by low efficiency level.

The global energy consumption can be significantly reduced as result of the introduction of energy efficient tungsten bulbs, compact fluorescent lamps and LEDs in the market.

The issues associated with electric energy saving by means of energy efficient light sources and their effective use has been the subject of the research for many years. These issues are increasingly wider and often discussed in recent years. The energy saving is facilitated by more and more common control systems: motion detectors (automatically turning OFF the lighting in empty rooms), twilight sensors, turning ON and OFF the lighting and lighting adjustment by means of a pilot. However the effects of saving activities depend on the individuals engaged in the scope of designing, construction and the use of lighting installations. In the near future, we can expect further development of LED lighting technology and facilitated application of control systems. These trends may contribute to further savings in electricity consumption.

REFERENCES

1. ABB Directories: Lighting. Constant lighting control, 2010.
2. **Buczaj M. 2011:** Eliminacja czynnika ludzkiego przez techniczne środki przekazu informacji w systemach nadzoru nad stanem chronionego obiektu. Motrol – Motoryzacja i Energetyka Rolnictwa, tom. 13, p. 34-42.
3. Directive 2002/91/EC issued by European Parliament and European Council on 16th December 2002 concerning the energetic quality of the buildings.
4. Pod redakcją **Piotra Borkowskiego. 2011:** Inteligentne systemy zarządzania budynkiem. Politechnika Łódzka.
5. **Markiewicz H. 2010:** Instalacje elektryczne. Wydanie VIII zmienione. WNT, Warszawa 1996.
6. **Markiewicz H. 1999:** Bezpieczeństwo w elektroenergetyce, WNT, Warszawa.
7. **Mikulik J. 2008:** Europejska Magistrala Instalacyjna EIB: rozproszony system sterowania bezpieczeństwem i komfortem, Stowarzyszenie Elektryków Polskich, Warszawa.
8. **Niestępski S. i inni 2011:** Instalacje elektryczne. Budowa, projektowanie i eksploatacja. Oficyna Wydawnicza Politechniki Warszawskiej.
9. **Petykiewicz P. 2001:** Nowoczesna instalacja elektryczna w inteligentnym budynku: przesłanki, zasady, techniczna realizacja, osprzęt. Centralny Ośrodek Szkolenia i Wydawnictw SEP, Warszawa.
10. **Plaksina O., Rausch Th. 2005:** Fieldbus Systems and their Applications, Vol. 6, Part 1.
11. Pod redakcją **Elżbiety Niezabitowskiej. 2010:** Budynek inteligentny - Tom I Potrzeby użytkownika a standard budynku inteligentnego, Wyd. Politechniki Śląskiej, Gliwice.

12. Pod redakcją **Elżbiety Niezabitowskiej. 2010:** Budynek inteligentny - Tom II Podstawowe systemy bezpieczeństwa w budynkach inteligentnych, Wyd. Politechniki Śląskiej, Gliwice.
13. Pod redakcją **J. Strojnego:** Podręcznik INPE dla elektryków, zeszyt 10: instalacja elektryczna w systemie KNX/EIB.
14. **Pracki P. 2011:** Projektowanie oświetlenia wnętrz, OWPW, Warszawa.
15. **Sumorek A., Buczaj M. 2010:** Przyszłość magistrali Local Interconnect Network. Motrol - Motoryzacja i Energetyka Rolnictwa, tom 12, p. 145-157.

ENERGOOSZCZĘDNE STEROWANIE
OŚWIETLENIEM W INTELIGENTNYM BUDYNKU

S t r e s z c z e n i e. Niniejszy artykuł odnosi się do zagadnień związanych z energią efektywnego zarządzania w zakresie energii elektrycznej. Analiza bilansu energetycznego wskazuje, że zużycie energii do celów oświetlenia odgrywa ważną rolę w tej równowadze.Wprowadzenie nowych energii elementów skutecznych rozwiązań oświetleniowych do kontroli odnosi się nie tylko w pełni automatyczny tzw inteligentnych budynków, ale jest niezwykle ważne dla użytkowników systemów opartych na konwencjonalnych instalacji elektrycznych.

S ł o w a k l u c z o w e: oświetlenie, sterowanie, energooszczędne, projektowanie, instalacja.

TEKA. COMMISSION OF MOTORIZATION AND ENERGETICS IN AGRICULTURE – 2012, Vol. 12, No. 1, 69–72

Assessment of average exhaust emissions from a farm tractor operating in a livestock building

Andrzej Karbowy, Adam Koniuszy, Paweł Sędłak

Department of Agrotechnical Systems Engineering; West Pomeranian University of Technology in Szczecin
Papieża Pawła VI Str. 1, 71 – 459 Szczecin, Poland; e-mail: adam.koniuszy@zut.edu.pl

Summary. The results of investigations of exhaust emissions in a livestock building from a farm tractor coupled with a feed wagon have been presented. The investigations were performed in an open space building divided into boxes with the livestock count of 60 cows.

Key words: microclimate, livestock building, engine load, exhaust emissions.

INTRODUCTION

Maintaining appropriate microclimate in the cow house is an important element of the livestock breeding system that influences its health and efficiency. Maintaining of the optimum conditions depends on many factors such as: breeding technology, feeding methods, design of the building, proper care and hygiene [7, 8].

Animals in the livestock buildings generate heat, carbon dioxide and water vapor to the environment. The level of these emissions depends on: animal weight, animal metabolism and ambient temperature [1]. The reduction of the emission of gases in farm production (flora and fauna) as well as the reduction of the emission from farm machinery have been addressed in the recommendations related to the admissible emissions contained in The UN Convention on Climatic Change [9].

The main parameters determining the microclimate of the livestock buildings are:
– temperature and relative humidity of the air,
– concentration of harmful gases,
– light intensity,
– ventilation and air exchange speed.

Aside from the main parameters determining the microclimate in the building the level of air contamination in the cow house also plays an important role. Admissible concentrations of gases deemed as most harmful in the livestock building are shown in Table 1.

Table 1. Admissible concentrations of air pollutants [Romaniuk, Overby 2004]

Gas	Concentration [mg×m^{-3}]	Amount [ppm]
Ammonia (NH_3)	15,4	20
Carbon dioxide (CO_2)	5930	3000
Hydrogen sulfide (H_2S)	7,5	5
Dust	10,0	¾

One of the sources of pollution in a livestock building is a farm tractor coupled with machinery servicing a group of animals in that building. The machinery operating with the tractor affects its exhaust emissions depending on the engine loads [5]. Aside from the loads that influence the emissions the technical condition of the tractor also plays an important role, particularly the piston-cylinder-ring assembly not to mention the injection system [11,10]. That is why it is important to properly select the feed wagon to the animal count and the tractor that a given farm owns.

RESEARCH METHODS

For the tests a farm tractor MF255 was used fitted with an straight engine AD3.152UR (table 2) combined with a feed wagon JF-STOLL VM 10-IS of the capacity of 10 m^3 and power demand of 45 kW. The measurements were realized in an open space building divided into boxes with the livestock count of 60 cows.

Table 2. Technical specifications of the AD3.152 UR engine

Basic technical specifications of the AD3.152 UR engine		
Parameter	Unit	Value
Number of cylinders, c	-	3
Engine displacement, V_{ss}	dm^3	2,502
Engine rated power, N_e	kW	34,6
Engine speed at rated power, n_N	Rpm	2250
Engine maximum torque, M_o	Nm	165,4
Engine speed at maximum torque, n_M	Rpm	1300,1400
Unit fuel consumption, g_e	$g \times kW^{-1} \times h^{-1}$	234

During the operation of the tractor coupled with the feed wagon load states were recorded through a TRS system *(Tractor Recording System)* [2]. Then, the most frequently occurring engine load ranges were obtained and a substitute simulation research cycle was determined. The measurements of the exhaust emissions were carried out on a chassis dynamometer through a multi-component exhaust gas analyzer CAPELEC CAP 3201IG/GO for each of the characteristic load ranges of the tested tractor. For the determination of the emissions of the individual exhaust gas components a specially developed methodology was applied [3].

RESEARCH RESULTS

Following the data recording the authors obtained 3175 records on the engine loads corresponding to 26,5 hours of work. The most frequently used engine speeds and loads of the tested tractor have been presented in the form of a two-dimensional probability distribution (Fig. 1).

The authors have observed that such auxiliary actions as u-turns, charging, wagon coupling are done outside of the building. For the calculations and analysis only those load states were selected that pertained to the tractor operating inside of the livestock building. In the presented graph it is the speed of n_s 2000 [rpm].

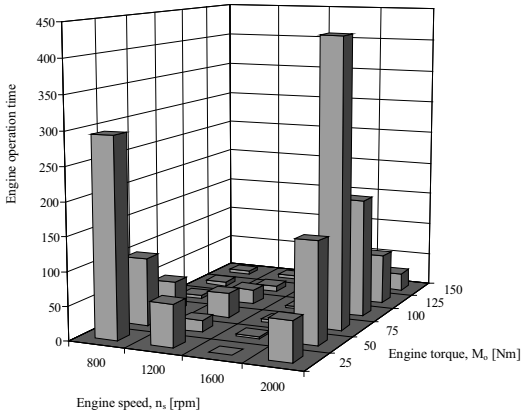

Fig. 1. Two-dimensional distribution of the operating time of the tractor engine (MF255)

Based on the above-presented results it has been ascertained that the substitute, simulating research cycle will have six different phases (sequences of loads) at the same engine speed (Table 3). The individual ranges of loads were assigned weight coefficients that were related to the operating time of the tested engine under the measured load.

Table 3. Substitute, simulation load cycle of the tested tractor

Number of phase		1	2	3	4	5	6
6 phase cycle	n_s [rpm]	2000	2000	2000	2000	2000	2000
	M_o [Nm]	55	60	70	80	90	100
	Weight coefficient	0,05	0,1	0,45	0,15	0,2	0,05

Based on the developed substitute engine cycle tests were performed on a chassis dynamometer where the emissions of the following were determined: CO_2, CO HC, NO_x as well as unit fuel consumption. In Fig. 2 the dependence of the unit fuel consumption on the effective power has been presented.

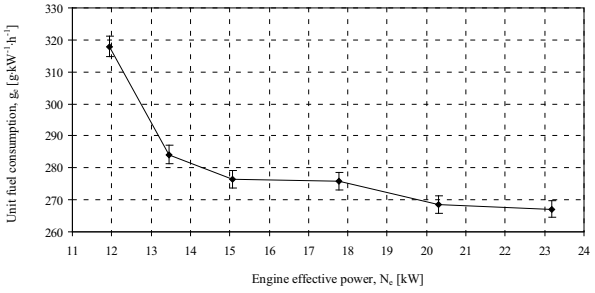

Fig. 2. Dependence of the unit fuel consumption on the tested engine effective power (AD3.152UR)

The authors observed that the lowest unit fuel consumption i.e. 267 $g \times kW^{-1} \times h^{-1}$ the tested engine achieved in the sixth phase of the cycle. The greatest unit fuel consumption was recorded in the first phase of the cycle. Along the subsequent phases the fuel consumption decreased. Also, in the sixth phase of the cycle the greatest emission of CO_2 was recorded - 8,3 $m^3 \times h^{-1}$ (Fig. 3). The smallest emission of the latter - 5,96 $m^3 \times h^{-1}$ was recorded for the first cycle.

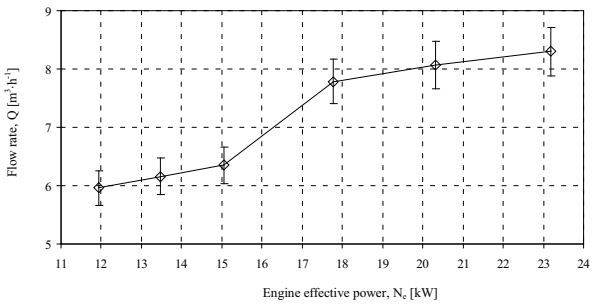

Fig. 3. Dependence of the CO_2 emissions on the tested engine effective power

Te subsequent phases of the research cycle showed an increase in the emission of CO_2 yet, for the first three cycles this increase is miniscule (amounts to approximately 0,35 $m^3 \times h^{-1}$). A significant growth of CO_2 was recorded between cycles three and four (1,45 $m^3 \times h^{-1}$). Then, the growth between cycle four and six amounted to approximately 0,5 $m^3 \times h^{-1}$. The sixth phase of the substitute cycle also showed the greatest emissions of the outstanding exhaust gas components i.e. CO, HC and NO_x (Fig. 4, 5).

An increase in the exhaust emissions was observed as the engine effective power of the tested engine grew, which is confirmed by investigations of other authors e.g. [Wasilewski 2004]. In cycles 1-4 the emission of CO was in the range from 0,02÷0,026 $m^3 \times h^{-1}$. In further cycles the emission of CO grew to reach 0,077 $m^3 \times h^{-1}$ in the sixth cycle, which is almost a double of the fourth cycle.

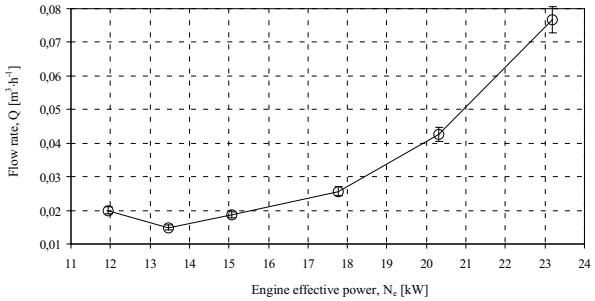

Fig. 4. Dependence of CO emission on the tested engine effective power

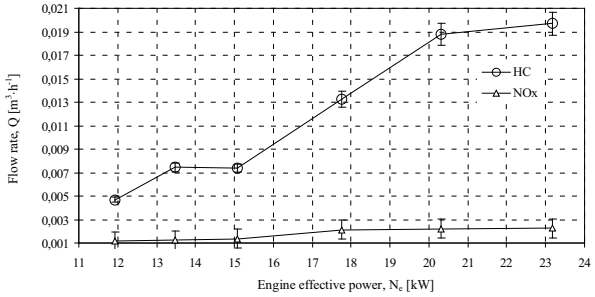

Fig. 5. Dependence of HC and NO_x emissions on the tested engine effective power

Similarly to CO_2, a significant increase in the emissions of HC and NO_x was recorded between cycles three and four. The emission of HC grew almost three times from 0,0074 $m^3 \times h^{-1}$ in cycle three to 0,0197 $m^3 \times h^{-1}$ in cycle six. The emission of NO_x doubled in the ranges analogical to HC.

In Table 4 the weighed averages have been listed of all the exhaust components measured in the test.

The use of a farm tractor coupled with farm machinery used in livestock buildings should be preceded by an analysis of the power demand in order to avoid elevated exhaust emissions including PM (particulate matter) to the ambient air in the building. Farm tractors used for the propulsion of the farm machinery inside livestock buildings should be fitted with modern aftertreatment systems [4]. Going on the assumption that CO_2 is not a toxic gas for living organisms (it only contributes to the greenhouse effect) we can state that all other exhaust gas components are of paramount importance. Based on the measurements of the amount of these gases in the air we can assess the real threat for the animals and humans directly exposed to the exhaust gases while feeding livestock with the use of a feed wagon in the livestock building. When comparing the exhaust emissions of farm tractors with other vehicles used in transport we must state that they have much higher exhaust emissions [6].

CONCLUSIONS

During the investigations the authors observed that the farm tractor operating in a livestock building generates high amounts of CO_2 as well as other exhaust components that are inhaled by the animals. This particularly pertains to NO_x and HC that can affect the animal health and the quality of meat and milk.

1. Besides, the method of assessment of the average values of exhaust emission proposed in the paper could be useful when designing the livestock building ventilation as this method takes into account the additional volume and type of exhaust gases coming from the operating tractor engine.
2. The developed substitute load cycle can serve to determine the optimum value of the effective power demanded by the tractor-wagon aggregate for the better welfare of livestock (optimum exhaust emission level).
3. The performed investigations showed that for the tested engine the optimum effective power amounts to 15 kW, which corresponds to the third load cycle. For these values of effective power the emissions of CO, CO_2, NO_x, HC are still low and the unit fuel consumption g_e is moderate.

Table 4. Weighed averages of the exhaust emissions obtained during the tests of the AD3.152.UR engine

Phase number		1	2	3	4	5	6	Weighed average
Emission, Q [$m^3 \times h^{-1}$]	CO_2	5,9591	6,1604	6,3477	7,7877	8,0685	8,304	6,9675
	HC	0,0047	0,0074	0,0074	0,0133	0,0188	0,0197	0,011
	CO	0,02	0,0149	0,0187	0,0257	0,0427	0,0767	0,0271
	NO_x	0,0012	0,0012	0,0014	0,0021	0,0022	0,0022	0,0017

REFERENCES

1. **Fiedorowicz G., Kuczyńska B., Łochowski B. 2008.** Mikroklimat pomieszczeń w oborach wolnostanowiskowych w okresie letnim. IBMER, Warszawa, p. 94-104.
2. **Koniuszy A., Nadolny R. 2007.** Sposób monitoringu pracy ciągnika oraz urządzenie do jego realizacji. Zgłoszenie Patentowe P 381892.
3. **Kuranc A. 2006.** Zastosowanie diagnostycznego analizatora spalin typu NDIR do pomiaru emisji spalin silnika o zapłonie samoczynnym. Inżynieria Rolnicza 5, p. 385-393.
4. **Lejda K. 2006.** An influence of exhaust gas recirculation on nox and other toxic components emission in diesel engines. TEKA Komisji Motoryzacji i Energetyki Rolnictwa Vol. VIA. Lublin
5. **Merkisz J. 2011.** Badanie emisji pojazdów w rzeczywistych warunkach ruchu. Silniki spalinowe 146, p. 3-15.
6. **Merkisz J., LijewskiP., Fuć P., Pielecha J. 2010.** Exhaust emission tests from agricultural machinery under real operating conditions. SAE Technical Paper Series 01-1949.
7. **Romaniuk W., Fiedorowicz G. 2002.** Nowoczesne technologie chowu krów mlecznych. IBMER, Warszawa.
8. **Romaniuk W., Overby T. 2004.** Systemy utrzymania bydła - poradnik, IBMER, Warszawa.
9. **Sadowski M 1996.** Strategie redukcji emisji gazów cieplarnianych i adaptacja polskiej gospodarki do zmian klimatu Instytut Ochrony Środowiska, Warszawa.
10. **Wasilewski J. 2004.** The influence of regulation parameters changes in a fuel injection system on co and hc emission levels in combustion gases of a tractor engine. TEKA Komisji Motoryzacji i Energetyki Rolnictwa. Vol. IV. Lublin.
11. **Wasilewski J. 2008.** An influence of injection pump wear of a tractor engine on exhaust gas toxicity. TEKA Komisji Motoryzacji i Energetyki Rolnictwa Vol. VIIIA. Lublin.

OCENA ŚREDNIEJ EMISJI SPALIN Z CIĄGNIKA PRACUJĄCEGO W BUDYNKU INWENTARSKIM

S t r e s z c z e n i e . Przedstawiono wyniki badań emisji spalin w budynku inwentarskiego z ciągnika rolniczego połączonego z wozem paszowym. Badania przeprowadzono w otwartym budynku z przestrzenią podzieloną na boksy ze zwierzętami w liczbie 60 krów.

S ł o w a k l u c z o w e : mikroklimat, budynek inwentarski, obciążenie silnika, emisja spalin.

TEKA. COMMISSION OF MOTORIZATION AND ENERGETICS IN AGRICULTURE – 2012, Vol. 12, No. 1, 73–77

Optimising the selection of batteries for photovoltaic applications

Jarosław Knaga, Tomasz Szul

Power Engineering and Agricultural Process Automation Department, Agricultural University of Krakow, ul. Balicka 116B, 30-149 Krakow; e-mail: j.knaga@ur.krakow.pl, t.szul@ur.krakow.pl

Summary. Methods were developed for determining the amount of energy generated by a PV module and for establishing an optimum battery capacity for applications in autonomous solar systems. The methods were applied for selection of batteries operating with the PV module with polycrystalline structure. Based on the analysis for a selected meteorological station, the optimum capacity of the battery to operate with the polycrystalline module was determined. Also, the unit cost of energy storage as a function of the battery depth of discharge was determined.

Key words: battery capacity, autonomous solar system, photovoltaic module, battery depth of discharge.

FOREWORD

The climate package adopted in 2008 by the EU Member States assumes, among others, increasing by 20 % electrical energy production from the so called "clean energy sources" [3]. One of the forms of energy production is direct processing of solar radiation into electricity in photovoltaic cells. Electrical energy generated in this way can be used to supply, e.g. street lights operating in the so called autonomous systems. In Poland, for road and street lighting around 1.8 TWh of electrical energy is used [17]. This results in CO_2 emission of ca. 1.3 M tons. Therefore, using this type of systems may have measurable benefit in reducing energy consumption and the resultant reduction of carbon emissions. Due to the nature of autonomous lighting systems, which rely solely on the energy supplied from solar cells, it is necessary to store the produced energy. This involves an appropriate selection of energy storage, i.e. battery capacity, which will have to operate in various weather conditions, with an uneven distribution of solar radiation thorough the year and the resultant varying consumption of energy by the consumer. There are elaborate literature sources on the selection of photovoltaic cells for the systems [15,18,8,6], however, the subject of energy storage received little attention. Most of the scholars describe extensively the methods for selecting starting and traction batteries [1,16,9,2], the methods for selecting battery capacity depending on the equipment power [5], yet nothing is said about the methods for selecting capacities of batteries for photovoltaic systems in terms of cooperation with the energy source.

OBJECTIVE

In view of the apparent lack of literature on the optimisation of selecting battery size to photovoltaic applications, this paper aims to develop methods allowing an optimum capacity determination for photovoltaic systems operating as autonomous power supply sources. Also an application example of battery selection is covered, in relation to 1 m^2 of the reception area of a photovoltaic panel made of polycrystalline silicon for a selected meteorological station.

RESEARCH METHODS

The main issue in a correct selection of a battery for photovoltaic systems is to determine the amount of energy the battery should store. The solar radiation energy may be determined based on the meteorological data on insolation, published at the website of the Ministry of Transport Construction and Maritime Economy [www.transport.gov.pl]. With this data source, the monthly amount of energy can be calculated from the formula [10,11,12].

$$E_m = \sum_{i=1}^{n} I_i \cdot g_i, \tag{1}$$

where:

I_i – solar radiation intensity W·m^{-2},

g_i – number of hours in a month with ith radiation intensity h.

Calculations of monthly sums are made for various inclination angles of the receiving plane. Based on those monthly radiation sums for all-year applications, such module inclination is decided at which the variability of sums in a year is the lowest possible. Afterwards, the amount of energy delivered by a photovoltaic module is determined in relation to 24 hours, for the least favourable month as can be determined from the formula (2):

$$E_{sd} = \frac{E_{m\,min}}{d}, \tag{2}$$

where:

$E_{m\,min}$ – solar radiation energy W·h·m^{-2},

d – number of days in a month in which there is minimum E.

The calculated E_{sd} value forms the basis for selection of a photovoltaic system for supplying a receiver in the all-year autonomy and determining the total operating autonomy period. The prerequisite for a battery selection is that it could store the total energy produced during the day in the best possible conditions. For this, yet in relation to the maximum insolation, the formulas (1) and (2) will be used. Capacity of the battery can be derived from the energy balance (3):

$$E_{dmax} \cdot \eta_{(T,I)} = q \cdot U \cdot z_{(n)} \cdot \eta_a, \tag{3}$$

where:

$E_{d\,max}$ – maximum 24-hour energy of solar radiation W·h·m^{-2};

$\eta_{(T,I)}$ – effectiveness of the photovoltaic module, depending on the radiation intensity and operating temperature [20,13,6];

q – battery capacity in Ah,

U – battery rated voltage,

z(n) – battery depth of discharge depending on the number of cycles,

η_a – energy storage effectiveness in a battery, depending on the temperature, charging system and battery itself.

The last stage is to calculate the autonomy period of the supply source, which can be expressed as the ratio of energy produced by a photovoltaic module during the day, in maximum insolation $E_{d\,max}$, to the average 24-hour energy E_{sd}:

$$W_a = \frac{E_{dmax} \cdot \eta_{1(T,I)}}{E_{sd} \cdot \eta_{2(T,I)}}, \tag{4}$$

where:

$E_{d\,max}$ – maximum 24-hour energy of solar radiation W·h·m^{-2},

E_{sd} – 24-hour energy of solar radiation W·h·m^{-2},

$H_{1(T,I)}$ – photovoltaic module effectiveness depending on the radiation intensity and operating temperature in extreme conditions,

$H_{2(T,I)}$ – photovoltaic module effectiveness depending on the radiation intensity and operating temperature in average conditions.

The methodology presented above was applied to select a battery for an autonomous photovoltaic system, in which photovoltaic cells with polycrystalline structure were used (the most popular in the market) [19], installed in a selected location.

ANALYSIS

While developing the method for selecting the battery capacity to operate in a solar autonomous system, meteorological data on the solar radiation distribution was applied, selecting a meteorological station located in south-east Poland in Podkarpackie province. The data refers to hour parameters of the total intensity of solar radiation on a surface for a typical meteorological year, calculated based on EN ISO 15927:4. Based on this data, total insolation was determined, depending on the inclination angle (0º, 30º, 45º, 60º) of the receiving surface oriented south in individual months of the year, as shown in the plot in Fig. 1.

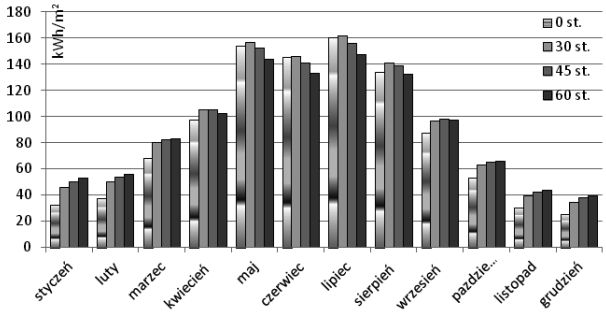

Fig. 1. Insolation distribution depending on the inclination angle of the receiving surface in a monthly configuration

The insolation is characterised by great variability in individual months and varies from 35 kWh/m^2 in December to 160 kWh/m^2 in July (Fig. 1). The value of insolation is affected by the inclination of the receiving area. An optimum inclination for the autumn and winter time (from October to March) should be 60º and 30º for other months. In the annual scale, considerable difference in the insolation is no longer observed, see Table 1.

Table 1. Annual insolation figures

Inclination angle	Insolation kWh·(m^{2}a)$^{-1}$
0º	1026
30º	1118
45º	1122
60º	1096

An important parameter regarding the operation (effectiveness) of photovoltaic cells is also the insolation distribution, depending on the solar radiation density [5,6], which, for the area in question, is shown in Figure 2.

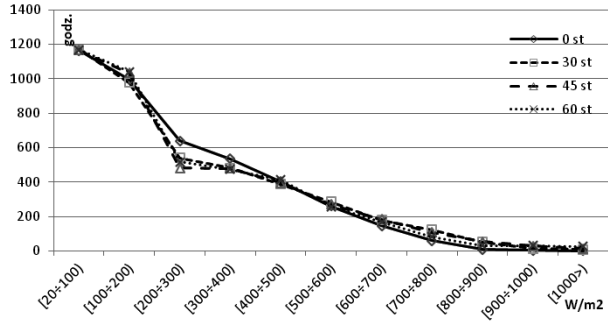

Fig. 2. Insolation distribution for selected inclination angle of the receiving surface versus insolation

The above graph allows determining the insolation figure vs. insolation, and it is shown by the area below the graph. As shown in the graph (Fig. 2), in over 50 % of the time of the average day length, the earth surface receives a stream of radiation with the density up to 200 W/m^2. With such a low solar energy stream, lower efficiency of the photovoltaic conversion should be considered [6,14].

Considering the effectiveness change of a solar cell [20] [11,12] with polycrystalline structure, the amount of energy was determined, which the cell is able to generate in a month. Bearing in mind the all-year autonomy of the system, the optimum inclination angle of the cell surface is 60º since it delivers most energy (Figure 3) in the autumn and winter time, and the least in the spring and summer period.

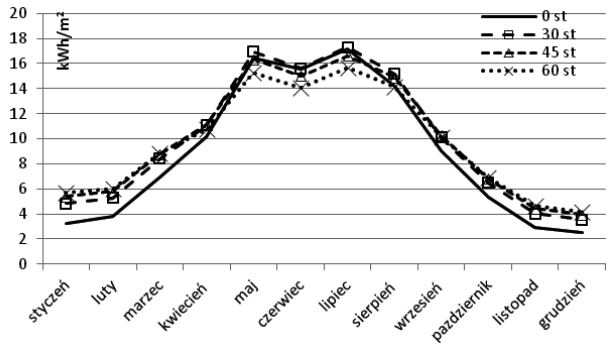

Fig. 3. Electricity production by a photovoltaic polycrystalline module

Assuming, in further calculations, the inclination angle of module plane of 60º, the average daily production of electricity was calculated together with the degree of use in the all-year autonomy system (Fig. 4). The graph is useful for determining parameters of a receiver supplied by an autonomous PV source.

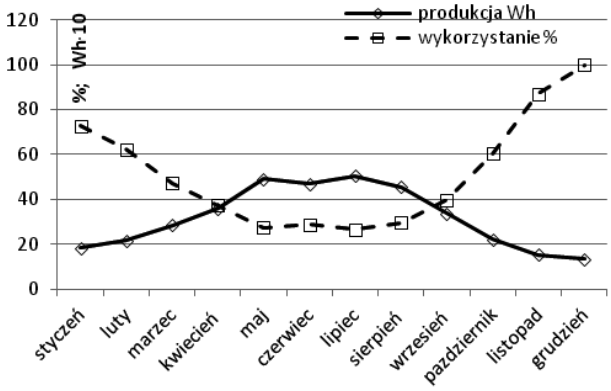

Fig. 4. Daily production of electricity from PV, and degree of use in the all-year autonomy system

A battery operating with a PV source should have optimally selected capacity, for the minimum cost of energy storage, ensuring, at the same time, storage of the energy delivered from the module.

To perform practical calculations of the cost of energy storage in a battery, data from commercial offers from various companies were used. Batteries with available technical documentation, specifying their life vs. depth of discharge, were chosen. The analysis of unit cost of energy supplied from a battery was started from determining the amount of energy per cycle (5):

$$E = \frac{q \cdot U \cdot z_c}{10^3}, \tag{5}$$

where:
E – energy output in a cycle [kWh],
q – battery capacity [Ah],
U – voltage at battery terminals [V],
z_c – battery depth of discharge per cycle.

The unit cost of energy supplied from a battery was determined from the relationship 6:

$$K_j = \frac{c \cdot 10^3}{E \cdot n(z_c)}, \tag{6}$$

where:
Kj – unit cost of energy [PLN/kWh],
c – battery market price [PLN],
E – energy output in a cycle [kWh],
$n(z_c)$ – number of cycles as a function of depth of discharge.

The relationships 5, 6 were adopted to simulate the unit cost of energy delivered by five different battery models with capacity above 200 Ah, and the results are shown in Fig. 5. Due to significant differences in the achieved results, the solar batteries were divided into two groups “a” and “b”, without specifying the manufacturers.

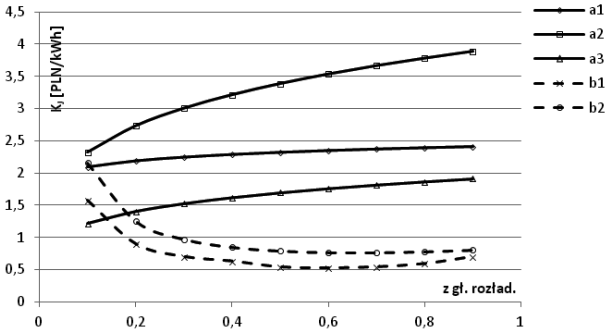

Fig. 5. Unit cost of energy storage as a function of the battery depth of discharge

Group "a" includes batteries for which the unit energy cost increases along with the depth of discharge. The lowest unit cost of energy from a battery in this group is with discharge to 10 %, and varies from 1.2 to 2.3 PLN/kWh, which is a few times higher than that of the energy from the power grid. Energy buffer of 10 % of the battery capacity is definitely too low for applications in autonomous solar systems. Therefore, 20 % depth of discharge was assumed for batteries in this group. For the "b" group batteries, however, the minimum unit cost can be found at the depth of discharge of 60 %. It has to be stressed that, for an optimum depth of discharge for this group, the unit energy cost varies from 0.5 to 0.75 PLN/kWh and is comparable with that of the energy from the power grid.

While designing battery capacity, it was assumed that the daily energy produced in the most effective solar conditions should be completely stored in the battery, at the optimum depth of discharge. Therefore, the maximum energy production by a PV in the best solar conditions was determined for further analysis of the system with all-year autonomy (Fig. 6).

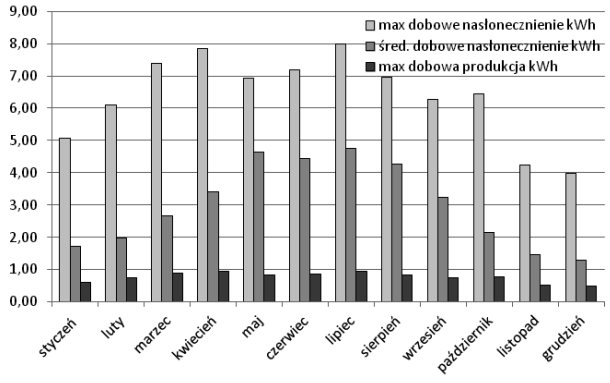

Fig. 6. Daily insolation: a) maximum, b) average, c) max energy production by a polycrystalline module; the values specified refer to 1 m^2 of the receiving area

From the relationship 3, battery capacity in two variants was determined, i.e. with the all-year and half-year autonomy, for the optimum depth of discharge, with the division into the "a" and "b" groups. The results of the battery capacity q calculations in relation to 1 m^2 of the receiving area are shown in the plot (Fig. 7).

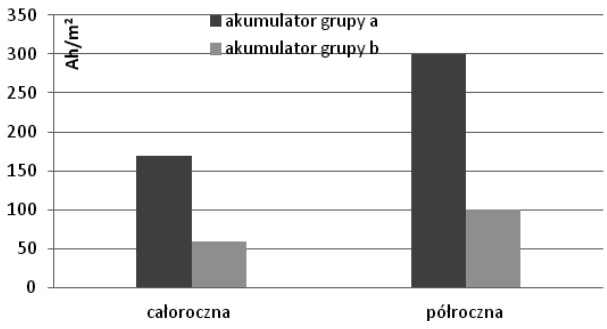

Fig. 7. Battery capacity

Legend: akumulator grupy a: group 'a' battery
akumulator grupy b: group 'b' battery
całoroczna: all-year
półroczna: half-year

Analysing the obtained results, it can be stated that for systems with all-year autonomy, the optimum battery capacity should be 60 Ah/m^2 for the "b" group batteries, and 170 Ah/m^2 for the "a" group batteries. For systems operating in the half-year autonomy (March-September), the capacity should be increased by 65 % for the "b" group and by 75 % for the "a" group respectively. For the battery capacities decided this way, the autonomy index W_a is 3.5 days for the all-year autonomy and 3 days for the half-year autonomy system, respectively.

CONCLUSIONS

The methods presented herein allows for the determining of the amount of energy generated by a PV module and establishing an optimum battery capacity for applications in autonomous solar systems. The methods developed were applied for selection of batteries operating with the PV module with polycrystalline structure. They can also be applied for other cell types in solar systems. Analysing the selected meteorological station, the optimum battery capacity operating with a polycrystalline module was established, which is 60 Ah/m^2 with the depth of discharge of 60 % and 170 Ah/m^2, with the depth of discharge up to 20 %. Also the unit cost of energy storage as a function of the battery depth of discharge was determined. The cost is from 1.2 to 2.3 PLN/kWh for the group of batteries marked as "a" and from 0.5 to 0.75 PLN/kWh for the "b" group. The very cost of energy storage in the batteries, in the best case, is comparable to the energy from the power grid, hence, at present, they are not a competitive alternative to the energy supplied from the power grid. It may be an alternative supply solution in places when no power grid supply is available.

The presented methods for selection of battery capacity allow for the achievement of 3.5 day-autonomy in the all-year operation, on condition that the energy drawn from the solar source will not exceed the average daily figures delivered by the PV module in the month with the lowest insolation.

REFERENCES:

1. **Binkiewicz A. 2009.** Dobór parametrów baterii litowo-polimerowych w mieszanych systemach zasilania. Opracowanie nr 334/Z5. Instytut Łączności. Państwowy Instytut Badawczy. Warszawa.
2. **Czerwiński A. 2005.** Akumulatory, baterie i ogniwa, Wydawnictwa Komunikacji i Łączności, Warszawa.
3. Dyrektywa Parlamentu Europejskiego i Rady 2009/28/ WE z dnia 23 kwietnia 2009 r. w sprawie promowania stosowania energii ze źródeł odnawialnych zmieniająca i w następstwie uchylająca dyrektywy 2001/77/ WE oraz 2003/30/WE.
4. **Fthenakis. 2003.** Practical Handbook of Photovoltaics: Fundamentals and Applications: Overview of Potential Hazards. Available at http://www.bnl.gov/pv/files/pdf/ar t_170.pdf.
5. **Klugman E., Klugmann-Radziemska E. 2005.** Ogniwa i moduły fotowoltaiczne oraz inne niekonwencjonalne źródła energii". Wydawnictwo Ekonomia i Środowisko. Białystok.
6. **Klugmann-Radziemska E. 2009.** Odnawialne źródła energii – Przykłady obliczeniowe. Wydawnictwo Politechniki Gdańskiej. Gdańsk.
7. **Knaga J. 2006.** Efektywność sterowania modułem fotowoltaicznym, Energetyka 9, s. 42–45.
8. **Lewandowski W. 2007.** Proekologiczne odnawialne źródła energii. Wydawnictwa Naukowo-Techniczne, Warszawa. ISBN: 978-83-204-3339-5.
9. **Michalski R., Janulin M. 2008.** Dobór parametrów eksploatacyjnych pojazdu z napedem elektrycznym, Nauka i Technika – Eksploatacja i Niezawodność nr 3, p. 69-73.
10. Ministerstwo Transportu, Budownictwa i Gospodarki Morskiej. Typowe lata meteorologiczne i statystyczne dane klimatyczne dla obszaru Polski do obliczeń energetycznych budynków http://www.transport.gov.pl/2-48203f1e24e2f-1787735-p_1.htm.
11. National Renewable Energy Laboratory (NREL). Energy Payback: Clean Energy from PV NREL Report No. NREL/FS-520-24619. Available at http://www.nrel.gov/docs/fy99osti/24619.pdf.
12. Norma EN ISO 15927-4 „Hygrothermal performance of buildings – Calculation and presentation of climatic data – Part 4 Data for assessing the annual energy for cooling and heating systems».
13. **Nowak W., Stachel A. 2011.** Kolektory słoneczne i panele fotowoltaiczne jako źródło energii w małych instalacjach cieplnych i elektroenergetycznych. Automatyka-Elektryka-Zakłócenia NR 4/2011 p. 55-64.
14. PHYWE Systeme GmbH & Co.KG. 2008. Characteristic Curves of a Solar Cell. Laboratory Experiments. Physics 4.1.09.
15. **Pluta Z. 2002.** Słoneczne instalacje energetyczne, Oficyna Wydawnicza Politechniki Warszawskiej, Warszawa.
16. **Przybyło H. 2009.** Zasady doboru akumulatorów. Wydawnictwo Technotransfer Sp.J.
17. **Ślęk B., Górczewska M. 2008.** Analizy i ekspertyzy dotyczące źródeł światła. Oświetlenie dróg, ulic i miejsc publicznych. Ministerstwo Gospodarki. Departament Energetyki.
18. **Trojanowska M., Knaga J. 2004.** Optymalizacja obciążenia modułu fotowoltaicznego SF 50, Inżynieria Rolnicza 2(57) p. 301-306.
19. **Tsuo, YS, Wang, TH, & Ciszek, TF. 1999.** Crystalline-Silicon Solar Cells for the 21st Century. Available at http://www.nrel.gov/docs/fy99osti/26513.pdf (raport o wilkości instalacji z ogniw polikrystalicznych).
20. **Wietrzny K. 2003.** Instalacje fotowoltaiczne. Instalator 1/2003.

OPTYMALIZACJA DOBORU AKUMULATORÓW DO ZASTOSOWAŃ FOTOWOLTAICZNYCH

Streszczenie. Opracowano metodykę pozwalającą na określenie ilości energii produkowanej przez moduł PV, oraz na określenie optymalnej pojemności akumulatora do zastosowań w autonomicznych układach solarnych. Metodykę wykorzystano przy doborze akumulatorów współpracujących z modułem PV o strukturze polikrystalicznej. Na podstawie analizy dla wybranej stacji metrologicznej określono optymalną pojemność akumulatora współpracującego z modułem polikrystalicznym. Określono również koszty jednostkowe magazynowania energii elektrycznej w funkcji głębokości rozładowania akumulatora.

Słowa kluczowe: pojemność akumulatora, autonomiczny układ solarny, moduł fotowoltaiczny, głębokość rozładowania akumulatora.

TEKA. COMMISSION OF MOTORIZATION AND ENERGETICS IN AGRICULTURE – 2012, Vol. 12, No. 1, 79–85

The automotive picture of Poznań against a background of other cities and national indexes

Karolina Kozak[*], *Miłosław Kozak*[**], *Jerzy Merkisz*[**], *Dawid Nijak*[*], *Bożena Wiśniewska*[*]

[*] Poznań City Hall, Poznań, Poland
[**] Poznań University of Technology, Poznań, Poland

Summary. Following the dynamic development of the automotive industry and economic changes in the last 20 years Polish transport-related needs and citizen mobility have changed as well. An increased demand for traveling and easy access to individual means of transport in the form of passenger cars put Poznań in the top ten of the largest cities of Poland in terms of the motorization level. The paper analyses the current situation of the level of motorization of the city of Poznań based on statistical data from Central Vehicle and Driver Register, Department of Motor Vehicles in Poznań and published by Central Office of Statistics. A synthetic analysis has been presented of the situation in Poznań against other largest cities of Poland and the average situation in the country. The paper also presents the analysis of the preferences of the citizens of Poznań in terms of engine capacity, type of fuel, engine type as and the most popular vehicle makes.

Key words: city of Poznań, motorization, statistics, mobile society.

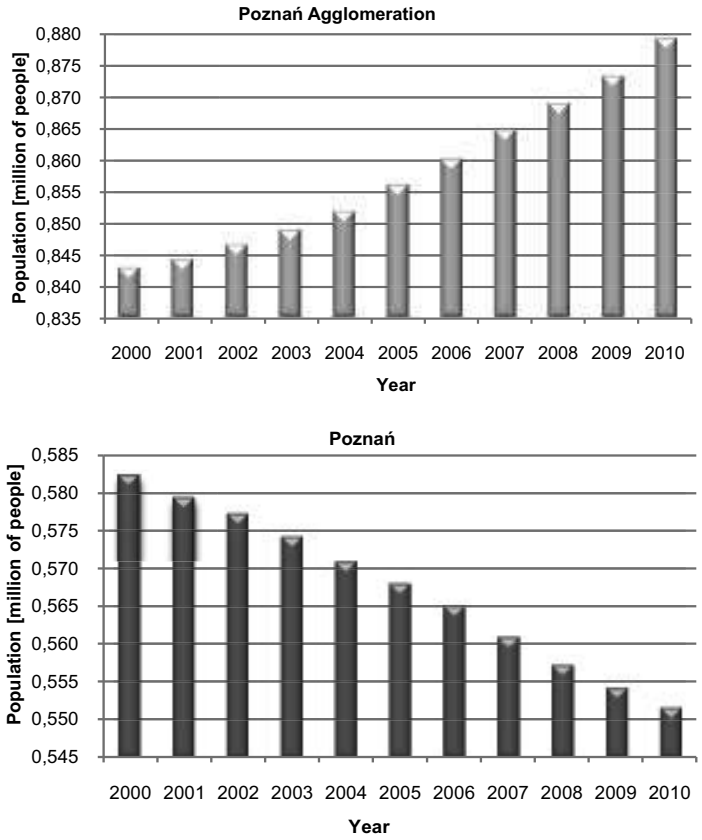

Fig. 1. Changes in the population of Poznań and the Poznań Agglomeration

INTRODUCTION

Poznań as one of the oldest cities and the fifth in terms of population in Poland is an important center for industry, trade, culture and higher education [1]. The population in 2010 was 551600 inhabitants [2]. This value is subject to a constant change (fig. 1). The city population is greatly affected by a negative human migration triggered by the so-called sub-urbanization [3]. The citizens move to adjacent towns preserving their employment in Poznań. The result of such actions is a growing population of the Poznań Agglomeration while the population of the city itself drops regularly.

Poznań is one of the strongest cities in Poland in terms of economy being at the same time one of the main centers for foreign investment [3]. In Poznań there are over 99000 economic entities while the number of foreign capital entities is one of the largest countrywide (approximately 2800) [3]. Hence, the unemployment rate, according to the September 2011 statistics is one of the smallest in Poland (fig. 2).

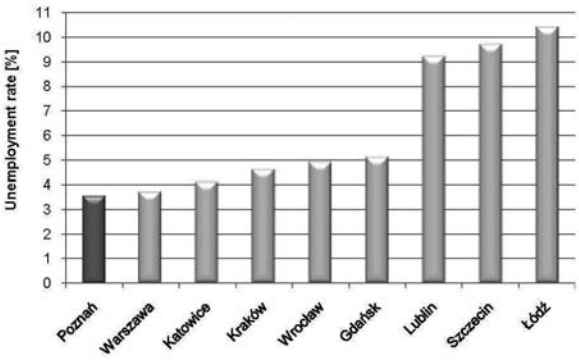

Fig. 2. Unemployment rate in the largest Polish cities– September 2011 [4]

The Poznań's geographical and economic location, both continentally and locally, on one of the most important transit routes connecting the western and the eastern part of Europe (halfway between Warsaw and Berlin) gives the city a privileged position. The city's economic, trade and business as well as residential function brings a necessity of intense development of transportation. At the same time the above-mentioned phenomena (economic development, suburbanization) not only result in longer travels but also generate new that arise not only from the home-work-home, home-campus-home routines but also from other motives (e.g. those related to recreation). The need to realize trips combined with a rapid development of the motorization and a relatively easy access to individual means of transport (passenger car) have contributed to significant changes in the functioning of road transportation and a creation of a mobile society [5]. As of the moment that passenger car became, as we call it, a common good, it is little wonder that in 2010 the basic means of transport, apart from public transit, was this very vehicle type. The share of vehicle traffic in overall transit in Poznań amounts to over 50% [6].

MOTORIZATION INDEX FOR THE CITY OF POZNAŃ

Recent social-economic changes in Poland have been accompanied by a dynamic growth of the number of vehicles driving on our roads [7]. According to the data of Central Office of Statistics (GUS) published in 2011 [8], the number of vehicle in the years 2005-2009 grew by 30% (from 12 339 353 units to 16 494 650 units). For the evaluation of the motorization level of society a motorization index is used that determines the number of vehicles per 1000 inhabitants. In the case of passenger cars, on average national scale this index currently amounts to 433, which, in comparison to the index obtained in 2005, constitutes a growth by 30%.

Referring the above national data to Poznań, the growing trend of the motorization index greatly exceeds the national average. According to the available data related to the number of registered vehicles in Poznań in the period from 2005 to 2009 we can observe an almost 40% growth in the motorization index. At the end of 2010 it reached a value of 516 (fig. 3). A particularly visible dynamic growth of the number of registered vehicles took place in the period from 2004 to 2008 i.e. the moment Poland became the EU member and an avalanche of vehicles were imported from the EU until the economic crisis in 2008. In this period the motorization index in Poznań grew almost by half. Indeed, after 2008 further growth of vehicles registered in Poznań continued, yet the value of this index was not this dynamic anymore. We can add that in 2010 in the city there were 370.000 vehicles registered, 2.6% more than the previous year [6].

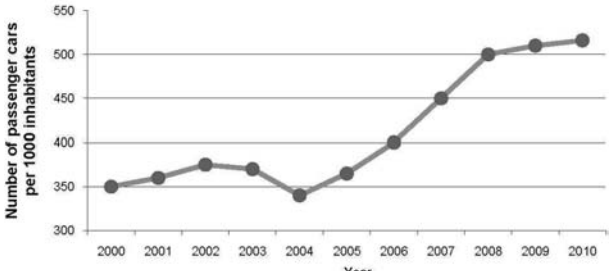

Fig. 3. Motorization index in Poznań in the years 2000-2010 [6]

The most up-to-date motorization indexes can be determined based on the data from Central Vehicle and Driver Register (CEPIK) [9]. The motorization index referred to the number of passenger cars (285 777 units as of 31.05.2011) at the assumption of 550 000 inhabitants in Poznań was 520 and in the poviat of Poznań (110 925 cars as of 31.05.2011 and 309 000 inhabitants): 359 [10]. Assuming for the calculations not only passenger cars but all the vehicles registered in Poznań the index would be higher and would amount to 652 (for 359 050 vehicles).

The value of the motorization index is subject to continuous changes. Each day new vehicles are registered and other are declared off the road. The lack of detailed

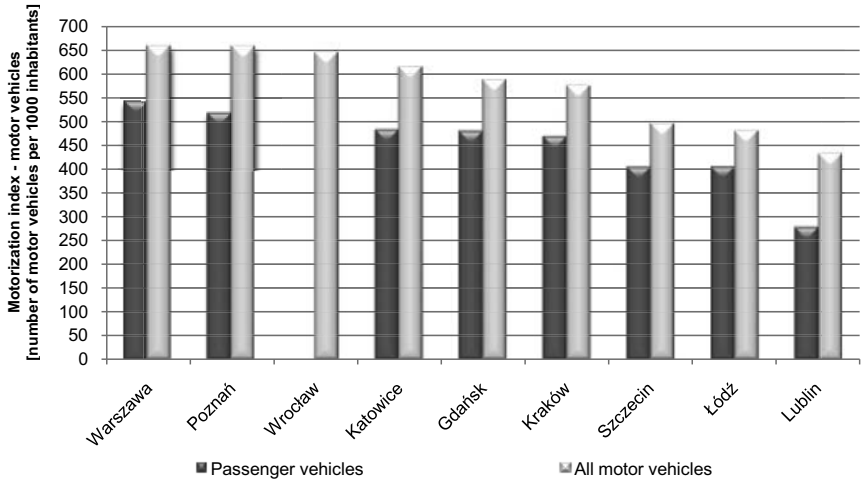

Fig. 4. Comparison of the motorization index in the largest Polish cities – data as of 2010 [12]

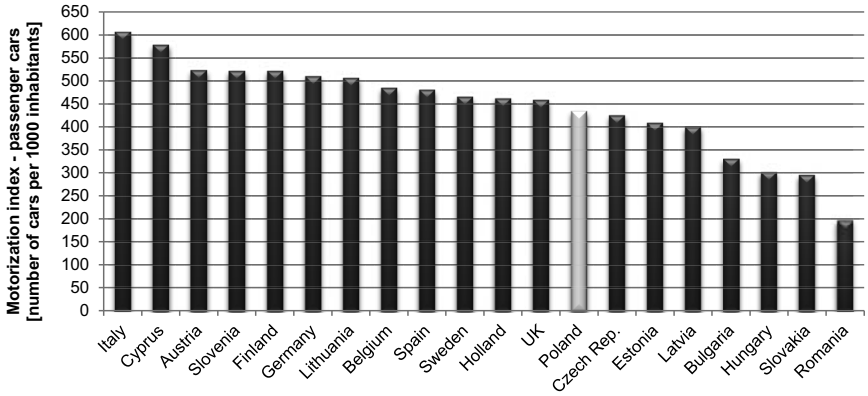

Fig. 5. Comparison of the motorization index (passenger cars only) in EU countries [8]

information on vehicles that are off the road and still recorded in the CEPIK record (physically not existing) significantly influences the state of knowledge on the actual state of motorization. Hence, small differences may appear in the available source data [9, 10, 11, 12]. What is more, the index value is also influenced by the assumed number of inhabitants. The differences between the indexes determined for Poznań based on the available sources respectively: 520 (CEPiK) and 516 (Department of Motor vehicles) can be deemed as insignificant.

It is worthwhile to compare the motorization indexes for Poznań with the available data for the largest cities of Poland and the average values for the EU member states (fig. 4 and 5). The analysis of the data leads to a conclusion that Poznań, immediately after Warsaw, has the largest number of passenger cars per 1000 inhabitants. Besides, the values of the motorization index for Poznań is comparable or even higher than the average values of this index for such EU member states as Austria, Belgium, Finland or Germany. Such a high level of motorization in Poznań has several reasons: low unemployment rate, relatively low prices of passenger vehicles in the second hand market, still insufficient, yet improving quality of public transit, growing but still acceptable cost of traveling (expressed in time and money) and the comfort of the users.

MOTORIZATION STRUCTURE IN THE CITY OF POZNAŃ

GENERAL INFORMATION

The largest group at 80% in the motorization structure of Poznań is passenger cars (Fig. 6). Another group is trucks (13%), motorcycles (3.2%) and mopeds (1.7%). Due to a very small share in the overall structure the last group referred to as 'other' (2.2%) contains: trailer trucks (0.9%), farm tractors (0.8%), buses (0.3%) and special heavy-duty vehicles (0.2%).

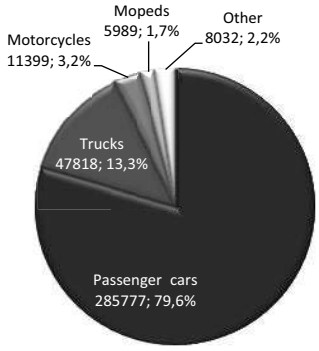

Fig. 6. Motorization structure of the city of Poznań as divided into type of vehicle and seen in per cent and quantity in 2011

The vehicle structure in Poznań in terms of year of manufacture and registration in the Department of Motor Vehicles has been presented in figure 7. Analyzing the presented data from 2004 we can observe a growing trend of the registered vehicles. In the years 2004-2008 this number doubled. In the analyzed period the number of registered vehicles was the highest in 2008. At the same time there was the highest number of newly registered vehicles, hence the highest number of vehicles from this year in Poznań. A clearly decreasing trend of the number of vehicles manufactured and registered in 2009 should probably be attributed to the economic crisis.

Another visible trend is that from 2004 the number of vehicles from a particular year of manufacture is lower than the number of vehicles registered in this particular year. Beginning from 2004 came a gradual increase in the number of registered vehicles, however, more pre-owned vehicles then new ones were registered. It is noteworthy that in 2004 as compared to the previous year the growth in the number of registered vehicles was over 50%. Such a high dynamics can be attributed to the avalanche of vehicles imported from the EU member states following the accession of Poland to the European structures in May 2004. The growing trend maintained until 2008 and then from 2009 we can observe a reduced number of registered vehicles in Poznań. The reason for this could have been the economic crisis or bad exchange rates – Euro in particular.

AUTOMOTIVE STRUCTURE IN POZNAŃ FOR PASSENGER CARS ANALYZED IN TERMS OF THEIR AGE

The total number of registered passenger cars in Poznań as of 30.11.2011 amounted to 285 777 units. The structure of passenger cars in Poznań in terms of their year of manufacture and year of registration in the Department of Motor Vehicles has been presented in figure

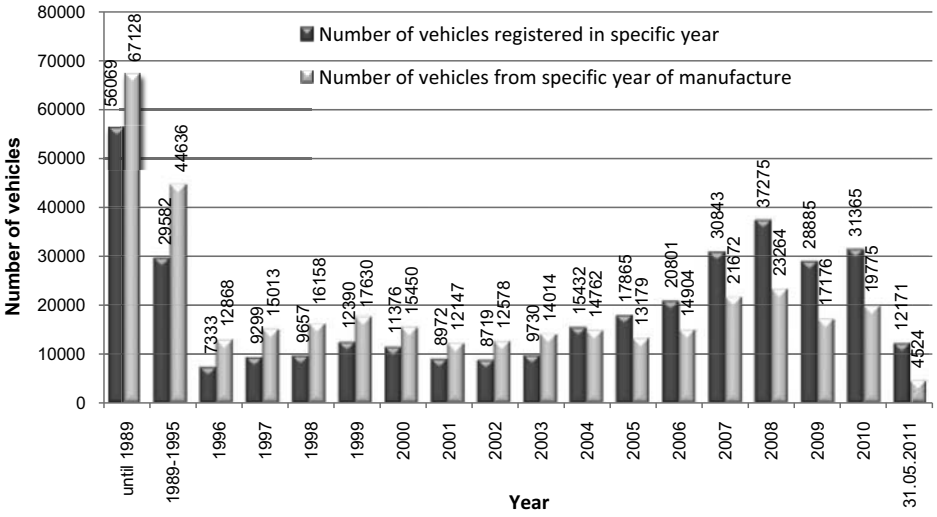

Fig. 7. Automotive structure in the city of Poznań as divided into year of manufacture and year of registration in the Department of Motor Vehicles in Poznań

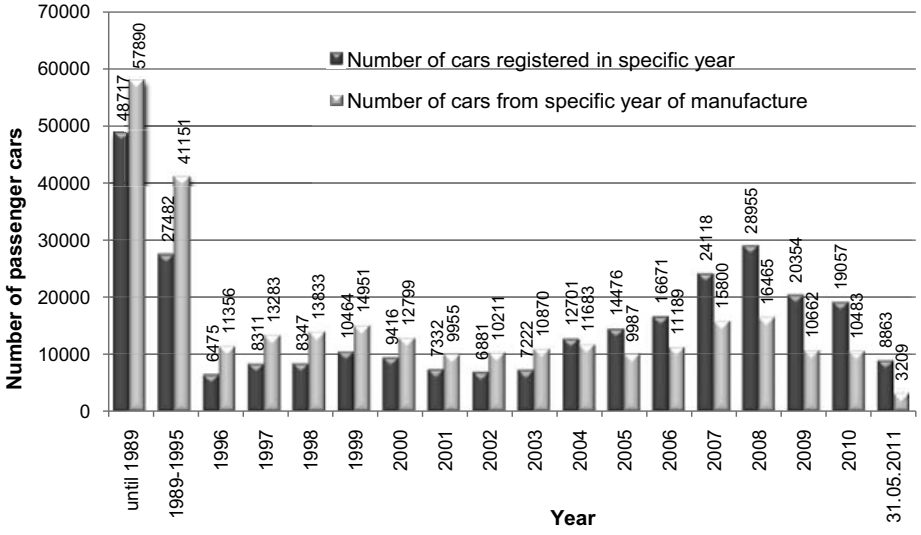

Fig. 8. Automotive structure of passenger cars in the city of Poznań as divided into year of manufacture and year of registration in the Department of Motor Vehicles in Poznań

8. When analyzing the presented data we can observe that the trend pertaining to the number of manufactured and registered passenger vehicles in Poznań is similar to the trend pertaining to all the vehicles registered in the city. In the years 2004-2008 the number of registered vehicles grew by more than 100%. Also, the number of vehicles manufactured in 2008 is the highest and the passenger cars from this year of manufacture are the highest in number in the city. A numerous collective group of vehicles are the vehicles registered in the period until 1989. Due to their age and low probability of everyday use these vehicles are not a common sight in the streets of Poznań. Almost 60.000 vehicles are vehicles over 20 years old and approximately 100.000 vehicles are 16 years of age and older. When comparing the structure of all vehicles and passenger cars only we can observe that the drop in the total number of registered vehicles in 2009 as compared to 2008 resulted practically only from the drop in the number of passenger cars.

The data from Institute of Automotive Market Research (Samar) [13] indicate that from January to May 2011 in the country 68 567 new vehicles [11] and 267 437 imported pre-owned vehicles were registered [13], which gives a total of 336 004 registered vehicles. This means that almost every fourth vehicle registered in the country was a new one. In the meantime in Poznań 8 863 passenger vehicles were registered, which constitutes almost 3% of all registered vehicles countrywide.

In order to show the Poznań statistics against the average national statistics fig. 9 presents the share of passenger vehicles in individual age groups. Based on the data we can observe that the average number of vehicles registered in Poznań in the age group up to 2 years is clearly higher than the national average. This means the citizens of Poznań buy more new vehicles than the national average.

A further analysis of the data in figure 9 indicates that, basically for all analyzed groups the vehicles registered in Poznań are younger as compared to the average statistics on the national level. In the case of passenger cars in the age group of up to 5 years the ones registered in Poznań constitute 24% and on the national level it is merely 12%. At the same time vehicles in the age group of over 16 years it is 35% in Poznań and almost 42% on the national level.

In the case of trucks the situation is similar. Vehicles up to 5 years constitute as much as 54% of the total number of those vehicles registered in Poznań and on the national level this value is merely 16%. The situation of trucks in the age group of over 11 years is quite contrary – in Poznań it is only 25% of the total number of heavy duty vehicles registered while on the national scale it is as much as 61%.

The age structure of the buses registered in Poznań and countrywide is similar to passenger cars with the only difference that the share of the vehicles in the age group above 16 years on the national scale is almost on the level of 60% whereas for Poznań this value is 42%.

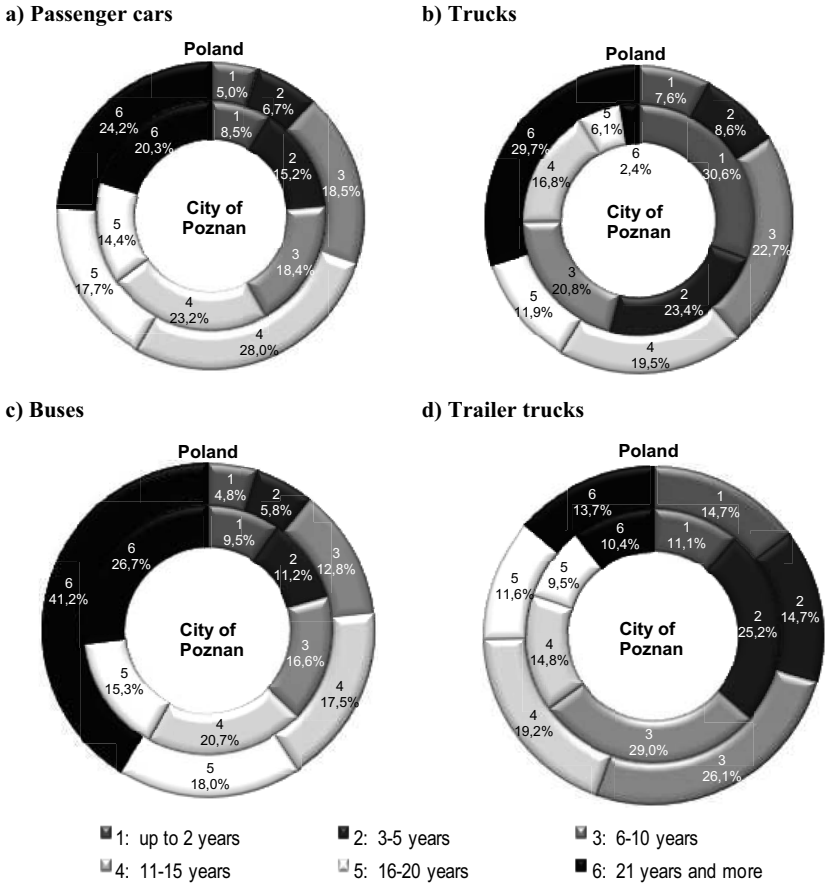

Fig. 9. Comparison of average vehicle shares in individual age groups in Poznań and countrywide

As for the trailer trucks, the general trend is similar to the other groups under analysis with the exception of the youngest vehicles (up to 2 years) that in Poznań are on the level of 11% while on the national scale it is almost 15%. The share of vehicles in the age group of up to 5 years in the total number of registered trailer trucks for Poznań is 36% while on the national scale it is almost 30%. Trailer trucks in the age group above 10 years constitute 35% in Poznań and over 44% on the national scale.

The above described status, i.e. a much younger vehicle fleet in individual categories could be a confirmation of the economic situation of Poznań and its citizens, which as mentioned earlier is one of the best in the country.

AUTOMOTIVE STRUCTURE OF THE CITY OF POZNAŃ FOR PASSENGER CARS – CITIZEN PREFERENCES

The preferences of the citizens of Poznań in terms of engine capacity, determined based on the number of passenger cars registered in the Department of Motor Vehicles in individual engine displacement categories, have been shown in figure 10. In the percentage structure of the passenger cars for engine capacity in Poznań small and medium sized (compact) vehicles dominate (engines of the capacity of 651 to 1600 cm^3 represent 64% of the total number of registered cars). The vehicles of engine capacity from 1601 cm^3 to 2000cm^3 constitute every fourth car registered in Poznań. The smallest group are cars of the engine capacity above 2501 cm^3 (total 4%).

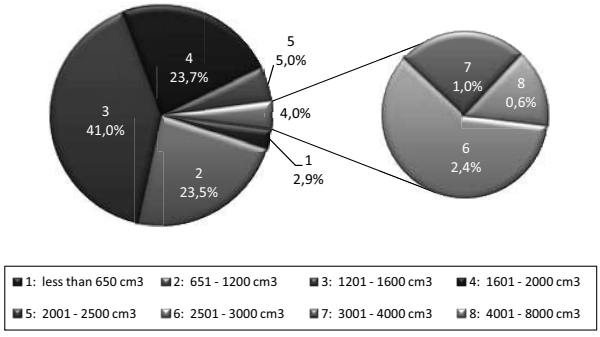

Fig. 10. Passenger cars registered in Poznań as divided into engine capacity [cm^3]

The drivers' preferences in terms of fuel and engine type in vehicles registered in Poznań have been shown in figure 11. From the data it results that the preferences of the drivers in Poznań in the above categories are spark ignition engines.

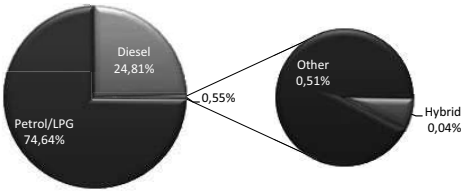

Fig. 11. Passenger cars registered in Poznań as divided into type of fuel

As a complement to the already presented analyses figure 12 presents a percentage structure of vehicle makes owned by the citizens of Poznań. For the sake of the analysis the vehicles of the makes that were registered in number not exceeding 10 000 units have been classified as 'other'.

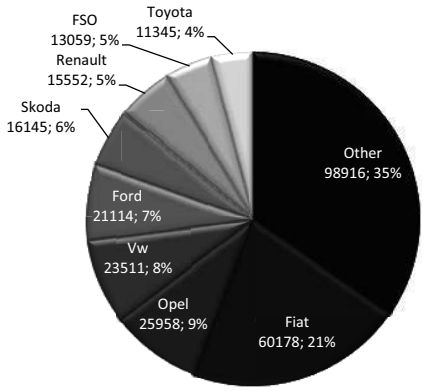

Fig. 12. The number of individual passenger car makes registered in Poznań

It is noteworthy that the most popular in the city of Poznań are the cars manufactured by Fiat that constitute over 21% of all registered vehicles. Further, the most popular makes in Poznań registered in the number of over 10.000 units are: Opel (9%), Volkswagen (8%), Ford (7%), Skoda (6%), Renault (5%), FSO (5%) and Toyota (4%). A large collective group is cars classified as 'other' (35%). In this group belong various makes whose individual share is miniscule as compared to the total number of registered vehicles. We should also remember that the database contains vehicles that probably do not exist anymore. For legal reasons it is impossible for these vehicles to be deleted from the database. In this context we need to indicate the vehicles manufactured by FSO – 5% of all passenger cars. A similar group are vehicles that are a rare sight in the streets of Poznań. These are: Trabant (1484 units), Wartburg (1329 units), Lada (1295 units), Zastava (956 units), Moskwicz AZLK (328 units). Beside the above indicated makes classified as 'other' there is another group that belongs to this classification due to its little number – luxury, niche vehicles: Lexus (374 units), Jaguar (359 units), Porsche (310 units), Pontiac (107 units), Cadillac (46 units), Lincoln (34 units), Bentley (13 units), Ferrari (9 units), Rolls Royce (5 units), Aston Martin (4 units) and Lamborghini (3 units).

CONCLUSIONS

The analysis of the here presented data allows a statement that the automotive structure in Poznań in most cases is positively far from the average values for Poland. In the case of the motorization index we obtain values that are higher than the average and the age of the registered vehicles is lower than the average values for the whole country. We should observe that the motorization

index for Poznań is comparable to values characteristic of better-developed EU member states. Such a situation in combination with a constantly growing trend and shortcomings in the infrastructure (e.g. park and ride lots or incomplete system of bypass roads) results in that the traffic conditions gradually deteriorate (higher congestion, costs of transport etc.). This unfortunately results in higher exhaust and noise emissions at the same time influencing the life of the citizens. A positive phenomenon that to some extent could compensate the growing traffic congestion and thus the growing pollution could be the higher (as compared to national average) number of vehicles in the age group of up to 5 years meeting at least the EURO-4 standard.

A constantly growing motorization index is a result of many factors. The most important seem to be: a relatively good (as compared to other cities) economic situation of the citizens of Poznań, advancement of the automotive industry and easy access to passenger vehicles as a means of transport, comfort and a common cult of a vehicle as a transport means, acceptable costs of traveling and suburbanization being a natural stage of the city development. The above-mentioned phenomena, with Poznań still remaining as the center for work, education and recreation leads to a realization of new traveling objectives.

REFERENCES

1. Poznań 2008 – Raport o stanie miasta. Oddział Statystyki, Analiz i Sprawozdawczości Wydziału Rozwoju Miasta, Urząd Miasta Poznania, Poznań 2009.
2. Statystyka regionalna. Główny Urząd Statystyczny. http://www.stat.gov.pl/gus/5840_5958_PLK_HTML.htm.
3. Poznań 2011 – Raport o stanie miasta. Oddział Statystyki, Analiz i Sprawozdawczości, Wydziału Rozwoju Miasta, Urząd Miasta Poznania, Poznań 2011.
4. Bezrobotni oraz stopa bezrobocia wg województw, podregionów i powiatów: styczeń-wrzesień 2011 r. Główny Urząd Statystyczny, Warszawa 2011.
5. http://pl.wikipedia.org/wiki/Motoryzacja.
6. Poznań 2010 – Sytuacja Społeczno-Gospodarcza. Oddział Statystyk, Analiz i Sprawozdawczości Wydziału Rozwoju Miasta, Urząd Miasta Poznania, Poznań 2011.
7. **Katarzyna Baryżewska, Małgorzata Mazurkiewicz, Roman Ulbrich:** Analiza wpływu kształtu układu drogowo – ulicznego miasta na emisje zanieczyszczeń odkomunikacyjnych i hałasu przy ustalonych parametrach brzegowych na przykładzie Zabrza. http://www.road.pl/GIS_emisja.htm.
8. Transport Drogowy w Polsce w latach 2005-2009, Informacje i opracowania statystyczne. Główny Urząd Statystyczny, Warszawa 2011, http://www.stat.gov.pl.
9. Dane pojazdów z Centralnej Bazy Pojazdów i Kierowców MSWiA, maj 2011.
10. Dane pojazdów z Wydziału Komunikacji Starostwa Powiatowego w Poznań, maj 2011.
11. Raport na temat przerejestrowań samochodów osobowych w I kwartale 2011 roku. Instytutu Badań Rynku Motoryzacyjnego Samar. http://www.samar.pl/__/3/3.a/62970/Raport-na-temat-przerejestrowań-samochodów-osobowych-w-I-kwartale-2011-roku.html?locale=pl_PL.
12. System Analiz Samorządowych SAS. www.sas24.org.
13. Rejestracje samochodów osobowych w maju 2011. Instytutu Badań Rynku Motoryzacyjnego Samar. http://www.samar.pl/__/3/3.a/63255/Rejestracje-samochodów-osobowych-w-maju-2011.html?locale=pl_PL.

OBRAZ MOTORYZACYJNY POZNANIA NA TLE INNYCH MIAST ORAZ WSKAŹNIKÓW OGÓLNOKRAJOWYCH

S t r e s z c z e n i e . W ślad za dynamicznym rozwojem motoryzacji oraz zmianami gospodarczymi zachodzącymi na przestrzeni ostatnich 20 lat w Polsce znaczącym zmianom uległy również potrzeby transportowe oraz mobilności mieszkańców. Zwiększony popyt na realizację podróży oraz łatwy dostęp do indywidualnego środka transportu, jakim jest samochód osobowy stawia Poznań w czołówce pod względem wartości wskaźnika motoryzacji wśród największych miast w Polsce. W artykule dokonano analizy stanu motoryzacyjnego Poznania na podstawie danych statystycznych z Centralnej Ewidencji Pojazdów i Kierowców, Wydziału Komunikacji Urzędu Miasta Poznania oraz publikowanych przez Główny Urząd Statystycznych. Zaprezentowano syntetyczną analizę sytuacji panującej w Poznaniu na tle największych miast w Polsce oraz średniej sytuacji w kraju. Przedstawiono także analizę preferencji mieszkańców Poznania w zakresie pojemności silnika, rodzaju stosowanego paliwa i napędu oraz najczęściej wybieranych marek samochodów osobowych.

S ł o w a k l u c z o w e : miasto Poznań, motoryzacja, statystyka, społeczeństwo mobilne.

TEKA. COMMISSION OF MOTORIZATION AND ENERGETICS IN AGRICULTURE – 2012, Vol. 12, No. 1, 87–91

The effect of binder addition on the parameters of compacted POPLAR wood sawdust

Ryszard Kulig, Stanisław Skonecki, Grzegorz Łysiak

Department of Food Machinery Operation, University of Life Sciences in Lublin
Doświadczalna 44, 20-280 Lublin, e-mail: ryszard.kulig@up.lublin.pl

S u m m a r y. The study discusses the results of tests investigating the effect of binder addition (calcium lignosulphonate, 0% to 20%) and moisture content (10% to 22%) on the parameters of compacted poplar wood sawdust. The susceptibility to compaction of the studied material, changes in material density and the mechanical strength of briquettes were analyzed. The addition of a binding agent increased compaction effort by 15.4% and briquette density – by 37% on average. Binder addition in the examined range resulted in an approximately 7-fold increase in the mechanical strength of briquettes at all analyzed moisture content levels.

K e y w o r d s: compaction, briquetting, binding agents, calcium lignosulphonate, poplar wood sawdust.

INTRODUCTION

The growing demand for solid biofuels [2, 16] supports the management of various types of by-products from the wood processing industry. Wood shavings, chips, bark, sawdust and wood powder account for 20÷30% of the initial mass of wood intended for processing. Most of those materials are characterized by problematic structure, low bulk density and low energy density, which is why they have to be processed into pellets or briquettes [5, 9, 10, 11].

Sawdust is a valuable raw material for the production of compacted biofuels. The particle size distribution of sawdust is generally suitable for pressure compaction without the need for further disintegration [1]. Sawdust from the wood of both coniferous and deciduous trees is used in the production process. Waste and by-products originating from various tree species have different lignocellulose composition. The most important consideration in the compaction process is lignin content whose average share in deciduous trees is 5% lower than in coniferous trees. Lignin is a natural binder which aggregates briquettes [18, 19, 20]. Sawdust from various tree species is often mixed in the production process to level out its lignin content. The above prevents technological problems, and it gives end products the required mechanical strength [3].

The above problem can also be solved by using organic and synthetic binders [12, 15]. Those compounds bind comminuted components (by acting like glue), thus improving the stability and quality of briquettes. As a result, the mechanical strength of briquettes is improved and the amount of energy required for the production process is reduced. Lignin binders are the most effective solution for compacting biological materials. They contain calcium and sodium lignosulphonates, processed starch and fatty acids. Lignin binders are used at various doses which generally do not exceed 3% of the material's weight. In line with the applicable regulations, the content of lignin binders in the production of solid biofuels should not exceed 2%. The discussed binders do not have a negative impact on biofuel combustion because they are burned in their entirety without producing additional ash, and they are completely neutral for the environment.

Binders improve material viscosity and lower its sensitivity to moisture, which supports the briquetting of materials with a higher moisture content without the risk of disintegration. This is an important consideration because sawdust from furniture and carpentry plants contains 10% to 20% of water on average. Sawdust from wet wood processed in sawmills is characterized by 50% moisture content, and it has to be dried to achieve a suitable moisture level for compacting [4, 8, 13, 17].

In view of the above, the objective of this study was to determine the values of pressure compaction parameters characterizing poplar wood sawdust with different moisture content levels and various quantities of a calcium lignosulphonate binder.

MATERIALS AND METHODS

The experimental material was poplar wood sawdust from a sawmill in the Lublin area. Sawdust was dried

in accordance with the requirements of standard PN-EN 14774-1:2010, to achieve a moisture content in the range of 10% to 22% (every 3% +/-0.2%). The required moisture content was determined using an equation for mass change over time based on the following dependence:

$$m_1 = m_0(\frac{100 - w_0}{100 - w_1}) \text{ (g)}, \quad (1)$$

where: m_0 – initial mass of material, g; m_1 – mass of material after drying, g; w_0 – initial moisture content of material, %; w_1 – moisture content of material after drying, %.

The binding agent (calcium lignosulphonate) was added to material samples with a various moisture content in the amount of 0.5%, 1%, 1.5% and 2%. Material without the binder served as the control.

The particle size distribution of sawdust was determined in accordance with standard PN-EN 15149-2:2011 using the SASKIA Thyr 2 laboratory sieve. The density of sawdust with a different moisture content was determined in bulk state according to standard PN-EN 15103:2010.

The material was subjected to pressure compaction in line with the method proposed by Laskowski and Skonecki [6] using the Zwick Z020/TN2S tensile test machine equipped with a pressing unit and a closed die with a cylinder (compaction chamber) diameter of 15 mm. Test parameters were as follows: mass of material sample – 2 g, cylinder (compacted material) temperature - 20ºC, piston speed - 10 mm·min^{-1}, maximum unit piston pressure – 114 MPa. Every compaction process was performed in three replications.

The results were used to develop a curve illustrating the correlation between compaction force and piston displacement. The values of maximum material density in compaction chamber ρ_c and total compactive effort L_c were determined based on the characteristic points of the compaction curve. The coefficient of material susceptibility to compaction k_c was calculated:

$$k_c = \frac{L_c'}{(\rho_c - \rho_n)} \text{ ((J·g}^{-1}\text{)/(g·cm}^{-3}\text{))}, \quad (2)$$

where: ρ_n – initial material density in compaction chamber, g·cm^{-3}; L_c' – unitary compactive effort, J·g^{-1}.

The density of the resulting briquettes was determined after 48 hours of storage ρ_a.

The compaction degree of the analyzed material in the chamber S_{zm} and the compaction of the resulting briquette S_{za} were determined as the quotient of density ρ_c and ρ_a, and initial density in the compression chamber ρ_n ($S_{zm} = \rho_c \cdot \rho_n^{-1}$, $S_{za} = \rho_a \cdot \rho_n^{-1}$). The degree of briquette expansion S_{ra} was calculated as the quotient of density ρ_a and ρ_c ($S_{ra} = \rho_a \cdot \rho_c^{-1}$) to evaluate the decrease in briquette density caused by turning expansion.

The mechanical strength of a briquette δ_m was determined in the Brazilian compression test [7, 14] using the Zwick Z020/TN2S tensile testing machine (with piston speed of 10 mm·min^{-1}). A briquette with diameter d and length l was compressed transversely to the axis until breaking point, and maximum breaking force F_n was determined. Mechanical strength δ_m was calculated using the following formula:

$$\sigma_n = \frac{2F_n}{\pi d l} \text{ (MPa)}. \quad (3)$$

The correlations between the binder content, the moisture content of the examined material and compaction parameters were analyzed in the STATISTICA program at a significance level of $\alpha_i = 0.05$. The form of the equations was selected by reverse stepwise regression. The significance of regression coefficients was determined by Student's t-test. Model adequacy was verified using Fisher's test.

RESULTS

BASIC PHYSICAL PROPERTIES OF MATERIAL

The results of the density of sawdust with different moisture content are presented in Table 1. The obtained data indicate that the bulk density of material in the analyzed range decreased by around -20% with an increase in moisture content.

Table 1. Correlation between the bulk density of material (ρ_s) and moisture content (w)

w (%)	10	13	16	19	22
ρ_s (g·cm^{-3})	0.142	0.137	0.132	0.122	0.114

The results of the particle size distribution of sawdust are presented in Figure 1. Particles measuring 1 to 1.6 mm had the highest percentage share of the analyzed samples, therefore, the material's granulometric composition was appropriate for pressure compaction.

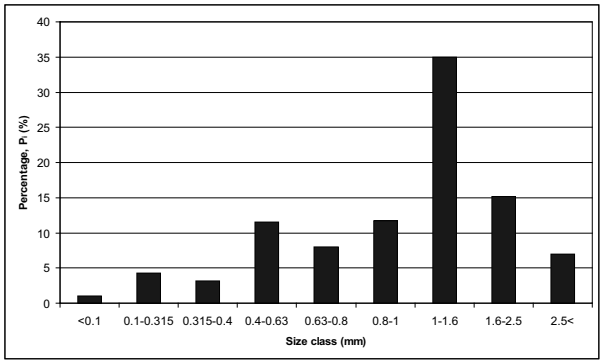

Fig. 1. Particle size distribution (P_i) of the studied material

Multiple regression equations describing the correlations between compaction parameters, the binder content and the moisture content of the experimental material are presented in Table 2. A regression analysis revealed that the studied correlations can be described by a quadratic equation of the second degree or a linear equation. The analyzed correlations are presented in Figures 2-6.

Table 2. Regression equations describing the correlations between density ρ_c, ρ_a, compactive effort L_c, coefficient k_c, degree of compaction S_{zm}, S_{za}, degree of expansion S_{ra}, mechanical strength δ_m and binder content Z_l and material moisture content w, and the values of determination coefficient R^2

Parameter	Regression equation	R^2
Density of material in the chamber, ρ_c	$\rho_c = -0.003Z_l^2 - 0.032Z_l + 0.03w + 0,001Z_l w + 1.391$	0.912
Briquette density after 48., ρ_a	$\rho_a = -0.044Z_l^2 - 0.059Z_l - 0.002w^2 + 0.015Z_l w + 0.837$	0.943
Compactive effort, L_c	$L_c = 3.151Z_l - 1.508w + 63.89$	0.911
Coefficient of susceptibility to compaction, k_c	$k_c = 0.932Z_l - 0.607w + 23.65$	0.956
Degree of material compaction, S_{zm}	$S_{zm} = -0.138Z_l + 0.287w + 8.290$	0.923
Degree of briquette compaction, S_{za}	$S_{za} = -0.369Z_l^2 - 0.61Z_l - 0.011w^2 + 0.135Z_l w + 5.778$	0.904
Degree of briquette expansion, S_{ra}	$S_{ra} = -0.024Z_l^2 - 0.021Z_l + 0.01w + 0.008Z_l w + 0.604$	0.945
Mechanical strength of briquette, δ_m	$\delta_m = 0.341Z_l - 0.037w + 0,875$	0.973

DENSITY OF MATERIAL IN THE CHAMBER AND BRIQUETTE DENSITY

An analysis of the results shown in Figure 2 and regression equations (Table 2) indicated that an increase in binder dose resulted in an insignificant drop in the maximum density of material in the chamber. The above was observed at every moisture level, and a more profound decrease in maximum density was reported at a lower moisture content of 10% and 13%.

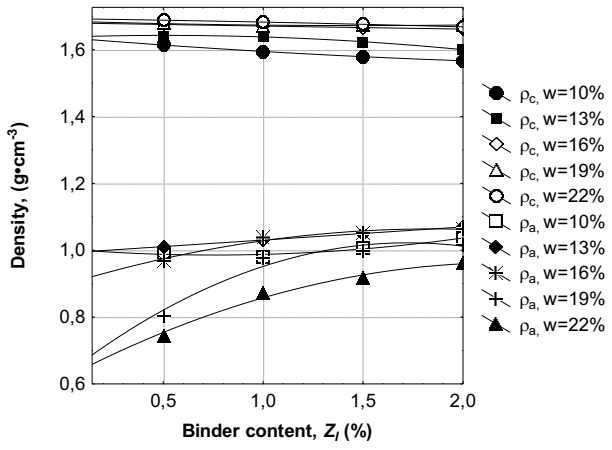

Fig. 2. Correlations between density of material in the chamber (ρ_c), briquette density (ρ_a) and binder content (Z_l) at different moisture content levels (w)

The variation of the analyzed parameter was determined in the range from 1.56 to 1.69 g·cm^{-3}. The highest density was observed in material samples with 22% moisture content.

Briquette density (after turning expansion – 48 h) increased from 0.62 (Z_l=0%; w=22%) to 1.07 (Z_l = 2%; w=13%) with the application of higher binder doses. The analyzed binding agent had the most significant impact on the density of briquettes made of material with a higher moisture content (19% and 22%). 1% and 2% addition of calcium lignosulphonate significantly reduced the effect of moisture content on the values of the examined parameter.

COMPACTIVE EFFORT AND SUSCEPTIBILITY TO COMPACTION

The application of higher binder doses probably increased the coefficient of friction between material particles and between particles and the walls of the compaction chamber. The above led to an increase in compactive effort and the coefficient of susceptibility to compaction (Fig. 3).

The value of parameter L_c for the analyzed samples ranged from 30.32 to 54.12 J, and the value of parameter k_c – from 10.82 to 20.02 (J·g^{-1})·((g·cm^{-3}))$^{-1}$. The values of the studied parameters were highest for the maximum binder dose (2%) and the lowest moisture content (10%). The above indicates that sawdust with a higher moisture content and without the addition of a binding agent is more susceptible to compaction.

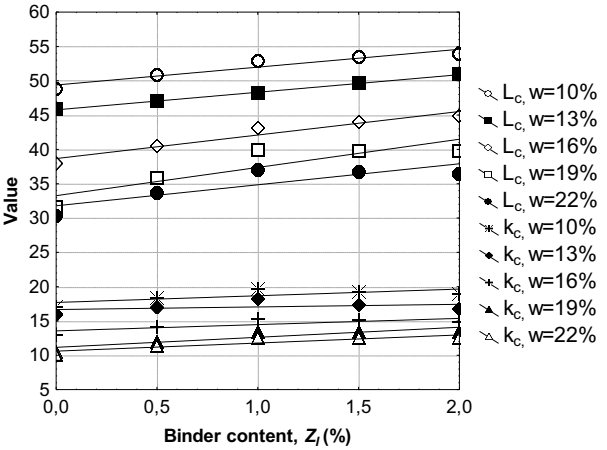

Fig. 3. Correlations between compaction effort (L_c), the coefficient of susceptibility to compaction (k_c) and binder content (Z_l) at different moisture content levels (w)

DEGREE OF BRIQUETTE COMPACTION AND EXPANSION

An analysis of the degree of material compaction in the chamber revealed that binder dose had an insignificant effect on the values of the studied parameter (Fig. 4).

On average, the maximum density of material in the chamber ρ_c was 13-fold higher than initial material density ρ_n. The highest maximum density was reported in material samples with 22% moisture content.

The results of briquette compaction analysis (Fig. 4) indicated that the density of a stored product was around 5-fold higher than the initial density in samples with 22% moisture content and no binder to around 8-fold higher one in samples with 2% binder content and the same moisture content. Binder addition increased the density of products made of materials with a higher moisture content. The highest compaction values were noted in briquettes made of material with 19% and 22% moisture content with 1%-2% addition of binder.

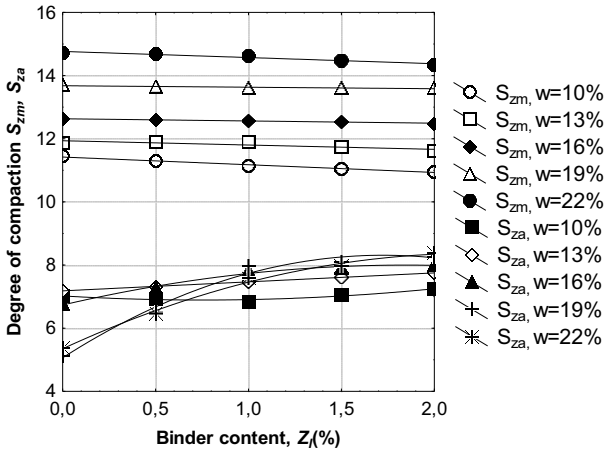

Fig. 4. Correlations between the degree of material compaction (S_{zm}), the degree of briquette compaction (S_{za}) and binder content (Z_l) at different moisture content levels (w)

The results of briquette expansion tests confirm the above observations (Fig. 5). In briquettes made of material with 19% and 22% moisture content, the addition of higher binder doses increased the analyzed parameter two-fold (from around 0.37 to around 0.6).

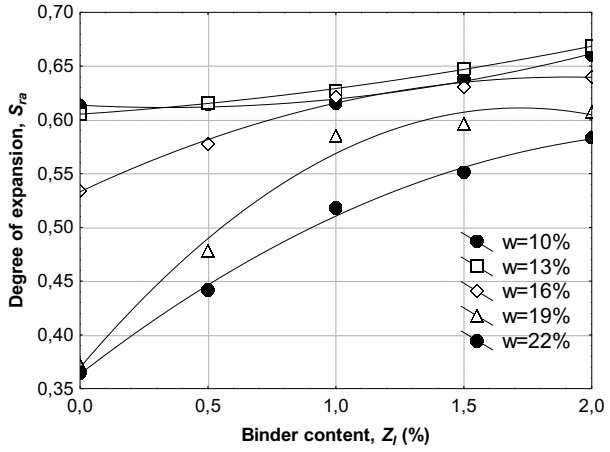

Fig. 5. Correlations between the degree of briquette expansion (S_{ra}) and binder content (Z_l) at different moisture content levels (w)

BRIQUETTE STRENGTH

The results of strength tests indicate that the mechanical strength of briquettes increased with the addition of a binding agent to poplar sawdust (Fig. 6).

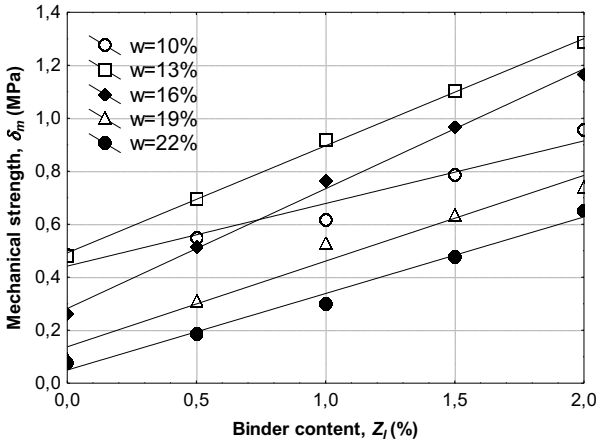

Fig. 6. Correlations between the mechanical strength of briquettes (δ_m) and binder content (Z_l) at different moisture content levels (w)

Mechanical strength values were determined in the range of 0.07 to 1.29 MPa. The highest strength values were reported in briquettes made of sawdust with 13% moisture content, and the lowest – in products with 22% moisture content, at every binder dose. It should be noted, however, that 1.5% addition of the binder to material with 22% moisture content produces briquettes whose strength is identical to that of products made of pure sawdust with 13% moisture content.

CONCLUSIONS

The following conclusions can be formulated based on the results of this study:

The addition of a binding agent in the analyzed dose range decreased the maximum density of material in the compaction chamber by an average of -4.1%, and increased briquette density by an average of 37%.

Sawdust's susceptibility to compaction decreased with a rise in binder dose. Compaction effort (with a binder content of 0%-2%) increased by 15.4%, and coefficient k_c increased by 12.5%, on average.

The degree of briquette compaction and expansion increased with a rise in binder dose at every binder content level. The highest increase was reported in the material with 19-22% moisture content where parameter S_{za} increased by 56.6% and parameter S_{ra} – by 61.1%, on average.

An increase in binder content led to an approximate 7-fold rise in the mechanical strength of briquettes, regardless of the moisture content of the investigated material.

REFERENCES

1. **Hejft R., 2002:** Ciśnieniowa aglomeracja materiałów roślinnych. Politechnika Białostocka. Wyd. i Zakład Poligrafii Instytutu Technologii Eksploatacji w Radomiu.

2. **Junginger M., Bolkesjø T., Bradley D., Dolzan P., Faaij A., Heinimö J., Hektor B., Leistad Ø., Ling E., Perry M., Piacente E., Rosillo-Calle F. Ryckmans Y., Schouwenberg P.P., Solberg B., Trømborg E., da Silva Walter A., de Wit M., 2008:** Developments in international bioenergy trade. Biomass and Bioenergy, 32, p. 717-729.
3. **Kaliyan N., Morey V.R., 2009:** Factors affecting strength and durability of densified biomass products. Biomass and Bioenergy, 33, p. 337-359.
4. **Kulig R., Laskowski J., 2011:** The effect of preliminary processing on compaction parameters of oilseed rape straw. Teka Komisji Motoryzacji I Energetyki Rolnictwa, vol. 11, p. 209-217.
5. **Leaver, R.H., 1988:** The pelleting process. Sprout-Bauer, Muncy, PA.
6. **Laskowski J., Skonecki S., 2001.** Badania procesów aglomerowania surowców paszowych – aspekt metodyczny. Inżynieria Rolnicza, nr. 2(22), p. 187-193.
7. **Li Y., Wu D., Zhang J., Chang L., Wu D., Fang Z., Shi Y., 2000.** Measurement and statistics of single pellet mechanical strength of differently shaped catalysts. Powder Technology, 113, p. 176-184.
8. **MacMahon M.J., Payne J.D., 1991:** The Pelleting Handbook. Borregaard Lignotech, Sarpsborg Norway.
9. **Mani S., Tabil L., G., Sokhansanj S., 2003:** An overview of compaction of biomass grinds. Powder Handling and Processing, vol. 15, p. 160-168.
10. **Mani S., Tabil L.G., Sokhansanj S., 2006.** Effects of compressive force, particle size and moisture content on mechanical properties of biomass pellets from grasses. Biomass and Bioenergy, 30(7), p. 648-654.
11. **Niedziółka I., Szymanek M., Zuchniarz A., Zawiślak K., 2008:** Characteristics of pellets produced from selected plant mixes. Teka Komisji Motoryzacji I Energetyki Rolnictwa, vol. 8, p. 157-162.
12. **Restolho J.A., Prates A., de Pinho M.N., M.D., 2009:** Sugars and lignosulphonates recovery from eucalyptus spent sulphite liquor by membrane processes. Biomass and Bioenergy, vol. 133, p. 1558-1566.
13. **Relova I., Vignote S., León M. A., Ambrosio Y., 2009:** Optimisation of the manufacturing variables of sawdust pellets from the bark of Pinus caribaea Morelet: Particle size, moisture and pressure. Biomass and Bioenergy, 33, p. 1351-1357.
14. **Ruiz G., Ortiz M., Pandolfi A., 2000.** Three-dimensional finite-element simulation of the dynamic Brazilian tests on concrete cylinders. Int. J. Numer. Meth. Engng., 48, p. 963-994.
15. **Sahoo S., Seydibeyo_M.O., Mohanty A.K., M. Misra M., 2011:** Characterization of industrial lignins for their utilization in future value added applications. Biomass and Bioenergy, vol. 135, p. 4230-4237.
16. **Schenkel Y., Crehay R., Delaunois C., Schummer J., 2003:** The agricultural sector and bioenergy production. Teka Komisji Motoryzacji I Energetyki Rolnictwa, vol. 3, p. 228-235.
17. **Skonecki S., Kulig R., Potręć M., 2011:** Ciśnieniowe zagęszczanie trocin sosnowych i topolowych – parametry procesu i jakość aglomeratu. Acta Agrophysica vol. 18, nr 1, p. 149-160.
18. **Thomas M., van Vliet T., van der Poel A.F.B., 1998.** Physical quality of pelleted animal feed. 3. Contribution of feedstuff components. Anim. Feed Sci. Tech., 70, p. 59-78.
19. **Wood J.F., 1987:** The functional properties of feed raw materials and their effect on the production and quality of feed pellets. Anim. Feed Sci. Tech., 18, p. 1-17.
20. **Van Dam J. E. G., Van den Oever M. J. A., Teunissen W., Keijsers E. R. P., Peralta A. G., 2004:** Process for production of high density/high performance binderless boards from whole coconut husk. Part 1: lignin as intrinsic thermosetting binder resin. Industrial Crops and Products, vol. 19, p. 207-216.

WPŁYW DODATKU LEPISZCZA NA EFEKTYWNOŚĆ ZAGĘSZCZANIA TROCIN TOPOLOWYCH

S t r e s z c z e n i e . Przedstawiono wyniki badań nad określeniem wpływu dodatku lepiszcza w postaci lignosulfonianu wapnia (od 0 do 2%) i wilgotności (od 10 do 22%) na parametry procesu zagęszczania trocin topolowych. W szczególności wyznaczono podatność surowca na zagęszczanie, zmiany gęstości materiału oraz wytrzymałość mechaniczną aglomeratów. Stwierdzono, że wraz ze wzrostem dodatku lepiszcza, rośnie wartość pracy zagęszczania przeciętnie o 15,4%. Natomiast gęstość aglomeratu wzrasta średnio o 37%. Wykazano, iż dodatek lepiszcza w rozpatrywanym przedziale powoduje około 7-krotny wzrost wytrzymałości mechanicznej aglomeratów w odniesieniu do wszystkich analizowanych wilgotności surowca.

S ł o w a k l u c z o w e : zagęszczanie, brykietowanie, lepiszcza, lignosulfonian wapnia, trociny topolowe.

TEKA. COMMISSION OF MOTORIZATION AND ENERGETICS IN AGRICULTURE – 2012, Vol. 12, No. 1, 93–102

Fourier transformation – an important tool in vibroacoustic diagnostics

Waldemar Kurowski

The Department of Mechanical Systems and Automation Engineering
Warsaw University of Technology, Faculty of Building, Mechanics and Petrochemical Industry
Adres: Jachowicza 2/4, 09 – 402 Płock, Poland, qurovski@wp.pl

Summary. The objective feature of the reflection allows for using measurable physical quantities that characterize the processes accompanying the operation of a mechanical device, as signals carrying encoded information. In order to decode this information, the signal has to be retrieved and converted into a characteristic, usually determined in frequency domain. Using the DFT procedure, the computer allows for calculations of the estimates of frequency characteristics. For the effective use of the numerical methods, one needs to know how the information encoded in the signal is generated during its processing. In order to investigate these problems, a model that reflects the A/C conversion and the periodization of the fragment of retrieved signal in a closed time frame was used. The investigation of this model has shown that the DFT procedure generates stripes representing the harmonic waves of a signal only for admissible frequencies, equal to the total multiplicity of the inverse of signal retrieval time. To present the wave of another frequency, the DFT procedure generates a substitute spectrum. Consequently, the discrete spectrums are a result of a superposition of waves representing the harmonic signal components of frequencies that belong to the admissible set as well as waves of frequencies that do not belong to this set and form substitute spectrums.

Key words: vibroacoustic diagnostics, numerical signal processing, Fourier transformation.

INTODUCTION

For construction and operation of mechanical devices information related to its technical conditions, its properties and processes taking place is necessary. In reference to mechanical devices the obtainment of such knowledge requires a realization of a research process consisting in acquiring and interpretation of information. This is the task of technical diagnostics [4, 5, 9, 10, 11, 14].

A reliable source of information on a mechanical device is research. It is known that 'the matter-characteristic, objective feature of the reflection is shown through generating and conveying information on the conditions of objects of the material world' [17]. This feature allows using measurable physical quantities that characterize the processes accompanying the operation of a device as diagnostic signals carrying encoded information. In order to decode this information the signal has to be retrieved and converted into a characteristic.

Most of the processes occurring in a device in operation that are the sources of the signals are series of events that repeat periodically. That is why the characteristics of these signals are usually determined in the frequency domain.

Computers of high computational power and modern algorithms allow cheap and quick calculations of different, sometimes very complex frequency characteristics of the diagnostic signal through numerical methods. For the effective use of the numerical methods of signal processing one needs to know how the information encoded in the signal is generated during its processing and how the information is distorted and presented in the signal characteristics.

THE SUBJECT OF INVESTIGATION

The subject of the investigation is a mechanical device composed of elements joined in kinematic pairs. An operating device can be perceived as a controlled acting system, schematically presented in figure 1. The system is characterized by an open flow of the stream of mass, energy and information that is divided into two components. The first appears at the output in the form of a working process. The other is an uncontrolled stream of mass, energy and information that accompanies this process. In a correctly functioning device the amount of mass and energy in the second component is miniscule in comparison to the mass and energy of the first one. Yet, the flow of information related to the functioning principle is similar to the first component [10, 17].

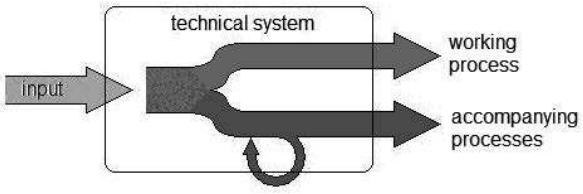

Fig. 1. Flow of stream of mass, energy and information

The second component of the flow stream appears in the form of processes that accompany the operation of the device. The most important are: deterioration, vibroacoustic and thermal processes. The cause-and-effect relation between the symptoms that characterize the conditions of the device and the processes that take place in this device as well as the relation between the processes emitted to the outside allows using 'reflection' for diagnostic purposes. The physical quantities that characterize these processes are used as signals carrying information on the device.

During the operation sources of wave distortions located in various kinematic pairs and parts of the mechanical device activate. Some of them have been shown in figure 2.

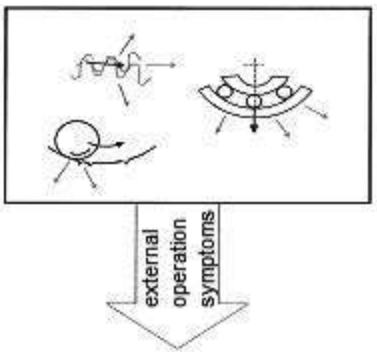

Fig. 2. Sources of wave distortions

The wave distortions generated by the sources, marked with $x_1(t),.....,x_n(t)$ in figure 3 are subject to feedback through propagation. Between the sources and the output of the system representing the investigated device forms a channel of flow of information. At the output of the channel appears signal $\vec{y}(t)$ whose coordinates are the selected physical quantities [10, 11].

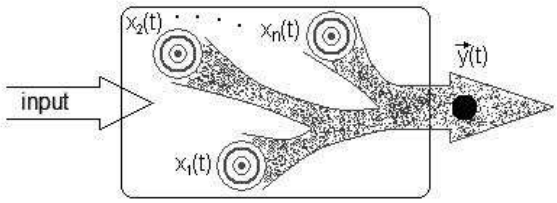

Fig. 3. The channel of the flow of information

In practice, individual time realizations of these quantities are used as diagnostic signals. The amount of information included in realization $f(t)$ depends on its versatility that shows through changes in time. Each change is one bit of information. The higher the frequency of these changes the more information in a time unit will be conveyed to the output of the flow channel. In this case the vibroacoustic signals (mechanical and acoustic vibrations) are the best choice out of all signal emissions by the operating device. An additional advantage of these signals is their accessibility outside of the device without distorting their operation [2,10, 17].

FOURIER TRANSFORM

In 1807, the baron Jean-Baptiste Joseph Fourier, a mathematician, engineer, member of the French Academy presented an essay treating on the fact that periodic, linear function $f(t)$ fulfilling the Dirichlet conditions can be expressed as a sum of series:

$$f(t) = a_0 + \sum_{n=1}^{\infty}\left(a_n \cos 2\pi\nu nt + b_n \sin 2\pi\nu nt\right), \quad (1)$$

where: $a_0 = \frac{1}{T}\int_{-T/2}^{T/2} f(t)dt$, $a_n = \frac{2}{T}\int_{=T/2}^{T/2} f(t)\cos 2\pi\nu ntdt$, $b_n = \frac{2}{T}\int_{-T/2}^{T/2} f(t)\sin 2\pi\nu ntdt$.

Coefficient a_0 is an average value, a_n, b_n are the coefficients of the harmonic distribution of function $f(t)$. Index $n = 1,2,...,\infty$ denotes the expressions of the series, T – period of function $f(t)$, $\nu = 1/T$ - frequency. Because: $\nu_n = \nu n = n/T$ and $\nu_{n+1} = \nu(n+1) = (n+1)/T$ the increment $\Delta\nu = \nu = 1/T = const$. Equation (1) presents function $f(t)$ as an infinite sum of cosine and sine functions of discrete frequencies growing by a step of $\Delta\nu$.

We can assume that for the non-periodic function $T\rightarrow\infty$, then $\Delta\nu\rightarrow d\nu$. Taking this assumption into account, after transforming series (1), we obtain a formula for the Fourier Transform [1, 3, 13]:

$$\mathbf{F}(\nu) = \int_{-\infty}^{\infty} f(t)\exp(-j2\pi\nu t)dt\,. \quad (2)$$

The integral (2) is a functional, in which the nucleus $\exp(-j2\pi\nu t)$, in function $f(t)$ seeks a harmonic wave of the frequency of $\nu\in[0,\infty)$ and describes it with a complex number, containing the time-averaged $t\in(-\infty,\infty)$ information on the amplitude and phase of this wave. In the complex coordinate system this number determines the point that is the end of a vector (in this paper the complex values will be typed in bold):

$$\mathbf{F}(\nu) = a(\nu)+jb(\nu), \quad (3)$$

of the phase module and angle:

$$\left|\mathbf{F}(\nu)\right| = \sqrt{a^2(\nu) - b^2(\nu)}, \quad (4)$$

$$\Psi(\nu) = arctg[b(\nu)/a(\nu)] + \pi m, \text{ where } m = 0,\pm1,\pm2,\ldots.$$

Vector **F**(v) presented in figure 4 is a spectrum of the harmonic wave of frequency v_n contained in function $f(t)$. Because operation (2) of the transformation of function $f(t)$ is repeated for all frequencies from the range $[0,\infty)$, transform **F**(v) show the course of signal $f(t)$ in the frequency domain.

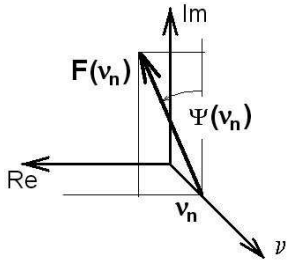

Fig. 4. The spectrum of the harmonic component of function $f(t)$

Using the phase module and angle from dependence (4), equation (3) can be notated according to the Euler theorem in the trigonometric form:

$$\mathbf{F}(v) = \left|\mathbf{F}(v)\right|\cos\psi(v) \pm j\left|\mathbf{F}(v)\right|\sin\psi(v) = \left|\mathbf{F}(v)\right|\exp[\pm j\psi(v)]. \quad (5)$$

Hence:

$$a(v) = \left|\mathbf{F}(v)\right|\cos\psi(v),\ -b(v) = \left|\mathbf{F}(v)\right|\sin\psi(v). \quad (6)$$

In the system of three coordinates: real part $a(v)$, imaginary unit $jb(v)$, frequency v - continuous course of the Fourier transform is a place of the geometrical end of vectors **F**(v) just like the ones in figure 4, distributed on the axis of frequency every $dv \to 0$. Taking the dependences (4) into account, we can present the transform in the form of two courses: module spectrum $\left|\mathbf{F}(v)\right|$ and spectrum of the phase angle $\psi(v)$.

Time realization $f(t)$ is always a real function of time. The results of the Fourier transformation of such a function will be a complex transform. Knowing the course of the cosine and sine functions we can prove that $a(v) = a(-v)$ and $-b(v) = b(-v)$. The Fourier transform of the real function fulfills the Hermite conditions. This means that the real part is even and the imaginary unit is odd. As a consequence the course of the module is an even function: $\left|\mathbf{F}(v)\right| = \left|\mathbf{F}(-v)\right|$ and the course of the phase angle is an odd function: $-\psi(v) = \psi(-v)$ [1, 3].

Time realization $f(t)$ and Fourier transform **F**(v) remain in the equivalence relation. The equivalent pair $f(t) \Leftrightarrow \mathbf{F}(v)$ fulfills the theorems of linearity and additiveness and mutual symmetry. The transform of the product of two functions $f_1(t) \cdot f_2(t)$ equals to the wreath product (convolution) of their transforms $\mathbf{F}_1(v)^*\mathbf{F}_2(v)$; the reverse theorem is also true.

THE MEASUREMENT WINDOW

An infinite period of function $f(t)$ manifests through infinite boundaries of integration of transformation (2). In diagnostic research of mechanical devices we retrieve a fragment of a signal $f(t)$:$t \in [-T/2, T/2]$. The finite retrieving time T becomes a basic period of function $f(t)$ and determined the frequency of the periodization of the retrieved fragment: $v_T = 1/T$. This is contrary to the assumption that $T \to \infty$ for non-periodic function $f(t)$ that the basis for the transformation of series (1) to the form of an integral (2) [1, 6, 8, 10].

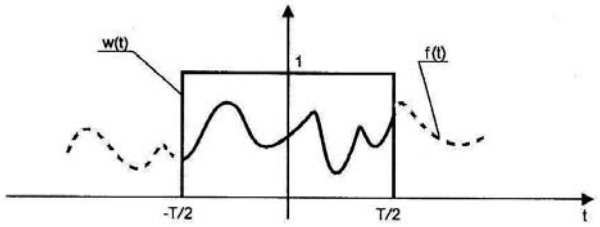

Fig. 5. Diagnostic signal in the measurement window

Range $[-T/2, T/2]$ determines a rectangular measurement window such that: $w(t) = 1$ for $t \in [-T/2, T/2]$ and $w(t) = 0$ for $t \notin [-T/2, T/2]$ presented in figure 5. The Fourier transformation is performed on signal $f(t)$:$t \in [-T/2, T/2] = [f(t):t \in (-\infty,\infty)] \cdot w(t)$:

$$\int_{-\infty}^{\infty} [f(t) \cdot w(t)] \cdot \exp(-j2\pi vt)dt, = \int_{T/2}^{T/2} f(t) \cdot \exp(-j2\pi vt)dt = \mathbf{F}(v)^* \mathbf{W}(v). \quad (7)$$

where the transform of the rectangular measurement window was $w(t)$:

$$\mathbf{W}(v) = \int_{-\infty}^{\infty} w(t)\exp(-j2\pi vt)dt = \int_{-T/2}^{T/2} \exp(-j2\pi vt)dt = T\frac{\sin \pi vT}{\pi vT}. \quad (8)$$

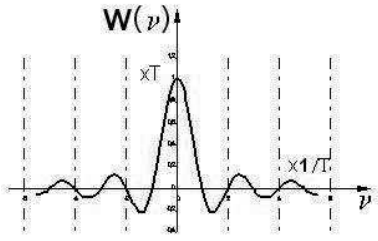

Fig. 6. Transform of the rectangular measurement window

The course of the transform **W**(v) for $v = 0$, presented in Figure 6, is suspended on the abscissa of the coordinate system. If signal $f(t)$ contains harmonic component of this frequency and amplitude that equals one then

this component should manifest in figure 6 in the form of a stripe of module spectrum $|\mathbf{F}(\nu)|$ on the ordinate. Because the signal was retrieved in finite time T, then as a result of the convolution (7) the stripe of the spectrum will be represented by local maximum of the course $\mathbf{W}(\nu)$ for $\nu = 0$. Because for $\nu \to 0$ $\lim \frac{\sin \pi \nu T}{\pi \nu T} = 1$ value T determines the scale that will adjust the height of this maximum against the length of the stripe.

In the spectrum of the module of the actual signal, the stripes denoting the amplitudes of the individual harmonic components occur for different frequency ν_n, where $n = 1,2,3,...$. The expression (8) will take the form:

$$\mathbf{W}(\nu) = T \frac{\sin \pi(\nu - \nu_n)T}{\pi(\nu - \nu_n)T}. \tag{9}$$

The stripe of the module spectrum for $\nu = \nu_n$ will be distorted by the rectangular measurement window identically as the stripe for $\nu = 0$.

The rectangular measurement window effect shows as a leakage and lateral waves of the Fourier transform of signal $f(t):t\in[-T/2,T/2]$. The leakage makes the differentiation of the neighboring stripes difficult and sometimes impossible and the lateral waves distort their value.

THE PROCESSING PRINCIPLES OF VIBROACOUSTIC SIGNALS

The time realization retrieved as a diagnostic signal is in fact an ergodic and stochastic process $f(\zeta,t)$, where: t – time, ζ - random variable. In a sufficiently long range function $f(t):t\in[-T/2,T/2]$ carries encoded information contained in process $f(\zeta,t)$. The processing that should enable reading of this information consists in determining of the non-random characteristics from function $f(t):t\in[-T/2,T/2]$. It is assumed that in range $[-T/2,T/2]$ this function is linear, stationary and fulfills the Dirichlet conditions [1, 10].

The characteristics can describe signal $f(t):t\in[-T/2,T/2]$ in three domains: value, time and frequency. In the diagnostic of mechanical devices the most frequent sample is the one consisting in transformation of the signal to the frequency domain with the use of the Fourier Integral. This is particularly the case in vibroacoustic signals.

Equivalence $f(t) \Leftrightarrow \mathbf{F}(\nu)$ means that the following relation is true: $|f(t)| \Leftrightarrow |\mathbf{F}(\nu)|^2$. The squared course of the module spectrum is a frequency image of the energy contained in signal *f(t)* and carries information of the intensity of the wave distortions that were activated while the mechanical device was in operation. This information, read and properly interpreted may form a message regarding the technical condition of the parts and kinematic pairs of the device where these sources are located [2, 10].

The sources of distortions are characterized by periodic repeatability of reversible events that manifest as wave phenomena. The values of frequencies determined based on the knowledge of the system composition and structure represented by the device can be deemed as common addresses of spectral components and sources that generated it. The addresses of a given pair source-component are usually different for each pair. The information resulting from relation $|f(t)|^2 \Leftrightarrow |\mathbf{F}(\nu)|^2$ regarding the value of the module of the spectral component of the signal is at the same time information regarding the energy resulting from the intensity of functioning of a given source of distortion. The schematics of the conveyance channel presented in figure 3 shows that signal $f(t):t\in[-T/2,T/2]$ carries information regarding the energy of different sources that are mixed due to mutual feedbacks. Course $|\mathbf{F}(\nu)|$ depicts the frequency decomposition of the signal that allows identifying and estimating the energy generated by given sources. That is why the Fourier transformation is an important tool in signal processing used in vibracoustic diagnostics of mechanical devices.

The computers allow calculations of the estimates of different characteristics that are difficult to determine through direct analogue measurement. The Fourier spectrum is a perfect example here. The database for the calculations of the spectrum is a series of values representing continuous time realizations of signal fragment $f(t):t\in[-T/2,T/2]$ [10, 11, 16].

MODEL OF A DISCRETE SIGNAL

The retrieved time realizations $f(t):t\in[-T/2,T/2]$ are continuous. A series of values from which the computer will calculate the Fourier transform is generated in two phases by the A/C converter from the retrieved signal:

1. sampling that consists in discretization of the function argument: $f(t):t\in[-T/2,T/2]$ in moments: $t_0,t_1,...,t_k,...,t_{N-1} \in[-T/2,T/2]$. The difference: $\Delta t = t_{k+1} - t_k = T_e$ determines the constant period of sampling and the frequency of sampling: $\nu_e = 1/T_e$. Values T and T_e, determine the number of samples: $N = T/T_e$ = int. that will fit into the measurement window,
2. quantization of realization $f(t):t\in[-T/2,T/2]$ in moments: $t_0,t_1,t_2,...,t_{N-1}$ that determines the value of signal $f(kT_e)$ for: $k = 0,1,2,...,N-1$.

The discrete function: $f(kT_e)$ represents a series of subsequent events each of which has an assigned number value. Separately, none of them carries any important information, but a series of N - events in timely order, does. In the database obtained during the A/C conversion information is stored regarding the signal in the measurement window in the moment of sampling. Other information that can exist in the signal is lost.

In order to analyze the process of generating the information during numerical processing we can use a model that reflects the A/C conversion and the periodization of the fragment of the retrieved signal in a closed time frame [10, 12,15]. For the creation of such a model we can use the Dirac comb:

$$\text{Ш}(t) = \bigcup_{\alpha=-\infty}^{\infty} \delta(t - \alpha T_e), \text{ where } \alpha = -\infty,...,-1,0,1,...,\infty,$$

shown in figure 7a. It is a series of impulses evenly distributed on the time axis maintaining a distance equal to signal sampling period $\Delta t = T_e = \text{const}$. The multiplication by the function of window $w(t)$ takes into account the retrieval of the signal of the period of $[-T/2,T/2]$ and limits the number of samples determined by the Dirac impulses to the value N:

$$f^{\bullet}(kT_e) = \left(f(t) : t \in (-\infty,\infty)\right),$$
$$\cdot w(t) \cdot \bigcup_{\alpha=-\infty}^{\infty} \delta(t-\alpha T_e). \tag{10}$$

The periodization of signal (10) we can reflect through convolution of signal $f^{\bullet}(kT_e)$ through Dirac comb Ш'$(t) = \bigcup_{\eta=-\infty}^{\infty} \delta(t-\eta T)$ in which the impulses are distributed on the time axis every $\Delta t = T = \text{const}$. and are numbered with an index: $\eta = -\infty,...,-1,0,1,2,...,\infty$:

$$f(kT_e) = \left(f(t) : t \in (-\infty,\infty)\right)$$
$$\cdot w(t) \cdot \bigcup_{\alpha=-\infty}^{\infty} \delta(t-\alpha T_e) * \bigcup_{\eta=-\infty}^{\infty} \delta(t-\eta T). \tag{11}$$

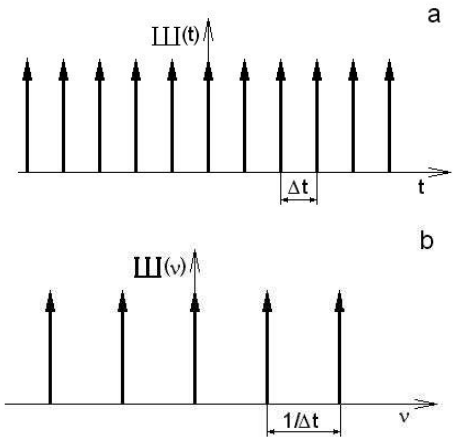

Fig. 7. Dirac comb in the time and frequency domain

Signal $f(kT_e)$ for $k = 0,1,2,...,N-1$ is a series of events that is why operations (10) and (11) marked ∪, are not algebraic addition but a summing of events.

DISCRETE FOURIER TRANSFORM

Taking into account the theorem on the transform of the algebraic product and convolution of two functions the Fourier transformation of signal $f(kT_e)$ can be notated as follows:

$$\mathbf{F}(\nu) = [\int_{-T/2}^{T/2} f(t)\exp(-j2\pi\nu t)dt \cdot \int_{-\infty}^{\infty} [Ш'(t)]\cdot\exp(-j2\pi\nu t)dt]* \int_{-\infty}^{\infty} [Ш(t)]\cdot\exp(-j2\pi\nu t)dt. \tag{12}$$

The Fourier integral from $-T/2$ to $T/2$ takes into account the algebraic multiplication through window $w(t)$. The result of the integration is the convolution of the function $f(t)\in(-\infty,\infty)$ transform and the transform of the rectangular measurement window occurring on the right side in formula (7).

The Fourier transform of the Dirac comb that is determined in the time domain remains the Dirac comb in the frequency domain [15]. It has a form of distribution of a period of $1/\Delta t$, shown in figure 7b. The transforms Ш(t) and Ш'(t) will be respectively:

$$\mathbf{Ш}(\nu) = \nu_e \bigcup_{\alpha=-\infty}^{\infty} (\delta - \alpha\nu_e), \quad \mathbf{Ш}'(\nu) = \nu_T \bigcup_{\eta=-\infty}^{\infty} (\delta - \eta\nu_T),$$

where: $\nu_e = 1/\Delta t = 1/T_e$, $\nu_T = 1/\Delta t = 1/T$ and $\alpha,\eta = -\infty,...,-1,0,1,...,\infty$.

Algebraic multiplication through comb **Ш**'(t) will result in a discretization of the spectrum to the form of a series of vectors referred to as stripes. Value $\nu_T = 1/T$ determines a constant distance between the stripes and determines the discrete spectrum resolution. The values $\eta\nu_T$ determine frequencies for which these stripes can appear. The rectangular measurement window limits the number of stripes to value N.

The convolution by **Ш**(ν) results in a periodization of the discrete spectrum. It is shown as a reproduction of the spectrum every ν_e value for an infinite number of times because $\alpha,\eta = -\infty,...,-1,0,1,...,\infty$. Frequencies ν_T and ν_e, occurring before the sums of events in the transforms of the Dirac combs **Ш'**(ν) and **Ш**(ν) determine the scale of the multiplication operation and do not influence the way the discrete spectrum is formed.

Figures 8a, b and c show the process of the formation of the discrete spectrum of the module of the tested signal represented by the real function of time.

According to the Hermit conditions, the spectrum of the module of the real function is even. In figure 8a spectrum $|\mathbf{F}(\nu)|$ and its even reflection $|\mathbf{F}(-\nu)|$ are symmetrical and form a unity that as a result of periodization is 'suspended' on the abscissa determined by stripes $0\cdot\nu_e$ and $1\cdot\nu_e$. The reproduction of the spectrum results in that the information in all ranges $[\alpha\cdot\nu_e, (\alpha+1)\cdot\nu_e)$, where $\alpha,\eta = -\infty,...,-1,0,1,...,\infty$ will be the same. That is why for the considerations only one range needs to be included: $[0,\nu_e)$. In this range $N = \nu_e/\nu_T$, stripes will fit that are numbered with index $n = 0,1,...,N-1$.

In figure 8b spectrum $|\mathbf{F}(\nu)|$, suspended on abscissa $\nu_e = 0\cdot\nu_e$ and its left hand reflection $|\mathbf{F}(-\nu)|$ suspended on abscissa $\nu_e = 1\cdot\nu_e$ are subject to superposition in frequency range $[0,\nu_e)$. The determined spectrum is a sum of superimposed courses: $|\mathbf{F}(\nu)|$ and $|\mathbf{F}(-\nu)|$. This phenomenon is called aliasing.

The middle of range $[0,\nu_e)$ is determined by the Nyquist frequency: $\nu_{Nyq} = 0{,}5\nu_e$. If in spectrum $|\mathbf{F}(\nu)|$ that is suspended on stripe $0\cdot\nu_e$ occurs a local maximum for frequency $\nu>\nu_{Nyq}$ then, due to symmetry, the same maximum will occur in spectrum $|\mathbf{F}(-\nu)|$, suspended on stripe

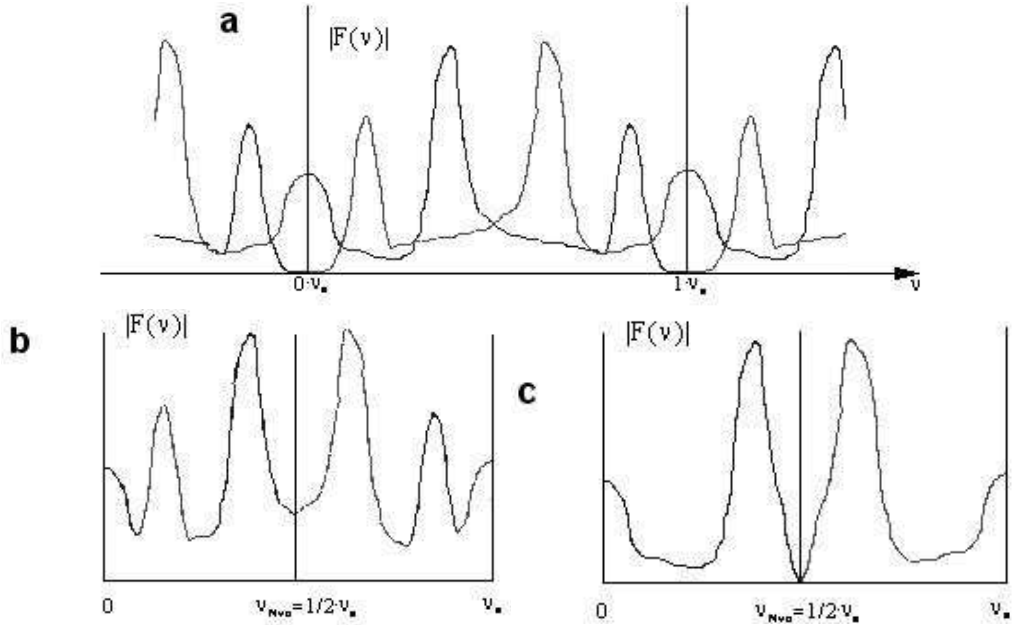

Fig. 8. Periodization, aliasing and filtering of the discrete spectrum

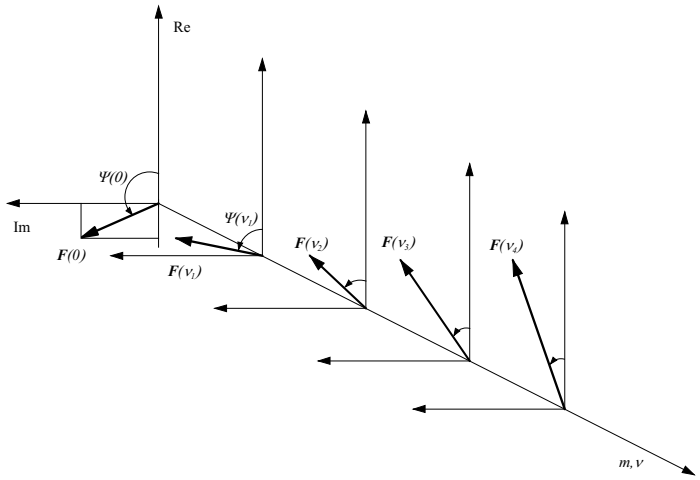

Fig 9. Signal discrete spectrum

$1 \cdot v_e$, for $v < v_{Nyq}$. As a result of aliasing in frequency range $[0, v_{Nyq})$ spectral information will be conveyed that is not contained in the signal. If we want to avoid that, we should use a low-pass filter of the signal that will damp the harmonic components of frequencies equal or greater than the Nyquist frequencies as shown in figure 8c.

If signal $f(kT_e)$ determined by formula (11) is subjected to low-pass filtering then in frequency range $[0, v_{Nyq})$ then at the most $N/2$ of the stripes of the discrete spectrum will fit that are numbered with an index: $n = 0,1,2,...,N/2-1$.

Replacing the integration with addition after $k = 0,1,2,...,N-1$ and substituting time and frequency in the discrete form from dependence (12) we can derive a formula for the discrete Fourier transform:

$$\mathbf{F}(nv_T) = \frac{1}{T}\sum_{k=0}^{N-1} f(kT_e) \cdot \exp(-j2\pi n v_T k T_e). \qquad (13)$$

In the dimensionless domain of indexes k and n, transformation (13) takes the form of Discrete Fourier Transform (DFT):

$$\mathbf{F}(n) = \frac{1}{N}\sum_{k=0}^{N-1} f(k) \cdot \exp(-j2\pi nk / N). \qquad (14)$$

Dependence (14) shows a system of equations for $n = 0,1,2,...,N/2-1$. The results of the solution of each equation is transform $\mathbf{F}(n)$ in the form of a complex number that determines the module and phase angle of a single stripe of a spectrum for frequency nv_T. The whole spectrum is a sum of harmonic components of a signal occurring on the frequency axis for values nv_T:

$$\mathbf{F}(v_n) = \bigcup_{n=0}^{N/2-1} \mathbf{F}(n). \qquad (15)$$

Figure 9 presents the signal discrete spectrum calculated from the DFT dependence.

SPECTRUM OBTAINED THROUGH THE DFT METHOD

While generating spectrum **F**(n) of signal $f(k)$ the discretization with period T_e results in a periodization of the spectrum with period $v_e = 1/T_e$. Sampling frequency $v_e = 1/T_e$ determines band $[0, v_{Nyq} = 1/2v_e)$ where the stripes of the discrete spectrum are contained.

The periodization of the signal $f(k)$ with period T results in a discretization of the spectrum with resolution $v_T = 1/T$. The DFT procedure generates stripes only for admissible frequencies nv_T of values equal to the total multiplicity of the inverse of signal retrieval time. The strips carrying original information on the harmonic components of the signal, are numbered with index $n = 0,1,2,...,N/2–1$.

The frequency structure of the signals generated by the sources of wave distortions that function in mechanical devices is unknown. The frequencies of the harmonic components that form the signal depend on the physical nature of the sources and they are independent from value T and $v_e = 1/T_e$. That is why we should expect that the frequencies of many components (possibly all) of the retrieved signal would not belong to the admissible set [7, 10, 11].

Figure 10a shows the signal in the form of a harmonic wave that was subjected to a discrete Fourier transformation. Because the retrieval time $T = n \cdot T_{f.h.}$ where $n = 2$ and $T_{f.h.}$ - the period, the frequency of the wave belongs to the admissible set. The spectrum of the module, presents the stripe for $n = 2$ shown in figure 10b. The reduction of time T results in that $T \neq n \cdot T_{f.h.}$ and frequency $v_T = 1/T$ of the wave does not belong to the admissible set. In order to present this wave the DFT procedure generates a substitute spectrum in the form of a set of waves of admissible frequencies that do not exist in the signal. The local maximum of the substitute spectrum shown in figure 10c occurs for admissible frequencies close to the value of $1/T_{f.h.}$. We can expect that the result of the superposition of waves of the substitute spectrum will be the approximate course of the signal.

The analysis of the results presented in Figure 10 gives grounds for a formulation of the following hypothesis: the waves of the discrete substitute spectrum are determined by the DFT procedure according to the Fourier series for a preset and limited set of admissible frequencies nv_T. The trueness of the hypothesis can be verified through comparing the spectrum of the signal obtained from the development into a Fourier series with the spectrum of this signal calculated with the DFT method.

After a transformation of the sum of the cosine and sine function in formula (1) the Fourier series can be notated in the form of a sine function taking into account the phase angle:

$$f(k) = \sum_{n=0}^{N/2-1} A_n \sin\left(\frac{2\pi nk}{N} + \psi_n\right). \tag{16}$$

In series (16) function $f(k)$ where $k = 0.1,2,...,N–1$ represents a discrete form of the investigated wave $f(t) = A\sin 2\pi vt$ retrieved in finite time T. The argument of the sine function determines the dimensionless domain of admissible frequencies that belong to range $[0, v_{Nyq})$ marked with index: $n = 0,1,2,...,N/2–1$. In comparison to series (1), in formula (16) the summing was limited to $N/2$ of the components. Symbol ψ_n denotes the phase angle of the n–th component of function $f(k)$.

Because in the experiment $T = const$ was assumed, the set of admissible frequencies preset for the development of function $f(k)$ will be constant. In order to obtain information that could confirm (or reject) the assumed hypothesis one should investigate different substitute spectrums. To this end we need to ensure the possibility of modification of the wave frequency without changing the retrieval time.

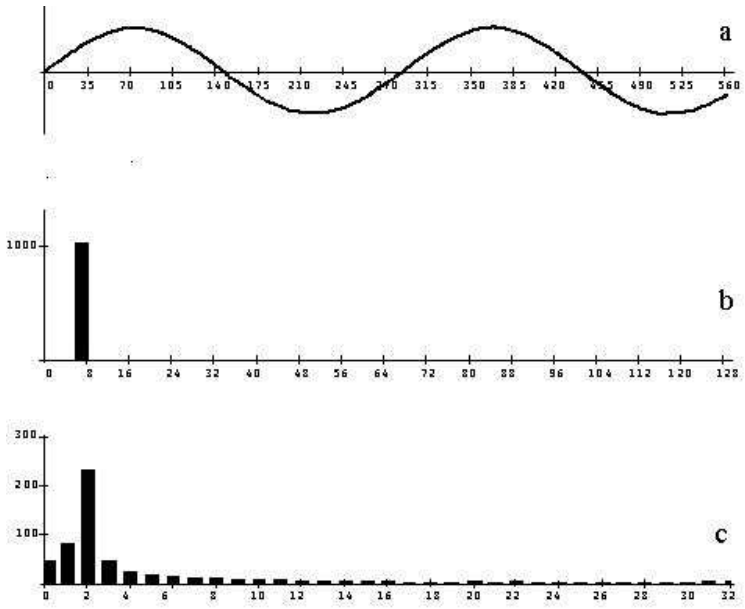

Fig. 10. The signal, its real and substitute spectrum

Let wave frequency $v = (1+\varepsilon)/T$. Then for $\varepsilon = 0$ - a single wave period equals T and its frequency $v \equiv v_T = 1/T$. For each value $\varepsilon \in (0,1)$ maintaining a constant retrieval time the frequency of the wave will not belong to the admissible set. After substituting the dependence: $v = (1+\varepsilon)/T$, $T = NT_e$ and $t = kT_e$, the argument of the sine function in formula (16), assumes the form $2\pi(1+\varepsilon)k/N$. Then:

$$f(k) = A\sin 2\pi(1+\varepsilon)\frac{k}{N} \tag{17}$$

Wave $f(k)$ has been determined for $A = 1$ and $N = 16$ samples numbered with index: $k = 0,1,2,...,15$. The modified wave presented in figure 11 was generated for: $\varepsilon = 2/3$. Taking the Nyquist criterion into account the spectrum was determined for $N/2-1$ of the frequencies marked with index $n = 0,1,...,7$.

Substitute spectrums of the module of the investigated wave calculated from the Fourier series and through the DFT method have been presented in figure 12. The stripes superimposed on the admissible frequency mesh show a spectrum obtained from formula (16) and the stripes in the immediate vicinity through the DFT method. The height of the stripes obtained with two methods is identical, which is confirmed by the adopted hypothesis.

DISCRETE SPECTRUM DISTORTION

The average value of the original wave of $\varepsilon = 0$, represented by the component of the spectrum for $n = 0$, equals zero. The performed modification of the frequency of this wave results in an unintended and incidental change of the average value of the retrieved fragment of the signal. That is why in the substitute spectrum in figure 12 the stripes for $n = 0$ are non-zero.

In figure 11 the axis of abscissa has been shifted so that the average value of the fragment of the wave for $\varepsilon = 2/3$ equaled zero. Figure 13 presents the courses of the discrete spectrum of the module of this fragment of the wave after shifting the axis of abscissa. The component of the spectrum for $n = 0$ equals zero and the stripes representing the outstanding components are the same as in figure 12 before the shift has been carried out.

From the course of transform $\mathbf{W}(v)$ in figure 6 and dependence (8) results that for the admissible frequencies n/T nv_T when $n = 1,2,... = \text{int}$, complex integer $\mathbf{F}(v)*\mathbf{W}(v) = 0$ because $\mathbf{W}(v) = 0$. For $n = 0$, this product is other than zero and the transform of the window influences the stripe of the spectrum through change of the scale. Formula (9) confirms that this statement is correct

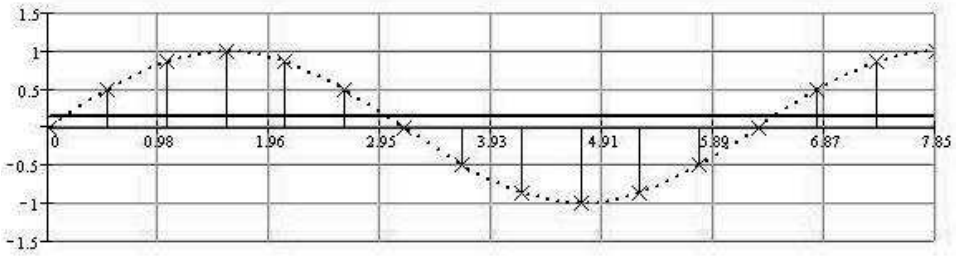

Fig. 11. Wave for $\varepsilon = 2/3$

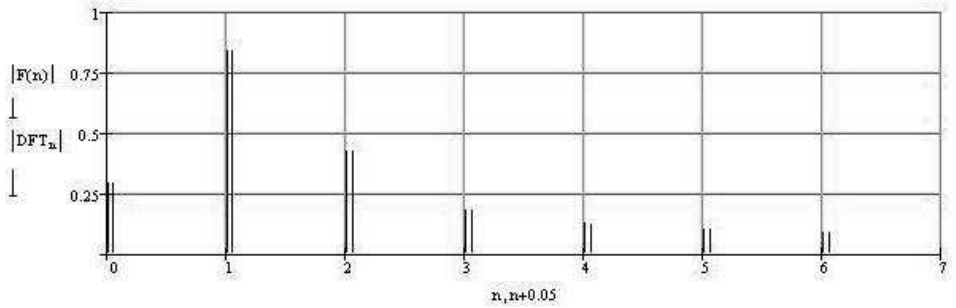

Fig. 12. Discrete wave spectrums for $\varepsilon = 2/3$

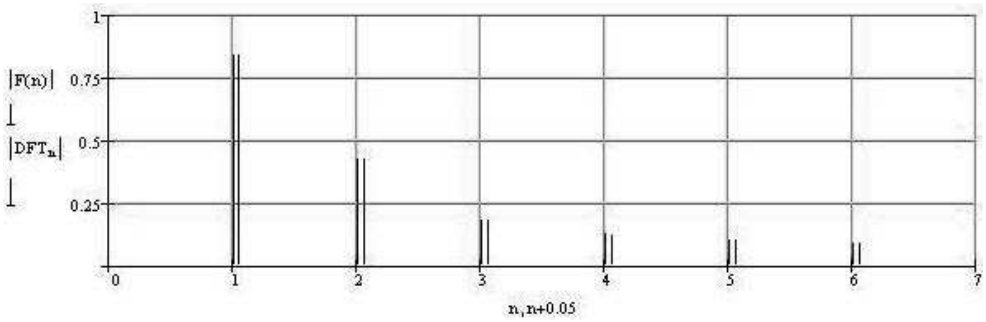

Fig. 13. Discrete wave spectrums for $\varepsilon = 2/3$ after resetting of the average value

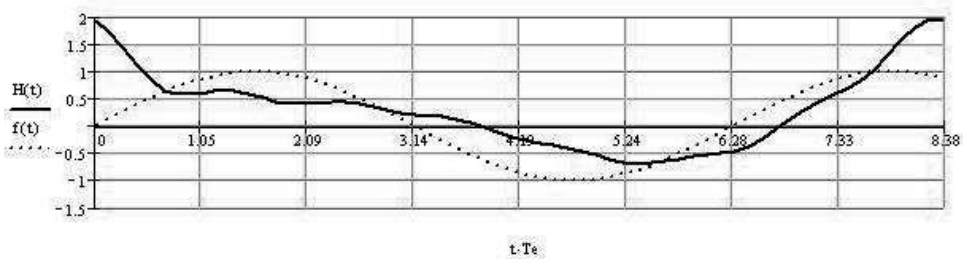

Fig. 14. The original and recovered waves for $\varepsilon = 2/3$

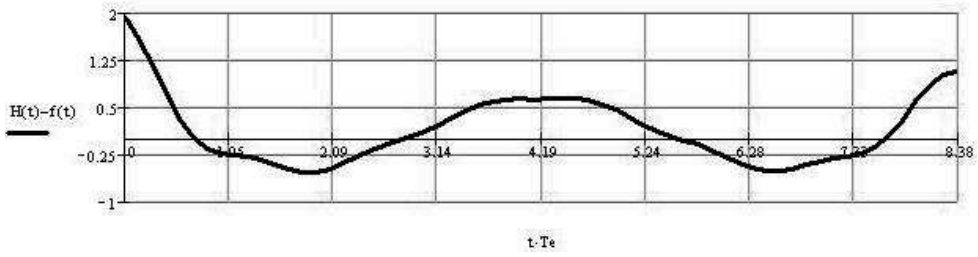

Fig. 15. Residuum of the original and recovered waves for $\varepsilon = 2/3$

for each stripe of the spectrum irrespective of value $n\nu_T$ for which it occurred on the condition that n = int.

Because in the discrete spectrum the total multiplicity of the inverse of the retrieval time determines the set of admissible frequencies, the discretization of the spectrum eliminates the distortions triggered by the rectangular measurement window in the form of a leakage and lateral waves. The filtering characteristics of periodical distribution **Ш**'(t) starts manifesting itself. Because dependence (7) remains true we can assume that the distortions of the discrete spectrums from the rectangular measurement window would display themselves in a different form than it directly results from this dependence.

In order to estimate the transfer of the information the original harmonic waves has been reproduced from the substitute spectrum. Figure 14 presents the comparison of the course of the wave generated for $\varepsilon = 2/3$ and the course of the wave that was a result of a superposition of the harmonic waves recovered from the stripes of the substitute spectrum. Figure 15 shows the residuum determined by the difference between the recovered and the original wave.

CONCLUSIONS

The discrete spectrums generated and emitted by mechanical devices in operation are a result of a superposition of waves representing the harmonic components of the signal of frequencies that belong to the admissible set as well as waves of frequencies that do not belong to this set and form substitute spectrums. Thus resulting distortions of the discrete spectrum are consequence of the existence of a rectangular measurement window of retrieval time of T.

The DFT procedure generates a substitute spectrum according to the Fourier series irrespective of the researcher's intention. The stripes of the spectrum are determined for admissible frequencies that belong to a limited range. The values of these frequencies and the boundary frequencies of this range are preset and determined by values T selected by the researcher. The substitute spectrum transfers approximately true frequency information in the form of a sum of untrue information that is not in the signal. The amount of information is limited by the width of the range $[0,\nu_{Nyq})$.

The superposition of the waves of the substitute spectrum, taking the phase shifts into account, recovers the course of the harmonic wave. The courses of the residuum determined from the comparison of the original wave and the same wave obtained from the substitute spectrum shows that the recovery is inaccurate and incomplete. This mainly results from the fact that the recovered wave is a result of limited number $N/2$ – waves of the substitute spectrum contained in frequency range $[0,\nu_{Nyq})$ not a infinite number of waves as the Fourier series requires.

The finite retrieval time, selected by the researcher, results in the fact that the average value of the processed fragment of the signal is mostly non-zero. The information transferred by the stripe of the discrete spectrum for $n = 0$ is incidental and thus unreliable. The distortion of the spectrum from the constant component can be eliminated by assuming this value to be zero by definition. From the courses of the residuum we can see that the wave recovered from the components of the substitute spectrum was more accurate as compared to the original wave. Such an action does not trigger a change of the components for $n>0$ and does not generate additional spectrum distortions.

The existence of the measurement window, which is an inevitable consequence of the limited retrieval time, as well as discretization of the signal during the A/C conversion are in opposition to the assumptions based on which from series (1) Fourier integral was derived (2). That is why the described distortions of the discrete spectrum are inevitable and with today's level of knowledge cannot

be eliminated nor reduced through adjustment windows used when determining the spectrums with analogue methods (spectrometers).

Each adjustment window is a function of weight. The signal multiplied by this function assumes a zero value at the beginning and at the end of the retrieval. This multiplication results in deletion of some information contained therein and addition of other, carried by the window function not contained in the signal. Product (7) assumes a form $\mathbf{F}(\nu)*\mathbf{W}_k(\nu)$ and transform of the adjustment window is $\mathbf{W}_k(\nu) \neq 1$. That is why the discrete Fourier transform of the fragment of the signal improved by the adjustment window, beside the harmonic components of the signal and substitute spectrums also includes the components contained in the window function. This results in an additional inaccuracy of the information contained in the discrete spectrum.

The distortions of the discrete Fourier spectrum of the retrieved fragment of the signal that come from the substitute spectrums can be reduced by extending of the retrieval time. It is known that for constant bandwidth $[0,\nu_{Nyq})$ as the retrieval time T grows the size of the set of admissible frequencies increases and the distance between them decreases. The number of the signal components that are probable to find their place in the set of admissible frequencies grows. As a result, the amount of information that can be accurately conveyed in the discrete spectrum increases. Also increases the number of the components of the substitute spectrums recovering the components of the signal of frequencies that do not belong to this set, which results in a better accuracy of the recovery.

For $T\rightarrow\infty$ frequency $\nu_T\rightarrow 0$ the admissible frequency set becomes infinitely large and the discrete spectrum approaches a continuous form. A practical realization of such a case is impossible due to an infinite length of the retrieval time. Even if that were possible, the determination of a discrete spectrum of an infinitely dense set of admissible frequencies would not eliminate the distortions.

REFERENCES

1. **Bath M. 1974:** Spectral Analysis in Geophisics. Elsvier Scientific Publishing Co.
2. **Batko W., Dąbrowski Z., Engel Z., Kiciński J., Weyna S. 2005:** Nowoczesne metody badania procesów wibroakustycznych, cz. I. Wyd. ITE – PIB, Radom.
3. **Bendat J.S., Piersol A.G. 1980:** Engineering Application of Correlation and Spectral Analysis. John Willey & Sons, New York, Chichester, Brisbane, Toronto, Singapore.
4. **Kurowski W.:** Teoriopoznawcze podstawy diagnostyki technicznej. Prace IPPT PAN, nr 76/1976.
5. **Kurowski W. 1976:** An Introduction to the Dynamic Diagnostics of Mechanisms. Nonlinear Vibration Problems, no 17, p. 225-269.
6. **Kurowski W. 1993:** Influence of a measurement time window on the FFT frequency spectrum. Journal of Theoretical and Applied Mechanics, 4, 31, p. 845-856.
7. **Kurowski W. 1995:** Informatical Properties of Discrete Spectrum. Archiwum Informatyki Teoretycznej i Stosowanej, Tom 7, z. 1-4, p. 95-104.
8. **Kurowski W. 1996:** Interferences in Discrete Spectrum. Archiwum Informatyki Teoretycznej i Stosowanej, Tom 8, z. 1-2, p. 191-239.
9. **Kurowski W. 1999:** Przedmiot i metoda poznania w diagnostyce technicznej. Zagadnienia Eksploatacji Maszyn, z.3(119), vol. 34, p. 551-564.
10. **Kurowski W. 2008:** Podstawy diagnostyki systemów technicznych. Metodologia i metodyka. Wyd. ITE – PIB, Warszawa – Płock.
11. **Kurowski W. 2010:** Inżynieria informacji diagnostycznej. Analiza sygnału. Wyd. ITE – PIB, Warszawa – Płock.
12. **Liferman J. 1980:** Les méthodes rapides de transformation du signal Fourier, Walsh, Hadamard, Haar. Wyd. Masson et Cie.
13. **Papoulis A. 1962:** The Fourier Integral and its Applications. McGraw-Hill Co., Inc., New York, San Francisco, London, Toronto.
14. **Pawłow B.W. 1967:** Badania diagnostyczne w technice. WNT, Warszawa.
15. **Zemanian A.H. 1969:** Teoria dystrybucji i analiza transformat. PWN, Warszawa.
16. **Zieliński T. P. 2009:** Cyfrowe przetwarzanie sygnałów. Od teorii do zastosowań. Wyd. Komunikacji i Łączności. Warszawa.
17. **Żółtowski B. 1996:** Podstawy diagnostyki maszyn. Wyd. Uczelniane AT-R Bydgoszcz.

TRANSFORMACJA FOURIERA – WAŻNE NARZĘDZIE W DIAGNOSTYCE WIBROAKUSTYCZNEJ

S t r e s z c z e n i e. Mierzalne wielkości fizyczne, charakteryzujące procesy towarzyszące funkcjonowaniu urządzenia mechanicznego, mogą być wykorzystane jako sygnały niosące zakodowane informacje. Aby je odczytać sygnał należy pobrać i obrobić. Obróbka polega najczęściej na transformacji sygnału do dziedziny częstotliwości metodą DFT. Wykorzystanie takiej obróbki wymaga wiedzy jak informacja diagnostyczna jest wytwarzana w dyskretnej charakterystyce sygnału. W tym celu należy badać model, który odzwierciedla pobranie sygnału w skończonym przedziale czasu, jego przetwarzanie A/C i periodyzację. Badania wykazują, że procedura DFT wytwarza prążki reprezentujące składowe harmoniczne sygnału tylko dla częstotliwości $n\nu_T$, które są całkowitą krotnością odwrotności czasu pobrania. Składowe o innych częstotliwościach są przedstawiane w postaci widm zastępczych. W konsekwencji, widma dyskretne są rezultatem superpozycji fal o częstotliwościach należących do zbioru dopuszczalnych i widma zastępczych reprezentujących fale, które do tego zbioru nie należą.

S ł o w a k l u c z o w e: diagnostyka wibroakustyczna, numeryczna obróbka sygnałów transformacja Fouriera.

TEKA. COMMISSION OF MOTORIZATION AND ENERGETICS IN AGRICULTURE – 2012, Vol. 12, No. 1, 103–107

Energy efficiency of ground heat exchangers co-operating with a compressor heat pump

Sławomir Kurpaska, Hubert Latała

University of Agriculture in Kraków, Institute of Agricultural Engineering and Computer Science,
University of Agriculture in Kraków, Poland Balicka 116B, 30-149 Krakow, Poland

Summary. The work presents results of an analysis of the coefficient of performance of a heat pump co-operating with ground heat exchangers. Three types of exchangers were examined: horizontal, vertical- made at the depth of 20 m (type I) and at the depth of 100 m (type II). It was proved that the highest value of the coefficient of performance (the COP) occurs for vertical exchangers (type I), slightly lower for horizontal exchangers and the lowest for vertical exchangers (type II). The statistical analysis, which was carried out, proved that the type of an exchanger significantly influences the value of the coefficient of performance; its average values are also statistically significant. Significance of the influence of temperature inside a facility on the value of the coefficient of performance was not proved.

Key words: compressor heat pump, vertical, horizontal ground heat exchanger.

INTRODUCTION

Constant search for methods of reducing energy outlays and alternative and more effective heat sources in technological processes and heating of facilities results from increased costs of obtaining heat from traditional carriers and from the care for the natural environment. Such activities are also influenced by policy of the European Community countries, which stimulates the use of renewable sources of energy. One of the methods of realization of this purpose is a heat pump, which co-operates with ground heat exchangers. Issues concerning the analysis of the effectiveness of the system, in which heat pumps are used, were the subject of the research in many scientific centres. Thus, [13] analysed operation effectiveness of the heat pump co-operating with vertical ground heat exchangers located in vertical poles, which constitute a foundation of housing estates. As a result of the research which they carried out, they determined usefulness of such a construction, they calculated a temporal and seasonal coefficient of energy efficiency of the system (calculated by means of the relation of the obtained thermal power with the supplied electric power). Kim et al. [4] presented a work containing results of the researched compressor heat pumps varied according to thermal efficiency and the applied thermal-dynamic factor. Air, water and soil were used as a lower heat source. In the constructed models, they included particular cycles of thermal-dynamic transformation of the circulation factor. On the basis of the tests which they carried out, they determined a percentage share of particular electric energy receivers (a compressor, a circulating pump) in shaping the value of the coefficient of energy efficiency of the system. Congedo et al. [1] using the CFD technology analysed the thermal issues in the ground, in which the ground heat exchangers co-operating with the heat pump were installed. As a result of the simulation which was carried out, influence of depth, ground conductivity and the flow speed of the circulation factor on the amount of heat obtained by the exchangers located in a flat and loop arrangement were determined. Temperature of ground at random depth and in random time was described by an equation of heat conductivity at the assumed periodical change of temperature of its outer layer. It was found that from among the analysed independent variables moisture of the ground influences the amount of the obtained heat the most, whereas from among the researched geometrical arrangements the loop system is recommended. Yang et al. [14] carried out a review of models used for describing phenomena occurring in the ground with the vertical heat exchangers. They concluded that there is a need to verify these models and the issues related to underwater flow which influence a change of central temperature should be added. Florides and Kalogiro S. [2] presented construction solutions of the ground heat exchangers and they characterised mathematical models used to describe phenomena in the ground. As a result of the analysis which they carried out, they stated that thermal-physical

properties of the ground centre influences the amount of the heat taken up by the ground exchangers whereas, span and spatial sitting of exchangers and thermal conductivity of the ground are decisive factors in the vertical exchanger. Partenay et al. [10] worked out a mathematical model of phenomena, which take place in the flowing circulation factor in the vertical ground exchangers. The compiled model was resolved with a numeric method (of definite elements) while a change of ground temperature during operation of the heat pump was the analysed issue. On the basis of the experimental tests which were carried out (a system of six vertical heat exchangers), correctness of this model was reported and a relation of the heat pump operation efficiency to temperature in the heat exchangers of the system (a steamer, a condenser) were found. Lee and Lam [6] carried out a computer simulation for the system composed of vertical exchangers co-operating with the heat pump. In the isolated space of the ground, relations of heat exchange with loops of particular meshes were worked out (with the method of definite differences). As a result of the analysis, they determined a periodical variability of the ground temperature as well as the value of the coefficient of heat transfer for the ground heat exchangers. Trillat et al. [12] presented results of experimental research in which the heat pump co-operated with solar collectors forming the so-called hybrid system. Energy effects of such a system along with its energy efficiency (the coefficient of performance) and calorific effect of the ground exchangers were determined whereas the authors recommended the considered system for heating facilities. On the basis of a long-term research, Huang and Lee [3] determined the consumption of electric energy used for driving a heat pump. Calculations were carried out in relation to a unitary growth of temperature of liquid stored in the buffer tanks of the heat pump. Ozgener and Hepbasli [9] analysed energy issues and financial outlays incurred on the use of the heat pump (co-operating with the vertical ground heat exchangers) for heating purposes. The authors worked out a simulation model, which may be used for an analysis of financial inputs at using the heat pump for heating facilities. Ozgener and Hepbasli [9] presented results of experimental research on using a heat pump for heating a greenhouse. They described thermal efficiency of vertical ground heat exchangers and temperature of air inside a greenhouse at supplying heat only from a heat pump. They also determined values of the coefficient of work efficiency of the system divided into days of various weather conditions. Ozgener and Hepbasli [7, 8] in the experimental research determined the work efficiency of the heat pump with the vertical heat exchangers used for heating a greenhouse. Moreover, they determined a value of the coefficient of work efficiency of the system (the COP), which they related with total energy supplied from the heat pump and to this part of energy, which was used for heating purposes of the above assumed temperature inside a greenhouse. Kurpaska's work [5] presents nomograms for determining construction and operation parameters in which the heat pump was working in a monovalent and hybrid system. The monovalent system constituted a co-operation of the heat pump with the grounded exchangers (both horizontal and vertical) whereas in the hybrid system a cumulative tank in which collected water was heated with solar collectors was the lower source of the pump.

The presented review of the literature explicitly results in actual analysis of the research issue, as the use of the heat pump in heating installations of facilities is one of future technical solutions. It is a consequence of the fact that the heat pump co-operating with a co-generative system (joint generation of heat and electric energy) is an ideal receiver of electric energy generated in this system. However, the system of obtaining heat from the bottom source, next to a type of the used pump decides on efficiency of using electric energy. Analysis of these issues is a main purpose of the presented work.

MATERIAL AND METHODS

Energy efficiency of the system the heat pump co-operating with the system of heat consumption and reception) decides on its economic cost-effectiveness.

Thus, this issue was analysed for a laboratory stand constructed in facilities of the Department of Production Engineering and Power Industry of the University of Agriculture in Kraków.

This stand (fig. 1) is composed of: a compressor heat pump, vertical ground exchangers: depth approx. 20 m (two U type exchangers and 2x U), depth 100 m (one U type exchanger and the other 2U type, horizontal exchangers in a geometric system: a single loop, a double loop and spiral arrangement. Two heat-air exchangers mounted in a laboratory foil tunnel constituted the system of heat reception.

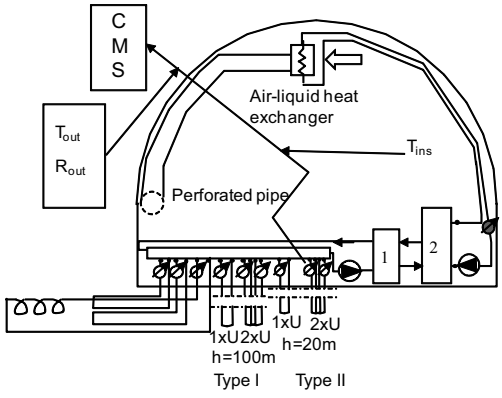

Ø impulse flow meter; •PT1000 resistance sensors; 1- heat pump; 2- buffer tank

Fig. 1. Scheme of the laboratory stand

During the experiments, necessary measurement amounts were monitored and recorded using an original Computer Measurement System. A stream of the flowing factor was measured with an impulse flowmeter, while temperature (of supply and return of the circulation factor) in particular exchangers as well as air temperature

(outside t_{out} and inside a facility t_{ins}) with a resistance sensor PT1000. Additionally, during the research, a demand for electric power used for driving elements of the researched system (a compressor, a circulating pump and circulation pumps of exchangers of the upper heat source) was determined and radiation intensity Rs was measured (with a pyranometer).

Using a definition of the heat pump operation, an equation of energy balance (including amount of heat obtained in a condenser of the analysed pump - Q) may by written down in the following form:

$$Q = W_{PC} + Q_{GZ}. \tag{1}$$

Operation efficiency of the heat pump in the system may be described with the coefficient of performance (coefficient of energy efficiency), which was defined pursuant to the standard PN-EN 255 in the following form:

$$COP_{grz} = \frac{Q_{GZ} + W_{PC}}{W_{PC}} = 1 + \frac{Q_{GZ}}{W_{PC}}. \tag{2}$$

In a differentiable time dτ, parameters necessary to describe the amount of heat obtained by the analysed ground heat exchangers, electric energy consumption (W_{PC}) and amount of heat obtained by exchangers located in the heated facility (Q_{GZ}) were measured.

Moreover, in the said time dτ the amount of heat obtained by the analysed ground exchangers was determined in relation to:

$$Q_{DZ} = \sum_{i=1}^{9}\left(\sum_{i=1}^{n} m_{cDZ,i} \cdot c_c \cdot \left(T_{z-DZ,i} - T_{p-DZ,i}\right)\right) d\tau_{PC}, \tag{3}$$

whereas for the system of heat reception in analogical time this relation takes the following form:

$$Q_{GZ} = \sum_{i=1}^{2}\left(\sum_{i=1}^{n} m_{cGZ,i} \cdot c_p \cdot \left(T_{z-GZ,i} - T_{p-GZ,i}\right)\right) d\tau_{PC+GZ}, \tag{4}$$

where: Q_{GZ} - heat supplied to the inside of the facility [J]; Q_{DZ} - heat obtained form the outside of the ground [J]; W_{PC} - electric power obtained by elements of the system [W]; τ_{PC}, τ_{GZ} -operation time of the heat pump (τ_{PC}) and of the upper source(τ_{GZ}) [s]; m_c - stream of the lower circulation factor (m_{cDZ}) and of the upper (m_{cGZ}) source [kg·s^{-1}], c_c - specific heat of the circulation factor [J·kg^{-1}·K^{-1}], $T_{z\text{-}DZ}$ and $T_{p\text{-}DZ}$- temperature of supply and return of the circulation factor of the lower heat source, $T_{z\text{-}GZ}$ and $T_{p\text{-}GZ}$ - temperature of supply and return of the circulation factor of the bottom heat source [°C].

RESULTS AND A DISCUSSION

The research was carried out in 2012. Fig. 2 presents an exemplary course of some measured values. Assuming pointlessness of all possible courses, visualisations of the measured parameters were limited to parameters of the liquid -air exchangers, which constitute an upper heat source in a tunnel, temperature inside and outside of the facility, difference between temperature of supply and return of the circulation factor and the state of work of the heat pump. Selected symbols include:

$T_{z\text{-}DZ1}$, $T_{z\text{-}DZ2}$- difference in temperature of the circulation factor, R_s - intensity of solar radiation outside the facility; V_{DZ1}, V_{DZ2}- indications of a water meter presenting amount of the factor flowing through exchangers supplying heat to the inside of the facility:, t_{ins}, t_{out} - respectively temperature inside and outside the facility, HP- operation state of the heat pump (value above zero means operation state of the heat pump).

According to what has been presented, in the period of 48 hours, the heat pump was working through 37 cycles of operation of the length within 11.5 to 32 minutes. Within this time, for driving technical devices of the system (a pump compressor, circulation pumps) almost 86 kWh of electric energy were used and 85.4 kWh of this amount was used for driving elements of the heat pump (a compressor, a circulating pump) whereas, approx. 0.6 kWh were used for circulation pumps obtaining heat from a buffer tank of the pump. In the presented period of time 460 MJ of heat where delivered to the facility.

Almost 500 cycles of pump operation were analysed (for all conditions of the experiment). For every cycle from the equation (2) a coefficient of performance was calculated.

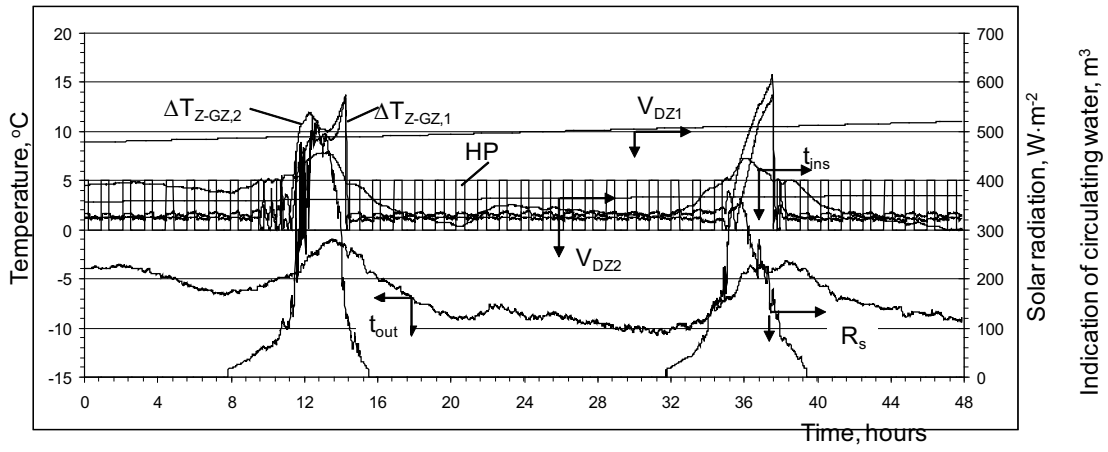

Fig. 2. Temporary course of some measured parameters in the expriment

Fig. 3 and 5 presents a calculated coefficient of operation efficiency of the pump co-operating with the analysed ground heat exchangers. Type I of vertical ground heat exchangers means exchangers located at the depth of 18 m while the type II means ground exchangers of 100 m depth.

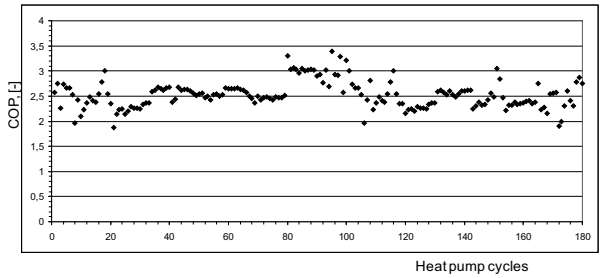

Fig. 3. Course of changes in energy efficiency of the heat pump co-operating with horizontal exchangers

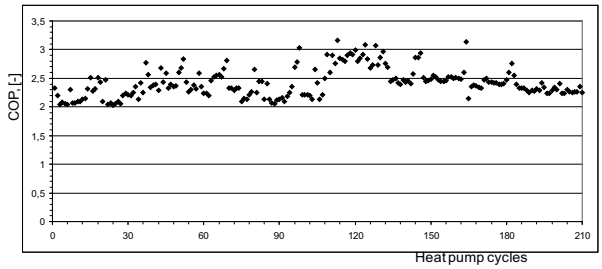

Fig. 4. Course of changes in energy efficiency of the heat pump co-operating with vertical ground exchangers of approx. 20 m depth

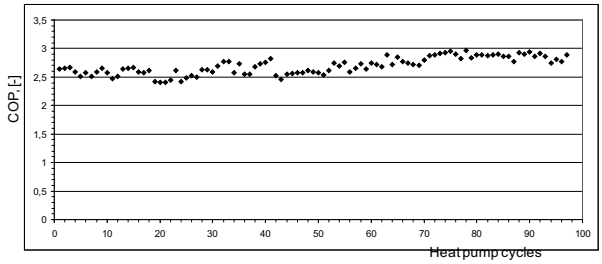

Fig. 5. Course of changes in energy efficiency of the heat pump co-operating with ground vertical exchangers at 100 m depth

When analysing the obtained courses, one may notice that the highest average value of the coefficient COP (the COP = 2.69) was obtained for the case when the heat pump was co-operating with the vertical ground exchangers located at 100 m depth. Whereas, when the pump co-operates with the horizontal exchangers, an average value of COP was 2.53, while for the vertical exchangers of approx. 20 m depth, the COP was 2.42. Comparable values of the surrounding climate were selected for the analysis. Thus, vertical exchangers made at the depth of 100 m are recommended as the lower heat source of the pump.

While analysing these relations, one may find that the co-operation of the heat pump with the vertical exchangers of 100 m depth is characterised also by a lower variability of the value of the coefficient of performance.

For the obtained data, at the level of significance α=0.05 a statistical analysis was carried out using the Statistica® packet. Fig. 6 presents results of average values along with a standard deviation of analysis.

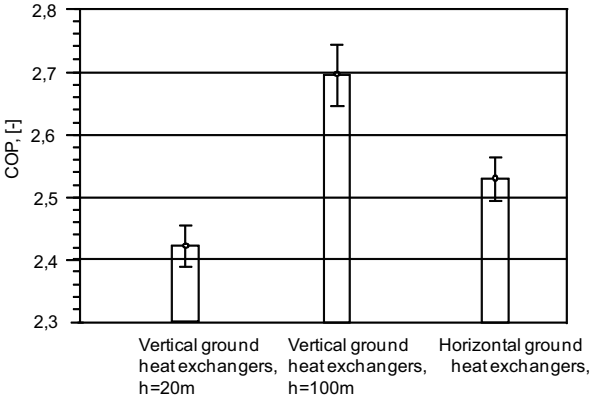

Fig. 6. Results of average values of the coefficient of performance with a standard deviation

The analysis of variance in a single classification, which was carried out proves that the assumed factors of the experiment (a type of the ground exchanger) significantly influence the analysed value of the coefficient of performance. Whereas, Duncan test proved that the average values of this coefficient differ in a statistically significant way.

Fig. 6 presents a graphic relation of the coefficient of efficiency of the heat pump (calculated from the equation 2) and temperature inside the facility.

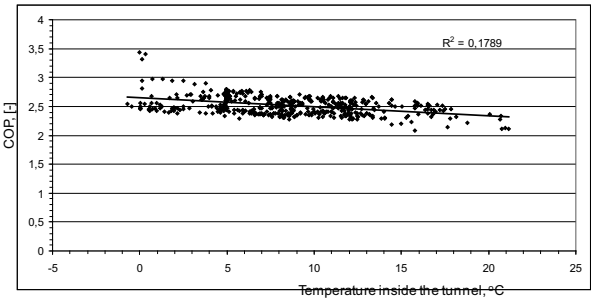

Fig. 7. Dependence of the heating efficiency coefficient on the temperature inside the object

One may notice that growth of temperature inside a foil tunnel means a slight decrease of the coefficient of efficiency of the heat pump. The statistical analysis did not prove significance of the regression coefficient. It means that there is no linear influence of temperature inside a foil tunnel on the value of the COP. Moreover, the value of the coefficient of determination (R^2=0.18) does not prove statistically significant relation of the COP with temperature inside a facility. It results from the relation of intensity of heat reception between exchangers and a surrounding air, since the higher temperature is around the heat exchangers, the lower value of the transfer coefficient gets. At the low difference of temperatures, the operation time of circulating pumps from the system

of heat reception increases. However, the power used for driving circulating pumps is many times lower than a demand for power by a compressor and a circulating pump of the lower heat source.

CONCLUSIONS

The highest average value of the COP was obtained for the vertical ground heat exchangers (type II), slightly lower for the horizontal exchangers and the lowest for vertical exchangers (type I). The analysis of variance proved that the assumed factors of the experiment (a type of the ground exchanger) considerably influence the analysed value of the COP and average values of this coefficient differ in a statistically significant way. Along with a temperature growth inside a foil tunnel, the value of the COP decreases slightly. However, the coefficient of regression is not statistically significant.

This research is founded by the Polish Ministry of Science and Higher Education, as a project: Energy and environmental aspects of renewable energy in horticultural object: N N313 445137.

REFERENCES

1. **Congedo P.M., Colangelo G., Starace G. (2012).** CFD simulations of horizontal ground heat exchangerS: A comparison among different configurations. Applied Thermal Engineering, p. 33-34, p. 24-32.
2. **Florides G., Kalogirou S. (2007).** Ground heat exchangers - a review of systems, models and applications. Renewable Energy, 32, p. 2461- 2478.
3. **Huang B. J., Lee C. P. (2004).** Long-term performance of solar-assisted heat pump water heater. Renewable Energy, 29(4), p. 633-639.
4. **Kim D.S., Morertti I., Hubert H., Monsberger M. (2011).** Heat exchangers and the performance of heat pumps- analysis of a heat pump database. Applied Thermal Engineering, 31(5), p. 911-920.
5. **Kurpaska S. (2008).** Constructional and operational guidelines for systems using a heat pump to heat horticultural objects (in Polish), Inżynieria Rolnicza, 2 (100), p. 155-162.
6. **Lee C.K., Lam H.N. (2008).** Computer simulation of borehole ground heat exchangers for geothermal heat pump systems. Renewable Energy, 33(6), p. 1286-1296.
7. **Ozgener O., Hepbasli A. (2005a).** Exergoeconomic analysis of a solar assisted ground-source heat pump greenhouse heating system. Applied Thermal Engineering, 25(10), p. 1459-1471.
8. **Ozgener O., Hepbasli A. (2005b).** Experimental performance analysis of solar assisted ground-source heat pump greenhouse heating system. Energy and Buildings, 37(1), p. 101-110.
9. **Ozgener O., Hepbasli A. (2005c).** Performance analysis of a solar-assisted ground-source heat pump system for greenhouse heating: an experimental study. Building and Environment, 40(8), p. 1040-1050.
10. **Partenay V., Riederer P., Salque T., Wurtz E. (2011).** The influence of the borehole short-time response on ground source heat pump system efficiency. Energy and Buildings, 43, p. 1280-1287.
11. PN EN 255-1: (2000) Air conditioners, liquid chilling packages and heat pumps compressors, will be driving electric - heating function - Terms, definitions and symbols.
12. **Trillat-Berdal V., Souyri B., Fraisse G. (2006).** Experimental study of a ground-coupled heat pump combined with thermal solar collectors. Energy and Buildings 38, p. 1477-1484.
13. **Wood Ch.J., Liu H., Riffat S.B. (2010).** An investigation of the heat pump performance and ground temperature of a piled heat Exchange system for a residual building. Energy, 35(12), p. 4932-4940.
14. **Yang H., Cui P., Fang Z. (2010).** Vertical-borehole ground –coupled heat pumps: A review of models and systems. Applied Energy, 87(1), p. 16-27.

EFEKTYWNOŚĆ ENERGETYCZNA WYMIENNIKÓW GRUNTOWYCH WSPÓŁPRACUJĄCYCH ZE SPRĘŻARKOWĄ POMPĄ CIEPŁA

Streszczenie. W pracy przedstawiono wyniki analizy wartości współczynnika efektywności pracy sprężarkowej pompy ciepła współpracującej z wymiennikami gruntowymi. Badano trzy typy wymienników: poziome, pionowe- wykonane na głębokość 20m (typ I) oraz na głębokość 100m (typ II). Wykazano, że największa wartość współczynnika COP występuje dla wymienników pionowych (typ I), nieco mniejsza dla wymienników poziomych i najmniejszą dla wymienników pionowych (typ II). Przeprowadzona analiza statystyczna wykazała, że rodzaj wymiennika wpływa istotnie na wartość COP; również średnie jego wartości są statystycznie istotne. Nie wykazano istotności wpływu temperatury wewnątrz obiektu na wartość współczynnika COP.

Key words: sprężarkowa pompa ciepła, pionowy, poziomy, wymiennik gruntowy.

TEKA. COMMISSION OF MOTORIZATION AND ENERGETICS IN AGRICULTURE – 2012, Vol. 12, No. 1, 109–113

Efficiency of the heat pump cooperating with various heat sources in monovalent and bivalent systems

Sławomir Kurpaska, Hubert Latała, Bogusława Łapczyńska-Kordon, Krzysztof Mudryk

Faculty of Power Engineering and Energetic, University of Agriculture in Krakow,
Balicka 116B, 30-149 Krakow, POLAND, rtkurpas@cyf-kr.edu.pl

Summary. This paper presents the findings of tests carried out on the efficiency of compressor heat pumps cooperating with various types of lower heat sources. Lower heat sources are as follows: horizontal ground heat exchangers, vertical exchangers and sources operating in the bivalent system. The system for receiving energy comprised a traditional heating system and liquid-air exchangers. A strong relationship between the heating efficiency of the analysed systems and temperature inside the structure was noted. Furthermore, it was indicated that for heat requirements of approximately 1 MJ×m^{-2} the applied bivalent system was fully capable of meeting this heat requirement.

Key words: coefficient of performance, heat pump, bivalent system.

INTRODUCTION

The limited amount of natural resources, including fossil fuels, and the capacity of the natural environment to accept pollution without dangerous changes occurring in the functioning of the global ecosystem, constitute the basis for taking measures in order to substitute fossil fuels with renewable sources of energy, including the use of heat pumps. Heat pumps may be operated mono- or bivalently. Under the monovalent system the heat source may be e.g. soil (heat exchangers both in horizontal and vertical systems). In turn, under the bivalent system, heat is transferred by the pump from the tank which stores the liquid which is heated up through the conversion of sunlight in the collectors. The possibility of using heat pumps in the heat systems of every heat reception system depends not only on energy and ecology but also on economic matters. Economic factors concern efficiency which depends on the type and condition of the lower hear source, as well as the manner of receiving the heat from the upper source. Research on the use of heat pumps has been carried out at many research centres. Hawlader et al [5] analysed the use of renewable sources of energy for heating glasshouses. Analyses were carried out on the operating efficiency of independent sources (heat pumps, solar collectors) and bivalent (hybrid) systems in the form of combined pump and solar collector action. The above researchers noted that under test conditions (a region with a high level of sun exposure) the lowest costs connected with the supply of heat were generated with the use of the bivalent system. Xu et al [16] analysed the energy effects of heat pumps in which use was made of atmospheric air heated up in flat liquid collectors as the lower heat source. Energy from the upper source was used for heating processing water. Kaygusuz and Ayhan [1999] described and analysed the heat pump cooperating system (atmospheric air was used as the lower source) with the upper source, in which the energy was stored in an accumulator filled with a body subject to phase transition. They defined the Coefficient of Performance (COP) system. Nagano et al. [13] elaborated an innovative system for visualising and analysing heat pump operating efficiency which makes use of the ground exchanger as a lower source. The heat pump was used for heating purposes in a prototype glasshouse. In the final analysis the researchers presented synthetic heat operating indicators (work efficiency, financial ratios), whilst the energy effects were calculated in terms of limitation of the emission of substances released from the combustion of conventional fuels. Hawlader et al [5] researched the energy effects of the system in which the heat pump cooperated with the solar collector. Energy from the upper source was used for heating liquid in the accumulator. The researchers defined the Coefficients of Performance for given system constituents. They also defined the rate of return on financial outlay.

Kaygusuz [8] performed system simulation tests in which the lower heat source drew energy from the conversion of sunlight in solar air collectors, whilst the heat pump cooperated with the accumulator, filled with

a solid subject to phase transition. The tests were carried out under laboratory conditions. Following analyses Kaygusuz defined the energy effects and indicated the legitimacy of conducting a thorough economic analysis for this system, which would be employed in real structures.

Yumruta and Unsal [17] elaborated a mathematical model for analysing heat pump cooperation, in which the lower heat source used water collected in the liquid accumulator located in the soil. The findings of water temperature variability simulation were depicted as a function of variable temperature of surrounding soil and total heat loss from the analysed accumulator. Hepbasli et al [6] defined the energy effects of the system in which the compressor heat pump cooperated with vertical ground heat exchangers. Following analyses the thermal efficiency of ground heat exchanger pipes and the Coefficient of Performance were defined. Esen et al [4] analysed the efficiency of heat pumps cooperating with ground heat exchangers. A mathematical model of heat exchange between the ground and piping constituting the lower heat source of the exchanger was developed. Research demonstrated a high degree of compliance between measured and calculated ground temperature with the use of a model. Trillat-Berdal et al [15] analysed heat pump operation in which the lower heat source was the intake of geothermal water and solar collectors. When using the existing numeric model they defined the operating parameters of the system under consideration and presented the energy and economic effects and the quantity findings of reducing the emission of harmful substances into the atmosphere. Knaga [10, 11] for the laboratory conditions analyzed the energy efficiency of compressor heat pump. Benli and Durmas [2], Ozenger and Hepbasli [14] analyzed the cooperation of the heat pump heating system installed in a greenhouse. Benli [1, 2], Boulard et al. [3] presented the results of analysis in which the heat pump working with heat storage material filled with the transition phase. Katsunori et al. [7] designed a system for using heat pumps for heated greenhouses and its effects compared with other heat sources. Research carried out by Kurpaska [12] presented the findings of an energy analysis connected with the selection of lower heat source for cooperation with the compressor heat pump.

On the basis of the above presented research findings one may state that they do not comprehensively include the entire analysis on which the taking of a decision to use a heat pump for heating a garden structure depends. For this reason the carrying out of such an analysis is the main purpose of the paper.

MATERIAL AND METHOD

The system under consideration comprises solar collectors, a tank for storing heated water, ground heat exchangers (horizontal and vertical), a compressor heat pump with buffer tank and a system of heat reception through a heating device located in the foil tunnel. The total length of the horizontal heat exchanger (with external diameter of 42 mm) was 300m, whilst the vertical exchangers (piping with the same diameter as in the case of the horizontal exchanger) constituted three boreholes, each 20 m deep, distributed in U layout (two sensors) and 2U layout – one ground sensor. In the foil tunnel, with overall surface area of 54m^2, a standard heating system and two liquid-air exchangers were installed. The heat reception system comprised a system of heating pipes (total surface area of 18.2m^2) and exchangers with heat exchange surface area equal to 6m^2 each. Figures 1 and 2 present the gauge position layout. During experimentation the following were measured: surrounding climate parameters, the flow stream medium in: solar collectors, lower and upper heat pump source, feed temperature, return of the circulating medium and electricity consumption by system elements (the heat pump compressor and the circulating pumps).

These levels were gauged continuously with the use of the authors' gauge system which also permitted the archiving of gauge levels.

The Coefficient of Performance was calculated as follows:

$$COP = \frac{Q_{wew}}{P_{PC} \cdot \tau_{PC} + \sum_{i=1}^{2} P_{wym,i} \cdot \tau_{wym,i}}, \quad (1)$$

where: Q_{wew}- heat delivered to the interior of the structure, J; P_{Pc}- electricity used by the heat pump, W; τ_{PC}, $\tau_{wym,i}$- respective operating time of the heat pump (τ_{PC}) and of circulating pumps in the heating system ($\tau_{wym,i}$), s; $P_{wym,i}$- electric power of the circulating pumps in the heating system, W.

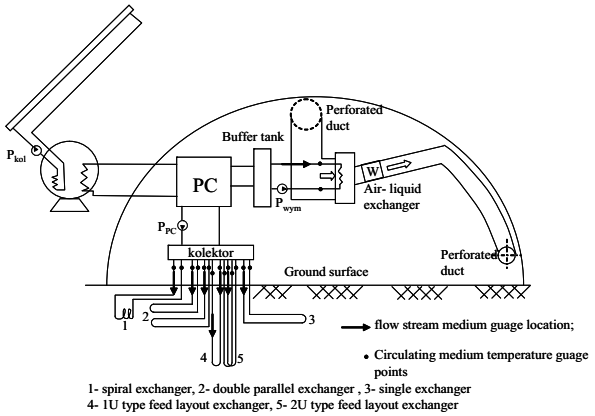

Fig. 1. Diagram depicting the gauge position and heat reception system

In turn, heat supplied to the interior of the structure (Q_{wew}) in $d\tau$ differential time is equal:

a) for liquid-air exchangers:

$$Q_{wew,wym} = \sum_{i=1}^{2}\left(\sum_{i=1}^{n} m_i \cdot c_p \cdot \left(t_{z,i} - t_{p,i}\right)\right) d\tau, \quad (2)$$

b) for traditional heating systems:

$$Q_{wew,sg} = m \cdot c_p \cdot \left(t_z - t_p\right) d\tau, \quad (3)$$

where: m- flow stream medium, kg×s^{-1}; c_p- medium specific heat capacity, J×kg^{-1}×K^{-1}; t_z, t_p- feed temperature and return of the heating medium, °C.

All calculations were carried out in relation to the unit surface area of solar collectors.

When analysing the composition of the bivalent system (collectors – storage tank – heat pump) sunlight energy reaching the solar collectors was defined (E_s) as well as the heat supplied by the following collectors: liquid ($Q_{kol,\,pl}$) and vacuum ($Q_{kol,\,pr}$). On this basis, within the given time range ($d\tau$) these levels were calculated by means of the following relationship:

$$E_s = \sum_{i=1}^{n} R_z \cdot F_{k,pl(pr)} \cdot d\tau\,, \tag{4}$$

$$Q_{kol,pl(pr)} = m_{pl(pr)} \cdot c_p \cdot \left(t_{z,pl(pr)} - t_{p,pl(pr)}\right) d\tau\,, \tag{5}$$

where: R_z- sunlight intensity, W×m^{-2}; $F_{k,pl(pr)}$- solar collector surface area, m^2; symbols: *pl* and *pr* refer to the appropriate flat plate collector ($_{pl}$) and vacuum collector ($_{pr}$).

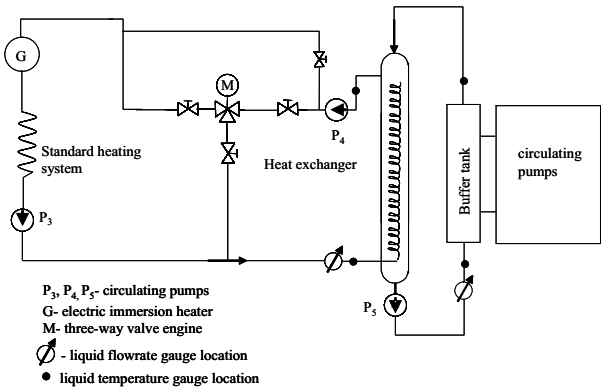

Fig. 2. Diagram depicting the hydraulic system feeding the standard heating system

When defining the heat pump operating efficiency in the bivalent system the following approach was employed:

$$\eta = \frac{Q_{wew,wym(sg)}}{\sum_{i=1}^{2} P_{kol,i} \cdot \tau_{kol,i} + P_{PC} \cdot \tau_{PC} + \sum_{i=1}^{2} P_{wym,i} \cdot \tau_{wym,i}}. \tag{6}$$

Where: $P_{kol,\,i}$, electric power of circulating pumps in the collectors, W; $\tau_{kol,i}$ pump operating time in the collector system, s.

Below are presented the findings of experiments carried out on: horizontal exchangers, vertical exchangers and the hybrid system.

RESULTS AND DISCUSSION

Research was carried out during the autumn and spring of 2008/2009. Figure 3 presents the thermal efficiency of the analysed heating systems installed in the structure. One may note their linear dependence between efficiency and temperature outside the structure. The reduced efficiency of heating systems at higher internal temperature and the absence of additivity in the thermal efficiency of individual heating systems (the total efficiency of individual heating systems is higher than the total efficiency of both exchangers) may be explained by the differentiated temperatures in feeding the circulating medium of both systems and the dependence of heat transfer intensity by the heating system on temperature inside the structure.

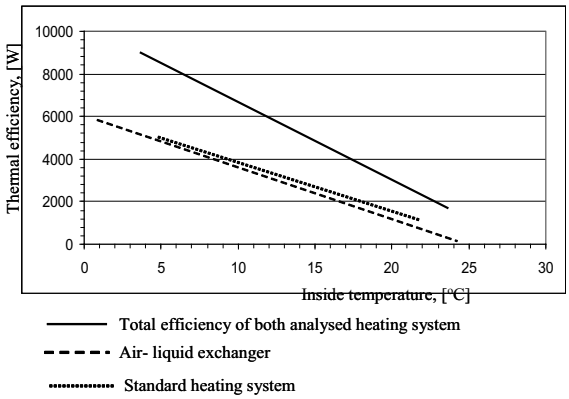

Fig. 3. Thermal efficiency of analysed heating systems

Figures 4 and 5 present COP for lower heat source in the form of horizontal heat exchangers (fig. 4) and vertical exchangers (fig. 5). As can be seen, average COP value depending on the type of exchanger is COP= 1.56 (horizontal ground heat exchangers) and 1.49 (vertical exchangers).

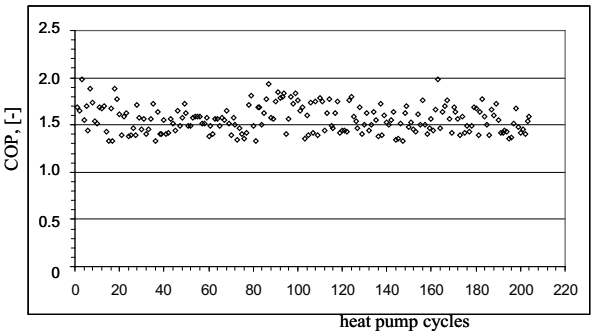

Fig. 4. Pump coefficient of performance during experiments with simultaneous heat distribution to the interior with the use of exchangers and of the traditional heating system (horizontal exchangers)

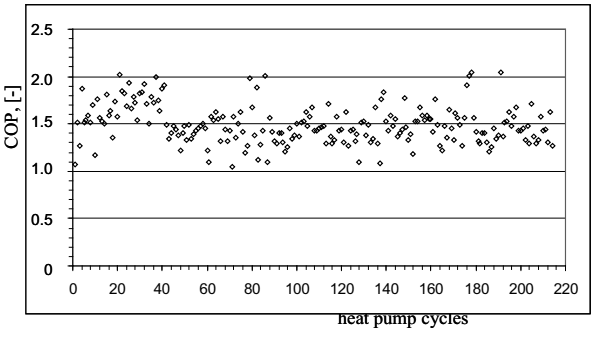

Fig. 5. Pump coefficient of performance during experiments with simultaneous heat distribution to the interior with the use of exchangers and of the traditional heating system (vertical exchangers)

Table 1 presents a synthetic calculation of differences depending on the types of lower heat source exchanges and the reception system.

Table 1. Relative differences (in relation to the traditional heat reception system) in the COP for the analysed experimental conditions

Type of lower heat source	Percentage difference in COP, %	
	Liquid-air exchangers	Exchangers + traditional heat distribution system
horizontal	18.7	21.2
vertical	17.3	23.1

An analysis of the presented calculation clearly shows that, irrespective of the type of lower heat source (vertical or horizontal ground heat exchangers), it is more advantageous to use additional liquid-air exchangers in the structure, apart from the traditional heat distribution system. It stems from data appearing in the table, as a result of applying the bivalent heat reception system, that growth in the COP of more than 21% is observed.

Concerning the bivalent system fig. 6 presents an example of average changes in liquid temperature in the tank together with designated heat pump operating cycles. During the experiment the accumulation tank contained 2.5m^3 of water. As a result of heat pump operations (total time over 11 cycles was 2.76 hours) average water temperature dropped (as a result of pump operations and heat loss into the environment) from approx. 35 °C to approx. 22 °C. In the presented time range (Fig. 6) the pump supplied almost 113 MJ of heat into the interior of the structure over 11 cycles. Scope of change of the amount of collected heat is between 400MJ and 1900MJ; each subsequent heat pump operating cycle collected less energy as a result of worse heat exchange of the lower source.

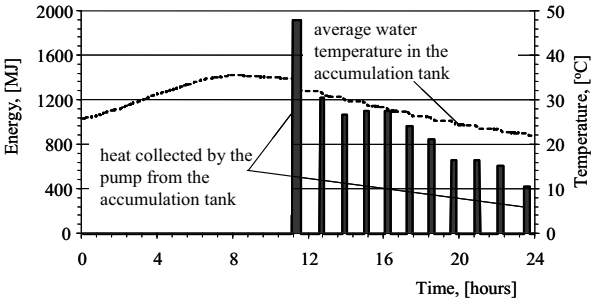

Fig. 6. The timing of water temperature changes in the tank and the amount of heat provided to the interior of the structure during the experiment in terms

When calculating the work efficiency of the bivalent system (Fig. 7) an analysis was carried out on all work cycles for differentiated capacities of the storage tank (between 2m^3 and 5m^3 of water). One notes the lack of dependency between the presented amounts and the sum of sunlight. It is true that solar energy as a result of conversion led to higher water temperature in the accumulation tank, but for the approved system operation cycle period there was no direct connection between these parameters (the sum of sunlight energy) and the average temperature of water in the lower source. Average efficiency value was 1.45 (heat pump) and 1.35 (for the entire hybrid system).

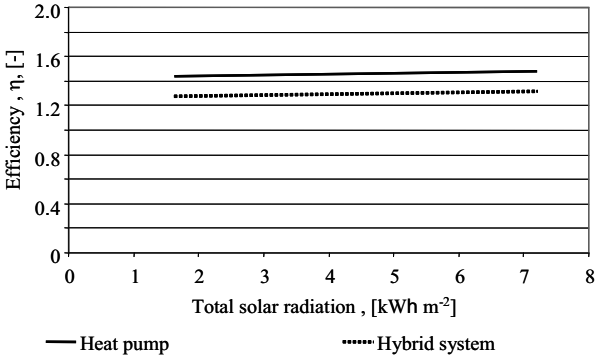

Fig. 7. Efficiency of the bivalent system and of the heat pump in total sunlight function

In turn, fig. 8 depicts the quantity of energy in the lower and upper heat pump heat source in reference to the structure's requirement for heat (the requirement for heat was calculated during liquid-air heat exchanger operations at 15°C, whilst energy was calculated for the system operating cycle period).

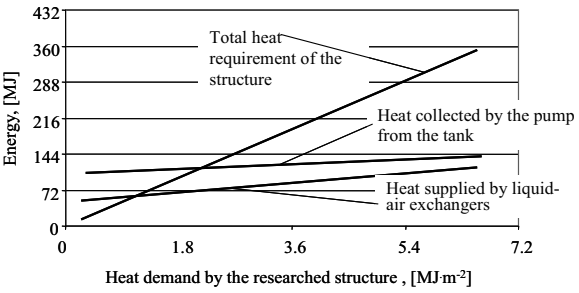

Fig. 8. Energy collected by the heat pump and energy supplied to the inside of the structure in terms of structure heat demand

When the structure requires a large amount of heat the energy supplied to the interior is less than the energy collected by the heat pump from the lower source. In turn, when the structure requires a small amount of heat (up to approx. 0.9 MJ·m^{-2}) the amount of heat supplied by the exchangers exceeded demand. Heat, which was collected by the heat pump from the accumulation tank could theoretically be enough to satisfy the heat demand of the structure at a level of approx. 1 MJ·m^{-2}.

CONCLUSIONS

1. The average COP of the pump cooperating with the ground exchangers, depending on their type, was between 1.49 (vertical exchangers) and 1.56 (horizontal ground heat exchangers).

2. Irrespective of the type of lower heat source (vertical or horizontal ground heat exchangers), it is more advantageous to use additional liquid-air exchangers in the structure, apart from the traditional heat distribution system.

3. Average efficiency value for each system was 1.45 (heat pump) and 1.35 (for the entire bivalent system).

REFERENCES

1. **Benli H. 2011.** Energetic performance analysis of a ground-source heat pump system with latent heat storage for a greenhouse heating Energy Conversion and Management 52, p. 581-589.
2. **Benli H, Durmus A. 2009.** Evaluation of ground-source heat pump combined latent heat storage system performance in greenhouse heating. Energy Buildings 41, p. 220-228.
3. **Boulard T, Razafinjohany E, Baille A, Jaffrin A, Fabre B. 2003.** Performance of greenhouse heating system with a phase change material. Agric Forest Meteorology, 52, p. 303-318.
4. **Esen H., Intali, Esen M. 2006.** Numerical and experimental analysis of a horizontal ground-coupled heat pump system. Building and Environment, 42(3), p. 1126-1134.
5. **Hawlader M.N.A., Chou S.K., Ullah M.Z. 2001.** The performance of a solar assisted heat pump water heating system. Applied Thermal Engineering, 21(10), p. 1049-1065.
6. **Hepbasli A., Akdemir O., Hancioglu E. 2003.** Experimental study of a closed loop vertical ground heat pump system. Energy Conversion and Management, 42(4), p. 527-548.
7. **Katsunori N, Takao K, Sayaka T. 2006.** Development of a design and performance prediction tool for the ground-source heat pump system. Applied Thermal Engineering 26, p. 1578-1592.
8. **Kaygusuz K., Ayhan T. 1999.** Experimental and theoretical investigation of combined solar heat pump system for residential heating. Energy Conversion and Management, 40(13), p. 1377-1396.
9. **Kaygusuz K. 1995.** Performance of solar- assisted heat pump systems. Applied Energy, 51(2), p. 93-109.
10. **Knaga J. 2007.** Changeability of heat output of heat pump with scroll type compressor, TEKA Commission of Motorization and Power Industry in Agriculture VIIA, p. 41-46.
11. **Knaga J. 2008.** Energy efficiency of small compressor assisted air-water type heat pumps, TEKA Commission of Motorization and Power Industry in Agriculture VIII 2008, p. 99-106.
12. **Kurpaska S. 2007.** Energy analysis for lower heat sources of heating pump while heating a plastic tunnel (in Polish). Inżynieria Rolnicza, 9(97), p. 103-111.
13. **Nagano K., Katsura T., Takeda S. 2006.** Development of a design and performance prediction tool for the ground source heat pump system. Applied Thermal Engineering, 26(14-15), p. 1578-1592.
14. **Ozgener O, Hepbaslı A. 2004.** Experimental performance analysis of a solar assisted ground-source heat pump greenhouse heating system. Renewable Energy, 37, p. 101-110.
15. **Trillat-Berdal V., Souyri B., Fraisse G. 2006.** Experimental study of a ground-coupled heat pump combined with thermal solar collectors. Energy and Buildings, 28(12), p. 1477-1484.
16. **Xu G., Zhang A., Deng S. 2006.** simulation study on the operating performance of a solar–air source heat pump water heater. Applied Thermal Engineering, 26 (11-12), p. 1257-1265.
17. **Yumruta R., Unsal M. 2000.** A computational model of a heat pump system with a hemispherical surface tank as a ground heat source. Energy, 25(4), p. 371-388.

EFEKTYWNOŚĆ POMPY CIEPŁA WSPÓŁPRACUJĄCEJ Z DOLNYMI ŹRÓDŁAMI CIEPŁA W SYSTEMIE MONO I BIWALENTNYM

S t r e s z c z e n i e. W pracy przedstawiono wyniki badań dotyczące efektywności sprężarkowej pompy ciepła współpracującej z różnymi rodzajami dolnych źródeł ciepła. Dolne źródła ciepła stanowiły: poziome gruntowe wymienniki ciepła, wymienniki pionowe oraz źródło pracujące w systemie biwalentnym. System odbioru ciepła składał się z tradycyjnego sytemu grzejnego i wymienników typu ciecz-powietrze. Stwierdzono, silną zależność między wydajnością cieplną analizowanych systemów a temperaturą wewnątrz obiektu. Ponadto, wyznaczono również, że do zapotrzebowania ciepła na poziomie ok. 1 MJ×m^{-2} zastosowany system biwalentny umożliwia w pełni pokrycie zapotrzebowania ciepła.

S ł o w a k l u c z o w e: współczynnik wydajności, pompa ciepła, system biwalentny.

TEKA. COMMISSION OF MOTORIZATION AND ENERGETICS IN AGRICULTURE – 2012, Vol. 12, No. 1, 115–120

Energy efficiency analysis of flat and vacuum solar collector systems

Sławomir Kurpaska, Hubert Latała, Jarosław Knaga

Faculty of Power Engineering and Energetic, University of Agriculture in Krakow, Poland
e-mail: rtkurpas@cyf-kr.edu.pl

Summary. This paper presents the findings of analyses depicting changes in solar radiation conversion efficiency in flat and vacuum solar collectors. It also sets out efficiency for the entire system based on a 24-hour cycle. On the basis of results, the model has been found which defines these efficiencies through experience (storage tank fluid capacity, surrounding temperature and total solar radiation). This model has also been validated and confirmed as useful for estimating efficiency and therefore, for selecting surfaces of the analyzed types of collectors in systems using these kinds of devices. Concerning the approved conditions, the time required for the reimbursement of investment costs has also been defined.

Key words: flat and vacuum solar collectors, conversion efficiency, solar radiation.

INTRODUCTION

The growing cost of energy, fear associated with the possibility of exhaustion of fossil energy sources, the need to increase the security of fuel and energy supply and concern for environmental protection have led to rapid growth of interest in the use of renewable energy. Solar radiation energy, which is converted into heat in flat and vacuum solar collectors, is being used more and more often as a component of renewable energy resources.

Of its many possible applications, heat obtained from solar collectors is also used in horticultural production, primarily for: supplementing the heating of structures under cover [10, 13], supplementary or basic heating of plastic tunnel bedding with the purpose of accelerating crop growth, preparation of processing water for the watering of plants, preparation of seedlings for planting, heating requirements for the post-harvest preparation of fruit and vegetables and heat treatment of soil pathogens [2]. A number of research centers has analyzed in detail matters relating to the conversion of radiation for various configurations and conversion system equipment. Adsten et al [1] analyzed the impact of solar collector locations (both flat and vacuum) in northern Europe for operating effectiveness. The impact of annual energy was determined and it was confirmed that the amount of obtained energy is closely related to the surrounding climate conditions. Apart from research on the use of individual collectors for energy purposes, specialist literature also provides the findings of research focusing on the coupling of collectors with heat pumps (so-called bivalent or hybrid systems). [7] researched the energy effects of the system in which the heat pump was coupled with the solar collector. The researchers defined the Coefficients of Performance for given system constituents. They also defined the rate of return on financial outlay and the COP for the entire system. [9] carried out an analysis of the use of renewable energy for a residential building, provided by solar collectors corresponding with a heat pump. They concluded that it was necessary to optimize system components because the configuration of the system and the dimensions of its components depend on local environmental conditions. Eisenmann et al [5] analyzed the possibility of saving materials in the production of collectors and, amongst other things, replacing them with other more available materials. Following research and the optimisation of collector construction, the above researchers noted a possible reduction of 25% in traditional material without negatively impacting the effectiveness of converting solar radiation energy into heat. Aye et al [3] studied the use of a compressor heat pump coupled with solar collectors for the purpose of heating processing water in residential buildings. In their analysis they compared aspects of energy and cost-effectiveness of the system under consideration in relation to separate constituent parts and indicated the conditions for which the proposed solution may be used in other facilities. Sozen et al [11] used neural networks for the purpose of analyzing the work effectiveness of flat solar collec-

tors; they used the following as input values: collector surface temperature, solar radiation intensity and duration, angle of declination, azimuth angle and inclination angle. In their summary they indicated the usefulness of the elaborated network architecture. Trillat-Berdal et al [12] analyzed the use of a heat pump coupled with solar collectors for the purpose of heating residential buildings. This system guaranteed the channeling of heated water (following the meeting of given conditions) through collectors to a buffer tank in which lower heat source exchangers were located. Heat exchanger performance and general system operating effectiveness were defined. They also analyzed heat pump operation in which the lower heat source was the intake of geothermal water and solar collectors. When using the existing numeric model they defined the operating parameters of the system under consideration and presented the energy and economic effects and the quantity findings of reducing the emission of harmful substances into the atmosphere. Kaygusuz [8] presented the findings of theoretical and experimental analysis of the heating system in which a heat pump (used for heating purposes) was coupled with solar collectors. The model took into account given system components, whilst experimental research demonstrated satisfactory comparison. The model permits the calculation of a collector surface, its efficiency and medium heating temperature. Badescu [4] presented the findings of theoretical analysis in which he considered two systems used for the heating of buildings, namely the hybrid system (solar collectors coupled with the heat pump) and the single system in which only the heat pump was used for heating the building. The coefficient of performance of the heat pump was defined and it was concluded that the hybrid system was more useful for the heating of facilities. Fuller [6] carried out a theoretical analysis and performed an experimental verification of the system in which use was made of water heated up in solar collectors for the heating of plastic tunnels. The water was collected in a storage tank and from there channelled (in a closed system) for the washing of the surface covering the facility. The energy effects of the system were defined and its usefulness in areas of high radiation was indicated.

Generalizing the results of research one may also state that the effectiveness of conversion depends not only on the system configuration but also on the parameters of the surrounding climate.

The main purpose of research involved an analysis of the effectiveness of conversion.

MATERIAL AND METHOD

EXPERIMENT SET-UP

Tests were conducted with the use of laboratory facilities located at the Agricultural University in Krakow (Figure 1).

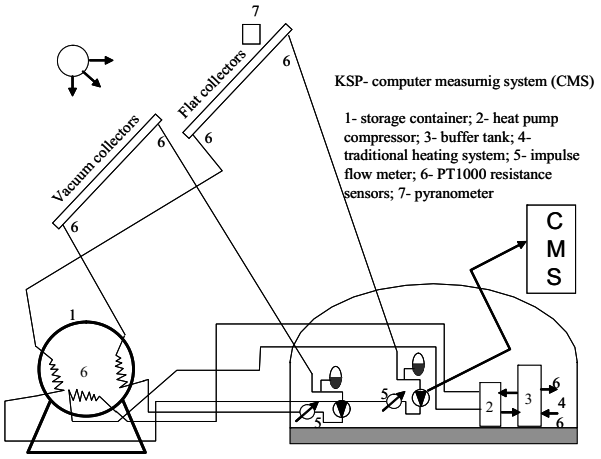

Fig. 1. Scheme of the laboratory stand

As indicated, the laboratory facility comprises flat (7.8m^2 effective surface) and vacuum (surface of 4.3m^2) solar collectors. The circulating medium flowed through a coil located in the buffer tank, which resulted in the higher temperature of the water in the tank. Heat reception from the tank (1) was attained thanks to heat pump operation (2), in which the lower source constituted an additional heat exchanger located in the buffer tank. Heat was supplied to the plastic tunnel heating system (4) from the buffer tank (3). During the performance of the experiments, whose purpose was to analyse the effectiveness of collector operation, one of the collector types (liquid or vacuum) did not participate in the conversion of solar radiation.

During research the following was used for measuring the analysed values: the liquid stream flowing through the impulse flow meter (5), water (inside container, circulating liquid) and air temperature measured with the use of copper-constantan thermocouples (6) and solar irradiation by pyranometer (7).

All the values were monitored and archived during sampling every 30 seconds with the use of the computer measurement system (CMS).

ANALYSIS

System efficiency analysis may be considered as the instantaneous efficiency (depending on dτ sampling time or long-term efficiency.

- Instantaneous efficiency of solar collectors

Heat obtained from the collector during dτ is equal to:

$$Q(\Delta\tau) = \dot{m} \cdot c_w \cdot (T_z - T_p) d\tau, \quad \text{J}. \tag{1}$$

In turn, conversion efficiency according to the standard expressed in the relationship between heat from the conversion and the sum of solar radiation energy, in other words:

$$\eta = \frac{Q(\Delta\tau)}{\Sigma R_{zewn} \cdot F_k \cdot d\tau}, \tag{2}$$

where: $\dot{m}$ - stream of circulating medium mass, kg×s^{-1}; c_w - medium specific heat, J×kg^{-1}×K^{-1}; T_z, T_p - respective feed temperature (T_z) and return (T_p) of the circulating medium; $\sum R_{zew}$ - sum of solar radiation, W×h; Fk- surface of tested collectors, respectively 4.3 m^2 (vacuum) and 7.8 m^2 (liquid collector).

- Long-term efficiency

In the considered system this efficiency expresses the relationship between the quantity of energy stored in the storage tank i.e. the difference between useful collector heat and total heat loss from the tank into the environment and the sum of solar radiation energy which reaches the collectors. In consideration of the above this dependency is expressed as follows:

$$\eta_{med} = \frac{\int_{h_E}^{h_W} Q(\tau)d\tau - A_S U_S \int_{day}^{h_W} \left[T_S(\tau) - T_{ot}(\tau)\right]d\tau}{F_k \int_{h_E} R_{zew}(\tau)d\tau}, \quad (3)$$

where: h_E, h_W- time of solar radiation penetration on the collector, A_S- surface heat loss of the storage tank, m^2; Us- replacement ratio of heat loss from the tank, W m^{-2} K^{-1}; T_S- instantaneous temperature of the liquid in the tank, ^{o}C; T_{ot}- tank surrounding temperature, ^{o}C, τ- time, s.

For the purpose of the analysis a period of time equal to 24 hours was approved as the long-term storage period.

In the presented dependency a difficulty arises in indicating the penetration ratio of tank heat into the atmosphere (U_S). The diagram of this system is indicated graphically in Figure 2.

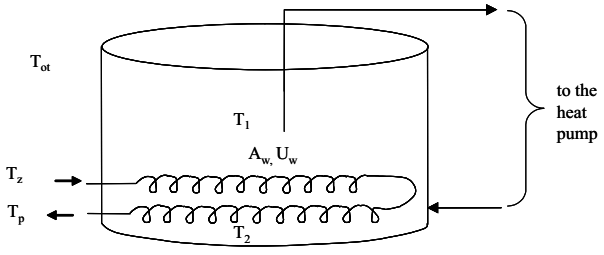

Fig. 2. Storage tank with coil: A_w - coil surface, m^2; U_w- ratio of heat penetration from the coil to water, W m^{-2} K^{-1}; T_1, T_2- tank liquid temperature, ^{o}C; m_w- stream of circulating medium flowing through the coil, kg s^{-1}

The following method was used for the purpose of designating the U_S coefficient. The tank is an exchanger in which there is liquid of a given mass (m) and specific heat (c_p). Water is heated in the tank following the transfer of heat from the medium which flows through the coil. There is thermal stratification in the tank, as a result of which a vertical temperature gradient takes place (t_1 and t_2 water temperature). In order to introduce the dependency defining change of tank water temperature, taking into account heat loss (Qstr), use has been made of standard heat balance. The dependency on indicating the U_S coefficient in d differential time was designated as follows (4):

$$U_S = \frac{m \cdot c_p \cdot \left(T_0 - T_{\Delta\tau}\right)}{A_S \cdot \left(T_{avg} - T_{ot}\right)d\tau}, \quad (4)$$

where: T_{avg}- is average liquid temperature at the beginning and at the end of the dτ interval, ^{o}C; T_0, $T_{\Delta\tau}$- is liquid temperature at the beginning (T_0) and at the end of the interval ($T_{\Delta\tau}$), ^{o}C.

On the basis of these findings a model dependency was established between efficiency defined through measurement and efficiency designated from the model. In order to define the differences, application was made of relative differences and mean square error calculated from the dependence:

$$\sigma = \left(\sum_{i=1}^{n} \frac{\left(\eta_{calc} - \eta_{\mathrm{mod}}\right)^2}{n} \right)^{0,5}, \quad (5)$$

where: η_{calc}, η_{mod}- calculated (η_{calc}) and designated efficiency (η_{mod}) from the proposed model, n- number of comparisons.

RESULTS AND DISCUSSION

Tests were carried out on varying volumes of water in the tank, between 1.25 m^3 and 1.78 m^3 (vacuum collectors) and between 2.22 m^3 and 3.75m^3 for flat collectors. The quantity of test liquid for flat collectors was, respectively: 2.22 m^3, 2.58 m^3, 2.9 m^3 and 3.22 m^3; and for vacuum collectors: 1.25 m^3, 1.4 m3, 1.6 m^3 and 1.78 m^3. Figures 3, 4 and 5 present examples of measured amounts.

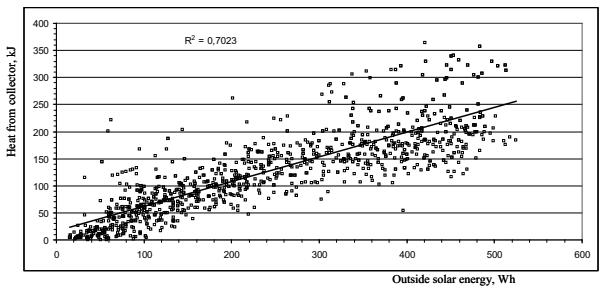

Fig. 3. Heat quantity generated in a solar vacuum collector in terms of total solar radiation

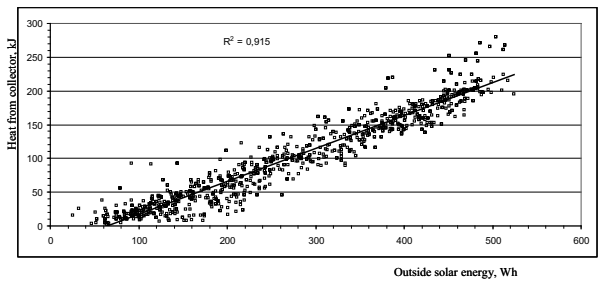

Fig. 4. Heat quantity generated in a flat vacuum collector in terms of total solar radiation

The dependency which arose as a result of the solar radiation conversion, between the quantity of heat generated in the collectors (in relation to unit surface) in terms of total solar radiation energy, is depicted in Figures 3 and 4, respectively, for vacuum collectors (Figure 3) and flat collectors (Figure 4).

Under test conditions the scope of heat quantity change spanned between 0.2 and 364.2 kJ×m^{-2} (vacuum collectors) and between 2.6 and almost 280 kJ/m^2 for flat collectors. In turn, average quantities of obtained heat stood at130 kJ×m^{-2} (vacuum collectors) and 103 kJ×m^{-2} (flat collectors). Taking into account the above data it stems that from the unit surface of a vacuum collector (based on average values) almost 18% more heat is obtained in comparison to flat collectors. This analysis was carried out for similar surrounding conditions (the sum of solar radiation energy, surrounding temperature).

Assuming the futility of providing all possible approaches, Figures 5 and 6 illustrate the impact of surrounding temperature and the sum of solar radiation on the change of effectiveness of the conversion of radiation for flat collectors. Calculations were performed in relation to the unit surface of flat collectors (Figure 5) and for storage tank fluid capacity at 2.25 m^3. The same course of change of effectiveness for vacuum collectors (for tank capacity equivalent to 1.25 m^3) is presented in Figure 6.

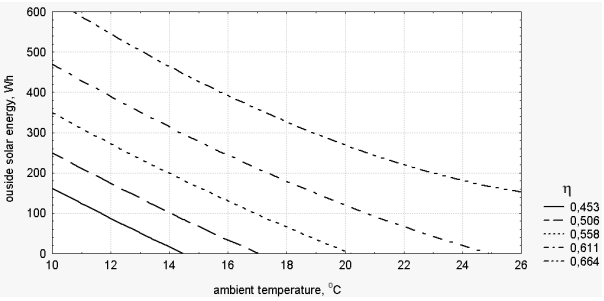

Fig. 5. Impact of surrounding temperature and the sum of solar radiation on the effectiveness of radiation conversion for flat collectors (liquid volume equivalent to 2.25m^3)

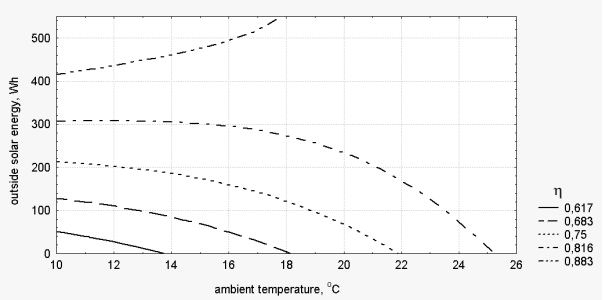

Fig. 6. Impact of surrounding temperature and the sum of solar radiation on the effectiveness of radiation conversion for vacuum collectors (liquid volume equivalent to 1.25m^3)

For maximum liquid volumes applied in the buffer tank (flat collectors, 3.22m^3 and vacuum collectors, 1.78m^3) the obtained calculations have been presented graphically in Figures 7 and 8.

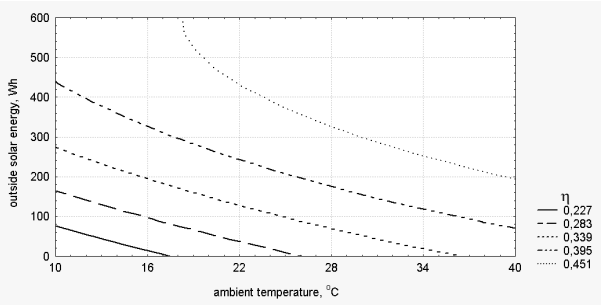

Fig. 7. Impact of surrounding temperature and the sum of solar radiation on the effectiveness of radiation conversion for flat collectors (liquid volume equivalent to 3.22m^3)

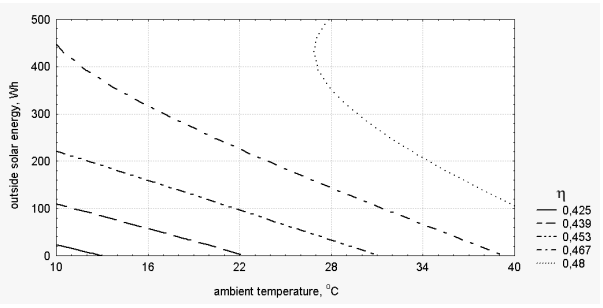

Fig. 8. Impact of surrounding temperature and the sum of solar radiation on the effectiveness of radiation conversion for vacuum collectors (liquid volume equivalent to 1.78m^3)

In analysing the obtained values one may state unequivocally that conversion effectiveness grows together with the growth of the sum of solar radiation and surrounding temperature. Under test conditions, the average efficiency value for tested collectors kept changing depending on liquid volume in the storage tank for: vacuum collectors – from 0.46 to 0.72 (respectively for tank capacity of 1.25 and 1.78 m^3), and ion the case of flat collectors from 0.4 (tank capacity of 2.25m^3) to 0.6 (for capacity of 3.22m^3). On the basis of obtained data it stems unequivocally that in order to obtain the highest level of efficiency through a solar collector system it is necessary to apply the above indicated liquid volumes in storage tanks. It was also noted that under the same conditions (for vacuum collectors almost 900 measure cycles were performed and 840 cycles for flat collectors), conversion effectiveness for vacuum collectors is on average 18% higher than in the case of flat collectors. The increase in conversion effectiveness as a positive function of temperature increase and the sum of solar radiation is the outcome of the growth in direct radiation share and reduced heat losses from the collector casing into the surroundings.

Following the performance of a series of tests, using non-linear estimation by means of the quasi-Newton method whilst retaining rates of convergence at 0.001, a dependence was found between independent variables (liquid volume in the tank - V_{zb}, surrounding temperature - t_{ot} and the sum of solar radiation energy R_{sl}). This connection for vacuum collectors is defined by the following dependence:

$$\eta = -0.5 \cdot V_{zb} + 1.24 \cdot t_{ot}^{0,023} + 3.85 \cdot 10^{-5} \cdot \sum R_{sl}^{1,19}; \quad R^2 = 0.87$$

for the scope of application: $1.25 \le V_{zb} \le 1.78$ m^3; $10.3 \le t_{ot} \le 37.5^{o}$C; 1.78; $15.2 \le R_{sl} \le 525$ Wh

In turn, for flat collectors this connection is expressed as follows:

$$\eta = -0.22 \cdot V_{zb} + 0.52 \cdot t_{ot}^{0,162} + 0.0168 \cdot \sum R_{sl}^{0,448}; \quad R^2 = 0.82$$

for the scope application: $2.25 \le V_{zb} \le 3.22$ m^3; $10.3 \le t_{ot} \le 37.5^{o}$C; 1.78; $15.2 \le R_{sl} \le 525$ Wh

These forms of dependence were selected on the basis of the largest coefficient of determination. In order to compare measured and calculated efficiency according to the proposed dependencies, in Figures 9 and 10 a global comparison between these values has been presented (for vacuum collectors Figures 9 and Figures 10 and for flat collectors).

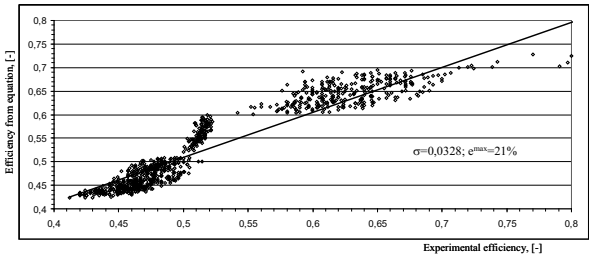

Fig. 9. Comparison between efficiency calculated from the proposed model and efficiency designated from vacuum collector tests

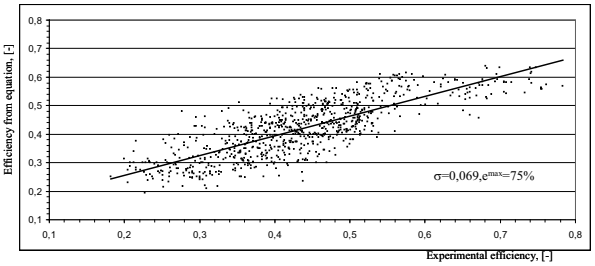

Fig. 10. Comparison between efficiency calculated from the proposed model and efficiency designated from flat collector tests

Calculated heat penetration coefficient form the tank to the surroundings (from model 4) stood at 2.4 W/m^{2}K. This illustrates unsatisfactory storage tank insulation.

Assuming the futility of providing all possible approaches, the decision was made to present in Figure 11 sample changes of long-term efficiency (η_{med}) calculated from the model (3) in terms of independent variables (surrounding temperature and sum of solar radiation). These dependencies are obtained for flat collectors and water volume in tanks equivalent to 2.22m^3. Under the test conditions this efficiency changes from 0.21 to 0.52. When analysing all combinations (type of collector, tank liquid volume), this scope ranges between 0.18 and 0.52 (flat collectors) and from 0.23 to 0.61 (vacuum collectors). Smaller values were obtained for larger liquid capacity in the storage tank.

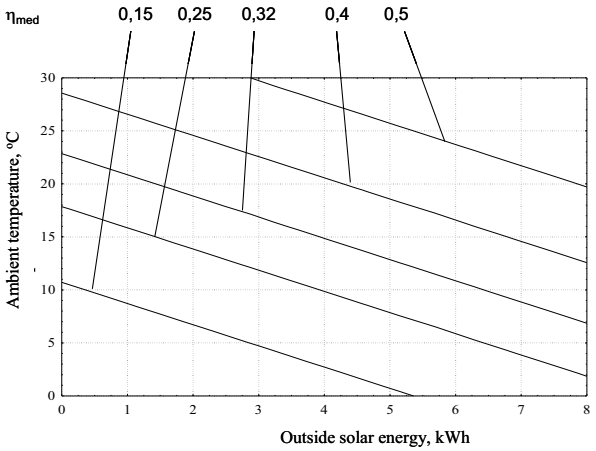

Fig. 11. Long-term efficiency (η_{med}) concerning surrounding temperature and sum of solar radiation energy

Changes in analysed efficiency are the outcome of reduction in temperature differences (collector temperature, tank temperature – surrounding temperature) and the larger share of direct radiation. The greater the values of these independent variables are, the smaller the heat loss from the collector, the storage tank and the more efficient conversion of direct radiation.

Summing up the research findings one may state that, considering their cognitive values (defined under operating conditions), they could also be applied. This stems from the fact that in each designed system which stems from its specifics, it is necessary to have an understanding of the efficiency of converting solar radiation into heat. The analysis also shows that vacuum collectors are more effective in converting radiation into useful heat. Conversion efficiency obtained through research demonstrates somewhat lower values than the parameters indicated by the producers of this equipment. However, the difference in the operating effectiveness of flat and vacuum collectors (higher efficiency) analysed during the summer (May - September) depended primarily on the surrounding temperature and solar radiation.

Of course, the attractiveness of the solution and the recommendation of a given type of collector depend on financial analysis. For this reason, in order to illustrate this topic, a calculation was made of payback on financial investment. The analysis took into account the following: the cost of purchasing the installation in entirety (vacuum or flat collectors included), average quantity of solar radiation (according to latitude of 54^o), installation operating time and cost of electricity. For calculation purposes, tank capacity corresponding to maximum collector efficiency and total respective solar collector surface (4 flat collectors) of 7.8 m^2 and 4.3m^2 (flat collectors) were assumed. The analysis findings, assuming that a flat collector set costs PLN 9,000 and a vacuum collector set costs PLN 12,000, indicated that return on investment would be 6.7 years and 6.5 years, respectively.

4. CONCLUSIONS

The following conclusions are based on the above analysis:

1. Depending on storage tank liquid volume, solar radiation conversion efficiency is between 0.46 and 0.72 for vacuum collectors and between 0.4 and 0.6 for flat collectors.
2. Under comparable experimental conditions, conversion efficiency for vacuum collectors is on average 18% higher than in the case of flat collectors.
3. The model defining the efficiency of solar radiation conversion in vacuum collectors is expressed as follows:

$$\eta = -0.5 \cdot V_{zb} + 1.24 \cdot t_{ot}^{0,023} + 3.85 \cdot 10^{-5} \cdot \sum R_{sl}^{1,19}; \quad R^2 = 0.87$$

for the scope of application: $1.25 \leq V_{zb} \leq 1.78$ m^3; $10.3 \leq t_{ot} \leq 37.5^{o}$C; 1.78; $15.2 \leq R_{sl} \leq 525$ Wh

for flat collectors:

$$\eta = -0.22 \cdot V_{zb} + 0.52 \cdot t_{ot}^{0,162} + 0.0168 \cdot \sum R_{sl}^{0,448}; \quad R^2 = 0.82$$

for the scope of application: $2.25 \leq V_{zb} \leq 3.22$ m^3; $10.3 \leq t_{ot} \leq 37.5^{o}$C; 1.78; $15.2 \leq R_{sl} \leq 525$ Wh.

4. Depending on the type of collector and liquid capacity in the storage tank, the daily efficiency of the analysed conversion system is between 0.18 and 0.61.
5. The payback period on financial investment in a solar radiation conversion system depending on the type of collector is, respectively, as follows: 6.5 years for vacuum collectors and 6.7 years for flat collectors.

REFERENCES

1. **Adsten M., Perers B., Wackelgard E. 2002.** The influence of climate and location on collector performance. Renewable Energy 25, p. 499-509.
2. **Al-Karaghouli A.A., Al-Kayssi A.W. 2001.** Influence of soil moisture content on soil solarization efficiency. Renewable Energy 24; 131-144
3. **Aye L., Charters W. W. S., Chaichana C. 2002.** Solar heat pump systems for domestic hot water. Solar Energy, 73(3), p. 169-175.
4. **Badescu V. 2002.** Model of a space heating system integrating a heat pump, photothermal collectors and solar cells. Renewable Energy, 27(4), p. 489-505.
5. **Eisenmann W., Vajen K., Ackermann H. 2004.** On the correlations between collector efficiency factor and material content of parallel flow flat-plate solar collectors. Solar Energy, 76 (4), p. 381-387.
6. **Fuller R. 2007.** Solar heating systems for recirculation aquaculture. Aquacultural Engineering, 36(3), p. 250-260.
7. **Hawlader M. N. A., Chou S. K., Ullah M. Z. 2001.** The performance of a solar assisted heat pump water heating system. Applied Thermal Engineering, 21(10), p. 1049-1065.
8. **Kaygusuz K. 1995.** Performance of solar-assisted heat-pump systems. Applied Energy, 51(2), p. 93-109.
9. **Kjellsson E., Hellström G., Perers B. 2010.** Optimization of systems with the combination of ground-source heat pump and solar collectors in dwellings Energy 35(6), p. 2667-2673.
10. **Kurpaska S., Latała H., Michałek R., Rutkowski K. 2004.** Funkcjonalność zintegrowanego systemu grzewczego w ogrzewanych tunelach foliowych. PTIR, Kraków, Monografia, pp. 118.
11. **Sozen A., Menlik T., Unvar S. 2008.** Determination of efficiency of flat-plate solar collectors using neural network approach. Expert System with Applications 35(4), p. 1533-1539.
12. **Trillat-Berdal V., Souyri B., Achard G. 2007.** Coupling of geothermal heat pumps with thermal solar collectors. Applied Thermal Engineering, 27(10), p. 1750-1755.
13. **Vox G., Schettini E., Lisi Cervone A., Anifantis A. 2007.** Solar thermal collectors for greenhouse heating., Acta Horticulturae 801: International Symposium on High Technology for Greenhouse System Management: Greensys 2007.
14. **Vasiliy Kudlenko, Dmitrij Devyatkin.** Cosmic Rays Muon Flux at the Sea Level by Highest Solar Activity. TEKA Kom. Mot. i Energ. Roln. – OL PAN, 2010, 10A, p. 339-344.

ANALIZA WYDAJNOŚCI ENERGETYCZNEJ PŁASKICH I PRÓŻNIOWYCH KOLEKTORÓW SŁONECZNYCH

Streszczenie. W artykule przedstawiono wyniki analiz obrazujących zmiany sprawności konwersji promieniowania słonecznego w płaskich i próżniowych kolektorach słonecznych. Określa on również wydajność całego systemu opartego na cyklu 24-godzinnym. Na podstawie wyników znaleziono model określający tę efektywność poprzez doświadczenie (zbiornik pojemność płynu, temperatura otoczenia i całkowite promieniowanie słoneczne). Model ten został również potwierdzony jako przydatny do oszacowania wydajności, a zatem przy wyborze powierzchni analizowanych typów kolektorów w systemach korzystających z tego rodzaju urządzeń. Określono również czas potrzebny na zwrot kosztów inwestycji w określonych warunkach.

Słowa kluczowe: płaskie i próżniowe kolektory słoneczne, wydajność konwersji, promieniowanie słoneczne.

TEKA. COMMISSION OF MOTORIZATION AND ENERGETICS IN AGRICULTURE – 2012, Vol. 12, No. 1, 121–125

Effect of fat content on the mechanical properties of texture of gingerbread pastry

Elżbieta Kusińska, Agnieszka Starek

Department of Food Engineering and Machinery, University of Life Sciences in Lublin, Poland,
e-mail: elzbieta.kusinska@up.lublin.pl

Summary. The paper presents the results of a study on the mechanical properties of gingerbread pastry texture with the use of the dual compression test TPA. The variable parameters in the experiment were the amount of fat added and the time of storage. The experiment was conducted for three consecutive days. Additionally, sensory assessment was performed for the purpose of selection of the optimum amount of fat addition on the basis of the textural properties.

Key words: gingerbread pastry, fat, texture, sensory assessment.

INTRODUCTION

Gingerbread occupies an equivalent position in the classification of confectionery products next to yeast pastry, puff pastry, shortcrust pastry, sponge-cake and others [7]. Gingerbread has a porous structure, is characterised by a spicy taste and flavour, and has brown colouring [4, 3, 18, 9]. It has health-prompting properties due to the spices added in its preparation (ginger, cloves, cinnamon, nutmeg, and allspice) [15, 2, 3]. The large content of spices puts the product in the category of bakery products with extended shelf-life [13].

Another component of gingerbread is fat, which - like carbohydrates - is primarily a source of energy [23]. Fats play also an important role in the process of regeneration and development of an organism [1, 8, 6, 24]. The content of fat in confectionery products has an effect on their properties, among other things it raises their nutritive value, ensures their crunchiness, and first of all it determines their consistency and taste [22]. Fats used in pastry-baking should have excellent sensory features, resistance to oxidation, and their consistency should comply with their intended use [10, 21].

In spite of its numerous taste values, gingerbread has certain shortcomings related with, among others, incorrect amounts of added components [12]. In the confectionery industry, textural parameters play an important role in the overall sensory and instrumental assessment of food. They depend on a number of raw material and production process features [11, 5]. To create new products and to improve those already produced, it is necessary to acquire knowledge on changes in the theological properties of semi-finished products and to relate those with the results of the sensory assessment [19, 20, 17]. Also, the analysis is necessary of correlation between the measured physical properties of the product and their sensory equivalents in each product under study [14].

OBJECTIVE AND SCOPE OF RESEARCH

The objective of the study was to determine and select the optimum values of the mechanical properties of the texture of gingerbread pastry during storage and in relation to the amount of fat added.

The scope of the study comprised the development of the recipe and the baking of pastries, instrumental measurement of the mechanical properties of their texture and sensory assessment of the products.

METHODS

The experimental material was four kinds of gingerbread with varied fat content (100g, 150g, 200g and 250g). Each of the gingerbreads studied was prepared using the following components: 5 eggs, 150g of sugar, 500g of wheat flour, 350g of liquid honey, 250g of 12% sour cream, margarine Kasia (in amounts varying for the various gingerbread kinds), 5g of soda, 30g of gingerbread spice mix. The prepared dough was placed in baking pans with dimensions of 10×38 cm and baked

at temperature of 160°C for 60 min. When the pastries cooled down, they were covered with aluminium foil and kept in a refrigerator at temperature of 6°C.

The experimental material prepared as above was subjected to instrumental testing with the use of the texturemeter TA.XT.plus, linked with a computer. The dual compression test TPA (Texture Profile Analysis) was performed, using 10 samples of crumb from each of the kings of gingerbread in the form of cubes with 2 cm side. The samples were compressed at tester head travel velocity of 50 mm·min^{-1} to 50% of their height. The basic texture parameters were read directly and calculated from the measurement curve:

– hardness, i.e. the maximum force during the first cycle of compression,
– elasticity, that characterises the degree of recovery of the initial form; it is the quotient of sample deformations during the first and second compression (E=L2/L1),
– cohesiveness characterising the forces of internal bonds that hold the product in one piece; it is the quotient of the areas beneath the graphs of forces of the first and second compression of the sample (Coh=W2/W1),
– chewability which is a measure of force required to chew a bite of food to make it ready for swallowing; it is defined as the product of hardness, cohesiveness and elasticity.

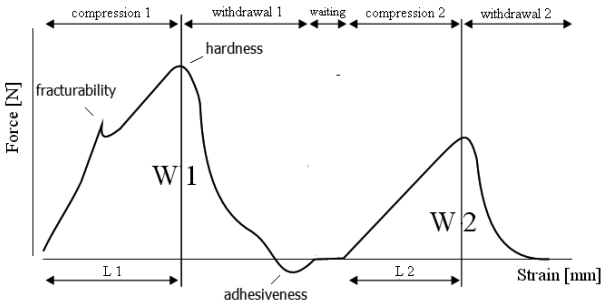

Fig. 1. Example of a graph obtained in the double compression test (TPA)

To observe changes taking place in the pastries during storage, the tests were conducted over three consecutive days.

Determination of the moisture content of the products and the sensory assessment were conducted in accordance with the Polish Standard PN-A-74252-1998. [16] The jury evaluated the uniformity of the batch, the external appearance, structure and texture, and the taste and flavour. They also estimated the quality of the gingerbreads.

RESULTS

The results of the study are presented in Figs. 2-5. Extension of the time of storage caused an increase of the hardness of the pastries. The highest hardness was achieved by the pastries after three days of storage (Fig. 2). Hardness decreased with increase in the amount of margarine added to the dough. The lowest effect on hardness during storage was noted when the margarine was added in the amount of 200g. The hardness of the pastry after 3 days of storage was higher by 0.51 N compared with the pastry after one day of storage.

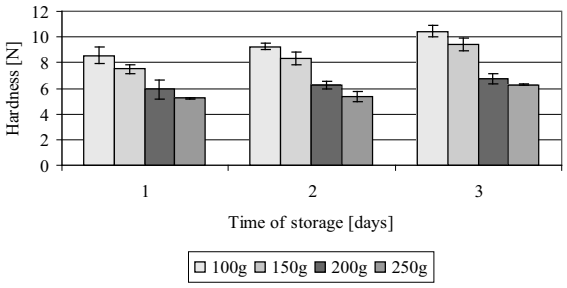

Fig. 2. Effect of fat addition on hardness of gingerbread in relation to time of storage

The effect of fat addition m [g] and time of storage t [days] on the hardness H [N] of gingerbread pastry was described by means of the equation:

$$H = 10.773 - 0.0271m + 0.707t, \quad (1)$$

R^2=0.94, $\alpha \leq 0.05$.

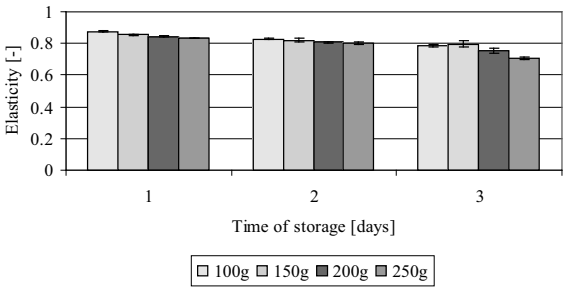

Fig. 3. Effect of fat addition on elasticity of gingerbread in relation to time of storage

The highest value of elasticity (Fig. 3) was noted on the first day for gingerbread with fat content of 100g, at 0.875, and the lowest on the third day for gingerbread with fat content of 250g – 0.707. Increase in the fat addition caused insignificant decreases in gingerbread elasticity during the first and second days of storage. Whereas on the third day a significant decrease of elasticity was observed between gingerbreads with fat content of 150g and 200g and those with 200g and 250g.

The changes in elasticity E [-] are described by the equation:

$$E = 0.958 - 0.000343m - 0.0448t, \quad (2)$$

R^2=0.884, $\alpha \leq 0.05$.

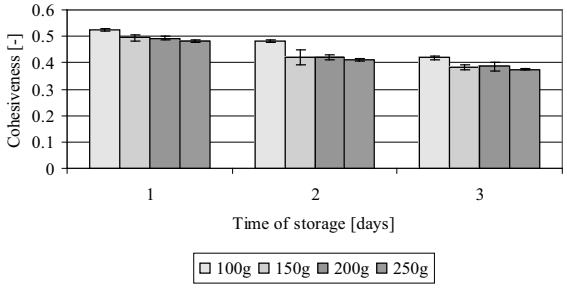

Fig. 4. Effect of fat addition of cohesiveness of gingerbread with relation to time of storage

For all the tested kinds of gingerbread, the cohesiveness decreased with the passage of time (Fig. 4). The highest value of that trait was noted after one day of storage for gingerbread with fat content of 100g (0.524), and the lowest for that in which the fat content was 250g, after three days of storage (0.374). For gingerbreads tested on the first day there were no significant differences in the values of cohesiveness. On successive days there appeared a significant decrease of cohesiveness between gingerbreads with margarine content of 100g and 150g. The decrease was at the level of ca. 12-13%.

The relations presented in Fig. 4 are described by the equation:

$$COH = 0.6047 - 0.00032m - 0.05405t, \quad (3)$$

R^2=0.914, $\alpha \leq 0.05$.

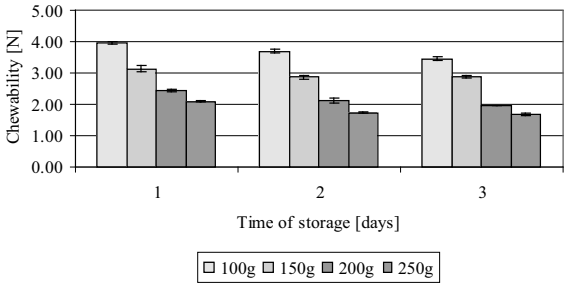

Fig. 5. Effect of fat addition on chewability of gingerbread in relation to time of storage

For each tested kind of gingerbread the value of chewability decreased with the passage of time of storage. As it can be seen in Fig. 4, on the first day of storage the value of that trait decreased by as much as 47% with increasing fat content. The value of chewability was the highest on the first day for the gingerbread with fat content of 100g, at 3.96 N, and the lowest for the gingerbread with fat content of 250g, on the third day since baking, at 1.68 N.

The changes in chewability *CH* [N] are described by the equation:

$$CH = 5.325 - 0.128m - 0.21t, \quad (4)$$

R^2=0.961, $\alpha \leq 0.05$.

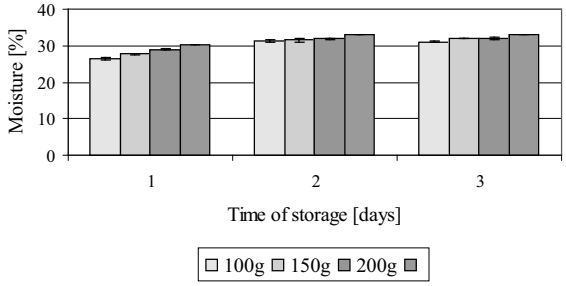

Fig. 6. Effect of fat addition on moisture of gingerbread in relation to time of storage

The lowest moisture (Fig. 6) was recorded for the crumb of gingerbread with 100g addition, on the first day of the study (26.43%), and the highest for that with fat content of 250 g, after two days of storage (33.13%). On the second and third days of storage the moisture changes did not differ statistically significantly.

The effect of fat addition *m* [g] and time of storage *t* [days] on the moisture content *M* [%] of gingerbread is described by the equation:

$$M = 11.57 + 14.541t + 0.0237m - 3.035t^2, \quad (5)$$

R^2=0.857, $\alpha \leq 0.05$.

The results of sensory assessment (Tab. 1) of the gingerbread pastries indicate that the gingerbread with fat content of 200g was classified in the first level of quality of confectionery products. The jury members declared that that batch of products was of good uniformity and homogeneity and no greater differences were noted among the individual items. The external appearance was characteristic for gingerbread pastry. The particular kinds of gingerbread differed slightly in crumb colour (the darkest was that with the lowest fat content). All of them had highly desirable taste, typical of that type of pastries, aromatic with well balanced intensity, ensuring consumption value. Gingerbread with traits desired by the consumer, one day after baking, should be characterised by the following mechanical properties of texture: hardness of 5.107–6.931N, elasticity of 0.837-0.847, cohesiveness of 0.482-0.503, chewability of 2.383-2.491N, and moisture of 28.113-29.152%. Studying the properties of texture one can largely eliminate the costly sensory evaluation, determined by personal references and sensitivity of sensory assessment, in favour of objective instrumental analysis, permitting rapid acquisition of a large number of repeatable results.

Table 1. Effect of fat content on sensory features of gingerbrea

Fat content	Quality factors pastry				Total points	Level of quality
	Batch uniformity	Appearance	Structure and texture	Taste and flavour		
100g	4	4	3	4	15	II
150g	4	5	4	4	17	II
200g	5	5	5	5	20	I
250g	4	4	4	3	15	II

CONCLUSIONS

1. The properties of the texture of gingerbread pastry are significantly affected by the amount of fat added and by the time of storage.
2. Extension of the time of storage caused a significant increase of gingerbread crumb hardness and moisture, and a decrease of elasticity, cohesiveness and chewability.
3. Hardness, elasticity and cohesiveness decreased with increasing level of margarine addition, while moisture increased.
4. The highest consumer rating was awarded to the gingerbread with fat content of 200g. It was qualified to the first level of quality of confectionery products.

REFERENCES

1. **Bartnikowska E., Obiedziski M., 1997.:** Unsaturated trans fatty acids - nutritional problem? Polish Journal of Food and Nutrition Sciences, 6 (47), p. 1-20.
2. **Cervenka L., Rezkova S., Hejdrychova J., Kralovsky J., Brozkova I., Kejchelova M., 2007.:** Study of moisture adsorption characteristics of gingerbreads and biscuits using a hygrometric method, Acta Alimentaria, 36, p. 319-328.
3. **Cervenka L., Rezkova S., Kralovsky J., 2008.:** Moisture adsorption characteristics of gingerbread, a traditional bakery product in Pardubice, Czech Republic, Journal of Food Engineering, 84, p. 601-607.
4. **Dojutrek Cz., Pietrzyk A., 1977.:** Wyroby ciastkarskie, WNT. Warszawa.
5. **Dziki D., Laskowski J., 2006.:** Influence of wheat grain mechanical properties on grinding energy reuirements. TEKA Komisji Motoryzacji i Energetyki Rolnictwa. 6A, p. 45-52.
6. **Erp-Baart M.A., Couet C., Cuadrado C., Kafatos A., Stanley J., Poppel G., 1998.:** Trans fatty acids in bakery products from 14 European countries, Journal of Food Composition and Analysis, 11, p. 161-169.
7. **Gasparska R., 1999.:** Klasyfikacja półproduktów i wyrobów cukierniczych, Przegląd Piekarski i Cukierniczy, 11, p. 54-56.
8. **Juttelstad A., 2004.:** The marketing of trans fat- free foods, Food Technology, 1 (58), p. 20.
9. **Kopta A., Łuszczak B., 1973.:** Technologia gastronomiczna dla ZSZ cz II. PWSZ, Warszawa.
10. **Krygier K., 2003.:** Podstawowa charakterystyka tłuszczów, Przegląd Piekarski i Cukierniczy, 5, p. 6-8.
11. **Kusińska E. 2007.:** Wpływ rodzaju dodanego tłuszczu na właściwości tekstualne i jakość ciasta drożdżowego, Problemy agrofizyczne kształtowania środowiska rolniczego i jakości surowców żywnościowych, Wydawnictwo Naukowe Fundacji Rozwoju Nauk Agrofizycznych, Lublin.
12. **Lipińska H., Lubczyńska H., Pisarek S., Woźniakowski A., 2002.:** Zbiór receptur ciastkarskich oraz podstawy technologii półproduktów i wyrobów, Wydawnictwo Handlowo-Usługowa Spółdzielnia „Samopomoc-Chłopska", Warszawa.
13. **Mathlouthi M., 2001.:** Water content, water activity, water structure and stability of food stuff, Food Control, 12, p. 409-417.
14. **Peleg M., 1998.:** Mechanical properties of dry btittle cereal products. In: The Properties of Water in Foods ISOPOW 6, Ed. Reid E. Blackie Academic and Professional, London.
15. **Piesiewicz H., Kwasek M., 1999.:** Przegląd Piekarniczy i Cukierniczy, Słodkie pieczywo korzenne, 12, p. 14-17.
16. Polska Norma: PN-A-74252-1998,.: Wyroby i półprodukty ciastkarskie, Metody badań.
17. **Schramm G. 1998.:** Reologia. Podstawy i zastosowania, Ośrodek Wyd. Nauk. PAN, Oddz. Poznań.
18. **Vytrasova J., Pribanova P., Marvanova L., 2002.:** Occurrence of xerophilic fungi in bakery gingerbread production, International Journal of Food Microbiology, 72, p. 91-96.
19. **Wanasink B. 2003.:** Response to "Measuring consumer response to food products", Sensory tests predict consumer acceptance, Food Quality and Preference, 14, p. 23-26.
20. **Wilkinson C., Dijksterhuis G.B., Minekus M. 2000.:** From food structure to texture, Trends in Food Science and Technology, 11, p. 442-443.
21. **Wójtowicz A., Mitrus M., 2010.:** Effect of whole wheat flour moistening and extrusion- cooking screw speed on the SME process and expansion ratio of precooked pasta products, TEKA Komisji Motoryzacji i Energetyki Rolnictwa, 10, p. 517-526.
22. **Wyczański S., 1989.:** Surowce i materiały pomocnicze w cukiernictwie, WSiP, Warszawa.
23. **Zalewski S., 2003.:** Podstawy technologii gastronomicznej, WNT, Warszawa.
24. **Żbikowska A., Marciniak-Łukasiak K., Krygier K., 2006.:** Wpływ zawartości izomerów trans w tłuszczach na jakość ciastek francuskich z mąk o różnej zawartości technologicznej, Żywność. Nauka. Technologia. Jakość, 2(47), p. 374-381.

WPŁYW ZAWARTOŚCI TŁUSZCZU NA WŁAŚCIWOŚCI MECHANICZNE TEKSTURY CIASTA PIERNIKOWEGO

Streszczenie. W pracy przedstawiono wyniki badań pomiaru mechanicznych właściwości tekstury ciasta piernikowego z użyciem testu podwójnego ściskania TPA. Parametrami zmiennymi w doświadczeniu były: ilość dodanego tłuszczu oraz czas przechowywania. Badania prowadzono przez trzy kolejne dni. Dodatkowo wykonano ocenę sensoryczną, która

pozwoliła na dobór optymalnej ilości tłuszczu na podstawie właściwości teksturalnych.

S ł o w a k l u c z o w e : ciasto piernikowe, tłuszcz, tekstura, ocena sensoryczna.

TEKA. COMMISSION OF MOTORIZATION AND ENERGETICS IN AGRICULTURE – 2012, Vol. 12, No. 1, 127–130

Effect of knife wedge angle on the force and work of cutting peppers

Elżbieta Kusińska, Agnieszka Starek

Department of Food Engineering and Machinery, University of Life Sciences in Lublin, Poland,
e-mail: elzbieta.kusinska@up.lublin.pl

Summary. The paper presents the method of measurement and the results of tests on cutting the fruits of two peppers cultivars - King Arthur and Bell. It was found that the knife wedge angle had a significant effect on the cutting force and work. Higher values of cutting force and work were obtained for red peppers than for yellow peppers. The cutting force and work were also related to the textural properties of the peppers.

Key words: peppers, cutting, knife wedge angle, cutting force, cutting work, texture.

INTRODUCTION

Peppers (*Capsicum annuum L.*) are a vegetable known and valued by consumers due to their high biological values and specific taste [4, 11]. The fruits of peppers are valued especially for their spice and medicinal properties [16]. Powdered peppers, also known as paprika, are used for colouring spice mixes for soups, smoked meats and for extruded products, as well as for extending the shelf life of ready-to-eat products (ready-to-eat dishes, cooled as well as frozen). The vegetable enhances the taste of food and constitutes a valuable component of healthy diet [1, 2, 13]. The fruits and seeds of peppers are a valuable raw material in the processing and pharmaceutical industries. They are included in the composition of numerous homeopathic preparations [17]. Peppers are particularly rich in organic micro-components with antioxidant properties that have a health-promoting effect on the human organism [7, 12]. Fresh fruits of peppers are the best source of antioxidants. Peppers can be subjected to a variety of technological factors, i.e. freezing, lyophilisation or freeze-drying, cooking, blanching. Proper selection of the parameters of those processes permits to avoid the degradation of valuable compounds [9].

The development of new technologies aimed at reducing the costs of production and at limiting the yield losses (ratio of the mass of cut products to the mass of intact products) permitted the improvement of fragmentation techniques [Kader 2002]. In the case of agricultural and food materials, cutting is a very frequently used form of fragmentation. Cutting forces not only determine the power requirements of the process under given conditions, but also affect the design of transport assemblies of processing machines. The possibility of calculating the cutting forces is a prerequisite for the design of properly operating and energy-saving machines in which the cutting process is realised [3]. In the fruit and vegetable processing industry cutting is applied to obtain products with desired shape and size [5]. The process of cutting fruits and vegetables depends primarily on the design of the cutting assembly, the shape of the cutting edge, the parameters of operation of the device, and on the physical properties of the plant material – its strength properties and structure. Also important are the conditions of cultivation, the duration and method of storage of the material, degree of ripeness, harvest conditions, cultivar-related traits, etc. [15, 19]. The working element that acts on the plant is the knife or cutting blade, whose operating parameters affect the values of operating drag of machines and the quality of cutting [6]. The operation of cutting knives can be considered as that of sharp wedged penetrating the material being cut. Flat knives with straight edge have found the most extensive application [18]. Studies concerned with the processes of cutting and fragmentation of materials comprise, in most cases, the determination of relations between the level of fragmentation of the material, its operating parameters and the energy expenditure [14, 8]. The diversity of designs and principles of functioning of cutting assemblies make it necessary that, for the purposes of their design and operation, determination was performed of the total or unit work of cutting [20].

OBJECTIVE AND SCOPE OF STUDY

The objective of the study reported herein was the determination of the effect of the knife wedge angle on the force and work of the process of cutting peppers. The variable parameters were the peppers cultivars and the orientation of the material being cut. Additionally, the textural properties of the two peppers cultivars were determined and compared.

METHOD

The experimental material was ripe fruits of two peppers cultivars: red peppers cv. King and yellow peppers cv. Bell. The material used in the study was fresh, healthy, free of mechanical damage. The fruits were harvested in the phase of full ripeness in the second decade of September, and tested on the following day. The peppers were subjected to preliminary treatment: washing, cutting along the pod, and removal of seeds. The material for the tests was cut from the central section of the peppers (i.e. in a zone with relatively constant circumference), in the form of half-rings with the height of 40 mm. The thickness of the meat was 5±2 mm. The process of cutting was conducted on the texture analyser, type TA.XT plus, maintaining constant orientation of the cutting knife. The knifes used in the tests were straight edge, with various wedge angles: 2.5°, 5°; 7.5°, 10°, 12.5°; 15°; 17.5° and 20°. Samples of peppers were placed parallel to the base of the analyser, skin down or skin up, and then they were loaded, in the perpendicular direction, with the cutting element at a constant velocity of 50 mm·min^{-1}. The results of the measurements were in the form of graphs representing the relation between the cutting force and knife displacement, from which the values of the cutting force and work were determined. The tests were performed in one hundred replications. Additionally, analysis of the texture of the peppers was performed, also by means of the TA.XT plus texture analyser, equipped with an adapter in the form of a cylinder with diameter of 25 mm. From each vegetable 10 specimens were prepared, in the form of cubes with the side of 5 mm. These were subjected to double compression at head travel velocity of 50 mm·min^{-1}. The process of compression was conducted at constant deformation of the specimens, of 50% of their height; the specimens were positioned skin down. Analysis of the measurement results, in the form of texture-grams, permitted the determination of the following texture parameters: hardness, brittleness, elasticity, cohesiveness, chewability.

RESULTS

The results of measurements of peppers cutting force and work are presented in Fig. 1-4.

The analysis of graphs representing the cutting force in relation to knife wedge angle with the peppers placed skin down revealed significant differences between the cultivars (Fig. 1), which was confirmed by the analysis of variance. The highest values of the cutting force were 53.211 N (cv. King Arthur) and 47.805 N (cv. Bell) for knife wedge angle of α=20°, while the lowest cutting force values were obtained for the knife wedge angle of α=2.5° (22.098 N and 26.641 N). Large differences between the cultivars appeared at the knife wedge angle of α=7.5° (73.95%).

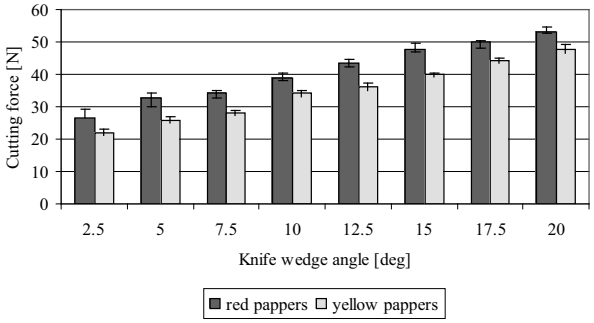

Fig. 1. Relation of cutting force of red and yellow peppers to knife wedge angle with the material positioned skin down

The relations presented in Figure 1 are described by equations (1) and (2):

$$F_{cr} = 25.19e^{0.1\alpha}, \quad (1)$$

$R^2 = 0.98$,

$$F_{cy} = 3.676\alpha + 18.273, \quad (2)$$

$R^2 = 0.99$,

where:
F_{cr} – cutting force of red peppers,
F_{cy} – cutting force of yellow peppers,
α – knife wedge angle.

For the fruits positioned skin up (Fig. 2), with knife wedge angle increase within the adopted range, the cutting force of yellow peppers grew1.82-fold and that of red peppers 1.73-fold, and in the case of material cut from the meat side, the corresponding increases were 2.16 and 1.99-fold. The lowest values of cutting force, 41.91 N (yellow peppers) and 50.845 N (red peppers), were recorded at knife wedge angle of α=2,5°, and the highest at α=20° (76.651 N for cv. Bell and 88.032 N for cv. King Arthur). The cutting force values for both cultivars were higher when the material was cut from the skin side than from the meat side, which was related with the structure of the skin.

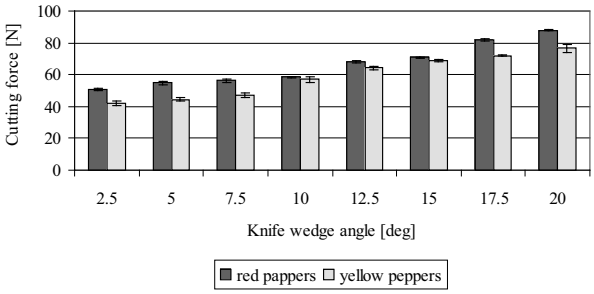

Fig. 2. Relation of cutting force of red and yellow peppers to knife wedge angle with the material positioned skin up

The relations presented in the Figure are described by equations (3) and (4):

$$F_{cr} = 45.433e^{0.079\alpha}, \quad (3)$$

$R^2 = 0.97$,

$$F_{cy} = 37.658e^{0.094\alpha}, \quad (4)$$

$R^2 = 0.97$.

In the experiments on peppers cutting, when the specimens were positioned skin down (Fig. 3) the lowest value of cutting work was 0.085 J for knife wedge angle α=2.5° for cv. Bell. With the reverse positioning of the material (Fig. 4) the cutting work for that peppers cultivar was greater by 45.21%. The highest values of cutting work were recorded for cv. King Arthur, for knife wedge angle α=20° when the cutting was from the side of the skin – 0.471 J. That value was higher by 0.079 J from that for cv. Bell tested with the same method. No significant differences between the results were observed when both peppers cultivars were cut with knives of wedge angles of α=10° and α=12.5°.

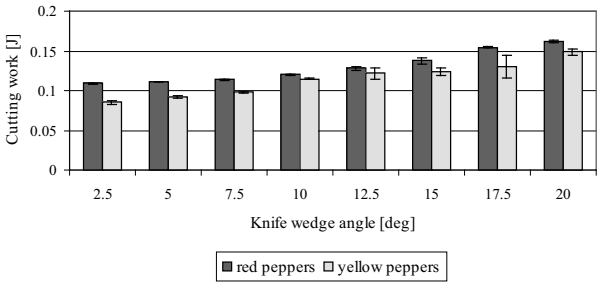

Fig. 3. Relation of cutting work of red and yellow peppers to knife wedge angle with the material positioned skin down

The relations presented in the Figure are described by equations (5) and (6):

$$W_{cr} = 0.097e^{0.06\alpha}, \quad (5)$$

$R^2 = 0.95$,

$$W_{cy} = 0.079e^{0.076\alpha}, \quad (6)$$

$R^2 = 0.97$,

where:
W_{cr} - cutting work of red peppers,
W_{cy} – cutting work of yellow peppers.

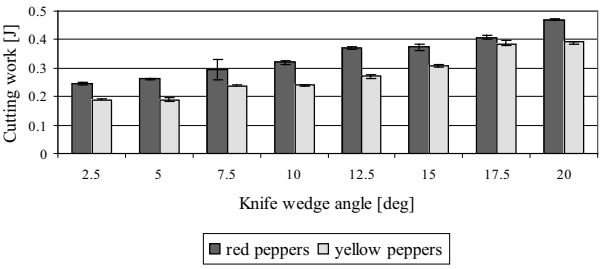

Fig. 4. Relation of cutting work of red and yellow peppers to knife wedge angle with the material positioned skin up

The relations presented in the Figure are described by equations (7) and (8):

$$W_{cr} = 0.224e^{0.09\alpha}, \quad (7)$$

$R^2 = 0.98$,

$$W_{cy} = 0.16e^{0.114\alpha}, \quad (8)$$

$R^2 = 0.97$.

Equations 1-8 were derived at significance level lower than/equal to 0.05.

Table 1 presents the results of measurement of the texture properties of the peppers.

Table 1. Texture properties of red peppers vs. King Arthur and yellow peppers vs. Bell

Variety	Hardness [N]	Brittleness [N]	Elasticity [-]	Cohesiveness [-]	Chewability [N]
Red peppers	81.909	41.824	0.497	0.326	13.271
Yellow peppers	62.096	39.274	0.536	0.326	10.85

Notably higher values of hardness, brittleness and chewability were obtained for the red peppers, elasticity of greater in the case of peppers cv. Bell, and cohesiveness was identical for both peppers cultivars.

The higher values of hardness and chewability and lower values of elasticity of the red peppers corresponded with the greater values of cutting force and work than in the case of the red peppers.

CONCLUSIONS

1. Increase of the knife wedge angle causes an increase in the values of peppers cutting force and work. The highest force value was obtained when cutting with a knife with wedge angle of α=20° - 88.032 N (red peppers cut with the skin up). When cutting with a knife with wedge angle of α=2.5° the lowest values of cutting force were obtained – 22.098 N (yellow peppers cut with the skin down).
2. Irrespective of the positioning of the specimens, in the case of cutting fruits of red peppers, higher values of the cutting force and work were obtained compared to fruits of yellow peppers. Cutting work values were the highest for peppers cv. King Arthur, 0.246 – 0.471 J, compared to cv. Bell at 0.188 – 0.392 J (positioned skin up).
3. The results of texture tests are related with the values of cutting force and work of peppers.

REFERENCES

1. **Buczkowska H., Dyduch J., Najda A., 2001.** Kształtowanie się zawartości niektórych składników chemicz-

nych w owocach papryki ostrej w zależności od odmiany i wielokrotności zbioru. Rolnictwo. Zeszyty Naukowe, 234(46), p. 27-32.
2. **De Marino S., Borbone N., Gala F., Zollo F., Fico G., Pagiotti R., Iorizzi M., 2006.** New constituents of sweet Capsicum annuum L. fruits and evaluation of their biological activity. Journal Agricultural. Food Chemistry, 54(20), p. 7508-7516.
3. **Dowgiałło A., 2006.** Modelowanie operacji cięcia materiałów rolno-spożywczych. Postępy Techniki Przetwórstwa Spożywczego, 1, p. 47-49.
4. **Gajc-Wolska J., Skąpski H., 2002.** Yield of sweet pepper depending on cultivars and growing conditions. Folia Horticulturae, 14(1), p. 95-103.
5. **Fellows P.J., 1996.** Food processing technology. Principles and practice (second end). CRC Press. U.K.
6. **Frączek J., Mudryk K., 2007.** Metoda pomiaru energochłonności procesu zrębkowania pędów wierzby. Inżynieria Rolnicza, 7(95), p. 47-53.
7. **Janeczko Z., 2003.** Owoce i warzywa jako źródło prozdrowotnych substancji o właściwościach antyoksydacyjnych. Folia Horticulturae, 1, p. 23-25.
8. **Kowalski S. 1993.** Badania oporów cięcia wybranych roślin. Zeszyty Problemowe Postępów Nauk Rolniczych, 408, p. 297-303.
9. **Krokida M.K., Philippopoulos C., 2006.** Volatility of apples during air and freeze drying. Journal Food Engineering, 73, p. 135-141.
10. **Lamikandra O., 2002.** Fresh-cut fruits and vegetables. Science, Technology, and Market. CRC Press, Boca Raton, Florida, USA.
11. **Márkus F., Daood H.G., Kapitány J., Biacs P.A., 1999.** Change in the caroteniod and antioxidant content of spice red pepper (paprika) as a function of ripening and some technological factors. Journal Agricultural Food Chemistry, 47(1), p. 100-107
12. **Materska M., Perucka I., 2005.** Antioxidant activity of the main phenolic compounds isolated from hot pepper fruit (Capsicum annuum L.). J. Agricultural Food Chemistry, 53, p. 1750-1756.
13. **Michalik Ł., Wierzbicka B., Kawecki Z., 2002.** Plonowanie i jakość papryki słodkiej w uprawie pod osłonami. Wartość biologiczna owoców papryki. Biuletyn Naukowy, 14, p. 89-99.
14. **Molendowski F., 2005.** Energochłonność procesu rozdrabniania surowców roślinnych na przykładzie rdzeni kolb kukurydzy. Zeszyty Naukowe Akademii Rolniczej. Wrocław.
15. **Nadulski R., 2001.** Wpływ geometrii narzędzia tnącego na przebieg procesu cięcia wybranych warzyw korzeniowych. Acta Agrophysica, 58, p. 127-135.
16. **Perucka I., Materska M., 2007.** Antioxidant vitamin contents of Capsicum annuum fruit extracts as affected by processing and varietal factors. Acta Scientiarum Polonorum. Technologia Alimentaria, 6(4), p. 67-74.
17. **Perucka I., Materska M., 2003.** Antioxidant activity and content of capsaicinoids isolated from paprika fruits. Polish Journal of Food and Nutrition Sciences, 12(53), p. 15-18.
18. **Sykut B., Kowalik K., Opielak M., 2005.** Badanie wpływu kątów ostrza i przystawienia na opory krojenia produktów spożywczych. Inżynieria Rolnicza, 9(69), p. 339-344.
19. **Szot B., Kęsik T., Gołacki K., 1987.** Badania zmienności właściwości mechanicznych korzeni marchwi w zależności od cech odmianowych, czynników agrotechnicznych i okresu przechowywania. Zeszyty Problemowe Postępów Nauk Rolniczych, 316, p. 227-246.
20. **Zastempowski M., Bochat A., 2011.** Badanie energochłonności cięcia materiału roślinnego. Inżynieria i Aparatura Chemiczna, 50(3), p. 91-92.

WPŁYW KĄTA ZAOSTRZENIA NOŻA NA SIŁĘ I PRACĘ CIĘCIA PAPRYKI

Streszczenie. W pracy przedstawiono metodykę pomiaru oraz wyniki badań cięcia owoców papryki dwóch odmian: King Arthur i Bell. Stwierdzono istotny wpływ kąta zaostrzenia noża na wartość siły cięcia i pracy cięcia. Wyższe wartości siły i pracy cięcia otrzymano dla papryki czerwonej niż żółtej. Siła i praca cięcia były również uzależnione od właściwości tekstualnych.

Słowa kluczowe: papryka, cięcie, kąt zaostrzenia noża, siła cięcia, praca cięcia, tekstura.

TEKA. COMMISSION OF MOTORIZATION AND ENERGETICS IN AGRICULTURE – 2012, Vol. 12, No. 1, 131–134

Energy of bean pods opening with phosphorous fertilization

Piotr Kuźniar

Department of the Farm and Food Production Engineering, University of Rzeszów
Zelwerowicza 4 st., 35-601 Rzeszów, Poland, pkuzniar@univ.rzeszow.pl

S u m m a r y. The study encompasses the results of research on a phosphorous fertilization impact on the energy necessary to open bean pods cultivated on dry seeds of varieties: Narew, Nida and Wawelska carried out in the years 2008-2010. Four doses of phosphorous were used: 0, 40, 80 and 120 kg·ha^{-1}. Nida variety was characterized with pods most vulnerable to cracking (opening energy 169.3 mJ), and pods least vulnerable to cracking were found in Narew variety (opening energy 262.5 mJ). Increasing phosphorous dose from 0 to 120 kg·ha^{-1} caused a decrease in the amount of energy necessary to open pods of the tested bean varieties, except for Wawelska variety, where an insignificant increase of this energy was observed.

K e y w o r d s: bean pod, opening energy, phosphorous fertilization.

INTRODUCTION

The main unfavourable feature of oil and leguminous plants is the tendency to crack their siliques and pods and flake their seeds before and after harvesting [5, 9, 14, 15]. Vulnerability of pods to cracking is a variety feature and is mainly determined by their structure and shape in cross section [7, 17, 18]. Among the elements of pod internal structure, their vulnerability to cracking is determined by, among others, content and structure of fibre in walls of their shells and seams which are considerably influenced by meteorological conditions in the period of growth as well as type and amount of the used fertilizers [3, 4, 6, 8, 10, 13, 19, 20].

The aim of this study was to evaluate an impact of diverse phosphorous fertilization on the amount of energy necessary to open pods of bean varieties cultivated on dry seeds.

MATERIAL AND METHODS

The research was conducted in 2008-2010. The bean was cultivated on the experimental field of the Department of the Farm and Food Production Engineering in Rzeszów. Four phosphorous doses were applied before sowing: 0, 40, 80, 120 kg·ha^{-1}. The tested bean varieties were characterized with a diverse size of seeds and pods (Tab. 1).

Table 1. Pod characteristics (average values) of tested bean varieties

Specification	Narew	Nida	Warta	Wawelska
Dimension of pods [mm]:				
Length	93,0	89,5	103,7	112,3
Width	10,1	10,4	10,0	11,2
Thickness	9,3	9,1	8,9	9,8
Number of seeds in pod	4,6	4,0	4,3	3,7

Energy required to open a pod was calculated with the pressure method [11, 16, 18] which is based on tearing a pod by compressed air (Fig. 1) from the relation:

$$E = \frac{3}{2} pV, \tag{1}$$

where:
E - energy of bean pods opening [J],
p - air pressure in the pod [Pa],
V - air volume inside the pod [m^3].

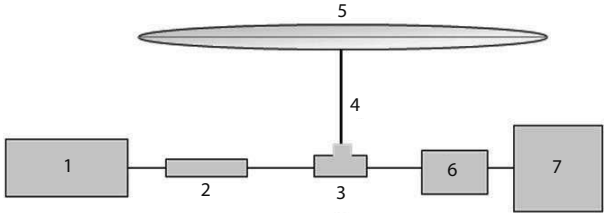

Fig. 1. Total device: 1 – compressed air bank, 2 – pressure gauge and cut-off-valve, 3 – T-tube, 4 – needle, 5 – pod, 6 – pressure sensor, 7 – computer

Air volume in a pod was determined with modified pictometric method [2, 11, 12].

Measurements were carried out on 20 pods for each variety with humidity in the range of 12.4-13.8%. The obtained results were statistically analyzed [1] with Statistica 9 program, with which variance analysis and LSD significance test were conducted.

RESULTS

Nida variety was the most vulnerable to cracking pods (Fig. 2). The statistically smallest amount of energy was necessary to open its pods, on average 169,3 mJ. The pods most resistant to cracking were found in Wawelska and Narew varieties for which opening energy amounted to 262.5 and 244.9 mJ, respectively.

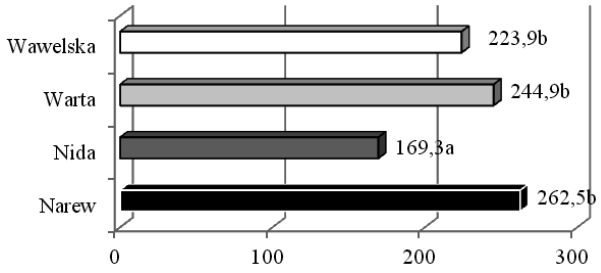

Fig. 2. Average from three years energy of pods opening [mJ] of tested bean varieties

*different letters signify significant differences for the significance level α = 0.05

The value of opening energy of bean pods of the tested varieties from years 2008-2010 for applied doses was presented in Table 2.

When analyzing the results contained in Table 2, it should be noted that pod opening energy of the tested varieties was diverse and depended on phosphorous dose and years. In case of Nida variety, changes of opening energy with the increase of phosphorous dose were not statistically important in any year of the research, whereas for Warta they were significant in 2009, and for Wawelska in 2009 and 2010. Only in case of Narew variety, significant changes in opening energy were observed in all the three years of research.

The pods were characterized with the lowest vulnerability in 2008. Narew and Nida pods were most prone to cracking in 2010, while Warta and Wawelska in 2010. A decrease of energy required to open pods of the tested bean varieties with the increase of phosphorous dose was observed (Tab. 2), with the exception of Wawelska which displayed a very slight increase of the amount in question.

The relation of pod opening energy of the tested bean varieties with phosphorous dose is well described by linear function (Fig. 3) in the form of:

$$E = a \cdot D + b, \tag{2}$$

where:
a, b - coefficients of equation,
D – phosphorous dose [kg·ha^{-1}].

Fig. 3. Relation of the pod opening energy of tested bean varieties to the dose of phosphorous

Coefficients of equations describing the relation of pod opening energy of the tested bean varieties with the phosphorous doses and their determination coefficients were presented in Table 3.

Table 2. Energy of pod opening [mJ] on tested bean varieties for applied doses of phosphorous

Variety	Years	Phosphorous doses [kg·ha^{-1}]				Average
		0	40	80	120	
Narew	2008 2009 2010	316,1ab 324,7b 345,0b	284,1b 284,6ab 112,9a	441,3b 256,9ab 177,2a	291,8a 181,8a 133,7a	333,3 III 262,0 II 192,2 I
	Average	328,6c	227,2ab	291,8bc	202,4a	262,5
Nida	2008 2009 2010	220,6a 203,8a 122,8a	193,8a 143,6a 126,1a	213,6a 169,4a 131,2a	273,0a 126,4a 107,3a	225,3 II 160,8 I-II 121,8 I
	Average	182,5a	154,5a	171,4a	168,9a	169,3
Warta	2008 2009 2010	185,1a 218,6a 290,1b	381,2b 202,4a 293,9b	332,2b 144,8a 201,3ab	361,2b 167,1a 162,2b	314,9 II 183,2 I 236,8 I
	Average	231,3a	292,5a	226,1a	230,2a	245,0
Wawelska	2008 2009 2010	259,7ab 205,5a 230,9a	204,4a 156,7a 185,9a	380,7b 189,9a 232,2a	357,4b 96,7a 187,8a	300,5 II 162,2 I 209,2 I
	Average	232,0ab	182,3a	267,6b	214,0b	224,0

*different letters in row and Roman numerals in column signify significant differences for the significance level α = 0.05

Coefficients of the analyzed equations indicate that the largest decrease of resistance to pod cracking with the increase of phosphorous dose occurred for Narew variety for which the increase of phosphorous dose of 1kg·ha^{-1} caused a decrease of 0.78 mJ of the energy necessary to open them.

Table 3. Values of coefficients of determination R^2 and coefficients of equation $E = a \cdot D + b$, describing dependence of opening energy of pods E on applied doses of phosphorous D

Variety	a	b	R^2
Narew	-0,7851	309,62	0,4888
Nida	-0,0597	172,90	0,0718
Warta	-0,1742	255,44	0,0804
Wawelska	0,0778	219,31	0,0127
Average	-0,2353	239,32	0,3979

Tomaszewska [19, 20] showed in her research that pods in the shells of which fibre layer consisted of sclerenchymatic cells is thicker or these cells are stronger, are more prone to cracking since during their drying larger stresses occur in the shell aiming at the pod opening. An increase of bean pod cracking vulnerability of the tested varieties with the increase of nitrogen dose may prove that there was an increase in thickness of shell fibre layer or strengthening of the structure of sclerenchymatic cells.

CONCLUSIONS

Pod opening energy of the tested bean varieties was diverse and depended on the used phosphorous doses.

Pods of Nida variety were most vulnerable to cracking. The energy in the mean amount of 169.3 mJ was sufficient to open them. Narew variety had pods most resistant to cracking, for them the opening energy amounted on average to 262.5mJ.

An increase of phosphorous dose from 0 to 120 kg·ha^{-1} caused a decrease in the amount of energy necessary to open pods of the tested bean varieties with the exception of Wawelska variety for which a statistically irrelevant increase of opening energy was observed.

Relation of the mean three year pod opening energy of the tested bean varieties with the applied phosphorous doses is described by linear function.

REFERENCES

1. **Burski Z., Tarasińska J., Sadkević R. 2003.** The methodological aspects of using multifactoral analysis of variance in the examination of exploitation of engine sets. TEKA Komisji Motoryzacji i Energetyki Rolnictwa Polskiej Akademii Nauk Oddział w Lublinie, 3, p. 45-54.
2. **Diehl K.C., Garwood V.A., Haugh C.G. 1988.** Volume measurement using the air-comparison pycnometer Trans. ASAE, 1, p. 284-287.
3. **Dorna H., Duczmal K. W. 1994.** Wpływ warunków klimatycznych na formowanie włókna w szwach strąków fasoli zwykłej (*Phaseolus vulgaris* L.). I Ogóln. Konf. Nak. Strączkowe Rośliny Białkowe. FASOLA, Lublin 25.11.1994, p. 135-138.
4. **Dutt B. K., Datta A. C, 1999.** Dynamic and quasi-static force and energy requirement for detachment and breakage of chickpea pedicel and pod. Transaction of the ASAE, 2, p. 309-318.
5. **Furtak J., Zaliwski A. 1986.** Badania nad zbiorem mechanicznym nasion fasoli. Roczniki. Nauk Rolniczych, ser. Technika Rolnicza, 2, p. 127-140.
6. **Hejnowicz Z. 1985.** Anatomia i histogeneza roślin naczyniowych. PWN Warszawa.
7. **Kuźniar P., Sosnowski S. 2002.** Relation between the bean pod shape factor and force required for pod opening. International Agrophysics, 2(16), p. 129-132.
8. **Kuźniar P., Strobel W. 2000.** Określenie wpływu grubości sklerenchymy strąków fasoli na ich podatność na pękanie. Acta Agrophysica, 37(14), p. 113-117.
9. **Kuźniar P., Sosnowski S. 2003.** Podatność strąków na pękanie a wielkość strat nasion fasoli podczas mechanicznego zbioru. Acta Agrophysica, 1(2), p. 113-118.
10. **Kuźniar P., Sosnowski S. 2003.** Wpływ wilgotności strąków fasoli i ich wielokrotnego nawilżania na siłę potrzebną do ich otwarcia. Acta Agrophysica, 2(1), p. 119-126.
11. **Kuźniar P., Sosnowski S. 2007.** The attempt of measuring the air volume in bean pods. TEKA Komisji Motoryzacji i Energetyki Rolnictwa Polskiej Akademii Nauk Oddział w Lublinie. 7A, p. 68-72.
12. **Kuźniar P. 2008.** The energy of bean-pod opening and the method of determining air volume therein. MOTROL- Motoryzacja i Energetyka Rolnictwa, 10, p. 73-77.
13. **Strobel W. 2003.** Porównanie cech fizycznych strąków różnych gatunków łubinu. Zeszyty Problemowe Postępów Nauk Rolniczych, 495, p. 73-80.
14. **Szot B., Tys J. 1979.** Przyczyny osypywania się nasion roślin oleistych i strączkowych oraz metody oceny tego zjawiska. Problemy Agrofizyki, 29.
15. **Szpryngiel M., Wesołowski M., Szot B. 2004.** Economical technology of rape seed harvest. TEKA Komisji Motoryzacji i Energetyki Rolnictwa Polskiej Akademii Nauk Oddział w Lublinie. 4, p. 19-29.
16. **Szwed G., Falęcki A., Tys J., 1996.** The method of pods crack resistance evaluation (in Polish). Lupin: scope of investigations and prospects of application. Polish Lupin Association and Institute of Bioorganic Chemistry, Polish Academy of Sciences, Poznań, p. 331-337
17. **Szwed G., Strobel W., Tys J. 1997.** Mechanizmy rządzące procesami pękania strąków łubinu. Mat. Konf. Łubin we współczesnym rolnictwie, Olsztyn 25-27.06.1997, p. 107-112.
18. **Szwed G., Tys J., Strobel W. 1999.** Pressurized methods for grading the vulnerability of pods splitting. International Agrophysics, 3(13), p. 391-395.
19. **Tomaszewska Z. 1954.** Wstępne badania nad anatomią strąków łubinu. Acta Agrobotanica, 2, p. 151-171.
20. **Tomaszewska Z. 1964.** Badania morfologiczne i anatomiczne łuszczyn kilku odmian rzepaku i rzepiku ozimego oraz przyczyny i mechanizm ich pękania. Hodowla Roślin, Aklimatyzacja i Nasiennictwo, 2, p. 147-180

Scientific paper financed from the funds for education in the years 2007-2010 developed as part of research project N N310 2242 33.

ENERGIA OTWARCIA STRĄKÓW FASOLI
PRZY ZRÓŻNICOWANYM NAWOŻENIU FOSFOROWYM

S t r e s z c z e n i e . Praca zawiera wyniki badań wpływu nawożenia fosforowego na energię potrzebną do otwarcia strąków fasoli uprawianej na suche nasiona odmian Narew, Nida, Warta i Wawelska wykonane w latach 2008-2010. Zastosowano cztery dawki fosforu: 0, 40, 80 i 120 kg·ha^{-1}. Najbardziej podatnymi na pękanie strąkami charakteryzowała się odmiana Nida (energia otwarcia 169,3 mJ), a najmniej podatne na pękanie strąki odnotowano u odmiany Narew (energia otwarcia 262,5 mJ). Zwiększenie dawki fosforu od 0 do 120 kg·ha^{-1} spowodowało spadek wartości energii potrzebnej do otwarcia strąków badanych odmian fasoli za wyjątkiem odmiany Wawelska, dla której odnotowano nieistotny wzrost tej energii.

S ł o w a k l u c z o w e : strąk fasoli, energia otwarcia, nawożenie fosforowe.

TEKA. COMMISSION OF MOTORIZATION AND ENERGETICS IN AGRICULTURE – 2012, Vol. 12, No. 1, 135–141

Influence of mineral fertilization on mechanical properties of the chosen elements of bean pod inner structure

Piotr Kuźniar

University of Rzeszów, Department of the Farm and Food Production Engineering,
Zelwerowicza 4 str, 35-601 Rzeszów, Poland, pkuzniar@univ.rzeszow.pl

Summary. The study presents characteristics of strength properties of the selected structure elements of bean pods of varieties: Narew, Nida, Warta and Wawelska with alternating fertilization with nitrogen and phosphorus. The abdominal seam bundles of bean pods were characterized with lower crippling stress, deformation and conventional modulus of elasticity than the vascular bundles of dorsal seam. At fertilization with phosphorous, abdominal and dorsal seam bundles of the pods of the analyzed bean varieties were characterized with larger deformation and lower strength to breaking and modulus of elasticity than when fertilized with nitrogen. The used macroelements had the largest influence on crippling stress and the smallest one on modulus of elasticity of fibre layer in a pod. The applied phosphorous doses exerted larger influence on the increase of stress and deformation than the nitrogen doses, and the modulus slightly increased with nitrogen fertilization.

Key words: bean pod, structure elements, crippling stress, deformation, modulus of elasticity.

INTRODUCTION

One of the unfavourable features of leguminous plants is a tendency to crack their pods and flake their seeds before and after harvesting [5, 13, 14, 17, 18].

Vulnerability of pods to cracking is a variety feature and is determined by their anatomic and morphologic structure. The main feature which facilitates cracking of a pod is the structure of its endocarp in which there is a fibre layer consisting of severely thickened sclerenchymatic cells situated diagonally to fruit's axis. Due to various arrangement of microfibers in cell walls during drying they shrink in various directions and the pod cracks along abdominal and dorsal seams. Fibre content and structure in vascular bundles and walls of the shell is the most significant among the elements of pod internal structure [2, 4, 10, 11, 16, 17, 20].

The aim of the study was to determine the influence of mineral fertilization on strength properties of the chosen structure elements of bean pods.

MATERIAL AND METHODS

The research was carried out in 2008-2010. Bean was cultivated in the experimental field of the Department of the Farm and Food Production Engineering in Rzeszów. Four nitrogen doses (0, 30, 60 and 90 kg·ha^{-1}) and phosphorus doses (0, 40, 80 and 120 kg·ha^{-1}) were applied before sowing. The research was conducted on pods of bean cultivated on dry seeds of the varieties: Narew, Nida, Warta and Wawelska, which were characterized by varied seed and pod size (Tab. 1).

Table 1. Pod characteristics (average values) of the tested bean varieties

Specification	Narew	Nida	Warta	Wawelska
Nitrogen fertilization				
Dimension of pods[mm]:				
Length	93,3	92,6	108,0	115,3
Width	10,0	10,0	9,6	10,8
Thickness	9,7	9,0	8,8	9,3
Number of seeds in a pod	4,8	4,2	4,5	3,9
Phosphorus fertilization				
Dimension of pods [mm]:				
Length	93,0	89,5	103,7	112,3
Width	10,1	10,4	10,0	11,2
Thickness	9,3	9,1	8,9	9,8
Number of seeds in a pod	4,6	4,0	4,3	3,7

Pod dimensions were calculated using an electronic slide calliper with the accuracy of 0.01 mm. Length was measured from the beginning of stalk to the peak, and width and thickness in cutting plane of perpendicular to main axis of the fruit, leading through its centre. Thick-

ness and width of a fibre layer and seam bundles were measured using an electronic dial gauge with the accuracy of 0.001 mm. Surface of cross section of the analyzed pod structure elements was calculated as a product of width and thickness.

Strength research covers such pod structure elements as:

– fibre layer,
– seam sclerenchyma bundles; abdominal and dorsal.

The research was conducted with the use of testing machine ZWICK with which, for the above mentioned pod structure, the following elements were determined: critical stress, modulus of elasticity (Young's modulus) and deformation [3, 6 - 9, 15, 19]. In order to separate fibre layer and seam sclerenchyma bundles from the other tissues, bundles were placed for 15 minutes in boiling water. Parenchyma tissues macerated in this way were removed (scraped off) with a blunt side of a scalpel so as not to damage sclerenchyma [12, 15]. For the purpose of resistance tests ca 2 mm straps were cut from a fibre layer parallel to the direction of fibre location.

Measurements were conducted on 20 pods for each of the tested varieties with their humidity within the range of 12.4-13.8%.

The result was statistically analyzed with Statistica 9 program with which variance analysis and LSD significance test were carried out [1].

RESULTS

The seams of Warta variety (Tab. 2) characterized with the vitally smallest width, thickness and cross section area of vascular bundles of abdominal and dorsal seam. The widest pod structure elements were observed in the Narew variety, and the thickest and with the largest cross section area were found in the Wawelska variety.

Except for the thickness in both the used types of fertilization and cross section area, abdominal seam bundles were characterized with significantly larger dimensions with nitrogen fertilization.

While analyzing data in Table 2, it also should be emphasized that pods of all the tested bean varieties displayed larger features in question for abdominal and dorsal bundles after application of phosphorous fertilization in comparison with nitrogen fertilization.

The influence of applied nitrogen doses (Tab. 3) on the analyzed geometric features of seam bundles of bean pods of the tested varieties was very diverse. Statistically significant changes were discovered only for the thickness of abdominal seam bundles of Nida pods and all the analyzed features of abdominal seam bundles of Warta pods. A similar relation can be observed by comparing mean values of these qualities from all the tested varieties. Discussed features of abdominal and dorsal seam bundles have the minimum value with no nitrogen dosage. The maximum values are reached with 30 and 60 kg nitrogen per hectare, and with the highest dose they decrease, yet they still are higher than at the first nitrogen dose.

The influence of applied phosphorous doses (Tab. 4) on the analyzed geometric features of abdominal and dorsal seam bundles of bean pods of the tested varieties was, similarly to nitrogen fertilization, highly diverse. Statistically significant changes were found only for the thickness of abdominal (increase) and dorsal (decrease)

Table 2. Mean values of dimensions and cross section area of abdominal (A) and dorsal (D) seam bundles of pods of the tested bean varieties

Specification	Seam bundles	Narew	Nida	Warta	Wawelska	Average
Nitrogen fertilization						
Width [μm]	A	674 bc	583 ab	511a	669 bc	609,3 II
	D	608 b	564 b	489 a	564b	556,1 I
Thickness [μm]	A	156 a	180 b	149 a	196 b	170,2 I
	D	158 ab	176 b	152 a	200 c	171,5 I
Surface of cross section [mm^2]	A	0,108 b	0,106 b	0,077 a	0,132 c	0,106 I
	D	0,097 b	0,101 b	0,076 a	0,114 b	0,097 I
Phosphorus fertilization						
Width [μm]	A	739 b	673 a	633 a	637 a	670,4 II
	D	626 a	606 a	574 a	612 a	604,3 I
Thickness [μm]	A	200 b	199 b	166 a	192 b	189,5 I
	D	187 a	186 a	168 a	209 b	187,7 I
Surface of cross section [mm^2]	A	0,151 c	0,133 bc	0,108 a	0,125 ab	0,129 II
	D	0,118 bc	0,114 ab	0,0980a	0,131 c	0,115 I

*different letters in row and Roman numerals in column signify significant differences for the significance level $\alpha = 0.05$)

Table 3. Values of dimensions and cross section area of abdominal (A) and dorsal (D) seam bundles of pods of tested bean varieties for applied doses of nitrogen

Specification	Dose [kg·ha^{-1}]	Narew	Nida	Warta	Wawelska	Average
Abdominal seam bundle						
Width [µm]	0 30 60 90	668 721 675 633	557 576 565 635	513 526 497 507	615 646 723 692	588,3 617,3 615,0 616,8
Thickness [µm]	0 30 60 90	127 a 173 b 155ab 170 b	162 189 176 193	148 147 168 134	209 202 195 177	161,7 177,7 173,1 168,8
Surface of cross section [mm^2]	0 30 60 90	0,086 0,128 0,108 0,108	0,091 0,110 0,101 0,123	0,077 0,079 0,082 0,068	0,131 0,132 0,142 0,123	0,096 0,112 0,108 0,106
Dorsal seam bundle						
Width [µm]	0 30 60 90	600 615 614 602	578 551 564 563	418 a 523 b 548 b 468 a	548 540 576 590	536,0 557,2 575,5 555,8
Thickness [µm]	0 30 60 90	157 168 151 155	157 168 197 182	116 a 166 b 162 b 164 b	208 206 195 190	159,6 176,9 176,5 172,9
Surface of cross section [mm^2]	0 30 60 90	0,096 0,106 0,095 0,094	0,090 0,093 0,114 0,105	0,050 a 0,089 b 0,088 b 0,077 ab	0,118 0,114 0,112 0,111	0,088 0,100 0,102 0,097

*different letters in column signify significant differences for the significance level α = 0.05

Table 4. Values of dimensions and cross section area of abdominal (A) and dorsal (D) seam bundles of pods of the tested bean varieties for applied doses of phosphorous

Specification	Dose [kg·ha^{-1}]	Narew	Nida	Warta	Wawelska	Average
Abdominal seam bundle						
Width [µm]	0 40 80 120	784 722 689 760	669 651 710 663	693 606 567 666	567 a 668 ab 611 ab 701 b	678,5 661,8 644,3 697,5
Thickness [µm]	0 40 80 120	179a 202 ab 192 ab 229 b	176 201 206 212	182 140 182 161	194 168 202 206	182,6 177,6 195,8 202,1
Surface of cross section [mm^2]	0 40 80 120	0,143 0,150 0,136 0,176	0,118 0,132 0,145 0,138	0,130 0,083 0,103 0,114	0,113 0,114 0,125 0,146	0,126 0,120 0,127 0,144
Dorsal seam bundle						
Width [µm]	0 40 80 120	589 628 649 637	603 644 582 594	622 b 519 ab 514 a 642 b	572 624 610 640	596,5 603,8 588,7 628,2
Thickness [µm]	0 40 80 120	187,9 ab 219,5 b 166,9 a 175,3 a	200,8 194,7 175,4 173,8	177,6 159,2 180,0 154,9	201,3 193,0 228,3 214,4	191,9 191,6 187,7 179,6
Surface of cross section [mm^2]	0 40 80 120	0,112 0,139 0,110 0,114	0,121 0,126 0,103 0,105	0,112 0,086 0,094 0,100	0,116 0,121 0,143 0,141	0,115 0,118 0,112 0,115

*different letters in column signify significant differences for the significance level α = 0.05

Table 5. Strength properties of fibre layer of abdominal (A) and dorsal (D) seam bundles of the pods of tested bean varieties

Specification	Seam bundles	Narew	Nida	Warta	Wawelska	Average
Nitrogen fertilization						
Critical stress [MPa]	A	99,6 bc	61,8 a	117,7 c	80,6 ab	89,9 I
	D	126,3	124,5	111,6	129,9	123,1 II
Deformation [%]	A	4,4	4,3	6,2	4,5	4,8 I
	D	7,1	7,7	7,7	6,4	7,2 II
Modulus of elasticity [MPa]	A	2528,8 c	1662,8 a	2060,9 ab	2184,7 bc	2109,3 I
	D	1937,3 ab	1856,7 ab	1595,9 a	2265,4 b	1913,8 I
Phosphorus fertilization						
Critical stress [MPa]	A	70,3 a	56,3 a	93,4 b	99,5 b	79,9 I
	D	101,5	117,5	113,4	121,5	113,5 II
Deformation [%]	A	6,6	5,7	7,2	6,2	6,4 I
	D	5,8	8,2	7,8	8,6	7,6 II
Modulus of elasticity [MPa]	A	1222,8 a	1408,4 ab	1369,6 ab	1774,8 b	1443,9 I
	D	2016,7 b	1567,6 a	1605,9 ab	1463,6 a	1663,5 II

*different letters in row and Roman numerals in column signify significant differences for the significance level $\alpha = 0.05$)

seam bundle and width of dorsal seam bundles of the Warta pods (increase) and width of abdominal seam bundles of the Wawelska variety pods (increase).

A relation between nearly all the tested varieties can be observed when comparing mean values of the analyzed qualities of abdominal seam bundles of bean pods. At first the relevant features of abdominal seam bundles decrease after the application of the second and the third phosphorous dose, and then they increase to values higher than at zero dose. The width of seam bundles of Narew, Nida pods and all the three features of this bundle in Warta pods constitute an exception. As regards dorsal seam bundles in comparison to abdominal seam, decreasing tendency occurs more frequently, especially for the width of this pod element.

Abdominal seam bundles of the Nida pods displayed the smallest stress, deformation and modulus of elasticity (tab. 5). In case of dorsal seam bundles the smallest stress and deformation was observed for the Narew variety pods, and the smallest modulus for the Warta pods. The abdominal seam bundles of the Warta pods were the most resistant to tearing and underwent the largest lengthening, while the largest modulus was present in the bundles of Narew (with nitrogen fertilization) and Wawelska (with phosphorous fertilization). The Wawelska variety pods displayed the largest crippling stress of dorsal seam bundle, Nida and Warta (with nitrogen fertilization) as well as Wawelska (with phosphorous fertilization) displayed the largest deformation, while the largest modulus was observed in the Narew variety.

Dorsal seam bundles (Tab. 5) demonstrated a significantly higher crippling stress, deformation and conventional modulus of elasticity than abdominal seam bundles. The exception constituted Narew variety in which abdominal seam bundles were characterized with a slightly higher value of modulus of elasticity (with nitrogen fertilization) and larger deformation (with phosphorous fertilization), as well as the Wawelska whose abdominal seam bundles displayed a higher modulus of elasticity with phosphorous fertilization. With phosphorous fertilization sclerenchyma bundles of seam bundles of the tested bean varieties manifested a lower resistance to tearing and modulus of elasticity, and larger deformation than with nitrogen fertilization. The exception was the Narew variety in which with phosphorous fertilization dorsal seam bundle underwent smaller lengthening and it was characterized with a slightly higher modulus of elasticity.

Table 6. Average values of thickness [μm] of the fibre layer of pods of the tested bean varieties

Fertilization	Narew	Nida	Warta	Wawelska	Average
Nitrogen	77,6 a	67,2 a	72,3 a	95,5 b	78,16
Phosphorous	92,3 b	68,2 a	70,3 a	102,8 c	83,39
Average	84,9 b	67,7 a	71,3 a	99,1 c	80,75

*different letters in row signify significant differences for the significance level $\alpha = 0.05$

The largest mean fibre thickness (99,1μm) was observed in the Wawelska variety pods (Tab. 6), whereas the Nida pods were characterized with the thinnest fibre

layer. The same diversity between varieties as regards thickness of the tested element of pod structure occurred with nitrogen and phosphorous fertilization, but with the latter this element of pod structure was slightly thicker

The influence of the applied nitrogen and phosphorous doses on the thickness of fibre layer is diverse for the tested bean varieties (Tab. 7). The thickness of this shell structure element of a bean pod of the Wawelska variety first decreased with the increase of the amount of sowed fertilizers reaching the minimal value at nitrogen dose of 30 kg·ha^{-1} and phosphorous dose of 80 kg·ha^{-1}, then increased reaching the maximum value with the largest doses of the used macroelements. A similar relation was observed for the Nida variety with nitrogen fertilization, where the difference in the thickness of fibre layer with the largest nitrogen dose was slightly lower than in that with zero dose. In the Wawelska variety with the increase of nitrogen dose a decrease of pod fibre layer thickness occurred, while in the Narew one firstly for the second nitrogen dose an increase of this pod element thickness and a decrease for the other doses were observed. The increase of nitrogen dose from 0 to 80 kg·ha^{-1} caused the increase of fibre layer thickness of the Nida and Warta pod shells, and for the dose of 120 kg·ha^{-1} this pod element was considerably thinner, similarly to the thickness with the zero phosphorous dose. In the Narew variety, the impact of phosphorous dose on the thickness of the relevant element of its pod structure was the most diverse. First a significant decrease in the relevant amount occured after the second dose, then an increase after the next dose and another decrease after the maximum phosphorous dose. Taking into account the mean values from the four bean varieties a slight falling tendency of pod fibre layer thickness with the increase of nitrogen dose can be observed.

Table 7. Thickness [µm] of the fibre layer of pods of the tested bean varieties for the applied doses of nitrogen and phosphorous

Fertilization	Dose [kg·ha^{-1}]	Narew	Nida	Warta	Wawelska	Average
Nitrogen	0	82,2 b	72,5 b	89,4 c	98,2	85,5 b
	30	83,8 b	58,6 b	73,6 b	88,5	76,1 ab
	60	79,1 ab	68,3 ab	71,8 b	95,8	78,8 ab
	90	65,4 a	69,5 ab	54,4 a	99,4	72,2 a
Phosphorous	0	104,4 b	63,7	69,3	106,1 ab	85,8
	40	80,5	71,2	69,7	98,4 ab	80,0
	80	a 96,9	71,7	75,9	92,8	84,3
	120	ab 87,2 ab	66,2	66,3	a 113,9 b	83,4

*different letters in column signify significant differences for the significance level α = 0.05

The pods of Wawelska variety were characterized by the fibre layer (Tab. 8) with the highest resistance to tearing and the largest deformation, whereas the highest module of elasticity was observed in the Warta pods. Fibre layer of Nida pods were characterized with the smallest value of the analyzed resistance parameters. The fibre layer of bean pods of Narew, Nida and Warta varieties was more resistant to tearing and underwent larger deformations with nitrogen fertilization. The modulus of elasticity reached higher values with nitrogen fertilization only for the Narew and Nida and lower ones for the Warta and Wawelska.

When analyzing mean values included in Table 9 and Figure 1 from four bean varieties of strength parameters of fibre layer it has to be emphasized that with the exception of deformation with nitrogen fertilization, these values significantly rise with the increase of sowed nitrogen and phosphorous. The used macroelements had the strongest

Table 8. Strength properties of fibre layer of pods of tested bean varieties

Specification	Narew	Nida	Warta	Wawelska	Average
Nitrogen fertilization					
Critical stress [MPa]	169,1 b	127,6 a	157,8 b	160,0 b	153,6
Deformation [%]	8,38 b	6,65 a	6,68 a	7,23 a	7,24
Modulus of elasticity [MPa]	1991,7 a	1932,2 a	2394,5 b	2216,4 ab	2133,7
Phosphorous fertilization					
Critical stress [MPa]	86,6 a	110,7 ab	132,3 b	180,6 c	127,6
Deformation [%]	4,18 a	5,60 b	6,01 b	9,17 c	6,24
Modulus of elasticity [MPa]	2089,3	1985,3	2199,4	1941,3	2053,8
Average of nitrogen and phosphorous fertilization					
Critical stress [MPa]	127,9 ab	119,2 a	145,0 b	170,3 c	140,6
Deformation [%]	6,28 a	6,13 a	6,35 a	8,20 b	6,74
Modulus of elasticity [MPa]	2040,5 a	1958,8 a	2296,9 b	2078,8 ab	2093,8

*different letters in row signify significant differences for the significance level α = 0.05

Table 9. Strength properties of fibre layer of pods of tested bean varieties for applied doses of nitrogen and phosphorous

Specification	Dose [kg·ha^{-1}]	Narew	Nida	Warta	Wawelska
Nitrogen fertilization					
Critical stress [MPa]	0 30 60 90	158,7 a 162,1 ab 140,4 a 215,2 b	144,1 122,7 128,1 115,6	89,6 a 20,5 a 231,8 b 189,2 b	148,0 157,6 176,3 157,9
Deformation [%]	0 30 60 90	8,03 8,88 7,85 8,78	7,18 b 6,63 ab 7,05 ab 5,75 a	5,80 a 6,23 a 8,05 b 6,65 a	7,15 7,23 7,40 7,15
Modulus of elasticity [MPa]	0 30 60 90	1940,3 1795,2 1811,9 2419,4	1976,6 1845,6 1818,7 2087,8	1654,9 a 2037,2 a 2983,7 b 2902,2 b	2069,1 2266,0 2356,9 2173,7
Phosphorous fertilization					
Critical stress [MPa]	0 40 80 120	51,9 a 70,6 a 78,0 a 145,9 b	87,6 100,1 125,8 129,4	110,1 149,3 127,3 142,6	157,4 165,2 209,0 190,9
Deformation [%]	0 40 80 120	2,64 a 3,71 a 3,92 a 6,43 b	5,15 5,53 5,83 5,90	5,78 6,35 6,28 5,65	9,73 8,55 8,78 9,63
Modulus of elasticity [MPa]	0 40 80 120	1987,1 2045,6 2063,2 2261,2	1731,8 1785,2 2164,1 2260,3	1939,9 2394,2 1997,5 2465,8	1581,4 a 1882,2 ab 2339,8 b 1961,9 ab

*different letters in column signify significant differences for the significance level α = 0.05

impact on critical stress and the weakest one on modulus of elasticity. The applied doses of phosphorous had larger influence on the increase of stress and deformation than the doses of nitrogen, and the modulus slightly more increased with nitrogen fertilization.

Dependence of mean values of strength parameters of fiber layer bean pods on the doses of nitrogen and phosphorus are well described by a linear function (Fig. 1)

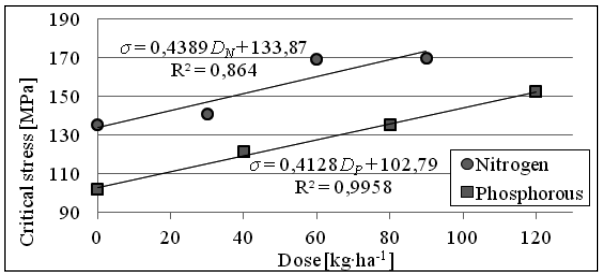

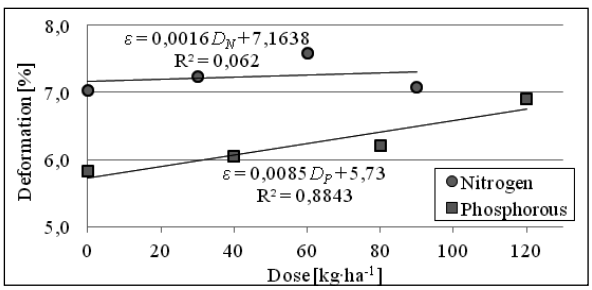

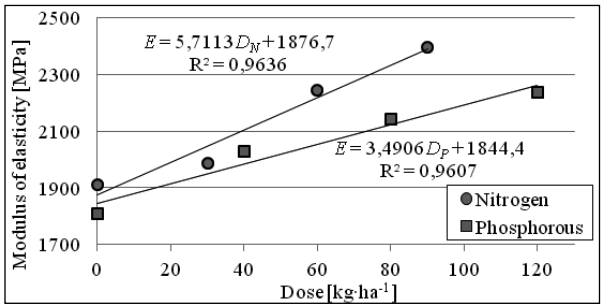

Fig. 1. Relation of mean values of strength parameters of fiber layer bean pods to the doses of nitrogen D_N and phosphorus D_P

CONCLUSIONS

1. Abdominal seam bundles of the tested bean varieties were characterized by larger width, thickness and cross section area as well as lower critical stress, deformation and modulus of elasticity than vascular bundles of dorsal seam.
2. In case of phosphorous fertilization abdominal and dorsal seam bundles of pods of the tested bean varieties were characterized with larger dimensions and deformation and lower strength to breaking and modulus of elasticity than with nitrogen fertilization. The exception constituted Narew variety in which, in

case of nitrogen fertilization, the dorsal seam was not lengthening as much and it was characterized with slightly larger modulus.
3. Abdominal seam bundles of Warta pods were the most resistant to breaking and underwent the largest lengthening, while these seams in the Wawelska variety beam pods were characterized with the highest modulus.
4. Fibre layer was thicker with phosphorous fertilization than with nitrogen fertilization, except for Warta variety pods.
5. The used macroelements had the strongest influence on critical stress and the weakest on modulus of elasticity of fibre layer in pod shell.
6. The applied phosphorous doses had a larger influence on the increase of stress and deformation than nitrogen doses, and modulus slightly more increased with nitrogen fertilization.

REFERENCES

1. **Burski Z., Tarasińska J., Sadkević R. 2003.** The methodological aspects of using multifactoral analysis of variance in the examination of exploitation of engine sets. TEKA Komisji Motoryzacji i Energetyki Rolnictwa Polskiej Akademii Nauk Oddział w Lublinie, 3, p. 45-54.
2. **Dorna H., Duczmal K. W. 1994.** Wpływ warunków klimatycznych na formowanie włókna w szwach strąków fasoli zwykłej (*Phaseolus vulgaris* L.). I Ogóln. Konf. Nauk. Strączkowe Rośliny Białkowe. FASOLA, Lublin 25.11.1994, p. 135-138.
3. **Dziki D., Laskowski J. 2006.** Influence of wheat grain mechanical properties on grinding energy requirements. TEKA Komisji Motoryzacji i Energetyki Rolnictwa Polskiej Akademii Nauk Oddział w Lublinie, 6A, p. 45-52.
4. **Esau K. 1973.** Anatomia roślin. PWRiL Warszawa.
5. **Furtak J., Zaliwski A. 1986.** Badania nad zbiorem mechanicznym nasion fasoli. Roczniki. Nauk Rolniczych, ser. Technika Rolnicza, 2, p. 127-140.
6. **Gładyszewska B., Stropek Z. 2010.** The influence of the storage time on selected mechanical properties of apple skin. TEKA Komisji Motoryzacji i Energetyki Rolnictwa Polskiej Akademii Nauk Oddział w Lublinie,10, p. 59-65.
7. **Gorzelany J., Sosnowski S. 2003.** Wpływ wybranych czynników na właściwości mechaniczne tkanki korzenia buraka cukrowego. Acta Agrophysica, 2, p. 73-82.
8. **Gorzelany J., Puchalski C. 2010.** Właściwości mechaniczne korzeni wybranych odmian buraków cukrowych. Inżynieria Rolnicza. 1 (119), p. 199-204.
9. **Guz T. 2008.** Thermal quarantine of apples as a factor forming its mechanical properties. TEKA Komisji Motoryzacji i Energetyki Rolnictwa Polskiej Akademii Nauk Oddział w Lublinie, 8a, p. 52-62.
10. **Hejnowicz Z. 1985.** Anatomia i histogeneza roślin naczyniowych. PWN, Warszawa.
11. **Kuźniar P., Sosnowski S. 2002.** Relation between the bean pod shape factor and force required for pod opening. International Agrophysics, 16(2), p. 129-132.
12. **Kuźniar P., Strobel W. 2000.** Określenie wpływu grubości sklerenchymy strąków fasoli na ich podatność na pękanie. Acta Agrophysica, 37, p. 113-117.
13. **Kuźniar P., Sosnowski S. 2003.** Podatność strąków na pękanie a wielkość strat nasion fasoli podczas mechanicznego zbioru. Acta Agrophysica, 2(1), p. 113-118.
14. **Kuźniar P., Sosnowski S. 2003.** Wpływ wilgotności strąków fasoli i ich wielokrotnego nawilżania na siłę potrzebną do ich otwarcia. Acta Agrophysica, 2(1), p. 119-126.
15. **Kuźniar P., Sosnowski S. 2010.** Energia otwarcia strąków fasoli właściwości wybranych elementów ich budowy. MOTROL - Motoryzacja i Energetyka Rolnictwa, 12, p. 99-107.
16. **Moś M. 1983.** Zmienność morfologicznych i anatomicznych cech strąka, jej wpływ na skłonność do pękania i plon nasion komonicy zwyczajnej (*Lotus corniculatus* L). Zeszyty Problemowe Postępów Nauk Rolniczych, 258, p. 197-203.
17. **Strobel W. 2003.** Porównanie cech fizycznych strąków różnych gatunków łubinu. Zeszyty Problemowe Postępów Nauk Rolniczych, 495, p. 73-80.
18. **Szot B., Tys J. 1979.** Przyczyny osypywania się nasion roślin oleistych i strączkowych oraz metody oceny tego zjawiska. Problemy Agrofizyki, 29.
19. **Szymanek M., Sobczak P. 2009.** Some physical properties of spelt wheat seed. TEKA Komisji Motoryzacji i Energetyki Rolnictwa Polskiej Akademii Nauk Oddział w Lublinie, 9, p. 310–320.
20. **Tomaszewska Z. 1954.** Wstępne badania nad anatomią strąków łubinu. Acta Agrobotanica, 2, p. 151-171.

Scientific paper financed from the funds for education in the years 2007-2010 developed as part of research project N N310 2242 33.

WPŁYW NAWOŻENIA MINERALNEGO NA WŁAŚCIWOŚCI MECHANICZNE WYBRANYCH ELEMENTÓW BUDOWY WEWNĘTRZNEJ STRĄKÓW FASOLI

Streszczenie. Praca przedstawia charakterystykę właściwości mechanicznych wybranych elementów budowy strąków fasoli odmian Narew, Nida, Warta i Wawelska przy nawożeniu azotowym i fosforowym. Wiązki szwu brzusznego strąków fasoli charakteryzowały się mniejszym naprężeniem niszczącym, odkształceniem i modułem sprężystości od wiązek przewodzących szwu grzbietowego. Dla nawożenia fosforowego wiązki szwu brzusznego i grzbietowego strąków badanych odmian fasoli charakteryzowały się większym odkształceniem oraz mniejszą wytrzymałością na rozrywanie i modułem sprężystości niż przy nawożeniu azotowym. Zastosowane makroelementy najsilniej wpłynęły na naprężenie niszczące a najsłabiej na moduł sprężystości warstwy włókien w łupinie. Na wzrost naprężenia i odkształcenia miały większy wpływ zastosowane dawki fosforu niż azotu, zaś moduł nieznacznie bardziej zwiększył się przy nawożeniu azotowym.

Słowa kluczowe: strąk fasoli, elementy budowy, naprężenie niszczące, odkształcenie, moduł sprężystości.

TEKA. COMMISSION OF MOTORIZATION AND ENERGETICS IN AGRICULTURE – 2012, Vol. 12, No. 1, 143–147

Rheological properties of extrusion-cooked starch suspensions

Marcin Mitrus, Agnieszka Wójtowicz, Tomasz Oniszczuk, Leszek Mościcki

Department of Food Process Engineering, Faculty of Production Engineering,
University of Life Sciences, Doświadczalna 44, 20-280 Lublin, Poland,
marcin.mitrus@up.lublin.pl

Summary. The influence of extrusion-cooking process parameters on the apparent viscosity of the extrusion-cooked starch suspensions was investigated. Baro-thermal treatment parameters showed changes in apparent viscosity of the obtained suspensions. The moisture content of the raw material and process temperature had the most strongly influence, much lesser impact was exerted by the extruder's screw speed. Apparent viscosity of extrusion-cooked starch suspensions varied within the range: (338-2504) mPa×s for potato starch, (481-3347) mPa×s for corn starch and (1419-3441) mPa×s for wheat starch.

Key words: starch, extrusion cooking, apparent viscosity, rheology.

INTRODUCTION

Native starch has different industrial applications, however, due to many disadvantages (e.g. insolubility in cold water), it's limited. Disadvantages of native starch can be reduced or even eliminated, through its modification by various methods. The simplest method of physical modification of starch is thermal or pressure-thermal treatment. As a result of heating the grain structure is destroyed and there is a partial starch gelatinization. During this process hydrogen bonds, that stabilize the tertiary and quaternary conformational structure of macromolecules, are disrupted [20]. Various forms of drying, extrusion or high pressure treatment are used for this purpose [2, 6, 21, 22].

Extrusion-cooking technique, widely used in food processing, comes from a well-known in the plastics extrusion techniques for thermoplastic materials. In general terms, extrusion-cooking of the raw material of plant origin is the extrusion of bulk material under high pressure and high temperature. This causes the significant changes in physical and chemical quality of the processed material. During pressure-thermal treatment, material is mixed, compacted, compressed, liquefied and plasticity in the end zone of the extruder. Extrusion pressure can reach up to 20 MPa and temperature of the slurry to 200°C. The scope of physical and chemical changes in processed raw materials depends mainly on the assumed parameters of the extrusion-cooking process and the construction of the extruder. Currently, various types of food fancy goods such as crisps, snacks, meat analogs, as well as pet food and aquafeed or thermoplastic starch are produced using that technique [12, 14, 15, 17].

Extrusion-cooking technique allows for the obtainment of pressure-thermally modified starches with different physical and chemical properties. Properties of the obtained modified starches can be created (within certain limits) depending on the process parameters used. The extrusion-cooker can be treated as a bioreactor. Such pressure-thermal process allows for the obtainment of modified starches with a wide range of degree of gelatinization, with different water absorption and solubility and the different rheological properties of starch pastes. These products may find wide application in food industry as food additives, very often by replacing chemically modified starchy products. Extrusion-cooked starch may find its use as a component of food products in the manufacture of instant products, different kinds of fillings in the confectionery industry, as a gelling agent, structure stabilizer and water- or fat-absorbent fillers. That may be very attractive from the consumer point of view. Application extrusion-cooking is a relatively cheap alternative in the production of modified starches.

Physical and chemical modifications of starch have an influence on the changes of rheological properties of starch suspensions. There are many methods of testing the food rheological properties [3, 7]. Apparent viscosity of the starch suspensions and pastes can be studied during the process of gelatinization [1, 5, 8, 18]. Most often viscosity of suspensions of native and modified starch is tested after heating process in order to gelatinization of starch [4, 13, 16, 19].

The objective of this research was to determine the effect of extrusion-cooking process parameters on the apparent viscosity of extruded starch suspensions prepared in room temperature.

MATERIALS AND METHODS

The basic raw material for investigations was: the commercial corn starch Meritena 100 type produced by T&L (Slovakia), wheat starch Meritena 200 type produced by SYRAL BELGIUM N.V. (Belgium) and potato starch Superior type produced by "PEPEES" S.A. in Lomza (Poland). During the extrusion-cooking process the 4 levels of moisture content of raw material (17, 20, 25 and 30%) were used. In order to obtain expected moisture content, starch was mixed with sufficient amount of water and stored for 24h in air tight polyethylene bags at room temperature to make whole sample material homogeneous.

Extrusion-cooking of potato starch was carried out using a modified single screw extrusion-cooker TS-45 (Polish design) with L/D = 16. The die with one opening with a diameter of 3 mm was used. During the study three temperature of extrusion process (100, 120 and 140°C) and a variable speed screw (60, 80, 100, 120 rpm) were used.

The suspensions (10% w/w dry mass basis) of grounded extrudates with distilled water were prepared by continuous stirring for 10 minutes, than apparent viscosity was measured using a Zwick testing machine BDO-FB 0,5 TH type, equipped with a back extrusion chamber 60 mm height and internal diameter of 50mm. A piston of 46 mm diameter and 20 mm height was used during measurements. The measurement cycle was 60 mm, test speed 100 mm/min, a slit width - 2 mm. The data was subjected to analysis of variance (ANOVA) by Duncan's test ($\alpha = 0.05$) using SAS 9.1 software

RESULTS

All native starches formed a unstable suspensions. Viscosity measurements of these suspensions were difficult because of starch sedimentation. Apparent viscosity of aqueous suspensions of native starches was about 3 mPas.

Extruded cereals starches formed opaque suspensions, while potato starch extrudates formed a transparent and translucent suspension. The suspensions obtained from starch contained 30% of moisture characterized ability to stratification. This was probably due to insufficient degree of fragmentation of the extrudates (Fig. 1).

Extruded wheat starch formed aqueous suspensions with a high apparent viscosity in the range from 1419 to 3441 mPas after 10 minutes of mixing. Extruded corn starch formed aqueous suspensions with a moderately high apparent viscosity in the range from 481 to 3347 mPas after 10 minutes of mixing. Extruded potato starch

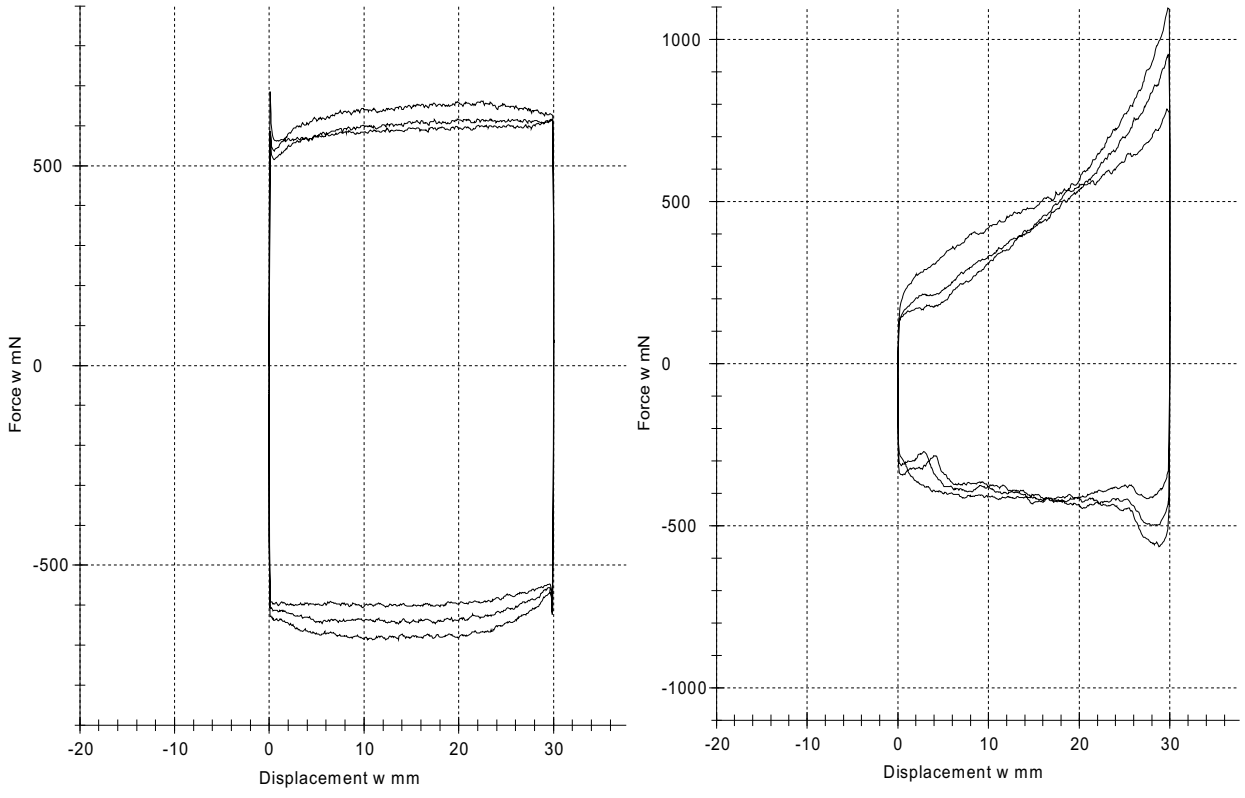

Fig. 1. Example of test results for corn starch extruded at 100°C with screw speed of 60 rpm; moisture content 17 and 30%, respectively

formed aqueous suspensions with a relatively low apparent viscosity in the range (338-2504) mPas after 10 minutes of mixing. Statistical analysis revealed significant effects of the raw material moisture content and screw speed on the apparent viscosity of extruded starch suspensions (tab.1).

Table 1. The results of measurements of the apparent viscosity of aqueous suspensions of wheat starch extruded at 140°C (the same letter in the row means no significant differences, the level of significance $\alpha = 0,05$)

Moisture content before extrusion [%]	**Apparent viscosity [mPa×s]**			
	60 [rpm]	80 [rpm]	100 [rpm]	120 [rpm]
17	3384^{a}	3343^{a}	3441^{a}	3068^{b}
20	2799^{b}	3563^{a}	3410^{a}	3657^{a}
25	2026^{c}	3029^{a}	2417^{b}	2734^{ab}
30	2484^{b}	3079^{a}	2537^{b}	2100^{c}
Screw speed [rpm]	**17%**	**20%**	**25%**	**30%**
60	3384^{a}	2799^{b}	2026^{c}	2484^{b}
80	3343^{a}	3563^{ab}	3029^{c}	3079^{bc}
100	3441^{a}	3410^{a}	2417^{b}	2537^{b}
120	3068^{b}	3657^{a}	2734^{c}	2100^{d}

The suspensions obtained from wheat starch extruded at higher screw speeds had a higher viscosity. The extrudates of wheat starch with higher moisture content formed suspensions with lower viscosity. The viscosity of the suspensions obtained from extruded wheat starch increased with increase of the extrusion temperature.

In a case of suspensions obtained from extruded corn starch it was found that an increase in moisture content of the processed material causes an increase in suspensions viscosity (fig. 2). The statistical analysis revealed insignificant effect of the extrusion-cooker screw speed on the apparent viscosity of extruded corn starch suspensions.

Potato starch extrudates produced at the higher screw speed formed the suspensions with lower viscosity. Increase in moisture content of the processed potato starch had a positive effect on the viscosity of the formed suspensions.

The extrusion-cooking process has great impact on physical and chemical properties of the processed starch, especially on its water absorption (WAI) and the solubility in cold water (WSI) [9, 10, 11]. Researches revealed that changes in WAI and WSI influenced on the apparent viscosity of the extruded starch suspensions (fig. 3).

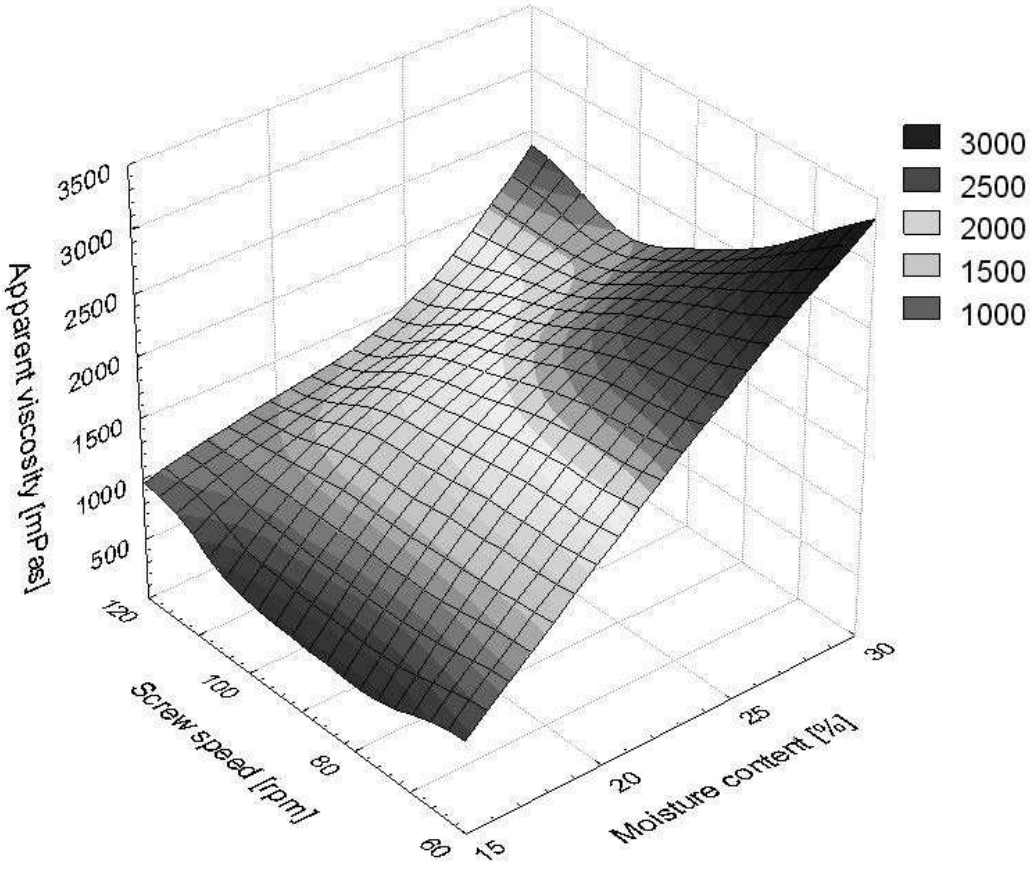

Fig. 2. Influence of the process parameters on the apparent viscosity of the corn starch-water suspensions for starch extruded at 120°C

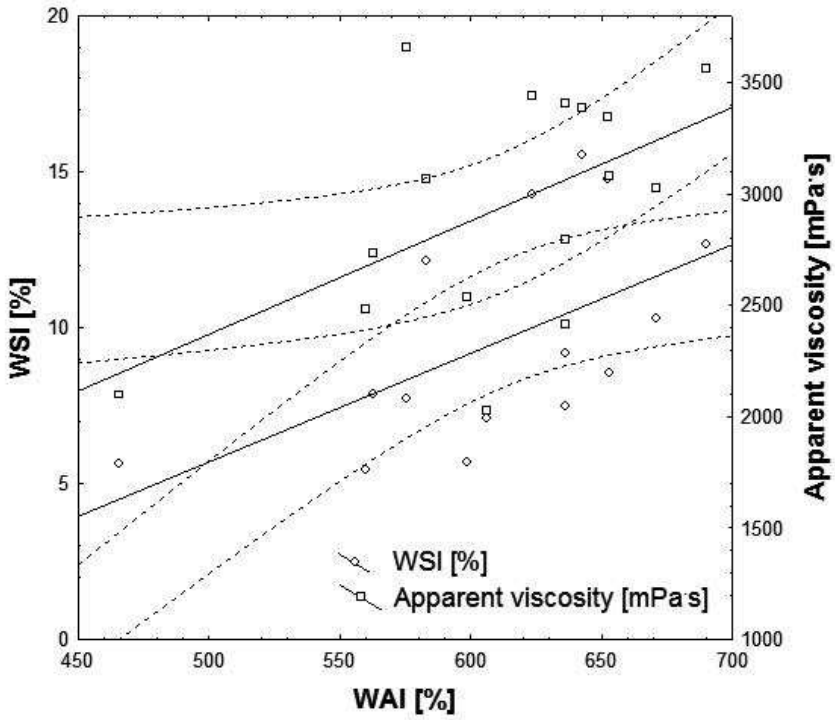

Fig. 3. Influence of WAI and WSI on the apparent viscosity of the extruded wheat starch suspensions

During the measurements was found that increase in starch water absorption involves an increase of viscosity of starch suspensions. This effect was observed for all types of the extruded samples. Increase of starch solubility in a cold water decreased viscosity of starch suspensions. Only for wheat starch increase of the suspensions viscosity with WSI increase was observed.

CONCLUSIONS

Extrusion-cooking process parameters determined the apparent viscosity of the extruded starch suspensions. The strongest effect was observed with the moisture content of starch before extrusion-cooking; the process temperature and the extruder screw speed were less affected. Probably this is due to the course of the starch gelatinization and degradation process and, in consequence, with the WAI changes and the solubility in cold water.

Extruded wheat starch formed aqueous suspensions with a high apparent viscosity in the range (1419-3441) mPas after 10 minutes of mixing. Extruded corn starch formed aqueous suspensions with a moderately high apparent viscosity in the range (481-3347) mPas after 10 minutes of mixing. Extruded potato starch formed aqueous suspensions with a relatively low apparent viscosity in the range of (338-2504) mPas, after 10 minutes of mixing.

REFERENCES

1. **Bhattacharya S., Sudha M.L., Rahim A. 1999.** Pasting characteristics of an extruded blend of potato and wheat flours, Journal of Food Engineering, 40, p. 107-111.
2. **Błaszczak W., Valverde S., Fornal J. 2005.** Effect of high pressure on the structure of potato starch, Carbohydrate Polymers, 59, p. 377-383.
3. **Bourne M.C. 2002.** Food Texture and Viscosity. Concept and Measurement, Elsevier Inc.
4. **Desse M., Ang S., Morris G.A., Abu-Hardan M., Wolf B., Hill S.E., Harding S.E., Budtova T., Mitchell J.R. 2009.** Analysis of the continuous phase of the modified waxy maize starch suspension, Carbohydrate Polymers, 77, p. 320-325.
5. **Han J-A., Be Miller J.N. 2007.** Preparation and physical characteristics of slowly digesting modified food starches. Carbohydrate Polymers, 67, p. 366-374.
6. **Kawai K., Fukami K., Yamamoto K. 2007.** Effects of treatment pressure, holding time, and starch content on gelatinization and retrogradation properties of potato starch-water mixtures treated with high hydrostatic pressure, Carbohydrate Polymers, 69, p. 590-596.
7. **Kobus Z., Kusińska E. 2010.** Effect of temperature and concentration on rheological properties of tomato juice, TEKA Commission of Motorization and Power Industry in Agriculture, Vol. X, p. 170-178.
8. **Loisel C., Maache-Rezzoug Z., Esneault C., Doublier J.L. 2006.** Effect of hydrothermal treatment on the physical and rheological properties of maize starch, Journal of Food Engineering, 73, p. 45-54.
9. **Mitrus M., Wójtowicz A. Mościcki L. 2010.** Modyfikacja skrobi ziemniaczanej metodą ekstruzji, Acta Agrophysica, 16(1), p. 101-109.
10. **Mitrus M., Oniszczuk T., Mościcki L. 2011.** Changes of specyfic mechanical energy during extrusion-cooking of potato starch, TEKA Commission of Motorization and Power Industry in Agriculture, Vol. XIc, p. 200-207.
11. **Mitrus M., Wójtowicz A. 2011.** Extrusion-cooking of wheat starch, TEKA Commission of Motorization and Power Industry in Agriculture, Vol. XIc, p. 208-215.

12. **Moscicki L. 2011.** Extrusion-Cooking Techniques. Applications, Theory and Sustainability, Wiley-VCH Verlag GmbH&Co. KGaA, Weinheim.
13. **Nuessli J., Handschin S., Conde-Petit B., Escher F. 2000.** Rheology and structure of amylopectin potato starch dispersions without and with emulsifier addition, Starch, 52, p. 22-27.
14. **Rejak A., Mościcki L. 2011.** Selected mechanical properties of TPS films stored in the soil environment, TEKA Commission of Motorization and Power Industry in Agriculture, Vol. XIc, p. 264-272.
15. **Singh S., Gamlath S., Wakeling L. 2007.** Nutritional aspects of food extrusion: a review, International Journal of Food Science & Technology, 42, p. 916-929.
16. **Singh N., Isono N., Srichuwong S., Noda T., Nishinari K. 2008.** Structural, thermal and viscoelastic properties of potato starches, Food Hydrocolloids, 22, p. 979-988.
17. **Sobczak P. 2006.** Sorbitol addition on extrusion process, TEKA Commission of Motorization and Power Industry in Agriculture, Vol. VIa, p. 163-169.
18. **Srichuwong S., Sunarti T.C., Mishima T., Isono N., Hisamatsu M. 2005.** Starches from different botanical sources II: Contribution of starch structure to swelling and pasting properties, Carbohydrate Polymers, 62, p. 25-34.
19. **Tako M., Hizukuri S. 2003.** Rheological properties of wheat (halberd) amylopectin, Starch, 55, 345-349.
20. **Van den Einde R., Bolsius A., Van Soest J., Janssen L.P.B.M., Van der Goot A., Boom R. 2003.** The effect of thermomechanical treatment on starch breakdown and the consequences for the process design, Carbohydrate Polymers, 55, p. 57-63.
21. **Wójtowicz A. 2011.** Influence of extrusion-cooking parameters on selected physical and textural properties of precooked maize pasta products, TEKA Commission of Motorization and Power Industry in Agriculture, Vol. XI, p. 441-449.
22. **Yan H., Zhengbiao G.U. 2010.** Morphology of modified starches prepared by different methods, Food Research International, 43, p. 767-772.

WŁAŚCIWOŚCI REOLOGICZNE ZAWIESIN SKROBI EKSTRUDOWANYCH

S t r e s z c z e n i e . W trakcie badań określano wpływ parametrów procesu ekstruzji na zmiany lepkości pozornej zawiesin skrobi ekstrudowanych. Parametry obróbki ciśnieniowo-termicznej miały duży wpływ na zmiany lepkości pozornej zawiesin ekstrudowanych skrobi. Najmocniej na lepkość oddziaływała wilgotność surowca i temperatura procesu, prędkość ślimaka ekstrudera miała mniejszy wpływ. Lepkość pozorna zawiesin ekstrudowanej skrobi zmieniała się w granicach: (338-2504) mPa×s dla skrobi ziemniaczanej, (481-3347) mPa×s dla skrobi kukurydzianej i (1419-3441) mPa×s dla skrobi pszennej.

S ł o w a k l u c z o w e : skrobia, ekstruzja, lepkość pozorna, reologia.

TEKA. COMMISSION OF MOTORIZATION AND ENERGETICS IN AGRICULTURE – 2012, Vol. 12, No. 1, 149–154

Equivalent fuel consumption of engines from swedish automotive companies

Jaromir Mysłowski

West Pomeranian University of Technology in Szczecin
70-310 Szczecin, Al. Piastów 19, e-mail templar_knight@wp.pl

Summary. The paper presents problems of specific fuel consumption as a parameter used to assess the use of the field of supply of the engine torque used to drive a truck with a high load capacity. A new rate of this assessment has been proposed in the form of equivalent fuel consumption and tests have been carried out with its use in the engines of the Scania and Volvo trucks.

Key words: engine, specific fuel consumption, load capacity.

INTRODUCTION

In accordance with the assumptions of the paper, one of the basic operating parameters of modern diesel engines and with direct injection i.e. the specific fuel consumption has been subject to the research. These engines are used to drive high load capacity trucks, and more and more often also to drive cars. The problem of reducing the fuel consumption by these engines is quite widely described in the literature [2,3,4,5,8,9,10,12,13,14 ,15,16,18,19], but there is a lack of publications referring to the tests of specific engines. After analysing the available data, the author has decided to address this issue. Performance tests on engine test bed and simulation tests have been carried out for a wider approach to the subject.

SPECIFIC FUEL CONSUMPTION

Operational fuel consumption is calculated on the basis of road test, which is carried out under certain traffic conditions, at constant or variable speed of the vehicle. This value is dependent on the vehicle and engine parameters as well as many operational factors, such as:

- technical condition of the engine and the vehicle components and
- mechanisms,
- weight and distribution of passengers, baggage and cargo,
- properties of the road, its shape and the type, quality and condition
- of the pavement,
- traffic conditions,
- atmospheric factors.

Knowledge of the minimum value of the fuel consumed by the engine allows for its conversion into the hourly rate, and then for planning the purchase of fuel for vehicles used in transport companies. The manner of driving process as an operational factor can be also taken into account, to a great extent conditioned by the subjective actions of the driver, depending on his / her mental and physical condition. The costs related to the purchase of fuel are among the highest expenses in the vehicle use [3, 9, 10, 12, 14, 16] Figure 1

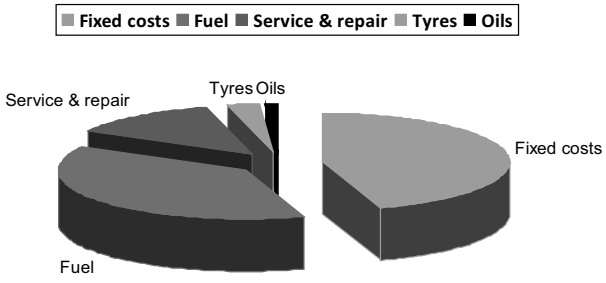

Fig. 1. Structure of the maintenance costs of vehicles [15]

In the theoretical analysis of the fuel consumption, it is possible to include the impact of only certain operational factors such as velocity profile, longitudinal profile of the road and the type and condition of the roadway affecting the value of the coefficient of rolling resistance.

Also, the road tests are carried out under strict conditions, which include: proper technical condition of the vehicle and the engine, specified loading of the vehicle with the weight of properly placed people and cargo, no wind and precipitation, road with a good surface ensuring good traction for the wheels. The data informing about the parameters and performance of vehicles the most often includes the nominal fuel consumption, which is a function of many variables. Consider the fact that the smaller the fuel consumption of the engine, the less the global quantity of toxic compounds emitted by the engine into the atmosphere. In this way, the key problem allowing for compliance with the demands of friendly operation is to reduce the fuel consumption by the engine that - next to the toxicity of exhaust gases and dynamic properties - are the measures of performance characteristics of the vehicle.

The most general rate of the economic efficiency of the engine operation (economy of a vehicle) is the fuel consumption measured in $dm^3/100$ km. However, this is an indicative and inaccurate rate, not taking into account such operating conditions as speed, its duration, load, road condition and service life. On the other hand, it is the most commonly used rate, given in the technical descriptions of vehicles. Sometimes, in relation to trucks, a monitoring fuel consumption at a certain speed of driving is given (e.g., V = 60 km/h) [16, 17, 19], whereas in relation to cars the average value of fuel consumption in urban and extra-urban driving is given.

Consider the fact that the smaller the fuel consumption of the engine, the less the global quantity of toxic compounds emitted by the engine into the atmosphere. In this way, the key problem allowing for compliance with the demands of friendly operation is to reduce the fuel consumption by the engine that - next to the toxicity of exhaust gases and dynamic properties - are the measures of performance characteristics of the vehicle. However, these are the results of simulation tests, carried out during a certain agreed operational cycle, not the road test results. With regards to the engines there is a more accurate rate - the specific fuel consumption, which is sometimes also given in technical descriptions, especially of trucks of high load capacity.

The specific fuel consumption expressed in g/kWh (g/ HPh) indicates what weight of fuel (and the chemical energy contained in it) is to be converted into mechanical work in order to produce one kilowatt-hour by the engine. It is a very positive rate that does not depend on the engine volume capacity (its size) and the type of fuel used and therefore one can compare different types of engines, designed for different purposes, powered by both petrol and diesel fuels or fuels derived from plants.

The manufacturers, due to the advertising reasons, the most often give the value of the minimum specific fuel consumption or, less often, its value at the engine speed corresponding to the rated power. Both the first and the second values - to a limited extent - characterise the engine in terms of economy, however this is much more useful information for practical purposes than the previous one.

Unfortunately, with regards to the fuel, the manufacturers are very sparing in giving information as to its curve run on the external characteristics of the engine, as is the case with the torque or engine power, not to mention the universal characteristics. Such data would allow for unambiguous determination as to which of the engines is more economical. The only possibility of obtaining this information is, therefore, to carry out simulation tests using data provided by manufacturers.

Accurate and quick determination of the specific fuel consumption and hence the parameter, on which the economy of the engine depends as well as its harmful impact on the environment are very important issues. This allows the user to plan the operating costs. A comprehensive picture of the specific fuel consumption at different engine operating conditions can be presented on the universal characteristics, where under the maximum torque curve there is a field of its supply [1, 9, 10, 16, 19]. Drawing the fields of operation on the universal characteristics, with constant load and speed for a specified gear, forms a time density characteristics of the engine operation, which enables a precise determination of the value of the specific fuel consumption [33,75,107,]. This gives the opportunity to assess the engine performance characteristics in the light of the requirements set.

TIME DENSITY CHARACTERISTICS OF SPECIFIC FUEL CONSUMPTION

The time density characteristics of the engine can be prepared using the results of road tests or field tests of a vehicle, drawing the operating ranges at a given load and engine speed on the universal characteristics of its engine or assuming in advance the model of the engine and properly dividing its universal characteristics [4, 6, 7, 9, 10].

For trucks of high load capacity moving on motorways or expressways, Scania company offers an universal division of the area of the universal characteristics into four fields according to the scheme assuming that the percentage share of the time density of the engine depends on the load capacity of the vehicle, and distinguishes two categories of vehicles [9, 10, 11, 13, 18]:

vehicles with the weight of 30 ÷ 40 tonnes	vehicles with the weight of 50 ÷ 60 tonnes
a) **I** - 9 %, **II** - 60 %, **III** - 6 %, **IV** - 25 %	b) - 9 % - 50 % - 6 % - 35 %

This way of dividing the universal characteristics has been shown in the Figure 2, where such division has been based on the following criteria:
– total engine operating time,
– engine operating time at various ranges of loads,
– time of driving in particular gears,
– number of clutch engagements.

A part of the set of measuring equipment designed for counting the engine operating time within specified ranges of its characteristics has been made in a simplified system of logic - running time meters.

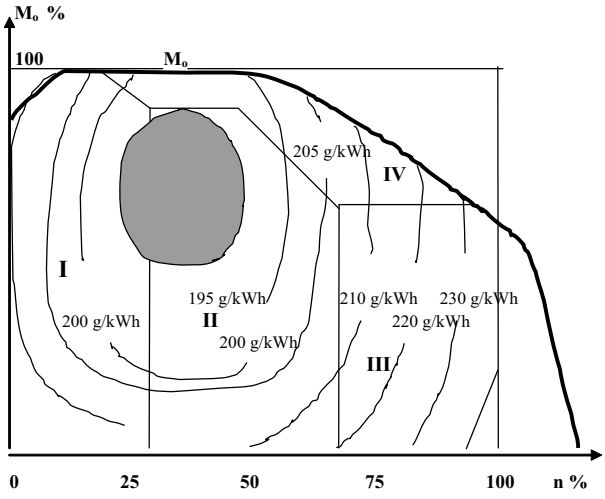

Fig. 2. Time density characteristics of the Scania DC 11 01 340 engine - grey colour denotes the minimum fuel consumption field

One should also bear in mind the fact that the field that in the assumption was based on the area of a rectangle of M_o – n (0 ÷ n_z) did not fully match the universal characteristics of the engine, limited from the top by the maximum torque curve and, in relation to the theoretical assumption, one could take into account only the specified percentage of the field of the mentioned rectangle. A part of the field above the maximum torque line has been subtracted at the speed corresponding to the idle speed and the speed above 75% of engine speed.

The time density characteristics prepared on the basis of the characteristics (Fig. 2) in the bar system (Fig. 3) considers only the fields actually used on the universal characteristics and thanks to that it can be seen what part of the universal characteristics does not coincide with the rectangle with the dimensions of M_{omax} – n.

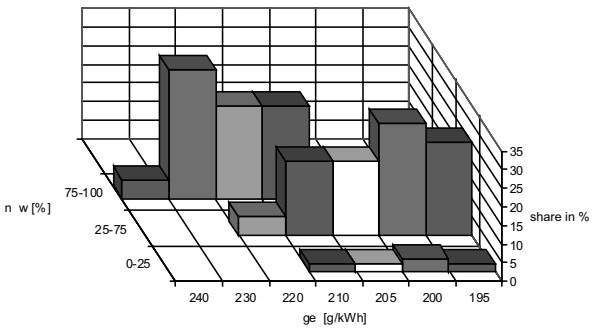

Fig. 3. Time density characteristics of the Scania DC 11 01 340 engine in the bar system

EQUIVALENT SPECIFIC FUEL CONSUMPTION

Due to the sought savings achievable thanks to the determination of precise fuel consumption by the engine, the desired information for the dispatchers of transport companies is to determine the quantity of fuel used by the engine of a truck driving a long way with a cargo. Hence the search for Scandinavian companies [2,8,10,18], the vehicles of which for example, drive a route from Gothenburg to Istanbul. The calculation of the likely fuel consumption is therefore an important issue. After the analysing this problem, the author has proposed application of a new measure of the economy of the engine operation in the form of ***equivalent specific fuel consumption*** as its equivalent value resulting from the time density characteristics of the engine load [18]. Assuming the engine model proposed by Scania, such calculation can be made using the weighted arithmetic mean with use of the time density characteristics [20]. For the Scania DC 11 01 340 engine, the characteristic of which in the bar system has been shown in the Figure 4, it looks as follows:

$$g_{ez} = \frac{\Sigma g_{ein} u_i}{\Sigma u_i}, \tag{1}$$

where:
$g_{ei\,n}$ - value of specific fuel consumption in i –field of the time density characteristics defined by the speed of the engine,
u_i - percentage share of the i –field in the time density characteristics.

For the Scania DC 11 01 340 engine, the value of the specific fuel consumption calculated with this method is:

Engine speed range 0−25% n_N

g_{ez} = (195×0.03+200×0.27+205×0.25+210×0.25+220×0.2):0.907 = 228.86 g/kWh.

Engine speed range 25-75% n_N

g_{ez} = 223.51 g/(kW×h).

Engine speed range 75-100% n_N

g_{ez} = 234.97 g/(kW×h).

Since the area under the torque curve (torque supply field) is 0.907 of the area of the rectangle with the dimensions of M_o - n_N, particular fields of the constant specific fuel consumption had to be referred to the actual field of torque supply. Thus, the equivalent specific fuel consumption for the whole area of the universal engine characteristics is:

$$g_{ez} = \Sigma\, g_{ez} : 3 = 687.34:3 = 229.11 \text{ g/(kW×h)}.$$

In order to determine what is the influence of the specific fuel consumption on the equivalent fuel consumption, for the Scania DC 11 01 340 engines, calculation of the hourly fuel consumption has been carried out based on the equivalent fuel consumption and the specific fuel consumption, obtaining the following results:

– for the equivalent fuel consumption and the engine power of 250 kW (340 HP):

$$G_h = \frac{g_e \cdot N_e}{1000} = \frac{229.11 \cdot 250}{1000} = 57.27\text{kg/ h}, \quad (2)$$
$$\text{i.e. } 57.27kg/h \cdot \frac{1}{0.82dm^3/kg} = 69.85dm^3/h,$$

– for the minimum specific fuel consumption and the engine power of 250 kW (340 HP):

$$G_h = \frac{192 \cdot 250}{1000} = 48\text{kg/h}, \quad (3)$$
$$\text{i.e. } 48.0kg/h \cdot \frac{1}{0.82dm^3/kg} = 58.53dm^3/h.$$

The difference is 11.32 dm^3, which at 10-hours operation of the vehicle during the driver's working day gives more than 113.2 dm^3 per day and is a significant quantity.

This calculation shows how much closer to the reality is to use, as the measure of economy of the engine operation, the equivalent specific fuel consumption, and not the minimum specific fuel consumption normally given in the descriptions of engines. In a similar way, the equivalent fuel consumption has been determined for 21 engines of the Scania and Volvo companies, obtaining:

– the average value of the minimum specific fuel consumption of 190.93 g/kWh, according to the manufacturer's data [2,8,11,13],
– the average value of the equivalent fuel consumption of 226.35 g/kWh, obtained from simulation tests. The difference between these two values tells about the method of use of the torque supply field of the engine during its operation and is the measure of economy of the engine operation. These were direct-injection engines, turbo-charged with the power of 180 to 486 kW at the rated speed of 1800 to 2400 1/min, and 71.5% of the engines fell within the range from 1800 to 1900 1/min. The maximum torque values ranged from 903 to 3895 Nm at the average engine speed of 1081 1/min (from 1000 to 1100 1/min). The curves of the value of the equivalent specific fuel consumption in ascending order have been shown in the Figure 4, where the trend line and the equation describing it have been given. The values of the maximum torque and the torque corresponding to the rated power have been given in ascending order in Fig. 5.

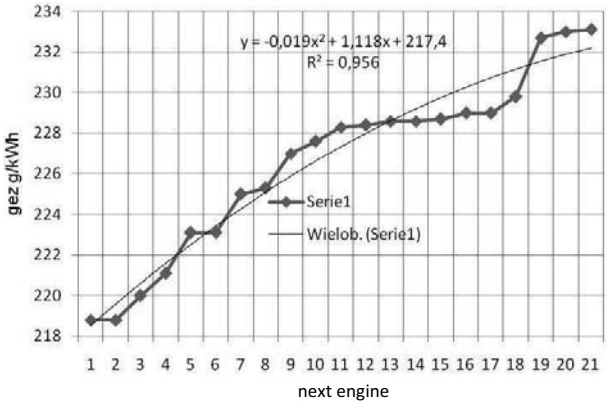

Fig. 4. Values of equivalent specific fuel consumption in ascending order

The trend line of the presented g_{ez} values is described by the equation:

$$y = -0.019\, x^2 + 1.118\, x + 217.4. \quad (4)$$

The values of maximum torque (series 1) are described by the equation:

$$y = 2.468\, x^2 + 74.78\, x + 977.1, \quad (5)$$

and the torque values corresponding to the rated power (series 2) with the equation:

$$y = -0.963\, x^2 + 108.5\, x + 617.2. \quad (6)$$

The equivalent specific fuel consumption is strongly related to both values of torque as the correlation coefficient between g_{ez} and Mo is 0.9535, and between g_{ez} and Mnz it is 0.9523. Given the fact that the engines of trucks should have the universal characteristics chosen in such a way that the field of their economic operation was at 75% of the rated load and at 75% of the rated engine speed for the tested engine group, these results were as follows:

– the average value of torque according to the manufacturers' data: 1657.95 Nm
– the average value of torque according to the simulation tests: 1266.022 Nm, hence the 1657.95 x 0.75 = 1243.46. The difference is 1.8% and therefore the engines assessed as a group are constructed in accordance with the adopted principles.

As for the average engine speed, at which there was a minimum fuel consumption according to the theoretical assumptions outlined above, it amounted to 1450 1/min, while from the simulation test it resulted in 1081 1/min, and so the difference corresponds to 34%.

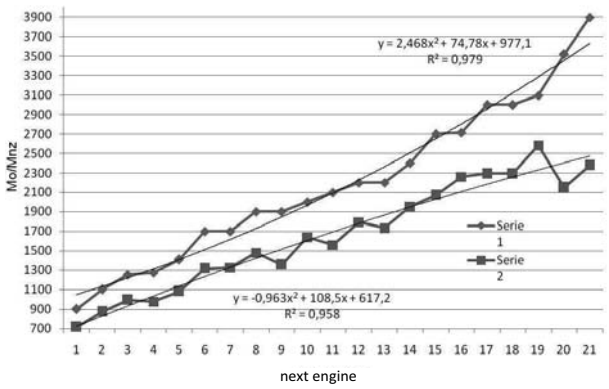

Fig. 5. Torque values of tested engines

The situation is the more advantageous that the maximum torque value occurs at lower engine speeds, which is desirable for operational reasons.

CONCLUSIONS

The presented results of research and tests support the assumption that the equivalent specific fuel consumption based on the universal characteristics (general) is a better rate of economy of the engine operation than the specific fuel consumption given on the external characteristics of the engine. After examining a greater number of engines it will be possible to make an attempt to generalise the obtained results.

REFERENCES

1. **Danilecki K. 2008:** Trends In the development of turbocharging systems in automotive vehicles. Combustion Engines. No. 2 (133). p. 61-67.
2. **Drukała D. 2000:** Volvo FH12- z piedestału na drogę. Polski Traker. Nr 5. p. 8-10. *[Volvo FH12-from the pedestal to the road. Polish Trucker].*
3. **Horodecki S. 1989:** Eksploatacyjne i organizacyjne przedsięwzięcia dla oszczędnego wykorzystania paliw w transporcie samochodowym. Kraków. Oszczędność paliw i energii. Wydawnictwo : PAN Oddział Kraków, Komisja Naukowo – Problemowa Motoryzacji. p. 77-87. *[Operational and organisational projects for economic use of fuels in road transport. Cracow 1989. Savings of fuel and energy. Publishing House: PAN – Polish Academy of Sciences, Cracow Branch of the Commission of Science and Problems in Motorisation. p. 77-87].*
4. **Jantos J. Siłka W. 1993:** Niektóre problemy symulacyjnych badań zużycia paliwa. Badania Symulacyjne w Technice Samochodowej. Lublin. Wydawnictwo Politechniki Lubelskiej i Krakowskiego Oddziału PAN. p. 192-198. *[Certain problems of simulation tests of fuel consumption. Simulation tests in automotive engineering. Lublin 1993. Publishing House of the Technical University of Lublin and Cracow Branch of the PAN Polish Academy of Sciences. p. 192-198].*
5. **Kiernicki Z. 2008:** Simulation method of operating parameters assessment used for comparative analysis. Combustion Engines. No. 1 (132).p. 73-78.
6. **Koniuszy A. 2008: The method of generating a** tractor engine time density characteristic. Combustion Engines. No. 2 (133). p. 54-60.
7. **Koniuszy A.:** The use of luster analysis method for the development of static load cycles of diesel engines in non road vehicles. Combustion Engines 2008. No. 4(135). p. 39-45.
8. **Majak M. 2000:** Volvo FH 12 ciężarówka roku 2000. Auto Transport. No. 2. p. 1-4. *[Volvo FH 12 Truck of the year 2000. Auto Transport 2000. No. 2. p. 1÷4]*
9. **Mysłowski J.K. 2009:** Improvement in the general efficiency of engines driving cars of great capacity. Journal of Kones '09. Stare Jabłonki, 23.09. p. 351-355.
10. **Mysłowski J.K., Talaga K. 2004:** Ocena prawidłowości wyznaczania jednostkowego zużycia paliwa. Ekologia pogranicza Gorzów Wlkp.–Łagów 09.23–26. Gorzów Wlkp. Instytut Badań i Ekspertyz Naukowych, p. 523-527. *[Assessment of the accuracy of determination of specific fuel consumption. Ecology of the borderline Gorzow Wielkopolski - Łagów 2004.09.23-26. Gorzow Wielkopolski. Institute for Research and Scientific Expertise, p. 523-527].*
11. **Mysłowski J, Mysłowski J.K. 2008:** A trial to improve fuel-efficiency rates of a turbo-charged engine. Journal of Kones. Power train and Transport. Warszawa, p. 375-380.
12. **Mysłowski J.K. 2008:** Alternative fuels for combustion engines, search for new ways of powered. Mechanical Engineering of the Baltic Region Kaliningrad State Technical University. Kaliningrad, N1 p. 86-94.
13. **Mysłowski J. 2003:** Simulation test of fuel consumption. Commission of motorisation No. 26-27 p. 323-328. POLISH ACADEMY OF SCIENCES CRACOW BRANCH, Cracow.
14. **Mysłowski J. Mysłowski J.K. 2003:** Simulation research of unitary fuel consumption of MAN engine. Lublin. POLISH ACADEMY OF SCIENCES BRANCH LUBLIN. Commission of motorisation and power industry in agriculture. Volume III p. 186-191.
15. **Siedlecki A.:** Jak oszczędzać paliwo. Transport- Technika Motoryzacyjna 2001, nr 4, p. 8-11. *[How to save fuel. Transport – Automotive Technology 2001, No. 4, p. 8-11].*
16. **Siłka W. 1997:** Energochłonność ruchu samochodu, Warszawa WNT. *[Energy consumption in vehicle movement. Warsaw WNT, 1997].*
17. **Siłka W. 2002:** Teoria ruchu samochodu, Warszawa WNT. *[Theory of vehicle movement. Warsaw WNT, 2002].*
18. **Rusak Z.:** Tytuł „Coach Of The Year 2004" dla MAN-a i Scanii. Autobusy 2003, nr 10, p. 2-4. *[Title of the "Coach of the Year 2004" for MAN and Scania. Coaches 2003, No. 10, p. 2-4].*
19. **Ubysz A. 2010:** Studium przebiegowego zużycia paliwa w samochodzie w ruchu rzeczywistym. Akademia Techniczno-Humanistyczna Bielsko–Biała. *[Study of mileage fuel consumption in a vehicle in real time. Academy of Technology and Humanism, Bielsko–Biała, 2010].*
20. **Walentynowicz J. 1986:** Planning experiment in inspections of internal - combustion engines. Combustion Engines. No. 2-3. p. 23-25.

EKWIWALENTNE ZUŻYCIE PALIWA W SILNIKACH POJAZDÓW SZWEDZKICH FIRM

S t r e s z c z e n i e . Przedstawiono problemy zużycia paliwa jako parametr wykorzystywany do oceny wykorzystania zasilania momentu obrotowego silnika używanego do napędu samochodu ciężarowego o dużej ładowności. Nowy sposób tej oceny został zaproponowany w formie równoważnego zużycia paliwa i został on przetestowany dla silników Scania i Volvo Trucks.

S ł o w a k l u c z o w e : silnik, zużycie paliwa, ładowność.

TEKA. COMMISSION OF MOTORIZATION AND ENERGETICS IN AGRICULTURE – 2012, Vol. 12, No. 1, 155–158

The flexibility of compression-ignition engines of scania trucks

Janusz Mysłowski

University of Technology in Koszalin
75-620 Koszalin,ul.Racławicka 15-17 e-mail mysjan@plusnet.pl

Summary. This paper presents an analysis of the improvement of flexibility coefficient of Scania engines designed for driving heavy goods vehicles. Linear trend was determined for the flexibility coefficient of present-day engines against the older generation ones.

Key words: engine, flexibility.

INTRODUCTION

The steady increase in the number of motor vehicles moving on public roads poses specific threats for the environment surrounding us. It is generally accepted in most discussions that vehicle's engine is the most unfavourable unit in it due to its adverse environmental effects.

The ongoing difficulties with fuels and energy trigger continuous searches for new energy carriers and entail attempts to reduce energy consumption [7,8,9].

The requirements set for present-day engines are frequently antagonistic, which is clearly visible when the ever-increasing number of motor cars and traffic difficulties connected with this, and on the other hand the necessity of reducing the quantity of consumed fuel and exhaust gases being expelled into environment, are taken into account. However, to ensure adequate truck dynamics requires larger and larger flexibility of their engines and application of appropriate drive train ratios [1]. The improvement of engine flexibility itself can bring significant results, the evidence of which should be considerations being quoted above. It is apparent that the method of feeding air and fuel to an engine may help improve engine flexibility The results presented below refer basically to the improvement of air feeding to engines [3].

FLEXIBILITY EVALUATION OF SCANIA ENGINES

Total flexibility of combustion engine is a product of torque flexibility and rotational speed flexibility (rotational speed range) according to the formula presented below.

A numeric expression of engine flexibility is flexibility coefficient. It may be determined, among others, on the basis of engine's external characteristics [1,6,10] in a manner given below:

$$E = e_M e_n = \frac{M_{o\max}}{M_N} \frac{n_N}{n_{Mo\max}}, \quad (1)$$

where: e_M – torque range (torque flexibility),
e_n – rotational speed range,
M_{omax} – maximum engine torque,
M_N – torque corresponding to rated power,
n_{Momax} – rotational speed of maximum torque,
n_N -– rated rotational speed.

The first part of the above product presents torque range (torque flexibility) and it depends on the course of engine's torque curve. This course depends on a number of factors, such as characteristic parameters of intake system, timing gear characteristics and feed system characteristics. By changing these parameters, the course of torque curve may be altered towards a user-desired direction so that the engine would be well adapted to performed tasks. The manner in which the flexibility and torque improvement is being implemented depends on performance abilities and profitability analysis of a given solution in case of specific engine.

When it comes to the possibilities of changing the second part of the above product, they are closely related to modification of its first part, consisting in the shift of

torque curve maximum position. The range of rotational speed depends on the position of this maximum and it is possible to control effectively the engine flexibility by changing it.

Analysis of the flexibility of engines of Scania trucks [4] over the last 10 years was carried out dividing these engines into 5-year-long periods of their operation, starting with the 90s of the last century. Comparison of the flexibility of the oldest engines is presented in Table 1.

Table 1. Flexibility of older generation Scania engines [1,4,6]

No.	Engine	e_M	e_n	E
1.	Scania D 8	1.158	1.600	1.852
2.	Scania DS 8 tb	1.143	1.600	1.828
3.	Scania D 11	1.172	1.833	2.148
4.	Scania DS 11 tb	1.004	1.571	1.577
5.	Scania 112	1.154	1.600	1.846
6.	Scania 112 M Tb	1.192	1.600	1.907
7.	Scania 142 M Tb	1.110	1.520	1.687
	Average	1.133	1.617	1.832

Explanations: tb – turbocharged engines

It clearly appears from the analysis of Table 1 that Scania turbocharged engines have worse dynamic properties when compared to unsupercharged engines. Average value of the flexibility coefficient of turbocharged engines amounted to 1.749, with 1.948 for unsupercharged engines, and was lower by 11.5%. This was the time of common introduction of turbo-supercharging which was not brought to perfection as it is at present. Next stage of the improvement of dynamic properties in Scania Company was common introduction of turbo-charging in the engines designed for driving heavy goods vehicles. This was primarily determined by economic reasons but simultaneously turbo-supercharging system was improved so that dynamic properties of engines increased in the manner being presented in Table 2 below.

Table 2. Flexibility of newer generation Scania engines [6,13]

No.	Engine	e_M	e_n	E
1.	Scania DSC 9 - 11	1.298	1.481	1.922
2.	Scania DSC 9 - 12	1.293	1.538	1.988
3.	Scania DSC 9 - 13	1.239	1.538	1.905
4.	Scania DSC 11 - 79	1.263	1.538	1.942
5.	Scania DSC 12 - 01	1.224	1.461	1.788
6.	Scania DSC 12 - 02	1.249	1.461	1.824
7.	Scania DSC 14 - 13	1.172	1.727	2.024
8.	Scania DSC 14 - 15	1.177	1.727	2.033
	Average	1.239	1.558	1.928

All the engines being described in Table 2 are turbocharged. Increase in the flexibility coefficient by 5% was mainly obtained through the increase of torque flexibility by 9.3%, i.e. by improving the charging system since the torque range coefficient decreased by 3.6% in relation to the engines being described in Table 1. This shows a clear-cut consistency of manufacturer in improving the applied method of engine charging, which greatly diverged [5,11].

Next Scania engines had much higher flexibility coefficients, which is presented in Table 3.

As in Table 2, all the engines described in Table 3 are turbocharged.

As far as flexibility is concerned, an increase was obtained from 1.835 (Tab. 1) to 2.253 (Tab. 3), i.e. by 22.9 %. This was obtained by increasing the torque flexibility and expanding rotational speed range (rotational speed flexibility). The flexibility of rotational speed increased by 7.2% in relation to the engines being described in Table 1, whereas the torque flexibility by 15.2.

Table 3. Flexibility of the latest generation Scania engines [13]

No.	Engine	e_M	e_n	E
1.	Scania TD 06 470	1.268	1.727	2.190
2.	Scania DC 11 D1 340	1.281	1.636	2.096
3.	Scania D12 D 279	1.300	1.817	2.363
4.	Scania D12 D 309	1.299	1.818	2.362
5.	Scania D12 D 338	1.291	1.636	2.113
6.	Scania D12 D 368	1.399	1.727	2.417
7.	Scania TD 12 12 420	1.347	1.794	2.327
8.	Scania DC 16 18 560	1.303	1.727	2.251
9.	Scania DC 16 21 620	1.308	1.727	2.260
10.	Scania DC 17 19 620	1.308	1.727	2.260
	Average	1.305	1.733	2.253

Comparison of the flexibility changes during twelve years is presented in Figure 1 [2,12].

Sequence numbers on the X axis correspond to engine numbers in respective tables, whereas symbols El1, El2, El3 represent respective tables.

Analysis of the trend line (linear trend, marked with a thick straight line) in Fig. 1 clearly indicates a downward trend for the first group of engines (decrease from 1.9 to 1.7), which resulted from their construction properties and rather poorly developed turbo-supercharging system. The improvement of this charging system resulted in an upward trend (trend line El2 in Figure 1, with an increase from 1.9 to 1.95). A small decrease may be noticed in

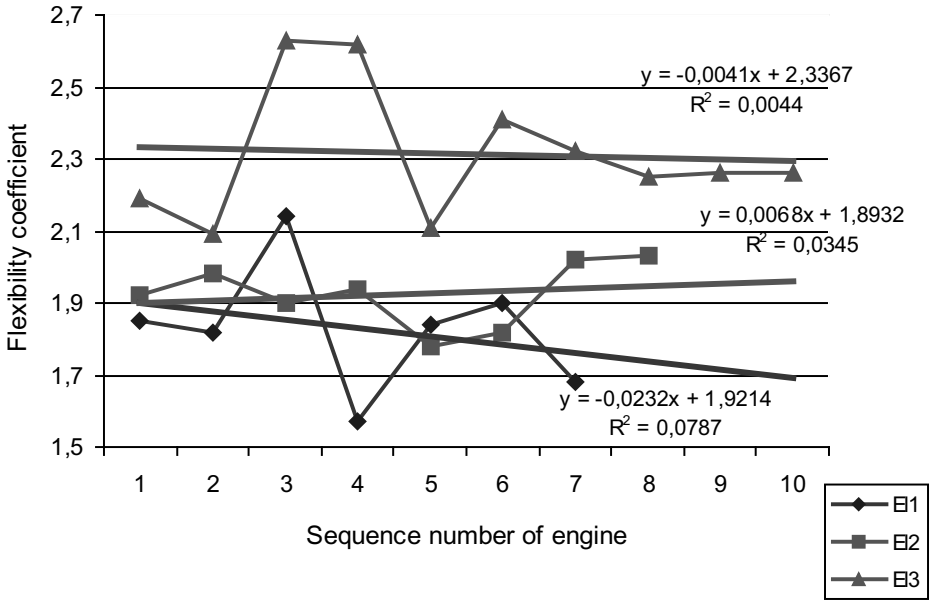

Fig. 1. Comparison of the flexibility of Scania engines under discussion

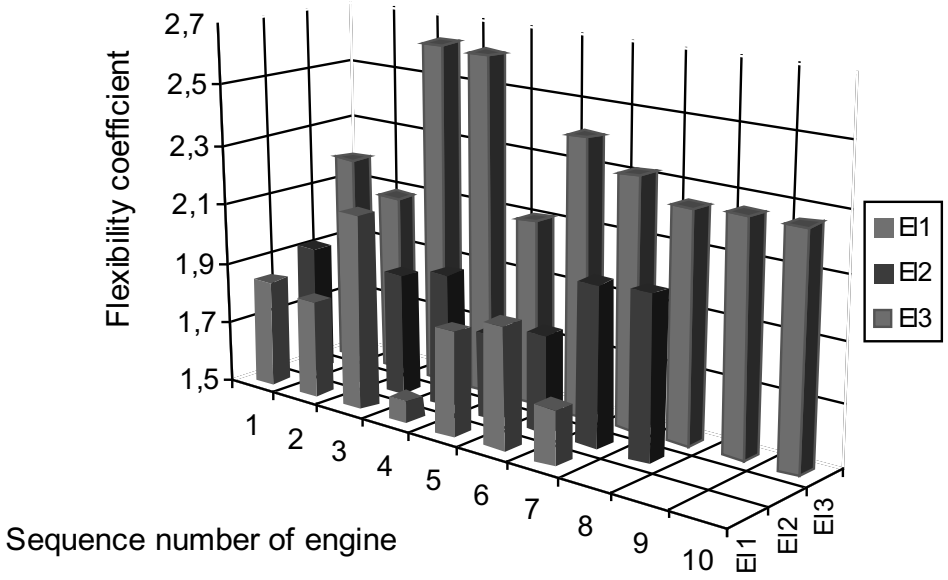

Fig. 2. Comparison of the flexibility coefficients of Scania engines as 3D column graph

flexibility in present-day engines (from 2.32 to 2.3) but the obtained flexibility values are higher by 18% to 26% than in case of the older generation engines. These results are more readable in the column graph presented in Figure 2.

CONCLUSIONS

The discussion presented in this paper allows for seeing how refinement of the feed systems and carburation in compression-ignition engines with tangential intake duct may affect the improvement of engine dynamic properties [11]. Similar trends will probably occur in engines with swirl intake duct (drallkanal) but their effects should be examined in the same way.

REFERENCES

1. **Dębicki M. 1969:** TEORIA SAMOCHODU.Teoria napędu.WNT Warszawa.
2. **Hozer J., Korol M., Korol J., Talaga L., Witek M. 1998:** Statystyka. Opis statystyczny. Uniwersytet Szczeciński, Szczecin.
3. **Luft S. 2003:** Pojazdy samochodowe.Podstawy budowy silników.WK i Ł, Warszawa.
4. **Majak M. 1998:** Scania pełna zmian. Transport – Technika Motoryzacyjna 4.
5. **Mysłowski Janusz. Mysłowski Jaromir 2006:** Tendencje rozwojowe silników o zapłonie samoczynnym. Wyd. AUTOBUSY, Radom.
6. **Mysłowski J.,Kołtun J. 2000:** Elastyczność tłokowych silników spalinowych. WNT Warszawa.

7. **Siłka W. 2002:** Teoria ruchu samochodu. WNT Warszawa.
8. **Siłka W. 1997:** Energochłonność ruchu samochodu. WNT Warszawa.
9. **Szczepaniak C. 1999:** Wybrane aspekty rozwoju motoryzacji. Politechnika Radomska, Radom.
10. **Wajand J.A., Wajand J.T. 2000:** Tłokowe silniki spalinowe, średnio- i szybkoobrotowe. WNT, Warszawa.
11. **Wajand J.T. 1989:** Wpływ rozpędzania pojazdu na przebiegowe zużycie paliwa. OSZCZĘDNOŚĆ PALIW I ENERGII.PAN Oddział Kraków, Komisja Naukowo - Problemowa Motoryzacji.Kraków.
12. **Walentynowicz J. 1996:** Stochastyczna identyfikacja wielowymiarowych charakterystyk i widm obciążenia silników spalinowych. WAT, Warszawa.
13. http://www.wagaciezka.com/viewtopic.php?t=10735.

ELASTYCZNOŚĆ SILNIKÓW O ZAPŁONIE SAMOCZYNNYM SAMOCHODÓW SCANIA

S t r e s z c z e n i e . W pracy przedstawiono analizę poprawy współczynnika elastyczności silników Scania przeznaczonych do napędu samochodów ciężarowych o dużej ładowności. Wyznaczono trend liniowy dla współczynnika elastyczności współczesnych silników na tle silników starszej generacji.

S ł o w a k l u c z o w e : Silnik, elastyczność.

TEKA. COMMISSION OF MOTORIZATION AND ENERGETICS IN AGRICULTURE – 2012, Vol. 12, No. 1, 159–162

Effect of selected factors on grain mass creep test under simulated load conditions

Rafał Nadulski, Elżbieta Kusińska, Zbigniew Kobus, Tomasz Guz

Faculty of Engineering and Food Processing Machinery, University of Life Sciences in Lublin
Doświadczalna Str. 44, 20-236 Lublin, Poland, e-mail: rafal.nadulski@up.lublin.pl

Summary. The paper presents the results of a study on the effect of vertical load, moisture and species of cereal on the course of grain mass creep test. The experiment demonstrated that the relative change in the height of grain column after a specific time, i.e. after 1, 2 and 8 days, depends on the species of grain, its moisture, and the value of the vertical load. The greatest range of changes in the height of the grain mass column (14.8%) was recorded after 8 days for oat grain with moisture of 22% under vertical load of 70 kPa.

Key words: grain, cereal species, moisture, vertical load, creep.

INTRODUCTION

At present a variety of designs of grain storage silos are in use [15, 1]. Harvested grain must meet specific quality requirements [4]. High quality of material stored in a silo can be maintained through active ventilation of the grain mass. Forced movement of air through a grain deposit involves flow resistance related with the porosity of the material. The airflow resistance of cereal grain and seeds is affected by the following factors: thickness of the layer of granular material, porosity, density, moisture of the material, size and shape of particles and the degree of compaction of the material, as well as the time of storage and the method of silo filling [11, 10, 12]. A majority of agricultural produce can be classified as viscoelastic bodies [7, 13], liquids as well as solids – amorphous bodies with high viscosity. The behaviour of such materials under certain conditions can be approximated by means of classical mechanical models [2]. Under other conditions those bodies display totally different responses to loads. In viscoelastic bodies a certain time has to elapse for a stabilised state of deformation to appear. In such bodies the phenomenon of creep occurs, causing permanent and irreversible deformation of the material [17, 5]. Creep consists in a change of the state of deformation of an element in time under the effect of constant strain acting at a constant temperature. The phenomenon is observed after a sufficiently long period of time and it occurs commonly in materials of plant origin, creating problems in their post-harvest processing.

The main factor determining the mechanical properties of kernels is water [3, 18]. High moisture content of kernels results in their susceptibility to plastic deformations. This can cause the appearance of internal damage and micro-damage to the seed coat. At low moisture content kernels are brittle and macro-damage to the external structures may take place. Changes in the shape of kernels are an important factor that determines grain quality and the conditions in the process of grain ventilation in a silo [6, 20].

During the storage of cereal grain and seeds in silos the bottom layers of the material are subjected to the greatest effect of vertical load and undergo deformation related with the rheological properties of grain mass [9, 8]. That problem is of particular importance during the storage of granular materials in silos with large dimensions [14]. This is indicated by studies by Kusińska and Szwed [19], simulating the conditions of storage of wheat grain in industrial silos with filling height of about 40 metres. The phenomena of self-sorting and increase of grain column pressure during the filling of silos cause compaction of the grain mass and a change in the tribological properties, which leads to a reduction of the ability of the material to return to its original shape after the removal of the load [3].

Analysis of the available literature shows that the behaviour of grain mass under the effect of loads appearing in large silos is still not sufficiently known.

OBJECTIVE AND SCOPE OF RESEARCH

The objective of the study was to perform, under laboratory conditions, a test of grain mass creep. The factors chosen as those that may have a significant effect on the behaviour of grain mass in the creep test included vertical load with values occurring in large silos, grain moisture and the species of the cereal.

METHOD

The experiment was performed on grain of winter wheat cv. Tonacja, winter rye cv. Słowiańskie, oat cv. Sławko, winter triticale cv. Pawo, and spring barley cv. Stratus. The initial moisture of the grain was ca. 13%. The grain was moistened in containers, adding water in the form of mist from a sprayer. When the moistening operation was completed, the containers were tightly sealed and then the grain was vigorously stirred. As a result of that operation three levels of grain moisture were obtained, of 14%, 18% and 22%. The moisture content of the grain was assayed in accordance with the standard PN79/R-69950. The the grain was poured into steel containers with diameter of 100 mm and height of 150 mm, equipped with a moving cover that permitted, through a system of four springs, to obtained the assumed level of load (Fig. 1).

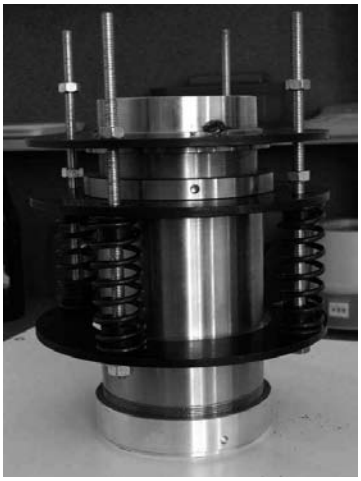

Fig. 1. Cylinder generating stresses in the grain mass

The grain mass was loaded obtaining a constant vertical load, and then stored at temperatures of 6°C and 22°C for 8 days. The experiment was conducted on grain mass subjected to vertical loads of 35, 52 and 70 kPa, and on a control sample, i.e. without any load applied. The design of the test system permitted the determination of the grain column height immediately after achieving the load desired load [12]. Then, changes in the grain column height were recorded after specific periods of time, i.e. successively after the first day, after two days and after 8 days. The parameters adopted as characterising the creep of the material was the relative change of grain column height ΔH after time t calculated from the formula:

$$\Delta H = \frac{(H - H_t) \cdot 100}{H}, \quad (1)$$

where:

ΔH – relative deformation of grain mass column after time t, %,

H_t – height of grain mass column after time t, mm,

H – initial height of grain mass column, mm.

Statistical analysis was conducted with the of the program Statistica ver. 6, StatSoft, Inc. [StatSoft, Inc. 2003]. Estimation of the effect of the variables (vertical load, cereal species, grain moisture) on the value of ΔH, i.e. the relative change of grain column height after time t was performed with the use of the module of variance analysis ANOVA.

RESULTS

The statistical analysis revealed that the relative deformation of the grain mass column ΔH after time t depended on the species of the cereal, grain moisture, and on the vertical load applied. In each case an increase of the value of the vertical load caused an increase in the value of ΔH. At grain moisture levels of 14% and 18% ΔH assumed values that did not exceed 5%. Extension of the time of grain mass loading caused a distinct increase in the value of ΔH.

Fig. 2 presents the range of changes of the height of grain mass column ΔH for rye grain with moisture of 22%. The effect of vertical load and time of storage on the relative deformation of grain mass column ΔH for wheat grain with moisture of 22% is presented in Fig. 3, and for triticale grain in Fig. 4. Comparing the grain of rye, wheat and barley with moisture of 22% the greatest range of changes in the value of ΔH was recorded for rye, for which ΔH after 8 days was from 5.5% to 11.1%.

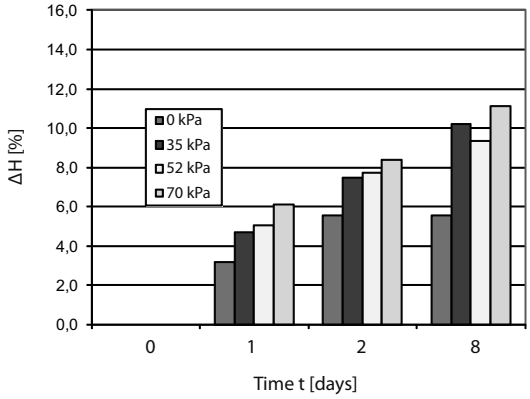

Fig. 2. Relative deformation of grain mass column ΔH for rye grain with moisture of 22% in relation to vertical load and time of storage

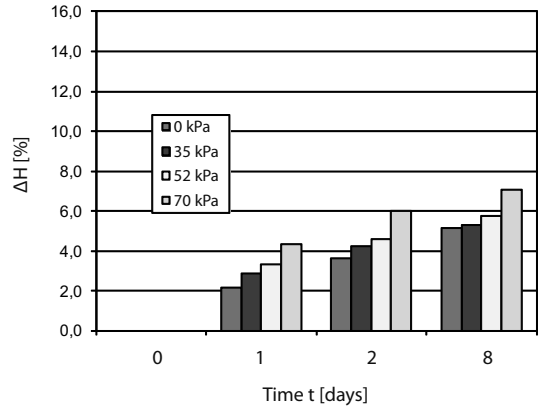

Fig. 3. Relative deformation of grain mass column *ΔH* for wheat grain with moisture of 22% in relation to vertical load and time of storage

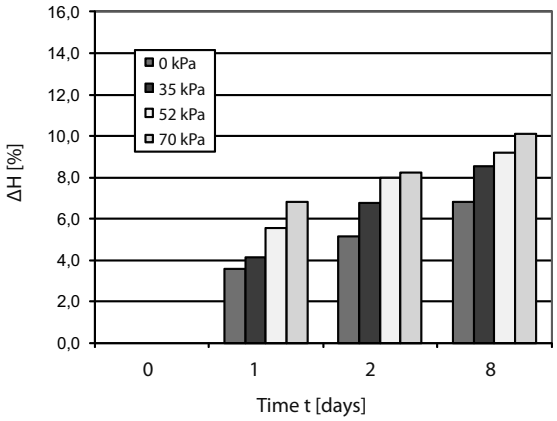

Fig. 4. Relative deformation of grain mass column *ΔH* for triticale grain with moisture of 22% in relation to vertical load and time of storage

Figures 5 and 6 present the range of changes of the relative deformation of grain mass column *ΔH* for grain of barley and oat with moisture of 22%. Note should be taken of the fact that in the case of non-loaded grain of barley small changes were observed in the values of *ΔH* with the passage of time, within the range from 1.3% to 1.9%.

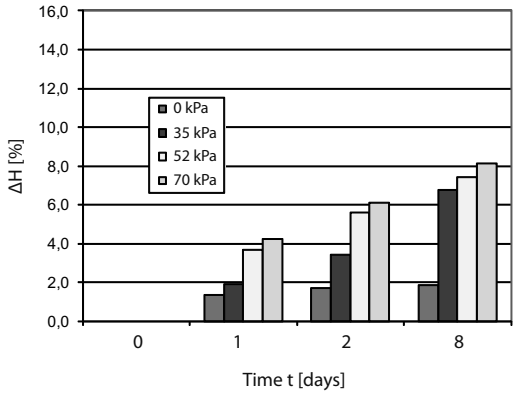

Fig. 5. Relative deformation of grain mass column *ΔH* for barley grain with moisture of 22% in relation to vertical load and time of storage

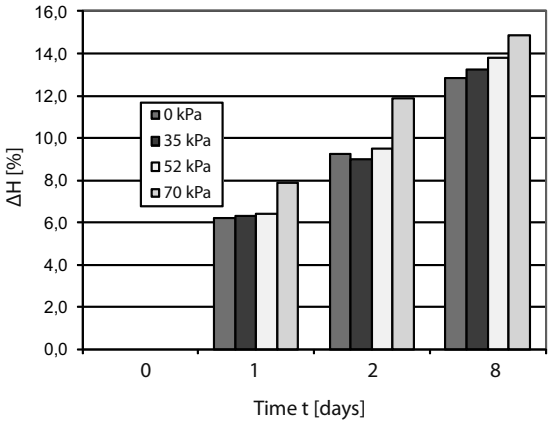

Fig. 6. Relative deformation of grain mass column *ΔH* for oat grain with moisture of 22% in relation to vertical load and time of storage

Among all the cereals tested at grain moisture of 22% the greatest range of changes of the relative deformation of grain mass column *ΔH*, amounting to 14.8%, was recorded after 8 days for oat grain subjected to a vertical load of 70 kPa.

After one day, among all of the cereals tested the smallest changes in the relative deformation of gain mass column *ΔH* occurred in the case of barley (from 1.3% to 4.2%) and wheat (from 2.2% to 4.3%), and the greatest for oat (from 6.2% to 7.8%). The study demonstrated that at grain moisture of 22% there appears a distinct and statistically significant effect of vertical load on changes in the grain column height *ΔH*. Among the cereal species tested, the greatest range of changes in the height of grain mass column was observed for oat, and the smallest for wheat. The experiment performed indicates the necessity of taking into account the phenomenon of grain material creep during the storage of cereal grain.

CONCLUSIONS

The study permitted the formulation of the following conclusions:

1. The creep test demonstrated that the relative deformation of grain mass column *ΔH* depends on the cereal species, moisture content of the kernels, vertical load applied, and on the duration of the loading.
2. In each case, with the passage of time an increase was observed in the relative deformation of grain mass column *ΔH*.
3. Increase in the value of vertical load causes a statistically significant increase of the relative deformation of grain mass column *ΔH* after 1, 2 and 8 days.
4. At grain moisture levels of 14% and 18% the relative deformation of grain mass column *ΔH* assumes values not exceeding 5%.
5. The greatest range of changes of the relative deformation of grain mass column *ΔH* (14.8%) was recorded after 8 days in the case of oar grain with moisture of 22% subjected to a vertical load of 70 kPa.

6. In the case of grain of the remaining species of cereals with moisture of 22%, after 8 days the range of changes of the relative deformation of grain mass column ΔH varied from 7.1% for wheat to 11.1% for rye.

REFERENCES

1. **Bowszys J., Tomczykowski J., 2007** Self-segregation of maize kernels during gravitational discharge from a silo. Teka Komisji Motoryzacji i Energetyki Rolnictwa, V (VII), p. 38-42.
2. **Didukh V., Igor Tsyz I. 2003** Investigation of density change of agricultural materials. Teka Komisji Motoryzacji i Energetyki Rolnictwa, 3. p. 79-90.
3. **Frączek J., Kaczorowski J., Ślipek Z., Horabik J., Molenda M. 2003.** Standaryzacja metod pomiaru właściwości fizyczno-mechanicznych roślinnych materiałów ziarnistych. Acta Agrophysica, Nr 92, Rozprawy i monografie, Lublin. ISSN. p. 1234-4125.
4. **Grundas S. Rudziewicz E. 2006** Physical and technological effects of wheat grain infestation by granary weevils. Teka Komisji Motoryzacji i Energetyki Rolnictwa, 6A, p. 61-69.
5. **Gumbe L. O. 1987** Mechanical properties of granular materials as related to loads in cylindrical grain silos. The Ohio State University. Dissertation. pp. 307.
6. **Guz T., Kobus Z., Kusińska E., Nadulski R., Oszczak Z. 2011.** Wpływ nacisków masy ziarna składowanego w silosie na zmiany cech geometrycznych pszenicy. Inżynieria Rolnicza, Nr 4 (129). p. 59-66.
7. **Horabik J. 2001** Charakterystyka właściwości fizycznych roślinnych materiałów sypkich istotnych w procesie składowania. Acta Agrophysica, 54, Lublin.
8. **Kolowca J. 2006a.** Właściwości reologiczne masy ziarna o zróżnicowanej wilgotności. Inżynieria Rolnicza, Nr 12 (87). p. 243-248.
9. **Kolowca J. 2006b.** Wpływ wielokrotnych obciążeń statycznych na stopień zagęszczenia i właściwości reologiczne masy ziarna. Inżynieria Rolnicza, Nr 13 (88). p. 193-199.
10. **Kusińska E. 2008** Hydraulic resistance of air flow through wheat grain in bulk. Teka Komisji Motoryzacji i Energetyki Rolnictwa, 8, p. 121-127
11. **Kusińska E., Kizun V. 2006** Wpływ zagęszczenia ziarna owsa i prędkości przepływu powietrza na opór hydrauliczny. Inżynieria Rolnicza, Nr 5(80), p. 403-410.
12. **Kusińska E., Nadulski R., Kobus Z., Guz T. 2011.** Opory przepływu powietrza podczas wietrzenia śruty pszennej. Inżynieria Rolnicza, Nr 4 (129). p. 159-165.
13. **Mohsenin N. 1987:** Physical Properties of Plant and Animal Materials, New York.
14. **Nadulski R., Kusińska E., Kobus Z., Guz T., Oszczak Z. 2011.** Analiza zmian objętości masy ziarnowej wybranych gatunków zbóż pod wpływem obciążenia. Inżynieria Rolnicza, Nr 4 (129). p. 237-242.
15. **Ramíreza A., Nielsenb J., Ayugaa F. 2010.** Pressure measurements in steel silos with eccentric hoppers. Powder Technology, Vol. 201(1), 12, p. 7-20.
16. StatSoft, Inc. 2003 STATISTICA (data analysis software system), version 6. www.statsoft.com.
17. **Steffe J. F. 1996** Rheological methods in food process engineering. Michigan State University, Freeman Press, ISBN 0-9632036-1-4, p. 418.
18. **Szot B. 1983** Czynniki kształtujące odporność ziarna pszenicy na obciążenia. Zeszyty Problemowe Postępów Nauk Rolniczych, Nr 258. p. 437-447.
19. **Szwed G., E. Kusińska. 2005** Zmiana niektórych cech geometrycznych ziarniaków pszenicy w wyniku niekorzystnych warunków przechowywania. MOTROL, Motoryzacja i Energetyka Rolnictwa, 7. p. 196-207.
20. **Waszkiewicz C. 1986** Badania nad wyznaczeniem oporów przepływu powietrza przez warstwę materiału ziarnistego. Roczniki Nauk Rolniczych. Nr 77-C-1. p. 207-215.

WPŁYW WYBRANYCH CZYNNIKÓW NA PRZEBIEG TESTU PEŁZANIA MASY ZIARNOWEJ W SYMULOWANYCH WARUNKACH OBCIĄŻEŃ

S t r e s z c z e n i e. W pracy przedstawiono wyniki badań dotyczące wpływu nacisku pionowego, wilgotności i gatunku zboża na przebieg testu pełzania. W wyniku przeprowadzonego eksperymentu stwierdzono, że względna zmiana wysokości słupa ziarna po określonym czasie tj. po 1, 2 i 8 dniach zależy od gatunku ziarna, jego wilgotności i nacisku pionowego. Największy zakres zmian wysokości słupa masy ziarnowej (14,8%) zarejestrowano dla owsa o wilgotności 22% po upływie 8 dni poddanego naciskowi pionowemu wynoszącemu 70 kPa.

S ł o w a k l u c z o w e: ziarno, gatunek, wilgotność, nacisk pionowy, pełzanie.

TEKA. COMMISSION OF MOTORIZATION AND ENERGETICS IN AGRICULTURE – 2012, Vol. 12, No. 1, 163–167

The influence of thermal processing on the course of the process of pressing juice from beetroot

Rafał Nadulski, Kazimierz Zawiślak, Karolina Strzałkowska, Dariusz Piekarski, Agnieszka Starak

Department of Food Engineering and Machinery, University of Life Sciences in Lublin, Doświadczalna Str. 44, 20-236 Lublin, Poland, e-mail: rafal.nadulski@up.lublin.pl

Summary. In this paper the influence was determined of thermal processing on the process of pressing juice from beetroot. The research was conducted with the use of three procedures for yielding juice. The achieved results indicate that utilised thermal processing, which consisted in freezing and pressing, after defrosting the resource, contributes to the increase in the efficiency of the process. At the same time no statistically significant differences in the content of the extract and the pH value of the yielded juice with the use of applied procedures were recorded.

Key words: beetroot, pulp, juice, pressing, freezing.

INTRODUCTION

In recent years the interest in pro-health food with maintained nutrients, which are necessary for a human organism, has increased. An important role in heart diseases prevention is played by fruit and vegetables as well as, achieved from them, juices rich in phitoelements [23]. Thanks to the increased consumption of fruit and vegetables 19% of cases of digestive system neoplasms, 31% of cases of ischaemic heart disease and 11% of cases of infarct could be prevented [11].

Consumers expect food which is minimally processed, which also concerns fruit and vegetables juices. New tendencies in producing fruit and vegetables juices regard the production of the so-called direct juices, naturally cloudy, from ecological and fermented resources [19, 6].

One of the vegetables with proved pro-health properties is beetroot (Beta vulgaris). In Poland beetroot is, except for carrots, the most wide-spread root vegetable in cultivation. An annual consumption of this vegetable in Poland is 12-14 kg per one inhabitant [2].

The root of beetroot contains proteins, sugars, mineral salts, vitamin C and B-group vitamins. It is a dietary vegetable – thanks to the high content of fibre which positively influences digestion processes. Beetroot owes its characteristic colour to the presence of betalain pigments which consist of betacyanins of red colour and betaxantines of yellow colour. Betanin, which has a higher ability to catch radicals than anthocyanins, belongs to betacyanins. Due to strong pro-health properties on the basis of beetroot juice preparations, which constitute a diet supplement, were developed and implemented.

The processing of the resource can significantly change its pro-health properties. The basic method for yielding liquid phase from plant materials is pressing [3, 25, 20, 9]. As research papers indicate, physical processing of juice after pressing (depectinisation, clearing, ultrafiltration and densification) causes the increase of mineral elements [12]. However, the research conducted by Nowak et al. [16] indicates the negative influence of unit operations on pro-health properties of celery and beetroot. Thus, we should seek such methods of processing of the resource which would minimise the negative influence of processing on the pro-health properties. Recently there has been a range of research related to the assessment of the quality of beetroot juice [1, 18], nevertheless, there is little research on the ways of achieving beetroot juice with the lowest quality changes [15].

In the preparation process of the resource for pressing enzymatic processing is utilised, which aims at increasing the efficiency of the process [17]. Lately a tendency to eliminate methods of chemical processing from the production processes can be observed [8]. That is why the interest of researchers has been directed to the utilisation of physical methods of initial pulp processing such as: pulsed electric field processing (PEF), ohmic heating (OH), radiation, sonification, microwave heating, pulp freezing [4, 7, 24, 10, 5, 13]. The use of the abovementioned forms of processing is aimed at preserving organoleptic and nutrition properties at the highest level, at the same time providing the proper level of efficiency.

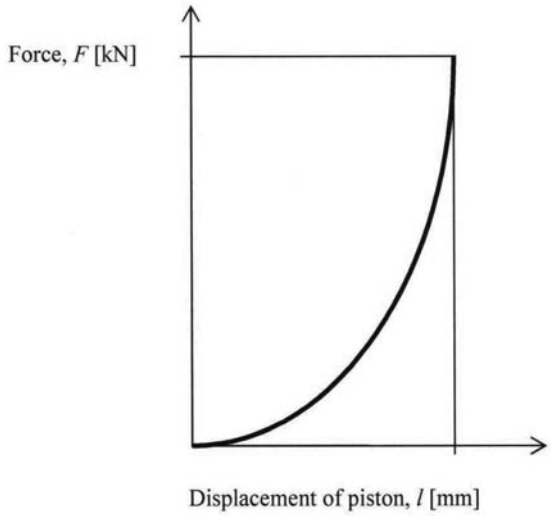

Fig. 1. Example of pressing curve of beet pulp

The aim of this research was to define the influence of the initial processing which consists in freezing and defrosting pulp or marc, on the efficiency and energy consumption of the pressing process. Energy consumption was defined solely in relation to pressing not taking into account energy input related to milling and freezing the resource. The scope of the research included the definition of efficiency and unit energy input of the pressing process and the assessment of the selected quality properties of the yielded juice by identifying the content of extract and juice pH value.

MATERIALS AND METHODS

The research was conducted on roots of beetroot variety Red Ball. It is a variety of high fecundity, for many years recommended for processing and storage [2]. For the purpose of the experiments healthy roots were used, without mechanical damage. Cleaned and peeled resource was milled with the use of milling machine MKJ250 produced by Spomasz Nakło with the use of a standard milling disc with 5 mm perforation. Pressing was conducted in a laboratory self-designed basket press, with the diameter of 80 mm and the capacity of approx. 600 cm^3, which cooperated with Instron 4302 apparatus [14]. Pressing was done with the use of a sieve with ~4 mm perforation and metal mesh. The speed of the piston stroke was defined at 10 $mm \cdot min^{-1}$. Pressing was conducted until the maximum force 9 kN was achieved, then the pressing was stopped. During the first pressing 200 g of vegetable pulp was pressed, whereas during the second pressing it was the marc which was created after the first pressing. The experiment was conducted according to established procedures:

- In procedure I the initial processing prior to the first pressing was milling the resource,
- In procedure II additionally before pressing the marc (second pressing) thermal processing was used, which consisted in freezing the marc in a temperature of -21°C, defrosting and bringing it to the temperature of the surrounding,
- In procedure III thermal processing (freezing and defrosting) of the resource was conducted both prior to the first pressing of pulp and the second pressing of marc.

From the Instron 4302 operating system a relation between the force of piston pressure and its stroke was gained (Fig. 1). After each test the amount of the yielded juice was defined, as well as the content of extract (PN-90/A-75101/02) and pH value (PN-EN 1132:1999) of the yielded juice [21, 23].

Yield of juice was calculated using the following equations:

$$W_j = \frac{M}{Mp},$$

where:

W_j – yield of juice, %,

M – mass of juice after pressing according to established procedure, kg,

M_p – mass of pulp or mass of marc according to established procedure, kg.

Whereas unit energy input was calculated using the following equations:

$$E_j = \frac{W}{M},$$

where:

Ej – unit energy input, $kJ \cdot kg^{-1}$,

W – work of pressing according to established procedure, kJ,

M – mass of juice after pressing according to established procedure, kg.

The conducted research allowed determining energy consumption and the efficiency of the pressing process, as well as defining the basic quality properties of the yielded juice. Statistical analysis of the research results

was carried out with the use of ANOVA one-way analysis of variance and Tukey's test.

RESEARCH RESULTS AND THEIR ANALYSIS

Thermal processing of beetroot pulp which consists in its freezing and then defrosting significantly influences the efficiency of pressing (Fig.2). In this case the efficiency of pressing is increased by over 70% (procedure III) in relation to pulp pressed directly after milling. Before the second pressing marc, according to procedure II and procedure III, was frozen and then defrosted before pressing. The efficiency of pressing juice from marc which was not frozen was previously just 5.6%, whereas from frozen marc and defrosted before pressing the efficiency of pressing was at the level of 59.4% (procedure II) and 36.7% (procedure III) (Fig. 3). In this case the efficiency was defined as the mass of juice in relation to the mass of marc after the first pressing. In the next diagram the overall efficiency of pressing for three applied research procedures is presented (Fig. 4). The highest efficiency of pressing was achieved for the process conducted according to procedure III. In this case the efficiency of pressing is higher by 11% in relation to the efficiency which is achieved according to procedure II and by 95% in relation to the efficiency achieved according to procedure III. The analysis of quality parameters of juice expressed by the assessment of juice pH value and the content of extract did not show any significant differences related to the manner of achieving the juice. The content of extract expressed on the Brix scale was from 9.53 to 9.97, whereas pH values of juice were within the range from 5.62 to 5.93 Table 1).

Table 1. Parametry jakościowe soku

Lp.	Procedure	Content of extract [°Brix]	Value pH
1	Procedure I	9,97±0,22a	5,62a±0,14
2	Procedure II	9,78±0,21ab	5,72±0,17a
3	Procedure III	9,53±0,18b	5,93±0,16a

The same letters in columns indicate that non-significant differences were obtained ($\alpha = 0{,}05$).

An important parameter for the assessment of the pressing process is its energy consumption. An essential role is played by energy input related to the initial processing of the resource before pressing. In this paper the analysis regarding energy consumption, milling and freeing the resources was omitted. From the analysis of the diagram (Fig. 5) it results that the lowest unit energy input of the first pressing was achieved for the resource which was frozen and defrosted before pressing (procedure III). During the second pressing the lowest values E_{j2} which amounted to 0.25 kJ kg^{-3} were achieved for procedure II, while for marc which was not frozen (procedure I) the value of unit energy input E_{j2} was 3.61 kJ kg^{-3} (Fig. 6). Taking into account both stages of pressing, the lowest value of unit energy input was achieved for procedure II – E_{jc} where the value was 3.61 kJ kg^{-3} (Fig.7).

The process of pressing juice from beetroot executed according to procedure II is characterised by high efficiency and at the same time low energy input as compared to the remaining procedures. However, in the technologi-

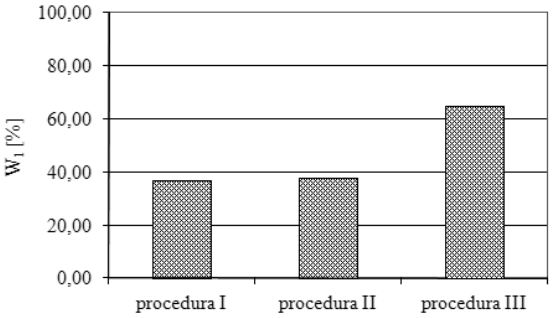

Fig. 2. Yield of juice W_1 during the first pressing in relation to the applied research procedure

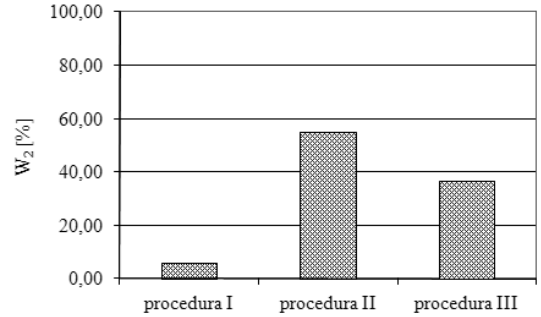

Fig. 3. Yield of juice W_2 during the second pressing in relation to the applied research procedure

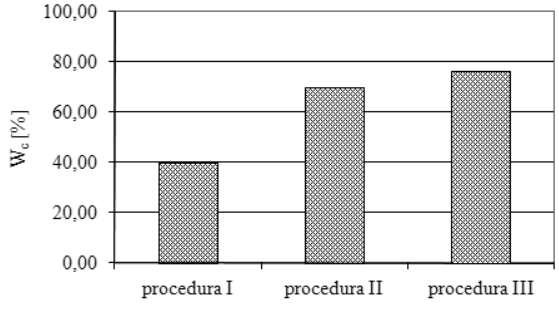

Fig. 4. Overall yield of juice W_c in relation to the applied research procedure

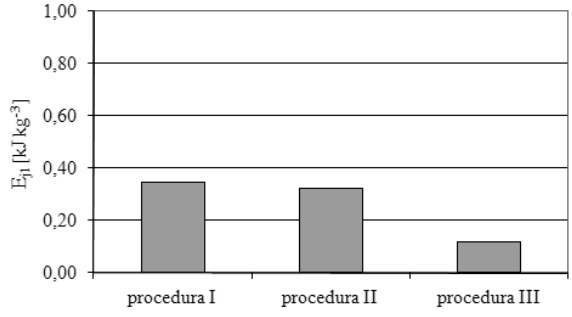

Fig. 5. Unit energy input E_{j1} during the first pressing in relation to the applied research procedure

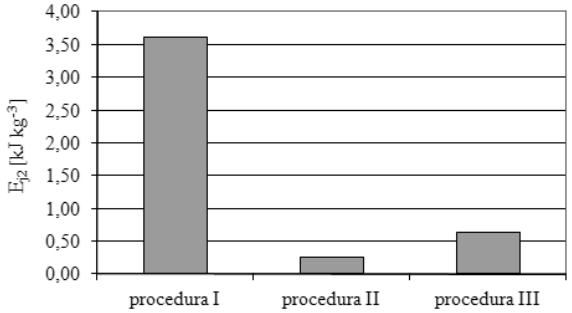

Fig. 6. Unit energy input E_{j2} during the second pressing in relation to the applied research procedure

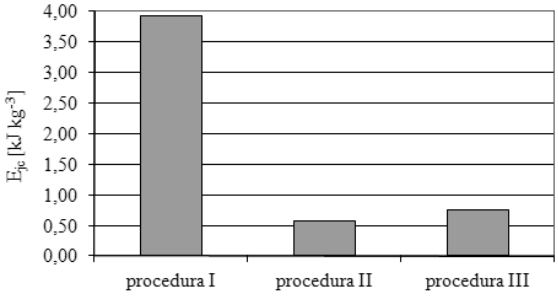

Fig. 7. Summary unit energy input E_{jc} of pressing in relation to the applied research procedure

cal process there exists an energy-consuming process of freezing marc, but taking into account the health aspect, procedure II may be recommended as a method for achieving juices with pro-health properties.

CONCLUSIONS

The conducted research allows for the formulation of the following conclusions:

1. Applied thermal processing increases the yield of beetroot juice. The highest efficiency of the process was achieved by pressing juice according to research procedure III. In this case there occurred a growth of yield by approx. 95% as compared to research procedure I.
2. Summary unit energy input are the lowest for pressing conducted according to research procedures II and III. Energy consumption of pressing beetroot juice drops almost seven times for method II as compared to procedure I.
3. No statistically significant differences in the content of the extract in the achieved juice with the use of different procedures were recorded. Also, no statistically significant differences in the pH value of the juice were recorded.
4. The conducted tests indicate the underlying sense for further research of the influence of the freezing process as the initial processing before pressing, especially having in mind the assessment of pro-health properties of the achieved beetroot juice.

REFERENCES

1. **Biegańska-Marecik R., Czapki J., Błaszczyk P. 2007.** Określenie wpływu odmiany i procesu technologicznego na występowanie smaku gorzkiego w buraku ćwikłowym. Żywność. Nauka. Technologia. Jakość 3(52): p. 62-70.
2. **Cierkoń K., Tendaj M. 2001.** Burak ćwikłowy - uprawa polowa. Hasło Ogrodnicze 6: p. 52-54.
3. **Dróżdż B. 2010** Energy analysis in oilseed processing industry. TEKA Kom. Mot. Energ. Roln., X: p. 47-58.
4. **Gerard K. A. Roberts J. S. 2004.** Microwave heating of apple mash to improve juice yield and quality. Lebensm.-Wiss u.-Technol. 37, p. 551-557.
5. **Innings F., Snah E. I. 1998.** Effect of pulsed electric fields on apple juice yield. Fruit Process 8(10), p. 412-416.
6. **Jaworowska G. Olczak A. 2010.** Napoje bezalkoholowe – nowe tendencje w produkcji. Przemysł Spożywczy 64: p. 36-39.
7. **Lebovka N. I., Praproscic I., Vorobiev E. 2003.** Enhanced expression of juice from soft vegetable tissues by pulsed electric fields; consolidation stages analysis. Journal of Food Engineering 59, p. 307-319.
8. **Lewicki P. 1998.** Tendencje w rozwoju technologii żywności. Przemysł Spożywczy 9, p. 31-35.
9. **Lewicki Piotr P., Lenart A, Mazur M. 1989.** Energochłonność pozyskiwania moszczu jabłkowego w prasach koszowych. Zeszyty Problemowe Postępów Nauk Rolniczych 355, p. 95-99.
10. **Lima M., Sastry S. 1999** The effects of ohmic heating frequency hot air drying rate and juice yield. Journal of Food Engineering 41(2), p. 115-119.
11. **Liu R. H. 2003.** Heath benefits of fruit and vegetables are from additive and synergistic combinations of phytochemical. Am. J. Clin. Nutr. 78: p. 517-520.
12. **Lubecka I., Pogorzelski E. 2006.** Wpływ procesu technologicznego na stężenia związków mineralnych w soku i koncentracie jabłkowym. Zeszyty Naukowe Politechniki Łódzkiej. Chemia Spożywcza i Biotechnologia 70(984): p. 43-52.
13. **Mitchel G. E., Isaacs A. R., Williams D. J., McLauchlan R., L., Nottingham S. M. 1991.** Low dose irradiation influence on yield and quality of fruit juice. J. Food Sci. 56(6), p. 1628-1631.
14. **Nadulski R. 2010.** Wpływ prędkości tłoka i stopnia rozdrobnienia surowca na wydajność i energochłonność tłoczenia miazg warzywnych. Zeszyty Problemowe Postępów Nauk Rolniczych 546: p. 237-243.
15. **Nadulski R., Wawryniuk P. 2009.** Ocena możliwości wykorzystania zamrażania jako obróbki wstępnej przed tłoczeniem miazg. Inżynieria Rolnicza 2(111): p. 123-130.
16. **Nowak D., Kidoń M, Syta M. 2008.** Ocena zmian właściwości przeciwutleniających suszy buraka ćwikłowego i selera w zależności od zastosowanych operacji jednostkowych. Żywność. Nauka. Technologia. Jakość 4(59): p. 227-235.
17. **Oszmiański J. 2002.** Technologia i analiza produktów z owoców i warzyw. Wydawnictwo Akademii Rolniczej, Wrocław, ISBN:8389189296, p. 140.
18. **Peroń S., Surma W. Gryszkin A. 2010.** Wpływ zawartości ekstraktu na wybrane cechy fizyczne soku

z buraków ćwikłowych oraz efektywność jego suszenia. Inżynieria Rolnicza 2(120): p. 103-109.
19. **Pierzynowska J., Prędka A., Drywień M., Ostrowska K. 2007.** Porównanie zawartości witaminy C w wybranych świeżych i przefermentowanych sokach warzywnych. Bromat. Chem. Toksykol. XL(4): p. 341-344.
20. **Płocharski W., Banaszczyk J. 1990.** Laboratory method for estimation of juice yield of apples. Fruit Science Reports Skierniewice. 1, p. 29-31.
21. PN-90/A-75101/02. Przetwory owocowe i warzywne. Przygotowanie próbek i metody badań fizykochemicznych. Oznaczanie zawartości ekstraktu ogólnego.
22. PN-EN 1132:1999. Soki owocowe i warzywne. Oznaczanie pH.
23. **Rimm E. B. Ascherio A., Giovannuci E. 1996.** Vegetable, fruit and cereal fiber intake and risk of coronary heart disease among men. Journal of American Medical Association 275: p. 447-451.
24. **Wang W-C., Sastry S. K. 2004.** Effects of moderate electrothermal treatments on juice yield from cellular tissue. Innovative Food Science and Emerging Technologies 3, p. 371–377.
25. **Wcisło G. 2006.** Application of the cold stamping method for rapeseed oil extraction. TEKA Kom. Mot. Energ. Roln. 6, p. 175-181.

WPŁYW OBRÓBKI CIEPLNEJ NA PRZEBIEG PROCESU TŁOCZENIA SOKU Z BURAKÓW ĆWIKŁOWYCH

S t r e s z c z e n i e. W pracy określono wpływ obróbki cieplnej na proces tłoczenia soku z buraków ćwikłowych. Badania realizowano z wykorzystaniem trzech procedur pozyskiwania soku. Otrzymane wyniki wskazują, że zastosowana obróbka cieplna polegająca na zamrażaniu i tłoczeniu po rozmrożeniu surowca przyczynia się do zwiększenia wydajności procesu. Równocześnie nie stwierdzono statystycznie istotnych różnic zawartości ekstraktu i wartości pH soku otrzymanego przy pomocy stosowanych procedur.

S ł o w a k l u c z o w e: burak ćwikłowy, miazga, sok, tłoczenie, zamrażanie.

TEKA. COMMISSION OF MOTORIZATION AND ENERGETICS IN AGRICULTURE – 2012, Vol. 12, No. 1, 169–173

Analysis of higher harmonics generation by non-linear loads

Krzysztof Nęcka

Department of Power Engineering and Agricultural Processes Automation, Agricultural University of Cracow
Balicka Str. 116B, 30-149 Kraków, Poland, e-mail: krzysztof.necka@ur.krakow.pl

S u m m a r y. This paper presents the recorded oscillograms of the commonly used current and voltage supplying non-linear loads. Contribution of individual higher harmonics (up to and including the 15th component) of the current supplying household and production equipment and their effects on the harmonics content in a low-voltage grid were analysed.

K e y w o r d s: non-linear load, rms value, distortion factor, higher harmonics.

INTRODUCTION

In recent years, due to the dynamic growth of the number and changes in the structure of used electrical loads, it has been discovered that the effects of voltage distortion in field distribution grids are becoming more and more severe [6]; Metody ograniczania …; [12]. The reason for this is an intense growth in the number of loads with power-electronic input circuits which convert AC energy into the same type of energy, but with different parameters than those of the power grid, or convert it into DC voltage and current. Such devices allow for the reduction of energy consumption but, on the other hand, introduce interference to the power grid, which distorts the voltage waveforms [1, 7].

Ideal voltage and current waveforms in AC power grids are sinusoidal in shape, changing in the function of time according to the pulsation $\omega = 2 \cdot \Pi \cdot f$, where f is the basic grid frequency, which - according to the *Connection Regulation* - should be 50 Hz ± 1% for 95% of the week time. Supplying non-linear loads causes the voltage waveforms to become a sum of waveforms with a basic frequency and with waveforms being their total multiplication.

Determining the voltage distortion level requires knowledge on the current distortion levels, which is an individual feature of a device and of the short-circuit impedance of the system as well [11].

The aim of the paper was to analyse higher harmonics in the current supplying household and production equipment and their effects on the higher harmonics content in the LV power grids.

MATERIAL AND METHODS

The objective of the study was met with own test results involving the measurement of individual higher harmonics in the current supplying individual electrical loads with the aid of the AS3-mini grid analyser. Distortion of voltage and current waveforms in a power grid supplying the loads affected was assessed based on the measurements performed in 15/0.4 kV transformer stations in rural areas of southern Poland using AS3 Plus analysers. The analysers used in the tests allowed measurement of higher harmonics up to and including the 15th component and for recording the supply current and voltage oscillograms.

RESULTS

- **Analysis of higher harmonics content in the current supplying individual electrical loads**

Most of today's household appliances, such as TVs, PCs, CFLs, etc., as well as controlled production equipment, draw a current in a non-linear manner. As shown in the oscillograms (Fig. 1), current is often drawn in the form of a short impulse in each half of the sinusoid. The household appliances tested, in contrast to production equipment, were characterised by low unit power output, 180 [W] on average. Since they often operate at the same time and there are quite a number of them, they pose considerable load to the power supply grid, drawing current which is highly distorted from the sinusoid. In

2010, in the Małopolska Province, the energy consumption in agriculture, for production purposes only, was of some 115 GWh, whereas the total demand for energy in households, including farmers' households, was 2673 GWh. As compared to the previous year, the increase observed was 1.7 and 5.2% respectively [3, 4].

Consumption of a distorted current increases its rms value (I_{RMS}) in relation to the basic frequency from a few to several per cent (Table 1). Such a high increase of the rms value of current for non-linear loads may lead to pronounced consequences on the local and global scale. It may, for example, lead to undesired activation of circuit breakers protecting given circuits and cause overheating of transformers and the entire power grid, since no effects of higher harmonics were considered in their design. Unfortunately, the effects of voltage and current distortions are usually not immediately visible. In the long run, however, they cause a significant increase of the operating cost by reducing the nominal device's lifespan.

The content of individual current harmonics introduced to the power grid by common household and production loads can be viewed based on the tests illustrated in Table 1 and 2. The values of the basic component of the drawn current (h_1) for individual loads and higher harmonic current values are shown in percentages of the basic component. The last column shows the rms value of the current drawn (I_{RMS}), which, for a linear load, equals the basic component.

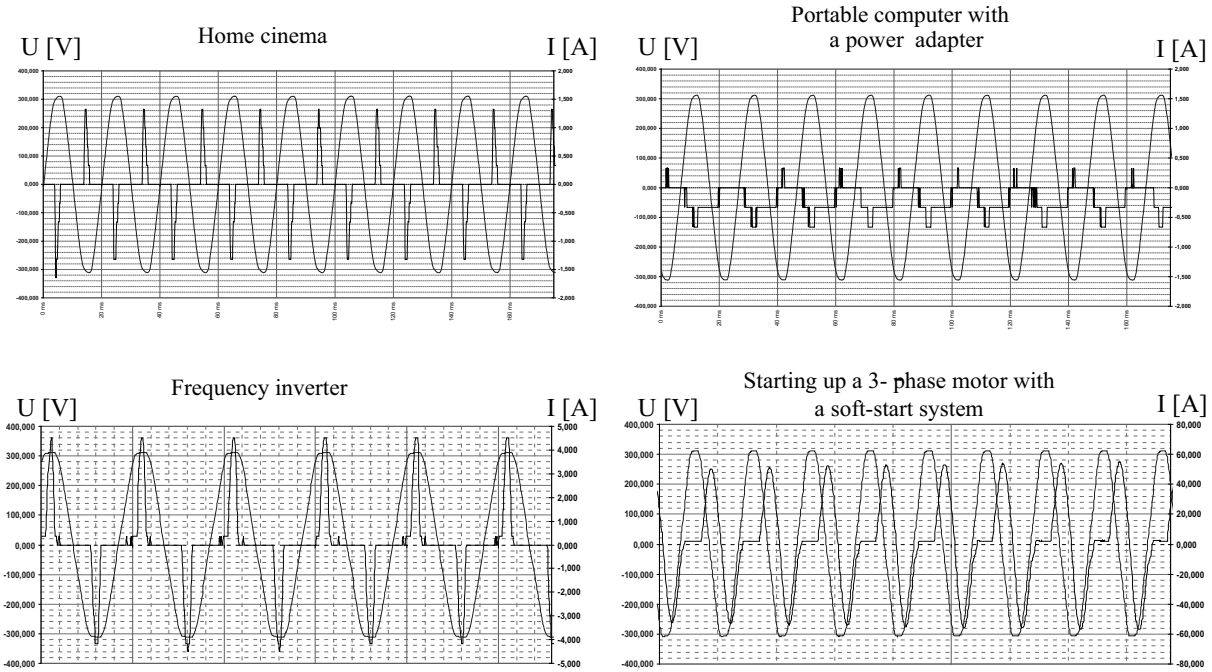

Fig. 1. Oscillograms of current and voltage supplying selected household appliances and production equipment

Table 1. Relative current values of higher odd harmonics in percentages of the basic component

Load:	Odd harmonic number								I_{RMS}[A]
	h_1 [A]	h_3	h_5	h_7	h_9	h_{11}	h_{13}	h_{15}	
		[%]							
TV	0,3	77,0	43,4	0,0	0,0	0,0	0,0	0,0	0,4
home cinema	0,2	50,0	42,4	0,0	0,0	0,0	0,0	0,0	0,3
PC	0,7	82,0	57,1	23,0	0,0	0,0	16,2	0,0	1,0
portable computer with a power adapter	0,2	83,6	66,8	54,3	0,0	0,0	0,0	0,0	0,3
microwave oven	6,0	30,2	8,0	3,8	0,3	0,0	0,0	0,0	6,3
CFLs switch on	0,1	67,2	23,2	23,2	23,2	23,2	20,0	20,0	0,2
CFLs after stabilising light flux intensity	0,2	70,4	0,0	0,0	0,0	0,0	0,0	0,0	0,2
vacuum cleaner max. rpm	4,9	14,6	0,0	0,0	0,0	0,0	0,0	0,0	5,0

vacuum cleaner min. rpm	3,1	66,4	31,8	17,7	9,4	4,2	2,2	0,0	3,9
lawn mower	4,2	8,0	4,5	0,0	0,0	0,0	0,0	0,0	4,2
manure pump	2,2	0,0	12,0	0,7	0,0	0,0	0,0	0,0	2,2
3-phase motor start up with as soft-start system	5,6	6,0	15,1	5,8	0,8	2,5	1,7	0,6	7,7
3-phase motor after the start up	6,3	0,0	10,8	0,5	0,0	0,0	0,0	0,0	6,3
start up of a 3-phase motor with an inverter	1,1	83,5	65,7	44,7	22,2	0,0	11,1	20,5	1,7

Table 2. Relative values of a current of higher even harmonics in percentages of the basic component

Load:	Even harmonic number						
	h_2[%]	h_4[%]	h_6[%]	h_8[%]	h_{10}[%]	h_{12}[%]	h_{14}[%]
microwave oven	12,4	5,6	2,8	0,0	0,0	0,0	0,0
CFLs switch on	16,2	11,1	16,2	16,2	16,2	11,1	16,2
3-phase motor start up with as soft-start system	82,8	34,3	1,9	5,2	2,7	0,0	0,0

According to the carried out tests, most of the non-linear loads draw current with higher odd harmonics while operating. The even harmonics were observed only in the current drawn by a microwave oven, and while switching on CFLs and starting up a 3-phase motor with a soft-start system reducing the starting current.

For the electrical loads tested, except for the motors, the third harmonic is dominating. The relative value of the third harmonic's current and of the basic component varied from 0% for 3-phase motors to 84% for PCs and the frequency inverter.

Currents containing the third harmonic and multiples of it are highly problematic, since they are summed arithmetically in the power grid, and they are not zeroed as for the basic component of the current and harmonics of the other order. Therefore, currents in the neutral conductor are often considerably higher than the phase currents, even by up to 170% [2].

- **Analysis of higher harmonics content in transformer stations supplying rural subscribers**

A commonly adopted measure of voltage and current distortion time waveforms in power grids is the value of the THD factor (total harmonic distortion), which determines the relative value of the current or voltage of higher harmonics according to the formula:

for voltage: for current:

$$THDU = \frac{\sqrt{\sum_{h=2}^{n} U_h^2}}{U_1}, \qquad THDI = \frac{\sqrt{\sum_{h=2}^{n} I_h^2}}{I_1}, \qquad (1)$$

where:

U_h, (I_h) – rms value of the h[th] voltage (current) harmonic,

U_1, (I_1) – rms value of the 1[st] voltage (current) harmonic.

Pursuant to the valid *Regulation of the Minister of Economy and Labour* [Dz. U. z 2005 r., nr 2, poz. 6], the THD factor of supply voltage THDU, including higher harmonics up to 40, should be less or equal 8%. The admissible levels of individual harmonics fall within the range from 1.5 to 6% [8, 9].

Standards for the maximum levels of current harmonics are determined by the *American Institute of Electrical and Electronic Engineers, IEEE – 519 - 1992* [5]. Those requirements are currently not applicable in Poland, but according to Szymański [11], future technical standards will be based on them. According to the IEEE 519 standard, the maximum level of THDI distortion factor for current drawn by the loads depends on the product of the short-circuit current I_{zw} of the supply system and the load current I_{obc} and should not exceed the values given in Table 3. The requirements apply to the values of the following harmonics, up to the order of 11.

Table 3. Maximum values of odd harmonics in a current according to IEEE-519

I_{zw}/I_{obc}	<20	20...50	50...100	100...1000	>1000
THDI dla n<11	4%	7%	10%	12%	15%

Distributions of the observed relative values of the current and voltage of individual harmonics as a percentage of the basic component in the transformer stations tested in rural areas of the Małopolska Province are shown in box plot graphs - Figures 2 and 3. They are drawn based on conventional measures of distribution locations. A box height is restricted by a confidence interval for the average distribution, and its branches show the scatter of the values observed. Inside a box, a line is marked which indicates the average value of individual higher harmonics.

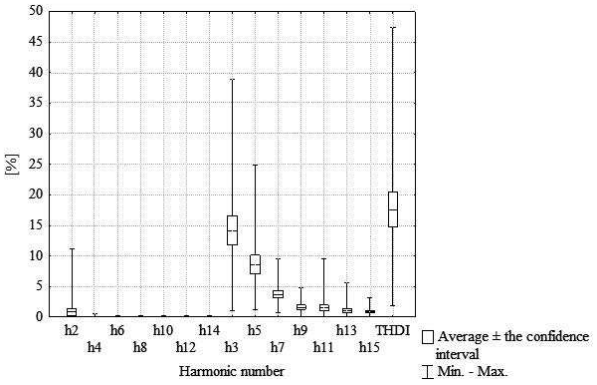

Fig. 2. Box plots showing distributions of relative current values of individual harmonics as a percentage of the basic component

In the transformer stations tested (Fig. 2), a dominating share of odd harmonics was found. The highest level was recorded for harmonics 3 and 5, the average values of which were 14.2 and 8.6% respectively. The total harmonics content ratio in the current was 17.6% on average, varying from 1.8 to 47.4%. According to the analysis performed, it may be impossible to meet the requirements of IEEE-519 in rural transformer stations without using active filters or other equally expensive systems for compensation of distorted power.

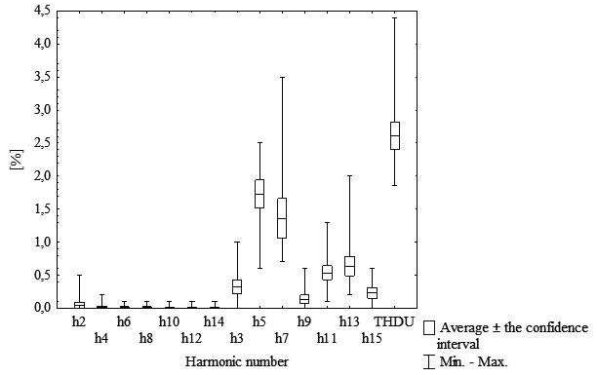

Fig. 3. Box plots showing distributions of relative voltage values of individual harmonics as a percentage of the basic component

In the objects tested, the THDU factor (Fig. 3) varied from 1.9 to 4.4% without exceeding the level of 8% allowed by law. However, there are still fears that, in the nearest future, supply voltage distortions, mainly in rural areas, may become a serious problem. Non-linear loads being a source of higher harmonics are commonly used both in households and production facilities. Furthermore, many farms are planning to purchase them in the days to come [Pabiańczyk 2010].

CONCLUSIONS

Non-linear loads commonly used in households draw current with a basic frequency and with frequencies being its total multiple, compromising the quality of electrical energy in the LV power grid. For the loads studied, the third harmonic was observed to have a dominating role, with the peak value exceeding 80% of the basic component. Also, the occurrence of a fifth harmonic of 67% was specific for them.

The increasing popularity of production facilities with power electronic input circuits is also the cause of generating higher harmonics in the current drawn from the power grid. Drawing current with non-sinusoidal waveforms distorts the supply voltage. Its value is currently at the level below 5% - not exceeding the limit value.

Since the number of loads with power electronic input circuits increases rapidly, the necessity to compensate current distortions may not be excluded. It is a very expensive undertaking, particularly in rural LV systems with considerable scattering of the distorting loads.

REFERENCES

1. **Baranecki A., Niewiadomski M., Płatek T. 2004.** Odbiorniki nieliniowe – problemy i zagrożenia. Wiadomości Elektrotechniczne. Nr 3. p. 24-26.
2. **Desmet J., Baggini A. 2003.** Dobór przekroju przewodów neutralnych w instalacjach o wysokiej zawartości harmonicznych. [online]. [dostęp 15–06–2010]. Dostępny w Internecie:http://www.bttautomatyka.pl/~lm/ssdservice/elektrotechnika/harmoniczne/kable_i_harmoniczne.pdf.
3. GUS 2010. Zużycie paliw i nośników energii w 2009 r. Główny Urząd Statystyczny. Warszawa.
4. GUS 2011. Zużycie paliw i nośników energii w 2010 r. Główny Urząd Statystyczny. Warszawa.
5. IEEE Standard 519-1992. 1993. Recommended Practices and Requirements for Harmonic Control in Electrical Power Systems. The Institute of Electrical and Electronics Engineers.
6. **Ludwinek, K., Siedlarz, A. 2011.** Analiza zawartości wyższych harmonicznych w prądach i napięciach maszyny elektrycznej współpracującej z siecią zasilającą. Pomiary, Automatyka, Robotyka R. 15. Nr 7-8. p. 60-69.
7. **Malska W., Łatka M. 2007.** Wpływ odbiorników nieliniowych na parametry jakości energii elektrycznej. Wiadomości Elektrotechniczne. Nr 10. p. 12-14.
8. Metody ograniczania wpływu wyższych harmonicznych. Rozwiązania Danfoss Drives [online]. [dostęp 4–04–2012]. Dostępny w Internecie: http://www.danfoss.com/NR/rdonlyres/C7869CC4-6719-45E9-8B69-AB27B43B7A6A/0/L_Web_Harmonics_DKDDPB41A149.pdf.
9. **Pabiańczyk J. 2010.** Świetlówki kompaktowe – co dalej? Spektrum. Nr 1-2. p. 17-20.
10. Rozporządzenie Ministra Gospodarki z dnia 20 grudnia 2004 r. w sprawie szczegółowych warunków przyłączenia podmiotów do sieci elektroenergetycznych, ruchu sieciowego i eksploatacji sieci oraz standardów jakościowych obsługi odbiorców. Dz.U. z 2005 r. nr 2, poz. 5 i 6.
11. **Szymański J. 2003.** Harmoniczne prądu wytwarzane przez prostowniki wejściowe przemienników

częstotliwości. Prace Naukowe. Politechnika Radomska. Elektryka. Nr 1(6).

12. **Trojanowska M., Nęcka K. 2007.** Analiza jakości napięcia zasilającego gospodarstwa wiejskie. Inżynieria Rolnicza. Nr 7 (95). p. 221-227.

ANALIZA WYTWARZANIA WYŻSZYCH HARMONICZNYCH PRZEZ ODBIORNIKI NIELINIOWE

S t r e s z c z e n i e . W pracy przedstawiono zarejestrowane oscylogramy prądu i napięcia zasilającego powszechnie stosowane odbiorniki nieliniowe. Dokonano analizy udziału poszczególnych wyższych harmonicznych (do 15-stej składowej włącznie) w prądzie zasilającym odbiorniki gospodarstwa domowego i produkcyjnego, oraz ich oddziaływania na zawartość harmonicznych w sieci elektroenergetycznej niskiego napięcia.

S ł o w a k l u c z o w e : odbiornik nieliniowy, wartość skuteczna, współczynnik odkształcenia, wyższe harmoniczne.

TEKA. COMMISSION OF MOTORIZATION AND ENERGETICS IN AGRICULTURE – 2012, Vol. 12, No. 1, 175–180

Biodegradation of TPS mouldings enriched with natural fillers

Tomasz Oniszczuk[1], Agnieszka Wójtowicz[1], Marcin Mitrus[1], Leszek Mościcki[1], Maciej Combrzyński[1], Andrzej Rejak[1], Bożena Gładyszewska[2]

Department of Food Process Engineering[1], Department of Physics[2], Lublin University of Life Sciences
Doświadczalna 44, 20-236 Lublin, Poland; e-mail: tomasz.oniszczuk@up.lublin.pl

Summary. The aim of the present study was to investigate the biodegradation of thermoplastic starch (TPS) mouldings in the soil. Samples, produced from mixtures of potato starch, glycerin and added fillers (natural fibers) were obtained in two steps: TPS granules by extrusion-cooking, than the extrudates were processed by injecting moulding technique to get mouldings. The varied weight loss of mouldings was observed during storage, depending the time of storage and raw materials composition. Those collected after 12 weeks of storage in the soil had the highest weight loss. It was noticed that the increased addition of glycerol in the mouldings had an effect on the higher degradation rate. To the contrary, the addition of fillers to the mouldings' composition, especially flax fibers, slowed down the process.

Key words: thermoplastic starch, extrusion-cooking, biodegradation, natural fibers.

INTRODUCTION

Extrusion-cooking, popular in food processing, causes the destruction of starch and leads to its thermoplastic nature. Mixing and processing of starch with other components allows to form new materials – thermoplastic starch (TPS) used in packaging sector [6, 8, 17, 19, 20, 21].

TPS can be used as stand-alone packaging material or as an additive that improves the degradation of plastics. Its application is possible due to the relatively short time of degradation to CO_2 and water. Biocomposites that are enriched with starch are mainly used in making films, containers, and in the production of foams used for filling of empty space contained in the packs [10, 14].

Packaging materials made from thermoplastic starch can be produced by two methods: single- and two-stage. A single-stage method involves prior formation of the components mixture and its application to the devices producing the packaging material. An example of such a device is an extruder, the universal machine widely used in plastic film production. A single-stage method is also used in the production of the mentioned before foams and fillers [5, 12, 13, 15].

In the case of two-stage method of production, the first step consists the production of TPS pellets – half-products processed by extrusion-cooking [11, 16]. The second stage is the production of packaging material, which can be performed with conventional equipment used in plastic processing, including film-blowing extruders and injection moulding machines.

MATERIALS AND METHODS

MATERIALS

The basic raw material was potato starch type Superior produced by AVEBE b.v. (NL), mixed with a technical glycerol of 99% purity produced by Odczynniki Chemiczne-Lublin (PL) – the plasticizer, and cellulose fibers vivapur type 102 (JRS GmbH, D) and flax fibers (Polish rural producers) – as the fillers.

PREPARATION OF MIXTURES

All ingredients were mixed using a laboratory ribbon mixer. The effective mixing time of 20 minutes was set after repeated attempts. The share of glycerol was 20%, 22% and 25% by the weight in the mixture, whereas the contribution of fibers in the prepared mixtures was 5% and 10%. After mixing, samples were left in sealed plastic bags for 24 hours in order to maintain the homogenous mixture. Immediately before the extrusion the blends were mixed once again for 10 minutes, which guaranteed getting looser structure of the mixture.

EXTRUSION-COOKING

TPS granules enriched with natural fibers were produced using a modified single screw extrusion-cooker type TS-45 (ZMCh Metalchem, PL) with L/D = 18/1, equipped with an additional cooling section of the barrel and a forming die with a hole diameter of 3 mm. Extrusion-cooking process temperature was set at the range from 60°C to 110°C and maintained appropriately adjusting the intensity of the flow of cooling liquid [1, 2, 3, 4].

HIGH-PRESSURE INJECTION MOULDING

The high-pressure injection moulding machine ARBURG 220H90-350 type, L/D=20.5 was used. The injection speed was maintained at (70-90) mm/s, the injection time: 5 sec., the process temperature ranged from 100° C to 180°C. Since the injection-moulded samples were used in the production, it gave the basic matrix in the form of 'shoulders', useful in the subsequent run-time tests of mechanical properties of moulded samples and their biodegradability. For biodegradability tests mouldings processed at 160°C were selected.

ASSESSMENT OF BIODEGRADABILITY TEST

The mouldings prepared with a moisture content of about 4% were placed in special baskets and stored in plastic boxes covered with 15 cm layer of garden soil with a moisture content of 70% and pH 6.5 for 2, 4, 8 and 12 weeks [18]. In order to ensure constant initial soil moisture, the content of soil and the process of water loss were determined twice a week (Fig. 1, 2).

The boxes with samples were kept in autumn in an unheated room at constant humidity at 15°C. Afterwards, mouldings were cleaned, weighed and dried to a moisture content of 4%. The determination of mass loss was carried out in the final stage of storage intervals [7, 9].

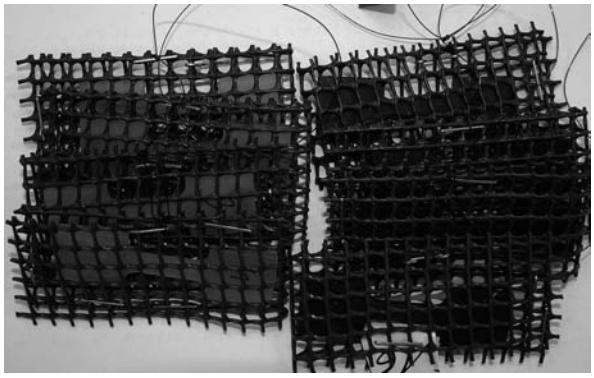

Fig. 1. The mouldings placed in the boxes with soil

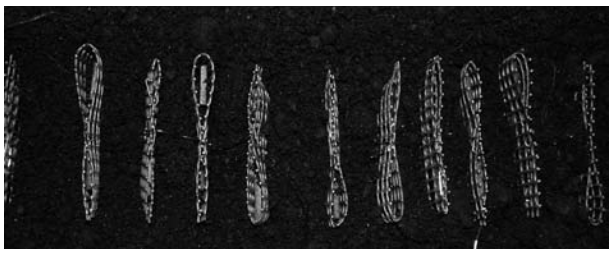

Fig. 2. The distribution of samples in the boxes to the ground

RESULTS

The highest weight loss was observed after 12 weeks storage period for the whole range of the investigated samples. The results of the weight loss in mouldings containing 20% of glycerol and the addition of flax fibers are shown in Figure 3.

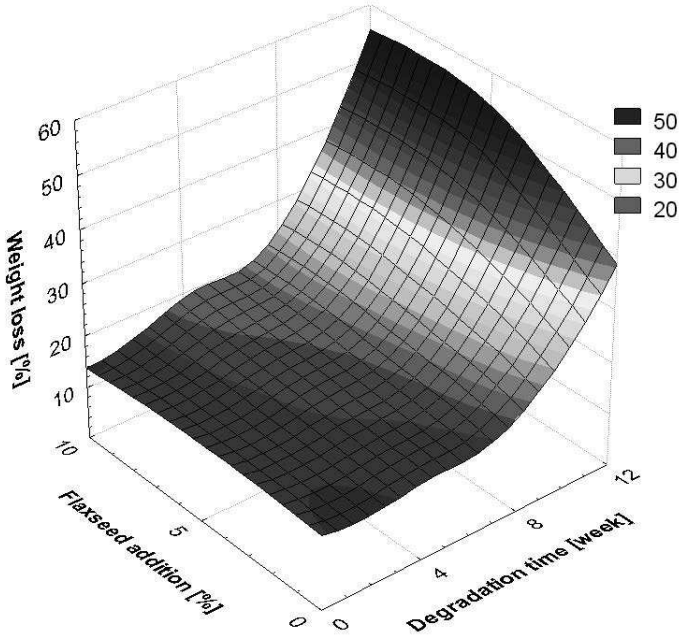

Fig. 3. The influence of storage time and the amount of flax fibers on the weight loss of the mouldings containing 20% of glycerol

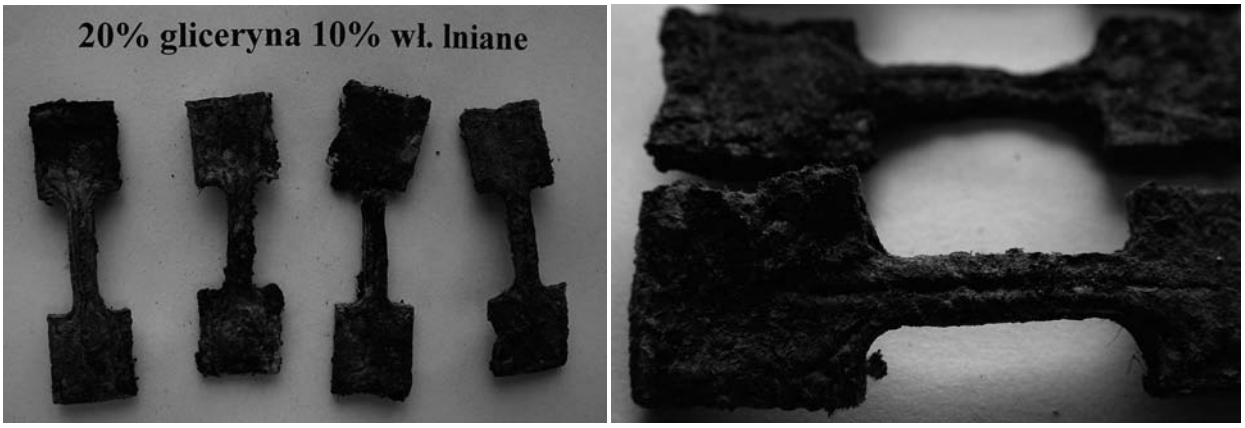

Fig. 4. Samples with flax fibers after 12 weeks of storage

For all the samples after the first two weeks of storage, the recorded weight loss ranged from about 13% (for the samples containing 20% of glycerol) to approximately 23% (for the samples containing 25% of glycerol).

In the case of starchy samples without natural fibers, stored for 12 weeks, a greater weight loss at a higher content of glycerol in the formulation of granulates was observed. Moreover, the moulding's surface underwent decomposition faster in contact with moist soil than in its inner layer (the moulding's core).

The addition of flax fibers influenced the degree of biodegradation. It was observed with the increase of the flax fibers content in the blend an increase in the weight loss of tested mouldings.

The highest weight loss, which reached about 56%, was observed in samples containing 10% of flax fibers after 12 weeks of storage. The samples processed without the addition of flax fibers characterized smaller weight loss, which was about 40% after 12 weeks (Fig. 4).The increase in the amount of plasticizer in the samples (22% and 25% of glycerol) increased the rate of biodegradation during the first 8 weeks of the experiment (Fig. 5, 6).

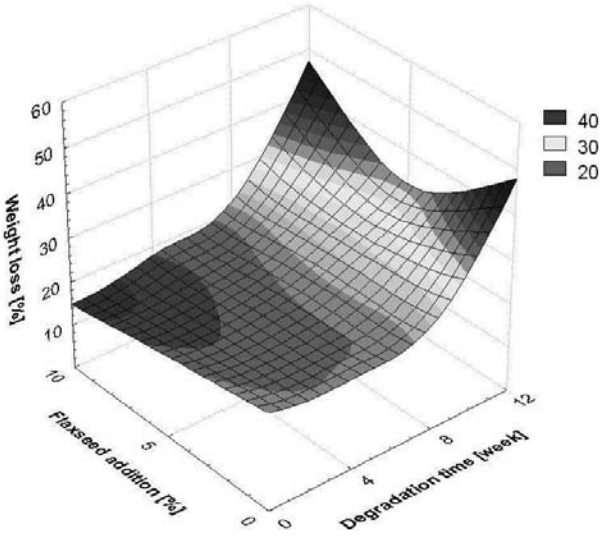

Fig. 5. The influence of storage time and the amount of flax fibers on the weight loss of the mouldings containing 22% of glycerol

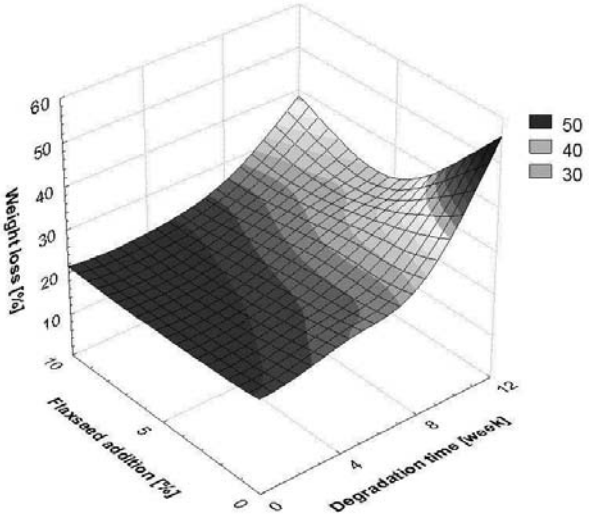

Fig. 6. The influence of storage time and the amount of flax fibers on the weight loss of the moulding 25% of glycerol

Weight losses of samples were greater than in the mouldings made from granulates containing 20% of glycerol. Mouldings with 22% of glycerol and 5% of flax fibers indicated the smallest weight losses during storage, reaching about 32% after 12 weeks (Fig. 5). The increase in the content of fibers from 5% to 10% in samples caused the increase in the weight loss by approximately 16%.

Samples made of granulate containing cellulose fibers of 5% and 10%, as well as those with the addition of 20% of glycerol, indicated similar properties to the samples containing flax fibers (Fig. 7).

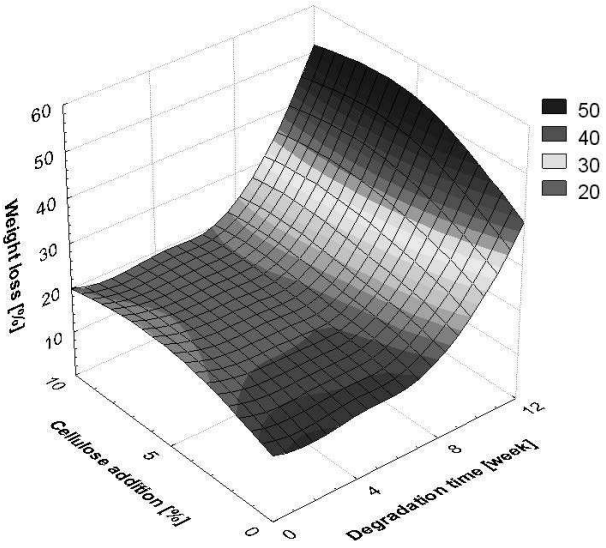

Fig. 7. The influence of storage time and the amount of cellulose fibers on the weight loss of the mouldings containing 20% of glycerol

The addition of cellulose fibers influenced their biodegradation process. As it was observed, the increase of cellulose fibers in the blend resulted in the increase in the weight loss. The highest weight loss, which ranged from about 51% - 53%, was observed for the mouldings containing 5% and 10% of cellulose fibers after 12 weeks of storage (Fig. 8).

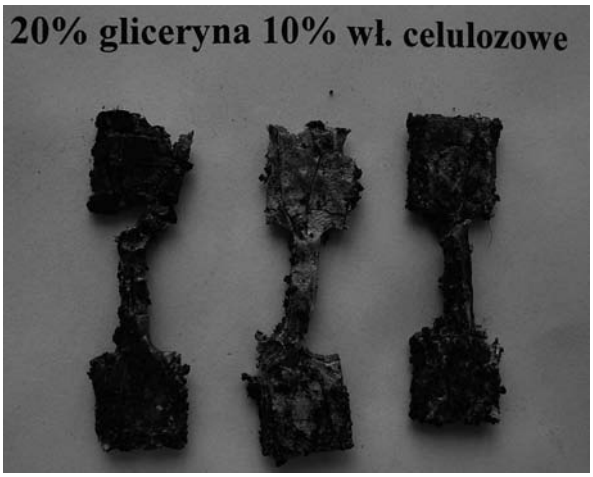

Fig. 8. Samples with cellulose fibers after 12 weeks of storage

Figure 9 presents a similar tendency, where the weight loss for tested samples produced from granulates containing cellulose fibers is similar to the weight loss for those containing flax fibers.

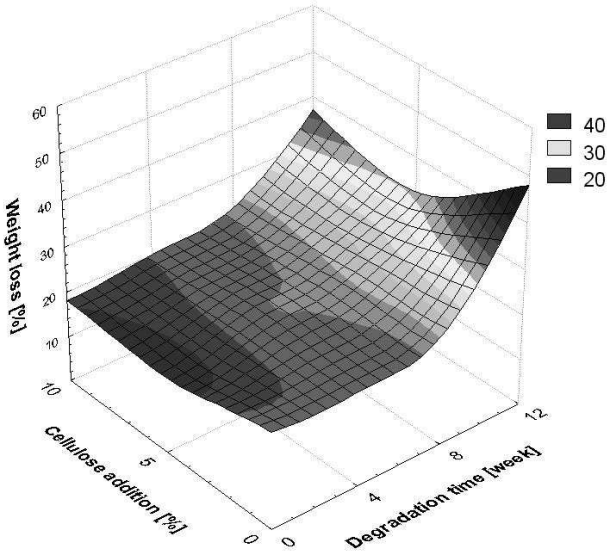

Fig. 9. The influence of storage time and the amount of cellulose fibers on the weight loss of the mouldings containing 22% of glycerol

Within the course of the experiment it was proved that the mouldings containing cellulose fibers displayed the same quality as those with flax fibers. Numerous cracks and groves which occurred on the surface of compacts as the result of consecutive biodegradation were observed (Fig. 10).

Figure 11 presents the influence of storage time and amount of cellulose fibers on the weight loss of the mouldings.

The highest weight loss was observed for the samples made of granulate containing 25% of plasticizer without the addition of fibers. After 12 weeks the weight loss was about 57%. The addition of cellulose fibers resulted in the decrease of weight loss in comparison to the samples produced without fibers.

Samples prepared without the addition of fibers and those containing cellulose were fragile and prone to cracking during storage according to the weight loss. Samples containing flax fibers displayed good resistance to the damage.

Fig. 10. The mouldings containing flax (a) and cellulose (b) fibers after 2 weeks storage time

CONCLUSIONS

It was indicated that the weight losses were higher with the increase of glycerol content in the mouldings. The highest weight loss (ca. 57%) was observed in the samples with 25% of glycerol.

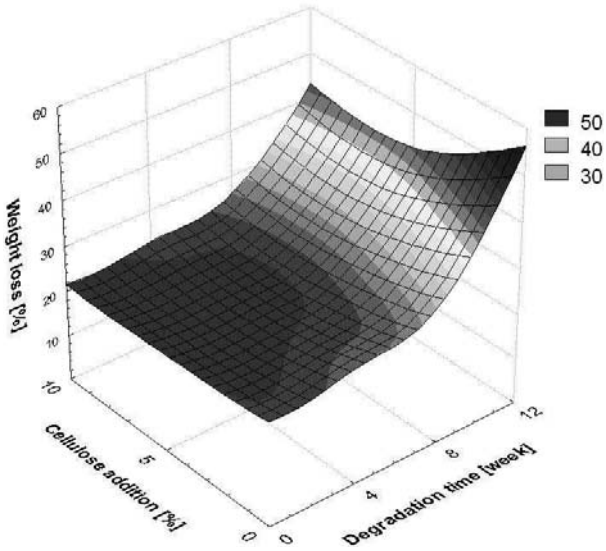

Fig. 11. The influence of storage time and the amount of cellulose fibers on the weight loss of mouldings containing 25% of glycerol

The increase in the content of flax fibers slowed down the process of decomposition in the first two weeks of storage. Numerous changes visible on the surface of mouldings in the early stage of storage (cracks, grooves, etc.) are considered to be the result of the consecutive biodegradation process.

The addition of flax and cellulose fibers resulted in quicker biodegradation process in soil, which was observed in the final stage of storing (after 12 weeks).

ACKNOWLEDGEMENTS

This scientific work was supported by Polish Ministry of Science and Higher Education founds on science in the year 2010-2012 as research project NN 313 275738

REFERENCES

1. **Averous L., Moro L., Dole P., Fringant C. 2000.** Properties of thermoplastic blends: starch – polycaprolactone, Polymer, 41, p. 4157.
2. **Bledzki A.K., Gassan J. 1999.** Composites reinforced with cellulose based fibres, Prog. Polymer Science, 24, p. 221.
3. **Bogracheva T.Y., Wang Y.L., Wang T.L., Hedley C.L. 2002.** Structural studies of starch with different water contents, Biopolymers, 64, p. 268.
4. **Brittritto M.M., Bell J.P., Brinkle G.M., Huang S.J., Knox J.R. 1979.** Synthesis and biodegradation of polymers derived from hydroxyacids, Journal of Ap-

plied Polymer Science, Applied Polymer Symposium, 35, p. 405.
5. **Dyadychev V., Pugacheva H., Kildeychik A. 2010.** Co-injection molding as one of the most popular injection molding Technologies for manufacture of polymeric details from secondary raw materials, TEKA Commision of motorization and Power Industry in Agriculture, PAN, Volume Xc, p. 57-62.
6. **Janssen L.P.B.M., Moscicki L. (Eds) 2008.** Thermoplastic Starch, Wiley-VCH Verlag GmbH & Co. KGaA, Weinheim, p. 1-29.
7. **Kikolski P., Dłuska-Smolik E., Bolińska A. 2005.** Metodyka oceny biodegradowalności polimerów opakowaniowych w badaniu ich przydatności do odzysku organicznego w wyniku kompostowania, Polimey, 3.
8. **Kowalczuk M.M. 2009.** Prace badawcze nad polimerami biodegradowalnymi. opakowanie, 9, p. 46-48.
9. **Łabużek S., Pająk J., Nowak B. 2005.** Biodegradacja modyfikowanego polietylenu w warunkach laboratoryjnych, Polimery, 9, p. 675.
10. **Mitrus M. 2012.** Starch Protective Loose-Fill Foams, Thermoplastic elastomer. InTech, Rijeka, p. 79-95.
11. **Mitrus M. 2007.** Badania właściwości mechanicznych skrobi termoplastycznej, Acta Agrophysica, 9(2), p. 423-430.
12. **Mitrus M. 2006.** Investigations of thermoplastic starch extrusion cooking process stability, TEKA Commission of motorization and Power Industry in Agriculture PAN, Volume VIa, p. 138-144.
13. **Mitrus M. 2004.** Wpływ obróbki barotermicznej na zmiany właściwości fizycznych biodegradowalnych biopolimerów skrobiowych, PhD Thesis, UP Lublin.
14. **Mitrus M., Mościcki L. 2009.** Physical properties of thermoplastic starches, Int. Agrophysics, 23, p. 305-308.
15. **Mitrus M., Oniszczuk T. 2007.** Wpływ obróbki ciśnieniowo – termicznej na właściwości mechaniczne skrobi termoplastycznej, Właściwości geometryczne, mechaniczne i strukturalne surowców i produktów spożywczych, Wyd. Nauk. FRNA, Lublin, p. 149-150.
16. **Moscicki L. (Ed) 2011.** Extrusion-Cooking Techniques, Wiley-VCH Verlag GmbH & Co. KGaA, Weinheim, p. 177-188.
17. **Mościcki L., Mitrus M., Wójtowicz A. 2007.** Technika ekstruzji w przemyśle rolno – spożywczym, PWRiL, Warszawa.
18. **Oniszczuk T. 2006.** Wpływ parametrów procesu wtryskiwania na właściwości fizyczne skrobiowych materiałów opakowaniowych, PhD Thesis, UP Lublin.
19. **Sobczak P. 2006.** Sorbitol addition on extrusion process, TEKA Commission of Motorization and Power Industry in Agriculture PAN, Volume VIa, p. 163-169.
20. **Thomas D.J., Atwell W.A. 1997.** Starch Analysis Methods. In: Starches. Eagan Press, St. Paul, Minnesota, p. 13-18.
21. **Żakowska H. 2003.** Opakowania biodegradowalne, Centralny Ośrodek Badawczo-Rozwojowy Opakowań, Warszawa, p. 20-65.

BIODEGRADACJA WYPRASEK SKROBI TERMOPLASTYCZNEJ WZBOGACONYCH NATURALNYMI WYPEŁNIACZAMI

Streszczenie. Badaniom poddano formy sztywne w postaci wyprasek wytworzonych ze skrobi termoplastycznej (TPS). Granulaty zostały wyprodukowane z mieszanek skrobi ziemniaczanej, gliceryny oraz dodatku wypełniaczy w postaci włókien naturalnych. Następnie formy sztywne w postaci wyprasek wytworzono metodą wtrysku wysokociśnieniowego z granulatów TPS charakteryzujących się zróżnicowaną zawartością gliceryny (plastyfikatora) i włókien (substancje wzmacniające). Podczas pomiarów zaobserwowano zróżnicowany ubytek masy wyprasek zależny od czasu ich przechowywania w glebie. Po 12 tygodniach przechowywania w glebie stwierdzono najwyższy ubytek masy próbek. Zwiększenie dodatku gliceryny w wyprasce wpływało na większe tępo biodegradacji natomiast dodatek wypełniaczy szczególnie włókien lnianych proces ten spowalniał.

Słowa kluczowe: skrobia termoplastyczna, ekstruzja, biodegradacja, włókna naturalne.

TEKA. COMMISSION OF MOTORIZATION AND ENERGETICS IN AGRICULTURE – 2012, Vol. 12, No. 1, 181–184

Influence of process conditions and fillers addition on extrusion-cooking efficiency and SME of thermoplastic potato starch

Tomasz Oniszczuk[1], Agnieszka Wójtowicz[1], Marcin Mitrus[1], Leszek Mościcki[1], Maciej Combrzyński[1], Andrzej Rejak[1], Bożena Gładyszewska[2]

Department of Food Process Engineering[1], Department of Physics[2], Lublin University of Life Sciences
Doświadczalna 44, 20-236 Lublin, Poland; e-mail: tomasz.oniszczuk @ up.lublin.pl

Summary. The aim of this paper is to present the results of the efficiency process and SME measurements during the extrusion-cooking of thermoplastic potato starch enriched with flax fibers, cellulose and ground bark.A modified single screw extrusion-cooker TS-45 with L/D = 18 and with an additional barrel cooling section was used in the experiments. The effect of the screw speed and the quantity and type of natural fillers added to the blends containing 20% of glycerol as plasticizer on the efficiency of the baro-thermal processing as well as energy consumption was the main concept of the investigation. It was proved that the increase of screw speed influences on higher process efficiency and SME values irrespective the type and amount of fillers, whereas additive level in the recipes had a slight effect on the tested characteristics.

Key words: thermoplastic starch, fillers, extrusion-cooking, energy consumption – SME.

INTRODUCTION

Thermoplastic starch (TPS) based products are fully degradable and are successfully used in agricultural, horticultural and food sector for packaging of dry foods [3, 22, 23]. The production of TPS-based products is possible with commonly known machinery and equipment used by plastic manufacturers and these products may be complementary to alternative plastics, however they do not have a wide application because of the utility of certain defects [12, 23]. In recent years large-scale studies aimed the increased share of starch in high quality starch-plastic composites. The main reasons for such modifications are environmental regulations of EU requirements for the improvement of recyclable or biodegradable packaging materials. Most of plastic wastes are resistant to degradation, due to the content of polymers which remain in the environment for a long time. TPS may be an effective additive which accelerates the degradation process by shortening polymer chains and reducing decomposition time [4, 13]. The issue of using starch of different origins (mostly maize, wheat, potato, tapioca) for the production of TPS biodegradable packaging materials is discussed in numerous scientific papers. Unfortunately, mechanical properties of TPS-based materials are weaker than conventional plastics. In order to improve their physical properties or material strength as well as the elasticity of the obtained products, various fillers should be added to raw material blends in the amount ranging from 1 to even 50%, according to the type of additives used. Flax, hemp, jute, coir, cotton fibers and wastes from wood industry seem to be most commonly applied materials.

Due to the new trends in biopolymers, the investigations of TPS processing for packaging materials using different types of starches and additives [1, 2, 5, 15] were carried out at the Department of Food Process Engineering, University of Life Sciences in Lublin.

The aim of this work was to investigate the influence of process conditions and different fillers (i.e. flax fibers, cellulose and ground bark addition) on extrusion-cooking efficiency and SME of thermoplastic potato starch.

MATERIALS AND METHODS

Potato starch produced by AVEBE b.v. (NL), mixed with 20% of glycerol of 99% purity produced by Odczynniki Chemiczne – Lublin (PL) was used as the basic raw material. The additives: cellulose fibers vivapur type 102 of JRS GmbH (D), flax fibers and ground bark (Polish rural producers) were applied in the amount ranging from 10% to 30%. Potato starch (16% of the moisture content) and the additives were mixed in laboratory ribbon mixer for 20 minutes. Next, the blends of different compositions were stored for 24 hours in plastic bags before tests [9]. The share of fibers for the prepared blends was 10%, 20% and 30% of the sample mass. The prepared samples were

again mixed for 10 minutes, prior to extrusion, which guaranteed getting loose structure of the compounds.

The study was performed using a modified single screw extrusion-cooker type TS 45 (Polish design) with L/D=18/1, equipped with an additional cooling section of the barrel and a forming die with a 3mm hole diameter. Granulates were produced using the extruder screw speed of 60 rpm, 80 rpm and 100 rpm. Extrusion-cooking process temperature was set in the range of 60°C - 110°C and maintained appropriately, adjusting the intensity of the flow of cooling liquid. The processing temperature was measured by thermocouples installed along the barrel; the results were recorded. Rotational speed of the screw was monitored using an electronic tachometer DM-223AR Wireless [9, 19, 20, 21].

The efficiency of TPS extrusion-cooking process according tothe screw speed and the addition of different types of fibers applied wasevaluated by setting the weight of TPS pellets obtained at a given time for all the mixtures according to following formula [17, 18]:

$$Q = \frac{m}{t}[kg \cdot h^{-1}], \quad (1)$$

where:

Q - process efficiency,

m – sample mass obtained during the measurement [kg],

t - measurement time [h].

Power measurement was performed using a standard wattmeter connected to the motor unit of the extruder. After consideration the motor load, screw speed and process efficiency the specific mechanical energy index (SME) according to the formula given in literature [2, 6, 7, 8, 9, 11, 14, 16] was evaluated:

$$SME = \frac{N \cdot O \cdot P}{N_m \cdot 100 \cdot Q}[kWh \cdot kg^{-1}], \quad (2)$$

where:

N - screw speed [min^{-1}],

N_m - the maximum screw speed [min^{-1}],

P - power [kW],

O - motor load [%],

Q –process efficiency [$kg \cdot h^{-1}$].

The measurements were made in six repetitions for each series of tests. Correlation coefficients were determined according to the influence of screw speed and the amount of fillers on efficiency process and SME values. Trend lines and regression equations were designated.

RESULTS

The efficiency of TPS extrusion-cooking process was directly correlatedwith the screw speed; the higher the screw speed applied, the higher the efficiency process was obtained, with correlation coefficients ranging from 0.99 for samples without the additive to 0.93 with addition of 30% cellulose fibers. The increasing content of cellulose fibers in the formulations for the sample processed at 60 rpm caused a slight increase of efficiency process (cor. coefficientof 0.82).The opposite tendencies to lower the efficiency with the increased level of cellulose fibers were observed for the screw speed of 80 and 100 rpm (-0.86 and -0.82, respectively). The highest process efficiency of 37.4 $kg \cdot h^{-1}$ was determined during the extrusion of potato TPS pellets contained 10% of cellulose fibers processed at the highest screw speed of 100 rpm (Fig. 1). The lowest efficiency (23.3 $kg \cdot h^{-1}$) was observed for blends without and with the content of 10% of cellulose fibers, processed at 60 rpm screw speed.

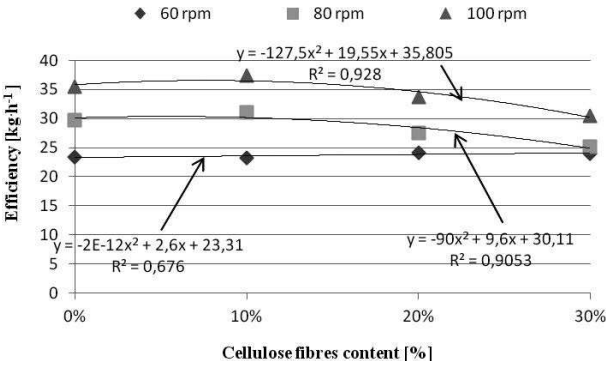

Fig. 1. Effect of screw speed and cellulose fibers content on the efficiency process of potato TPS pellets

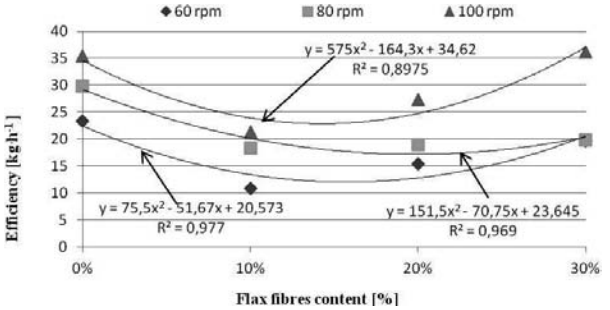

Fig. 2. The influence of the screw speed and flax fibers content on the efficiency of the extrusion-cooking of potato thermoplastic pellets

The results of process efficiency for blends with flax fibers are presented in Fig. 2. A bit similar effect was observed for samples with addition of flax fibers. The efficiency of process increased when increasing screw speed was applied (cor. coefficients ranging from 0.86 at 30% of flax fibers to 0.99 without the additive).The lowest efficiency of extruded blends was registered for the samples with the content of 10% of flax fibers.

The application of ground bark to all kinds of mixtures resulted in the decrease of efficiency of the extrusion-cooking (correlation coefficients -0.77, -0.96 and -0.83 for 60 rpm, 80 rpm and 100 rpm, respectively). Differences between trials were small and calculated to the value of 1,0 $kg \cdot h^{-1}$. The results are presented on the Fig. 3. A strong impact of screw speed applied during processing onthe process efficiencywas observed, with correlation coefficients varying from 0.99 for samples without additives to 0.95 for samples with 30% of bark.

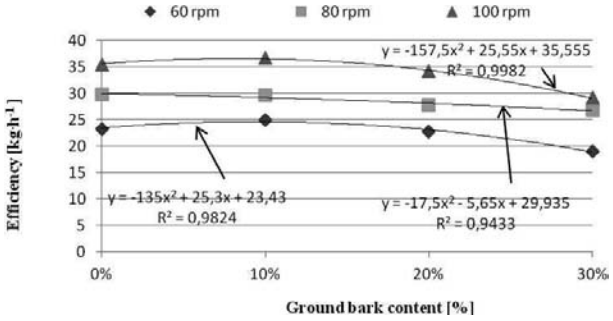

Fig. 3. The influence of the screw speed and ground barkcontent on the efficiency of the extrusion-cooking of TPS pellets

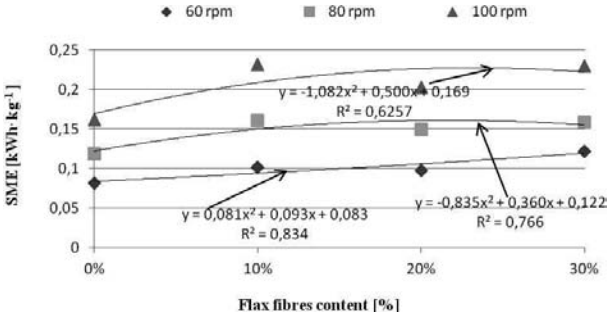

Fig. 5. The influence of the addition of flax fibers and the screw speedused on SME values

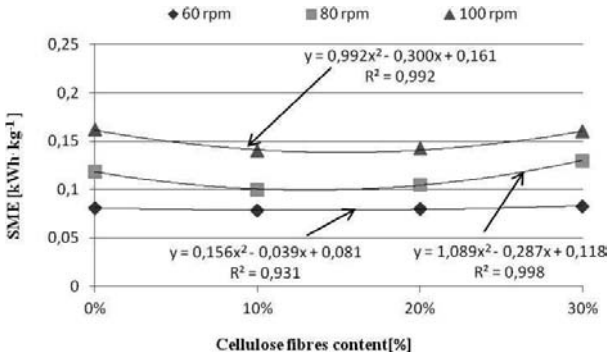

Fig. 4. The influence of cellulose fibers addition and the screw speedon the energy consumption

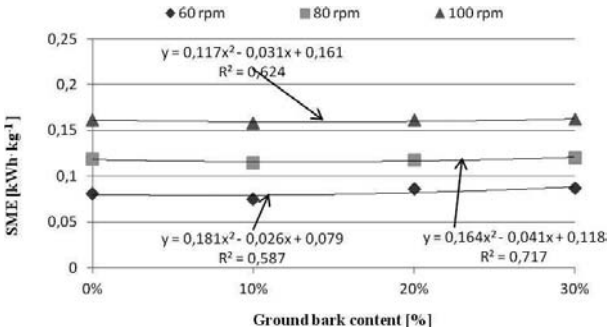

Fig. 6. The influence of the addition of ground bark and screw speed on the SME values

The application of the extrusion-cooking technology to produce TPS pellets takes into account another important factor - the specific mechanical energy SME required to obtain the unit of final product [18]. During the measurements it was found out that the consumption of energy strongly depended on the screw speed used during processing. SME values were higher with increasing screw rotations (0.98-0.99), irrespective of the type of additive applied.

Fig. 4 presents the results of SME for samples with the addition of cellulose fibers. For samples processed at 60 rpm there was no impact of additive level on SME values. For higher rpm applied, the addition of cellulose fiber in amount of 10% lowered SME, but a higher level of the additive slightly increased SME during processing.

For TPS samples contained flax fibers, the increase of SME with a higher level of additive in the recipe with correlation coefficients 0.91, 0.72 and 0.69 for 60, 80 and 100 rpm, respectively was observed (Fig. 5). A higher SME in these samples may be affected by the filamentous nature of flax fibers and due to its greater length; samples with this additive display greater resistance during processing. The highest SME values of 0.23 kWh·kg^{-1} were noticed for the sample containing 30% of flax fibers processed at 100 rpm of the screw.

It was noticed that SME values were similar during processing of biopolymers containing cellulose fibers and ground bark. The addition of ground bark as a filler had no significant impact on the energy consumption (Fig. 6). Higher values of SME were recorded during processing of potato TPS pellets containing ground bark at higher screw rpm, with 0.99 correlation coefficient evaluated for each level of additive in the recipe.

CONCLUSIONS

The efficiency of the extrusion-cooking of potato thermoplastic starchwas directly correlated to the screw speed applied; the higher the screw rotation, the higher the efficiency was obtained. The addition of natural fillers decreased the process efficiency.

The values of SME were strongly affected by the screw speed during extrusion-cooking, where a higher rpm resulted in higher SME.

The obtained SME results were similar during processing of biopolymers containing cellulose fibers and ground bark.

The increased level of additive resulted in higher SME during processingonly for samples with flax fibers. The highest energy consumption of 0.23 kWh·kg^{-1} was noticed during the production of potato TPS pellets containing 30% of flax fibers, processed at 100 rpm of the screw.

ACKNOWLEDGEMENTS

This scientific work was supported by Polish Ministry of Science and Higher Education founds on science in the year 2010-2012 as research project NN 313 275738

REFERENCES

1. **Czerniawski B., Michniewicz J. 1998.** Opakowania żywności. Agro Food Technology, Czeladź.
2. **Dyadychev V., Pugacheva H., Kildeychik A. 2010.** Co-injection molding as one of the most popular injection molding Technologies for manufacture of polymeric details from secondary raw materials, TEKA Commision of motorization and Power Industry in Agriculture, PAN, Volume Xc, p. 57-62.
3. **Funke U., Bergthaller W., Lindhauer M.G. 1998.** Processing and characterization of biodegradable products based on starch. Polymer Degradation and Stability, 59, p. 293.
4. **Janssen L.P.B.M., Mościcki L. 2006.** Thermoplastic starch as packaging material. Acta Sci. Pol., Technica Agraria, 5(1).
5. **Leszczyński W. 1999.** Biodegradowalne tworzywa opakowaniowe. Biotechnologia, 2, p. 50.
6. **Mitrus M. 2005.** Changes of specific mechanical energy during extrusion cooking of thermoplastic starch. TEKA Commission of Motorization and Power Industry in Agriculture, 5, p. 152-157.
7. **Mitrus M. 2006.** Investigations of thermoplastic starch extrusion cooking process stability. TEKA Commission of Motorization and Power Industry in Agriculture, 6A, p. 138-144.
8. **Mitrus M. 2012.** Starch protective loose-fill foams. in: Thermoplastic elastomers, ed. El-Sonbati A., InTech, Croatia, p. 79-94.
9. **Mościcki L., Mitrus M. 2001.** Energochłonność procesu ekstruzji. TEKA Commission of Motorization and Power Industry in Agriculture, 1, p. 186-194.
10. **Oniszczuk T. 2006.** Effect of parameters of injection moulding process on the structural properties of thermoplastic starch packaging materials. PhD Thesis, Department of Food Process Engineering, Lublin Agricultural University, Lublin.
11. **Ryu G.H., Ng P.K.W. 2001.** Effects of selected process parameters on expansion and mechanical properties of wheat flour and cornmeal extrudates. Starch, 53, 147-154.
12. **Sikora T., Gimeza M. 2008.** Elementy towaroznawstwa. WSiP, Warszawa, p. 102.
13. **Suprakas S. R., Mosoto B. 2005.** „Biodegradable polymers and their layered silicate nanocomposites: In greening the 21st century materials world". Canada Research Chair on Polymer Physics and Nanomaterials, Chemical Engineering Department, Université Laval, Sainte-Foy, Que., Canada G1K 7P4.
14. **Sobczak P. 2006.** Sorbitol addition on extrusion process, TEKA Commission of Motorization and Power Industry in Agriculture PAN, Volume VIa, p. 163-169.
15. **Stasiek J. 2007.** Wytłaczanie tworzyw polimerowych. Zagadnienia wybrane. Wyd. Uczelniane Uniwersytetu Technologiczno-Przyrodniczego w Bydgoszczy, Bydgoszcz.
16. **Wójtowicz A., Mitrus M. 2010.** Effect of whole wheat flour moistening and extrusion-cooking screw speed on the SME process and expansion ratio of precooked pasta products. TEKA Commission of Motorization and Power Industry in Agriculture,10, p. 517-526.
17. **Wójtowicz A. 2008.** Influence of legumes addition on proceeding of extrusion-cooking process of precooked pasta. TEKA Commission Motorization and Power Industry in Agriculture,, 8a, p. 209-216.
18. **Wójtowicz A., Mościcki L. 2008.** Energy consumption during extrusion-cooking of precooked pasta. TEKA Commission of Motorization and Power Industry in Agriculture, 8, p. 311-318 (80:20).
19. **Żakowska H. 1997.** Materiały degradowane – alternatywa dla tradycyjnych opakowań z tworzyw sztucznych? (2). Przemysł Fermentacyjny i Owocowo-Warzywny, 12, p. 36-38.
20. **Żakowska H. 2005.** Recykling odpadów opakowaniowych. Wyd. COBRO, Warszawa.
21. **Żakowska H. 2006.** Światowy postęp w produkcji opakowań przydatny do kompostowania. Opakowanie, 2, p. 15-17.
22. **Żakowska H. 2004.** Ocena ekologiczna opakowań prowadzona w COBRO. Ważenie-Dozowanie-Pakowanie 4, p. 28-30.
23. **Żakowska H. 2003.** Opakowania biodegradowalne. Wyd. COBRO, Warszawa.

WPŁYW PARAMETRÓW PROCESU I DODATKU WYPEŁNIACZY NA WYDAJNOŚĆ I ENERGOCHŁONNOŚĆ EKSTRUZJI TERMOPLASTYCZNEJ SKROBI ZIEMNIACZANEJ

Streszczenie. W pracy przedstawiono rezultaty badań wydajności i energochłonności procesu ekstruzji termoplastycznej skrobi ziemniaczanej z dodatkiem wypełniaczy w postaci włókien celulozowych,lnianych oraz mielonej kory. W badaniach zastosowano zmodyfikowany ekstruder jednoślimakowy TS-45 o L/D=18 z dodatkowym chłodzeniem końcowej części cylindra urządzenia. Badano wpływ prędkości obrotowej ślimaka ekstrudera oraz ilości i rodzaju stosowanego wypełniacza w mieszance zawierającej 20% gliceryny jako plastyfikatora na wydajność oraz energochłonność procesu ekstruzji mieszanek skrobi termoplastycznej. Wraz ze wzrostem prędkości obrotowej ślimaka ekstrudera rosła energochłonność oraz wydajność procesu ekstruzji w przypadku wszystkich rodzajów zastosowanych mieszanek surowcowych.

Słowa kluczowe: skrobia termoplastyczna, wypełniacze, ekstruder, energochłonność.

TEKA. COMMISSION OF MOTORIZATION AND ENERGETICS IN AGRICULTURE – 2012, Vol. 12, No. 1, 185–189

Influence of process conditions on quality and energy consumpion during extrusion-cooking of carp feed

Tomasz Oniszczuk[1], Leszek Mościcki[1], Agnieszka Wójtowicz[1], Marcin Mitrus[1], Andrzej Rejak[1], Kazimierz Zawiślak[2], Paweł Sobczak[2], Jacek Mazur[2], A. Oniszczuk[3]

[1]Department of Food Process Engineering, University of Life Sciences in Lublin; [2]Department of Food Engineering and Machinery, University of Life Sciences in Lublin; [3]Department of Inorganic Chemistry, Medical University in Lublin, e-mail:tomasz.oniszczuk@up.lublin.pl

Summary. The paper presents the results of influence of the extrusion-cooking process conditions on the energy requirement and water stability of carp feed. The feed was obtained from standard mixtures of raw materials having various initial moisture content (25%, 27% and 29%, respectively), with the application of baro-thermal treatment using a single screw extrusion-cooker type TS-45. The results of the examinations showed that higher moisture content of raw materials influenced the decrease of the specific mechanical energy SME. The efficiency of the extrusion process increased both with the higher screw speed and higher moisture content of raw materials. The highest water stability was obtained for the carp feed produced from the mixture of 25% m.c. processed at 80 rpm.

Key words: extrusion-cooking, specific mechanical energy, water stability, single screw extrusion-cooker.

INTRODUCTION

The development of freshwater fish farming in Poland requires that more attention should be paid to the process of fish nutrition and more efficient use of fish feed. It pertains to different age groups and species of reared fish. In order to implement a suitable fishery management, the knowledge of biology, fish dietary needs, nutrition methods and quality of feed ingredients is required [2, 3, 6, 9].

Cost-effectiveness of fish rearing and the specificity of carp feeding depend to a large extent on the stability of feed in the water. Feeding fish with less stable feed containing expensive, wholesome components that may undergo lixiviation or dilution, leads to severe losses in the aquatic environment, mainly due to the deterioration of oxygen balance in ponds and increased load of organic matter. Due to constant technological progress, the feed industry offers more efficient and nutritious feed.

A variety of production processes is applied in the manufacture of aquatic feed. In the past dry or wet pelleting was the most popular method [18,19]. Since the quality of pellets for the fish is not suitable due to low water stability and limited nutritional effects, the recent years have seen the replacement of such a feed type by extruded one [7, 10, 11,14]. Extrusion technique allows to introduce various types of components that still have not been used in the production of fish feed. These components have a significant impact on the improvement of physical properties of feed, the efficiency of rearing as well as death rate and health of fish. To understand the basic physical properties of extruded fish feed with different additives, it is necessary to perform a series of measurements that will help identify the main utility characteristics of extrudates and implement appropriate adjustments to the manufacturing parameters in order to obtain high quality products [4, 11, 13, 16, 21].

The aim of this study was to examine the influence of process conditions on functional properties of the extrusion-cooked carp feed as well as the consumption of energy during processing.

MATERIALS AND METHODS

A standard mixture of carp feed was used in the experiment (Table 1). The basic raw materials and components were delivered by Animex Grupa Drobiarska S.A., Zamość, Poland. The balancing of feed recipe and the production technology were developed on the basis of commonly available nutritional standards, computer program, as well as following the recommendations of the personnel of the of Department of Food Engineering and Machinery, Lublin University of Life Sciences. The feed was produced by extrusion-cooking on a single screw extrusion-cooker TS-45 (polish design), fitted with a plasticizing unit of L/D ratio of 16/1.

Table 1. The composition of the mixture

Component	Percentage content [%]
Maize	12.0
Wheat	19.0
Soybean	32.0
Fishmeal	20.0
Fodder yeast	5.0
Rapeseed oil	9.0
II-calcium phosphate	0.8
Chalk Fodder	1.2
Premix[1]	1.0

[1]Premix (1kg): VITAMIN A - 4 400.00 IE, VITAMIN D3 – 680.00 IE, VITAMIN E – 6.00 mg, VITAMIN B1 – 0.60mg, VITAMIN B2 – 1.20mg, BIOTIN – 40.00mcg, VITAMIN B6 – 0,8mg, VITAMIN B12 – 6000.00mcg, VITAMIN K – 0.8mg, NIACIN – 20.00mg, FOLIC ACID – 0.16mg, Ca PANTOTHENATE – 4.00mg, Mn – 16mg, Zn – 20mg.

Raw materials used in the production of the carp feed were grinded with a hammer mill H-111/3 type, using sieves with the openings of 2 mm. 10 kg of the sample was prepared and mixed for 10 minutes in a ribbon mixer. After mixing the ingredients, their moisture content was tested. The mixtures were once again placed in the mixer and moistened by adding water to the final moisture content of 25%, 27% and 29% d.m. The moisture content was determined by a drying method according to PN-76/R-64752.

During the production of feed, the following process parameters were adopted: heat treatment temperature from 110°C to 140°C (various in different extruder sections)**,** the degree of screw compression 1:3, screw speed 80, 100 and 120 rpm, rotational speed of the knife: 1200-1500 rpm, die with 3 holes of 2.5 mm diameter each [12].

The final stage of production was vacuum coating of feed with soybean oil, in which the premix had been dissolved. Fat liquidation was performed in a vacuum mixer of the authors' own construction equipped with a stirrer. Oil and the premix were injected inside by a spray nozzle at 0.08 MPa. The process of fat liquoring and stirring lasted 10 minutes.

The examination of extrusion-cooker's efficiency was performed by determining the mass of the extrudates obtained in 5 minutes for all the applied mixtures of raw materials and process parameters. The measurements were carried out six times for each series of tests, the results being the average of the measurements. The efficiency was expressed in $kg \cdot h^{-1}$ according to the formula:

$$Q = \frac{m}{t} \cdot [kg \cdot h^{-1}], \quad (1)$$

where:

Q – extruder's efficiency,

m – weight of extrudate obtained during, the measurement [kg],

t – measurement time [h].

The measurement of energy consumption was conducted by a standard wattmeter connected to the extrusion-cooker's motor unit. Taking into account the specifications of the engine installed in the extrusion-cooker TS-45, and determining the motor load and efficiency measured at consecutive attempts, the values were converted into the value of specific mechanical energy (SME) according to the formula [1, 5, 8, 10, 15, 17, 20]:

$$SME = \frac{N \cdot O \cdot P}{N_m \cdot 100 \cdot Q} [kWh \cdot kg^{-1}], \quad (2)$$

where:

N - screw speed [rpm],

N_m - max. srew speed [rpm],

P - power [kW],

O - motor load [%],

Q - process efficiency $[kg \cdot h^{-1}]$.

The examination of water stability of carp feed

Water stability of the obtained carp feed was assessed using the Hastings-Hepher method in own modification. The aim of the research was to determine the loss of the extrudate mass during the bath at temperature similar to water temperature in the pond, simultaneously stimulating water movements which caused the fall of feed onto the bed. The device equipped with base, electric engine, electric regulator of rotations and two containers with water, where containers with the examined samples were immersed, was used for the experiment. The extrudate was weighed to 0.01 g twice. The weighed samples were placed in two containers made of wire net with the mesh diameter of 0.1 x 0.1cm and 3x6x9cm linear size. One liter of water at temp. 20°C, 22°C and 24°C was placed to each of the containers. The containers with feed were suspended and the device put into motion with the frequency of 1 rotation of the container per 8 seconds. The testing lasted 60 minutes, after which the containers were put away for draining and dried at the temperature of 110°C to obtain constant weight. Next, the weight of the samples was compared with the weight of the feed before testing. The obtained results were expressed as water stability measurement. The stability was calculated from the following formula:

$$S = \frac{m_g}{m_n} * 100[\%], \quad (3)$$

and after:

$$m_w = \frac{m * W}{100} [g], \quad (4)$$

$$m_n = m - m_w [g], \quad (5)$$

where:

S – water stability [%],

m_g – sample mass after testing and drying [g],

m_n – dry granulate [g],
m_w – water mass in granulate used in testing [g],
m – granulate weight after soaking [g],
W – moisture [g].

All measurements were carried out in 6 replications [18,20].

RESULTS

All fish feeds were assessed in terms of their usefulness. Physical properties of these feeds, in particular their water stability and influence on aqueous environment contribute to the growth rate of fish and better living conditions in the pond. During the extrusion process, the influence of the initial moisture content of mixtures designed for the production of feed on their efficiency and the consumption of energy was observed [7]. It was proved that the efficiency of the extrusion process increased both with the higher extruders' screw speed and the growth of moisture content of the mixture. The highest efficiency of the extrusion process (30.5 kg·h^{-1}) was observed for the mixture of 29% of moisture content produced at 120 rpm, whereas the lowest efficiency was observed for the mixture of 25% of moisture content produced at 80 rpm^{-1}. Results are presented on the Fig. 1.

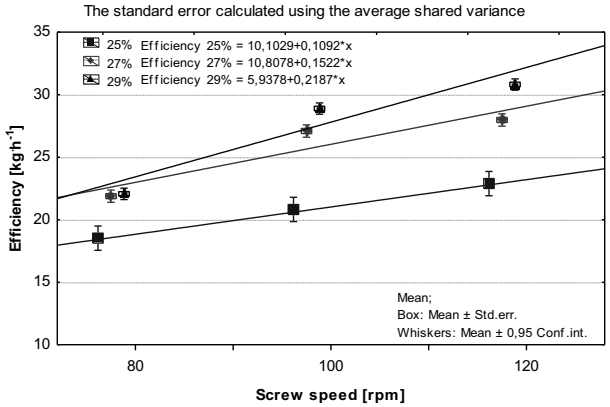

Fig. 1. The influence of the mixture moisture content and screw speed on the efficiency of the extrusion-cooking of carp feed

The application of extrusion techniques to the production of selected blends requires the determination of SME values, necessary to obtain a single mass of the product, which indicates whether the production is profitable. SME values depended on the changes of extrusion parameters, i.e. changes in screw speed and the moisture content of the mixtures. SME values decreased together with the growth of moisture content of raw mixtures.

The highest SME values (0.21 kWh·kg^{-1}) were observed at the extrusion of the mixture with 25% humidity, with the application of 120 rpm of screw speed. The lowest SME values (0.099 kWh·kg^{-1}) were observed at the extrusion of the mixture with 29% of moisture content with the application of 80 rpm screw speed of extruder (Fig. 2).

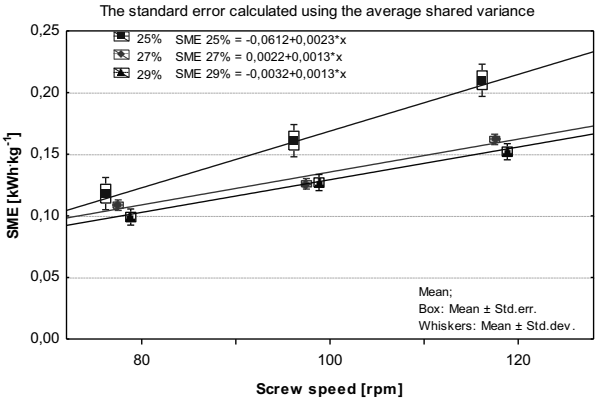

Fig. 2. The influence of the mixture moisture content and the screw speed on SME during the processing of carp feed

Sorensen et al. [18] observed that SME values ranged from 0.034 kWh·kg^{-1} to 0.039 kWh·kg^{-1} at the production of trout feed *(Oncorhynchusmykiss)*, where single screw extruder with conditioner was applied. Lower SME values observed by Sorensen were the result of the composition of feed, a higher content of fishmeal characterized by a limited number of fibers. The application of conditioner, which enables thermal processing of particular components, gives the possibility to dose more fat inside the conditioner. Water stability of the extrudates, which determines its quality, was another physical property measured. The experiment of the process of water stability of carp feed was carried out for water at 20°C, 22°C and 24°C. The extrudates produced at 80 rpm indicated the highest water stability, allowing for the whole range of moisture content of applied mixtures.

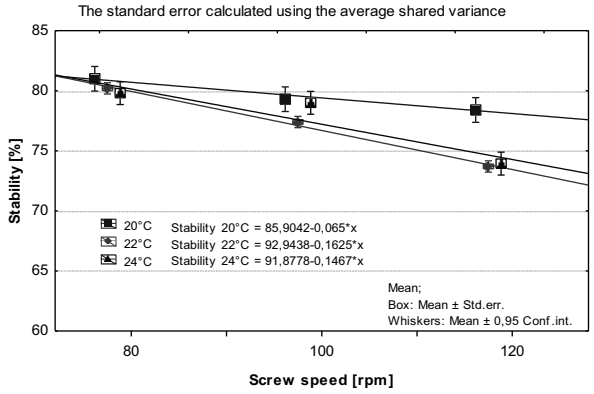

Fig. 3. The influence of the screw speed and pond's water temperature on the water stability of the extruded carp feed (mixture of 25% m. c.)

The growth of the screw rotations by 20 rpm caused the decrease of water stability by a few percent. The extrudates produced from mixtures of 25% humidity indicated the highest stability ranging from 78 to 81% (Fig. 3).

In the case of mixtures containing 25% of moisture content and processed at 80 rpm, the temperature of water applied for testing the feed slightly influenced water stability of carp feed.

The increase of the screw speed influenced the decrease of water stability in all the applied mixtures. The lowest water stability (67% – 70%) was observed at 120 rpm and the moisture content of mixtures at 27% and 29%, respectively (Fig. 4, 5).

The result may be considered satisfactory: the guarantees enough time for fish to eat the extrudate and contributes to smaller contamination of the reservoir. Pound's water temperature has important influence on the fish growth during intensive feeding, especially in summer. Fish belonging to the carp family have a tendency to feed together with the growth of temperature: the feed is eaten faster, which contributes to smaller contamination of the pond/reservoir.

Slightly lower values of water stability of the extrudates were observed for the mixtures tested at 24°C (the differences indicated approximately 2%). The mixtures containing 27% of moisture content and processed at the maximal speed of screw indicated the biggest difference (approximately 7%) depending on water temperature applied for testing.

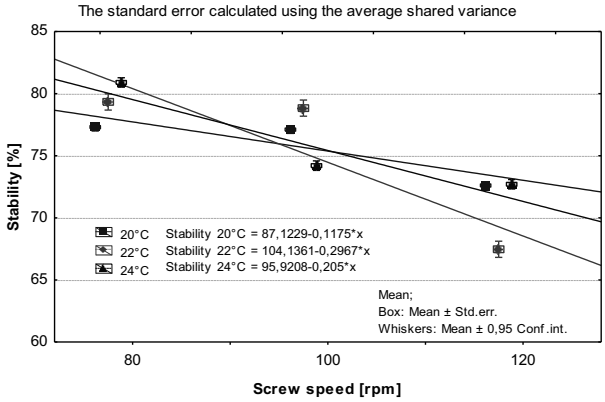

Fig. 4. The influence of pond's water temperature and the screw speed on water stability of the extruded carp feed (mixture of 27% m. c.)

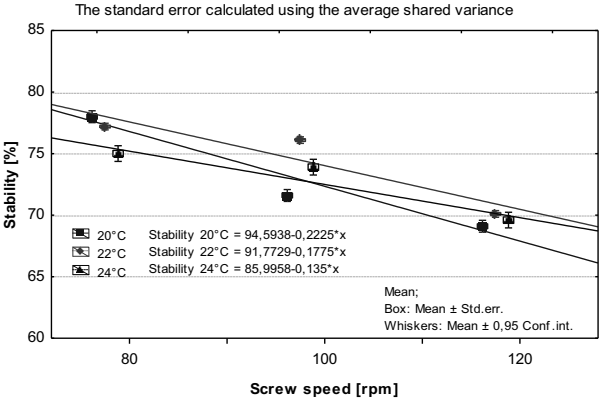

Fig. 5. The influence of the pond's water temperature and the screw speed on water stability of the extruded carp feed (mixture of 29% m. c.)

CONCLUSIONS

The efficiency of the extrusion-cooking of carp feed was higher when the mixture of raw materials with higher initial moisture content was processed at higher screw speed. However, an increase of the screw rpm usually resulted in higher energy consumption (SME) during extrusion-cooking, application of more water to the mixture (at softer level) can optimize the costs of processing and keeping proper level of the products quality. That has to be done on the compromise level.

The carp feed produced from the mixture with 25% of moisture content indicated the highest water stability. Water stability of extrudates decreased with the growth of screw speed. Pond's water temperature used during testing did not show substantial influence on the water stability of the extrusion-cooked carp feed.

REFERENCES

1. **Chung-Wen Su 2007.** Effects of eggshell powder addition on the extrusion behaviour of rice. Journal of Food Engineering, 79, p. 607-612.
2. **Dudkiewicz D. 2002.Technologia i** wyposażenie do produkcji ekstrudowanych pasz dla ryb. Magazyn Przemysłu Rybnego, 1, p. 5-9.
3. **Guziur J., Białowąs H., Milczarzewicz W. 2003.** Rybactwo stawowe. Oficyna Wydawnicza „Hoża", Warszawa.
4. **Harper J.M. 1981.** Extrusion of Foods. vol. 1, CRS Press Inc., USA.
5. **Janus P. 2002.** Metoda pomiaru energii użytecznej w procesie technologicznym przetwórstwa żywności oparta na stratach poszczególnych silnika elektrycznego i maszyny roboczej. Acta Scientiarum Polonorum. Technologia Alimentaria 1(1), p. 103-111.
6. **Koreleski J., Świątkiewicz S. 2006.** Zakaz stosowania antybiotyków – co dalej? Pasze Przemysłowe, 2/3, 22-29.
7. **Korol W. 2006.** Wymagania w zakresie zapewniania jakości handlowej w produkcji i obrocie pasz. Pasze Przemysłowe, 2/3, p. 29-35.
8. **Kulig R. 2007.** Effect of conditioning methods on energy consumption during pelleting. TEKA Commission of Motorization and Power Industry in Agriculture, 7a, p. 52-58.
9. **Lee K-J., Dabrowski K., Rinchard J., Gomez C., Guz L. 2004.** Supplementation of maca (*Lepidiummeyenii*) tuber meal in diets improves growth rate and survival of rainbow trout Oncorhynchusmykiss (Walbaum) alevins and juveniles. Aquaculture Research, 35, p. 215-223.
10. **Le Roux D., Vergnes B., Chaurand M., Abecassis J. 1995.** A thermomechanical approach to pasta extrusion. Journal of Food Engineering, 26, p. 351-368.
11. **Mościcki L., Mitrus M., Wójtowicz A. 2007.** Technika ekstruzji w przemyśle rolno-spożywczym. PWRiL, Warszawa.
12. **Mościcki L. 1998.** Produkcja karmy dla zwierząt domowych i ryb. Przegląd Zbożowo-Młynarski, 5.

13. **Mościcki L. 2000.** Technika ekstruzji w przetwórstwie rolno-spożywczym. Wyd. specjalne, Przegląd Zbożowo-Młynarski, Warszawa.
14. **Oniszczuk T. 2002.** Metodyka badań ekstrudowanych karm dla ryb. Inżynieria Rolnicza, 4(37), p. 257-263.
15. **Ryu G.H., Ng P.K.W. 2001.** Effects of selected process parameters on expansion and mechanical properties of wheat flour and cornmeal extrudates. Starch, 53, p. 147-154.
16. **Salah Mesalhy A. Mohamed Fathi M. George J. 2008.** Echinacea as immunostimulatory agent in Nile Tilapia (OreochromisNiloticus) via earthen pond experiment. 8TH International Symposium on Tilapia in Aquaculture.
17. **Singh N., Smith A.C. 1997.** A comparison of wheat starch, whole wheat meal and oat flour in the extrusion cooking process. Journal of Food Engineering, 34, p. 15-32.
18. **Sorensen M., Storebakken T., Shearer K.D. 2005.** Digestibility, growth and nutrient retention in rainbow trout *(Oncorhynchusmykiss)* fed diets extruded at two different temperatures. Aquaculture Nutrition, 11, p. 251-256.
19. **Szumiec J., Stanny L. 1975.** Ocena stabilności pasz granulowanych stosowanych w żywieniu karpi. Gospodarka Rybna, 12, p. 3-5.
20. **Szymanek M. 2008.** Energy-consumption at sweet corn threshing, TEKA Commission of Motorization and Power Industry in Agriculture, 8, p. 241-246.
21. **Thomas M., Van der Poel A.F.B. 1996.** Physical quality of pelleted animal feed 1. Criteria for pellet quality, Animalfeed Science and Technology, 61, p. 89-112.

WPŁYW WARUNKÓW PROCESU NA JAKOŚĆ I ENERGOCHŁONNOŚĆ EKSTRUDOWANEJ KARMY DLA KARPIA

Streszczenie. W pracy przedstawiono wyniki badań wpływu prędkości obrotowej ślimaka ekstrudera oraz wilgotności surowców na zapotrzebowanie energii jednostkowej oraz stabilność wodną karmy dla karpia w zależności od temperatury wody stosowanej w teście stabilności wodnej ekstrudatu. Karmę wytwarzano ze standardowych mieszanek surowcowych o zróżnicowanej wilgotności początkowej mieszanki (25%, 27% i 29%) oraz stosując obróbkę ciśnieniowo-termiczną przy użyciu zmodyfikowanego ekstrudera jednoślimakowego TS-45. W wyniku przeprowadzonych badań stwierdzono, że wzrost wilgotności mieszanek przeznaczonych do ekstruzji wpływał na spadek SME. Wydajność procesu ekstruzji zwiększała się wraz ze wzrostem prędkości obrotowej ślimaka ekstrudera oraz wraz ze wzrostem wilgotności mieszanki. Najwyższą stabilnością wodną charakteryzowała się karma wyprodukowana z zastosowaniem 80 obr.min-1 ślimaka ekstrudera przy wilgotności mieszanki surowcowej 25%.

Słowa kluczowe: ekstruzja, właściwości fizyczne, stabilność wodna, ekstruder jednoślimakowy.

TEKA. COMMISSION OF MOTORIZATION AND ENERGETICS IN AGRICULTURE – 2012, Vol. 12, No. 1, 191–194

Influence of moisture content on selected physical properties of rape seeds and the processes of cleaning and separation

Marian Panasiewicz, Rafał Nadulski, Kazimierz Zawiślak, Jacek Mazur, Paweł Sobczak

Department of Food Process Engineering and Machines; University of Life Sciences in Lublin
e-mail: marian.panasiewicz@up.lublin.pl

Summary. The aim of the research was the determination of change of physical properties of rape seeds during drying process in diverse time-temperature conditions. Kana rape seeds were used for research, at 6% storage moisture content, as well as additionally moistened ones up to 17% postharvest moisture content. The samples were convection-dried at temperature levels (60, 80, 100ºC) for 20 and 40 minutes. After the drying, the physical properties of rape seeds were determined. The results of research showed that high drying temperature or large initial moisture content are not recommended for long storage time. However, the estimate of results showed that rape seeds which are designed for direct processing can be dried at a higher temperature then the temperature applied in present practice.

Key words: rape seeds, drying temperature, physical properties, cleaning, pneumatic separation.

INTRODUCTION

Polish tradition of growing rape seeds, constant growth of its economic significance, which stems from wide possibilities of using oils within the scope of the production of solid food products and liquid plant oils, chemical materials and biofuels for running diesel engines, have caused the necessity for a more versatile and effective use of this valuable plant resource [5, 3, 12]. Any actions aimed at increasing the amount of pressed oil (the so-called extra virgin oil), require seeking new, not yet used in industrial processing of rape seeds, methods for their preparation and initial processing prior to the pressing process [2, 16, 17]. The procedures, which are described as postharvest processing, are the processes of cleaning and drying seeds. These processes influence both the change in physical and technological properties of seeds, increased costs as regards electricity consumption, and the quality of final products [15, 20, 17, 13]. Rape seeds before storing should be cleaned and dried to the moisture content below 7%. Previous research and practice indicated that in seeds with high water content there occur many unfavourable processes negatively influencing further storing and processing [1, 6, 14]. Improper execution of the drying process, especially the use of too high temperatures, leads to changes in physical and chemical properties of rape seeds. As it has been indicated by previous experiments in this scope, seeds of higher moisture content should be dried at low temperatures. High temperatures negatively influence utility and technological values of the resource leading to, among others, decreasing mechanical durability of seeds, at the same time increasing their vulnerability to damage [14, 4, 18].

The aim of this research was to indicate the influence of the moisture content on selected physical properties of Kana variety rape seeds. The scope of this research included the measurement of these parameters for grain with the storing moisture content (W=6%) and seeds additionally moistened to the postharvest moisture content (W=17%). Additionally moistened seeds underwent the process of convection drying in different ranges of time and drying temperatures, then measurements related to defining and assessing selected physical properties of seeds were conducted.

MATERIAL AND METHODS

For the purposes of the research Kana variety rape seeds were used. This variety is characterised by a high degree of oil content, proved high output content of oil, as well as generally good technological quality of this resource. Seeds with the initial moisture content W=6% were additionally moistened to the postharvest moisture content W=17%. In order to additionally moisten seeds to the established moisture content an adequate amount of water was added, which was calculated from the formula (1):

$$Mw = \frac{M1 - M0}{100\% - M1} * m, \qquad (1)$$

where: M_w – mass of water necessary for additional moistening, [g],

M_l – moisture content of grain after additional moistening, [%],

M_o – initial moisture content of grain, [%],

m – mass of sample, [g], [Lis et al. 1983].

In order to equalise the required moisture content in the total mass, the conditioned samples were stored in hermetic containers in a cooling chamber at a constant temperature approx. 3°C and underwent multiple mixing during the day. Next, the seeds were dried in a laboratory drier at temperatures T=60, 80, 100 and time t=20min and 40min. Control samples constituted seeds of the moisture content 6% and 17% before drying. The seeds were placed on perforated metal sieves, in a thin 0.5cm layer. The drying process was conducted in a laboratory drier with turbo-circulation. After completing the process of seeds drying and cooling, the specific physical properties, i.e.: the moisture content, angle of slide and angle of repose, tapped bulk density and loose bulk density, mass of 1000 seeds and average particle size were defined. All the tests were conducted according to the Polish Norms, in five repetitions (the results were presented as averages).

RESULTS AND DISCUSSION

In order to indicate the range of changes in physical properties which are especially important in further processing, which determines the quality of seeds and their technological value, it is necessary to define selected groups of geometrical and mass properties of the resource [18]. The defined initial parameters (Tab. 1.) were used as the database against which the results achieved during the conducted tests after the processes of drying were compared. The research, conducted according to the established aim and methodology, has indicated high sensibility of rape seeds in relation to varied time periods and drying temperatures. Changes were recorded for all the tested groups of physical properties.

Table 1. Comparison of physical properties of Kana variety rape seeds of moisture content 6% and 17%

Physical properties	Kana – winter rape seeds variety	
Moisture content [%]	6.0	17.0
Angle of slide [°]	16.83	22.48
Angle of repose [°]	21.33	26.77
Loose bulk density [kg·m^{-3}]	631.16	618.84
Tapped bulk density [kg·m^{-3}]	701.23	665.79
Weight of 1000 seeds [kg]	0.00637	0.00711
Average particle dimension [m]	0.00168	0.00188

The above table presents basic physical properties of the tested Kana variety rape seeds with two extreme levels of moisture content. Seeds with lower moisture content (dry) had a smaller angle of slide and angle of repose, as well as average particle size and mass of 1000 seeds. When it comes to mass characteristics, lower values of density (both in tapped bulk density and loose bulk density) were achieved for samples of seeds with moisture content W=17%.

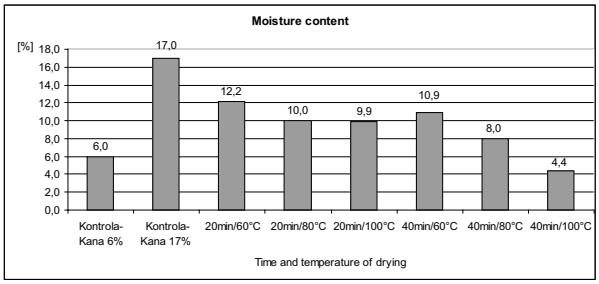

Fig. 1. The range of moisture content changes in the tested seeds, achieved during drying in different ranges of time and temperature

In the general assessment of the quality of seeds which are treated as a processing resource, their moisture content is taken into account, which has a significant influence on storing seeds and their utility for further processing. The range of seed moisture content changes presented in Fig. 1. illustrates the intensity of water loss during the process of seeds drying. From the analysis of the moisture content distribution it results that drying at a temperature of 100ºC and time 40min is unfavourable because the moisture content of seeds decreased far below the require storing moisture content and was only W=4.4%. Differences in the level of values of tapped bulk density and loose bulk density were also recorded. Density of seeds (Fig. 2a) generally increased together with elapsing time and increasing temperature and were within the range from 619.2kg·m^{-3} to 891.7 kg·m^{-3}. Seeds dried at the highest temperature for the longest time recorded an especially significant increase in tapped bulk and loose bulk states. Different drying parameters of specific samples of rape seeds had a significant influence on changes of the angle of slide and the angle of repose. The lowest values of the angle of slide (as compared to the control sample), were achieved for seeds dried in the highest range of time and temperature (40min/100°C). Its value was 15.67° (in relation to the control test 22.48°). Milder drying conditions (e.g. 40min/60°C or 20min/60°C), also influenced the change of values of the angle of slide and repose, however these decreases had a lower range of changes (Fig. 2b.). In the seeds processing industry the mass of one thousand seeds and the average particle size are the main indicators of ripeness of seeds, and at the same time indicators of technological value.

As predicted, these changed together with the change of drying parameters, i.e. the more intensive drying, the lower the values of these properties (Fig. 3a and b).

a)

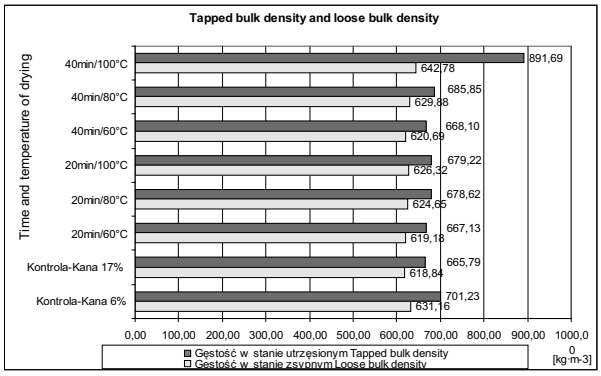

b)

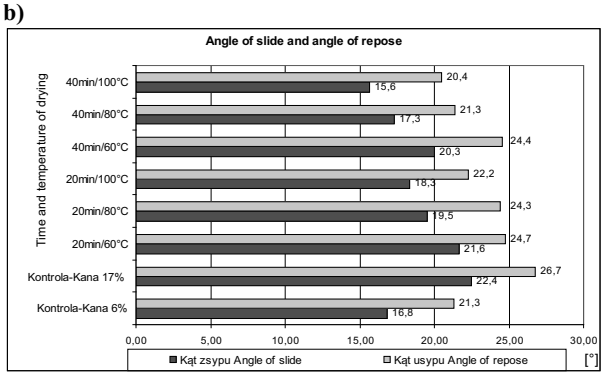

Fig. 2. The range of changes of physical properties: a) tapped bulk density and loose bulk density; b) angle of slide and angle of repose

a)

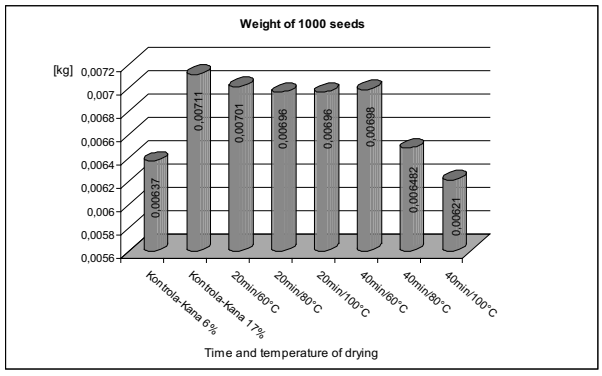

b)

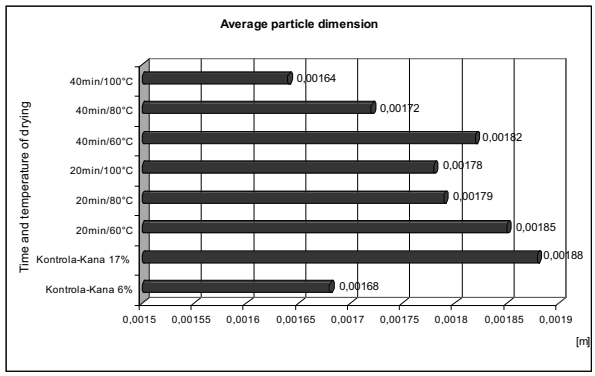

Fig. 3. The range of changes of physical properties: a) weight of 1000 seeds; b) average particle dimension, achieved in diverse time-temperature conditions of drying process

The achieved research results and their analysis explicitly indicate the influence of drying time and temperature on a selected group of physical properties of tested rape seeds. Every change, even in a narrow range, of conditions of the drying process influenced a decrease or increase of particular physical properties of seeds.

The scope of recorded changes, conditioned by transpiration, has led both to favourable and unfavourable influences on further preparation and processing of seeds. The achieved research results constitute a valuable database important both in the process of cleaning and separation, drying and storing seeds, and in further processing related to acquiring oil (cold pressed oil, extraction, rafination, etc.) It should be presumed that drying conditions may also influence the effectiveness of the pressing process and the quality of pressed oil. It should be added that clarification of the abovementioned relations will be undertaken in the next cycle of research.

CONCLUSIONS

On the basis of the conducted research the following conclusions were formulated:

The conducted research related to the scope of changes of selected groups of physical properties in relation to the moisture content of seeds present a possibility to assess them in the aspect of application of different times and temperatures of rape seeds drying, as well as further preparation and processing.

A very high temperature of drying and long duration of this procedure influence the speed and intensity of drying, as well as significant changes (mostly unfavourable) of the majority of tested physical properties of seeds, and at the same time their technological value.

The research results indicate that in case of seeds with a high harvest moisture content (within the range W=17%), it is necessary to precisely select and apply parameters of the drying process, thanks to which the required storing moisture content (6-7%) will be achieved in an effective and energy-saving way, at the same time maintaining high technological value of the resource.

From the practical point of view and technological requirements of processing it seems that the most favourable drying conditions for moist rape seeds after harvesting require drying time t=40min and temperature T=80°C. These parameters condition an effective decrease in the moisture content of seeds to the required storing value, i.e. ~7%. It should be added that the suggested drying conditions must be additionally adjusted and take into account technical-technological parameters of the applied drying machines.

REFERENCES

1. **Gawrysiak-Witulska M. 2005:** Wpływ temperatury i techniki suszenia na wybrane wyróżniki jakościowe nasion rzepaku. Inżynieria Rolnicza 11(71), p. 129-135.
2. **Górecka A., Wroniak M., Krygier K. 2003:** Wpływ ogrzewania nasion rzepaku na jakość wytłaczanego oleju. Rośliny Oleiste. Tom XXIV: p. 567-576.
3. **Kachel-Jakubowska M. 2009:** Influence of acid number and peroxide number kontent on the quality of rape seeds for consumption and biofuel industry. TEKA Kom. Mot. Energ. Roln.-OL PAN, 2009, 9, p. 114-120.
4. **Lis T., Lis H., Szot B., Siarkowski Z. 1983:** Próba oceny wpływu wilgotności na wybrane właściwości fizyczne ziarna pszenicy ozimej Grana. Zeszyty Problemowe Postępów Nauk Rolniczych 253: p. 65-78.
5. **Niewiadomski H. 1993:** Technologia tłuszczów jadalnych. WNT. Warszawa.
6. **Panasiewicz M., Mazur J., Zawiślak K., Sobczak P. 2009:** An influence of preliminary rapeseed processing on oil extrusion. TEKA Kom. Mot. Energ. Roln.-OL PAN, 2009, 9, p. 217-222.
7. Polska Norma PN –EN ISO 666: 2004. Nasiona oleiste – Oznaczenia wilgotności i zawartości substancji lotnych.
8. Polska Norma PN – ISO 7971 – 2:1998. Ziarno zbóż – Oznaczanie gęstości w stanie zsypnym, zwanej „masą hektolitra".
9. Polska Norma PN – R 74017:1968. Ziarno zbóż i nasiona strączkowe jadalne – Oznaczanie masy 1000 ziaren.
10. Polska Norma PN – Z-04002-07:1998. Oznaczanie kąta nasypu pyłu.
11. Polska Norma PN – Z-04002-08:1974. Oznaczanie kąta zsypu.
12. **Roszkowski A. 2006:** Agriculture and Fuels of the Future. TEKA Kom. Mot. Energ. Roln.-OL PAN, 2009, 6, p. 131-134.
13. **Wojalski J., Domagała A., Kaleta A., Janus P. 1998:** Energia i jej użytkowanie w przemyśle rolno-spożywczym. Wydawnictwo SGGW.
14. **Szot B. 2008:** Ocena podstawowych właściwości fizycznych nasion rzepaku jarego. Acta Agrophysica 12(1): p. 191-205.
15. **Tańska M., Rotkiewicz D. 2003:** Wpływ różnych czynników na jakość nasion rzepaku. Rośliny Oleiste. Tom XXIV: p. 595-616.
16. **Topilin G., Yakovenko A., Uminski S., Nowak J. 2009:** A hydrodynamic installation for the production of biodiesel fuel. TEKA Kom. Mot. Energ. Roln.-OL PAN, 2009, 9, p. 342-346.
17. **Topilin G., Yakovenko A., Uminski S., Nowak J. 2009:** Production of biodiesel fuel for self-propelled agricultural machinery. TEKA Kom. Mot. Energ. Roln.-OL PAN, 2009, 9, p. 352-356.
18. **Tys J., Sobczuk H., Rybacki R. 2002:** Influence of dryling temperature on mechanical properties of rape seeds (in Polish). Oilseed Crops. IHAR, XXIII, p. 417-426.
19. **Yang X., C. Bern, C.R. Hurburgh. 1990:** Airflow resistance of cleanings removes from corn. Trans. of A.S.A.E., p. 1299.
20. **Zając G. 2009:** Methyl esters of rape oil as an addition to diesel fuel. TEKA Kom. Mot. Energ. Roln.-OL PAN, 2009, 9, p. 407-417.

Scientific research financed from the resources for science for the years 2011-2014 as the research project N N313 757140.

WPŁYW WILGOTNOŚCI NA WYBRANE WŁAŚCIWOŚCI FIZYCZNE NASION RZEPAKU ORAZ PROCES CZYSZCZENIA I SEPARACJI

S t r e s z c z e n i e. Celem przeprowadzonych badań było określenie zmian właściwości fizycznych nasion rzepaku w zależności od wilgotności i zastosowanych warunków procesu suszenia (zróżnicowany czas i temperatura). Do badań wykorzystano nasiona rzepaku odmiany Kana o wilgotności przechowalniczej 6% oraz dowilżone nasiona tej odmiany do wilgotności pozbiorowej 17%. Próbki poddano suszeniu konwekcyjnemu w temperaturach 60, 80 i 100°C oraz czasie 20 i 40min. Po procesie suszenia określono właściwości fizyczne. Uzyskane wyniki badań wskazują, że wysoka temperatura suszenia oraz duża wilgotność początkowa wpływają niekorzystnie na właściwości fizyko-mechaniczne nasion rzepaku powodując w większości przypadków ich znaczące pogorszenie, co ma istotne znaczenie w przypadku dłuższego przechowywania. Ma to też istotny wpływ na proces separacji pneumatycznej nasion. Ocena wyników badań wskazuje, że nasiona rzepaku przeznaczone do bezpośredniego przerobu mogą być suszone w nieco wyższych, od stosowanych w praktyce temperaturach.

S ł o w a k l u c z o w e: nasiona rzepaku, temperatura suszenia, właściwości fizyczne, czyszczenie i separacja pneumatyczna.

TEKA. COMMISSION OF MOTORIZATION AND ENERGETICS IN AGRICULTURE – 2012, Vol. 12, No. 1, 195–199

The analysis of the influence of initial processing of oat caryopses on the course and energy consumption of the flaking process

Marian Panasiewicz, Jacek Mazur, Paweł Sobczak, Kazimierz Zawiślak

Department of Food Engineering and Machines, University of Life Sciences in Lublin

Summary. The paper presents results of measurements of the energy consumption flaking process of dehulled oat grains depending on the method and parameters of moistening and moisture content. Measurement of energy consumption was determined according to the methodology at the different working gap size. The energy consumption of flaking process depends on the size of the working slot crusher. Its highest value was recorded at flaked grains at the working gap A_1= 0.1 mm. However, differences in power changes between the slits A_1 = 0.1 mm and A_2 = 0.2 mm ranged from 6% (for samples of moisture content M_5 = 18%), up to 32% (for dry grain M_1 = 10%). The most preferred method is moistening oats grain by the steam for less energy consumption in the flaking process. Regardless of the assumed initial moisture content, the lowest power values for their flaking were obtained for the samples moisted by steam for the time t_1 = 5 min.

Key words: energy consumption, flaking, oat grain, hydrothermal treatment.

INTRODUCTION

In the processing of cereal resources, especially grits cereals, one of the most important issues is the knowledge of the application of hydrothermal procedures. They constitute the foundation for the initial grain processing before dehusking or flaking 4;7;14;15. A particularly important role, especially in the production of grits, breakfast flakes and the so-called breakfast cereal products, is played by different methods of conditioning grain and seeds [2, 3, 5, 12]. These procedures to a large extent influence both the course and the efficiency of processing, as well as trigger a range of changes in physical properties of the processed resources. As the final result, both factors determine the quantity and the consumption quality of ready-made cereal products or semi-products [12, 11, 10, 6].

Contrary to conditioning applied in the milling industry, which has been a scientific issue for a long time, the subject matter of research and practice of further use of hydrothermal processing procedures in the production of grits, breakfast cereals or preparation of cereal products have been the subjects of intense research only since the last decade. The research brings about higher interest in this subject matter and progress in scientific research and utilitarian experiments, which are aimed at finding wider possibilities of the application of cereal resources in the food industry [1, 8, 11, 17].

Although these processes are known and applied in processing cereal into flour, in the processing of grain and seeds into low-processed cereal products (except for highly-processed products which are produced with the use of methods of pressure agglomeration) they are only known in fragmentary studies mainly devoted to selected cereal and seeds of none-cereal plants. The application of these processes to a randomly selected resource in strictly defined conditions allows for achieving favourable changes in its physical properties, which is especially important in processing procedures. The group of more important properties includes structural-mechanical properties, whose properly directed alternation by hydrothermal processing is one of the basic tasks in preparatory processes of grain which undergo subsequent processing operations in cereal-milling and fodder industries. It particularly concerns preparing grain for grinding, dehusking and flaking processes or recently popular methods of the so-called preparation of grain and seeds [10, 11, 18, 14, 15]. It should be stressed that the application of a given method of hydrothermal processing and selection of its technological parameters (particularly the range and sequence of the procedure) are often the most important secrets of all eminent companies which process cereal resources. It results, among others, from the fact that these are complex processes, in which the influence and the scope of interactions of individual factors are interconnected and interrelated. Experiments within the scope of processing of cereal resources indicate that their adequate preparation, which consists in achieving technological features which would be close to the optimum

for a given process is as important (or even the most important), as the correct determination of parameters for proper processing, including the process of flaking [13, 2, 4].

THE AIM AND SCOPE OF THE RESEARCH

The primary aim of the research was to measure energy expenditures of the process of flaking in relation to the final moistness of dehusked oat grain, changing parameters of its moistening with water and steam, and the working aperture of the grinding machine. The scope of the influence of the final moistness and selected methods of hydrothermal processing of oat caryopses were defined in relation to energy expenditures and work which was necessary for the execution of the process of flaking. The detailed scope of the research included preparation of the resource for the research, which consisted in separating the medium fraction and additional moistening of the resource with water and steam, as well as measuring energy consumption of the process of caryopses flaking with different working apertures of the grinding machine. The achieved research results were statistically processed.

RESEARCH METHODOLOGY

For the purposes of the research dehusked oat caryopses - variety Jantar were used, after the process of dehusking these were sorted in a sieve sifter, in which the holes had a longitudinal shape with the following sizes: 3.0x3.25 mm (upper sieve), and 1.8x2.25 mm (lower sieve). The initial moistness of caryopses was M=10%. Caryopses prepared in this manner were processed hydrothermally, which involved:

a) additional moistening with water leading to five levels of final moistness (M_1=10%, M_2=14%, M_3=18%, M_4=22% and M_5=26%) [PN-91/A-74010] [16];
a) moistening caryopses with steam with differentiated levels of initial moistness within the range M_{i1}=10%, M_{i2}=12%, M_{i3}=14%, M_{i4}=16% and M_{i5}=18%.

The time of caryopses processing with steam was t_1=5 min, t_2=10 min and t_3=15 min.

After conducting hydrothermal procedures, samples of caryopses which were additionally moistened to reach particular levels of final moistness, went through the process of grinding in the grinding machine with smooth rollers. The working apertures of the grinding machine were A_1=0.1 mm, A_2=0.2 mm and A_3=0.3 mm. During the process of flaking the measures of energy consumption in relation to the method of conditioning, final moistness of caryopses and the applied aperture in the grinding machine were conducted.

THE TEST STAND AND THE MEASUREMENT OF ENERGY CONSUMPTION OF THE FLAKING PROCESS

The measurement of energy consumption of the flaking process was conducted for two groups of the resource, i.e. caryopses additionally moistened with water and caryopses additionally moistened with steam. Processing with steam was carried out in a laboratory roaster-mixer, applying the pressure of steam p_s=0.28 MPa.

Following the process of moistening with steam, the grain was placed in a hermetic container and seasoned for 30 minutes. The samples prepared in this way, which weighed 1 kg, underwent the process of flaking at the laboratory test stand, which consisted of a grinding machine, an inverter, and a computer with software and equipment (Fig. 1).

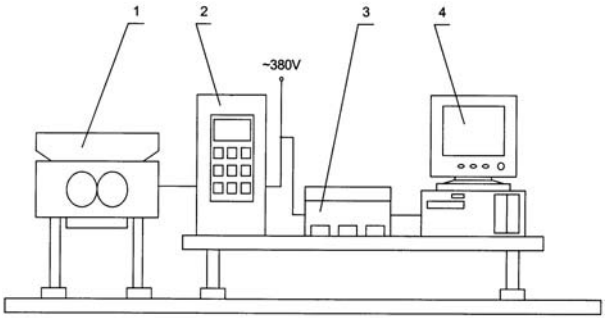

Fig. 1. A schematic of the stand for measuring energy consumption of the flaking process of grain resources: 1-grinding machine, 2-inverter, 3-power converter type Lumel PP83, 4-computer with a PCL-711B card

The process of flaking was carried out in a grinding machine "Tytan" H-759 adjusted to laboratory research, powered by a 2.2 kW engine with rated voltage of 380V, current rating of 5.2 A and power coefficient of 0.82. The working parts of the grinding machine were 2 smooth rollers with the diameter of 240 mm and the width of 50 mm. The circumference velocity of the rollers was 0.252 $m \times min^{-1}$. Smooth and seamless feeding of the working aperture of the grinding machine with the resource was done thanks to a belt conveyor with the capacity of 40 $g\ s^{-1}$. After the start up of the grinding machine and stabilising its operation, the feeding conveyor (belt conveyor) and the computer with the power converter, which recorded the values of energy consumption necessary for grinding a sample of 1 kg grain, were turned on at the same time. The measurement was conducted during five repetitions for a given moistness and method of moistening resources. The arithmetic mean achieved after 5 repetitions was assumed as the result.

RESULTS OF THE RESEARCH AND THEIR ANALYSIS

The achieved research results indicated the complex character of correlations between parameters of hydrothermal processing of caryopses and energy consumption of the flaking process. It was ascertained that differentiated levels of grain moistness, hydrothermal processing and the working aperture of the grinding machine influenced both the technological value of the resource

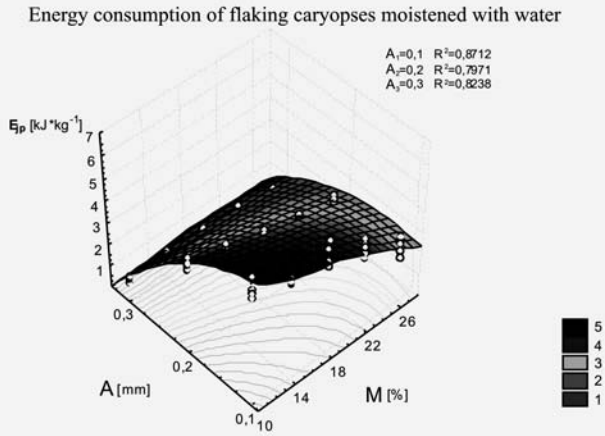

Fig. 2. The range of changes in energy consumption of the flaking process of caryopses which were moistened with water in relation to varied levels of moistness and the working aperture of the grinding machine A From the analysis of the achieved research results, which illustrate a complex pattern of connections and interrelations which occur between the conditions and parameters of oat grain moistening, flaking processes and energy consumption of these processes, it results that the variant closest to the optimum seems to be the moistening of the resource with steam for the period t_2=10 min and working aperture of the grinding machine A_2=0.2 mm

and the course of the flaking process, as well as energy consumption of flaking. The biggest influence on energy consumed for flaking was ascertained in relation to the size of the working aperture of the grinding machine. In the case of caryopses moistened with water the highest value was recorded during flaking caryopses with the working aperture A_1=0.1 mm and A_2=0.2 mm (Fig. 2). The differences in the scope of energy consumption between apertures A_1=0.1 mm and A_2=0.2 mm fluctuated from 6% (for samples with moistness M_5=18%), to 32% (for dry caryopses M=10%). For these two working apertures the value of energy consumption for grinding caryopses decreased together with an increase in their moistness. The only exception is grinding caryopses with the working aperture A_3=0.3 mm, where the lowest energy consumption, which was measured for the same level of moistness of the resource under research, was recorded.

A more favourable way, different from moistening caryopses with water before flaking, which leads to significant decrease in energy expenditures during flaking turned out to be the method of hydrothermal processing under differentiated conditions including different levels of initial moistness of the resource and time of moistening the resource with steam (Fig. 2).

The presented research results indicate that the time of moistening the grain with steam in a significant way influences the value of energy expenditures for the execution of the process of flaking, while similarly to grain moistened with water, the scope and character of changes of this parameter is reflected by complex parametric interrelations. The lowest energy demand for flaking was recorded for the variant in which the grain was moistened with steam for the period t_3=15 min and grinded in the working aperture A_2=0.2 mm and A_3=0.3 mm. In this case the demand for energy, depending on the initial moistness of the grain before steaming fluctuated within the range *8.13-8.70 kJ *kg^{-1}* (for A_2=0.2 mm) and *7.85-8.13* kJ*kg^{-1} (for the aperture A_3=0.3 mm) (Fig. 3b and c). As compared to the shortest moistening time t_1= 5 min, the demand for energy for the same sizes of the working aperture A_2=0.2 mm and A_3=0.3 mm, taken at different levels of initial moistness was *12.68-18.11 kJ*kg^{-1} and 9.21-13.22 kJ*kg^{-1}* , respectively.

The achieved, quite big differences of energy consumption of the process of flaking, related to the compared extreme values of grain moistening time (t_1=5 min and t_3=15 min), prove that longer moistening times (steaming), lead to very intensive influence of steam on the change of the internal structure of grain, and especially on its structural-chemical properties. The detailed analysis of the obtained research results with the use of Tukey's multiple comparison confidence intervals indicates that the values of means regarding energy consumption of the process of grain flaking which was moistened for a short period of time (t_1=5 min), are considerably different from mean values of this parameter for the remaining times of moistening (t_1=5 min and t_3=15 min).

Table 1. Multiple comparison confidence intervals (Tukey's test), for the two-way analysis of variance – time of caryopses moistening with steam* working aperture of the grinding machine

t_1, t_2, t_3 [min]	A [mm]	a	b	C	D	e	f
10	0.3	****					
15	0.2	****	****				
15	0.1	****	****	****			
10	0.2		****	****			
5	0.3			****	****		
10	0.1				****	****	
5	0.1					****	****
15	0.3					****	****
5	0.2						****

a,b,c,d,e,f homogeneous groups; the same literal indicator determines the lack of crucial difference between means within a given group at the level of significance α=0.05.

a)

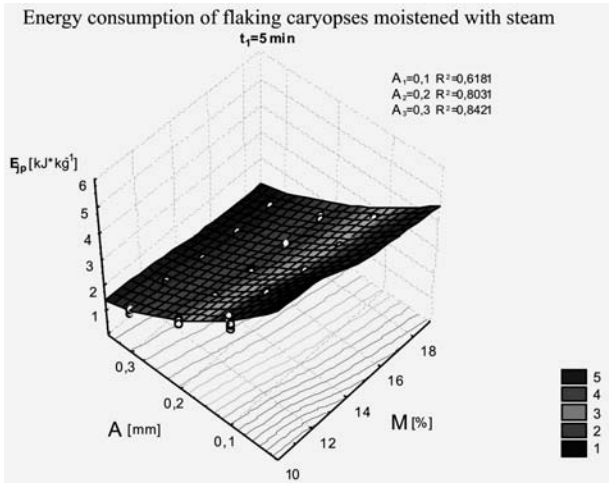

b)

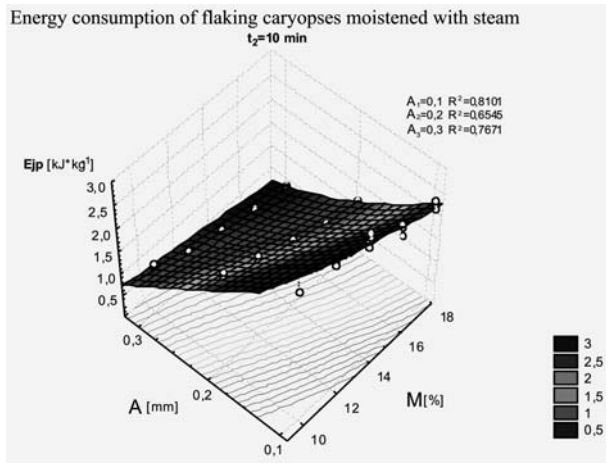

c)

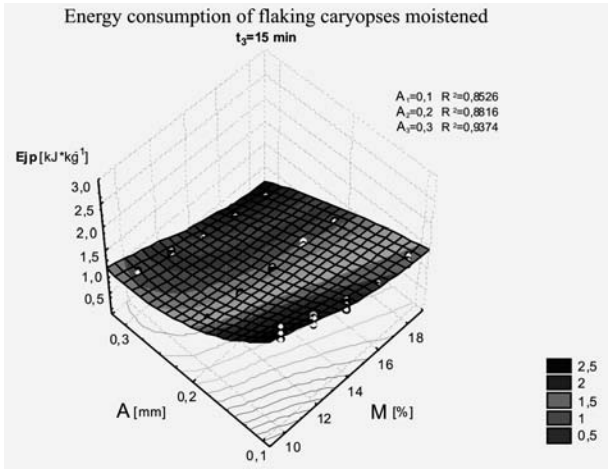

Fig. 2. Energy consumption of flaking caryopses moistened with steam in relation to the working aperture of the grinding machine A; time of moistening:

a) t_1=5 min, b) t_2=10 min c) t_3=15 min

CONCLUSIONS

After conducting the research the following conclusions were drawn up:

1. Flaking oat caryopses is a complex process whose course and energy consumption are influenced by many factors.
2. The analysis of research results regarding energy consumption of the caryopses flaking revealed a vast range of changes of this parameter, which mainly results from the diversity of the working aperture and the time of moistening and not so much from the level of the initial moistness of the resource.
3. As regards the method of moistening and parameters of hydrothermal processing, the lowest energy consumption (for research ranges) was recorded for grain moistened with steam for the period t_3=15 min (irrespective of the size of the working aperture). Shortening of moistening time caused an increase in expenditures of energy on flaking while a simultaneous, noticeable influence of initial moistness of grain was recorded.
4. The biggest influence on energy consumption of the process of flaking was ascertained in relation to the size of the working aperture, while the highest values were recorded for the aperture A_1=0.1 mm (irrespective of the time of moistening and the initial moistness). The differences in the range of changes of energy consumption between apertures A_1=0.1mm and A_2=0.2mm fluctuated from 6% (for samples of moistness M_5=18%) to 32% (for dry caryopses M_1=10%).
5. In the assessment of energy consumption of flaking (the lowest demand for energy) and the course of the process, the best effects (close to the optimum in this scope of research) were ascertained for the variant in which the time of moistening was t_2=10 min and the working aperture was A_2=0.2 mm.
6. In the case of long-term moistening of a resource with steam (t_3=15min) only slightly lower values of energy consumption, similarly to samples moistened through the period t_1=5min and t_2=10min, were achieved. Consequently, long-term and energy-consuming moistening with steam is unprofitable.
7. The conducted statistical analysis of research results, which included changes of energy during the flaking of caryopses in relation to different factors determining the process, allowed for the specifying of the full image of interrelations between these factors.

REFERENCES

1. **Frączek J., Hebda T. 2000.** Ocena sprężystości wybranych nasion na podstawie pomiaru ich twardości. Inżynieria Rolnicza 9(20), p. 73-84.
2. **Gąsiorowski H. 2000.** Wartość użytkowa owsa nagiego, Przegląd Zbożowo-Młynarski, nr 7, p. 15-16.
3. **Gąsiorowski H. 1998.** Współczesny pogląd na walory fizjologiczno-żywieniowe owsa. Przegląd Zbożowo-Młynarski, nr 12, p. 2-3.

4. **Gunsasekaran S., Farkas D.F. 1988.** High-pressure hydratation of corn. Trans. of the ASAE, Vol.31, nr 5, p. 1589-1593.
5. **Grochowicz J., Zawiślak K. 2002.** Badania porównawcze energochłonności rozdrabniania nasion w mlewniku walcowym i rozdrabniaczu bijakowym. Katedra Inżynierii i Maszyn Spożywczych, Maszynopis AR Lublin.
6. **Grundas S., i inni 1998.** Charakterystyka cech technologicznych ziarna uszkodzonego mechanicznie w wyniku nawilżania. Przegląd Zbożowo-Młynarski, nr 4, p. 23-26.
7. **Jurga R. 2001.** Przygotowanie ziarna do przemiału. Przegląd Zbożowo-Młynarski, nr 6, p. 40-43.
8. **Kiryluk J., Różycka K. 1996.** Wpływ wilgotności i zabiegów hydrotermicznych na właściwości przemiałowe owsa. Przegląd Zbożowo-Młynarski, nr 3, p. 26-27.
9. **Kowalewski W. 1998.** Wpływ surowca na jakość płatków owsianych. Poradnik Młynarza, nr 8, p. 31-32.
10. **Kowalewski W., Gąsiorowsaka T., Gąsiorowski H. 1993.** Ocena skuteczności obróbki hydrotermicznej płatków owsianych. Przegląd Zbożowo-Młynarski, nr 9, p. 14.
11. **Kowalewski W. 1998.** Technologia przerobu owsa na płatki dla zakładów małej i średniej zdolności przerobowej. Przegląd Zbożowo-Młynarski, nr 8, p. 13-16.
12. **Korpysz K., Roszkowski H. 1993.** Gniecenie-energooszczędna metoda przygotowania śruty. Przegląd Tech. Rol. i Leś. nr 3, p. 18-20.
13. **Obuchowski W., Strybe K. 2001.** Możliwość modyfikacji układu białkowego i węglowodanowego ziarna na drodze obróbko hydrotermicznej. Przegląd Zbożowo-Młynarski, nr 9, p. 14-16.
14. **Panasiewicz M. 2001.** Dobór parametrów nawilżania parą wodną surowców zbożowych. Inżynieria Rolnicza, nr 10(30), p. 269-274.
15. **Panasiewicz M., Grudziński J. 2001.** Różne metody przygotowanie owsa przed przerobem. Inżynieria Rolnicza, nr 2(22), p. 291-296.
16. Polskie Normy do oznaczania wilgotności ziarna. PN-91/A-74010.
17. **Romański J., Niemiec A. 2001.** Wpływ wilgotności ziarna pszenicy na energię rozdrabniania w gniotowniku modelowym. Acta Agrophysica 46, p. 153-158.
18. **Wojdalski J., Domagała A., Kaleta A., Janus P. 1998.** Energia i jej użytkowanie w przemyśle spożywczym. Wydawnictwo SGGW, Warszawa.

ANALIZA ZABIEGÓW OBRÓBKI WSTĘPNEJ ZIARNIAKÓW OWSA NA PRZEBIEG I ENERGOCHŁONNOŚĆ PROCESU PŁATKOWANIA

S t r e s z c z e n i e. W pracy przedstawiono wyniki badań pomiarów nakładów energetycznych procesu płatkowania obłuszczonych ziaren owsa w zależności od metody i parametrów nawilżania oraz wilgotności wyjściowej. Pomiar energochłonności określano dla poszczególnych, założonych w metodyce wielkości szczeliny roboczej gniotownika. Największy wpływ na energochłonność płatkowania stwierdzono w odniesieniu do wielkości szczeliny roboczej gniotownika. Jej najwyższą wartość odnotowano przy płatkowaniu ziarniaków przy szczelinie roboczej A_1=0,1mm. Natomiast różnice w zakresie zmian poboru mocy pomiędzy szczelinami A_1=0,1mm i A_2=0,2mm wahały się od 6% (dla prób o wilgotności M_5=18%), do 32% (dla ziarniaków suchych M_1=10%). Najbardziej korzystną metodą w odniesieniu do zużycia energii w procesie płatkowania okazało się nawilżanie ziarniaków owsa parą wodną. Niezależnie od założonego metodycznie poziomu wilgotności początkowej surowca najniższe wartości mocy idącej na ich płatkowanie uzyskiwano dla próbek nawilżanych parą przez czas t_1=5 min.

S ł o w a k l u c z o w e: nakłady energetyczne, płatkowanie, owies, obróbka hydrotermiczna.

TEKA. COMMISSION OF MOTORIZATION AND ENERGETICS IN AGRICULTURE – 2012, Vol. 12, No. 1, 201–204

The impact of intake canal geometry on kinematics of load in combustion chamber

Piotr Piątkowski

Technical University of Koszalin, Department of Mechanical Engineering,
75-620 Koszalin, Racławicka 15-17, e-mail: piotr.piatkowski@tu.koszalin.pl,

Summary. The results of analysis of technical possibilities to increase engine efficiency were presented in this article. This problem was connected with kinematics properties of air inflow to the combustion chamber. The possibilities of intake airflow modulation have a positive impact on the level of engine usable parameters and emission. This issue was presented in the results of experimental research. The results of baseline research gave information about the flow resistance. On the basis of results of experimental research conclusions were made.

Key words: supply system, engine, filling of combustion chamber.

INTRODUCTION

The efficiency of engine is the most important priority during the designing of modern engines. Those questions corresponding to the decrease of fuel consumption and decrease of impact on natural environment have become extremely important. Efficiency is also important today, where intensification of transport use has a negative impact on air clarity and economic growth is the cause for increase of fuel consumption.

The direction of sparkle ignition (SI) engine development was based on the development of automotive market and introduction of new technology which gave many new products. Now the most important aims are: the decrease of fuel consumption and fulfilling more and more radical norms of emission relating to toxic gases emissions and keeping of high level of usable engine parameters as torque and power [13].

Photochemical smoke over the city is today the „normal" effect of chemical reaction under sunrays in the big and highly industrialized cities.

In most countries the administration setup of limitation of emission was established. The toxic gases [10] are; hydrocarbons (C_nH_m), carbon monoxide (CO), nitro oxide (NO_x), molecular parts (PM) and sulfur oxide (S – mainly from the fuel pollution).

Currently, in the phase of continuous development are systems which are able to increase energy efficiency of SI engines, as well as produce better energy - ecological parameters [3,4]. By applying a combination of a few different modern constructional systems, the considerable decrease of fuel consumption and exhaust gases emission could be achieved (Fig. 1 and 2).

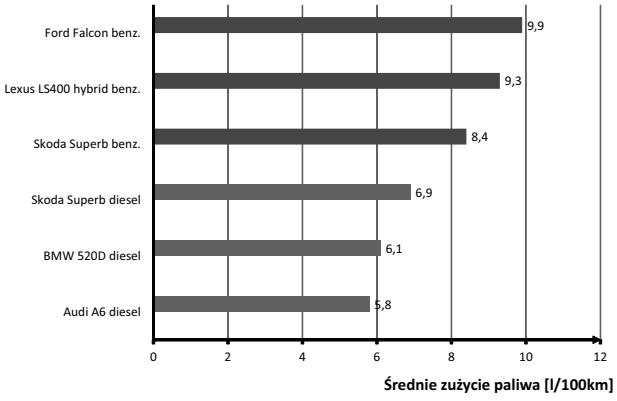

Fig. 1. The average fuel consumption by the modern cars with automatic transmission [17] (test type - ADR 81)

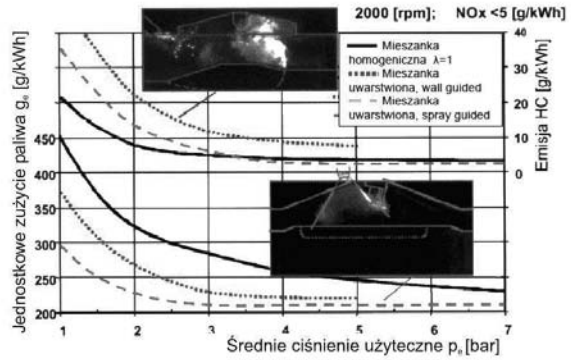

Fig. 2. Comparison of specific fuel consumption and hydrocarbons emission for GDI engine by the injection and mixture type [5]

The alternative fuels as a source of energy for the modern engine are still being developed by the quality and exploitation requirements. It can be a cause of more effective use of this fuel as renewable source of energy in the future. Except this, now we have many possibilities of adopting engine feeding system to specific properties of fuel [11, 14].

Indirect measures of these are achieved by low levels of fuel consumption and low toxic gas emissions as well as the increase (or keeping) of engine parameters like torque and power.

Many researchers [1, 8, 9, 15] were engaged in the research on the impact of intensification of vortex in combustion chamber on heat transfer in SI engine. Others were engaged in the research on the impact of turbulence on heat creation [2, 6, 16] and stabilization of burning process in piston engines [7]. The results of this type of research in different ways have indicated the impact of swirl on engine work conditions. The authors agree that the vortex has a positive impact on air-fuel mixture formation by achievement of more homogeneous form. This conclusion was made by the achievement of decrease of level emissions of carbon monoxides and hydrocarbons. Also, the increase of nitro oxide was achieved. However, the impact of vortex on heat transfer was not clear. The possibilities of intensification of preliminary swirl in intake canal are seldom mentioned in research works. This intensification can be very important in cases of;

– formation of homogenous mixture,
– low RPM level,
– engines with a relatively small capacity of one cylinder
– use of alternative fuel by engine feeding system.

EXPERIMENTAL STAND

The experimental stand was based on the real intake system of four strokes, four cylinders SI engine with displacement of 1598 cm. The diameter of intake canal for experimental stand was 34 mm. The cause of difference between engine and model was accessibility of tubes on the local market.

The effect of swirl was achieved by using the flexible element with the 65 mm length, width 32 mm and thickness 0,4 mm steel tape assembled inside the tube. The real view of this element was presented in Figure 3.

On the basis of these assumptions the airflow experimental model in the intake canal was built. The picture of experimental stand was illustrated in Figure 4.

The value of airflow resistance (Δp) was assigned on the equation;

$$\Delta p = \rho \cdot g \cdot n \cdot l \text{ [Pa]}, \tag{1}$$

where:
ρ – density of liquid in manometer [g/ccm],
g – earthly acceleration [m/s^2],
n – manometer ratio,
l – number of gradations.

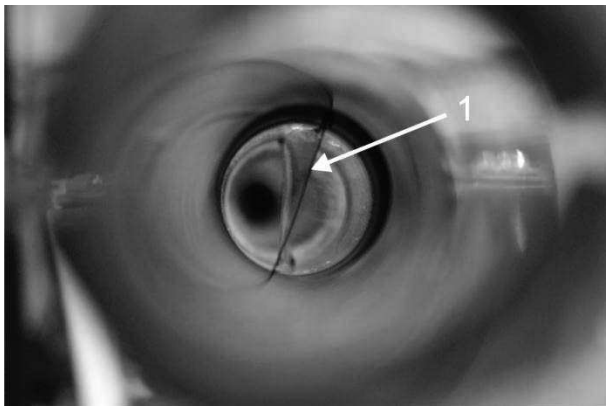

Fig. 3. The picture of canal with flexible geometry [9]; 1 – steel tape

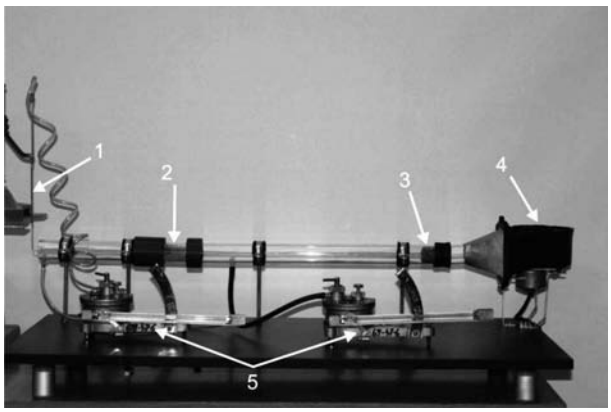

Fig. 4. The experimental stand; 1 – Prandtl's pipe, 2 – flexible tape, 3 – airflow stabilizer, 4 – ventilator, 5 – Recknagel's micro manometers

The value of velocity was achieved on the basis of dynamic pressure in two self-orthogonal plane. Measure points were based on the divided field of tube surface. The diameter of tube was divided by nine rings with 2 mm width. And so, the four measure points for each ring were achieved.

The airflow velocity (v) for each measure point was calculated by the equation:

$$v = \sqrt{\frac{2 \cdot g \cdot \rho \cdot n \cdot l}{1,3}} \text{ [m/s].} \quad (2)$$

The average value of velocity for the field of tube surface was achieved from;

$$\overline{v} = \frac{1}{A} \cdot \sum_{n=1}^{9} \frac{\left(v_{n1} + v_{n2} + v_{n3} + v_{n4}\right)}{4} \cdot A_n, \text{ [m/s],} \quad (3)$$

but:

$$A_n = \pi \cdot \frac{\left(d_{n1}{}^2 - d_{n2}{}^2\right)}{4}, \text{ [m}^2\text{],} \quad (4)$$

where:

A – field of surface of orthogonal canal intersection [m^2],

A_n – field of surface for n –ring,

n – number of the ring,

$v_{n1\div4}$ – airflow velocity for the successive n - ring and measure point,

d_{n1} – outside diameter for n – ring,

d_{n2} – inside diameter for n – ring.

THE RESULTS OF EXPERIEMENTAL RESEARCH

The research concerned the assessment of impact of flexible geometry canal on airflow velocity and flow resistance. Also changing of airflow extreme of velocity positioning was important for evaluation of velocity profile. As it was mentioned, the steel tape was a flexible element of intake canal. One end of tape was fixed to the tube by the first ring, but the second end of tape could change its position by the moving of second ring.

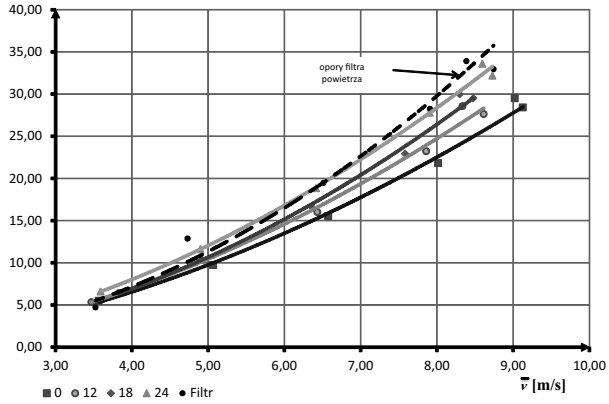

Fig. 5. The airflow resistance (Δp) by average airflow velocity ($\overline{v}$) and different angle of twist tape (0, 12, 18, i 24°) and air filter flow resistance

In this way, steel tape was twisted. The second ring was able to provide steel length compensation, too. The angle of tape twist was from 0÷24°, however the obtained average velocities were from 3,5÷9,2 m/s. The composition of experimental research results concerning the assessment of airflow resistance by average velocity and the angle of tape twist were presented in Figure 5.

A very important conclusion from analysis of Figure 5 is that the use of flexible element of intake canal has no significant impact on airflow resistance and the airflow resistance is even less than for the clear air filter flow. The difference between the lowest and the highest resistant value for the tape twist 24° for achieved airflow velocity was only a bit more than 5 Pa, while the measure deviation of airflow resistance was 0,96 Pa.

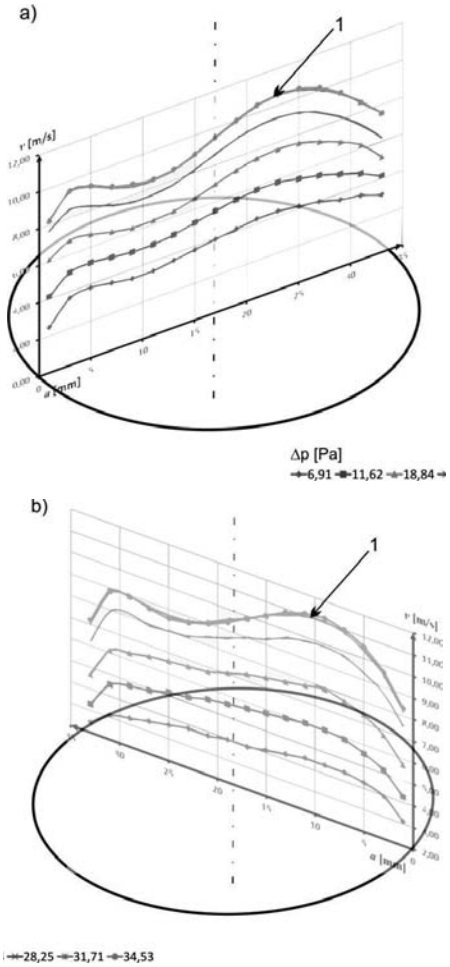

Fig. 6. The composition of velocity profiles of airflow for two mutually perpendiculars planes (a, b) inside the canal; 1 - the highest of airflow velocity (11,2 m/s)

These results are very promising for achieved change of airflow velocity profile for the cross intersection. Suitable velocity profile can help to deliver cylinder load without the meeting with valve head and the intensity of turbulence will decrease, than it can decrease filling loses.

From the analysis of results illustrated in Figure 6 we can see that by the change of angle tape's twist, the change of airflow velocity profile was achieved. It was very effective for the angle of tape twist 24°. There the two of extreme for velocity profile next to inside tube's walls appeared. This experiment can be very useful for implementation of flexible intake canal for air inflow to combustion chamber to the piston engines. In this way,

we can get not significant increase of flow resistance (about 7%). Suitable positioning of flexible element inside intake canal for intake valves has a positive impact on effect of load swirl penetration from intake's canal to the combustion chamber.

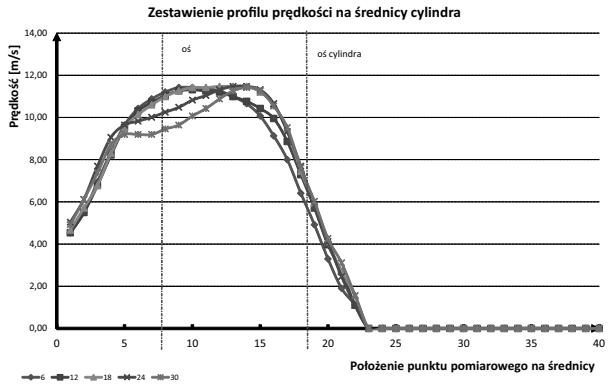

Fig. 7. The view of change of airflow velocity profile during inlet to the cylinder for parallel canal

It will be very useful for the mixture preparation. On the composition of speed profile (Fig. 6) the displacement of the minimum from the center was achieved. The cause of this was unexpected not axial deformation of tape during the twist – what will be involved during the next experimental research.

In Figure 7 the change of airflow speed profile during inlet to combustion chamber was illustrated. There we can see positive action of swirl from intake canal, which displaced of center of intake airflow to the center of cylinder. It will be very helpful from the points of view of the mixture preparation and combustion process.

CONCLUSIONS

On the basis of experimental research results the conclusions are the following;

1. Implementation of geometrically flexible element of intake canal has no significant impact on the flow resistance (it is even lesser than the impact of air filter).
2. The velocity of airflow and the angle of tape twist have impact on the kind of velocity profile change.
3. The change of airflow velocity profile can be a cause of decrease of turbulence from valve head.
4. Effect of load swirl during filling of combustion chamber have impact on achievement of better condition of mixture preparation (mixture more homogeneous)

REFERENCES

1. **Algifri AH., Bhardwaj RK, Rao YVN. 1988:** Heat transfer in turbulent decaying swirl flow in a circular pipe. Int J Heat Mass Transfer, 31(8) pp. 1563–8.
2. **Alkidas A.C. 2007:** Combustion advancements in gasoline engines, Energy Conversion&Mana-gement, 48, pp. 2751-61.
3. **Burski Z. Mijalska-Szewczak I. 2008:** Evaluation of energy-consumption in the vehicles of EU international communication infrastructure, TEKA VIIIa, Lublin.
4. **Burski Z. 2008:** Stanadrization of a vehicle's power effectiveness on the basis of indicator of similarity of speed distribution, TEKA VIII, Lublin.
5. **Friedl H., Kapus P. 2002:** Kierunki Rozwoju Silników ZI, Silniki Spalinowe 2.
6. **Fuerhapter A, Piock WF, Fraidl GK. 2003:** CSI – controlled auto ignition – The best solution for the fuel consumption – versus emission tradeoff? SAE Paper NO. 2003-01-0754.
7. **Goto Y., Narusawa K. 1996:** Combustion stabilization of spark ignition natural gas engine, JSAE Review 17, pp. 251-8.
8. **Loosley DJ. 1961:** Heat transfer from a centrally located source in a vortex flow, MSThesis, AFIT, WPAFB.
9. **Mc Kelvey R. 1960:** Heat transfer from a heated cylinder in vortex type flow, MSThesis, AFIT, WPAFB.
10. **Wasilewski J. 2008:** An influence of injection pump wear of a tractor engine on exhaust gas toxity, TEKA VIIIa, Lublin.
11. **Piątkowski P. 2007:** Wpływ parametrów zasilania w układach dwupaliwowych na efektywność energetyczną tłokowego silnika spalinowego, Rozprawa doktorska, Koszalin.
12. **Piątkowski P., Lewkowicz R. 2010:** Wpływ kinematyki ładunku napływającego do komory spalania na efektywność procesu spalania w silnikach tłokowych, Motrol nr 12, pp. 115-121.
13. **Uzdowski M. 2010:** Ekologiczne aspekty zmian konstrukcyjnych w tłokowych silnikach spalinowych, MOTROL 12, p. 158-167, Lublin.
14. **Uzdowski M. 2010:** Możliwości wykorzystania biogazu do zasilania silników spalinowych, MOTROL 12, p. 167-173, Lublin.
15. **Yilmaz M., Comakli O., Yapici S. 1999:** Enhancement of heat transfer by turbulent decaying swirl flow. Energy Conversion Manage; 40:1365–76.
16. **Zhang D., Hill P.G. 1996:** Effect of swirl on combustion in a short cylindrical chamber, Combustion and Flame 106, p. 318-332.
17. http://australian-clean-energy-facts.com.

WPŁYW GEOMETRII KANAŁU DOLOTOWEGO NA KINEMATYKĘ RUCHU ŁADUNKU W PRZESTRZENI ROBOCZEJ SILNIKA TŁOKOWEGO

S t r e s z c z e n i e. W artykule przedstawiono wyniki badań eksperymentalnych oraz analizy literatury pod względem możliwości technicznej realizacji pracy silnika z uwagi na ograniczenie emisji spalin oraz zmniejszenie zużycia paliwa. W pracy przedstawiono zagadnienia związane z możliwością wykorzystania zjawiska zawirowania ładunku na tle uzyskiwanych wartości parametrów pracy. Zamieszczone wyniki badań eksperymentalnych przeprowadzone na stanowisku modelowym pozwoliły uzyskać odpowiedź na zagadnienia oporów przepływu oraz pozwoliły określić wnioski dotyczące technicznej możliwości implementacji do silnika badawczego.

S ł o w a k l u c z o w e: układ zasilania, silnik, napełnianie, komora spalania

TEKA. COMMISSION OF MOTORIZATION AND ENERGETICS IN AGRICULTURE – 2012, Vol. 12, No. 1, 205–210

The use of icme process to design a rocker arm for special-purpose vehicles

Stanisław Pysz, Robert Żuczek[1)]

[1)]Foundry Research Institute, 73 Zakopianska St., 30-418 Krakow, Poland,
pysz@iod.krakow.pl, zuczekr@iod.krakow.pl

S u m m a r y. The conversion of elements from welded part to casting, using advanced foundry alloys gives a possibility to improve properties of newly designed construction. Application of computer techniques CAD/CAE allows to integrate the work of designers, constructors, foundrymen in one production process called ICME. In order to reduce the weight of particular suspension elements and rise of the dimensions tolerance, the high strength AlZnMgCu alloy was used on rocker arm cast. The design of the new rocker arm was based on the real steel element, complete computer analysis of exploitation environment was performed; additionally the casting technology was verified in order to produce a lower rocker arm of a special-purpose vehicle.

K e y w o r d s: numerical simulation, high strength aluminum castings, material and design conversion, suspension of mobile vehicles.

INTRODUCTION

Reducing the weight of the structure while maintaining its original functionality, or decreasing the expected maximum values of stress fields operating in individual sections of the structure contributes significantly to improved performance properties of the selected item [1,2]. The conversion of structure or of both the structure and material requires the use of most advanced materials and modern manufacturing technology, as well as close cooperation between the designer and process engineer. The world trends are aimed at significant reduction in workload of performance parts, e.g. by replacement of parts welded or bolted with monolithic cast structures. The development of modern casting technology and new alloys with improved properties significantly contribute to more vivid interest in the cast structures. The use of better and better computational models enables an integration of the materials science with the design process and making a new structure (ICME – Integrated Computational Materials Engineering) [3-7]. This provides great advantages, including shortening of the design and lead time to get a new product through a comprehensive analysis of numerous variants of the solution without the need for a costly and energy-intensive research conducted on real models.

This article presents only a part of the research using an integrated calculation process for the development of a new design of the rocker arm as a part cast from aluminium alloy.

BASIC ASSUMPTIONS

The design of the suspension system in mobile off-road vehicles implies the use of high-strength materials with a high safety factor. The examined components of the suspension system must be fully functional in every available area, and possible failure of one of the elements should guarantee continuation of the vehicle operation or possibly quick and easy replacement [8,9]. The possibility of structure and material conversion was examined on a transportation and rescue vehicle with an unladen weight not exceeding m = 3500 kg. The selected type of suspension system consists of six independently mounted wheels, including two drive wheels.

The lower rocker arm is a welded construction composed of 13 elements, and the whole structure weighs about 10.5 kg, while the upper rocker arm is welded from 9 elements and weighs approximately 8.5 kg. To make welded rocker arms, special tooling is needed to ensure the repeatability and dimensional consistency. The biggest problem is high labour input. The possibility of using casting as a replacement part is expected to considerably increase both the quality of workmanship and repeatability.

The design of a new construction of the rocker arm was based on the existing kinematic structure of the

suspension (Figure 1), with particular emphasis put on the collision-free mating of the newly developed structure with the already existing suspension components, maintaining the so far existing mounting points.

The accepted load diagrams assume a uniform distribution of forces acting on individual wheels of the vehicle during transit through the rough terrain, including the loss of stability and extreme inequality of each wheel contact with the substrate [10].

For numerical analysis, an AlZnMgCu alloy was selected. The AlZnMgCu alloys are characterised by higher mechanical properties compared to the commonly used aluminium alloys with silicon. The tensile strength R_m after heat treatment varies within the range of 400-500 MPa. The disadvantage of these alloys is definitely lower resistance to fracture and poor ductility.

The main alloying elements are zinc and magnesium. The zinc-to-magnesium ratio in these alloys is greater than unity (Zn: Mg> 1). Iron and silicon are considered impurities. Other elements such as Zr, Mn, Cr have little effect on the structure strengthening, while Ti and Be serve as grain refiners. It is also assumed that Cu, depending on the content of Zn and Mg, is strengthening the structure, improving also the stress corrosion resistance.

RESEARCH

For the strength analysis, a 3D virtual model of a single-wheel suspension system, consisting of the upper and lower rocker arms, hydroactive actuator and steering knuckle, has been designed. Figure 1 shows model of the suspension system with the rocker arms so far made from the welded steel pipes and profiles.

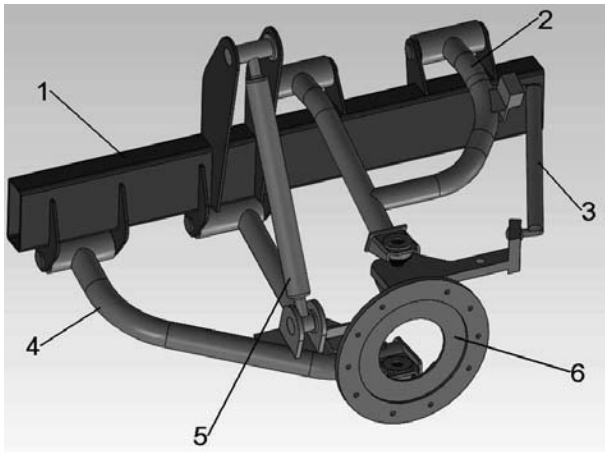

Fig. 1. Model of single-wheel suspension system in the examined vehicle: 1 – part of the vehicle frame, 2 – upper rocker arm; 3 – anti-roll bar, 4 – lower rocker arm; 5 – hydroactive actuator, 6 – steering knuckle

To identify the values of forces acting on individual nodes in the examined suspension system components, running on an experimental track with constant speed v = 15 km / h was simulated. During the simulation, maximum response values were determined for each node of the analysed fragment of the suspension system, assuming several criteria for the acting load.

Additionally, a load diagram was examined for the suspension system of the vehicle during heavy braking on concrete in such a way as to obtain a delay of 8 m/s^2.

The design of cast rocker arms was developed with reference to the technology of their manufacture, assuming three different profiles of cross-sections, i.e. channel section, horizontal T-section, and vertical T-section. Models with more cast arm profiles developed in a CAD system are shown in Figure 2.

To analyse the cast structure loading mode, it is necessary to introduce data collected for the AlZnMgCu alloy. Laboratory investigations were carried out to determine parameters such as R_m, R_{p02}, and A_5. The fatigue behaviour of the AlZnMgCu alloy was also tested using modified low cycle fatigue test (MLCF) at different levels of the cyclic loading determined by finite element method (FEM) on an MTS 810 testing machine.

Models developed for simulation were imported to ANSYS. Based on the accepted kinematic suspension scheme and the preset pattern of loads acting on the suspension system during the drive, preliminary numerical calculations were conducted for the cast lower rocker arm.

Analysis covered all the conceptual designs shown in Figure 2 and the design of a welded rocker arm. The newly developed design was analysed as a part cast from the AlZnMgCu aluminium alloy, while welded rocker arm was analysed as a steel element.

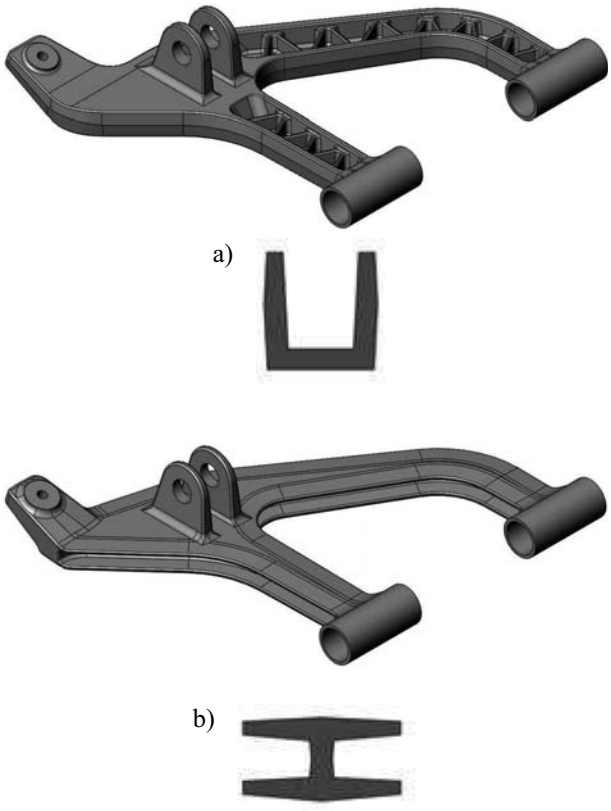

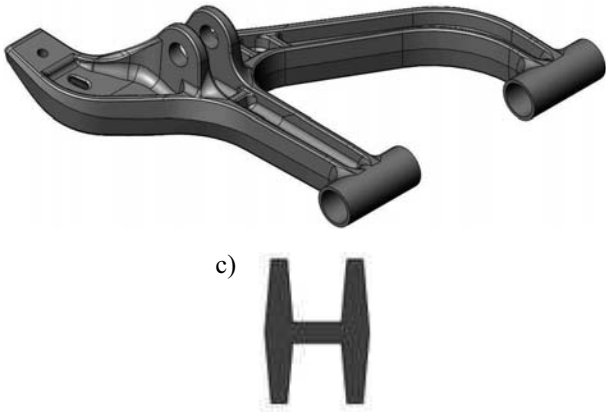

Fig. 2. 3D models of rocker arm with arm cross-sections ready for numerical analysis: a) – channel section (ribbed), b) – double-T horizontal section, c) – double-T vertical section

RESULTS

Based on CAD models, the weight of the newly developed structure was estimated and its percentage reduction relative to the actual structure of rocker arm made from prefabricated welded steel. For the designs shown in Figure 2, the obtained reduction of weight was:
– for cast channel section - 37.5%,
– for cast double-T horizontal section - 38.9%,
– for cast double-T vertical section - 29.4%.

Thus, the pre-designed structures have allowed triple weight reduction in cast component compared with the welded construction.

The results of the response of component forces in each node of the lower rocker arm set in a global coordinate system (GCS) are shown in Table 1.

Tab. 1. Responses obtained for selected loading modes at the lower rocker arm/ steering knuckle mounting point

Criterion	Component F_X,[N]	Component F_Y,[N]	Component F_Z,[N]
Loading mode I	-15 550	-7 547	14 559
Loading mode II	-12 915	-15 895	14 172
Loading mode III	-20 302	53 368	8 009
Loading mode IV	191	-10 847	9 604
Loading mode V	25 000	-5 000	-10 000

The heaviest load acting on the suspension system during simulation tests was obtained in the case of load operating on the outer surface of the wheel, i.e. in loading mode III. For the examined patterns of kinematic excitation, a maximum dynamic surplus coefficient was determined for the static vertical force operating on a wheel of approximately k_d = 2.5. Under the conditions of the dynamic loads applied, the adoption of this factor results in a higher value of the force acting on a suspension system than the force acting in the case of a quasi-static load. Then, the load acting on a single rocker arm will be twice as high as the static uniform load acting on all wheels of the vehicle [11, 12].

The algorithm for a modified low cycle fatigue test MLCF allows the estimation of mechanical properties of the material in a single test based on the results of analysis of the fatigue curve characterised by a gradually increasing value of the amplitude of force until failure of the specimen [13]. The accommodation limit R_{AK} is defined as a stress value below which the strain increment is less than or equal to 0.1%. Table 2 compares the results obtained during MLCF tests performed on rod-shaped specimens with a diameter of 6.5 mm.

Tab. 2. The mechanical properties obtained in laboratory studies for an AlZnMgCu alloy (ε_{max} – the maximum allowable strain for $20x10^6$ cycles).

Tensile strength R_m [MPa]	Elongation A_5 %	Yield strength $R_{0,2}$ [MPa]	Elastic modulus E [MPa]	Fatigue strength Z [MPa]	Accommodation limit R_{AK} [MPa]	ε_{max}
431	1.18	417	68669	159	151	0,3

Table 3 compares the data obtained for an AlZnMgCu alloy with the strength parameters of the material currently used.

Tab. 3. Basic mechanical properties of the rocker arm material adopted for the numerical analysis of a loading process

Material	Elastic modulus [MPa]	Tensile strength [MPa]	Yield strength [MPa]	Density [kg/m^3]
AlZnMgCu alloy	72000	430	417	2795
Structural steel	205000	945	890	7850

The results of calculations of the stress distribution for loading mode III are shown in Figure 3. The adopted load limit has been reduced to 400 MPa to better illustrate the distribution of the maximum stress fields in a welded steel rocker arm and in the preliminary cast structure design.

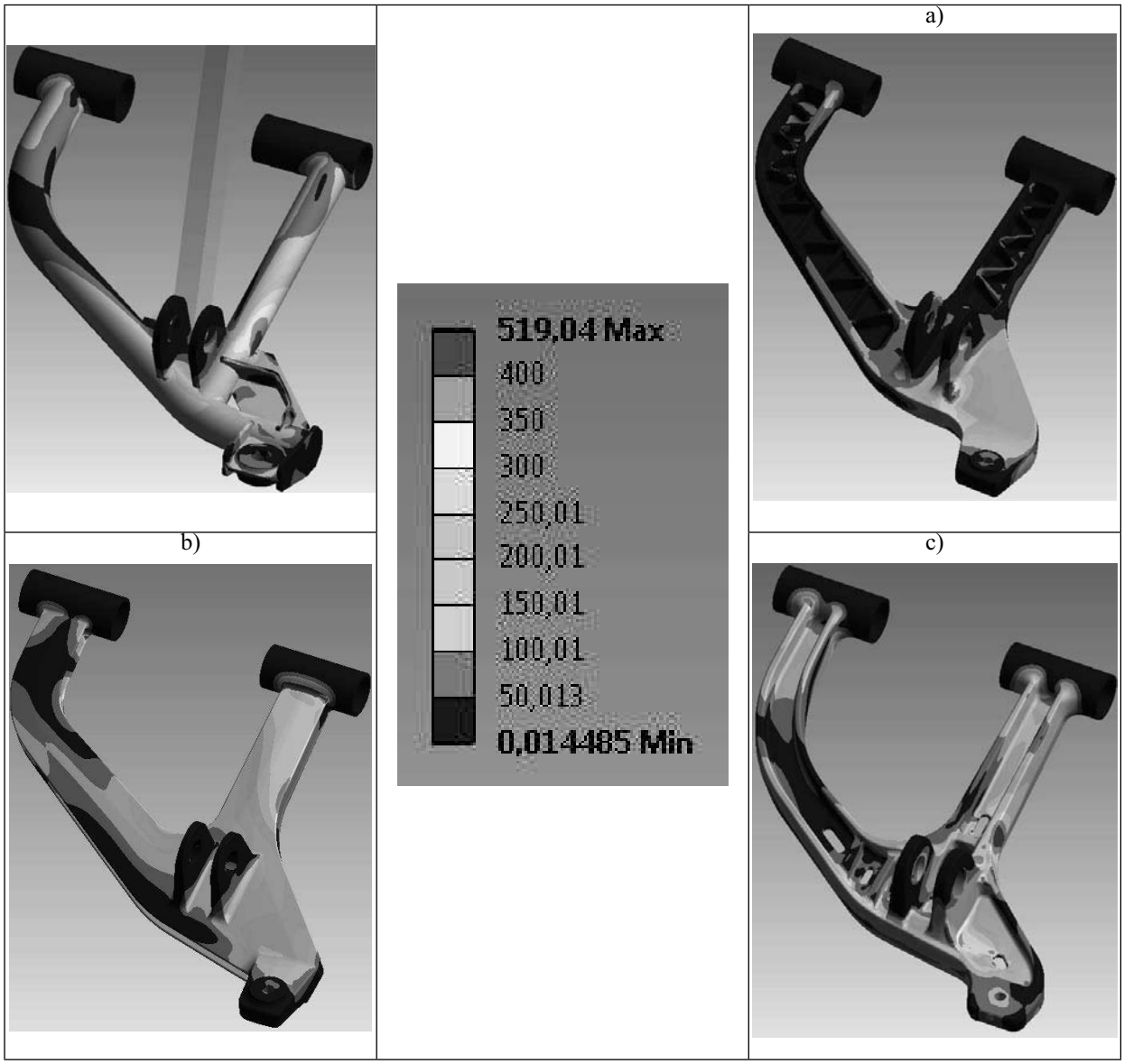

Fig. 3. Analysis of stress distribution in a welded steel rocker arm and in the conceptual cast structure design for loading mode III

Calculations have shown that, given the casting process potentials and the effect of the proposed cross-section shape on the distribution of the maximum stress field values, an optimal shape has the design of a double-T vertical profile (model c in Fig. 2). The design optimisation in terms of the reduced weight of an element while maintaining at the same level the expected maximum stress values or, if possible, reducing them in a substantial way, helped to decrease the weight of the cast aluminium rocker arm to 7.9 kg, which means a 25% reduction in weight obtained on a single element [14].

The maximum reduced stress values (according to von Mises), occurring in the sensitive areas of the analysed structure of the lower rocker arm casting, determined for each loading mode, are compared in Table 4, while distributions of the stress field values are shown for selected loading modes in Figure 4.

Tab. 4. Maximum stress values for different loading modes

	Loading mode I	Loading mode II	Loading mode III	Loading mode IV	Loading mode V
Maximum stress [MPa]	189	198	301	131	221

The maximum displayed values of the stress fields have been reduced to 150 MPa to enhance the visibility of the most overloaded areas.

The next step in an optimisation of the geometry of the converted lower rocker arm design allowed reducing the maximum values of stresses occurring in the casting during loading at a given dynamic surplus coefficient. The maximum values of stresses occurring in the original welded design of the lower rocker arm, estimated from the results of numerical analysis (Figure 2), reached the values

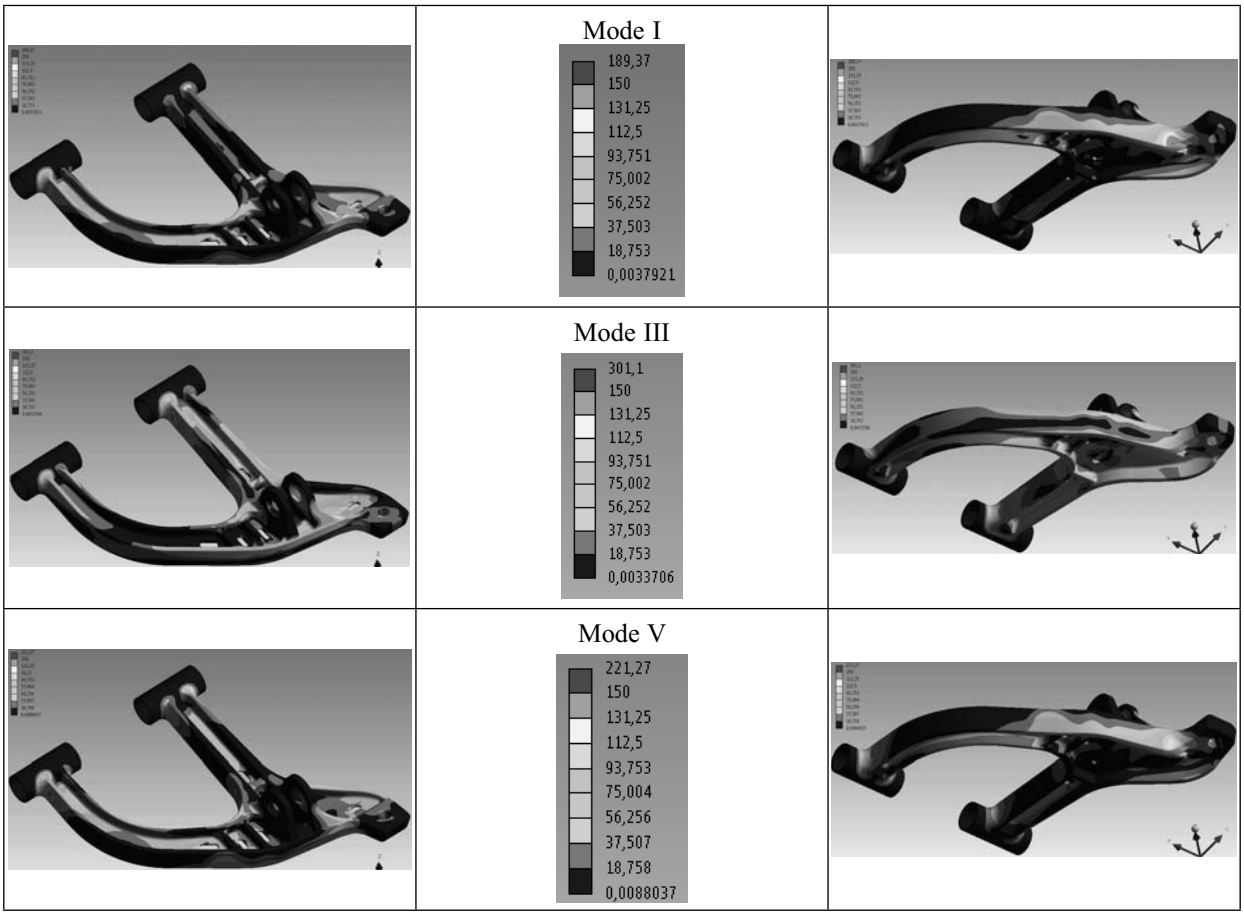

Fig. 4. Distribution of the generalised stress fields for selected loading modes after the reduction of casting weight

of about 520 MPa for loading mode III. In the case of the rocker arm cast from an AlZnMgCu alloy, the maximum stress values for the same loading mode were 301 MPa. As the analysis shows, the maximum stress in the newly developed structure constitutes about 72% of the yield strength, whereas in the case of the welded construction, this value constituted about 60% of the yield strength.

An analysis of the distribution of maximum stresses shows that, at the adopted loading modes, stresses are concentrated in the predetermined areas of controlled damage, i.e. precisely there where they were expected to occur, without affecting the rocker arm and actuator mounting points.

The newly designed cast rocker arms were introduced to the suspension model and tested for a collision-free cooperation of the whole system. Figure 5 shows a CAD model of the suspension system with the newly designed rocker arms.

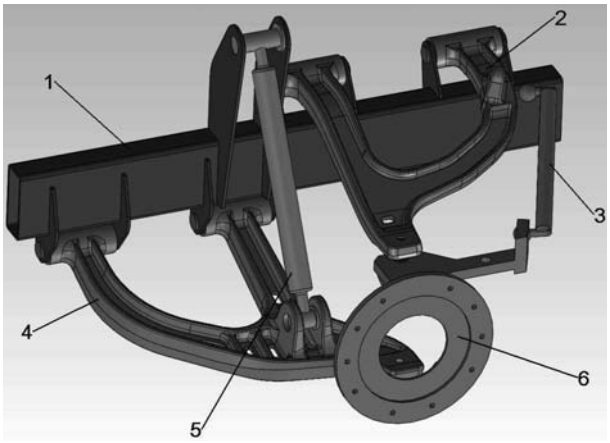

Fig. 5. Model of single-wheel suspension system in the examined vehicle with the newly designed cast rocker arms

CONCLUSIONS

1. Based on numerical calculations, the design of a rocker arm was developed, whose cross-section is a double-T vertical profile.
2. The maximum value of reduced stresses (von Mises) for the most unfavourable loading mode is 300 MPa, which represents 72% of the yield strength of an AlZnMgCu alloy.
3. The maximum stress location is in the areas of the preset controlled damage, and thus in the areas where damage can occur without affecting the rocker arm and actuator mounting points.
4. Optimising the design and the use of aluminium alloys for cast parts enabled reducing the weight to 7.9 kg, i.e. by 25%, compared with the welded structure.
5. The conducted analysis shows that the developed cast rocker arm design meets the performance requirements adopted for special-purpose vehicles.

REFERENCES

1. **Wasilewski J. 2006:** An analysis of smoke emissions from a rape biofuel fed tractor engine, TEKA, Polish Academy of Sciences, vol. VI, p. 169-174.
2. **Kozak M., Merkisz J. 2005:** The mechanics of fuel sulphur influence on exhaust emissions from diesel engines, TEKA, Polish Academy of Sciences, , vol. V, p. 96-106.
3. **Allison J., Li Mei, Wolverton C., Su XuMing 2006:** Virtual Aluminum Castings: An Industrial Application of ICME, JOM, November.
4. **Allison J., Backman D., Christodoulou L. 2006:** Integrated Computational Materials Engineering: A New Paradigm for the Global Materials Profession, JOM, Nov.
5. **Allison J.E.:** Integrated Computational Materials Engineering (ICME): The Next Big Thing in Structural Materials, Ford Research and Advanced Engineering, Ford Motor Company, Dearborn, MI 48124.
6. **Allison J.E. 2010:** Integrated Computational Materials Engineering (ICME) for Mg : International Pilot Project, Ford Motor Company, April.
7. **Warrick R. J., Althoff P., Druschitz A. P., Lemke J. P., Zimmerman K. 2000:** Austempered Ductile Iron Castings for Chassis Applications, Society of Automotive Engineers, 2000 World Congress, Detroit, March 6–9.
8. **Pysz S., Karwiński A., Czekaj E. 2009:** An analysis and comparison of properties of Al-Si alloy automotive castings made by rapid prototyping and standard lot production, TEKA, Polish Academy of Sciences, vol. V, p. 251-258.
9. **Pirowski Z., Gościański M. 2009:** Konstrukcja i technologia wytwarzania odlewanych lemieszy do pługów obracalnych i zagonowych, MOTROL – Motoryzacja i Energetyka Rolnictwa, Lublin, t. 11, p. 159-167.
10. **Wierciński J. i inni 1985:** Wypadki drogowe - elementy analizy technicznej i opiniowania, WKiŁ Warszawa.
11. **Petrov L., Yakovenko A., Melnik A., Nowak J. 2009:** Working out the equation of the „Graviment" tractor movement by the method Ostrogradsky-Jacoby, TEKA, Polish Academy of Sciences, , vol. V, p. 240-243.
12. **Burski Z, Krasowska-Kołodziej H. 2012:** Modelling of the kinetic energy loss in a vehicle on the basis of cumulative frequency of speed profile parameters, Econtechmod, vol. 1, no 2, Lublin-Lviv-Cracow, p. 3-7.
13. **Maj M., Piekło J. 2009:** MLCF-an optimised program of low - cycle fatigue test to determine mechanical properties of cast materials, Archives of Metallurgy and Materials, Vol. 54 (2), p. 393-397.
14. **Żółkiewicz Z., Zółkiewicz M. 2009:** Lost foam process – the chance for industry, TEKA, Polish Academy of Sciences, vol. V, p. 431-436.

WYKORZYSTANIE ZINTEGROWANEGO SYSTEMU PROJEKTOWANIA DO OPRACOWANIA KONSTRUKCJI WAHACZA DLA POJAZDU SPECJALNEGO PRZEZNACZENIA

S t r e s z c z e n i e . Zamiana elementów spawanych na jednolite konstrukcje odlewane, przy zastosowaniu nowoczesnych tworzyw odlewniczych przyczynia się do poprawy właściwości użytkowych nowoopracowanej konstrukcji. Wykorzystanie nowoczesnych technik komputerowych pozwala zintegrować działania konstruktorów, technologów i wykonawców poszczególnych elementów w ujednoliconym procesie ICME. W opracowanej konstrukcji wahacza zastosowano wysokowytrzymały stop AlZnMgCu, w celu obniżenia masy poszczególnych elementów zawieszenia i zwiększenia dokładności wymiarowej uzyskanych konstrukcji wahacza. Przeprowadzone badania obejmowały zakres opracowania nowej konstrukcji na podstawie istniejącego elementu stalowego wraz z szeregiem analiz wytrzymałościowych i weryfikacji komputerowej opracowanej technologii odlewania dla wahacza dolnego stosowanego w pojazdach specjalnego przeznaczenia.

S ł o w a k l u c z o w e : symulacje numeryczne, wysokowytrzymałe odlewy aluminiowe, konwersja materiałowo-konstrukcyjna, zawieszenie pojazdów mobilnych.

TEKA. COMMISSION OF MOTORIZATION AND ENERGETICS IN AGRICULTURE – 2012, Vol. 12, No. 1, 211–218

Efficiency of biomass energy used for heating purposes in a residential building in comparison with other energy sources

Grzegorz Redlarski, Janusz Wojdalski**, Adam Kupczyk**, Janusz Piechocki****

* Gdansk University of Technology, Faculty of Control and Electrical Engineering, Department of Mechatronics and High Voltage Engineering
** Warsaw University of Life Sciences, Faculty of Production Engineering, Department of Production Management and Engineering
*** University of Warmia and Mazury in Olsztyn, Faculty of Technical Sciences, Department of Electric and Power Engineering

Summary. This paper discusses the results of analyses investigating the energy efficiency of biomass in comparison with other popular energy carriers used for heating, ventilation and water heating in residential buildings. The compared energy sources were lignite, natural gas, heating oil and electricity produced by conventional and integrated power generation plants. The most efficient variant relying on biomass and the least efficient variant that involves electricity generated by a conventional power plant were described in detail for the harsh climate zone of Suwałki region in Poland (climate zone V).

The demand for energy in a residential building was analyzed, taking into account six variants of heating. Primary energy consumption ranged from 82.65 kWh×(m^2×year)$^{-1}$ for biomass to 481.05 kWh×(m^2×year)$^{-1}$ for electric energy generated in the grid system. Intermediate values were obtained for the other energy carriers analyzed in the study. Biomass-generated energy accounts for approximately 17% of the primary energy from the public grid that is needed to power the studied building.

Key words: biomass, energy efficiency, residential building, primary energy carriers, microgeneration.

SYMBOLS AND ABBREVIATIONS

A_f – heated area in a building or apartment, m^2,
c_w – specific heat of water - 4.19 kJ×(kg×K)$^{-1}$,
$E_{el,pom,H}$ – annual demand for final electric energy to supply auxiliary heating and ventilation devices, kWh×(year)$^{-1}$,
$E_{el,pom,W}$ – annual demand for final electric energy to supply auxiliary water heating devices, kWh×(year)$^{-1}$,
EK – index of annual demand for final energy in a building, kWh×(m^2×year)$^{-1}$,
EP – index of annual demand for primary energy in a building, kWh×(m^2×year)$^{-1}$,
j.o. – unit of reference (person),
k_t – correction factor for hot water temperature other than 55°C,
L_i – number of units of reference (persons)
$Q_{H,nd}$ – demand for energy in a residential building, kWh×(year)$^{-1}$,
$Q_{H,gn}$ – monthly indoor heat gain and solar gain, kWh×(month)$^{-1}$,
$Q_{H,ht}$ – monthly heat loss caused by heat transfer and ventilation, kWh×(month)$^{-1}$,
q_{int} – thermal load of premises with indoor gain, W×m^{-2},
Q_{int} – monthly indoor heat gain, kWh×(month)$^{-1}$,
$Q_{K,H}$ – annual demand for final energy in heating and ventilation systems, kWh×(year)$^{-1}$,
$Q_{K,W}$ – annual demand for final energy in the water heating system, kWh×(year)$^{-1}$,
Q_P – annual demand for primary energy in heating, ventilation, water heating systems and auxiliary devices, kWh×(year)$^{-1}$,
$Q_{P,H}$ – annual demand for primary energy in heating and ventilation systems, kWh×(year)$^{-1}$,
$Q_{P,W}$ – annual demand for primary energy in the water heating system, kWh×(year)$^{-1}$,
Q_{s1} – solar gain through windows in vertical partitions, kWh×(month)$^{-1}$,
Q_{s2} – solar gain through roof windows, kWh×(month)$^{-1}$,
Q_{sol} – solar gain, kWh×(month)$^{-1}$
$Q_{W,nd}$ – demand for water heating energy, kWh×(year)$^{-1}$,
t_M – number of hours per month, h×(month)$^{-1}$,
t_{UZ} – operating time (day),
V_{CWi} – unitary daily consumption of hot water, dm^3×(day×j.o.)$^{-1}$,
w_{el} – index of non-renewable primary energy expenditure required to generate and supply electric energy to the analyzed building,
w_H – index of non-renewable primary energy expenditure required to generate and supply heating energy to the analyzed building,
w_W – index of non-renewable primary energy expenditure required to generate and supply water heating energy to the analyzed building,

$\eta_{H,d}$ – annual seasonal distribution efficiency of a heat carrier in a building,
$\eta_{H,e}$ – annual seasonal efficiency of heat control and heat consumption in a building,
$\eta_{H,g}$ – annual seasonal efficiency of heat generation from the energy supplied to a building's boundary layer (final energy),
$\eta_{H,gn}$ – heat gain index in heating mode,
$\eta_{H,s}$ – mean annual efficiency of heat storage in capacitators of the building's heating system (within or outside the boundary layer),
$\eta_{H,tot}$ – total efficiency of a building's heating system,
$\eta_{W,d}$ – mean annual efficiency of hot water distribution in a building,
$\eta_{W,e}$ – mean annual heat efficiency (equal to 1.0),
$\eta_{W,g}$ – mean annual efficiency of heat generation from the energy supplied to a building's boundary layer (final energy),
$\eta_{W,s}$ – mean annual efficiency of hot water storage in capacitators of the building's hot water system (within or outside the boundary layer),
$\eta_{W,tot}$ – total efficiency of the water heating system,
Θ_{CW} – hot water temperature in the feed valve, 55°C,
Θ_{O} – cold water temperature, 10 °C,
ρ_{W} – water density, 1000 kg×m^{-3}.

INTRODUCTION

The looming danger of depletion of non-renewable energy sources, rapid climate change, the advances made in technologies that rely on alternative energy sources, including biomass [11, 19, 25], and environmental pollution [5, 28] spur new research into the energy efficiency of biomass [1, 2, 3, 14, 25, 27]. The Act on Energy Efficiency of 15 April 2011 (Journal of Laws No. 94, item 551) defines energy efficiency as *the ratio of total energy input to a building, machine or equipment under standard operating conditions to the amount of energy consumed by that building, machine or equipment to deliver the anticipated effect*. In this paper, the concept of energy efficiency is understood as the amount of non-renewable primary energy required to meet heating, ventilation and hot water needs of a building. The methodological aspects of energy efficiency have been discussed in detail by Patterson [20]. According to the law of energy conservation in a closed system, generation capacity (or reserve energy from an energy store) is needed for the required amount of energy to be supplied to a recipient at any given moment. This requirement is apparently easy to fulfill, but in practice, it is fraught with numerous technical, logistic and transport problems. To illustrate, the transport of large quantities of raw materials, such as bituminous coal, lignite, crude oil, natural gas or biomass (Table 1), requires complex logistic (coordination of deliveries), transport (geographic distance) and technical (infrastructure) processes. Those requirements often pose a substantial barrier due to high investment costs, ineffective distribution systems or environmental concerns [10].

In view of the above, the energy efficiency of various sources should be analyzed in a broader context. The selection of optimal generation methods and energy sources requires comprehensive evaluations [13] that account for legal and economic aspects [8, 9], physical properties [12]

Table 1. Percentage of primary energy sources used in Poland

No.	Year / Energy source	2000	2005	2007	2008	Unit
1	**Bituminous coal**					
	Domestic consumption	84890	78722	84587	80415	×10^6 kg
	Consumption in electric power plants, CHP plants and heat plants	51628	50903	52937	48968	×10^6 kg
2	**Lignite**					
	Domestic consumption	59487	61589	57528	59371	×10^6 kg
	Consumption in electric power plants, CHP plants and heat plants	59149	61075	56895	58646	×10^6 kg
3	**Crude oil**					
	Domestic consumption	18081	18191	20024	21036	×10^6 kg
4	**Methane-rich natural gas**					
	Domestic consumption	10119	12694	12728	13036	hm^3
	Household consumption	3052	3414	3341	3347	hm^3
5	**Nitrogen-rich natural gas**					
	Domestic consumption	3028	3514	3535	3386	hm^3
	Household consumption	699	450	462	432	hm^3

Source: Own study based on [Directive 2002/91/CE]

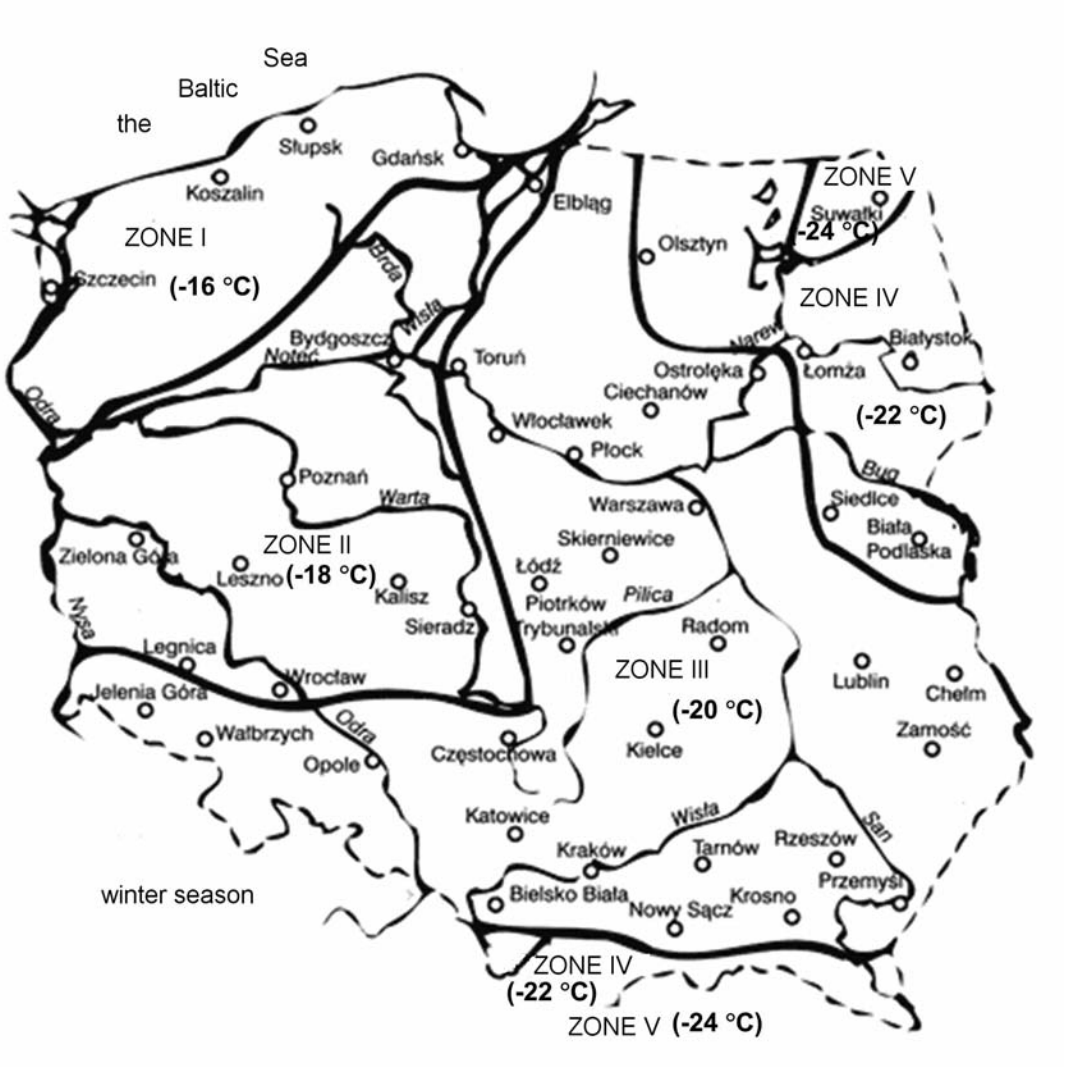

Fig. 1. Climate zones in Poland in the winter season, from October to March (as per standard PN-76/B-03420)

and the latest technological solutions [6, 7]. Alternative sources of energy should play an important part in this process, especially because they eliminate logistic and transport concerns in the generation process (energy is generated at the site of use). Unconventional energy sources should deliver additional benefits to justify their use. At present, alternative sources of energy have a low output, therefore, their use is generally limited to small buildings or sites with low energy requirements.

According to the available data, Polish housing and service sectors are responsible for more than 40% of final energy consumption, and this value is growing. The above can be attributed to the relatively low level of awareness about energy saving measures and energy performance of residential buildings. The energy efficiency of biomass and other energy sources under severe climatic conditions has never been compared in Polish literature.

The objective of this study was to present and discuss the results of energy efficiency analyses of biomass and popular energy carries used for heating purposes in a typical single-family house. The article focuses on both scientific and utilitarian aspects of the analyzed problem. The materials and methods are overviewed in the first part of this paper, whereas the second part discusses the results and proposes practical solutions.

MATERIALS AND METHODS

The energy efficiency analysis of the Polish housing sector was performed on the example of a typical single-family house (Table 2) in the city of Suwałki (this information is needed to calculate solar gains) in Poland's most energy-intensive climate zone V (Fig. 1).

The reference building used in this study was a single-family, two-storey house inhabited by a family of five (this information is needed to determine hot water demand). The structure and technical systems in the analyzed building were consistent with the requirements and guidelines of the relevant laws, in particular the Regulation of the Minister of Infrastructure of April 2009 amending the regulation on the technical requirements set for buildings and their surroundings (Journal of Laws of 7 April, 2009, No. 75, item 690).Various calculations were performed to

determine the benefits delivered by the analyzed energy sources in the building (Table 2) [21, 22, 23, 24]. The calculation procedure was consistent with the provisions of the Regulation of the Minister of Infrastructure of 6 November 2008 on the calculation methodology for determining the energy performance of a building or an apartment or a part of a building that constitutes a technically integral whole and the manner of developing energy performance certificates and templates (Journal of Laws of 2008, No. 201, item 1240).

In line with the above regulation, the demand for energy is determined by a number of factors, including thermal insulation of walls, structural parameters, performance of energy supply systems and functional properties (for example, the number of inhabitants, temperatures and air exchange rates in the building). An analysis of demand for energy from various sources (at a constant level of energy consumption in the building) supports the determination of differences in primary energy expenditures, defined as the amount of non-renewable energy supplied by technical systems, for heating, ventilation and water heating purposes in the building.

Table 2. Main parameters of the analyzed building.

Building parameters	
Built-up area	116 m^2
Cubic capacity	535.1 m^3
Net floor area with controlled temperature	184.6 m^2
Location	climate zone V
Air-conditioning system	none
Ventilation system	natural
Cubic capacity of heated rooms	458.6 m^3

The measured parameters were expressed as follows:

– index of annual demand for final energy in the building:

$$EK = (Q_{K,H} + Q_{K,W}) \cdot A_f^{-1},$$

– primary energy index:

$$EP = Q_p \cdot A_f^{-1},$$

– total efficiency of the building's heating system:

$$\eta_{H,tot} = \eta_{H,g} \cdot \eta_{H,s} \cdot \eta_{H,d} \cdot \eta_{H,e},$$

– total efficiency of the water heating system:

$$\eta_{W,tot} = \eta_{W,g} \cdot \eta_{W,s} \cdot \eta_{W,d} \cdot \eta_{W,e},$$

– annual demand for final energy in heating and ventilation systems:

$$Q_{K,H} = Q_{H,nd} \cdot \eta_{H,tot}^{-1},$$

– annual demand for final energy in the water heating system:

$$Q_{K,W} = Q_{W,nd} \cdot \eta_{W,tot}^{-1},$$

– annual demand for primary energy in heating and ventilation systems:

$$Q_{P,H} = w_H \cdot Q_{K,H} + w_{el} \cdot E_{el,pom,H},$$

– annual demand for primary energy in the water heating system:

$$Q_{P,W} = w_W \cdot Q_{K,W} + w_{el} \cdot E_{el,pom,W}$$

– annual demand for primary energy:

$$Q_P = Q_{P,H} + Q_{P,W},$$

– solar gain:

$$Q_{sol} = Q_{s1} + Q_{s2},$$

– monthly indoor heat gain:

$$Q_{\text{int}} = q_{\text{int}} \cdot A_f \cdot t_M \cdot 10^{-3},$$

– annual demand for water heating energy:

$$Q_{W,nd} = V_{CWi} \cdot L_i \cdot c_w \cdot \rho_W \cdot$$
$$\cdot (\Theta_{CW} - \Theta_O) \cdot k_t \cdot t_{UZ} \cdot (1000 \cdot 3600)^{-1},$$

– annual demand for heating and ventilation energy:

$$Q_{H,nd} = \sum\nolimits_n (Q_{H,ht} - \eta_{H,gn} \cdot Q_{H,gn}).$$

The discussed method may be applied to analyze the consumption of primary energy from various sources and to evaluate the resulting benefits. The following variants were analyzed to determine the demand for primary energy and energy consumption in the studied building:

– *variant* 1 – the source of energy for central heating and water heating systems was lignite with calorific value of 2.680 kWh/kg (9.648 MJ/kg),
– *variant* 2 – the source of energy for central heating and water heating systems was grid electricity,
– *variant* 3 - the source of energy for central heating and water heating systems was biomass with calorific value of 4.280 kWh/kg (15.408 MJ/kg),
– *variant* 4 – the source of energy for central heating and water heating systems was natural gas with calorific value of 9.970 kWh/m^3 (35.892 MJ/m^3),
– *variant* 5 – the source of energy was heat produced in an integrated cycle combining lignite firing in the central heating system with solar energy supplied by thermal solar collectors in the water heating system,

– *variant* 6 – the source of energy for central heating and water heating systems was heating oil with calorific value of 10.080 kWh/l (36.288 MJ/l).

RESULTS

Owing to the vast abundance of material produced by the analyses (*variant* 1 ÷ *variant* 6), only two extreme cases (representing the highest – *variant* 2, and the lowest – *variant* 3, consumption of primary energy) are described in the successive parts of this paper. For easier interpretation, the obtained results were sorted in view of the adopted technical configuration, i.e. they were described separately for heating and ventilation systems and the water heating system. The results illustrating the demand for heating and ventilation energy and water heating energy are presented in Table 3.

Table 3. The results of heat calculations for the analyzed building.

Results of heat calculations for the analyzed building	
Air flow rate	566.5 $m^3 \times h^{-1}$
Seasonal demand for heat	26330.9 $kWh \times year^{-1}$
Index of seasonal demand for heat	57.4 $kWh(m^3 \times year)$
Shape factor	0.7 m^{-1}
Limiting factor of seasonal demand for heating energy	34.5 $kWh \times (m^3 \times year)^{-1}$
Solar gain	9561.1 $kWh \times year^{-1}$
Indoor solar gain	430.1 $kWh \times year^{-1}$
Annual demand for water heating energy	2408.73 $kWh \times year^{-1}$

Source: own study

BIOMASS ENERGY

The results of comprehensive calculations that account for the use of auxiliary energy to power circulating pumps in the central heating system and automated boiler controls clearly indicate that biomass energy is the most efficient of the analyzed variants (with the lowest consumption of primary energy at 82.65 $kWh \times (m^2 \times year)^{-1}$). The input values and the results of the analysis of the heating and ventilation system are presented in Table 4. The results reported for the water heating system are shown in Table 5.

The physical parameters representing the demand for primary energy relative to a unit of area in the evaluated building constitute important information in the light of the Regulation of the Minister of Infrastructure (2008) [23, 22]. The value, percentage share and demand for primary energy for heating, ventilation, water heating and auxiliary devices are given in Table 6. The calorific value and the use of various types of biomass have also been discussed by [15, 16, 17].

Table 4. Use of biomass energy for heating and ventilation in the analyzed building

Input values		
1	Energy carrier	Fuel - biomass
2	Selected generation variant	Biomass (straw) boiler with rated output of up to 100 kW, manually operated
3	Selected control variant	Water-circulating heating system with column or panel radiators – in a central heating system
4	Selected transmission variant	Water-circulating heating system with a local generation source and insulated installation
5	Selected storage variant	No buffer tank
6	Overall system efficiency	0.49
Results of analysis		
1	Demand for final energy	53859.63 $kWh \times year^{-1}$
2	Demand for auxiliary energy	1107.6 $kWh \times year^{-1}$
3	Demand for primary energy	14094.73 $kWh \times year^{-1}$

Source: own study

Table 5. Use of biomass energy for the water heating system

Input values		
1	Energy carrier	Fuel - biomass
2	Selected generation variant	Low-temperature boiler with rated output of up to 50 kW
3	Selected control variant	Centrally controlled water heating system with circulation, limited operating time and full piping insulation
4	Selected transmission variant	Small systems with up to 30 water supply points
5	Selected storage variant	Energy-efficient water tank
6	Overall system efficiency	0.58
Results of analysis		
1	Demand for final energy	4167.92 $kWh \times year^{-1}$
2	Demand for auxiliary energy	108.82 $kWh \times year^{-1}$
3	Demand for primary energy	1160.05 $kWh \times year^{-1}$

Source: own study

Table 6. Demand for primary energy in the analyzed building

No.	Primary energy	Heating and ventilation	Hot water	Auxiliary devices	Total
1	Value [kWh×(m^2×year)$^{-1}$]	58.36	4.52	19.77	82.65
2	Share [%]	70.61	5.46	23.92	100

Source: own study

The high share of primary energy needed to power auxiliary devices in the building (Table 6) results from the use of automatic control systems which are supplied solely by grid electricity.

GRID ELECTRICITY

The use of grid electricity is the least energy efficient variant which requires the highest expenditure of primary energy (481.05 kWh×(m^2×year)$^{-1}$). Detailed data for the applied technologies and the reported demand for heating and ventilation energy are presented in Table 7. The input values and the noted results for the water heating system are shown in Table 8 (solutions that would increase the overall demand for energy in the building were not analyzed).

Table 7. Use of grid electricity for heating and ventilation in the analyzed building

Input values		
1	Energy carrier	Electricity – integrated generation
2	Selected generation variant	Electric heaters: convection, surface and radiation heaters, electric floor heating
3	Selected control variant	Electric heaters: convection, surface and radiation heaters
4	Selected transmission variant	Heat source in the room
5	Selected storage variant	No buffer tank
6	Overall system efficiency	0.97
Results of analysis		
1	Demand for final energy	27139.66 kWh×year^{-1}
2	Demand for auxiliary energy	0 kWh×year^{-1}
3	Demand for primary energy	81418.98 kWh×year^{-1}

Source: own study

Table 8. Use of grid electricity for the water heating system

Input values		
1	Energy carrier	Electricity – integrated generation
2	Selected generation variant	Electric storage heater (with lossless storage tank)
3	Selected transmission variant	Water is heated locally at supply points. No water circulation in the system.
4	Selected storage variant	No tank
5	Overall system efficiency	0.98
Results of analysis		
1	Demand for final energy	2457.88 kWh×year^{-1}
2	Demand for auxiliary energy	0 kWh×year^{-1}
3	Demand for primary energy	7373.65 kWh×year^{-1}

Source: own study

The demand for primary energy in the studied building is presented in Table 9, separately for every type of energy use.

Table 9. Demand for primary energy in the analyzed building

No.	Primary energy	Heating and ventilation	Hot water	Auxiliary devices	Total
1	Value [kWh/(m^2×year)]	441.10	39.95	0	481.05
2	Share [%]	91.70	8.30	0	100

Source: own study

The results shown in Table 9 indicate that nearly 92% of energy is used for heating and ventilation, and that the relevant energy expenditure is more than seven times higher in comparison with the biomass variant (Table 6). Such a high demand for electricity can be attributed to a high index of renewable energy expenditure which is set at 3.0 pursuant to the cited Regulation of the Minister of Infrastructure (2008). The above solution was probably introduced by the legislator with the aim of reducing electricity consumption in residential buildings because the public power grid has a relatively low generation efficiency (0.36 ÷ 0.44). High levels of consumption deplete non-renewable sources of energy (mostly coal) and significantly increase harmful emissions to the natural environment, including CO_2 emissions.

CONCLUSIONS

The two extreme cases analyzed in this study were biomass, an unconventional source of energy (with pri-

mary energy consumption of 82.65 kWh×(m^2×year)$^{-1}$), and electricity supplied by the public power grid (with primary energy consumption of 481.05 kWh×(m^2×year)$^{-1}$). With regard to the remaining energy carriers, energy consumption values were noted in between the above extremes. The results reported for all tested variants are compared in Figure 2. This comparison points out at significant variations in the quantity of primary energy needed to supply identical residential buildings. Biomass-generated energy accounts for only 17% of the primary energy from the public grid that is needed to power identical buildings. The above fact implies that the demand for primary energy can be reduced by approximately 83%. Measures aiming to economize energy consumption would be particularly valuable in sites located far from generation sources because they would eliminate transfer losses [18]. Such solutions would also limit the depletion of primary energy sources and lower harmful emissions to the environment.

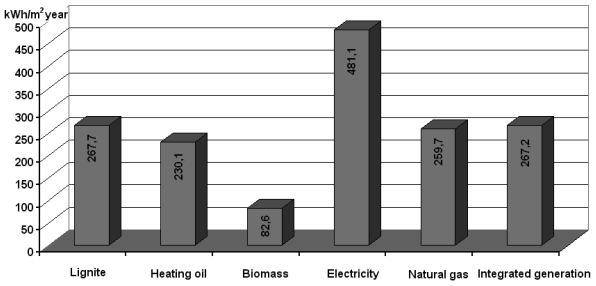

Fig. 2. Primary energy consumption values for all the analyzed variants in a residential building.

Source: own study.

Due to accelerating climate changes and their adverse consequences, the search for the most efficient sources of energy will be a key global challenge in the coming years. The efficiency of energy carriers used for heating, ventilation and water heating in residential buildings is an issue of particular concern. The results of analyses examining the most popular to the most technically demanding solutions (*variant* 1 ÷ *variant* 6), also in the harshest climate zone (V), indicate that biomass is the most efficient energy carrier. The results of our analysis can significantly contribute to planning processes in agriculture and the power industry by illustrating that the consumption of primary sources of energy can be modified and, consequently, economized. They can also provide a valuable input for administrative decisions regarding preferential treatment for selected energy-saving solutions and sources of renewable energy.

REFERENCES

1. **Balat M. 2007:** An Overview of Biofuels and Policies in the European Union. Energy Sources. Part B: Economics. Planning. and Policy. 2: 2. p. 167-181.
2. **Bartnik R. 2009:** Elektrownie i elektrociepłownie gazowo parowe. Efektywność energetyczna i ekonomiczna. WNT. Warszawa (pp. 256 p.).
3. **Demirbas A. 2007:** Modernization of Biomass Energy Conversion Facilities. Energy Sources. Part B: Economics. Planning. and Policy. 2: 3. p. 227-235.
4. Directive 2002/91/CE of the European Parliament and of the Council of 16 December 2002 on the energy performance of buildings (OJ L001. p. 65. 2003). http://www.nape.pl (retrieved in January 2012).
5. **Gustavsson L. Joelsson A. 2007:** Energy conservation and conversion of electrical heating systems in detached houses. Energy and Buildings. 39. p. 717-726.
6. **Horyński M. 2008:** Heating system control in an intelligent building. TEKA Kom. Mot. i Energ. Roln. 8. p. 83-88.
7. **Horyński M. 2009:** Reasonable energy management in an intelligent building. TEKA Kom. Mot. i Energ. Roln. 9. p. 78-84.
8. **Izdebski W. Osiak J. Skudlarski J. 2010a:** Economical aspects of straw briquettes production. TEKA Kom. Mot. i Energ. Roln.. 10. p. 101-106.
9. **Izdebski W. Osiak J. Skudlarski J. 2010b:** Residential building heating costs using the energy from grain combustion.. TEKA Kom. Mot. i Energ. Roln. 10. p. 107-111.
10. **Izdebski W. Osiak J. Skudlarski J. 2010c:** The organizational and economical aspects of thermal energy production from grain biomass for the needs of individual farms. TEKA Kom. Mot. i Energ. Roln.. 10. p. 112-117.
11. **Kowalska A. 2010:** Overview of technological methods of energy production from biomass. TEKA Kom. Mot. i Energ. Roln.. 10. p. 209-215.
12. **Kraszkiewicz A. 2008:** Ocena ciepła spalania i wartości opałowej wybranych sortymentów drewna robinii akacjowej na tle klas grubości. MOTROL – Motoryzacja i Energetyka Rolnictwa. 10. p. 67-72.
13. **Kupczyk A. Piechocki J. Kupczyk M. 2011:** Rozwój biogazowi rolniczych w Polsce na tle wykorzystania odnawialnych źródeł energii. Gospodarka Materiałowa i Logistyka. 1. p. 24-30.
14. **Marecki J. 2001:** Perspektywy rozwoju elektroenergetyki w Polsce do 2020 yearu. Komitet Problemów Energetyki przy Prezydium PAN. Gdańsk.
15. **Niedziółka I. Szymanek M. 2010:** An estimation of physical properties briquettes produced from plant biomass. TEKA Kom. Mot. i Energ. Roln. 10. p. 301-307.
16. **Niedziółka I. Zuchniarz A. 2006:** Analiza energetyczna wybranych rodzajów biomasy pochodzenia roślinnego. MOTROL – Motoryzacja i Energetyka Rolnictwa. 8A. p. 232-237.
17. **Niedziółka I. Szymanek M. Zuchniarz A. Zawiślak K. 2008:** Characteristics of pellets produced from selected plant mixes. TEKA Komisji Motoryzacji i Energetyki Rolnictwa. 8. p. 157-162.
18. **Niernsee M. 2010:** Kryteria doboru lokalizacji nowych elektrowni węglowych – praktyczne podejście w warunkach polskich. Energetyka. 1. p. 83-88.
19. **Osiak J. Skudlarski J. Izdebski W. 2009:** Assessment of profitability levels of agricultural biomass production for purposes of the professional energy sector. TEKA Kom. Mot. i Energ. Roln. 9. p. 205-210.

20. **Patterson M.G. 1996:** What is energy efficiency? Concepts. indicators and methodological issues. Energy Policy. vol. 24. 5. p. 377-390.
21. PN-76/B-03420.1978: Wentylacja i klimatyzacja. Parametry obliczeniowe powietrza zewnętrznego. Polski Komitet Normalizacji i Miar. Wyd. II. Warszawa 1978.
22. PN-EN ISO 13790:2008. Energetyczne właściwości użytkowe budynków – obliczanie zużycia energii do ogrzewania i chłodzenia. Polski Komitet Normalizacyjny. Warszawa 2008.
23. Rozporządzenie Ministra Infrastruktury z dnia 6 listopada 2008 w sprawie metodologii obliczania charakterystyki energetycznej budynku i lokalu mieszkalnego lub części budynku stanowiącej samodzielną całość techniczno-użytkową oraz sposobu sporządzania wzorów i świadectw ich charakterystyki energetycznej (Dz. U. z 2008 r. Nr 201. poz. 1240). Http://isap.sejm.gov.pl (dostęp: styczeń 2012).
24. Rozporządzenie Ministra Infrastruktury z dnia 12 marca. 2009a. zmieniające rozporządzenie w sprawie warunków technicznych. jakim powinny odpowiadać budynki i ich usytuowanie (Dz. U. z dnia 7 kwietnia 2009)Http://isap.sejm.gov.pl (dostęp: styczeń 2012).
25. **Ruszel. M. 2009:** Polish Perspective of Climate and Energy Package. New-Energy. 4. p. 5-8.
26. **Stolarski M. Krzyżaniak M. Graban Ł. 2011:** Evaluation of energy-related and economic aspects of heating a family house with dendromass in the north-east of Poland. Energy and Buildings. 43. p. 433-439.
27. **Unal H. Alibas K. 2007:** Agricultural Residues as Biomass Energy. Energy Sources. Part B: Economics. Planning. and Policy. 2: 2. p. 123-140.
28. **Upton B. Miner R. Spinney M. Heath L.S. 2008:** The greenhouse gas and energy impacts of using wood instead of alternatives in residential construction in the United States. Biomass and Bioenergy, 32. p. 1-10.

WYDAJNOŚĆ ENERGII BIOMASY STOSOWANEJ DO CELÓW GRZEWCZYCH W BUDYNKU MIESZKALNYM W PORÓWNANIU Z INNYMI ŻRÓDŁAMI ENERGII

S t r e s z c z e n i e. W artykule omówiono wyniki analiz badających efektywność energetyczną biomasy w porównaniu z innymi popularnymi nośnikami energii wykorzystywanymi do ogrzewania, wentylacji i ogrzewania wody w budynkach mieszkalnych. Porównywane źródła energii to: węgiel brunatny, gaz ziemny, olej opałowy i energia elektryczna produkowana przez konwencjonalne i zintegrowane elektrownie. Najbardziej efektywny wariant wykorzystujący biomasę i najmniej efektywny wariant oparty na energii elektrycznej wytworzonej przez konwencjonalną elektrownię zostały szczegółowo opisane dla strefy nieprzyjaznego klimatu Suwalszczyzny w Polsce (klimat strefa V).

Zapotrzebowanie na energię w budynku mieszkalnym było analizowane, biorąc pod uwagę sześć wariantów ogrzewania. Zapotrzebowanie energii zawierało się w zakresie od 82,65 $kWh\times(m^2\times rok)^{-1}$(w przypadku nośnika energii - biomasy) do 481,05 $kWh\times(m^2\times rok)^{-1}$) (energia elektryczna – wytworzona w systemie elektroenergetycznym). Pozostałe nośniki energii dotyczą stanów pośrednich. Biomasa stanowi około 17% energii pierwotnej, która byłaby wymagana do zasilenia budynku, w przypadku jej doprowadzania z krajowego systemu elektroenergetycznego.

S ł o w a k l u c z o w e: biomasa, wydajność energetyczna, budynek mieszkalny, nośniki energii, mikrowytwarzanie.

TEKA. COMMISSION OF MOTORIZATION AND ENERGETICS IN AGRICULTURE – 2012, Vol. 12, No. 1, 219–224

Influence of keratin addition on selected mechanical properties of TPS film

Andrzej Rejak[1], Leszek Mościcki[1], Agnieszka Wójtowicz[1], Tomasz Oniszczuk[1], Marcin Mitrus[1], Bożena Gładyszewska[2]

Department of Food Process Engineering[1], Department of Physics[2], Lublin University of Life Sciences
ul. Doświadczalna 44, 20-280 Lublin; e-mail: andrzej.rejak@up.lublin.pl

Summary. The aim of this study was to investigate the influence of process parameters of extrusion-cooking of thermoplastic starch (TPS) enriched with keratin hydrolyzate on selected physical properties of packaging films obtained. TPS granulates were processed using single screw extrusion-cooker TS-45 (Polish design). The mixtures of raw materials contained: starch, glycerin and hydrolyzed keratin. The obtained granulates were finally processed by film blowing process in a plastic extruder, especially designed in the Department of Food Process Engineering of University of Life Sciences in Lublin. Mechanical tests of films were performed to evaluate strain and elongation during extension tests.

Key words: starch, film, keratin, extrusion, blowing, strain, elongation.

INTRODUCTION

The increasing demand for disposable packaging contributed to the significant development of the packaging market, but also created a problem with its utilization after use. A particular difficulty makes plastic materials, whose large amounts are polluting the natural environment. The antidote is recycling, but it carries a large cost and requires adequate segregation of waste.

Nowadays, the problem of ecology is the leading theme in EU countries. There is a clear trend that aims to replace a variety of materials for their organic counterparts. This phenomenon is reflected also in packaging sector. Currently the leading product as packaging material is a plastic film, whose main ingredients are polypropylene, polyethylene and other plastics, which are totally indecomposable in the environment. The solution to the problem of disposals of such material is the use of biodegradable materials through photochemical transformation with chemical or biological reagents. More and more scientists are looking for materials that are both degradable and durable and have become an alternative to plastics.

The best ecological way to reduce packaging waste is the production of biodegradable packaging materials [6, 8]. The initial step in the process of biodegradation of conventional plastics packaging can be done by modifying the material or the additive having the capacity to absorb solar radiation [9, 21]. Recently has been introduced on an industrial scale production of packaging materials made from polyolefin polymers with modified starch, otherwise known as thermoplastic starch (TPS) [1, 2 3]. They belong to a generation of biodegradable materials based on natural resources.

Starch is relatively cheap raw material and completely biodegradable [3, 4]. Materials from the starch exhibit a tendency to brittleness unfortunately, are not resistant to water and over time lose their mechanical properties due to the process of recrystallization [11]. Starch may be plasticity by baro-thermal treatment provided with the appropriate mix of plasticizers [12, 13, 18, 19, 20].

MATERIALS AND METHODS

Tests of TPS film blowing and its physical properties measurements were conducted in the laboratories of Department of Food Process Engineering (DFPE) of University of Life Sciences. The obtained granulates were finally processed on a laboratory production lines, specially designed in FPED, produced by SAVO Wiązowna, using a film blowing technique (Fig. 1).

The basic raw materials for production of biodegradable films were: potato starch "Superior" of ZPZ Łomża, technical glycerin of ZPCH Lublin and an emulsifier - keratin hydrolyzate produced by "Proteins" Łódź. Compositions of mixtures used in the experiments are presented in Table 1.

Fig. 1. Film blowing equipment [8]

TPS granulates were processed using a modified single screw extrusion-cooker TS-45 (Polish design), with L/D = 16, the screw speed varied from 40 to 80 rpm and the temperature in the range 70–120°C. Determination of selected physical properties of TPS granulates was helpful in order to establish the range of temperatures and screw speed during film extrusion.

Table 1. Recipes of granulates applied for biodegradable film blowing

Sample	Potato starch [%]	Glycerine [%]	Keratin [%]
SGK-1	78	20	2
SGK-2	75	20	5
SGK-3	70	20	10

During the extrusion with blowing of TPS the film sleeves were obtained with different diameters and thicknesses, depending on the composition of the TPS granulates, extrusion-blowing temperature range (59-130°C) and the screw rotation (60, 70 and 80 rpm). During the tests the die-mold with a nozzle diameter of 80 mm and the working slot of 1 mm was used.

The obtained films were evaluated to mechanical properties tests, during which the specified breaking force and elongation were measured [15, 16, 17]. Strength tests were carried out on Zwick universal testing machine type BDO-FBO0.5TH (Ulm, Germany) (Fig. 2). During multiple measurements followed properties of film samples were determined: σM - maximum strain, σB - strain at break, εM - elongation at maximum strain, and εB - elongation at break [5, 7, 14]. Test strips (length of 100 mm and width of 20 mm) were cut from the film depend on recipe. Tests samples were prepared longitudinal and transversal to the direction of film blowing. The measurements were conducted in five replications. Results were analyzed with Statistica 6.0 [10] according to keratin addition and screw speed used..

Fig. 2. Universal testing machine type Zwick BDO-FB0.5TH.

RESULTS

Different film sleeves were obtained depending on the composition of TPS granulates and process parameters. Film extrusion-blowing conditions depend on keratin addition are shown in Table 2.

Table 2. Processing parameters of biodegradable film blowing

Sample	Screw speed [rpm]	Motor load [A]	Temperature of extruder sections [°C]						
			Barrel				Die-head		
			I	II	III	IV	1	2	3
SGK-1	60	8.6	59	76	118	109	92	112	111
	70	8.6	69	73	117	119	115	107	103
	80	9.7	67	73	117	119	120	122	110
SGK-2	60	9.1	61	72	120	124	120	120	108
	70	9.1	62	71	122	123	114	119	104
	80	9.1	61	70	120	121	112	117	103
SGK-3	60	8.2	60	75	124	123	118	119	107
	70	8.2	65	80	128	120	110	110	105
	80	9.3	61	75	128	123	115	108	107

All the obtained films were flexible; very good properties presented films processed with different screw rotation on the base of SGK-1 and SGK-2 granulates, in which the keratin was added respectively in 2 and 5%. Films obtained from these granulate characterized good flexibility during blowing, had a semi-transparent color and after cooling remained relatively resilient, with no crumbling. Satisfactory results were also obtained during the extrusion-blowing of films with application of granulates with 10% of keratin, however the film was very soft, which greatly impeded their blow.

After blowing, all the film samples were tested to determine a tensile strain and elongation during extension. Film samples were analyzed not only according to keratin

addition level and varied screw speed during the extrusion-blowing, but also depend on direction of cutting of samples for tensile tests: longitudinal and transversely to the direction of film blowing. Films obtained from SGK-1 and SGK-2 granulates were characterized by good flexibility as well during blowing as the tests of strength. These films have high resistance to rupture, as evidenced by the breaking force values are illustrated in Figure 3, higher than in other examined samples of films, both the tensile samples cut transversely and longitudinally to the direction of extrusion.

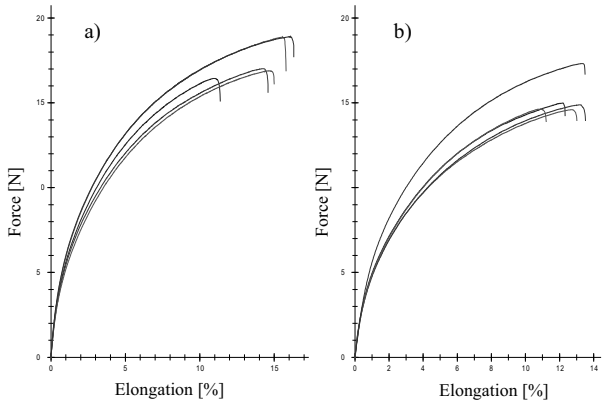

Fig. 3. Breaking force and elongation during extension test of a) longitudinal and b) transversal samples of SGK-1 film processed at 60 rpm

The results of measurements of maximum tensile strain of the transversal film samples during extension tests depending on the screw rotation used and keratin participation in a mixture of raw materials are shown on the Figure 4. Maximum strain values were 4.23-4.67 MPa in the transversal samples of films with 2% of keratin in the formulation of TPS granulates. Increasing the amount of keratin to 10% decreased the maximum strain to the level of 1.75-2.28 MPa. The significant dependence of screw speed during extrusion the maximum strain on the was not observed in this case.

Maximum tensile strain valuesdetermined by extension test of the longitudinal samples were similar, ranged from 1.61-2.08 MPa for films SGK-3 with 10% addition of keratin to 3.31-5.24 MPa for films SGK-1 with 2% addition of keratin (Fig. 5). Increasing share of keratin in the formulations caused a decrease in the maximum strain of the samples. The use of high screw rpm increased the maximum strain of the longitudinal film samples during extension.

Figure 6 shows the results of measurements of the strain at break during extension test of transversal film samples. The values of this parameter were slightly lower than the maximum strain and ranged from 1.57 to 4.40 MPa, depending on the screw rotation used during the extrusion and the amount of keratin in TPS granulates.

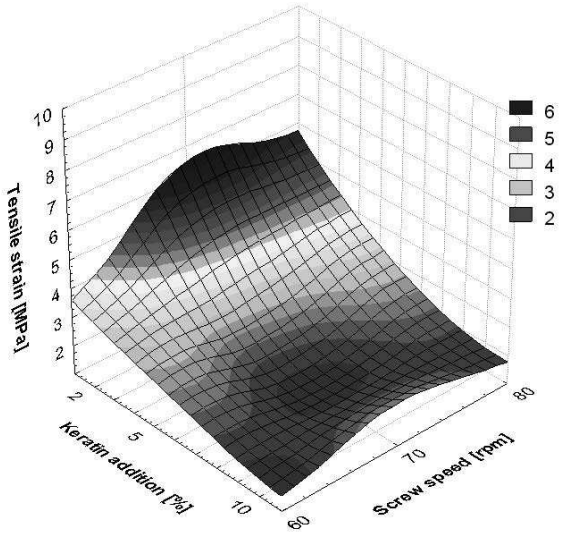

Fig. 5. Maximum tensile strain σM at longitudinal samples during extension test

There was a tendency to reduce strain during breaking with increasing addition of keratin, as evidenced by negative correlation coefficients determined for this feature.

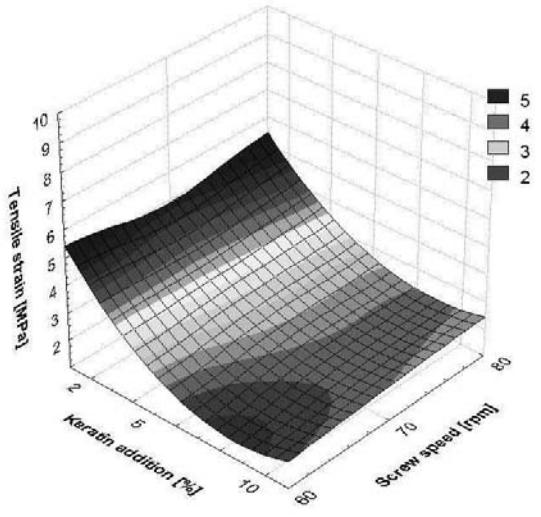

Fig. 4. Maximum tensile strain σM at extension test of transversal samples

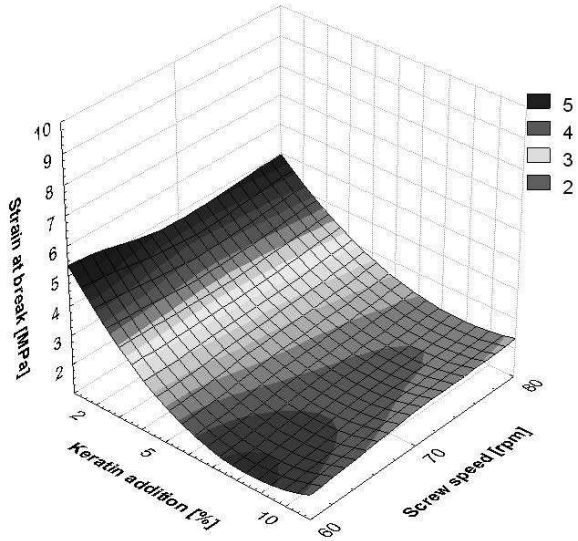

Fig. 6. Tensile strain at break σB at extension test of transversal samples

The results of measurements of film strain at break during longitudinal extension in the direction of extrusion-blowing are summarized in Figure 7. For longitudinal samples higher values were indicated than for transversal samples. In attempts at SGK-1 containing 2% of keratin, decrease of a strain at break was observed with increasing screw speed during extrusion. The opposite tendency was observed for other samples, when a small increase in strain was noted at higher screw speed applied during film production.

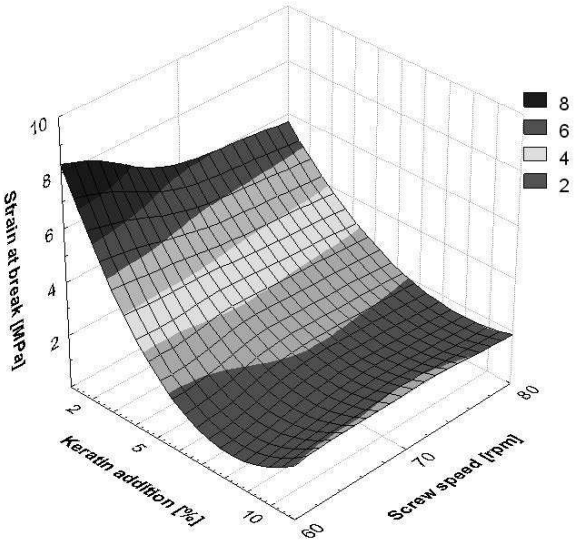

Fig. 7. Tensile strain at break σB at longitudinal samples during extension test

Differentiated relationships were observed during determination of the film elongation, according to the sample direction, the content of keratin and screw rotation used during production. Figure 8 shows the results of measurements of the maximum film elongation for transversal samples to the direction of its extrusion-blowing.

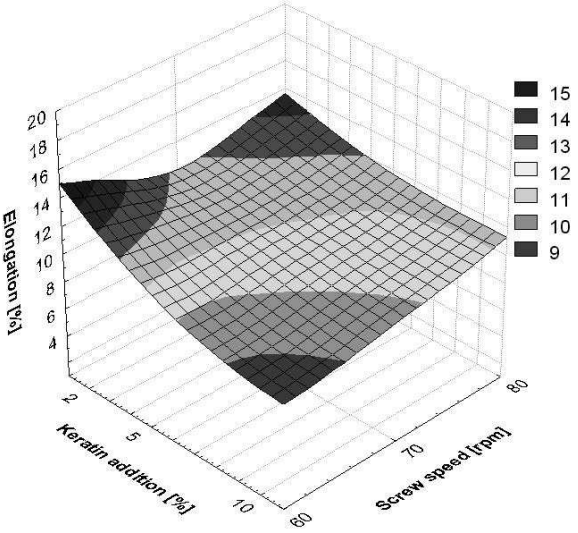

Fig. 8. Maximum elongation at extension test of transversal samples

Elongation of the films ranged from 8.62 to 13.83%, and the maximum flexibility was measured for SGK-1 film containing 2% addition of keratin, produced at low screw speed. Similar results of maximum elongation of film samples cut longitudinal to the extrusion direction were obtained (see Figure 9). The values obtained according to the addition of keratin and screw rotation used during extrusion showed that again, the lowest keratin addition in the recipe allowed for greater flexibility of films. The elongation for this sample ranged from 10.89% when using 60 rpm during extrusion to 13.84% at a maximum screw speed. The results obtained for the sample of SGK-3 are presented on the Figure 10.

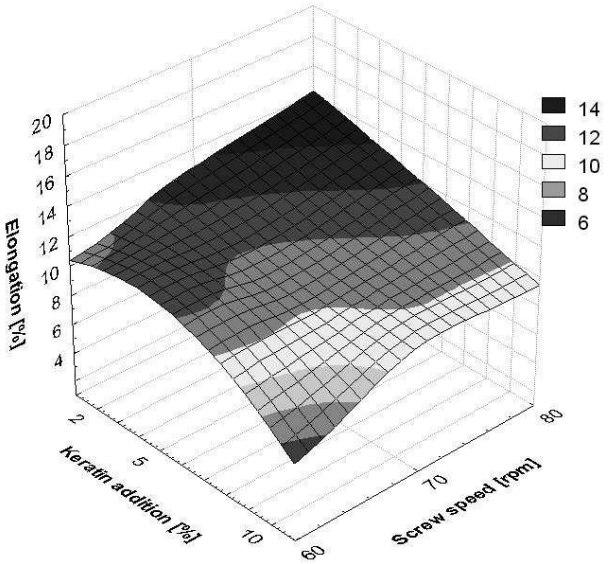

Fig. 9. Maximum elongation at extension test of longitudinal samples

The lowest elongation both for samples selected across and along the direction of extrusion was noted with a film obtained by using low screw rotation and with the greatest participation of keratin in the formulation. Also for this film the lowest value of the breaking force was measured (not exceeding 10 N). Large keratin addition weakened the internal structure of the film that was less flexible (elongation 6-8%) and less resistant to damage.

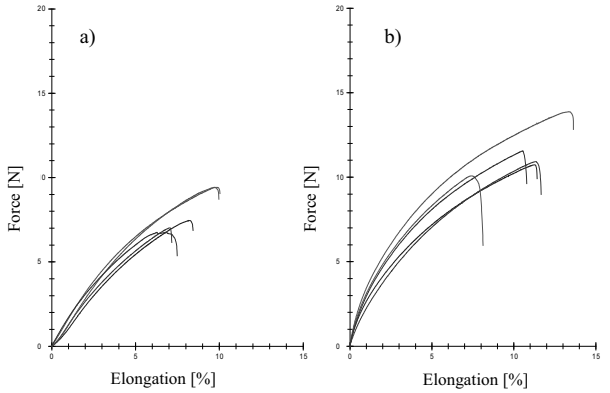

Fig. 10. Breaking force and elongation of a) longitudinal and b) transversal samples during extension test of SGK-3 film processed at 60 rpm

The results of measurements of the film elongation at break during extension of transversal samples depended on the applied processing screw speed and the amount of the additive are presented on the Figure 11. Elongation at break ranged from 8.22 to 13.75%, as previously the highest elongation characterized films produced at the highest screw speed and the lowest addition of keratin. Increasing the screw speed during extrusion-blowing affected the flexibility of film and higher elongation values of all the samples reached for longitudinal samples along the direction of film extrusion.

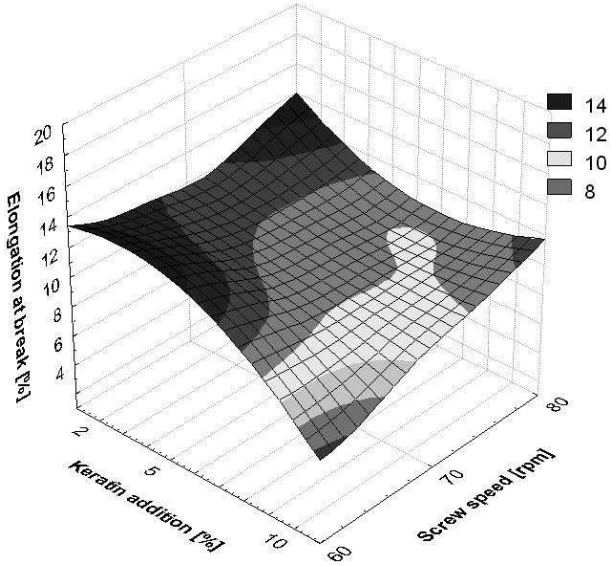

Fig. 11. Elongation at break εB at transversal samples during extension test

The values of this parameter were slightly lower than for samples cut transversal to the film sleeve blowing direction. The results of the elongation at break of film are summarized on the Figure 12.

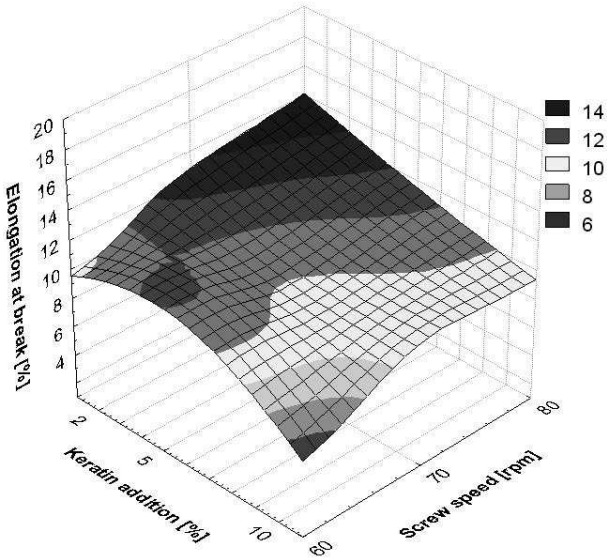

Fig. 12. Elongation at break εB at longitudinal samples during extension test

Analysis of the results showed that at 5 and 10% addition of keratin increasing maximum strain - σM and strain at break - σM for transversal films during extension tests were observed with increasing a screw speed during extrusion, as evidenced by high values of correlation coefficients in Table 3.

For the film samples containing 2% of keratin there was unclear effect of the screw rotation speed on the studied properties. While the results of elongation during extension tests indicated an increase the maximum elongation - εM and elongation at break - εB during tests of longitudinal samples of blow film with increasing screw speed.Increasing content of keratin in the blends of raw materials affected the lowering of the value of all parameters, as evidenced by negative correlation coeffi-

Table 3. Correlation coefficients of the mechanical properties of TPS film depending on the content of keratin

Keratin [%]	σM at trans-versal extension	σM at longitudinal extension	σB at trans-versal extension	σB at longitudinal extension	εM at trans-versal extension	εM at longitudinal extension	εB at trans-versal extension	εB at longitudinal extension
2	0,397	0,797	-0,309	-0,952	-0,318	0,990	-0,364	0,995
5	0,945	0,676	0,990	0,427	0,911	0,717	-0,873	0,578
10	0,969	0,402	0,971	0,488	0,990	0,875	0,990	0,877

Table 4. Correlation coefficients of the mechanical properties of TPS film depending on the screw rotation during extrusion

Screw speed [rpm]	σM at trans-versal extension	σM at longitudinal extension	σB at trans-versal extension	σB at longitudinal extension	εM at trans-versal extension	εM at longitudinal extension	εB at trans-versal extension	εB at longitudinal extension
60	-0,918	-0,990	-0,909	-0,886	-0,977	-0,884	-0,940	-0,818
70	-0,952	-0,838	-0,918	-0,932	-0,990	-0,975	-0,998	-0,932
80	-0,927	-0,985	-0,929	-0,936	-0,954	-0,999	-0,635	-0,999

cients with high values (above 0.8) determined for whole range of the screw rotation used [22]. Data summarized in Table 4 demonstrates the negative impact of increasing amount of keratin on the mechanical properties of the obtained TPS films, irrespective on the screw speed used during extrusion.

CONCLUSIONS

The detailed study and analysis of the obtained results have allowed for the following conclusions:

It is possible to produce biodegradable starchy films of satisfactory properties while using extrusion-cooking process for the production of TPS granulates (half-product) and extrusion-blowing technique for films (final product), however implementing carefully selected process conditions.

Addition of keratin in amounts up to 5% significantly improved the ability of film elongation (film SGK-1, SGK-2).

Addition of keratin at 10% resulted in excessive softness of the film, substantially reduced its strength.

The screw speed had a significant impact on the physical properties of TPS films.

ACKNOWLEDGEMENTS

This scientific work was supported by Polish Ministry of Science and Higher Education founds on science in the years 2010-2012 as a research project N N313 275838.

REFERENCES

1. **Averous L., Boquillon N. 2004.** Biocomposites based on plasticized starch: thermal and mechanical behaviours. Carbohydrate Polymers 56, p. 111-122.
2. **Avérous L., Fringant C., Moro L. 2001.** Starch-based biodegradable materials suitable for thermoforming packaging. Starch/Stärke 53, p. 368-371.
3. **Bhatnagar S., Hanna M. 1996.** Starch-based plastic foams from various starch sources. Cereal Chemistry 73(5), p. 601-604.
4. **Bourtoom T., Chinnan M. 2008.** Preparation and properties of rice starch-chitosan blend biodegradable film. LWT - Food Science and Technology 41, p. 1633-1641.
5. **Broniewski T., Kapko J., Płaczek W., Thomalla J. 2000.** Metody badań i ocena właściwości tworzyw sztucznych. WNT-Warszawa.
6. **Czerniawski B. 2001.** Postęp techniczny w dziedzinie opakowań z tworzyw sztucznych. Opakowanie, 1, p. 26-28.
7. **Gładyszewska B., Stropek Z. 2010.** The influence of the storage time on selected mechanical properties of apple skin. TEKA Commission of Motorization and Power Industry in Agriculture 10, p. 59-65.
8. **Janssen L., Mościcki L. (Eds.) 2009.** Thermoplastic Starch. Wiley-VCH, Germany.
9. **Korzeniowski A., Foltynowicz Z., Kubera H. 1998.** Postęp rozwoju opakowalnictwa na świecie. Opakowanie, 5, p. 12-16.
10. **Kuna-Broniowska I., Gładyszewska B., Ciupak A. 2011.** Storage temperature influence on Young modulus of tomato skin. TEKA Commission of Motorization and Power Industry in Agriculture 11, p. 218-228.
11. **Lawton J.W. 1996.** Effect of starch type on the properties of starch containing films. Carbohydrate Polymers 9, p. 203-208.
12. **Leszczyński W. 1999.** Biodegradowalne tworzywa opakowaniowe. Biotechnologia, 2/45, p. 50-64.
13. **Mościcki L., Wojtowicz A. 2000.** Kierunki rozwoju opakowań ekologicznych. Zeszyty Naukowe Politechniki Opolskiej, 254, p. 177-184.
14. **Park H., Lee S., Chowdhury S., Kang T., Kim H., Park S., Ha C. 2002.** Tensile properties, morphology, and biodegradability of blends of starch with various thermoplastics. Journal of Applied Polymer Science 86, p. 2907-2915.
15. PN-69/C-89043. Tworzywa sztuczne. Oznaczanie cech wytrzymałościowych przy statycznym rozciąganiu.
16. PN-83/C 89091. Folie z tworzyw sztucznych. Oznaczanie wytrzymałości na rozdzieranie.
17. PN-EN ISO 1798. Elastyczne tworzywa sztuczne. Oznaczanie wytrzymałości na rozciąganie i wydłużenie przy zerwaniu.
18. **Rejak A., Mościcki L. 2006.** Biodegradable foil extruded from thermoplastic starch. TEKA Commission of Motorization and Power Industry in Agriculture, 6, p. 123-130.
19. **Rejak. A. 2007.** Badania właściwości fizycznych skrobiowych folii biodegradowalnych. Acta Agrophysica, 9(3),p. 747-754.
20. **Roper H., Koch H. 1990.** The role of starch in biodegradable thermoplastic materials. Starch, 42/4, p. 123-140.
21. **Shi Q, Chen C, Gao L, Jiao L, Xu H, Guo W. 2010.** Physical and degradation properties of binary or ternary blends composed of poly (lactic acid), thermoplastic starch and GMA grafted POE. Polymer Degradation and Stability, doi: 10.1016/j.polymdegradstab.2010.10.002.
22. **Tarasińska J., Hanusz Z. 2008.** Remarks on the faulty regression in Excel. TEKA Commission of Motorization and Power Industry in Agriculture 8, p. 277-281.

WPŁYW DODATKU KERATYNY NA WYBRANE WŁAŚCIWOŚCI FIZYCZNE FOLII ZE SKROBI TERMOPLASTYCZNEJ

Streszczenie. Celem pracy było zbadanie wpływu wybranych parametrów procesu wytłaczania folii z granulatu skrobi termoplastycznej z dodatkiem hydrolizatu keratyny, na podstawowe właściwości fizyczne otrzymywanych folii opakowaniowych. Do produkcji folii skrobiowej zastosowano granulat otrzymany w procesie ekstruzji na ekstruderze jednoślimakowym TS-45 o L/D=16. Do wytworzenia granulatu użyto skrobię, glicerynę oraz polimer hydrolizat keratyny. W trakcie procesu wytwarzania granulatu stosowano obroty ślimaka ekstrudera w zakresie od 40 do 80 obr.min^{-1} oraz temperaturę w zakresie 70 – 120°C. Następnie z uzyskanego granulatu wytłaczano folię metodą rozdmuchu na specjalnie do tego celu wytłaczarce, zaprojektowanej w Katedrze Inżynierii Procesowej UP w Lublinie. Badano cechy wytrzymałościowe folii tj. naprężenie i wydłużenie podczas testów na rozciąganie.

Słowa kluczowe: skrobia, folia, keratyna, ekstruzja, wytłaczanie, naprężenie, wydłużenie.

TEKA. COMMISSION OF MOTORIZATION AND ENERGETICS IN AGRICULTURE – 2012, Vol. 12, No. 1, 225–229

The influence of the knife's geometric parameters on the unitary energy of a cutting process of salix viminalis

Henryk Rode, Jacek Szpetulski

Warsaw University of Technology; Faculty of Construction, Mechanics and Petrochemistry;
Department of Mechanical Systems Engineering and Automation;
Address: 2 Jachowicza Street, 09 – 400 Płock, Poland; email: hrode@op.pl

Summary. Research results of the cutting process of a stem of an energy plant – Salix Viminalis - are presented in the following case study. The study also presents the influence of the knife's geometric parameters on the unitary energy of the cutting process of the stems of Salix Viminalis, with different moisture.

Key words: cutting process, energy plants, unitary energy of cutting a stem, geometric parameters of a knife, moisture.

INTRODUCTION

There has been a great interest in energy plants recently. It is mainly due to the rigorous requirements concerning environmental protection, as well as the search for new ecological and cheap sources of energy [2, 6, 7]. The plants are characterized by high biomass increase in relatively short time and the biomass burning process is more ecological due to the lower content of sulphur dioxide [1, 3]. The weight of the ash left after the burning process is twenty times lower than the ash from the fossil fuel. The other advantage of the usage of energy plants is the fact that the carbon dioxide balance is almost zero because it is absorbed during the plants' growth. The expected and systematic increase of energy plants plantations causes the fact that the problem of the harvest and processing, which also means the cutting process of the plants, is becoming quite significant. The knowledge about the influence of such factors as geometric parameters of a knife, moisture and morphological constitution of the plants on the unitary energy of the cutting process is necessary for proper design and optimalization of this process [4, 5, 9, 10, 12, 14, 22]. These factors have also a significant influence on the proper functioning of agricultural machines' cutting units.

THE PURPOSE OF THE RESEARCH

The aim of the research was to determine the influence of the knife's edge angle towards the plant's stem on the unitary energy of cutting Salix Viminalis. The research was carried for stems with three different diameters and three different moistures. The notion unitary energy means the total energy needed for the realisation of the cutting process falling on the unit area of the section of the cut plant.

THE SUBJECT OF STUDY

The subject of the studies is a popular energy plant - Salix Viminalis. Salix viminalis is an energy willow species. It is characterized by a quick increase of timber mass (about 14 times bigger than in case of naturally grown forests) [8, 19, 20, 21]. It is also characterized by very high fuel value. Its other advantages are low soil requirements, easy vegetative reproduction (shoots), resistance to frost and pests and low fertilizer and pesticides requirements (possibility of fertilization with sludge). Thanks to its quick increase of timber mass it is particularly useful in strengthening river banks in form of fascines. The willow's sprouts achieve the height of even 7 metres, which is why it is the best to process them into silvers, briquettes and pellets, and then burn them in stoves. The ash weigh does not exceed 1% of the burnt weight. Moreover, it also functions as phytoremediation – soil and water natural purification of heavy metals and other chemical combinations.

Fig. 1. Salix Viminalis – stem's cross-section

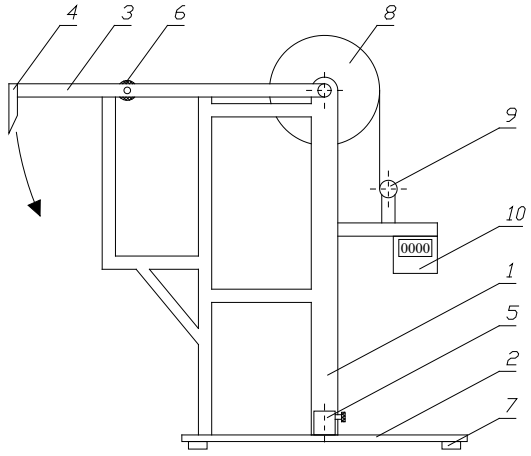

Fig. 2. Measuring device of pendulous type: 1 – mast with frame, 2 – main plate, 3 – pendulum, 4 – knife, 5 – holder of plant sample with fastening handwheel, 6 – stop dog, 7 – adjustable foot, 8 – rotary disk, 9 – linear transducer, 10 – digital recording device

RESEARCH STATION AND THE COURSE OF RESEARCH

Studies of the cutting process of energy plants have been carried out in the Institute of Mechanical Engineering - Technical University of Warsaw in Płock for many years [23, 24, 25]. The studies concern determining the influence of selected parameters of cutting units, as well as the plants' constitution and condition on the quality of the cutting process and its energy consumption [15, 18, 17, 16].

Currently the studies are carried out with the usage of a laboratory station, constructed for this purpose [Rode, Szpetulski 2010], which also allows to determine how putting the knife edge at different angles towards the stem affects the unitary energy falling on the unit area of the plant's cross – section.

Research station of pendulous type for cutting process research is located in the laboratory at Warsaw University of Technology in Płock. It is equipped with a digital recording device which reads the value of electric signal [mV] from the linear transducer. The transducer is an electromechanical device, which changes linear motion into electric signal proportional to the shift. The linear motion is transmitted in the transducer onto a turn of a measuring drum. The signal is measured at the frequency of 400 Hz and, then, is recorded in the memory of digital recording device equipped with measurement display.

During the research the height of the knife edge's final position after cutting the plant's stem is recorded and then compared to the height the same knife edge reached while dead movement without cutting process. The result of a subtraction of those heights multiplied by pendulum's reduced mass constitutes the energy of the cutting process.

METHODOLOGY AND THE COURSE OF RESEARCH

The plants from the plantation were selected at random. Then, they were selected according to their diameters and moistures. The samples of the stem of Salix Viminalis for the study were as follows – three different diameters of stems without forks: 10mm, 13cmm and 16mm with three different moistures: 15%, 23% and 44%.

The 80 mm long samples with different diameters and without forks were prepared for cutting . Each measurement was carried out at least 7 times [Mulas, Rumianowski 1997]. The cutting of the plant took place with the following parameters: knife velocity V = 4,7 m/s, knife edge thickness = 100 μm, type of knife edge: even with a cut from the top, knife edge angle α = 26°30'.

The study included determining the unitary energy for different positions of the knife's edge towards the stem with different moistures.

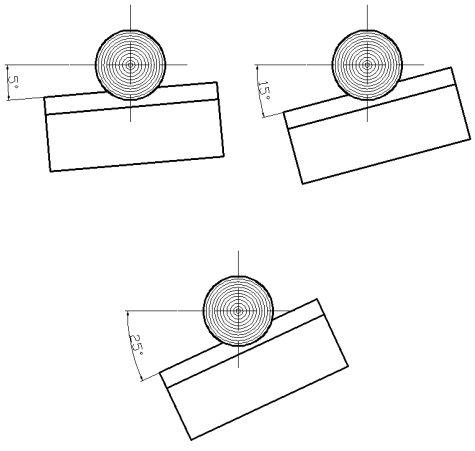

Fig. 3. Position of the knife's edge towards the stem of the cut plant

RESEARCH RESULTS AND ANALYSIS

The unitary energy of cutting Salix Viminalis increases with the diameter's increase. This tendency does not depend on moisture. Irrespective of the stem's moisture the unitary energy also increases with the increase of the knife's edge angle towards the stem. Fig. 4 presents an exemplary process of changes of the unitary energy in the knife's edge angle towards the stem function for 3 chosen diameters with the moisture of 23%. Those functions have a very similar process for the other moistures, e.i.: 15% and 44%.

Irrespective of a chosen stem's diameter, the moisture increase causes the unitary energy decrease for every knife's edge angle concerned. Fig. 5. presents an exemplary process of changes of the unitary energy in moisture function for a stem with diameter of 13mm. Those functions have a very similar process for the other diameters, i.e.: 10 and 16 mm.

As a result of cutting the studied samples of Salix viminalis, breaks occurred: almost totally cut samples, the middle of the cut samples and lengthwise samples. It depends on the physical features of the stems and their dimensions. The crucial parameter regarding the breaks

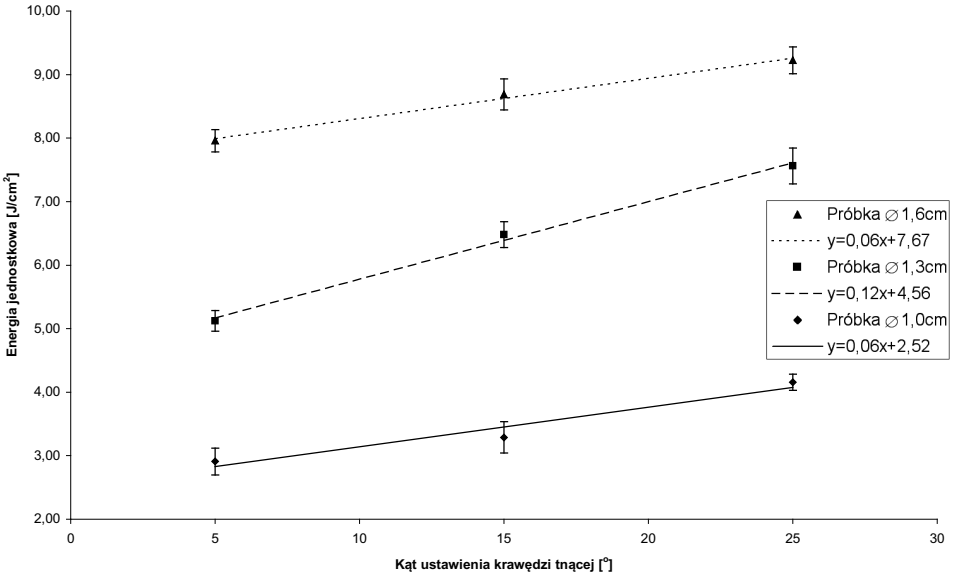

Legend: energia jednostkowa [kJ/m2] – unitary energy; kąt ustawienia krawędzi [^{0}] – knife's edge angle ♦ sample Ø 10; ■ sample Ø 13 ▲ sample Ø 16

Fig. 4. The course of changes of unitary energy of cutting in the knife's edge angle towards the stem function for 3 different diameters of stems of (Salix Viminalis) and for the moisture of 23%

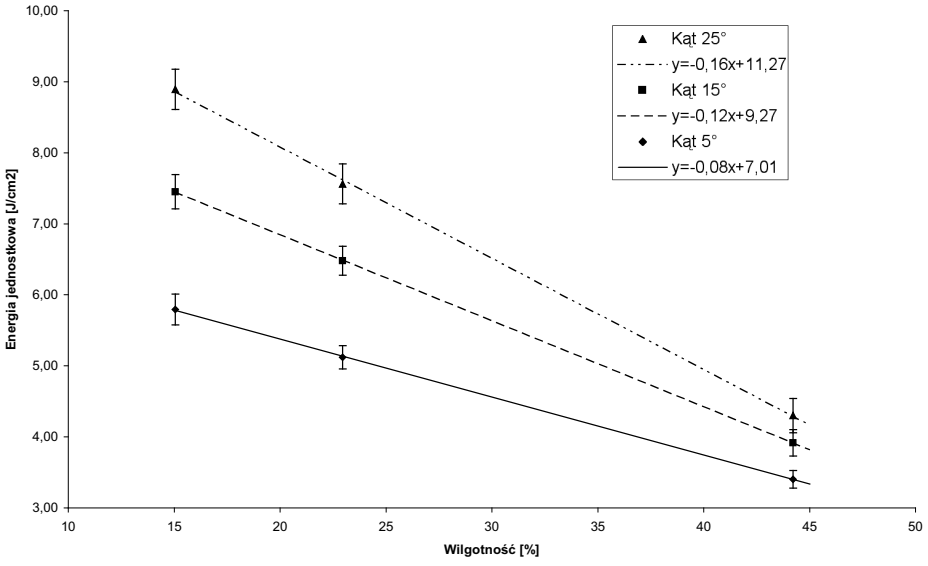

Legend: energia jednostkowa [kJ/m2] – unitary energy; wilgotność [%] – moisture ♦ angle 5°; ■ angle 15°; ▲ angle 25°

Fig. 5. The course of changes of unitary energy of cutting in the moisture function for 3 different angles of the knife's edge position towards the stem of Salix Viminalis and for the diameter of 13 mm

was moisture. The bigger diameter and lower moisture the more often breaks occurred.

Fig. 6. The break in an almost totally cut sample

Fig. 7. The break in the middle of the cut sample

CONCLUSIONS

The curried out studies allowed to determine the unitary energy of the cutting process of Salix Viminalis for different angles of the knife's edge position towards the cut stems with three different diameters and three different moistures.

As a result of the research it can be stated, that:

1. The angle of the knife's edge position towards the cut stem and the stem's moisture has a significant influence on the unitary energy of the cutting process of a plant.
2. The unitary energy of cutting increases together with the increase of the angle of the knife's position. It may result from the fact that the contact surface is bigger so the frictional resistance is bigger. This tendency is the same for every studied stem's diameter and moisture.
3. The graphs with courses of changes of the unitary energy of the cutting in moisture function show a clear decrease of the unitary energy when the moisture increases. This tendency is the same for every studied stem's diameter and knife's edge angle.
4. Analysing the results of the study of the cutting process, it can be stated that the samples' moisture has much bigger influence on the unitary energy than the angle of the knife's position.
5. The optimal parameters of the cutting process resulting from the research are as follows: small angle of the knife's position and high moisture.

The method of studying the cutting process may also be used to study other energy plants.

REFERENCES

1. **Baran D., Kwaśniewski D., Mudryk K. 2007:** Wybrane właściwości fizyczne trzyletniej wierzby energetycznej. Inżynieria Rolnicza, nr 8(96), p. 7-12.
2. **Dreszer K., Michałek R., Roszkowski A. 2003:** Energia odnawialna – możliwości jej pozyskiwania i wykorzystania w rolnictwie. Wydawnictwo PTIR, Kraków – Lublin – Warszawa.
3. **Dubas J., Grzybek A., Kotowski W., Tomczyk A. 2004:** Wierzba energetyczna – uprawa i technologie przetwarzania. Wyższa Szkoła Ekonomii i Administracji. Bytom.
4. **Frączek J., Mudryk K. 2006:** Metoda określenia oporów cięcia pędów wierzby energetycznej. Inżynieria Rolnicza, nr 8(83), p. 91-98.
5. **Górski J. 2001:** Proces ciecia drewna elektryczną pilarką. Rozprawy Naukowe i Monografie. Wydawnictwo SGGW, Warszawa.
6. **Gradzik P., Grzybek A., Kowalczyk K., Kościk B. 2003:** Biopaliwa. Warszawa.
7. **Grzybek A. 2002:** Biomasa jako alternatywne źródło energii. Warszawa.
8. **Juliszewski T., Kwaśniewski D., Baran D. 2006:** Wpływ wybranych czynników na przyrosty wierzby energetycznej. Inżynieria Rolnicza, nr 12(87), Kraków, p. 225-232.
9. **Kowalski S. 1993:** Badania oporów cięcia wybranych roślin. Zeszyt Prob. Post. Nauk Rol. 408, p. 297-303.
10. **Kwaśniewski D., Mudryk K., Wróbel M., 2006:** Zbiór wierzby energetycznej z użyciem piły łańcuchowej. Inżynieria Rolnicza, nr 13(88), p. 271-276.
11. **Lisowski A. i** inni. 2010: Technologie zbiorów roślin energetycznych. Wydawnictwo SGGW, Warszawa.
12. **Lisowski A. 2006:** Ścinanie i rozdrabnianie wierzby energetycznej, Technika Rolnicza Ogrodnicza Leśna 4, p. 8-11.
13. **Mulas E., Rumianowski R. 1997:** Rachunek niepewności pomiaru. WPW, Warszawa.
14. **Popko H., Miszczuk M. 2004:** Badania oporów krajania niektórych produktów spożywczych.. Zeszyt Prob. Post. Nauk Rol. 354.
15. **Rode H. 2008:** Badania procesu cięcia wybranych roślin energetycznych, Rozdział w monografii Wybrane zagadnienia mechaniki w budowie urządzeń technicznych. p. 286-297. Politechnika Warszawska, Płock.
16. **Rode H. 2011:** The energy of a cutting process of a selected energy plant. Teka Komisji Motoryzacji i Energetyki Rolnictwa. vol. XI, Lublin, p. 326-334.
17. **Rode H., Szpetulski J. 2010:** The study of the willow viminalis cutting process. Bioagrotechnikal Systems Engineering. vol.6(22), Płock, p. 63-75.
18. **Rode H., Witkowski P 2011:** Moisture influence on the unitary energy of a cutting process of selected energy plants. Teka Komisji Motoryzacji i Energetyki Rolnictwa. vol. XI, Lublin, p. 317-325.

19. **Rudko T., Stasiak M. 2004:** Właściwości mechaniczne pędów wierzby energetycznej. III Zjazd Naukowy. Referaty i doniesienia. Dąbrowice 27-29.09.2004.
20. **Szczukowski S., Tworkowski J., Stolarski M.J. 2004.** Wierzba energetyczna. Wydawnictwo Plantpress Sp. z o.o., Kraków.
21. **Szczukowski S., Tworkowski J., Wiwart M., Przyborowski J. 2002:** Wiklina (Salix Sp.) Uprawa i możliwości wykorzystania. Wydawnictwo Uniwersytetu Warmińsko-Mazurskiego, Olsztyn.
22. **Szymanek M. 2007:** Analysis of cutting process of plant material. Teka Komisji Motoryzacji i Energetyki Rolnictwa – OL PAN, VIIA, p. 107-113.
23. **Żuk D. 1979:** Określenie koniecznej prędkości elementów tnących w maszynach do ścinania źdźbeł i łodyg. Maszyny i Ciągniki Rolnicze nr 3/1979. Warszawa.
24. **Żuk D. 1986:** Proces cięcia źdźbeł zbóż. Prace Naukowe Politechniki Warszawskiej - Mechanika z. 95. Warszawa.
25. **Żuk D., Rode H. 1992:** Propozycje oceny energetycznej zespołów tnących. Prace Naukowe Politechniki Warszawskiej - Mechanika z. 152. Warszawa.

WPŁYW PARAMETRÓW GEOMETRYCZNYCH NOŻA NA ENERGIĘ JEDNOSTKOWĄ PROCESU CIĘCIA WIERZBY ENERGETYCZNEJ

S t r e s z c z e n i e . Praca zawiera wyniki badań procesu cięcia łodygi rośliny energetycznej - wierzby konopianej (Salix Viminalis). Przedstawiono wpływ parametrów geometrycznych noża na energię jednostkową cięcia łodyg wierzby konopianej przy różnych wilgotnościach rośliny.

S ł o w a k l u c z o w e : proces cięcia, rośliny energetyczne, energia jednostkowa cięcia, parametry geometryczne noża, wilgotność.

TEKA. COMMISSION OF MOTORIZATION AND ENERGETICS IN AGRICULTURE – 2012, Vol. 12, No. 1, 231–235

The study of the rotary cutting process of energy plants

Henryk Rode, Paweł Witkowski

Warsaw University of Technology; Faculty of Construction, Mechanics and Petrochemistry
Department of Mechanical Systems Engineering and Automation
Address: Jachowicza 2, 09 – 400 Płock, Poland; email: horde@op.pl

Summary. The article presents the new research station for studying the rotary cutting process of energy plants. It is based on a power unit of a rotary mower. The article also discusses the results of the pilot studies of the cutting process of Salix Viminalis and Reynoutria Sachalinesis with the inertial method.

Key words: rotary mower, unitary energy of cutting, rotary cutting process, Salix Viminalis, Reynoutria Sachalinesis, energy plants.

INTRODUCTION

There is a tendency towards ecological behaviour nowadays. It is not only fashion but also a necessity. Using the biomass energy, instead of energy obtained from fossils, protects the environment against greenhouse effect [3, 7, 8]. In order to make this tendency last, the acquisition of energy from energy plants should be profitable. That is why the problem of the harvest, processing and breaking up these plants and preparing them for further usage is becoming quite significant [5, 16]. The features influencing the unitary energy of cutting are: plant's dimensions, shear strength, friction factor and moisture [12, 13]. The studies of the cutting process of energy plants should be useful Chile designing cutting units and choosing parameters of working units for harvest machines [10, 15, 23].

THE PURPOSE OF THE RESEARCH

The aim of the latest research series was to determine the influence of selected parameters of rotary cutting unit and the plants' constitution and stand on the quality and energy consumption of the cutting process [17, 18, 19, 24, 25, 26].

The pilot studies were carried out mainly in order to test a newly constructed laboratory station, at the Institute of Mechanical Engineering - Technical University of Warsaw in Płock [19]. The research included determining unitary energy of the cutting process of Salix Viminalis and Reynoutria Sachalinesis with different stems' diameters forming a kind of a nest.

The notion unitary energy means the total energy needed for the realisation of the cutting process falling on the unit area of the section of the cut plant.

THE SUBJECT OF STUDY

Energy plants are those, which are characterized by high biomass increase in relatively short time. The plants are also characterized by low soil requirements, high resistance to diseases and pests and high fuel value [1, 4]. Due to the growing number of energy plants plantations in our country, Salix Viminalis and Reynoutria Sachalinesis were selected for the pilot studies.

Salix viminalis is the most popular plant from energy willow species. It is characterized by a quick increase, productivity and low energy consumption during the production process. It is also characterized by quite low labour inputs as far as obtaining biomass is concerned. Moreover, it also functions as phytoremediation - soil and water natural purification. It can also be used as a protective belt from toxic emission [9, 20, 21, 22].

Reynoutria sachalinesis comes from Asia. It is a perennial plant, which grows to 300 - 400 cm. The leaves are 15 – 40 cm long, nearly heart-shaped. The flowers are small, white or beige, up to 3mmm long, produced on short panicles. Male flowers have 7-8 stamens and female flowers have one carpel. The fruit is a nut. Up to 580 GJ of energy can be obtained from 1 ha of crop. It accumulates heavy metals from soil. The root system is very deep. The plant grows in riverside bushes and flood meadows [2].

Fig. 1. View of Salix viminalis' stem in a cross-section

Fig. 2. View of Reynoutria sachalinesis' stem in a cross-section

RESEARCH STATION

The measurement of the unitary energy of cutting was carried out at a research station for studying energy plants rotary cutting process (Fig.3.)

The station consists of two, independently working, units (cutting unit and transporting unit). The units are set in a construction frame (1). The cutting unit consists of inertial knives placed on the circumference of the working plate – diameter 50cm (8). The knives are set with knife holders (10). The working plate (8) is set with screws to the working hub (7), which is placed on the working roller with the usage of bearings. The torque transmission from the electric motor (5) to the cutting unit proceeds through the working roller, which is connected with the motor by means of the overload coupling (9). The transporting unit consists of the electric motor (4), which pulls the truck (3) along the slideway (2) by a line (12). The truck's construction allows to set the research material of different dimensions and constitutions. The inverter controls rational speed of the motor (5) which drives the cutting unit. The inverter keeps a constant voltage ratio to the frequency – from initial frequency to the basic frequency. The inverter, which controls rational speed of the motor driving the transporting unit, adjusts voltage characteristics to the frequency not linearly but according to the respective load at a given moment. The value of the rational speed of the motor which drives transporting unit (4) as well as the motor's of the cutting unit (5), is achieved through putting the adequate frequency. A required frequency value is put into a computer programme (Drive View), which is designed for LG inverters.

The load increase on the motor, which drives the cutting unit, resulting from the research material cutting, causes the increase of the current strength needed for running this process. It is then registered in the computer programme (Drive View) as a graph illustrating the power consumption in time function (Fig. 4). The results analysis allows to determine unitary energy necessary for the proper course of the plants cutting process.

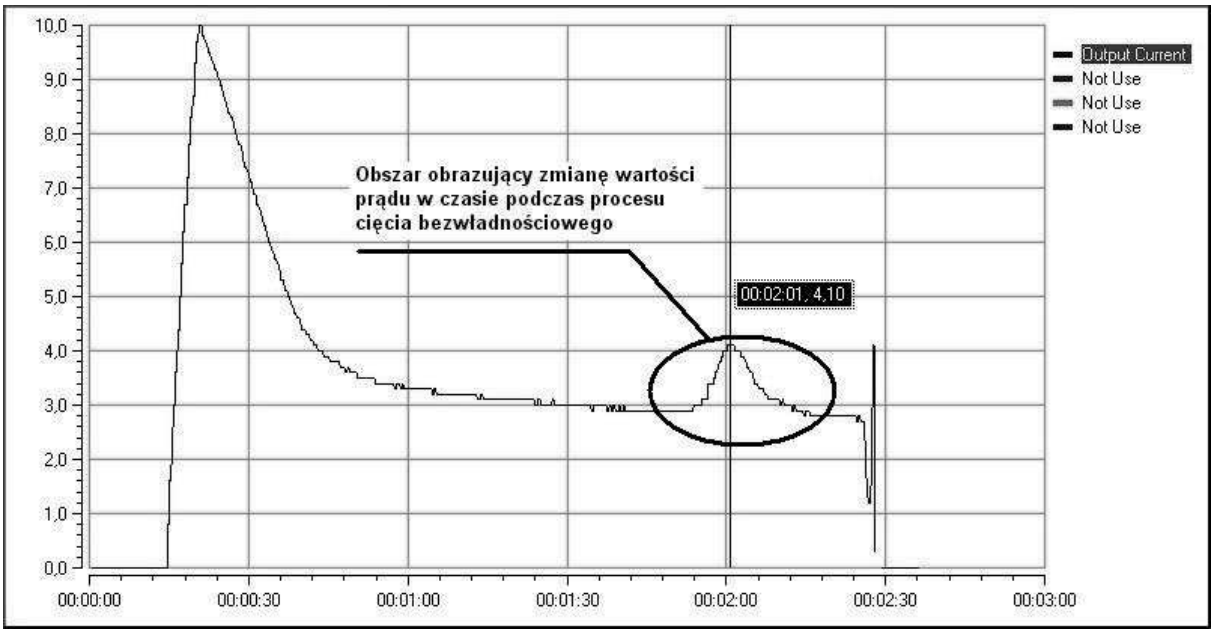

Legend: the area illustrating the voltage value change during the rotary cutting process.

Fig. 4. An exemplary graph illustrating power consumption in time function

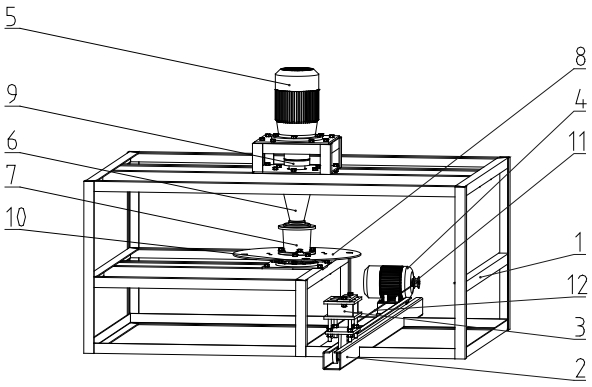

1. construction frame,
2. truck slideway,
3. truck,
4. electric motor for truck shift,
5. electric motor of the cutting unit,
6. working roller's housing
7. working hub,
8. working roller,
9. overload coupling,
10. knife holder,
11. spool,
12. line.

Fig. 3. Research station for studying energy plants rotary cutting process

METHODOLOGY AND THE COURSE OF RESEARCH

For the study of the rotary cutting process the samples of Salix Viminalis and Reynoutria Sachalinesis were prepared. The researched plants came from the Experimental Station at the Faculty of Agriculture and Biology – University of Life Sciences in Skierniewice [Stacja Doświadczalna Wydziału Rolnictwa SGGW]. A 25 cm long sample was cut from the stem and set in such a way so that the cutting could take place at the height of 10cm from the ground. The cutting process in the field takes place at such a height. The samples of the researched plants were set on the truck in two rows (Fig. 5). The photos of the plants cross section were taken each time after the cut. On the day of carrying out the study the moisture of the researched plants was determined. Salix Viminalis samples with moisture of 15% and Reynoutria Sachalinesis of 12% were chosen. Each measurement was carried out at least 7 times [Mulas, Rumianowski 1997].

The cutting process at the research station was carried out with the following parameters:
- Rational speed of the cutting unit n=1710 r.p.m.
- Linear velocity of the truck shift V= 0,03m/s.
- Linear velocity of inertial knives V= 44,75 m/s.
- Inertial knife's weight m= 6505g.
- Knife edge angle α = 29°20'.
- Type of knife edge: even with a cut from the top.

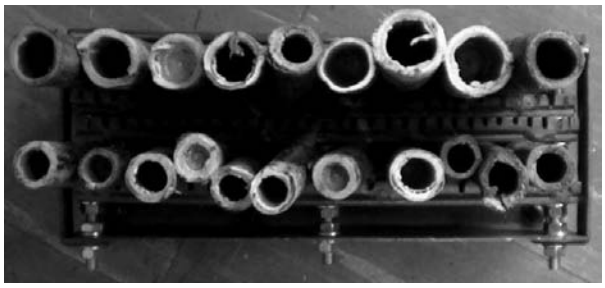

Fig. 5. The energy plants samples set on the truck

RESEARCH RESULTS AND ANALYSIS

It can be stated, by analysing the results, that very low increase of surface area of the cut Salix Viminalis stems, forming a kind of a nest, causes a high increase of the unitary energy of the cutting process. With the 90% increase of the cut surface area the energy increases by 250% (Fig.6.). Such a rapid increase may be caused by the ligneous constitution of the stems section, which with relatively low moisture (15%) were fibrous and required a total cut in order to split the tissues.

In comparison with Salix Viminalis the demand for unitary energy is relatively low in the case the Reynoutria Sachalinesis cutting. It may be connected with the inner section of the studied plant. Reynoutria Sachalinesis is empty inside (section of a pipe) and its morphological constitution is similar to bamboos. Changing the size of the cut surface area does not cause a rapid increase of the unitary energy. With a 50% increase of cross – section the unitary energy increases only by 20% (Fig.7.). Relatively low moisture (12%) caused the fact that the plant's stems were fragile, they broke during the cutting

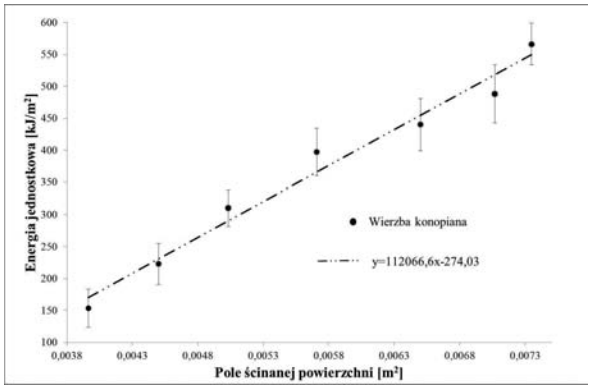

Legend: energia jednostkowa – unitary energy [kJ/m²]; pole ścinanej powierzchni – cut surfie are [m²]; ♦ wierzba konopiana – Salix Viminalis

Fig. 6. The course of changes of unitary energy of Salix Viminalis in the cut surface area function

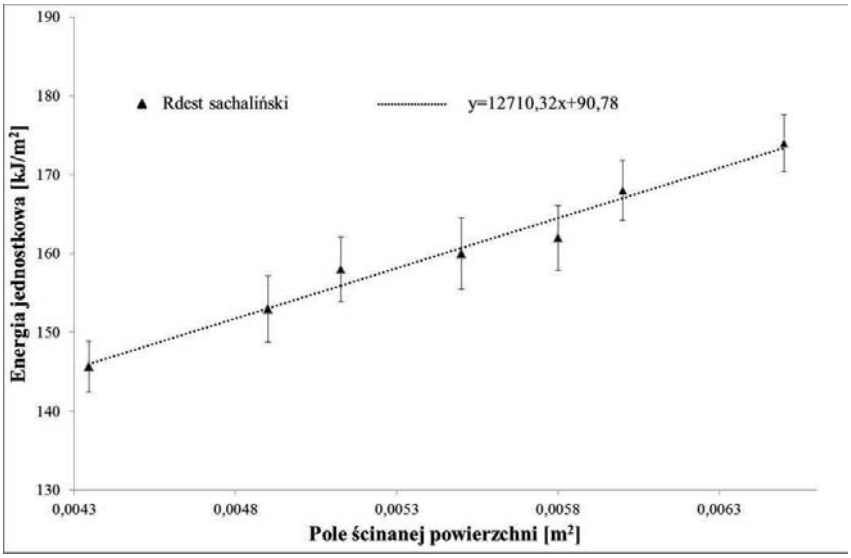

Legend: energia jednostkowa – unitary energy [kJ/m2]; pole ścinanej powierzchni – cut surfie are [m2]; s rdest sachaliński – Reynoutria Sachalinesis

Fig. 7. The course of changes of unitary energy of Reynoutria Sachalinesis in the cut surface area function.

process and did not weight down the knife in the final cutting phase.

CONCLUSIONS

The study of the rotary cutting process of energy plants are the continuation of studies carried out on the research station of pendulous type. The new research station allows for the study of the cutting process in the natural-like conditions. It also allows for using chipper disk as well as circular saw [Górski 2001, Kwaśniewski et al. 2006].

The presented pilot studies only slightly show the possibilities of the new research station and the results should be treated as initial ones.

REFERENCES

1. **Baran D., Kwaśniewski D., Mudryk K. 2007:** Wybrane właściwości fizyczne trzyletniej wierzby energetycznej. Inżynieria Rolnicza, nr 8(96), p. 7-12.
2. **Burnie G. i** inni, 2005: Botanica. Rośliny ogrodowe. Kónemann.
3. **Dreszer K., Michałek R., Roszkowski A. 2003:** Energia odnawialna – możliwości jej pozyskiwania i wykorzystania w rolnictwie. Wydawnictwo PTIR, Kraków – Lublin –Warszawa.
4. **Dubas J., Grzybek A., Kotowski W., Tomczyk A. 2004:** Wierzba energetyczna – uprawa i technologie przetwarzania. Wyższa Szkoła Ekonomii i Administracji. Bytom.
5. **Frączek J., Mudryk K. 2006:** Metoda określenia oporów cięcia pędów wierzby energetycznej. Inżynieria Rolnicza, nr 8(83), p. 91-98.
6. **Górski J. 2001:** Proces ciecia drewna elektryczną pilarką. Rozprawy Naukowe i Monografie. Wydawnictwo SGGW, Warszawa.
7. **Gradzik P., Grzybek A., Kowalczyk K., Kościk B. 2003:** Biopaliwa. Warszawa.
8. **Grzybek A. 2002:** Biomasa jako alternatywne źródło energii. Warszawa.
9. **Juliszewski T., Kwaśniewski D., Baran D. 2006:** Wpływ wybranych czynników na przyrosty wierzby energetycznej. Inżynieria Rolnicza, nr 12(87), Kraków, p. 225-232.
10. **Kowalski S. 1993:** Badania oporów cięcia wybranych roślin. Zeszyt Prob. Post. Nauk Rol. 408, p. 297-303.
11. **Kwaśniewski D., Mudryk K., Wróbel M., 2006:** Zbiór wierzby energetycznej z użyciem piły łańcuchowej. Inżynieria Rolnicza, nr 13(88), p. 271-276.
12. **Lisowski A. i** inni. 2010: Technologie zbiorów roślin energetycznych. Wydawnictwo SGGW, Warszawa.
13. **Lisowski A. 2006:** Ścinanie i rozdrabnianie wierzby energetycznej, Technika Rolnicza Ogrodnicza Leśna 4, p. 8-11.
14. **Mulas E., Rumianowski R. 1997:** Rachunek niepewności pomiaru. WPW, Warszawa.
15. **Popko H., Miszczuk M. 2004:** Badania oporów krajania niektórych produktów spożywczych. Zeszyt Prob. Post. Nauk Rol. 354.
16. **Rode H. 2008:** Badania procesu cięcia wybranych roślin energetycznych, Rozdział w monografii Wybrane zagadnienia mechaniki w budowie urządzeń technicznych. s. 286-297. Politechnika Warszawska, Płock.
17. **Rode H., Witkowski P. 2011:** Moisture influence on the unitary energy of a cutting process of selected energy plants. Teka Komisji Motoryzacji i Energetyki Rolnictwa. vol. XI, Lublin, p. 317-325.
18. **Rode H.** 2011: The energy of a cutting process of a selected energy plant. Teka Komisji Motoryzacji i Energetyki Rolnictwa. vol. XI, Lublin, p. 326-334.
19. **Witkowski P. 2011:** Stanowisko do badań procesu cięcia roślin. Rozdział w monografii Inżynieria mechaniczna – innowacje dla przedsiębiorstw. p. 129-132. Politechnika Warszawska, Płock.
20. **Rudko T., Stasiak M. 2004:** Właściwości mechaniczne pędów wierzby energetycznej. III Zjazd Naukowy. Referaty i doniesienia. Dąbrowice 27-29.09.2004.

21. **Szczukowski S., Tworkowski J., Stolarski M.J. 2004.** Wierzba energetyczna. Wydawnictwo Plantpress Sp. z o.o., Kraków.
22. **Szczukowski S., Tworkowski J., Wiwart M., Przyborowski J. 2002:** Wiklina (Salix Sp.) Uprawa i możliwości wykorzystania. Wydawnictwo Uniwersytetu Warmińsko-Mazurskiego, Olsztyn.
23. **Szymanek M. 2007:** Analysis of cutting process of plant material. Teka Komisji Motoryzacji i Energetyki Rolnictwa – OL PAN, VIIA, p. 107-113.
24. **Żuk D. 1979:** Określenie koniecznej prędkości elementów tnących w maszynach do ścinania źdźbeł i łodyg. Maszyny i Ciągniki Rolnicze nr 3/1979. Warszawa.
25. **Żuk D. 1986:** Proces cięcia źdźbeł zbóż. Prace Naukowe Politechniki Warszawskiej - Mechanika z. 95. Warszawa.
26. **Żuk D., Rode H. 1992:** Propozycje oceny energetycznej zespołów tnących. Prace Naukowe Politechniki Warszawskiej - Mechanika z. 152. Warszawa.

BADANIE PROCESU CIĘCIA ROTACYJNEGO ROŚLIN ENERGETYCZNYCH

S t r e s z c z e n i e. W artykule przedstawiono nowe stanowisku do badań procesu cięcia rotacyjnego roślin energetycznych bazujące na zespole napędowym kosiarki rotacyjnej. Omówiono także wyniki badań wstępnych procesu cięcia wierzby konopianej i rdestu sachalińskiego.

S ł o w a k l u c z o w e: kosiarka rotacyjna, energia jednostkowa cięcia, cięcie rotacyjne, wierzba konopiana, rdest sachaliński, rośliny energetyczne.

TEKA. COMMISSION OF MOTORIZATION AND ENERGETICS IN AGRICULTURE – 2012, Vol. 12, No. 1, 237–241

The application of labview software for the control of a model of a tracking photovoltaic system

Mariusz Sarniak

Warsaw University of Technology, Faculty of Civil Engineering, Mechanics and Petrochemistry
Department of Mechanical Systems Engineering and Automatization
Address: Al. Jachowicza 2/4, 09–402 Płock, Poland, e-mail: sarniak@pw.plock.pl

S u m m a r y. The paper presents the design of a test stand for tracking photovoltaic systems. For the control of the stand the authors used a universal measurement and control card LabJack U12 and the control algorithms were realized in the LabVIEW environment. The test stand was adapted for testing of different types of cells and different types of control.

K e y w o r d s: photovoltaic conversion, tracking system, photovoltaic cell, and photovoltaic panel.

INTRODUCTION

The tests on tracking photovoltaic systems are usually conducted on prototype or low series load bearing structures [12, 13, 6, 15]. An even greater variety is encountered in the control mechanisms in the case of both the actuators and the control algorithms. In general, we can distinguish two types of control algorithms in the tracking photovoltaic systems: systems that track the maximum solar radiation in set time intervals and systems that set the receiver plane perpendicularly to the direct radiation according to the astronomical algorithms [11, 9, 21].

In all the cases there are many important aspects that require in-depth fundamental research. The results of the tests on the test stand can be the rationalization of the selection of the design and functional parameters of the tracking photovoltaic systems.

AIM OF THE WORK

The aim of the task is to construct a test stand that will enable the performance of a variety of fundamental research of the tracking photovoltaic systems. The element supervising the functioning of the control system is a universal measurement card LabJack U12 supported by LabVIEW that enables programming of the algorithms in G graphic language [1].

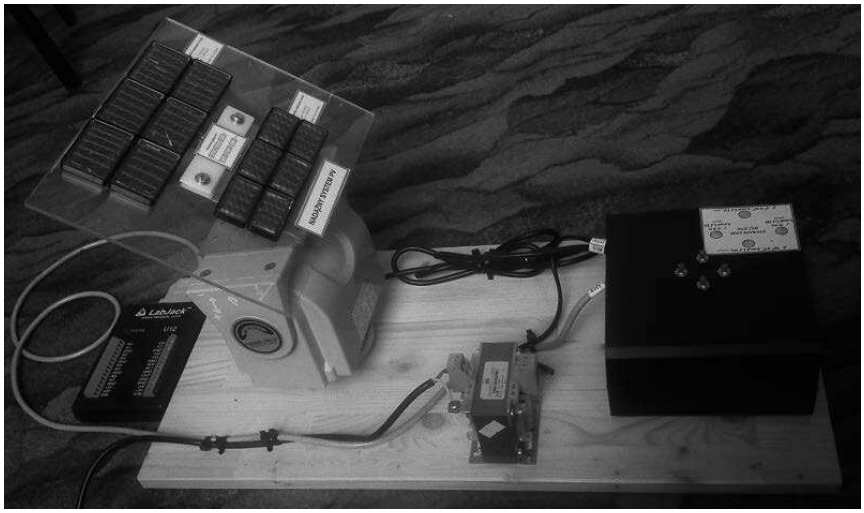

Fig. 1. Image of the test stand

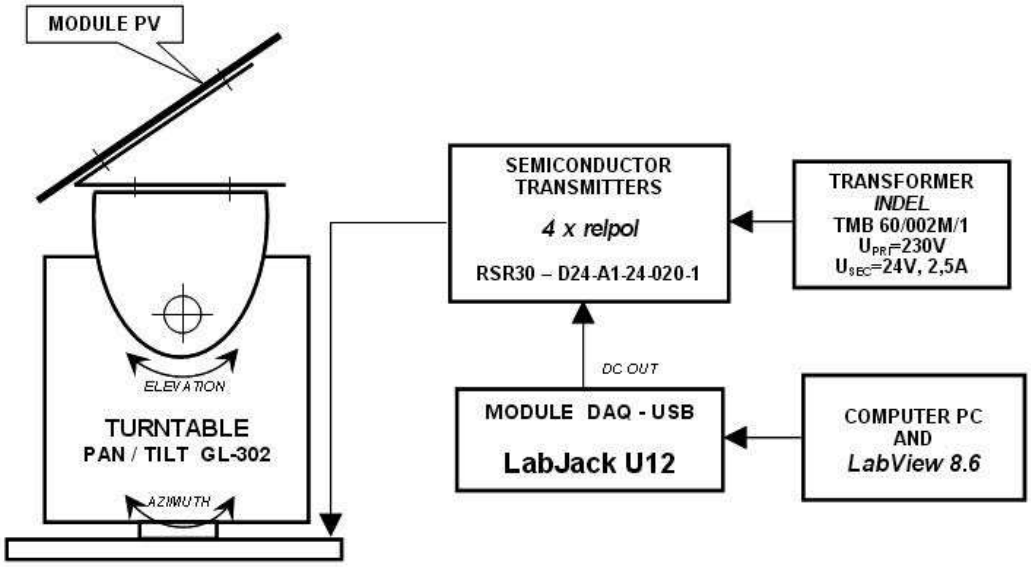

Fig. 2. Schematics of the test stand

DESCRIPTION OF THE TEST STAND

For the needs of the research of the tracking photovoltaic systems a stand was built as seen in Fig. 1. The actuator is an adapted PAN / TILT camera GL-302 tracker motor on which the photovoltaic panel was fixed.

Detailed schematics of the connections of the test stand has been presented in Fig. 2. The control is realized through a universal control and measurement card LabJack U12 supported by a PC computer connected via a USB port. The power supply of the control system is realized through a 24 V adapter and semi-conductor relays RELPOL RSR30. The stand also enables manual operation of the tracker motor. The control algorithms are built in the G graphic language in the LabVIEW 8.6 environment.

The tracker motor operates in two planes: azimuth (rotation angle - γ) and elevation (angle of incidence - β). Owing to the use of a special support and end switches of the tracker motor the following ranges of rotation have been obtained: for the angle of rotation in the azimuth plane (γ): 45^0-315^0 (measured from the north direction clockwise) and for the angle of incidence (β): 0^0-90^0. For the used power supply and control systems the rates of rotation of the model of a tracking photovoltaic system were determined experimentally in both planes: azimuth plane (for angle γ) – 4.41 [^{0}/s] and elevation plane (for angle β) – 4.95 [^{0}/s]. On the test stand two sets composed of six serial photovoltaic cells are fitted. The cells are made from polycrystallic silicon of the parameters: 450 mV and 100 and 200 mA respectively.

METHODOLOGY OF RESEARCH

Fig. 3 presents the schematics of the geometrical codependence in the system between the direct radiation and the plane of the radiation receiver.

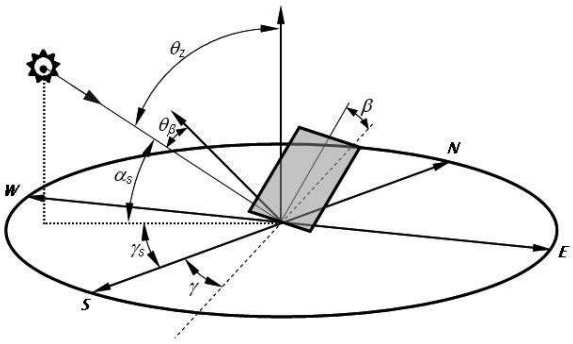

Fig. 3. Geometry of the solar radiation system–plane of the radiation receiver, where: β – angle of incidence of the receiver against horizon; γ – receiver azimuth– deviation from the local parallel of longitude measured against south (to the east it is negative, to the west– positive); γ_S – the Sun azimuth– deviation of the direct solar radiation from the south; θ_β – angle of radiation on the plane of the receiver measured between the direct solar radiation and the regular for the receiver; θ_Z – angle of zenith being at the same time the angle of solar radiation on the horizontal plane; α_S – the Sun elevation – the angle of the direction of the radiation to the plane of the horizon

The aim of the control systems of the tracking photovoltaic systems is to set the plane of the receiver so that the direct component of the solar radiation falls on the plane perpendicularly [2, 3, 4, 20]. Converting this aim into a mathematical notation we can show it as follows:

$$\gamma = \gamma_s, \tag{1}$$

$$\beta = \theta_z \quad \text{that is} \quad \beta = 90^0 - \alpha_s. \tag{2}$$

Another approach in seeking of the optimum position of the plane of the radiation receiver is determining of the Sun position through radiation sensors. A detailed analysis of the functioning of the control systems allows

establishing the time interval between the settings of the individual positions. The idea behind such an approach to the control of the tracking photovoltaic systems is a compromise between the energy benefit resulting from the application of the control system and the energy consumption used for this very control. Such an analysis, apart from the solar radiation and temperature should also take into account the direction and strength of the wind while using the trackers in the location where the system is fitted [7, 10, 17, 14].

The mapping of the Sun trajectory in the sky during the day can be presented graphically in the coordinates $\alpha_S=f(\gamma_S)$. It is a graph of the Sun position that is a set of lines for individual days of the months and the latitude. Detailed mathematical relations and graphs of the Sun position for the characteristic locations in Poland can be found in literature e.g. [5, 16, 6]. Fig. 4 presents a diagram made in LabVIEW that realized the algorithm of the setting of the fitting plane of the photovoltaic cells in line with the direct solar radiation.

The icon marked 'ALGORITHM' in the diagram contains a set of mathematical relations described in detail in literature [16, 21] that were placed in a special block of the G graphic programming language referred to as 'Formula Node'. As seen in Fig. 4 the input parameters in the proposed algorithm is time and location and the output quantities - the angle of incidence of the receiver (β) and the solar azimuth (γ_S). The output values of these angles are then converted into times of rotation of the trackers in the elevation and azimuth planes. Another stage of the algorithm is the use of two 'flat sequences' of the G graphic language. In both flat sequences to control the digital outputs of the LabJack U12 measurement card special functions 'LJ EDO' were used provided by the card manufacturer that make the LabVIEW software compatible with LabJack U12. The effect of the operation of the algorithm is the actuation of the tracker motors for a preset time, which realizes the displacement of the photovoltaic cell.

The influence of the application of the control of the tracking photovoltaic systems will be presented in the form of example current/voltage (I-V), characteristics performed according to the methodology described in detail in the author's college handbook [Sarniak 2008].

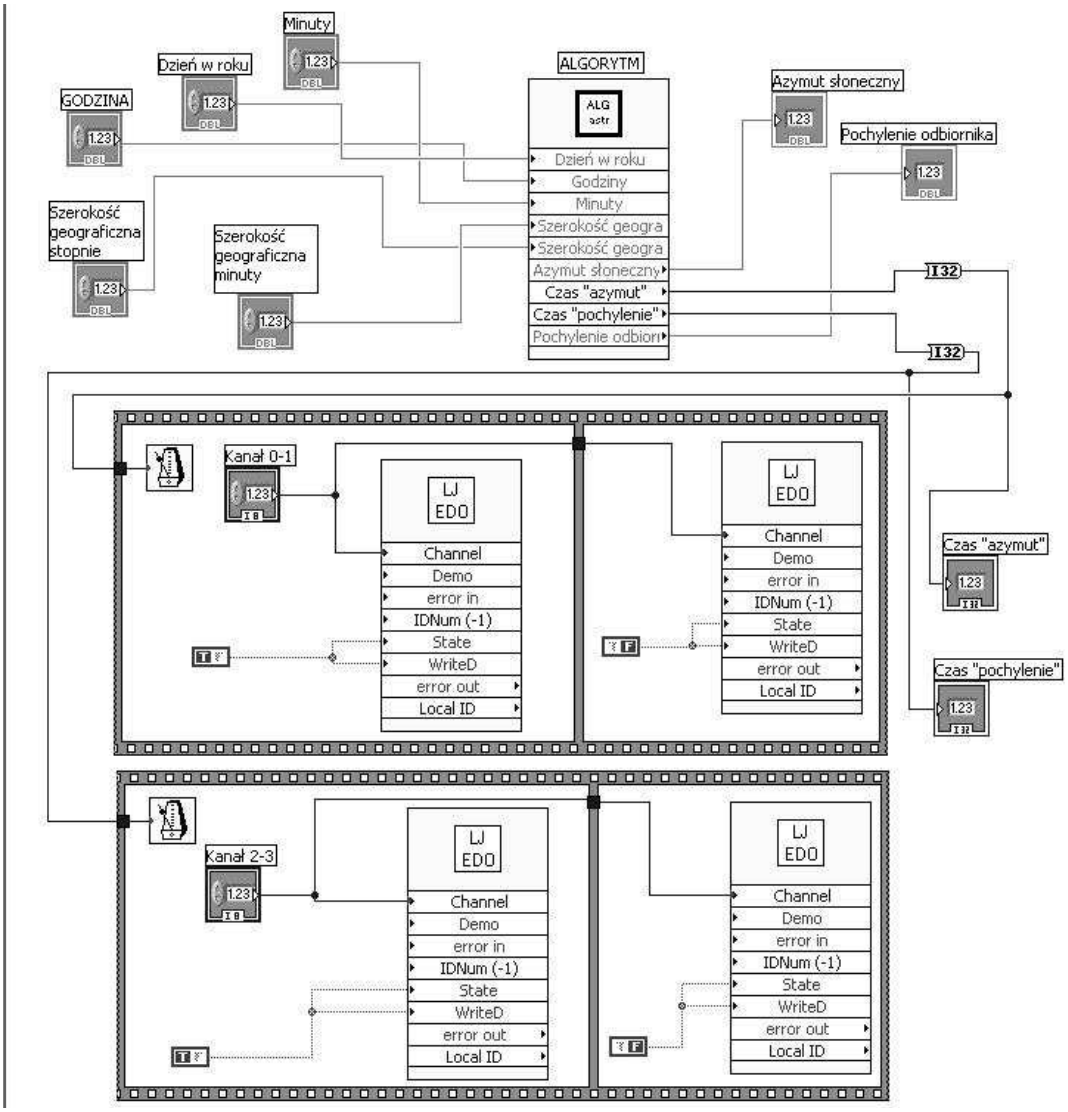

Fig. 4. Diagram presenting the control algorithm of a tracking photovoltaic system model built in LabVIEW 8.6

RESEARCH RESULTS

As a result of the operation of the algorithm the theoretical optimum positions of the plane of the photovoltaic module were determined for the example tests, as shown in table 1.

Table 1. Theoretical optimum positions of the photovoltaic module for the test location of the model test stand

Hours of measurements performed on 16.03.2012r.	Results of the calculations for the location: 52°28'N 19°40'E	
	γ_S [°]	β [°]
$9^{\underline{00}}$	131.69	64.63
$12^{\underline{00}}$	183.14	53.99
$15^{\underline{00}}$	233.27	66.95

For these three positions the current/voltage (I-V) characteristics were measured and compared with their courses for the stationary photovoltaic system. In literature [e.g. Pluta 2000] it is recommended that the stationary photovoltaic systems be fitted azimuthally directed south and the angle of incidence be set on the level equaling the earth's latitude.

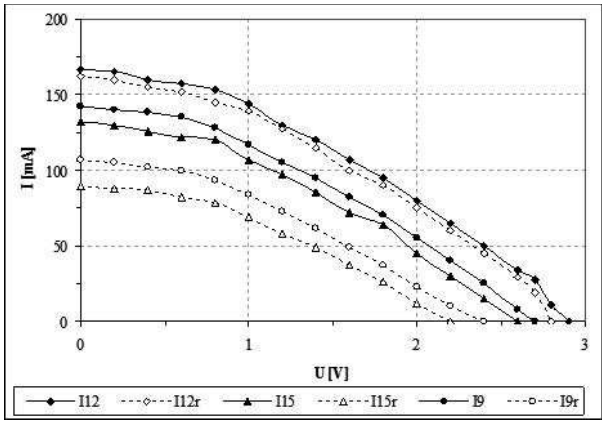

Fig. 5. Current /voltage (I-V) characteristics performed on 16.03.2012 at $9^{\underline{00}}$, $12^{\underline{00}}$ and $15^{\underline{00}}$

Fig. 5 presents the I-V characteristics for three hours ($9^{\underline{00}}$, $12^{\underline{00}}$, $15^{\underline{00}}$) of the day (16.03.2012). These characteristics were performed for the location given in table 1. The solid lines denote the I-V characteristics for the optimum settings resulting from the calculation algorithm and the dotted lines the I-V characteristics for the stationary all-year setting. The all-year position of the tested panel was set using the manual control on the model test stand. The preliminary tests on the model test stand were conducted at full sun operation i.e. direct sun radiation dominating. The I-V characteristics shown in Fig. 5 were developed for the cells of the following electrical parameters: 450 mV and 200 mA.

CONCLUSIONS

1. The I-V characteristics made for $12^{\underline{00}}$ hrs only slightly deviates from the one that was made for the all-year position. This is a result of the fact that angular values of the photovoltaic cell position calculated from the algorithm are very close to the all-year ones.

2. Significant differences can be observed for the measurements for $9^{\underline{00}}$ and $15^{\underline{00}}$. They can be estimated here at the level of 45-50 [mW] of the maximum power. In this case the purposefulness of tracking photovoltaic systems is confirmed.

3. Better electrical parameters of the I-V characteristics for $9^{\underline{00}}$ in relation to $15^{\underline{00}}$, despite apparent time symmetry to the noon, probably result from the negative temperature coefficient for pollycrystallic silicon used in the model of the photovoltaic system,.

4. The preliminary investigations presented in this paper substantiate the need for further, more detailed research of this issue in terms of the possibilities of a more efficient use of the photovoltaic systems.

5. The investigations into tracking photovoltaic systems can be very wide in range. Tins range includes a variety of types of the photovoltaic modules in a variety of solar radiation conditions. The economic aspect is also important showing in which cases it is economically beneficial.

6. The effect of further research on the model test stand will be the determination of the optimum control algorithm for the tracking photovoltaic system and final programming of the single-circuit microprocessor such as ATMega644p in the BASCOM language for the control of the autonomous system.

REFERENCES

1. **Buczaj M., Humorek A. 2011:** The use of LabVIEW environment for the building of supervision system controlling the climatic and technical parameters in farm rooms. TEKA Kom. Mot. i Energ. Roln. – OL PAN, v. 11, p. 18-28.
2. **Chochowski A., Czekalski D. 2005:** Pomiary pyranometryczne na stanowisku SGGW-Ursynów. Polska Energetyka Słoneczna nr 2/2005, p. 15-19.
3. **Chwieduk D. 2006:** Modelowanie i analiza pozyskiwania oraz konwersji termicznej energii promieniowania słonecznego w budynku. Instytut Podstawowych Problemów Techniki PAN, Warszawa.
4. **Jarzębski Z. M. 1990:** Energia Słoneczna, konwersja fotowoltaiczna. PWN, Warszawa.
5. **Kaiser H. 1995:** Wykorzystanie energii słonecznej. Wydawnictwo AGH, Kraków.
6. **Kapica J. 2011:** Application of a microcontroller in simulation of the photovoltaic generators. TEKA Kom. Mot. i Energ. Roln. – OL PAN, v. 11, p. 173-180.
7. **Klugmann E.1999:** Energetyka fotowoltaiczna. PWN, Warszawa.

8. **Klugmann E., Klugmann-Radziemska E. 1999:** Alternatywne źródła energii. Energetyka fotowoltaiczna. Wydawnictwo Ekonomia i Środowisko, Białystok.
9. **Klugmann E. Klugmann-Radziemska E. 2005:** Ogniwa i moduły fotowoltaiczne oraz inne niekonwencjonalne źródła energii. Wydawnictwo Ekonomia i Środowisko, Białystok.
10. **Marecki J. 1995:** Podstawy przemian energetycznych. WNT, Warszawa.
11. **Messenger R. A., Ventre J. 2010:** Photovoltaic Systems Engineering. Third Edition. 527 pp. CRC Press Inc.
12. **Myczko A., Karłowski J., Lenarczyk J. 2010:** Porównanie efektywności energetycznej zestawu modułów fotowoltaicznych stacjonarnych i pracujących w układzie nadążnym w warunkach gospodarstwa rolnego. Problemy Inżynierii Rolniczej nr 4/2010.
13. **Nalepa K., Neugebauer M., Spławiej P., Chmielewski R. 2009:** Wykorzystanie mikrokontrolera jednoukładowego do sterowania optymalnym ustawieniem płaszczyzny ogniwa fotowoltaicznego w stosunku do słońca. Inżynieria Rolnicza 8(117)/2009.
14. **Nawrocka A., Grundas S. 2010:** Applications of semiconductor nanoparticles in power industry. TEKA Kom. Mot. i Energ. Roln. – OL PAN, v. 10, p. 284–293.
15. **Nowicki J. 1980:** Promieniowanie słoneczne jako źródło energii. Arkady, Warszawa.
16. **Pluta Z. 2000:** Podstawy teoretyczne fototermicznej konwersji energii słonecznej. Oficyna Wydawnicza Politechniki Warszawskiej, Warszawa.
17. **Roszkowski A. 2006:** Agriculture and fuels of the future. TEKA Kom. Mot. i Energ. Roln. – OL PAN, v. 6, p. 131-134.
18. **Sarniak M. 2006:** Badanie wpływu przestrzennego ustawienia paneli fotowoltaicznych na przebiegi charakterystyk prądowo-napięciowych. Wybrane Problemy Inżynierii Mechanicznej. Instytut Inżynierii Mechanicznej w Płocku, rozdział 15 w monografii, p. 176-183.
19. **Sarniak M. 2008:** Podstawy fotowoltaiki. Oficyna Wydawnicza Politechniki Warszawskiej, Warszawa.
20. **Sarniak M. 2011:** The testing of energy efficiency of a prototype hybrid solar panel. TEKA Kom. Mot. i Energ. Roln. – OL PAN, v. 11, 335-342.
21. **Smoliński S.1998:** Fotowoltaiczne źródła energii i ich zastosowania. Wydawnictwo SGGW, Warszawa.
22. PN-EN ISO 9488: 2002: Energia słoneczna – Terminologia.

ZASTOSOWANIE OPROGRAMOWANIA LABVIEW DO STEROWANIA MODELEM NADĄŻNEGO SYSTEMU FOTOWOLTAICZNEGO

S t r e s z c z e n i e. W pracy przedstawiono projekt stanowiska do badań nadążnych systemów fotowoltaicznych. Do sterowania stanowiskiem wykorzystano uniwersalną kartę pomiarowo-sterującą LabJack U12, a algorytmy sterowania są realizowane w systemie LabVIEW. Stanowisko jest przystosowane do badania różnych typów ogniw i różnych algorytmów sterowania.

S ł o w a k l u c z o w e: konwersja fotowoltaiczna, system nadążny, ogniwo fotowoltaiczne, panel fotowoltaicznym.

TEKA. COMMISSION OF MOTORIZATION AND ENERGETICS IN AGRICULTURE – 2012, Vol. 12, No. 1, 243–246

The method of selection of optimum fitting parameters for stationary photovoltaic systems and optimum control parameters for tracking photovoltaic systems

Mariusz Sarniak

Warsaw University of Technology, Faculty of Civil Engineering, Mechanics and Petrochemistry
Department of Mechanical Systems Engineering and Automation
Address: Al. Jachowicza 2/4, 09–402 Płock, Poland; e-mail: sarniak@pw.plock.pl

Summary. The paper presents a simplified method of selection of the optimum fitting parameters for stationary photovoltaic systems and optimum control parameters for tracking photovoltaic systems. The method consists in the stationary analysis of the available files of the database from complete 30-year observations for 43 meteorological stations in Poland. The application of the presented method has been shown on the example the meteorological station located in Płock Trzepowo. Based on the data for the selected station a set of optimum parameters has been developed.

Key words: solar radiation intensity, solar collector, photovoltaic conversion, photovoltaic panel.

INTRODUCTION

In the paper the authors proposed a simplified method of determining of the optimum parameters for the fitting of stationary photovoltaic systems and determining of the control ranges for tracking photovoltaic systems based on the available meteorological data gathered during long-term observations. The basic criterion when selecting the parameters is the maximum value of the solar radiation hitting the surface of the photovoltaic module [6, 13, 14, 16].

On the web page of the Ministry of Transport, Construction and Maritime Economy (*www.transport.gov.pl*) data files have been made available, generated from the Institute of Meteorology and Water Management that determine the 'typical meteorological years'. The data in these files come from observations carried out in 61 meteorological stations 43 of which have had full data streams from 30-year observations in the years: 1971-2000. 'Typical meteorological years' have been developed based on the EN ISO 15927:4 standard [18].

For the needs of the proposed method, data from the following files have been used: *wmo123600iso.txt* and *wmo123600iso_stat.txt* for the nearest meteorological station located in Płock Trzepowo located at: $52^0$35' N, $19^0$44' E. The data files contain values of solar radiation both total and dispersed for the horizontal plane and the values for the planes of different angles of incidence. The files have been imported and processed through built-in functions of a spreadsheet.

SELECTION OF THE FITTING PARAMETERS FOR THE STATIONARY PHOTOVOLTAIC SYSTEMS

Theoretical analyses of the optimum angle of incidence β_{opt} of the solar radiation receiver in terms of the criterion of the maximum energy benefit have shown a close relation of this angle to the period of operation for which the calculations were carried out [9, 8, 4]. If we take into account only the direct component of the solar radiation then the optimum angle of incidence of the solar collector oriented to the south we can calculate from the dependence [12, 2, 3]:

$$\beta_{opt} = \varphi - \delta, \tag{1}$$

where:

ϕ - Latitude assumed as positive for the northern hemisphere,

δ - Solar declension – angular sun orientation against the plane of the equator at astronomical noon.

The solar declension on a given day we can calculate from the Cooper's approximate formula:

$$\delta = 23,45 \cdot \sin\left(360 \cdot \frac{284 + n}{365}\right), \tag{2}$$

where:

n – consecutive month in the year.

In practice, average value of the solar declension is assumed for the analyzed period of operation. Most often

it is the value of the solar declension for the day recommended in a given month i.e. such a day for which the solar declension equals the average monthly value [11, 5]. Table 1 presents the calculations of the optimum angle of incidence β_{opt} for the photovoltaic system, whose plane is oriented to the south. These results take into account only the direct component of the solar radiation. The calculations were made for the latitude $52^0 35'$ N at which the meteorological station Płock Trzepowo is located.

Table 1. Results of calculations β_{opt} for the location $52^0 35'$ N – Płock Trzepowo

Month	Solar declension for the recommended day in a given month δ [^{0}]	Optimum angle of incidence of the surface of the photovoltaic system β_{opt} [^{0}]
I	-20,9	73
II	-13,0	66
III	-2,4	55
IV	9,4	43
V	18,8	34
VI	23,1	29
VII	21,2	31
VIII	13,5	39
IX	2,2	50
X	-9,6	62
XI	-18,9	71
XII	-23,0	76

These results have a high error rate because additionally diffusion and reflection components get to the surface of the photovoltaic system [15, 10, 1].

In order to determine the optimum angle o incidence for a stationary photovoltaic system fitted in the plane oriented to the south an analysis has been performed of selected data collected in file *wmo123600iso_stat.txt* for the said station Płock Trzepowo. In the field of the databases values of solar radiation are available for different positions of the plane of the receiver - as schematically presented in fig. 1.

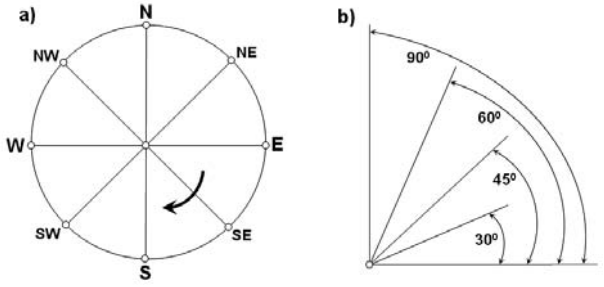

Fig. 1. Schematics of different data gathered in the files of the meteorological stations: a) data available for the azimuth position-γ, b) data available for the angle of incidence against horizon-β

Table 2 presents the query for data from the monthly report of the total solar radiation for the meteorological station located in Płock Trzepowo. The greatest values of the solar radiation have been found and presented in individual months for several constant orientations of the plane of the fitting of the radiation receiver. The marking of the receiver plane setting in table 2 is composed of the letter determining the azimuth position and the number determining the angle of incidence against the horizon frequently referred to as the elevation angle as seen in the schematics in figure 1.

Table 2. List of greatest monthly values of the total solar radiation for the meteorological station located in Płock Trzepowo

Month	Orientation for MAX	The total of the monthly solar radiation [Wh×m^{-2}]					
		MAX	S-0	S-30	**S-45**	S-60	S-90
I	S-60	28802	20395	25779	27654	28802	28655
II	S-60	42967	30207	39039	41718	42967	40940
III	S-60	86369	66187	81598	85468	86369	79220
IV	S-45	92869	86049	92757	92869	90760	80643
V	S-30	136746	131342	136746	134467	128998	110993
VI	S-30	138354	136926	138354	134864	128949	112163
VII	SE-30	141089	137722	139657	136483	130894	114754
VIII	S-30	121894	115339	121894	120862	116985	102266
IX	S-45	91266	80249	89763	91266	90412	82022
X	S-60	59882	45519	55905	58808	59882	56383
XI	S-60	31186	21617	27917	30008	31186	30550
XII	S-60	21823	18380	20563	21337	21823	21822
Total:		**993247**	889932	969972	**975804**	958027	860411
Loss against MAX:			10,4%	2,34%	1,76%	3,55%	13,37%

If we want to use the maximum monthly sums of the solar radiation we should change the setting of the receiver 7 times during the year. The adoption of a constant annual receiver orientation S-45 results in only 1.76 % of the losses of the total solar radiation as compared to the maximum values.

THE SELECTION OF THE CONTROL PARAMETERS FOR THE TRACKING PHOTOVOLTAIC SYSTEMS

Optimistic claims of the manufacturers related to the apparent 40 % increase in the efficiency of tracking photovoltaic systems in comparison to the stationary ones have been verified experimentally in [9]. When designing this type of systems one needs to take into account the losses of the energy used for the control process and only then present the energy balance as a reliable one.

The energy losses are dependent on many factors: the frequency of adjustment of the plane angle of incidence of the photovoltaic system, the direction and strength of wind, ambient temperature etc. Most of these factors cannot be influenced but we can optimize the frequency of adjustments of the angle of incidence of the photovoltaic system towards the sun.

A proposal of a simplified method of optimization consists in a monthly averaging of the collected data (based on 30 years of observations) from the meteorological stations related to the solar radiation intensity for different combinations of the positions of the receiver as presented in figure 1. The next step is determining the maximum values of the solar radiation intensity for individual hours in each month. Based on such an analysis the results were obtained of the optimum positions of the plane of the solar radiation receiver plane as shown in table 3.

CONCLUSIONS

1. The analysis of the data collected in the period of 30 years from the meteorological station located in Płock Trzepowo has shown that for the stationary photovoltaic system the optimum angle of incidence aiming south is 45^0.

2. In the case of tracking photovoltaic systems, the analysis of the data from the meteorological station enables determining of a set of parameters for the control in two planes as shown in table 3.

3. In the winter months when the solar radiation is mostly diffuse, the changes in the setting of the plane of the photovoltaic system are not frequent: December-January a fixed position, February-November three positions.

4. In the summer months when the direct solar radiation component is prevalent, the optimum positioning

Table 3. Optimum orientation of the plane of the solar radiation receiver for the highest radiation intensity averaged to a representative day of each month in a calendar year

Hours of the model day for a given month (hours UTC)	Month I	II	III	IV	V	VI	VII	VIII	IX	X	XI	XII
4												
5												
6						E-60	E-60		E-60			
7					E-60		E-45	E-60				
8				SE-60		E-45	SE-45		SE-60		SE-90	
9		SE-60	SE-60		SE-45	SE-30	SE-30	SE-45	SE-45	SE-60		
10								SE-45				
11				S-45	S-30		S-30	S-30	S-45	S-60	S-60	
12		S-60	S-60			S-30	SW-30					
13							SW-45		SW-45			
14	S-60	SW-60	SW-60		SW-45	SW-45	W-45	SW-45	SW-60	S-60	SW-60	S-60
15				SW-60					W-60			
16												
17					W-60	W-60	W-60	W-60				
18												

of the photovoltaic plane requires several shifts in the position per day e.g. in July that is nine shifts.

5. The described method can be used for any given number of locations countrywide using the data from the closest meteorological station for the calculations.

REFERENCES

1. **Chochowski A., Czekalski D. 2005:** Pomiary pyranometryczne na stanowisku SGGW-Ursynów. Polska Energetyka Słoneczna nr 2/2005, p. 15-19.
2. **Chwieduk D. 2006:** Modelowanie i analiza pozyskiwania oraz konwersji termicznej energii promieniowania słonecznego w budynku. Instytut Podstawowych Problemów Techniki PAN, Warszawa.
3. **Jarzębski Z. M. 1990:** Energia Słoneczna, konwersja fotowoltaiczna. PWN, Warszawa.
4. **Kaiser H. 1995:** Wykorzystanie energii słonecznej. Wydawnictwo AGH, Kraków.
5. **Kapica J. 2011:** Application of a microcontroller in simulation of the photovoltaic generators. TEKA Kom. Mot. i Energ. Roln. – OL PAN, v. 11, p. 173-180.
6. **Klugmann E.1999:** Energetyka fotowoltaiczna. PWN, Warszawa.
7. **Klugmann E., Klugmann-Radziemska E. 1999:** Alternatywne źródła energii. Energetyka fotowoltaiczna. Wydawnictwo Ekonomia i Środowisko, Białystok.
8. **Marecki J. 1995:** Podstawy przemian energetycznych. WNT, Warszawa.
9. **Myczko A., Karłowski J., Lenarczyk J. 2010:** Porównanie efektywności energetycznej zestawu modułów fotowoltaicznych stacjonarnych i pracujących w układzie nadążnym w warunkach gospodarstwa rolnego. Problemy Inżynierii Rolniczej nr 4/2010.
10. **Nalepa K., Neugebauer M., Spławiej P., Chmielewski R. 2009:** Wykorzystanie mikrokontrolera jednoukładowego do sterowania optymalnym ustawieniem płaszczyzny ogniwa fotowoltaicznego w stosunku do słońca. Inżynieria Rolnicza 8/2009. p. 117.
11. **Nawrocka A., Grundas S. 2010:** Applications of semiconductor nanoparticles in power industry. TEKA Kom. Mot. i Energ. Roln. – OL PAN, v. 10, p. 284–293.
12. **Ney R. 1994:** Energia odnawialna. Nauka Polska nr 1/1994.
13. **Nowicki J. 1980:** Promieniowanie słoneczne jako źródło energii. Arkady, Warszawa.
14. **Pluta Z. 2000:** Podstawy teoretyczne fototermicznej konwersji energii słonecznej. Oficyna Wydawnicza Politechniki Warszawskiej, Warszawa.
15. **Sarniak M. 2006:** Badanie wpływu przestrzennego ustawienia paneli fotowoltaicznych na przebiegi charakterystyk prądowo-napięciowych. Wybrane Problemy Inżynierii Mechanicznej. Instytut Inżynierii Mechanicznej w Płocku, rozdział 15 w monografii, p. 176-183.
16. **Sarniak M. 2008:** Podstawy fotowoltaiki. Oficyna Wydawnicza Politechniki Warszawskiej, Warszawa.
17. **Smoliński S.1998:** Fotowoltaiczne źródła energii i ich zastosowania. Wydawnictwo SGGW, Warszawa.
18. **Tymiński J. 1997:** Wykorzystanie odnawialnych źródeł energii w Polsce do 2030 roku. Aspekt energetyczny i ekologiczny. Wydawnictwo IBMER, Warszawa.
19. PN-EN ISO 9488: 2002: Energia słoneczna – Terminologia.
20. EN ISO 15927-4: 2003: Hygrothermal performance of buildings - Calculation and presentation of climatic data - Part 4: Data for assessing the annual energy for cooling and heating systems, CEN.

METODA DOBORU OPTYMALNYCH PARAMETRÓW MONTAŻU DLA STACJONARNYCH I STEROWANIA DLA NADĄŻNYCH SYSTEMÓW FOTOWOLTAICZNYCH

Streszczenie. W pracy przedstawiono uproszczoną metodę doboru optymalnych parametrów montażu dla stacjonarnych i sterowania dla nadążnych systemów fotowoltaicznych. Metoda polega na analizie statystycznej dostępnych plików baz danych z pełnych 30-letnich obserwacji dla 43 stacji meteorologicznych na terenie Polski. Zastosowanie prezentowanej metody pokazano na przykładzie stacji meteorologicznej Płock Trzepowo. Na podstawie danych dla wybranej stacji opracowano zbiór optymalnych parametrów.

Słowa kluczowe: natężenie promieniowania słonecznego, kolektor słoneczny, konwersja fotowoltaiczna, panel fotowoltaiczny.

TEKA. COMMISSION OF MOTORIZATION AND ENERGETICS IN AGRICULTURE – 2012, Vol. 12, No. 1, 247–250

Characteristic load states of a tractor engine under farm operating conditions

Paweł Sędłak, Adam Koniuszy, Tomasz Stawicki

Chair of Agrotechnical Systems Engineering; West Pomeranian University of Technology Szczecin
Papieża Pawła VI nr 1, 71 – 459 Szczecin; e-mail: adam.koniuszy@zut.edu.pl

Summary. The paper presents the results of the in-use investigations of a U912 tractor operating in the conditions of an average farm in the Province of Lubuskie. In-use investigations of tractor engines under actual operating conditions allow an obtainment of a great deal of important information from the point of view of the end-user and the manufacturer. They determine the scale of mechanical loads on the engine and characterize the engine speed ranges at which they occur. An exact exploration of the load conditions and the characteristics of operation lead to an improvement of the engine design and optimize its durability and reliability of its individual elements.

Key words: farm tractor, combustion engine, in-use investigations.

INTRODUCTION

Empirical tests on farm tractors under actual farm operating conditions allows for an obtainment of valuable information on the engine loads that they must withstand while in operation. The loads that come from the coupled machinery and tools are realized by a combustion engine supplying mechanical energy. The value of the loads depends on many factors that are characteristic of the individual operating conditions. Field plowing, one of the hardest tasks for the same kind of plow may generate different power demand, which may result from different terrain conditions, type of soil, humidity, wheel slip, type of plowing etc. Different loads are generated during transport and other light tasks in agriculture [1, 2, 11]. A combustion engine of a farm tractor must thus have sufficient power output and dynamics in order to be able to fulfill such different conditions of operation – as opposed to combustion engines fitted in road vehicles [10]. An example analysis of the obtained in-use test results of the farm tractor engine loads is significant when evaluating the reliability and durability of the individual engine elements and fuel economy of the engine operation [3, 7].

The obtained results of the in-use tests of the farm tractors may be helpful improving the existing designs of both the engines and farm tractors as a whole as well as they may turn out invaluable in designing new machinery (engines). The changes may reduce the loads on the individual engine elements and reduce the fuel consumption, noise level, exhaust emissions and result in a more effective use of the farm tractors [4, 5, 6]. Despite the fact that in-use investigations are time consuming and costly we can still observe a growing interest of the manufacturers in this type of research.

RESEARCH METHODS

The in-use tests were conducted on a U912 farm tractor used in the farm located in the northeastern part of the province of Lubuskie in the strzelecko-drezdenecki powiat, municipality of Dobiegniew. This farm mostly grows winter cereals - rapeseed, wheat, rye and spring cereals - barley and oat and has an area of 87,6 ha. The tests were carried out in the period – July, August, and September when the tractor was most intensely used in fieldwork and for transporting of the crops. In the monitored period the tractor effectively operated for 100,3 hours. The URSUS 912 tractor is fitted with a Z8401.1 engine. In Table 1 its technical parameters have been specified.

Table 1. Technical specifications of the Z8401.1 engine

Basic technical data of the Z8401.1 engine		
Parameter	Unit	Value
Number of cylinders, c	-	4
Engine displacement, V_{ss}	dm^3	4,562
Rated power output, N_e	KW	57,1
Engine speed at rated power output, n_N	rpm	2200
Maximum torque, M_o	Nm	277,6
Engine speed at maximum torque, n_M	rpm	1450
Unit fuel consumption, g_e	$g \times kW^{-1} \times h^{-1}$	240

For the recording of the selected operating parameters of the tested engine the authors used a tractor recording system TRS-1 developed in the Chair of Agrotechnical Systems Engineering at West Pomeranian University of Technology in Szczecin [9]. The device generates time density TD characteristics of a piston combustion engine under actual operating conditions.

After a proper installation the device allows a fully automatic unassisted measurement. The activation of the measuring systems begins with the engine start-up and the end of the measurement takes place as the engine is switched off. TRS-1 measures and records in real time the engine speed, the amount of consumed fuel and the time of operation. The system is also fitted with a GPRS that enables the recording of the instantaneous location, covered distance and speed of the vehicle. The recorded quantities are stored on a removable data carrier from which the data is subsequently transferred to a PC computer for statistical processing.

Due to a small size of the measurement equipment and a full automation of the recording the tractor user operated the tractor similarly to previous years (which is of significance in terms of the representativeness of the collected data). The tractor user only indicated the kind of work performed in the subsequent days. The results obtained under such conditions can be deemed as typical use of a farm tractor on a farm coupled with similar machinery. The aim of the performed tests was to explore the distribution of engine speeds and torque of the tested engine under farm operating conditions while performing different tasks.

RESEARCH RESULTS

In the monitored period the engine was used for crop transport works (transport from the field to the farm premises and from the premises to the buying stations), and other works such as soil braking, disking, fertilizing etc. That is why in the figures the engine speed and torque were listed for these two tractor applications and the collective value for the whole period. Figure 1 presents the distribution of engine speeds for the transport task Fig. 1a and during 'other' works Fig. 1b.

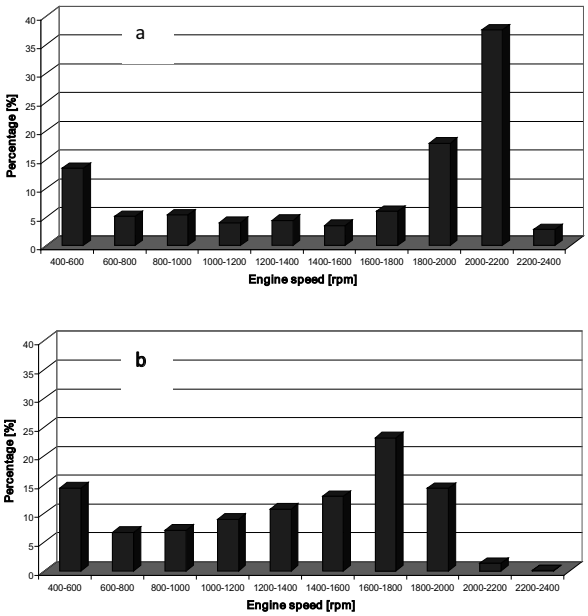

Fig. 1. Distribution of the Z8401.1 engine speed during: a) transport, b) 'other' works

From the analysis of the collected information on the use of the tested tractor and the time of performance of the individual tasks it results that these works were performed for 46,1 hours and other works for 54,2 hours. Such a high share of the works related to transport could be explained by high agrotechnical season during the tests when the tractors are coupled with trailers and collect grain from the harvester to transport it to the storage buildings.

As we can see in the results shown in Fig. 1 the distribution of engine speeds is different for transport tasks and 'other' tasks. The dominating speed for the transport task is the range from 2000 to 2200 rpm, which constitutes 37,5% of the total time of tractor operation with this task. For other works the dominating range is 1600-1800 rpm, which constitutes 23,2% of the total operating time. In both cases of the engine operation we can observe a great share of the engine operation at idle i.e. engine speed of 400-600 rpm (13,4% for transport tasks and 14,3% for 'other' tasks). Such a high share of this range is caused by the fact that he machines need to be coupled with the tractor and maintenance for 'other' works needs to be carried out (the driver does not switch off the engine). In the case of the transport tasks this is caused by waiting in a line for the buying station.

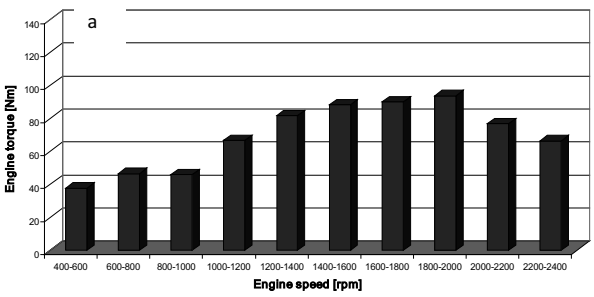

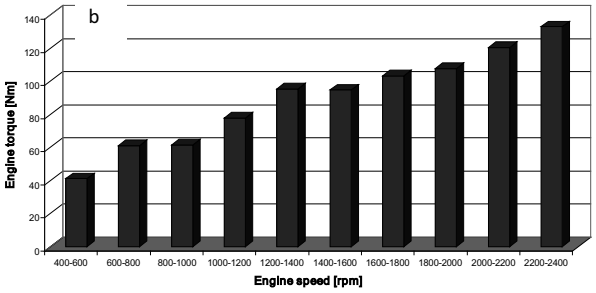

Fig. 2. Distribution of the Z8401.1 engine torque during: a) transport task, b) 'other' works

Fig. 2. in the form of graphs shows the distribution of the average torque as a function of speed and Fig. 3 the share of the individual ranges of torque in time. Approximately 75 % of the time in the transport task the engine worked with the torque in the range from 20 to 100 Nm (Fig. 2a). When performing transport tasks the torque was most frequently within the range of 60-80 Nm and constituted 25,8% of the total operating time. This torque is approximately 25% of the rate torque, which suggests a very small employment of the engine potential. When performing 'other' works we can distinguish two ranges of torque that were most frequently used. These were 20-80 Nm (38,5 % of the item) and 140-200 Nm (25,1 %). The first range corresponds to works at light field tasks (fertilizing, spurting) and the other to groundbreaking or disking [8].

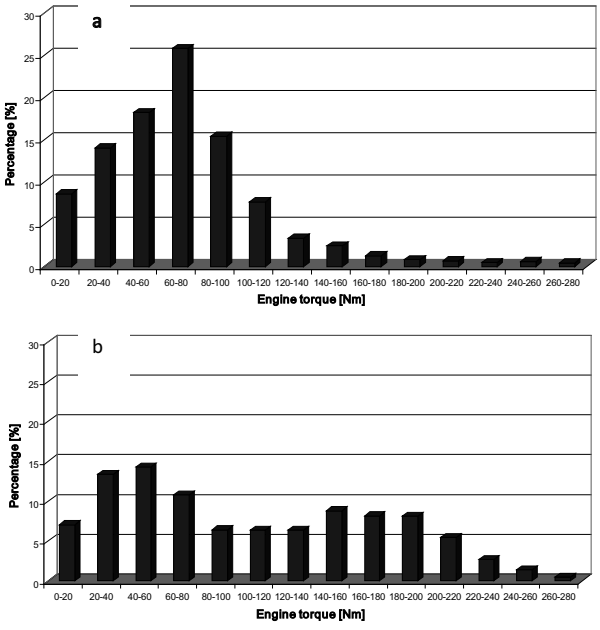

Fig. 3. Distribution of torque in the total work time a) transport, b) 'other' works

Figures 4, 5 and 6 show the average of the tested values in the whole period of the conducted investigations. The analysis of the obtained results from the in-use investigations of the Z8401.1 engine has shown that irrespective of the performed tasks (fieldworks, transport) there is a great share of the engine operation at idle (400-600 rpm) in the whole period of its operation (13,95 %).

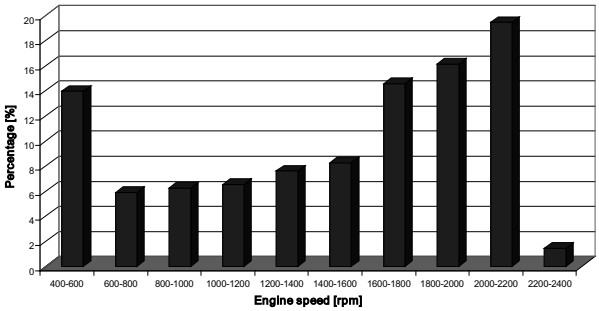

Fig. 4. Distribution of the average Z8401.1 engine speeds

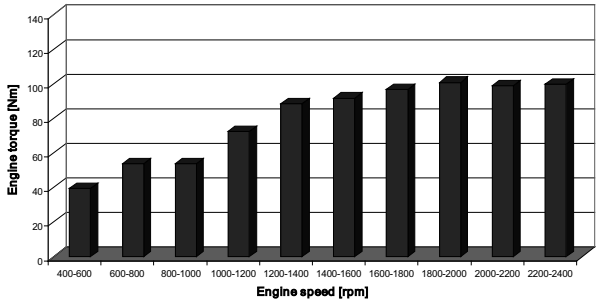

Fig. 5. Distribution of the average torque of the Z8401.1 engine for the individual engine speeds

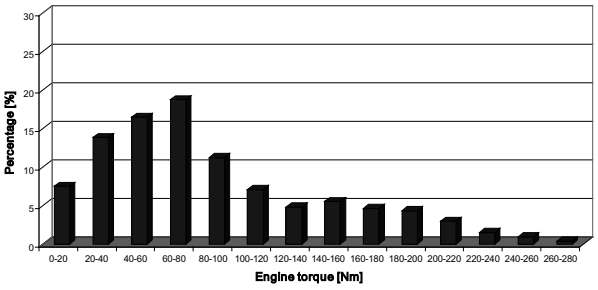

Fig. 6. Distribution of the average torque in the total operating time

Another range of the engine speeds i.e. 1600-2200 is over 50 % of the total operating time (including the engine speed of 2000-2200 - 19 %). Such a great share of the engine speed of 2000-2200 is caused by the fact that the tractor was used for road transport of the crops and was driven at its maximum road speed. At the same time the engine operated with the torque of 60-80 Nm. As results from Fig. 6 the tested farm tractor operated mostly at the torque within the range of 20 to 80 Nm (49 % of the total operating time – which constitutes approximately 49 hours). The operation at the torque from 140 to 200 Nm is 14,5 % of the time (approximately 14,5 hours).

CONCLUSIONS

1. The conducted in-use investigations of the Z8401.1 engine have shown that the farm tractor operated at idle for approximately 13,95% of the total operating time.

2. The dominant range of the engine speed was 2000-2200 rpm.
3. In the tested period the engine most frequently ran at the torque from 60 to 80 Nm (18,7 %) of the total operating time.
4. The employment of the engine power in the farm under analysis is very low and indicates an improper selection of the type of tractor to the agricultural tasks.
5. The results of the performed investigations confirm the purposefulness of this type of investigations as regards optimizing the selection of machines for tasks and designing machines for specific tasks in terms of maximum employment of their potential.

REFERENCES

1. **Ambrozik A., Piasta Z. 1988:** Ocena pracy silnika spalinowego w oparciu o uogólnioną użyteczność jego wskaźników. Silniki Spalinowe 4, p. 33-36.
2. **Banasiak J., Bieniek J., Detyna J. 2002:** Aktualne problemy użytkowania maszyn rolniczych. Eksploatacja i Niezawodność 2 (14), p. 63-72.
3. **Bieniek A., Graba M., Lechowicz A. 2011:** Control of agricultural engine injection system in aspect of ecological property improvement. Combustion Engines 3/2022 (146), PTNSS-2011-SC-192.
4. **Chłopek Z., Biedrzycki J. 2011:** Research of the work states of car engines in conditions simulated a traffic in cities. Combustion Engines 3/2022 (146), PTNSS-2011-SC-132.
5. **Czarnigowski J., Droździel P., Kordos P. 2002:** Charakterystyczne zakresy prędkości obrotowych wału korbowego podczas pracy silnika spalinowego w warunkach eksploatacji samochodu. Eksploatacja i Niezawodność 2 (14), 55-62.
6. **Hansson P.-A., Noren O., Bohm M. 1999:** Effects of Specific Operational Weighting Factors on Standardized Measurements of Tractor Engine Emissions. Journal Agricultural Engineering Research 74, p. 347-353.
7. **Koniuszy A. 2008a.** A new method of usability evaluation of agricultural tractors based on optimum working index [OWI]. TEKA Komisji Motoryzacji i Energetyki Rolnictwa. OL Pan. 8a, p. 93-99.
8. **Koniuszy A. 2008.** Usabilityanalysis of static load cycles for assessment of tractor engine operation economy. TEKA Komisji Motoryzacji i Energetyki Rolnictwa. OL Pan. 8, p. 107-113.
9. **Koniuszy A. 2010.** Identyfikacja stanów obciążeń ciągnika rolniczego. Wydawnictwo Uczelniane ZUT, Szczecin.
10. **Liscak S., Las P. 2001:** Actual Situation of Bus Fleet Renovation in Conditions of the Slovak Republic. Journal of KONES, Internal Combustion Engines, vol. 8, no. 1-2.
11. **Wisłocki K. 1989:** Rozkład warunków pracy w optymalizacji silnika spalinowego i pojazdu. Silniki Spalinowe 4, p. 26-33.

CHARAKTERYSTYCZNE STANY OBCIĄŻEŃ SILNIKA CIĄGNIKOWEGO EKSPLOATOWANEGO W WARUNKACH GOSPODARSTWA ROLNEGO

S t r e s z c z e n i e . W artykule przedstawiono wyniki badań eksploatacyjnych ciągnika U912 eksploatowanego w warunkach przeciętnego gospodarstwa rolnego województwa lubuskiego. Badania eksploatacyjne silnika ciągnikowego w warunkach rzeczywistych umożliwiają uzyskanie bardzo wielu informacji istotnych z punktu widzenia zarówno użytkownika jak i producenta. Pozwalają one określić skalę obciążeń mechanicznych jakim jest poddawany obiekt oraz scharakteryzować zakresy prędkości obrotowych przy jakich one występują. Dokładne poznanie wymuszeń oraz charakterystyki eksploatacji pozwala poprawiać konstrukcję silnika jak i optymalizować trwałość i niezawodność poszczególnych węzłów.

S ł o w a k l u c z o w e : ciągnik rolniczy, silnik spalinowy, badania eksploatacyjne.

TEKA. COMMISSION OF MOTORIZATION AND ENERGETICS IN AGRICULTURE – 2012, Vol. 12, No. 1, 251–255

The analysis of the usability of selected stationary load cycles for the assessment of the tractor engine economy

Paweł Sędłak, Wiesław Janicki, Krzysztof Matuszak

Department of Agrotechnical Systems Engineering. West Pomeranian University of Technology Szczecin
Papieża Pawła VI 1, 71 – 459 Szczecin, e-mail: *pawel.sedlak@zut.edu.pl*

Summary. The paper analyzes the operating indexes of an AD3.152 engine obtained during three stationary load cycles: an 8-phase cycle and two variants of a 5-phase cycle. The obtained results have been presented and compared based on the weighted averages.

Key words: combustion engine, engine economy, stationary load cycles.

INTRODUCTION

The operating conditions of a combustion engine are closely related to its application. Engines of road vehicles are subject to entirely different loads than stationary ones. The engines of road vehicles are characterized by a high variability of engine loads and speeds as compared to stationary engines for which the loads are frequently changed without changing the engine speed. Because constant operating conditions in the most advantageous ranges of engine speeds cannot be ensured their fuel economy differs and highly depends on proper operation by the personnel. The operation of an engine within the range of engine speeds corresponding to the highest overall efficiency ensures the lowest fuel consumption (highest engine economy). The fulfillment of these conditions is very often impossible due to the nature of the work performed [6, 3]. In order to optimize the process of engine operation and provide evaluation many synthetic operating models have been developed describing their typical application. The highest number of models has been developed for vehicle engines used in transportation. These models serve to determine the ecological characteristics of these engines (high requirements related to the exhaust and noise emission). Ever since the emission limiting standards have been adopted, unified testing procedures were introduced allowing comparison of the engines in terms of environmental impact. The application of the already existing test cycles to a group of vehicles such as farm tractors may lead to great inaccuracies resulting from the different nature of the operation of road vehicles and the said farm tractors. Many variables influence the operation of a farm tractor. These are: geographical location, terrain, soil firmness, changes in humidity, climatic conditions, types of performed works let alone the tractor operator himself [1, 9]. That is why tractor operation models should be developed that take into account the specificity of the performed works and the geographical location.

In the paper the authors attempted to explain whether the indexes of the tractor engine obtained according to the regional model of operation (5-phase) differ from the indexes obtained during tests carried out according to the European Union method of the 8-phase cycle [PN-EN ISO 8178-4] and 5-phase Deutz cycle developed in Germany for farm tractors.

RESEARCH METHODS

The object of the research was a three cylinder, four-stroke diesel engine (AD3. 152). The engine used for the research is a unit fitted in low-power farm tractors widely applied in Polish farms. The engine was fitted in a dynamometer of the Chair of Agrotechnical Systems Engineering of the West Pomeranian University of Technology in Szczecin. The dynamometer was fitted with a HZW Froud brake and other necessary equipment.

The tests were conducted according to three stationary load cycles. The first load cycle that the engine was subject to was the 8 – phase load cycle applicable in the EU member states representative of the off road vehicles and self propelled machinery powered with diesel engines. The second was a 5-phase Deutz load cycle developed in Germany for the assessment and analysis of the exhaust emissions from farm machinery (as the

authors reckon, this test better reflects the nature of the works in agriculture). The third test cycle was a 5-phase load cycle developed in the Chair of Agrotechnical Systems Engineering of the West Pomeranian University of Technology in Szczecin reflecting the local operation of farm tractors [2, 4]. This cycle was developed based on the specificity of the local farms and geographical conditions of West Pomerania [5]. The test stand measurements were carried out according to the PN-91/R-36102 standard [8] [7].

The values of the settings of the torques and engine speeds for individual phases of the cycles have been shown in table 1, 2 and 3.

Table 1. Settings of the torques and engine speeds in the 8-phase cycle

Phase	Engine speed n_s/n_{znam}	Torque M_o/M_N	Weight coefficient
I	1	1	0,15
II	1	0,75	0,15
III	1	0,5	0,15
IV	1	0,1	0,1
V	0,6	1	0,1
VI	0,6	0,75	0,1
VII	0,6	0,5	0,1
VIII	0,3	0	0,15

Table 2. Settings of the torques and engine speeds in the 5-phase Deutz cycle.

Phase	Engine speed n_s/n_{znam}	Torque M_o/M_N	Weight coefficient
I	0,95	0,88	0,31
II	0,85	0,48	0,18
III	0,53	0,4	0,19
IV	1	0,15	0,2
V	0,4	0	0,12

Table 3. Settings of the torques and engine speeds in the 5-phase regional cycle

Phase	Engine speed n_s/n_{znam}	Torque M_o/M_N	Weight coefficient
I	0,9	0,8	0,08
II	0,9	0,45	0,06
III	0,65	0,7	0,45
IV	0,65	0,45	0,17
V	0,3	0	0,25

RESULTS OF TESTS

The unit fuel consumption was not analyzed and was not calculated for: phase VIII of the 8 – phase cycle, phase V of the Deutz and regional cycles as these phases characterize the engine idle speed, at which the effective

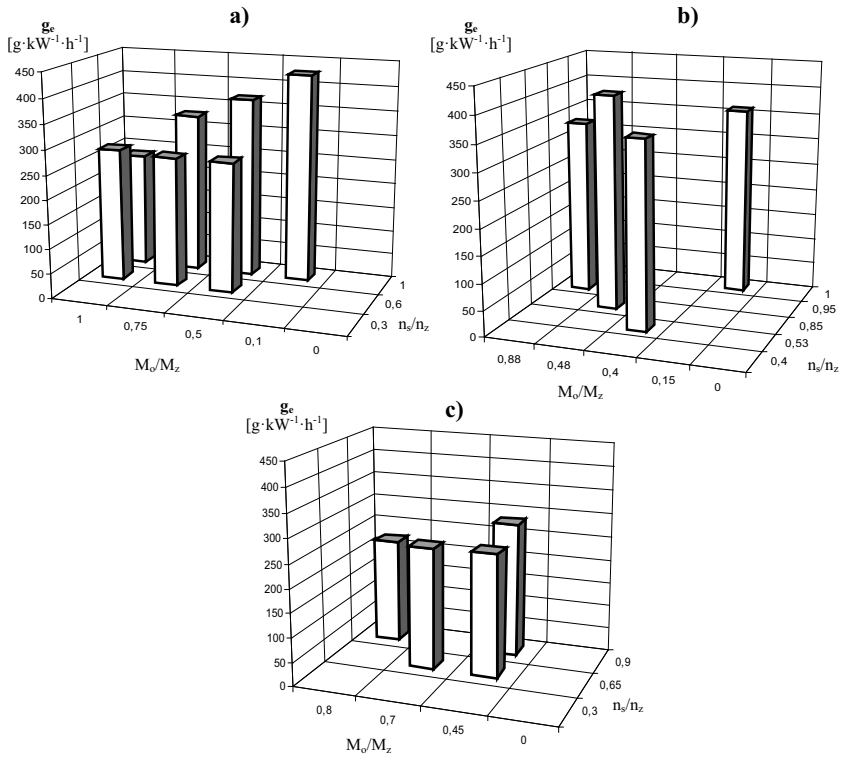

Fig. 1. Average values of the unit fuel consumption in the cycles: a) 8-phase, b) Deutz 5-phase, c) regional 5-phase

power is not generated. Based on the performed measurements and calculations it has been ascertained that the lowest unit fuel consumption 237,52 g·kW^{-1}·h^{-1} was obtained in phase I of the 8-phase load cycle (Fig. 1a). In phases VII, VI and V the unit fuel consumption was higher by 13,8% (phase VII), 13,5% (phase VI) and 16,9% (phase V) respectively as opposed to phase I of this cycle. For phase III the unit fuel consumption was higher than for phase I by 58,2% (phase III) and 40,3% (phase II) respectively. The greatest increase (by 82,6%) as compared to the unit fuel consumption in phase I was obtained for phase IV of the 8-phase load cycle and it amounted to 466,43 g·kW^{-1}·h^{-1}.

Based on the performed measurements of the AD3.152 engine the authors calculated that the highest unit fuel consumption i.e. 409 g ·kW^{-1}·h^{-1} was obtained in phase II of the Deutz 5-phase load cycle (Fig. 1 b). In the other 3 phases of the cycle the unit fuel consumption was lower by 18,4% (phase I), 13% (phase III) and 12,3% (phase IV) respectively. The lowest unit fuel consumption of 333,11 g· kW^{-1}·h^{-1} was obtained in phase I of the load cycle.

The average values of the unit fuel consumption for the 5-phase regional load cycle have been shown in Fig. 1c. The lowest unit fuel consumption obtained in phase I was 221,18 g·kW^{-1}·h^{-1}. For phase II a growth was observed (by 17,2%) of the unit fuel consumption as compared to phase I and a growth by 16,3% was observed for phase III. The highest unit fuel consumption, higher by 28,3% than phase I was observed in phase IV and amounted to 283,5 g·kW^{-1}·h^{-1}. The weighted average unit fuel consumption for the tested engine for each of the cycles is: for the 8-phase cycle 308,8 g·kW^{-1}·h^{-1}, for the Deutz cycle 358 g·kW^{-1}·h^{-1} and for the 5-phase regional cycle 258 g·kW^{-1}·h^{-1} respectively.

The average values of the hourly fuel consumption were calculated for the individual phases of the load cycles and have been shown in graphs in Fig. 2 (a –8 phase cycle; b –Deutz cycle, c – regional cycle). For the 8-phase load cycle the lowest value was observed for phase VII and amounted to 3,34 kg×h^{-1} and the highest was observed for phase II - 8,213 kg×h^{-1}.

Fig. 2b presents the average hourly fuel consumption in the Deutz load cycle. The highest hourly fuel consumption of 6,69 kg×h^{-1} was obtained in phase I of the load cycle. In the other phases due to a lower engine load a drop in the fuel consumption took place by: 38% (phase II), 39% (phase III), 58% (phase IV) respectively. The lowest hourly fuel consumption occurred for phase IV of the cycle and amounted to 2,79 kg×h^{-1}.

Fig. 2c presents the obtained average values of the hourly fuel consumption for the individual phases of the regional 5-phase cycle. The lowest hourly fuel consumption was observed for phase IV – 3,06kg×h^{-1} and the highest for phase I – 5,2 kg×h^{-1} (higher by 69,9% as compared to cycle IV).

In all the cycles the authors observed the occurrence of the lowest hourly fuel consumption in the last but one phase of the individual cycles. The weighted average hourly fuel consumption for the tested engine for each of the cycles is: 8-phase - 6,34 kg×h^{-1}, Deutz - 4,71 kg×h^{-1} and for regional 5-phase - 3,81kg×h^{-1}.

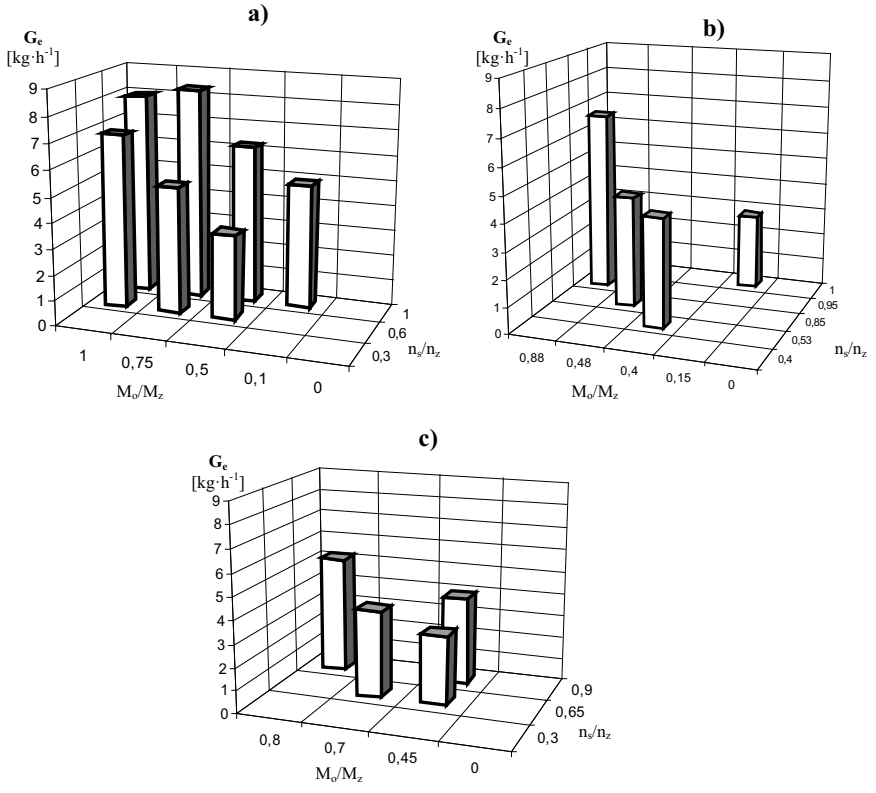

Fig. 2. Average values of the hourly fuel consumption in the cycles: a) 8-phase, b) Deutz 5-phase, c) regional 5-phase

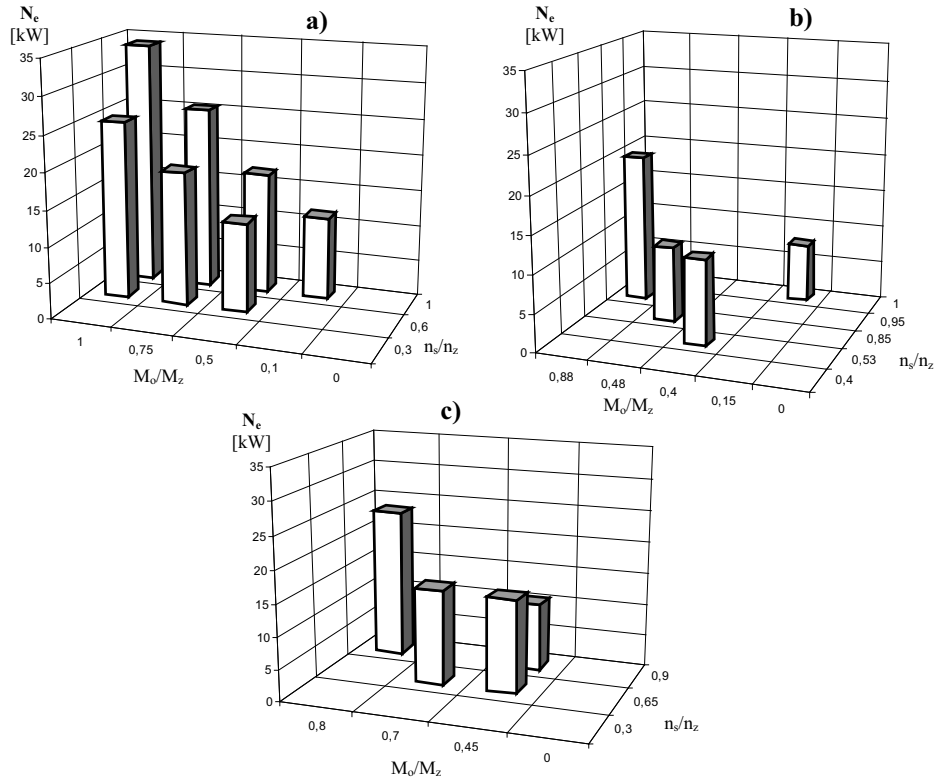

Fig. 3. Average values of the effective power in the cycles: a) 8-phase, b) Deutz 5-phase, c) regional 5-phase

Fig. 3 presents the average values of the effective power obtained for the tested engine in the individual phases of the test cycles.

In the 8-phase cycle the lowest power of 11,5 kW was obtained in phase IV, the highest of 33,9 kW in phase I of the cycle. The highest effective power was obtained in phase I of the Deutz cycle i.e. 19,82 kW. The other analyzed phases have shown a reduction of the effective power. The lowest effective power of 7,68 kW was obtained in phase IV of the tested load cycles. In the regional 5-phase cycle the lowest value was obtained in phase IV and amounted to 10,54 kW. The highest power of 23,4 kW was obtained in phase I. The weighted average effective power for the tested engine for each of the cycles is for the 8-phase cycle 21,3 kW, Deutz cycle 13,2 kW and regional 5-phase cycle 18,9 kW.

Due to a different number of phases, values of torque and engine speed in the individual test cycles we cannot directly compare the results obtained in the individual phases. Taking the coefficients o weight assigned by the cycle authors to the subsequent phases we can determine the weighted averages of the selected indexes of the operation of the given AD3.152 engine. Figures 4,5,6 show the weighted average indexes of work i.e.: effective power N_e, hourly fuel consumption G_e and unit fuel consumption g_e. Analyzing the obtained results we can state that the tested cycles are different in terms of the indexes of the engine work, particularly g_e – the index of the engine economy.

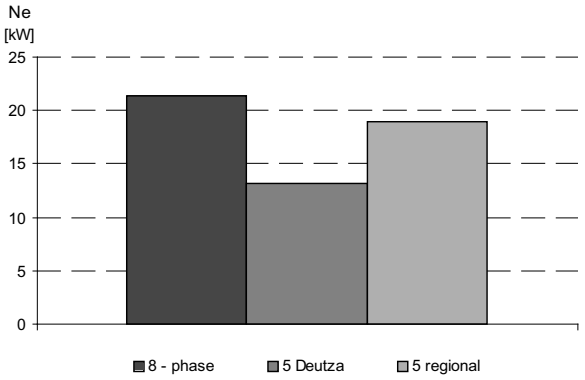

Fig. 4. Weighted average values of the effective power index N_e [kW]

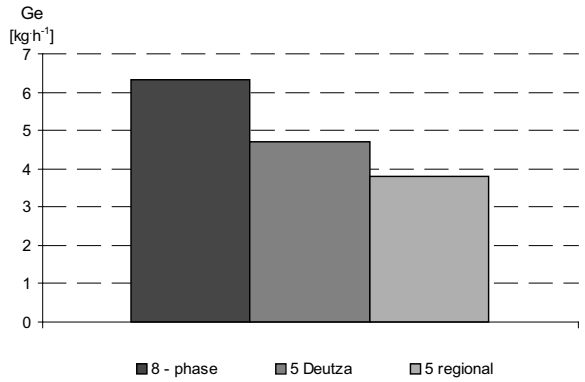

Fig. 5. Weighted average values of the hourly fuel consumption index G_e [kg×h^{-1}]

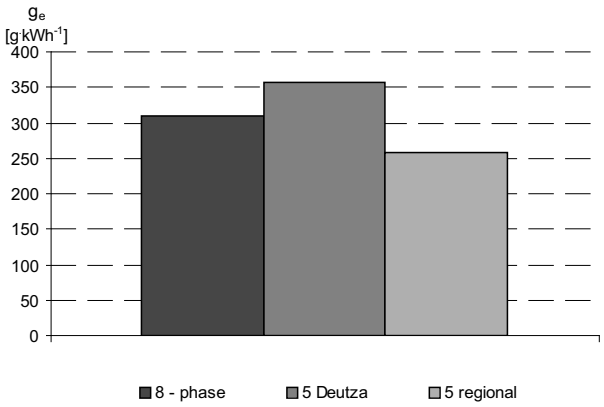

Fig. 6. Weighted average values of the unit fuel consumption index g_e [g·kW^{-1}·h^{-1}]

The highest weighted average effective power N_e was obtained by the engine operating according to the 8 – phase cycle. This power amounted to 21,3 kW. In the Deutz cycle the weighted average effective power was 13,2 kW. For the regional 5-phase cycle developed for the area of the West Pomeranian the weighted average effective power was 18,89 kW.

When analyzing the weighted average hourly fuel consumption we can observe that the 5 – phase cycles show a lower fuel consumption as compared to the 8 – phase cycles. The results obtained for the 5 – phase cycles are G_e= 4,71 kg×h^{-1} for the Deutz cycle and G_e=3,81 kg×h^{-1} for the regional 5 – phase cycle. For the 8 – phase cycle G_e was determined on the level of 6,34 kg×h^{-1}. The difference between the 8- phase cycle and the 5 – phase cycles falls in the range from 25,7% to 39,9%.

The highest weighted average unit fuel consumption g_e was for the Deutz cycle and amounted to 358 [g·kW^{-1}·h^{-1}]. For the 8 – phase cycle the unit fuel consumption was lower by 13 % as compared to the Deutz cycle. The lowest value was calculated for the regional 5 – phase cycle - 258 [g·kW^{-1}·h^{-1}], which is a value lower by 24 % as compared to the Deutz cycle.

The most important index related to the economy level of the engine operation is unit fuel consumption. The lower the unit fuel consumption the better the overall efficiency the engine has. The regional 5 – phase cycle ensures the obtainment of the lowest unit fuel consumption hence, the operation of the engine according to this model leads to a fuel economy and contributes to the reduction of the exhaust emissions.

CONCLUSIONS

1. The weighted average engine work indexes obtained in the tested cycles (AD3.152) were significantly different from each other, thus confirming the assumption that stationary load cycles should be developed depending on the region and specificity of the engine application.
2. From the performed research it results that the weighted average hourly fuel consumption and effective power obtained in the 5-phase load cycles were lower than the values obtained in the 8 – phase cycle.
3. The analysis has shown that the obtained work indexes of the engine operating according to the regional 5 – phase cycle are more advantageous in terms of economy as compared to the other two analyzed load cycles.

REFERENCES

1. **Cupiał K., Grzelka J., Dużyński A., Grzelka P. 2005.** The traction survey and monitoring of a vehicle using a satellite navigation system. TEKA Komisji Motoryzacji i Energetyki Rolnictwa. Vol. V. Lublin p. 37-47.
2. **Hansson A., Noren O., Bohm M. 1999.** Effects of Specific Operational Weighting Factor on Standrdized Measurements of Tractor Engine Emission. Journal of Agricultural Engineering Research, Volume 4 (74), p. 37-43.
3. **Hansson A., Lindgren M., Noren O. 2001.** A Compersion Between Different Methods of calculating Average Engine Emission for Agricultural Tractor. Journal of Agricultural Engineering Research, Volume 1 (80), p. 347-353.
4. **Koniuszy A., Nadolny R. 2007.** Sposób monitoringu pracy ciągnika oraz urządzenie do jego realizacji. Zgłoszenie Patentowe P 381892.
5. **Koniuszy A. 2010.** Identyfikacja stanów obciążeń ciągnika rolniczego. Wydawnictwo Uczelniane ZUT, Szczecin.
6. **Merkisz J. 2004.** Tendencje rozwojowe silników spalinowych. Silniki spalinowe 118, p. 28-39.
7. PN-91/R-36102 1991. Ciągniki i maszyny rolnicze. Badania stanowiskowe silników.
8. PN-EN ISO 8178-4. 1999. Silniki spalinowe tłokowe. Pomiar emisji spalin. Cykle badawcze silników o różnym zastosowaniu.
9. **Rychlik A., 2006.** Metody pomiaru zużycia paliwa pojazdów użytkowych. Eksploatacja i niezawodność4 (32) p. 37-41.

ANALIZA PRZYDATNOŚCI WYBRANYCH STACJONARNYCH CYKLI OBCIĄŻEŃ DLA OCENY EKONOMICZNOŚCI SILNIKÓW CIĄGNIKÓW

S t r e s z c z e n i e. Praca analizuje parametry eksploatacyjne silnika AD3.152 uzyskane w ciągu trzech stacjonarnych cykli obciążeń: 8-fazowego i dwóch wariantów 5-fazowego cyklu. Uzyskane wyniki zostały przedstawione i porównane w oparciu o średnie obciażeń.

S ł o w a k l u c z o w e: silnik spalinowy, ekonomiczność silnika, stacjonarne cykle obciążeń.

TEKA. COMMISSION OF MOTORIZATION AND ENERGETICS IN AGRICULTURE – 2012, Vol. 12, No. 1, 257–261

The techniques of producing energy from biomass[1]

Wiktoria Sobczyk, Anna Kowalska**

*AGH University of Science and Technology, Cracow, Poland

Summary. The paper describes the sources of biomass and techniques of producing energy from burning biomass: conventional burning, burning in fluidized bed, pyrolysis and gasification. Thermal processing of waste biomass from agricultural production and from the food industry allows to receive energy carriers in the form of liquid or gaseous fuels. Development of alternative energy sources creates a chance of maintaining energy independence. It is also compatible with the idea of sustainable development.

Key words: conventional energy, alternative energy, biomass, wood, straw, fluidized burning, energy plants.

INTRODUCTION

The depletion of energy minerals deposits and recurring oil crises have caused an increasing interest in alternative energy sources. The electric power, the flywheel of the world's economy, is produced mainly in thermal, hydro-electric, nuclear and wind power stations [10]. Thermal power plants produce over 60% of global energy. Unlike thermal power plants, water power stations do not pollute the natural environment. However, they require suitable lay of the land and significant water potential.

Production of bioenergy from alternative sources has been developing for many years in Western Europe, USA and Japan. Basket willow, Pennsylvanian mallow, miscanthus, rose (*Rosa multiphlora*) and grain straws are used for this purpose.

Poland has a significant technical potential of biomass and possibilities of its use for energy production purposes increase every year. Willow cultivation is especially popular [11, 9]. From one hectare of energetic willow plantation one may harvest 20 tonnes of dry mass which has the calorific value of 8 m^3 of heating oil or 10 tonnes of coal. It is estimated that a 30-are plantation (i.e. on fallow lands) can fulfill annual energy needs of a small farm. In the agricultural sector the harvest of willow is conducted in the winter months which is the time of low demand for workforce. Cultivation of multi-hectare plantations on fallow lands could therefore reduce unemployment. The willow as an energy carrier is practically inexhaustible (after 30 years the soil has to be reclaimed and a new plantation can be started) [16].

The produced biomass requires processing. This is associated with construction of new production plants and modernisation of existing boiler rooms used for burning coal or heating oil. The ecological aspect has still greater meaning for the power sector's activity. Objects and installations have to fulfill European Union's standards regarding the permissible concentrations and emissions of pernicious gases. Because of this fact the interest of power plants and CHPs (combined heat and power plants) with biomass increases and new markets open for farmers.

Realisation of projects associated with eco-energy sector is financially supported by EKO-Fund Foundation.

THE ORIGIN OF BIOMASS

Plant resources are a source of different kinds of fuels: solid fuels, bio-alcohol, bio-oil, bio-gas. The process of fuel production begins with acquiring adequate raw material. This can be plant waste from energetic plantations, plants with high sugar content, oil plants.

In agriculture one can mention: straw, hay, beetroot pomaces. Forestry, wood mills and paper industry are also in possession of many different raw materials: chips, sawdust, brushwood, bark (fig. 1), lignin waste water.

[1] The paper has been prepared within the AGH University of Science and Technology – statutory research work No 11.11.100.482

Fig. 1. Tree bark

Broad spectrum of materials is offered by agricultural and food industry: waste from sugar factories, distilleries, breweries, straw, food waste [1].

Recently plantations of fast-growing plants and trees have gained large popularity. These include: willow, plane tree, poplar, eucalyptus, sugar cane, rape, sunflower, flax, chosen species of grass (i.e. Sudan grass), grains, potatoes, corn, manioc, sugar beet, soybean, peanuts, sorgo.

On breeding farms one may find waste from animal-farming: liquid manure, bio-gas. The municipal management provides waste sediments, household waste, waste paper, sewage treatment plant waste [5, 6].

TECHNIQUES OF ENERGY PRODUCTION BURNING WOOD WASTE

The form of the fuel has fundamental meaning during the burning process. Wood waste are optimal for burning after being disintegrated into chips. Large contact area in relation to the wood's mass creates a possibility of rapid heating to the ignition temperature and their complete burning. This is the condition for proper use of heat from the burned wood. The best way to use fine industrial waste (chips, sawdust) is to briquette them [2].

Choosing the right furnace for particular forms of wood is also an important factor:

– long pieces of wood should be burned in furnaces with mechanical loading,
– in automatic furnaces one should burn wood in pieces and in form of compressed granulates, pellets (fig. 2) or briquettes (fig. 3) [7, 14].

Fig. 2. Pellets from Olimp wood produced by the company Stelment

Fig. 3. Briquette from oak pulp

– in furnaces with pneumatic loading and separation of carbon black one should burn sawdust (fig 4) [12].

Fig. 4. Sawdust

Burning of wood proceeds in three stages:

– drying and heating,
– degasification,
– proper burning.

During the degasification the flammable gases (hydrogen and carbon monoxide) burn up quickly and rise the temperature. After the gasification phase charcoal is created (fig. 5). It burns in ca. 800°C.

Fig. 5. Charcoal

The proper burning proceeds almost without visible smoke. When the humidity of the fuel is high, special vaults are used to make the flame return and increase the drying process speed in the burning chamber [12]. Through the application of blowing the flame can be extended which improves the quality of burning [13].

After modernisation of Power Plant Jaworzno II a modern thermal-electrical power plant was created. Old Soviet Pk-10p no. 1, 2 and 3 boilers were replaced with two fluidized boilers of "Compact" type manufactured

by Foster Wheeler. Two turbine sets of WK-50 type were replaced by thermal-condensative sets of 13CK70 type produced by ABB Zamech Ltd. Co-incineration of coal and biomass proceeds in CFB 260 boilers:

– meat and bone dust
– forest biomass: wood chips of calorific value up to 15 MJ/kg,
– "Agro" biomass - sunflower shells and rape oilseed cakes (fig. 6, 7), hop (fig. 8), post-distillation grain dried material, grain bran, beetroot and fruit pomace (fig. 9), grinding grain (fig. 10),
– liquid "Agro" biomass – glycerin.

Fig. 6. Briquette from sunflower shells

Fig. 7. Rape oilseed cake

Fig. 8. Hop pellet

Sunflower shells have calorific value of 17-19 MJ/kg while rape oilseed cake even up to 20 MJ/kg.

Fig. 9. Pellet from beetroot pomace

Fig. 10. Pellet from grinding grain

Fluidized combustion of biomass occurs when fine particles of suspended matter are blown by the air coming from underneath them. Very good mixture of air and fuel particles is created and the large area of their contact increases the intensity of burning (the temperature may reach even 800°C). Thanks to this fact, during burning of biomass the emissions of nitrogen oxides are significantly reduced in comparison to grid furnaces.

PYROLYSIS AND GASIFICATION

Processing of the given raw material occurs during the following processes: gasification, pyrolysis, granulating, indirect burning, leaching, fermentation, pressing or esterification. In the final process we receive a fuel that can be processed into thermal or electric energy as well as into mechanical work.

The biomass is relatively low carbonificated, has high concentration of organic compounds and low ash content. These characteristic of biomass are the main reasons of its attractiveness as a fuel for gasification. The fact that it is not unequivocally defined when it comes to quality can be viewed as its flaw. The efficiency of gasification process (the relation between the chemical energy of the produced gas and the chemical energy in fuel) for the most simplistic installations oscillates around 20%, but for the more advanced ones reaches even 90% [8].

Utilization of waste biomass from agricultural production and from the food processing industry is an

important issue. One of the possibilities is to use it for energy production, even if it is direct burning. Thermal processing of biomass allows to produce energy carriers in the form of liquid or gaseous fuels. This is possible during the pyrolysis and gasification processes. Gasification can be carried out in a few different ways: it can be methane fermentation or gasification for production of generator gas with the use of different gasifying media.

Gasification is a well-known and commonly used technology of processing biomass into gaseous fuels. Gasification consists of a number of thermodynamic processes (exchange of heat and mass and omnidirectional exothermic and endothermic chemical reactions which occur in high temperature) and leads to conversion of solid fuel into gaseous form. Water vapour, air, oxygen or carbon dioxide can act as the gasifying media [13].

Gasification of solid biomass is conducted in a similar way as the gasification of coal. The differences result from higher reactivity of the biomass, higher oxygen content in the structure and lower ash melting temperature [15]. The gasification process can be divided into areas of varying temperature: drying, degasification, pyrolysis and proper gasification that occurs in the combustion and reduction zone. Because the biomass is essentially build of carbon, hydrogen and oxygen, in reality the biomass gasification process produces synthesis gas which contains the following flammable components: hydrogen, carbon monoxide, small quantities of methane and incombustible compounds: mainly carbon dioxide, water vapour and nitrogen [8].

The amount and quality of the synthesis gas from biomass gasification depend mainly on the type of biomass, but also on the gasifying medium, temperature, pressure and method of gasification. In the case when oxygen is the gasifying medium, the hydrogen content in the produced gas exceeds 40% and carbon monoxide content is up to 40%. On the other hand, when water vapour is the gasifying medium, hydrogen content exceeds 50% and carbon monoxide content exceeds 15%.

The high level of biomass humidity is not a problem in the gasification process because of a method called hydrothermal gasification in which the humidity of biomass may reach even 95%. In this technology the biomass is transformed into hydrogen and carbon dioxide with the presence of water of critical parameters. The organic substance of the biomass switches into carbon dioxide and hydrogen comes from both the biomass and from water [8]. The generalised schema of the energy system with biomass gasification has been shown in Figure 11.

Pyrolysis is an independent thermal process or it can constitute as a stage in the gasification process. Pyrolysis can be described as thermal decomposition of the biomass without presence of external oxidizing and reducing media.

Depending on the type of pyrolysis one may receive different solid, liquid or gaseous products. Gaseous energy carriers are used for production of thermal energy and for powering internal combustion engines which in turn power the generators that produce electrical energy (hot fumes are the source of thermal energy). Other technologies of gas purification are in use as well. They lead to an increase in the flammable contents share in the gas of up to 99,9% [8, 4].

THE ADAVANTAGES OF BIOMASS AND BIOGAS

Using waste from the overproduction of food is doubtlessly one of the advantages of producing energy from biomass. This energy is clean and does not lead to creation of any significant environmental pollutants. Let us remind that biomass contains 0,01% of sulphur and after its burning the remained ash has a mass of 1% of the original raw material mass (in comparison - hard coal has between 0,5 and 5% of sulphur and leaves between 10 and 15% of ash). Emission of nitrogen compounds is also seriously reduced because of significant lowering of combustion temperature. The greatest reduction of emission occurs during balancing the carbon dioxide emissions which are responsible for the greenhouse effect. CO_2 emission during burning is equal to the concentration of CO_2 produced during the natural decay of biomass [4].

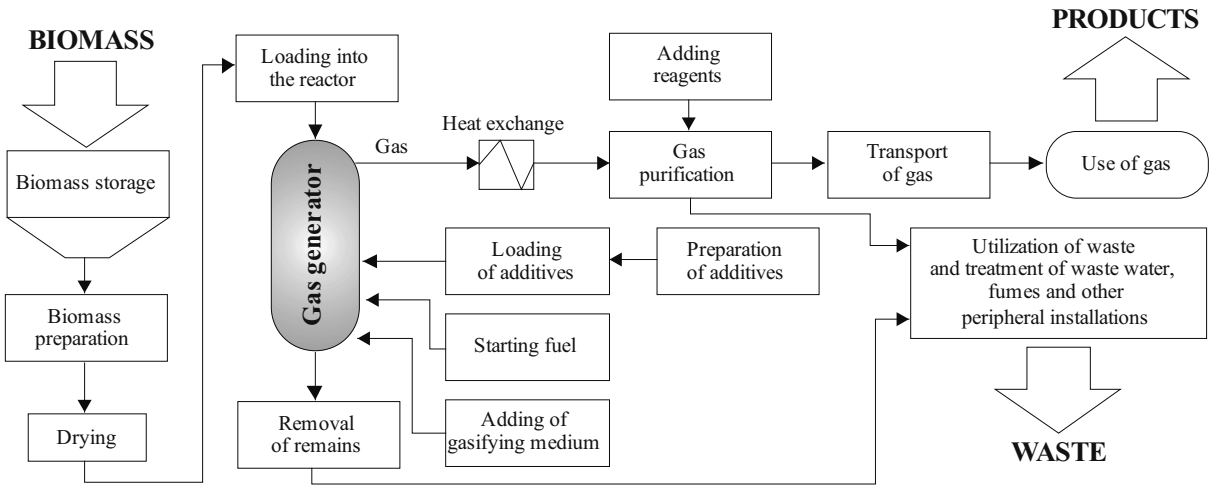

Fig. 11. Energy system of integrated biomass gasification [Piechocki 2010, changed]

The development of alternative energy technologies provides energy safety to the country because of diversification of energy producers' offer. The energy production is decentralized and does not require construction of power lines (there are no transmission-related losses). In comparison to the energy produced using conventional methods it supports economical water management. Production costs of energy from biomass are comparable to the costs of producing electricity from the power grid. Moving further, it should be pointed out that in the poor and developing countries it allows to improve the hygiene and health conditions through cessation of spilling fecal matter directly onto the fields (Chinese and Indian provinces) what has once been a cause of dangerous diseases epidemics.

There are not many flaws of this kind of energy production but they are significant. The calorific value of biomass is two times lower than that of hard coal. Biomass processing installations are capital-intensive investments (large investment costs during the construction phase). Furthermore, it is necessary to strictly follow the fermentation regimes (temperature, acidity, hermetic conditions during the processes). The biomass is usually highly moist which causes problems during its transport and storage. Bio-fuels production requires higher capital expenditures in comparison to the fuels produced during oil processing. Additionally, there are no tax exemptions for the producers of energy from biomass.

CONCLUSIONS

Production of energy from conventional sources causes significant damage to the environment. The reserves of fossil fuels are reduced every year and the energy becomes more expensive. The development of alternative energy sources opens a chance for an increase in the country's energy independence, for regional development and creating new jobs. It allows for pro-ecological modernization of the energy systems. For example, the cultivation of energetic willow can be a profitable and interesting area of agricultural development.

The biomass can come from diversified sources: there are special energy plants cultivations and wastes from plant products production and processing.

A lot of attention is paid to the environmental factors when considering energy production. During burning of biomass one may derive from additional benefits, like significant reductions of detrimental substances emissions. Biomass is a cheap, ecological and clean energy source. Looking for alternative sources of energy is also compatible with the sustainable development principles.

REFERENCES

1. **Bowszys T., Sądej W., Wierzbowska J., 2007:** Use of agricultural and communal waste products in fertilization of oilseed rape grown for biofuel. TEKA Komisji Motoryzacji i Energetyki Rolnictwa PAN, vol. VIIA, p. 43-50.
2. **Jakubiak M., Kordylewski W., 2008:** Pelety podstawowym biopaliwem dla energetyki. Archiwum Spalania, vol. 8, nr 3-4.
3. **Kalina J., 2004:** Zgazowanie paliw stałych. Gospodarka Paliwami i Energią, nr 15.
4. **Kaszak M., 2006:** Efektywność energetyczna produkcji nośników energii z biomasy. Praca inż. ATR WM, MiBM.
5. **Kowalik P., 1997:** Światowe tendencje w wykorzystaniu biomasy do produkcji ciepła, elektryczności i paliw samochodowych. Gospodarka paliwami i energią 1/1997.
6. **Kowalska A., 2008:** Overviev of technological methods of energy production from biomass. TEKA Komisji Motoryzacji i Energetyki Rolnictwa PAN, vol. X, p. 209-215.
7. **Kulig R., 2007:** Effects of conditioning methods on energy consumption during pelleting. TEKA Komisji Motoryzacji i Energetyki Rolnictwa PAN, vol. VIIA, p. 59-67.
8. **Piechocki J., Sołowiej P., Neugebauer M., 2010:** Gazyfikacja biomasy odpadowej z produkcji rolniczej. Inżynieria Rolnicza 5 (123).
9. **Sobczyk W., 2007:** Plonowanie wierzby wiciowej - w świetle badań. Polityka Energetyczna, tom 10, zeszyt specjalny 2, Kraków, p. 547-556.
10. **Sobczyk W., 2008:** Wykorzystanie alternatywnych źródeł energii w Zawoi Przysłopie (Małopolska). Folia Scientiarum Universitatis Technicae Resoviensis nr 229, Budownictwo i inżynieria środowiska, z. 47, p. 457-463.
11. **Sobczyk W., 2011:** Evaluation of harvest of energetic basket willow. TEKA Komisji Motoryzacji i Energetyki Rolnictwa PAN, vol. XI, p. 343-352.
12. **Soliński I., 2001:** Biomasa energia odnawialna. Biblioteka Szkoły Eksploatacji Podziemnej. Seria z lampką górniczą nr 9, Kraków.
13. **Tymiński J., 1997:** Wykorzystanie odnawialnych źródeł energii w Polsce do 2030 roku - aspekt energetyczny i ekologiczny. IBMER, Warszawa.
14. **Wach E., 2009:** Poradnik użytkownika pelet drzewnych. Projekt Komisji Europejskiej - Pellets@las. FORCE Technology.
15. **Warowny W., Kwiecień K., 2006:** Paliwa z biomasy i ich wykorzystanie. Przemysł Chemiczny nr 12.
16. **Zaród J. 2006:** Racjonalne zagospodarowanie odłogów i nieużytków w województwie zachodniopomorskim, w: Adamowicz (red.): Zrównoważony i trwały rozwój wsi i rolnictwa. Wyd. SGGW, Warszawa.

TECHNIKI POZYSKIWANIA ENERGII Z BIOMASY

Streszczenie. W pracy opisano źródła biomasy oraz techniki pozyskiwania energii ze spalania biomasy: spalanie konwencjonalne, fluidalne spalanie, pirolizę i gazyfikację. Obróbka termiczna biomasy odpadowej z produkcji rolniczej i przetwórstwa spożywczego pozwala otrzymać nośniki energetyczne w postaci paliw płynnych lub gazowych. Rozwój alternatywnych źródeł energii stwarza szansę na utrzymanie niezależności energetycznej. Jest także zgodny z ideą ekorozwoju.

Słowa kluczowe: energia alternatywna, rośliny energetyczne, biomasa, drewno, słoma, spalanie fluidalne.

TEKA. COMMISSION OF MOTORIZATION AND ENERGETICS IN AGRICULTURE – 2012, Vol. 12, No. 1, 263–267

The influence of the operating conditions of farm tractors on the wear of crankshaft slide bearings

Tomasz Stawicki, Adam Koniuszy, Paweł Sędłak

Department of Agrotechnical Systems Engineering, West Pomeranian University of Technology Szczecin
Papieża Pawła VI Str. 1, 71 – 459 Szczecin, Poland, e-mail: tomasz.stawicki@zut.edu.pl

S u m m a r y. The paper presents selected results of in-use investigations of a farm tractor U 912 and a harvester BIZON SUPER Z056. Based on the recorded engine operating states of both the tested machines the number of start-ups and the time of operation were recorded. The results of tribological investigations have also been presented performed in the friction pair: crankshaft journal - slide bearing. Based on the analysis of the collected material the authors attempted to determine whether the dynamic (non-steady) states of the operation of slide bearings, characteristic of engine start-ups can result in a significant reduction of their life until the moment its normative durability is depleted.

K e y w o r d s: farm tractor, operation, slide bearings, friction, wear.

INTRODUCTION

The process of machine use is characterized by a high dynamics of changes in the operating states, which influenced the elements of the kinematic pairs. The durability and reliability of the machinery to a large extent depend on the above and it is this particular dynamics causing that the kinematic pair usable potential is consequently reduced. In such machines as farm tractors there exists uncertainty in modeling of the operating conditions, which is the result of changes in the engine thermal states, variations in the motion resistance and the ambient conditions [1, 14]. To other determinants of the process of operation that decide about the specificity of the farm application of machines we can include differences in the operation routines of drivers and irregular frequency of use throughout the year. Scientific works frequently point to a relatively small efficiency of farm tractors (average operating times 300 h/year, which translates into extended periods of depreciation – up to 40 years) and ineffective use of their engines, whose average loads range from 60-70 % of the rated power [4, 3].

The analysis of the operation on the durability of the kinematic pairs is particularly needed in relation to friction pairs that due to their proneness to failure, repair costs and operating safety are treated as weak links (critical pair). In the case standalone farm machinery that would be the engine crankshaft slide bearings. These friction pairs are designed for liquid lubrication. It is, however, impossible in the overall range of external shocks.

During start-up, stoppage and operating overloads, non-steady states of the slide bearing operation occur that make the hydrodynamic liquid lubrication of the bearing impossible [13]. In such a situation direct metal-to-metal contact may occur at the points of actual friction and adhesive grafts may occur as a result of molecular forces that will lead to a quicker material wear in the friction pairs [7, 2]. Since, under non-steady states of operation, the motion resistance may grow abruptly (at dry friction the friction coefficient may exceed the value characteristic of liquid friction over 100 times [7]) this may significantly reduce the durability of the friction pair, even if the collective operating time under such conditions is relatively short in relation to the total operating time of a given friction pair. The above considerations constituted a basis for further studies of the problem of determining of the influence of the operating conditions on the durability of slide bearings of the crankshaft in farm machinery.

RESEARCH METHODS

The investigated problem was realized in two stages. The first stage was the analysis of information on the operating parameters of standalone farm machinery. The object of the research were: farm tractor U 912 and a harvester BIZON SUPER Z056 used in one of the farms in the province of Zachodniopomorskie (West

Pomerania). In the case of the farm tractor the operating tests were carried out in the period 07.2006-10.2008 and the data related to the harvester were obtained during harvest works in 2009 and 2011. For the recording of the engine operating states TRS (Tractor Recording System) was used developed in the Chair of Basics of Technology at the University of Agriculture in Szczecin [6]. This system allows recording of the following data related to the engine operating states and conditions of operation:
– Engine start-up and stoppage time,
– Engine time of operation,
– Engine speed,
– Hourly fuel consumption,
– Geographical location of the Machinery.

Due to the character of the research the object of particular interest were data on the engine start-ups and engine times of operation. Since, during the engine start-up and stoppage there are engine speeds for which hydrodynamic liquid lubrication is impossible it was assumed that their number may reduce the durability of the crankshaft journal-slide bearing pair.

In the second stage of the investigations tribological tests were carried out in the friction pair that reflected the crankshaft journal - slide bearing pair. The authors aimed at determining the influence of the sliding velocity on the wear of the bimetal tape before its shaping into a half-bearing. The flat samples of the bearing material operated with steel rollers (counter sample material: steel 40 HM, 51-53 HRC) on the length of the friction contact corresponding to the width of the sample l = 7 mm. The wear tests were carried out for the following operating parameters of the test pair:
– Velocity of slide v : 0,6; 0,9; 1,2; 1,45 [m · s^{-1}],
– Load P = 300 N,
– Friction distance 2500 m,
– Lubrication medium: engine oil *Superol M CC 30*, *15W/40.*

The selection of the velocity of slide was made based on the preliminary tests for which the parameters of the test working pair were analyzed at the engine speeds characteristic of the start-up phase for diesel engines (it is assumed that the engine speed when starting up should be in he range of 100-200 rpm). For each of the applied speeds 6 test runs were performed.

RESEARCH RESULTS

The research cycle of the U 912 farm tractor extended over a period of over two years of operation i.e. from 03.07.2006 to 14.10.2008. Through the TRS system installed in the machinery, information was obtained on the parameters of the tractor operation through data recording with a 30-second resolution. The operation of the measurement system was initiated when the engine was started and lasted until the engine stopped. Based on the analysis of the obtained data the authors ascertained that *the collective tractor operating time in the whole research cycle was almost 301 hours, which corresponds to 1009 engine start-ups.*

The obtained results indicate low effectiveness of the tractor use in the given farm, which is characteristic of Polish farms [Kocira 2005, Pawlak 2005]. In the analyzed period the tractor was used with different intensity and the hours of operation and number of start-ups showed a similar trend of changes in analogical agricultural seasons (Fig. 1), adequately to the nature of the realized farm work. An exception is December 2008 when the recorded operating time and number of start-ups are not the resultants of the farm work. At that time the tractor was used for collecting timber for heating purposes.

The results of the in-use investigations of the harvester in the form of number of start-ups and engine

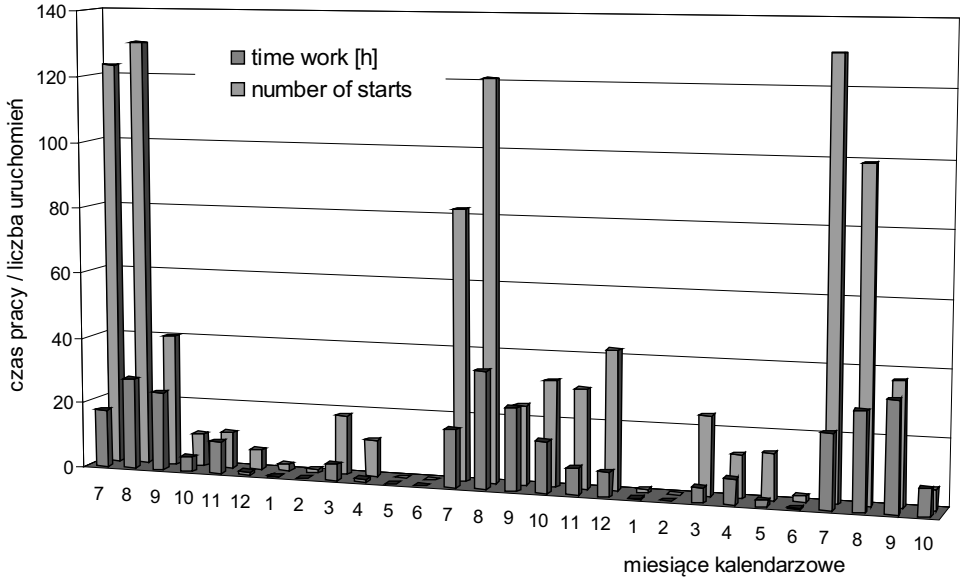

Fig. 1. Number of star-ups and engine operating time in the whole research cycle (3 July 2006 to 14 October 2008)

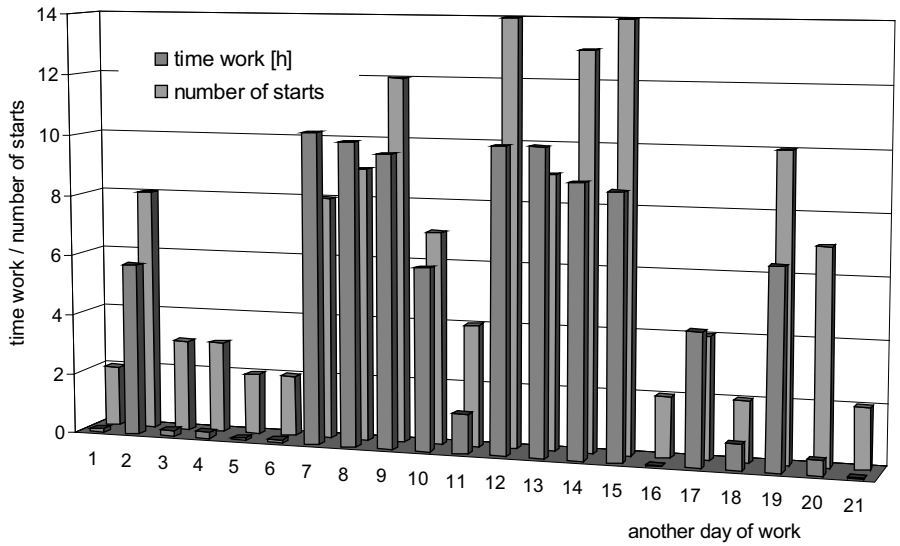

Fig. 2. Number of start-ups and engine operating time of the harvester during summer field works in 2009

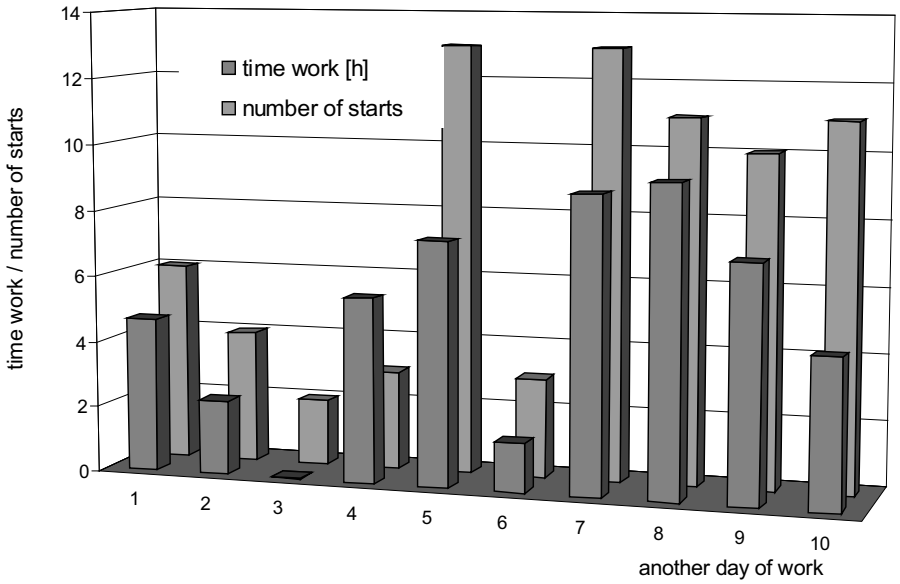

Fig. 3. Number of start-ups and engine operating time of the harvester during summer field works in 2011

operating time in relation to the days of its use have been presented in Fig. 2 and 3.

As results from the obtained data, *in the fieldwork in 2009 the harvester operated for 93 hours and was started 137 times and in 2011 its operating time was 51 hours and the engine was started 76 times*. The recorded engine operating time in 2011 was over 80 % shorter than in the agricultural season 2009, which was the result of limited services rendered by the owner of the machine, and harvesting only in his own farm. The presented data clearly confirm the lack of effectiveness of use of the harvester, as it is generally assumed that the rational time of operation of a harvester should be 20-25 years, which at the normative durability of 3000 hours, denotes an annual use on the level of 150-120 hours [8, 11].

The presented results of the tests on the U 912 farm tractor and the BIZON harvester correspond to the specificity of use of agricultural machinery. The specific conditions of operation lead to a quicker moral (functional) wear of the machinery rather than their physical wear. This results from the small effectiveness of use of the machine potential and the dynamics of introducing new generations of technologically advanced machinery. This generates a problem of particular importance i.e. ensuring an appropriate level of long-term reliability of the farm machinery in the long run (40 years and more). The efforts of the service technicians should obviously minimize the potential failure through, for example adhering to the repair intervals that should be realized depending on the actual needs. Helpful may also be the data on the engine operating states as well as the tribological

data related to the intensity of the destruction processes of the kinematic pair, characteristic of these operating states.

As mentioned earlier in the paper, engine start-ups generate the occurrence of dynamic states of the operation of the slide bearings of the crankshaft. The knowledge as to the number of these states together with the intensity of the material wear of the friction pairs during start-up can be used to forecast the intervals between the crankshaft rebuilds (honing to further repair undersize). This constituted an assumption for the experimental exploration of the triboligical characteristics of the sliding material pair crankshaft journal - bearing and its relation to the operating conditions in the life cycle.

Through the results of the tribological tests the authors attempted to determine the measure of the linear wear of the samples made from the slide bearing material depending on the velocity of slide of the counter sample simulating the crankshaft journal. Under the conditions of actual operation of the crankshaft journal - slide bearing pair, when the elements come into contact the friction contact is distributed, while the here discussed wear tests began from concentrated friction contact of the roller (counter sample) with the sample coat. The tests were performed for the steady loads on the pair and four selected velocities, which is naturally far from the operating shocks. The assumed rigor of the laboratory tests reduced and simplified the tests and shortened their duration and at the same time provided interesting information in relation to the energy interactions in the friction pair under the conditions of combined friction, characteristic of the non-steady states of the operation of sliding pairs.

Table 1 presents the results of the wear tests obtained for all the performed test runs. The results were averaged, and, based on these results, the characteristics of the changes of the linear wear of the samples as a function of velocity and slide were developed (Fig. 4) [12].

Table 1. Wear tests results

Velocity of slide [m · s $^{-1}$]	Linear wear in the tests [mm]						Average wear [mm]	Standard deviation s [mm]
	1	2	3	4	5	6		
0,6	0,393	0,588	0,547	0,292	0,569	0,297	0,448	0,137
0,9	0,289	0,231	0,277	0,151	0,170	0,162	0,213	0,061
1,2	0,109	0,228	0,131	0,282	0,108	0,164	0,170	0,071
1,45	0,219	0,203	0,241	0,227	0,182	0,271	0,224	0,031

The greatest wear of the samples was determined for the lowest velocity of the counter sample. Also in this case the authors observed a great spread of the results in the measurement trial. An explanation of such a status quo can be provided in the data contained in the bibliography. In the results of tribological studies it is stressed that low relative velocities < 0,8 m · s $^{-1}$, at unit stresses above 10 Mpa facilitate adhesive grafts [7]. As the tests were carried out on concentrated friction contact and at relatively low velocities of slide, in the case of the lowest applied velocities both of the above conditions were fulfilled.

Great development and separation of the adhesive grafts with the effect of generating of the wear products leads to a seizure of kinematic pairs and in extreme cases when the friction process begins to dominate inside the surface layer it can lead to emergency stoppage of the friction pairs [10, 5]. During the tests, the recorded changes of the moment of friction for tests performed at the velocity of 0,6 m · s $^{-1}$ are characterized by the least stable course. The observed changes in the motion resistance correspond to the highest intensity of the damaging occurrences in the tested pair, which could be attributed to the courses of the wear processes consisting in destruction of the adhesive grafts [10].

In the range of the assumed slide velocities, the lowest wear occurred for the velocity of 1,2 m · s $^{-1}$. Taking the observed relations we can conclude that it is purposeful to seek start-up engine speeds that are optimum in terms of durability. It is noteworthy to relate this to the daily practices. The circumferential velocities of the

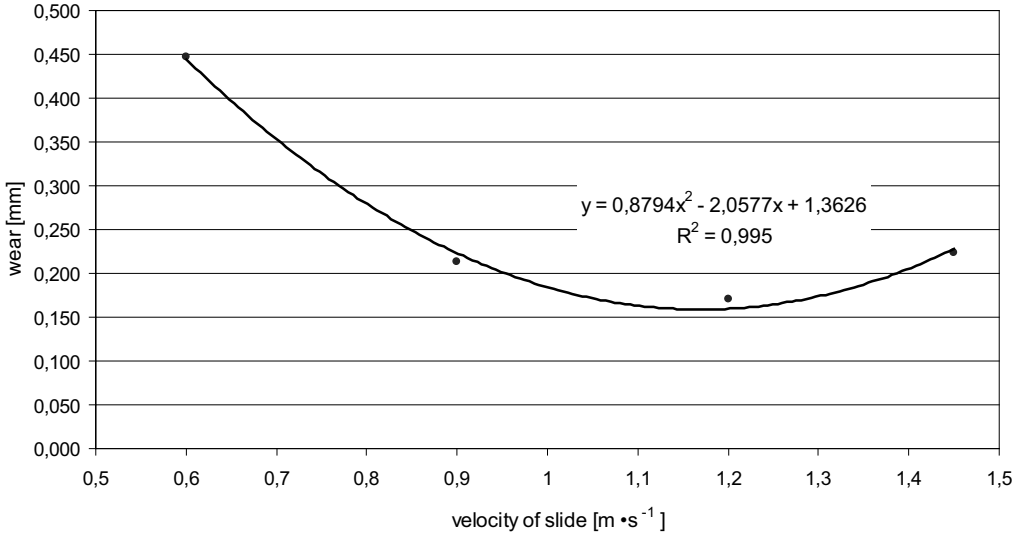

Fig. 4. Linear bearing material's wear depending on the velocity of slide of the roller simulating the crankshaft journal

points located on the surface of the crankshaft journals of nominal diameters of 80 and 90 mm, for, as assumed, the proper start-up engine speeds of 100-200 rpm are 0,42-0,84 m · s^{-1} (80 mm journal) and 0,47-0,94 m · s^{-1} (90 mm journal). These are, thus, in the context of the obtained results of wear tests disadvantageous slide velocities. The presented estimate calculations, due to the assumed order of the diameters of the crankshaft journals, can correspond to the farm tractors of higher power output. In the case of widely applied farm tractors of low and medium power class (as mostly used in Poland - URSUS 912, C 385, C 360, or MF 235) at the start-up engine speeds as mentioned above, the obtained velocities of slide of the crankshaft journals will be much lower, hence the risk of intensification of the wear process of the kinematic pairs will be higher. The obtained adjustment of the trend line for the empirical data ($R^2 >$ 0,8) indicates the possibility of forecasting of the slide bearing material wear for the slide velocities other than those used in the tests.

CONCLUSIONS

1. The results of the in-use tests point to a need of analysis of the operation of engines of farm machinery in terms of their usable specificity conditioned by the nature of the agricultural works.
2. The recorded times of the operation of the engines and the number of start-ups (in the case of the farm tractor it was over three times higher than the number of hours of operation and in the case of the BIZON harvester 1,5 times higher than the number of hours of operation) juxtaposed with the general duration of the research indicate a possible significant influence of the start-ups on the durability of the crankshaft journal-slide bearing kinematic pair.
3. The wear tests indicate that optimum start-up engine speeds be sought in order to reduce the wear of the friction pairs under the non-steady conditions of operation of the slide pair.

REFERENCES

1. **Chłopek Z. 1999.** Modelowanie procesów emisji spalin w warunkach eksploatacji trakcyjnej silników spalinowych. Prace Naukowe Politechniki Warszawskiej, p. 173.
2. **Hebda M. 2007.** Procesy tarcia, smarowania i zużywania maszyn, Wydawnictwo Instytutu Technologii Eksploatacji – PIB, Warszawa, p. 620.
3. **Dyer J. A., Desjardins R.L. 2003.** Simulatet Farm Fieldwork, Energy Consumption and Related Greenhouse Gas Emissions in Canada. Biosystems Eng. 85(4): p. 503-513.
4. **Kim J.H., Kim K.U., Wu Y.G. 2000.** Analysis of transmission load of agricultural tractors. J. Terramechanics 37: p. 113-125.
5. **Kocira S. 2005.** Wykorzystanie maszyn rolniczych w gospodarstwach o różnej wielkości ekonomicznej. Problemy Inżynierii Rolniczej, 3(49): p. 15-22.
6. **Koniuszy A., Nadolny R. 2007.** Sposób monitoringu pracy ciągnika oraz urządzenie do jego realizacji. Zgłoszenie Patentowe nr: P 381892.
7. **Lawrowski Z. 2008.** Tribologia tarcie, zużywanie i smarowanie, Oficyna Wydawnicza Politechniki Wrocławskiej, Wrocław, p. 322.
8. **Muzalewski A.** 2008 Zasady doboru maszyn rolniczych. IBMER, Warszawa, 92. Dostępny w Internecie (20.01.2012).
9. http://www.arimr.gov.pl/fileadmin/pliki/zdjecia_strony/185/Zas_dob_masz_rol_300309.pdf.
10. **Nosal S. 2009.** Analiza pojęć związanych z zacieraniem adhezyjnym. Nowa definicja zacierania. MOTROL, Mot. i Energ. Rol. 11c: p. 141-150.
11. **Pawlak J. 2005.** Wykorzystanie ciągników i maszyn samojezdnych w rolnictwie polskim. Problemy Inżynierii Rolniczej, 4(50): p. 51-56.
12. **Polański K. 2010.** Wpływ nieustalonych stanów pracy na trwałość węzła ślizgowego czop-panewka. Praca magisterska - materiały niepublikowane ZUT w Szczecinie, p. 57.
13. **Woropay M., Landowski B., Jaskulski Z. 2004.** Wybrane problemy eksploatacji i zarządzania systemami technicznymi, Wydawnictwo Uczelniane Akademii Techniczno-Rolniczej, Bydgoszcz, p. 351.
14. **Yusupov R. Ch., Deev V. Y., Zaynishev A. V., Solomonenko M. V. 2003.** Optimisation of parameters of diesel's regulator and loading. TEKA, TEKA Kom. Mot. Energ. Roln, 3, p. 263-270.

WPŁYW WARUNKÓW EKSPLOATACYJNYCH CIĄGNIKÓW ROLNICZYCH NA ZUŻYCIE ŁOŻYSK WAŁU KORBOWEGO SLAJDÓW

S t r e s z c z e n i e . W artykule przedstawiono wybrane wyniki w użyciu badań gospodarstwa ciągnika U 912 oraz kombajn zbożowy Bizon Super Z056. Na podstawie zapisanych stanów pracy silnika obu maszyn badanych liczba nowopowstających oraz czas pracy zostały zarejestrowane. Wyniki badań tribologicznych zostały również przedstawione wykonywane w parze tarcia: Dz wał korbowy - łożysko ślizgowe. Na podstawie analizy zebranego materiału autorzy próbowali ustalić, czy dynamicznych (nie wzrasta) stany eksploatacji łożysk ślizgowych, charakterystyczne dla silnika typu start-up może doprowadzić do znacznego obniżenia ich życia do chwili jego trwałość normatywny jest wyczerpany.

S ł o w a k l u c z o w e : ciągnik rolniczy, praca, łożyska ślizgowe, tarcie, zużycie.

TEKA. COMMISSION OF MOTORIZATION AND ENERGETICS IN AGRICULTURE – 2012, Vol. 12, No. 1, 269–273

Impact of parasite resistance on operation of ignition system in motor vehicle

Sebastian Styła

Department of Computer and Electrical Engineering, Lublin University of Technology,
20-618 Lublin, 38a Nadbystrzycka Street; e-mail: s.styla@pollub.pl

S u m m a r y. The paper presents the impact of parasite resistance occurring as the result of ageing of elements, humidification of the vehicle electric system or physical damage on the correct functioning of ignition systems in motor vehicles. The methods have been presented for detecting this type of failures and for analyzing the obtained results. The tests have been performed by means of typical diagnostic instruments available in every motor vehicle diagnostic *station. The mechanical and electronic* ignition systems have been used for testing. Furthermore, the paper presents the system proposed in order to automatically detect small changes in the resistance significantly affecting the functioning of the whole ignition system.

K e y w o r d s: resistance, ignition system, ignition coil, ignition advance angle, oscillogram.

INTRODUCTION

The automotive electric and electronic technologies were developed parallel to combustion engines over the last century. This process encompassed the following basic phases: the development of electrical ignition systems and electric energy sources, the application of electrical lighting and starting methods. In spite of such dynamic progress, an average car today resembles its design from those years in one respect: most troubles are associated with still unreliable mixture ignition. However as a result of the introduction of electric and electronic solutions it was possible to resolve many problems associated with the construction of ignition systems.

The conditions of work as well as more and more stringent legal regulations in the scope of the equipment and requirements in the scope of safety and reliability of motor vehicles constitute big challenge to their designers and manufacturers. The electrical installation of a motor vehicle shall meet the conditions described in relevant standards [18, 19, 20]. Their scope encompasses the following features [4, 5, 6, 9]: operational and fire protection safety, durability, reliability, simplicity, resistance to vibration, humidity, shocks as well as to extremely high and low temperatures. Simultaneously these devices shall be characterized by low manufacturing costs, parts interchangeability as well as small sizes and weight. Incorrect functioning may result in vehicle immobilization or, in certain cases, even in hazard to persons travelling in the car and to other road users. Therefore the capability to get a correct diagnosis and to repair an element in accordance with proper procedure is extremely important in case of a failure. In order to achieve this goal, it is necessary to combine relevant diagnostic parameters with the vehicle element under testing [12, 13].

Owing to difficult working conditions in vehicle electrical installation, its failures are possible as a result of an additional resistance called parasite resistance occurring in these systems. The parasite resistance is generated under the influence of ageing electrical elements of vehicles, high air humidity or physical damages. These damages frequently result in the inefficiency of the whole circuit. In case of the ignition system, this inefficiency may lead to the engine immobilization. The value of resistance causing such inefficiencies may be equal to only a few ohms.

THE CHARACTERISTICS OF IGNITION SYSTEMS UNDER TESTING

The ignition of fuel and air mixture is the basic condition required for engine operation. Furthermore this ignition shall take place at proper time. The achievement of rated operating conditions of the motor vehicle i.e. proper engine power, durability, emission characteristics and fuel consumption [13, 16] is warranted in case of correct operation of this system. Therefore the symptoms of this system failure can be observed already in course of the operation. It must be remembered that the reasons and symptoms of specified inefficiency depend mainly on the

ignition system design applied in this vehicle. The application of electronic control in the ignition systems [1, 2, 16], new designing and simulation techniques [10, 11, 15], new design solutions as well as the creation of diagnostic procedures using the hardware operating in OBD standard [7, 8] made it possible to significantly increase the reliability of these circuits. However it was impossible to completely eliminate the problems in course of their diagnosing.

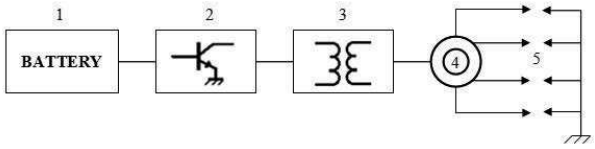

Fig. 1. Mechanical ignition system with an electronic interrupter: 1 – battery, 2 – ignition module, 3 – ignition coil, 4 – high tension distributor, 5 – spark plugs

Two popular ignition systems applied in passenger cars have been used in the tests i.e. (i) mechanical ignition system with high tension distributor and with an electronic interrupter (Fig. 1) and (ii) electronic ignition system without distributor and with individual ignition coils for each cylinder (Fig. 2).

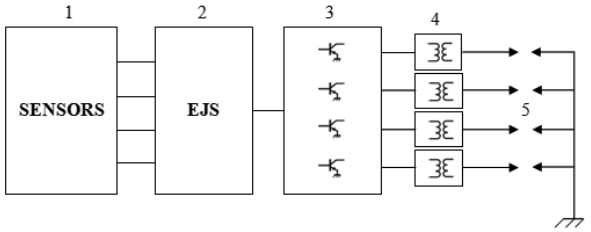

Fig. 2. Electronic ignition system with individual ignition coils for each cylinder: 1 – sensors, 2 – engine controller, 3 – ignition module, 4 – ignition coils, 5 – spark plugs

The parasite resistance was simulated in the both systems by means of a slide resistor connected between the ignition module and ignition coil (on low voltage side).

Table 1. Oscillograms on the low voltage side of mechanical ignition system

Value of parasite resistance	Voltage oscillogram on primary side of ignitron coil	Voltage oscillations oscillogram in course of spark discharge
0 Ω	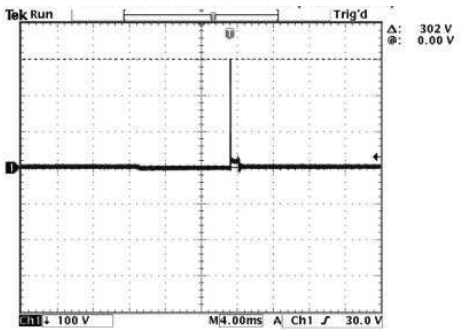	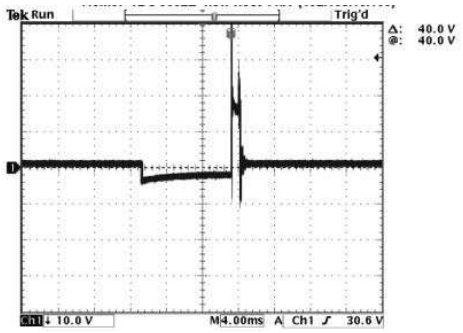
0,7 Ω	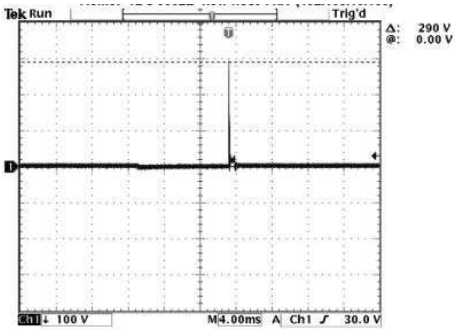	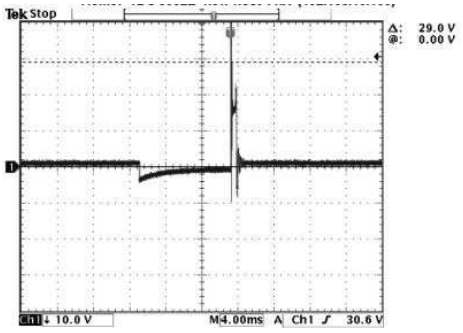
2,2 Ω	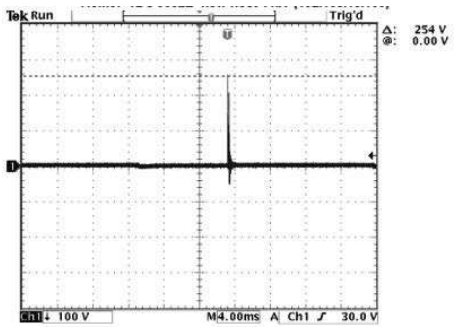	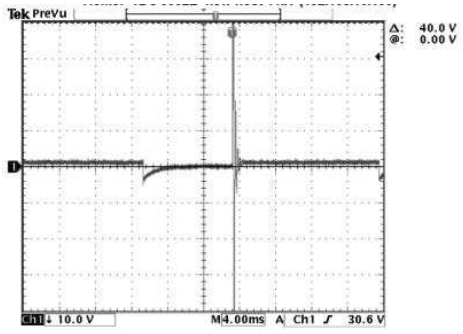

4,0 Ω (no spark discharge)	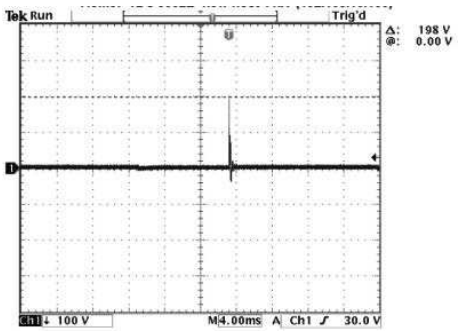	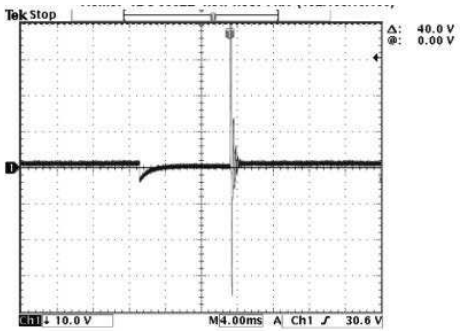

Such location of parasite resistance has been applied in order to determine the impact of an additional resistance occurring in the conductors, on the contacts or ignition coil on the functioning of the whole circuit.

The preliminary tests revealed that there was no significant impact of the resistance change on high voltage side on the correct operation of the ignition system. Furthermore no symptoms indicating to this type of failure have been recorded in the installations equipped with OBD airborne diagnostic system.

LABORATORY TESTS

The occurrence of parasite resistance in the low voltage circuit of the ignition system may contribute to unstable engine operation or even to the lack of fuel and air mixture in case of high values of parasite resistance. On the basis of the shapes of oscillograms obtained on the low voltage side of the ignition system, it is possible to determine the accurate value of parasite resistance as well as its limit value as the determinant to qualify if the system is efficient or not. The examples of curves for mechanical and electronic ignition system are illustrated in Tables No 1 and 2. The determination of corresponding parameter and its combination with the type of failure makes it possible to create a diagnostic monitor which will be used for automatic detection of the value of parasite resistance its impact, using OBD airborne diagnostic standard.

Analyzing the obtained results, we can see certain repeatability of measurements regardless of the con-

Table. 2. Oscillograms on the low voltage side of electronic ignition system without distributor

Value of parasite resistance	Voltage oscillogram on primary side of ignitron coil	Voltage oscillations oscillogram in course of spark discharge
0 Ω	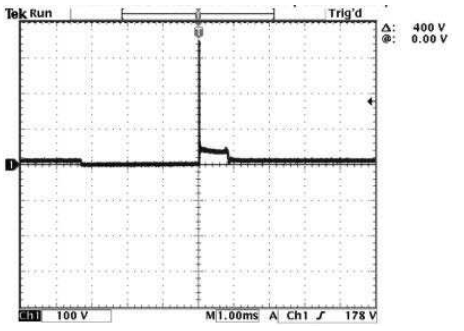	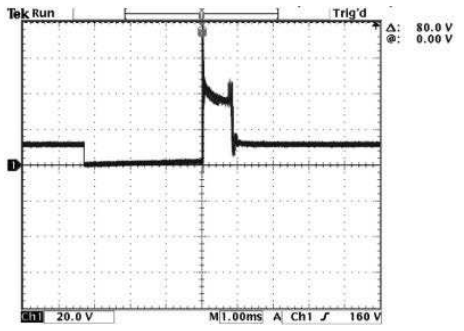
0,9 Ω	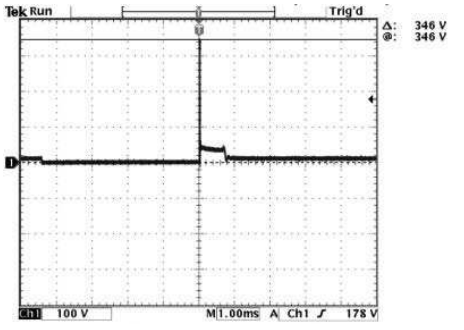	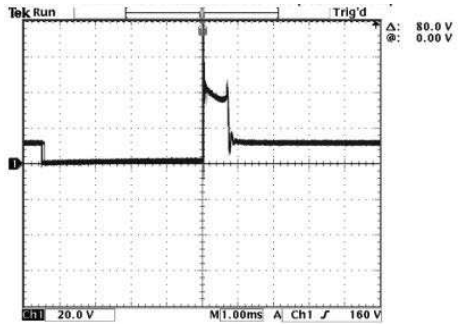

2,7 Ω	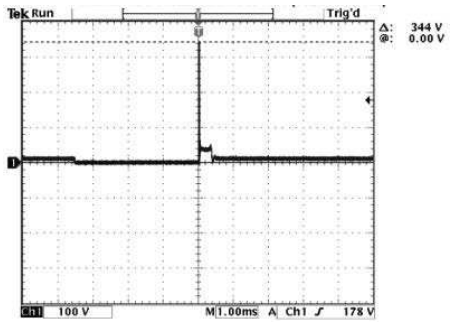	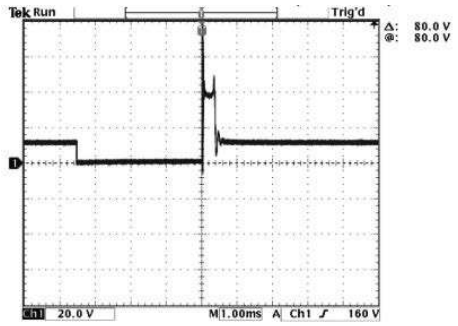
3,9 Ω	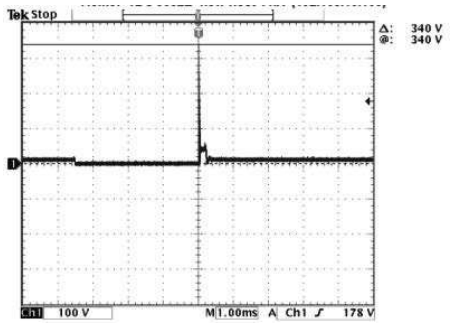	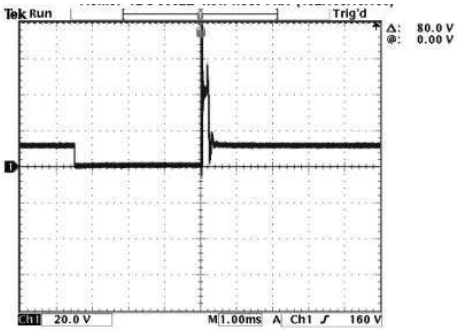
6,6 Ω (no spark discharge)	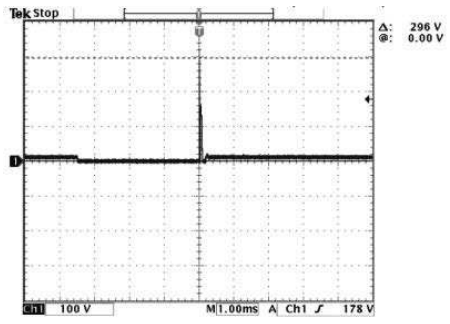	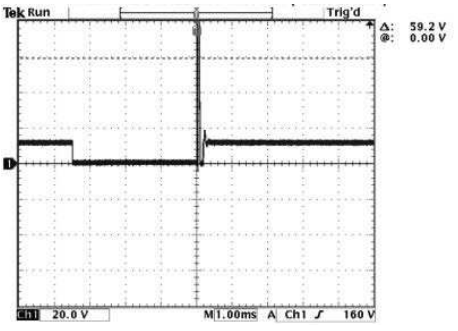

struction and generation of applied ignition system. Two parameters can be used in order to determine the of parasite resistance and to qualify the system as inefficient, i.e. (i) voltage "peak value" in course of discharge as the parameter significantly reducing its value if an additional resistance occurs (ii) another method consists in the analysis of the shape of oscillations occurring after electric discharge on spark plug.

The impact of parasite resistance discussed above on the shape and distribution of the spark between electrodes of the spark plug has been illustrated in Fig. 3. The impact of energy supplied to spark plugs is crucial for reliable ignition of fuel and air mixture. Its reduction directly contributes to unstable operation of the combustion engine as well as to increased levels of toxic compounds emitted by the vehicle into the ambient atmosphere.

CONCLUSIONS

The application of electronic control systems in engine operation contributed to the increase of reliability of the circuits responsible for the ignition of fuel and air mixture. However it was impossible to eliminate all

a) b) c) d)

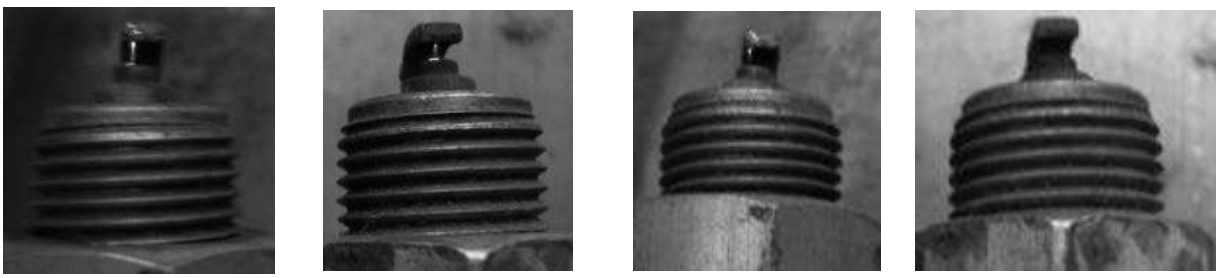

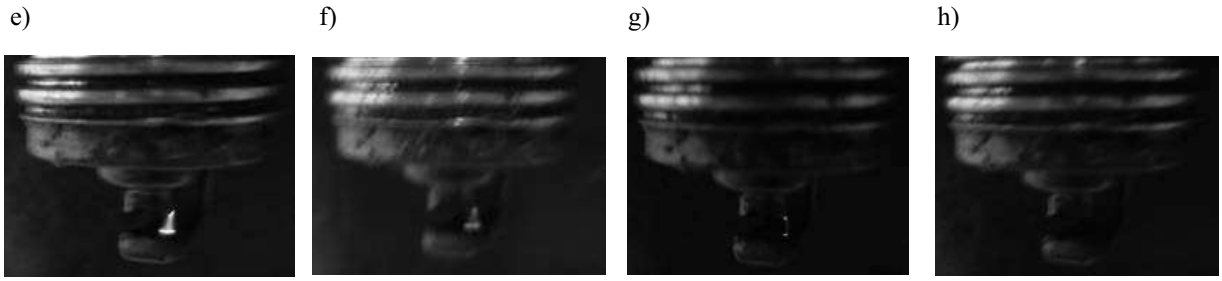

Fig. 3. Spark discharges on spark plugs for various values of parasite resistance: (mechanical system) - a) 0Ω; b) 0,7 Ω; c) 2,2 Ω; d) 4 Ω; (electronic system without distributor) - e) 0 Ω; f) 0,9 Ω; g) 3,9 Ω; h) 6,6 Ω

problems. From the tests presented in this study it appears that the ignition energy is significantly affected by an insignificant value of parasite resistance occurring in the low voltage circuit of ignition system. Such failures are possible as the result of ageing of elements, humidification of the installation or physical damages. The diagnostics of such failures and their localization is extremely difficult.

A possible solution consists in the combination of corresponding diagnostic parameter (in this case the value of ignition voltage on primary side of ignition coil) with the value of parasite resistance at which the ignition system ceases to operate correctly. Therefore it is possible to create a diagnostic monitor automatically detecting this type of failure and operating in OBD standard. Furthermore, the risk of vehicle immobilization caused by an incorrectly operating ignition system could be reduced in case of application of CAN or LIN communication bus [3, 17].

REFERENCES

1. Bosch, Informator techniczny: Sterowanie silników o zapłonie iskrowym. Zasada działania. Podzespoły, WKŁ, Warszawa, 2002.
2. Bosch, Informator techniczny: Sterowanie silników o zapłonie iskrowym. Układy Motronic, WKŁ, Warszawa, 2004.
3. Bosch, Informator techniczny: Sieci wymiany danych w pojazdach samochodowych, WKŁ, Warszawa, 2008.
4. **Dziubiński M., Ocioszyński J., Walusiak S.:** Elektrotechnika i elektronika samochodowa, WU Politechniki Lubelskiej, Lublin, 1999.
5. **Dziubiński M.:** Elektroniczne układy pojazdów samochodowych, Wydawnictwo Naukowe Gabriel Borowski, Lublin, 2004.
6. **Herner A., Riehl H. J.:** Elektrotechnika i elektronika w pojadach samochodowych, WKŁ, Warszawa, 2009.
7. **Merkisz J., Mazurek ST.:** Pokładowe systemy diagnostyczne pojazdów samochodowych, Warszawa, WKŁ 2007.
8. Poradnik serwisowy nr. 5/2003: Diagnostyka pokładowa standard OBD II – EOBD.
9. **Rokosch U.:** Układy oczyszczania spalin i pokładowe systemy diagnostyczne samochodów. OBD, Warszawa, WKŁ 2007.
10. **Styła S., Walusiak S., Pietrzyk W.:** Wykorzystanie pakietu LabView w procesie projektowania sterownika silnika spalinowego. XIII Konferencja pod patronatem Komitetu Elektrotechniki PAN i Institute of Electrical and Electronics Engineers "Zastosowania Komputerów w Elektrotechnice'2008", Materiały, Poznań, 2008, p. 193-194.
11. **Styła S., Walusiak S., Pietrzyk W.:** Computer simulation possibilities in modeling of ignition advance angle control in motor and agricultural vehicles, TEKA Komisji Motoryzacyjnej i Energetyki Rolnictwa PAN o/Lublin, tom VIII '2008, p. 231-240.
12. **Trzeciak K.:** Diagnostyka samochodów osobowych, WKŁ, Warszawa, 2002.
13. **Tylicki H., Wilczarska J., Bartol M.:** Metodyka diagnozowania stanu maszyn, MOTROL: Motoryzacja i Energetyka Rolnictwa PAN o/Lublin, tom 8, 2006, p. 230–239.
14. **Walusiak S., Pietrzyk W., Sumorek A.:** Ocena diagnostyczna stanu technicznego pojazdów samochodowych w wybranej stacji diagnostycznej, MOTROL: Motoryzacja i Energetyka Rolnictwa PAN o/Lublin, tom 5, 2003, p. 219-226.
15. **Walusiak S., Podleśny M., Pietrzyk W.:** Microprocesor model to control ZI motors, TEKA Komisji Motoryzacyjnej i Energetyki Rolnictwa PAN o/Lublin, Tom VI A '2006, p. 199-206.
16. **Wendeker M.:** Sterowanie zapłonem w silniku samochodowym, LTNPL, Lublin, 1999.
17. **Zimmermann W., Schmidgall R.:** Magistrale danych w pojazdach. Protokoły i standardy, Warszawa, WKŁ 2008.
18. PN-85/S-76001 – „Pojazdy silnikowe -- Wyposażenie elektryczne -- Ogólne wymagania i badania".
19. PN-S-76021:1998 Instalacja elektryczna pojazdów samochodowych -- Wymagania i metody badań.
20. PN-S-76021:1998/Az1:2001 Instalacja elektryczna pojazdów samochodowych -- Wymagania i metody badań.

WPŁYW REZYSTANCJI PASOŻYTNICZEJ
NA DZIAŁANIE UKŁADU ZAPŁONOWEGO SAMOCHODU

S t r e s z c z e n i e . W artykule przedstawiono wpływ rezystancji pasożytniczej powstającej pod wpływem: starzenia się elementów, zawilgoceniem instalacji elektrycznej pojazdu lub uszkodzenia mechanicznego, na poprawną pracę układu zapłonowego pojazdów samochodowych. Przedstawiono sposoby wykrywania tego typu uszkodzeń oraz analizowania otrzymanych wyników. Badania przeprowadzono za pomocą typowych przyrządów diagnostycznych znajdujących się w każdej stacji kontroli pojazdów. Do badań wykorzystano mechaniczny i elektroniczny układ zapłonowy. W artykule podano ponadto propozycję układu automatycznie wykrywającego niewielkie zmiany recytacji, które znacząco wpływają na działanie całego układu zapłonowego.

S ł o w a k l u c z o w e : rezystancja, układ zapłonowy, cewka zapłonowa, kąt wyprzedzenia zapłonu, oscylogram.

TEKA. COMMISSION OF MOTORIZATION AND ENERGETICS IN AGRICULTURE – 2012, Vol. 12, No. 1, 275–279

New elements in vehicle communication "media oriented systems transport" protocol

Andrzej Sumorek, Marcin Buczaj

Department of Computer and Electrical Engineering, Lublin University of Technology, Poland

Summary. Until recently, no significant breakthroughs have occurred in the area of functional efficiency of automotive vehicle communication protocols. The transmission speed for "high-speed" communications busses and protocols is still much slower than those of a typical computer network. Neither the High-Speed CAN (1 Mbps bandwidth) nor TTP protocol (10 Mbps bandwidth), can be compared to the 1 Gbps bandwidth that is typical for widely used computer networks. Other difficulties are that these vehicle communication networks are nonstandard and frequently use proprietary protocols (e.g., communication methods, communication medium and data formats). In contrast, computer networks have much more advanced capabilities. They are capable of a range of functions, from sending simple serial messages to maintaining sessions based on multi-media data. These functions remain lacking in the automotive vehicle communication protocols. One of the protocols in which functionality and bandwidth has reached much higher levels than competitive protocols is the Media Oriented System Transport. The purpose of this publication is to review new functions introduced in its latest version.

Key words: Media Oriented Systems Transport, Vehicle Information Network.

INTRODUCTION

Communication protocols and buses used in automotive vehicles went through a different development process than typical solutions used in computer communication. The main focus of automotive communication interfaces was initially the exchange of simple diagnostic messages. The function of such systems was to monitor and regulate the amount of pollution emitted by the vehicle. The second step of the evolution of the buses was to limit the number of failures by limiting the number of connections and the length of the wiring [19]. The next developmental step was to increase the safety and functionality of the vehicle by increasing the bandwidth between the larger number of communication ports. At this point, two major development trends of communication buses can be identified. The first of them was to replace the mechanical connection with connections between multiple devices using buses (Drive-by-Wire, X-by-Wire) [14]. The main concern with such a solution is limiting the failure rate. The second development direction was to increase the user comfort by integrating multi-media subsystems. A simple user interface is frequently implemented to manage complex automotive multimedia systems. The integration of various dedicated devices (e.g., telephone, DVD player, MP3 player) into a single system is difficult.

One of the key solutions to solving the problem of communication between various devices is the bus and protocol Media Oriented Systems Transport (MOST). The Media Oriented Systems Transport bus was created as a result of experience with the previous bus, Domestic Digital Bus (D2B) [10].

Similar to the previous D2B, the MOST bus uses an optic fiber link as the primary communication medium. This optical solution allows for even the slowest version to achieve the throughput similar to the highest speed rated in other communication networks, such as FlexRay (10-20 Mbps) [2].

EVOLUTION OF „MOST" BUS

As mentioned before, the MOST evolved directly from the D2B. The D2B was developed with the sole focus of supporting multimedia devices. Similarly, the main functions of MOST are multi-media and telematics [21]. As a result, the MOST bus is located at the boundary of the vehicle control subsystems (Fig. 1)). Safety mechanisms implemented in MOST protocols (checksum, ability to create a redundant interconnecting ring, from 25 to 150 Mbps bandwidth, error rate in the

range of 10^{-10} [21]) allow utilization of MOST for almost any configuration.

The protocol of data exchange in MOST25 is much more complex than other protocols (e.g., CAN, LIN) [12, 15]. The basic communication unit of the protocol is created with 16 frames (Fig. 2). A single frame can be up to 64 bytes long and can be used to send data as synchronous, asynchronous, or control (Fig. 2). The most typical data type is synchronous, which represents multimedia data and occupies the largest configurable portion of the frame. Asynchronous data is used to support multi-media information such as GPS systems, information about accessed files, and data of capsulated protocols within the MOST system. The control data is responsible for managing communication between the network ports. Due to this fact, the data frame is 32 bytes long, and the frame has to be divided into 16 sub-frames by each individual communication unit (Fig. 2).

Later versions of the MOST protocol implemented increased transfer speeds. The basic MOST25 (25 Mbps) works with a sampling rate of 44.1 or 48 kHz, maintained in a 64 byte frame. The doubling of the throughput is achieved in MOST50 by increasing the size of the frame from 64 to 128 bytes (Fig. 2, 3). Further increase of the frame size results in achieving throughput of 150 Mbps in the protocol MOST150 (Fig. 3) [6, 7, 9].

In addition to a continuous increase of the bus throughput, frame modifications are introduced. Control data is sent as a set of four byte packets. Also, typical synchronous data types have been complemented with the addition of an isochronous type. For the isochronous data type, a feature reserving a required portion of the bus throughput is introduced. This feature is introduced in spite of the fact that the bus frequency is different from the data sampling rate. Handing of this new data

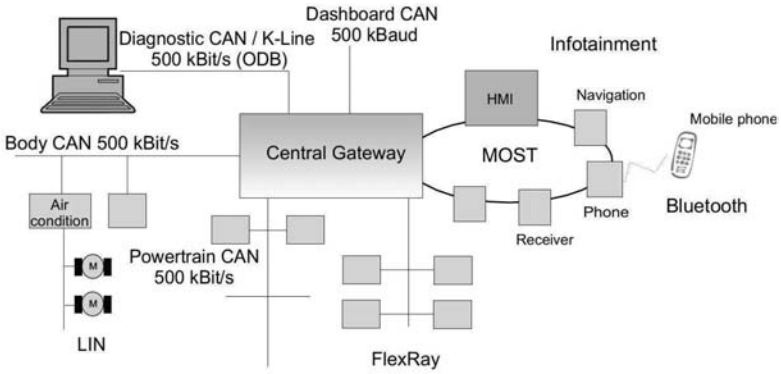

Fig. 1. Vehicle network with a ring of MOST bus [5]

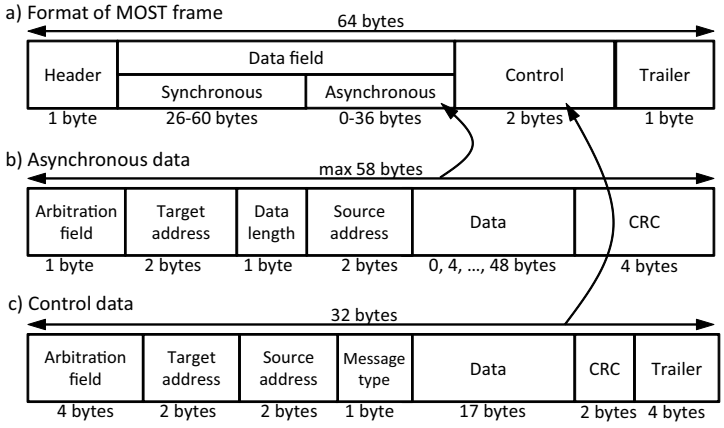

Fig. 2. MOST protocol - data format [5, 20, 19, 21, 16]

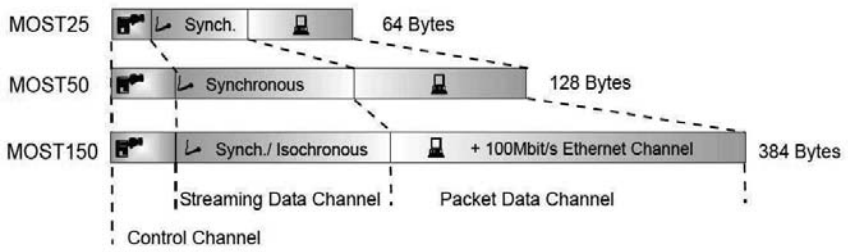

Fig. 3. Structure of MOST frame [6]

type is managed by three isochronous channel servicing protocols.

Undoubtedly the most significant changes were introduced in the area of handling digital data, which were typically managed by computer devices. The first of these types is QoS Isochronous IP (streaming), which is mainly used for transmitting audio/video data from application servers with a guaranteed bandwidth allocation [7, 9].

A second change is the way the asynchronous channel is handled. This channel can now share the bandwidth with a synchronous one, and sending 372 bytes in a single frame is possible. Under this MOST protocol, the asynchronous channel was renamed Packet or Ethernet.

Another key change was the elimination of an adaptive layer MAMAC (MOST Asynchronous Medium Access Control). In the previous MOST versions, MOST25 and MOST50, the MAMAC layer was responsible for the TCP/IP transmissions, which were performed within the asynchronous channel. The MAMAC layer was replaced with MHP (MOST High Protocol). The MHP layer allows use of the asynchronous channel to address the MDP data packets using 16-bit addresses or the MEP Ethernet data using 48-bit addresses. It is even possible to perform parallel addressing using both methods at the same time. MOST Ethernet Packets allow addressing methods identical to the Ethernet network [6].

NEW CAPABILITIES OF MOST150

Advanced driver assistance systems such as: collision warning, traffic sign monitoring, lane departure warning, lane guidance, pedestrian warning, night vision, adaptive cruise control or pre-crash warning require integration with a wide variety of vehicle subsystems. A typical application of the MOST protocol falls under the Infotainment network category (Fig. 1), which does not require as low a failure rate as that of advanced applications.

Fig. 4. Safety layer concept [3]

The MOST protocol appears to contain characteristics allowing for easy integration of existing multimedia networks with driver assistance network. Key characteristics of bus that allow this integration include [3]:

– high throughput – "driver assistance" systems are required to interface with a larger variety of sensors and actuators. MOST is equipped with synchronous/isochronous channels and asynchronous/packet channels capable of allocating a portion of the bandwidth to each of the required services. Having packet communication and IP protocol available allows for easy introduction of car-to-car, car-to-infrastructure communication. It also allows for communication with peripherals such as a fuel distribution, a GSM module or a garage/house control equipment [1, 4, 13];
– deterministic-function - the necessity to provide safety requires implementation of protocols based on stiff time bounded rules guaranteeing small and predictable delays. Additionally, all required parameters must be fulfilled over a wide temperature range (-40 C to 95 °C). The ability to simultaneously define a portion of bandwidth for multiple synchronous channels gives an ability to control both throughput and delays;
– high safety margin - communication cannot be susceptible to errors caused by: failure of network nodes, frame failures, and message delays. Even on the basic communication layer (Fig. 2), it is possible to monitor communication quality through cyclic redundancy check, sequence counter, message length, and time-out detection. An additional application layer gives additional functions of monitoring correctness of exchanged data (Fig. 4).

The features mentioned above confirm that MOST150 can function as a safe system within its own nodes or nodes of other networks. Based on these characteristics, MOST150 shows optimal fit as a network for the Advanced Driver Assistance Systems (ADAS).

The throughput in the range of 150 Mbps, introduced by MOST150, is the highest within any of the vehicle communication networks. This performance dates back to the year 2000 (Fig. 5). In spite of that, even faster solutions are being pursued with designers attempting to take advantage of the physical layer of the optic fibers. Such solutions are characterized by low weight, low sensitivity to interference, and relatively low cost.

Tests performed on increasing communication speed have been conducted in the Fraunhofer Institute. The POF-Plus (Plastic Optical Fiber), implemented within the MOST layer, demonstrated the ability to achieve a throughput of 1.25 Gbps. At the same time, the results indicated that the optical fiber connection solution functioned properly with lengths up to 11.2 meters and an absolute loss coefficient of 0.4 dB/m [17].

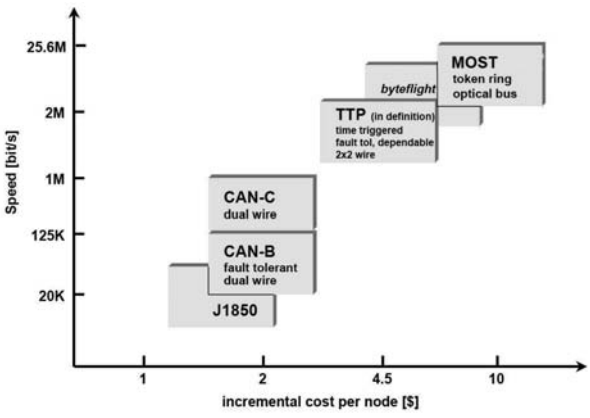

Fig. 5. Data rate of vehicle buses in 2000 [18]

Multimedia content frequently requires protection from unauthorized access or duplication. Two primary mechanisms of data protections are: DTCP (Digital Transport Content Protection) and HDCP (High-Bandwidth Digital Content Protection). Both of these were implemented in the MOST protocol. Version 3 of the DTCP protection is covered by Supplement B (M6 cipher), and protection DTCP-IP version 1 is covered by Supplement E (AES-128 cipher). Difficulties might arise in the case of HDCP protection, which exists under two versions. Version 1 is common for synchronous and uncompressed content, while Version 2 is dedicated to compressed and protected content (interface independent adaptation-IIA).

MOST utilizes two schemes of DTCP deciphering such that a synchronous channel is used for multimedia, audio, and video transport stream, and an additional synchronous channel is used for supplemental data required for the deciphering process (e.g., the cipher key inside of the Synchronous Added Data - SAD, Fig. 6). The HDCP IIA transport stream is protected such that audio requires additional deciphering from an elementary stream. This requires simultaneous transfer of the stream and the cipher key with the utilization of the isochronous channel. A difficulty might arise when accessing two sets of data which are protected using different methods. This circumstance could lead to exceeding the throughput of the packet channel [8].

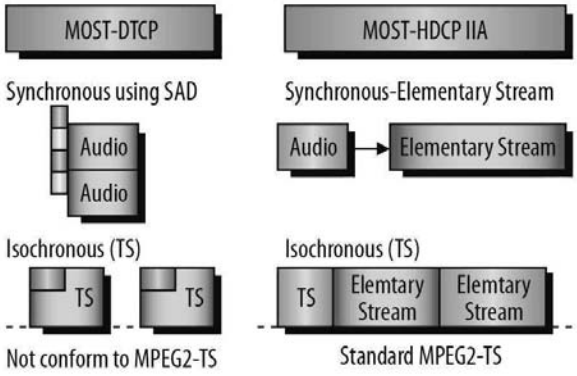

Fig. 6. Two transport mechanisms for protected content [8]

Internet access has become a necessity for people who require continuous access to real/time data. The internet also serves as a source of multimedia data and allows users to connect other mobile devices.

Due to the implementation of the Ethernet channel introduced in MOST150, the driver and passengers have access to functions based on: IP (internet protocol), TCP (Transmission Control Protocol), or HTTP (Hypertext Transfer Protocol). Physical access to the network is achieved by making a connection to the head unit (HU), which functions as a central router independent of the connection type (wire or wireless). The head unit can also act as a hot spot for WLAN devices such as a smart phone or tablet PC (Fig. 7). Due to the vehicle mobility, it is important to be able to utilize wireless networks protection such as ciphering.

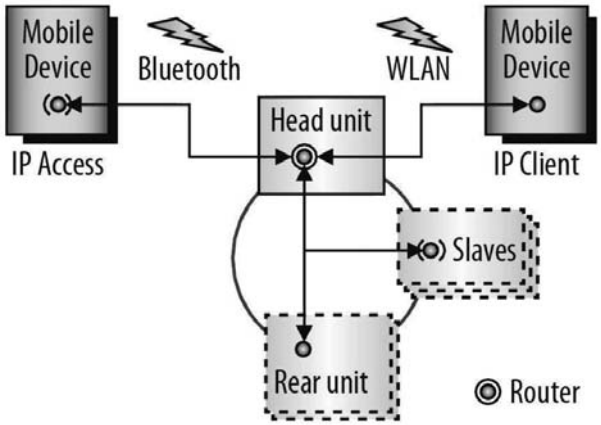

Fig. 7. Model of IP architecture of a vehicle infotainment system [11]

For communication between devices utilizing the IP protocol, the MOST150 Ethernet Packet Channel is used. Practical tests of the efficiency of packet type communication were conducted by Daimler. The results indicated the ability to achieve theoretical throughput of 142.8 Mb/s, with 107 Mb/s under practical conditions. This represents 75% utilization of the throughput capability. Introduction of the limitation of available throughput to 43.75 Mb/s resulted in achieving utilization of the throughput up to 82%. The future design direction of IP for the MOST network focuses on more effective utilization of higher level layers of the OSI model [11].

CONCLUSIONS

Years of development of the MOST network/protocol resulted in achieving a very mature solution capable of servicing a large variety of data types. To date, the use of MOST has moved beyond infotainment applications. The features of this network, as described in the article, lead to the following conclusions:

– The advanced communication frame fulfils requirements of both diagnostic and multimedia communication.
– The high throughput and the predictable behaviour of the protocol allows implementation or utilization of this protocol in future applications for advanced driver assistance systems.
– The protocol contains features allowing access to protected content, allowing compliance with copyright laws.
– The maximum throughput of 150 Mbps does not even approach the possible boundaries of the communication speed of the MOST protocol.

REFERENCES

1. **Boguta A., 2011:** Application of IP monitoring in the supervising system of a building. Teka Komisji Motoryzacji i Energetyki Rolnictwa, vol. XI, ISSN 1641-7739, pp. 9-17.

2. **Bosch R. GmbH, 2008:** Sieci wymiany danych w pojazdach samochodowych, Warszawa, Wydawnictwa Komunikacji i Łączności.
3. **Bott W., 2012:** MOST in Driver Assistance. Elektronik automotive 3/2012, pp. 49-50.
4. **Buczaj M., Daniluk M., 2010:** Wykorzystanie modułu GSM do zdalnego monitorowania i zarządzania pracą wybranych układów w pojazdach. Logistyka 6/2010, pp. 445-452.
5. **Grzemba A., 2008:** MOST - The Automotive Multimedia Network, Frazis Verlag GmbH.
6. **Grzemba A., 2011:** MOST - The Automotive Multimedia Network. From MOST25 to MOST 150 , Frazis Verlag GmbH.
7. **Karche M., 2011:** Testing the New MOST150 Capabilities. A How to for Testing and Validating the New Isochronous and IP/Ethernet Features of MOST150, SMSC Automotive Infotainment Systems, 05.11.2011.
8. **Klaus-Wagenbrenner J., 2012:** Crux of Matter, Elektronik automotive, March 2012, p. 56-57.
9. **Kohler H., 2008:** MOST150 – The Next Generation Automotive Infotainment Backbone, SMSC Automotive Infotainment Systems, Proceedings of Workshop on ICT in Vehicles - Palexpo, Geneva, p. 5-7.
10. **Leen G., Heffernan D., 2002:** Expanding Automotive Electronic Systems. Computer, vol 35.
11. **Leonhardi A., Walter U., Hauke R., Maniscalco M., 2012:** Let Me Entertain You. IP architecture of a MOST150-based infotainment system, Elektronik automotive, Special Issue - MOST, 2012, p. 58-60.
12. **Merkisz J., Mazurek S., 2007:** Pokładowe systemy diagnostyczne pojazdów samochodowych, Warszawa, Wydawnictwa Komunikacji i Łączności.
13. **Styła S., 2010:** Analiza możliwości i funkcjonalność elektronicznych liczników dystrybutorów paliw. Motrol - Motoryzacja i Energetyka Rolnictwa, tom 12, p. 139-144.
14. **Styła S., Walusiak S., Pietrzyk W., 2008:** Computer simulation possibilities in modelling of ignition advance angle control in motor and agricultural vehicles. Teka Komisji Motoryzacji Energetyki i Rolnictwa, 8, p. 231-240.
15. **Sumorek A., 2011:** Zróżnicowanie protokołów diagnostycznych, sterujących i multimedialnych w pojazdach. Logistyka 3/2011, p. 2583-2592.
16. **Sumorek A., Buczaj M., 2011:** The problems in fibre optic communication in the communication systems of vehicles. Teka Komisji Motoryzacji i Energetyki Rolnictwa, vol. XI, ISSN 1641-7739, p. 363-372.
17. **Weber N., Zerna C., 2012:** 1000 Mbit/s. From Theory to Practice. Elektronik automotive 3/2012, p. 18-31.
18. **Wense H-Ch., 2000:** Introduction to Local Interconnect Network, Munich, Germany, March 2000.
19. **Widerski T., 2005:** Samochodowe sieci informatyczne. Poradnik serwisowy, 5/2005, Warszawa, Wydawnictwo Instalator Polski.
20. **Widerski T., Kędzierski J., 2004:** Samochodowe sieci informatyczne (MOST), Auto Moto Serwis, 6/2004, Warszawa, Wydawnictwo Instalator Polski, p. 35-37.
21. **Zimmermann W., Schmidgall R., 2008:** Magistrale danych w pojazdach. Protokoły i standardy, Warszawa, Wydawnictwa Komunikacji i Łączności.

NOWE ELEMENTY PROTOKOŁU KOMUNIKACYJNEGO POJAZDÓW „MEDIA ORIENTED SYSTEMS TRANSPORT"

S t r e s z c z e n i e . Długotrwały rozwój protokołów komunikacyjnych pojazdów samochodowych nie zaowocował dotychczas nadzwyczajną wydajnością i funkcjonalnością rozwiązań. Prędkości transmisji osiągane przez protokoły i magistrale określane „high-speed" są niskie w porównaniu z przeciętnymi przepustowościami sieci komputerowych. Przepustowość rzędu 1 Mbps protokołu High Speed CAN lub 10 Mbps protokołu TTP jest znacząco mniejsza niż przepustowość 1 Gbps typowa dla kablowych sieci komputerowych. Kolejnym czynnikiem, który należy brać pod uwagę, jest zróżnicowanie metod komunikacji i formatów danych. O ile sieci komputerowe mogą przesyłać zarówno proste komunikaty szeregowe jak i prowadzić sesje oparte o dane multimedialne, to protokoły komunikacji pojazdów dopiero rozwijają takie uniwersalnej funkcje. Protokół, którego funkcjonalność i przepustowość jest bardziej rozwinięta niż u konkurencji to protokół i magistrala Media Oriented Systems Transport. Niniejsza publikacja ma za zadanie przybliżyć funkcje wprowadzone w jego ostatniej wersji.

S ł o w a k l u c z o w e : Media Oriented Systems Transport, Vehicle Information Network.

TEKA. COMMISSION OF MOTORIZATION AND ENERGETICS IN AGRICULTURE – 2012, Vol. 12, No. 1, 281–287

Regional differences in equipment of machinery park on farms

Anna Szeląg-Sikora

Institute of Agricultural Engineering and Informatics, University of Agriculture in Krakow

S u m m a r y. The aim of this paper was to analyze the level of machinery park equipment on the farms differing in their location. In the course of research carried out in the form of directed interview, the objects were chosen from the Małopolska Province and the West Pomerania Province. The obtained results allow for the conclusion that in the case of the surveyed holdings, there are differences in the level of machinery park equipment. Examples include value of installed capacity in tractors, where for the objects of the Małopolska Province is the average of 9.05 kW · ha^{-1} of cropland, while in the West Pomerania Province only 1.99 kW · ha^{-1} of cropland.

K e y w o r d s: agricultural machinery, tractors, machinery park, farm.

INTRODUCTION

One of the factors determining the competitive ability of Polish agriculture is the use of cost-effective production technology. The possibility of applying such technology forces the necessity of machinery park renewal, especially in commodity holdings, which will allow to obtain a better quality of products [14, 5]. Thus, the use of technical means of work in addition to improving the working conditions of the farmer and reducing the workload of manual should also have an impact on getting better production effects [Kocira 2008]. Obtaining a good quality of products enforces compliance with various standards, standardized national rules and EU regulations. By a set of technology standards, we mean a set of requirements and technological parameters, which include technical and technological equipment, functional solutions, the elements of technical infrastructure to meet the needs of animal welfare, but also protecting the environment. These standards relate to for eg. design, construction and maintenance of livestock buildings, installation, operation and control of animals, machinery and equipment used in the production and transport of animals [11]. So now the choice of individual elements of technical infrastructure of farms on the one hand is dictated by the needs resulting, among others, from the orientation of production, on the other hand, it must meet the relevant requirements in order to comply with standards. Undoubtedly, a reasonably sized and operated tractor-machine park improves production operations in accordance with the requirements of agrotechnical periods of agronomy and quality of treatments, and its costs are not borne by the holding over the current playback capabilities of existing hardware [13]. Known and used methods of selection of machines and machinery for farms (e.g. indicator, technological or factor) are quantitative methods that allow you to specify the number of units needed due to the agricultural area, crop structure and the term of agrotechnical and complex system of technological processes [3]. Another of the factors that are determinant of equipment level of the machinery park is the intensity of production. It may be one of the determinants of the changes taking place in the farm aimed towards the modernization of technical base [18]. The precision agriculture should also be mentioned, whose implementation can not do without the input of new solutions in the field of agricultural technology. Practical applications of precision agriculture require different applications of the doses of fertilizers, pesticides, seeds, or changes in equipment operating parameters (e.g. depth of plowing, sowing density, performance of air flow in the sprayers) [16]. The key of importance in improving food security will be played by the monitoring system (traceability) at each stage of production, processing and trade, which cannot be made without the use of precision agriculture components [Auernhammer 2006]. Monitoring is necessary, particularly to identify the time and place of contamination of plant protection products by nitrates and heavy metals, or use of illicit substances [6]. For this purpose it is necessary to correlate the positioning and communication system. So there is a problem of significantly wider agricultural information in the introduced process of modernization of

the machinery park, because on the quantity and quality of the gained information the management of the farm production process depends. Decisions regarding the purchase or sale of agricultural machinery, significantly affect the production technologies and, consequently, the economic health of the holding (agro firm) in the future [2].

Analysis of supply of selected agricultural machinery and equipment for the domestic market in the years 2001-2009 showed that, similarly to the production, import and export, it is characterized by high volatility, which certainly does not favor domestic producers in the planning of production [20]. Significant changes are observed in the production and distribution of agricultural machinery and methods of their manufacture and use. Currently, the final product usually arises from the assembly of finished parts ordered from subcontractors or purchased from specialized companies. In the production and trade, apart from the transnational corporations the important role is played by small and medium enterprises (SMEs) producing these accessories or short series of very specialized machines [Hołownicki 2008]. These dependencies are the result of many conditions. These will include factors related to the regionalization of agricultural production and, in relation to them, the size of economic and operational indicators [7]. Polish agriculture is characterized by a great diversity of farming conditions. This is evident in the wide range of agrarian structures and the considerable variations in the size of farms as well as livestock. Also, a significant influence on the specificity of Polish agriculture is undoubtedly exerted by geographical conditions, which to some extent limits the extent of the agricultural production. The level and structure of production are often determined by the experience possessed by the farmer and farm equipment in the technical appliances [17]. Taking into account the current situation of Polish agriculture, the number of family farms should be increased so that they gave full employment to at least 2 family members and sufficient parity income for agricultural families. Due to the development of mechanization, the transformation of agrarian sector is desirable, in the direction of the growing area of farms [7]. As numerous studies by other authors have pointed out [21, 15, 19, 12], the equipment of households in agricultural equipment, including the number, types, value and efficiency of machines and the number of used tractors and their power varies widely between farms, even of a similar production profile. The most differentiating factor, in terms of the mechanical appliances, is undoubtedly the size (area) of the farm. It is a major distinguishing feature of the scale of production. Specific features of agricultural production – i.e. the spatial nature, seasonality, diversity of products obtained, the quality of agricultural roads and the other - require that the farm is equipped in diverse and sometimes specialized technical means, e.g. for transport [9]. Efficiency of raw material and transport flows in the enterprises depends to a major extent on the proper equipment of farms in the technical means in the form of production and transport equipment, which are part of the logistics infrastructure [10].

The conducted study of literature in the field on the issues concerning the modernization of technical equipment of farms raises the question, whether the existing regional disparities in our country are also reflected in the level of technical equipment in facilities of farms? Therefore, can the available resources of land be the determinant of the quantitative status of ownership of agricultural machinery and tools? Are the resources invested in the machinery park comparable in two distant voivodships? Finding the answer to the above questions was undertaken as the objective of this work.

MATERIALS AND METHODS

To fully accomplish the adopted objective of the work, the target objects were selected from two distant sites: the Małopolska Province and the West Pomerania Province, these regions being undoubtedly different as to the nature of the conducted agricultural activities. The characteristics of technical equipment was based on background information gathered during research conducted in the form of directed interview with the owners of farms, using a previously prepared questionnaire. The study was conducted in 30 farms, with 15 objects from each of the voivodships. In addition to the grouping variable, which was the location, the farms were also divided according to the area. By creating various area groups comparing the size of each, in the two voivodships only two groups were separated, i.e. 5,1-15,0 ha and 15,1-30,0 ha.

In the studied objects the pattern of use was dominated by arable land and conducted agricultural activi-

Table 1. Characteristics of the surveyed holdings

Specification	Farms							
	Małopolska Province				West Pomerania Province			
	including area [ha]:							
	Average	**0-5 ,0**	**5,1-15,0**	**15,1-30,0**	Average	**5,1-15,0**	**15,1-30,0**	**30,1- 50,0**
Number of holdings	-	4	7	4	-	4	6	5
Area of agricultural land [ha]	11,40	3,85	10,71	20,14	52,83	14,13	23,75	119,20
Arable land	10,96	3,21	10,41	19,67	46,66	11,50	12,42	109,20
Grassland	0,43	0,63	0,30	0,48	6,17	1,63	4,33	12,00

[Source: own research]

ties were focused on plant production (Table 1). The characteristics of the tractor-machines park working in the surveyed farms is shown by calculating: quantitative equipment of the owned technical equipment, replacement value of machinery park, the rate of energy consumption and the performance of agricultural tractors (by giving the number, age, duration of use, annual use). Calculations were based on the methodology used in the Institute of Agricultural Engineering and Informatics at the Faculty of Production and Power Engineering, University of Agriculture in Krakow [8].

THE RESULTS AND DISCUSSION

One of the key pieces of equipment of the machinery park is mechanical traction, i.e. tractors. In the group used for comparative analysis, the quantitative average of equipment in tractors was comparable, i.e. at the level of about 2 pcs · farm^{-1}. Referring the number of tractors to the conversion factor of one hectare from the area of agricultural land, we see that these differences are important. In the group of objects from the West Pomerania Province, on average there were only 0.04 units per hectare, while in the second group there were 0.33 pc. Noticeable difference is also evident within the first adopted area group (5,1-15,0 ha of agricultural land), where, in the farms from the West Pomerania Province, the value is less than 10-fold. By analyzing the owned tractors by the classes, in each case they were dominated by tractors in class 9 kN (Table 2).

One of the characteristics of agricultural tractors, speaking indirectly about their „modernity", is their age. In the surveyed holdings, the average age in both the West Pomerania Province and the Małopolska Province was decreasing while increasing the area of agricultural land. Analyzing the average value, the younger tractors were owned by farmers from the West Pomerania Province,for an average of 4 years. The difference in the average level of four years was also noted in the analysis of time of use of farm tractors. It should be noted that the average age of tractors often is underestimated by the dominant number of tractors owned which were more than 15 years old, but in the whole group of tractors in the farms reported, the present „new" (1-5 years old) tractors were often purchased from the EU funds.

Proper selection of tractors should be reflected in the level of their annual usage. It is a indicator of the use of their productive potential, which indicates the degree of utilization of the merits of having these machines. In the analysis, the annual use of agricultural tractors was related to the area of one hectare of agricultural land, farm, and physical piece of tractor. Comparing the annual use of tractors in relation to the available resources of land, we can see that the households of the Małopolska Province with an increase in available resources have decreased yearly utilization of land. On average in this group the annual use of tractors stood at 35.87 cgh·ha^{-1}of cropland, and was three times higher than the average in the West Pomerania Province (cgh 12.03 · ha^{-1}of cropland). Such a large use of tractors on farms in the Małopolska Province - notwithstanding its smaller resources of the earth,

Table 2. Characteristics of tractor park

Specification		Farms							
		Małopolska Province				West Pomerania Province			
		including area [ha]:							
		Average	**0-5 ,0**	**5,1-15,0**	**15,1-30,0**	Average	**5,1-15,0**	**15,1-30,0**	**30,1- 50,0**
[pcs ·ha^{-1} of cropland]									
Tractros		0,21	0,33	0,24	0,14	0,04	0,013	0,10	0,02
in this:	class 6 kN	0,15	0,26	0,17	0,09	0,03	0,12	0,08	0,01
	class 9 kN	0,05	0,07	0,07	0,03	0,01	0,02	0,02	0,01
	class 14 kN	0,02	0,00	0,01	0,02	0,00	0,02	0,00	0,01
[pcs · farm^{-1}]									
Tractros		2,40	1,25	2,57	3,25	2,20	1,75	2,17	2,60
in this:	class 6 kN	1,73	1,00	1,86	2,25	1,40	1,50	1,67	1,00
	class 9 kN	0,60	0,25	0,71	0,75	0,53	0,25	0,50	0,80
	class 14 kN	0,20		0,14	0,50	0,20	0,25		0,60
[years]									
Age		22	29	21	20	18	24	19	15
Time of use		18	23	20	14	16	20	18	10
Annual usage									
[cgh·ha^{-1} of cropland]		35,87	45,64	32,40	31,56	12,03	18,67	31,40	6,73
[cgh·farm^{-1}]		408,80	175,50	347,14	750,00	619,33	280,00	693,33	802,00
[cgh·pcs.$^{-1}$]		170,3	140,4	135,0	230,8	281,5	140,0	320,0	308,5

[Source: own research]

was doubtless dictated by the structure of the crop, in which the important role was played by time-consuming cultivation of vegetables (often repeated agrotechnical treatments such as spraying, fertilizing). In each of the separate groups, both in terms of location and resources of agricultural land (area group), the value of the annual usage rate was increasing with the increasing of possessed area of agricultural land. In the households of the Małopolska Province it was in the range 175.50 - 750.00 and in the second region 280,00-802,00 cgh · farm^{-1}. In the equipment of the tested objects in most cases there were at least two tractors, so for comparative purposes Table 2 also contains data on the average annual use per one tractor. The results are varied within the grouping variable for the assumed location-voivodship. In the group 5,1-15,0 ha of area in the two voivodships the value of

Table 3. Quantitative equipment of machinery park

Specification	Farms							
	Małopolska Province				West Pomerania Province			
	including area [ha]:							
	Average	**0-5 ,0**	**5,1-15,0**	**15,1-30,0**	Average	**5,1-15,0**	**15,1-30,0**	**30,1- 50,0**
	[pcs ·ha^{-1} of cropland]							
Ploughs	0,09	0,26	0,09	0,04	0,02	0,07	0,05	0,01
Soil aggregate	0,06	0,13	0,08	0,03	0,01	0,03	0,01	0,01
Manure spreader	0,05	0,20	0,04	0,02	0,01	0,05	0,04	0,00
Fertilizer distributor	0,06	0,07	0,08	0,03	0,02	0,03	0,05	0,01
Grain drill	0,09	0,26	0,09	0,04	0,01	0,03	0,05	0,01
Point drills	0,02	0,00	0,03	0,02	0,00	0,00	0,01	0,00
Automatic planters	0,06	0,07	0,08	0,03	0,01	0,07	0,01	0,00
Spraying machines	0,08	0,26	0,08	0,04	0,01	0,05	0,02	0,01
Rotary mower	0,05	0,07	0,07	0,03	0,01	0,07	0,03	0,00
Pick-up balers	0,02	0,00	0,03	0,02	0,01	0,03	0,01	0,00
Potato diggers	0,02	0,20	0,00	0,01	0,01	0,02	0,02	0,00
Potato harvesters	0,06	0,07	0,08	0,04	0,01	0,03	0,01	0,00
Beet harvesters	0,00	0,00	0,00	0,00	0,00	0,00	0,02	0,00
Combine-harvesters	0,04	0,07	0,04	0,02	0,02	0,05	0,05	0,01
Delivery vans	0,07	0,07	0,09	0,04	0,00	0,02	0,01	0,00
Trailers	0,12	0,13	0,12	0,09	0,03	0,13	0,06	0,01
	[pcs · farm^{-1}]							
Ploughs	1,00	1,00	1,00	1,00	1,00	1,00	1,00	1,00
Soil aggregate	0,73	0,50	0,86	0,75	0,47	0,50	0,17	0,80
Manure spreader	0,53	0,75	0,43	0,50	0,60	0,75	0,83	0,20
Fertilizer distributor	0,67	0,25	0,86	0,75	0,93	0,50	1,00	1,20
Grain drill	1,00	1,00	1,00	1,00	0,67	0,25	1,00	0,60
Point drills	0,27		0,29	0,50	0,07		0,17	
Automatic planters	0,67	0,25	0,86	0,75	0,33	0,75	0,17	0,20
Spraying machines	0,93	1,00	0,86	1,00	0,67	0,75	0,33	1,00
Rotary mower	0,60	0,25	0,71	0,75	0,60	0,75	0,67	0,40
Pick-up balers	0,27		0,29	0,50	0,27	0,50	0,17	0,20
Potato diggers	0,27	0,75	0,00	0,25	0,27	0,25	0,50	
Potato harvesters	0,73	0,25	0,86	1,00	0,27	0,50	0,17	0,20
Beet harvesters					0,13		0,33	
Combine-harvesters	0,40	0,25	0,43	0,50	0,93	0,75	1,00	1,00
Delivery vans	0,80	0,25	1,00	1,00	0,20	0,25	0,17	0,20
Trailers	1,33	0,50	1,29	2,25	1,40	1,75	1,33	1,20

[Source: own research]

this ratio differed by 67.14 cgh·pcs^{-1}, in the case of the other comparable group (15,1-30,0 ha of cropland), this difference was 56,67 100 cgh · pcs^{-1} (Table 2).

The machinery park in the surveyed holdings include cultivation machinery and tools, machines for fertilization and plant protection and harvesting machine. There was no presence of machines and tools directly used in livestock production which is clear from the orientation of production test items, which were focused on plant production. Table 3 contains details of the number of machines, for comparative purposes the results are given in the [pcs · ha^{-1} of cropland] and [pcs · farm^{-1}].

As is clear from the data of Table 3 in each of the tested objects there was a plough in the equipment, an average farm in the Małopolska Province also owned a grain seeder, where for comparison in the second voivodship there were 0.67 pcs ·farm^{-1}. Among the harvesting machinery, in case of harvesters, in the West Pomerania Province they belonged to the equipment in almost every household, while in the Małopolska Province only in every other farm. In both groups the lack of sugar beet harvesters was noted, not counting the one exception in West Pomerania Province. This is undoubtedly dictated by the adverse changes that occur in our country when it comes to decreasing the cultivation area of this plant.

One of the indicators that can be a criterion in the selection of individual machines is the installed capacity in agricultural tractors. This is the parameter which the farmers are guided by in choosing the machines and related equipment. It is important to choose tractors and machinery to make it possible to leverage the existing capacity resources.

Table 4 contains the values of individual components of the total of the installed appliances in the examined farms. In each of the separate groups, agricultural tractors have the largest share. In the objects of the Małopolska Province, the average per hectare of arable land is 9.05 kW, while in the West Pomerania Province only 1.99 kW. Let's compare the two groups with the same area, i.e. 5,10-15,00 ha of cropland and 15,1-30,00 ha of cropland and we see that in the West Pomerania Province this ratio is much lower. Hence the conclusion that in these objects tractors have less power than the objects of the second group with the similar farming conditions (like the land resources). In the households of the Małopolska Province a significant share in the total power values were also cars that were used primarily to transport crops (vegetables) on the markets. Their average power was 40.13 kW· farm^{-1}, for comparison in the group from the West Pomerania Province it was only 0.15 kW · farm^{-1}.

The possessed machinery park is the value of capital invested in the farm, because the work includes the gross replacement value ratio computed in accordance with the approved methodology as the value of new machinery. Analyzing the results, it was noted that the average index value for one household only slightly differs for groups within the investigated objects by location and this difference is only about 20 t PLN.

It is noted that the differences in the value of index appear, when we examine the ratio of the gross replacement value of the existing resources of the land. In this situation, we see that the average per hectare of land in the West Pomerania Province is only 5.46 t PLN, while

Table 4. The installed appliances in the machinery park

Specification		Farms							
		Małopolska Province				West Pomerania Province			
		including area [ha]:							
		Average	**0-5 ,0**	**5,1-15,0**	**15,1-30,0**	Average	5,1-15,0	15,1-30,0	30,1- 50,0
		[kW·ha^{-1} of cropland]							
Total		14,95	15,98	17,57	10,44	3,46	9,89	7,43	1,96
in this:	vans	3,52	2,48	4,52	2,36	0,15	0,64	0,29	0,06
	tractors	9,05	9,92	10,06	6,73	1,99	6,34	3,77	1,28
	self-propelled	2,16	2,93	2,75	1,25	1,24	2,73	3,22	0,57
	other	0,21	0,65	0,23	0,10	0,08	0,18	0,15	0,05
		[kW·farm^{-1}]							
Total		170,39	61,45	188,26	248,08	178,03	148,33	164,00	233,10
in this:	vans	40,13	9,55	48,46	56,15	7,64	9,55	6,37	7,64
	tractors	103,16	38,15	107,83	160,00	102,61	95,15	83,25	151,98
	self-propelled	24,67	11,25	29,50	29,63	63,80	40,88	71,17	67,60
	other	2,43	2,50	2,47	2,30	3,98	2,75	3,22	5,88

[Source: own research]

in the Małopolska Province up till 22.97 t PLN. Noticeable differences are also between groups of the same area (5,10-15,00 ha of cropland and 15,1-30,00 ha of cropland) in both voivodships. Thus, it can be concluded that the households of the Małopolska Province are excessively invested in, and available resources of land may not be sufficient to generate revenues allowing for continuous recovery process - the modernization of the owned machinery park.

CONCLUSIONS

Currently, in the Polish agriculture there have been a number of changes, on the one hand connected with our country's accession to the European Union, and therefore with the need to compete with the agriculture of the EU countries, on the other hand changes are dictated by the opportunity to create a development that makes the EU subsidies available. From previous studies, among others by the author of this study, it has been shown that subsidizing agriculture is largely directed at the modernization of technical infrastructure. Farmers who have started using the EU funds, spend the money on technical investments by purchasing new machinery and tools. In this way, they "rejuvenate" the machinery park and thereby increase its value, and rationally access its individual elements. Responding to the questions posed at the beginning of this article it can be concluded that the objects included in the comparison groups differed as to the standard of machinery park equipment, as evidenced by the calculated values of the indicators. This diversity manifests itself primarily in the quantitative index of equipment in relation to individual machines, which in turn was reflected in the replacement value of machinery park calculated for each of the separate groups, both in location (in the West Pomerania Province - 5.46 t PLN · $ha^{-1}$of cropland , while in the Małopolska Province - 22.97 t PLN · $ha^{-1}$of cropland) and resources of agricultural land (for example, a group of area 5.00 - 15.00 hectares in the West Pomerania Province - 15.36 t·$ha^{-1}$of cropland, while in the Małopolska Province - 28.42 t·ha^{-1} of cropland). Differences also occurred in the indicators characterizing the tractors, whose average number was about 2 pcs · $farm^{-1}$ in both voivodships, however, in relation to the calculated land resources the values differed significantly. Contrary to expectations, while it might seem that the higher value of the annual use of farm tractors should occur in the West Pomerania Province, because of a greater acreage of arable land, the situation appeared to be reversed. The households from the Małopolska Province had a higher use of farm tractors, which on average in a year worked at 35.87 cgh · $ha^{-1}$of cropland, whereas at 12.03 cgh · ha^{-1} in the West Pomerania Province. Undoubtedly, that was due to the fact that farms in the Małopolska Province had a significant percentage of laborious vegetable crops.

In conclusion we can say that according to the conducted research, the standard of equipment in the machinery park is a major problem in the field of agricultural engineering. It seems reasonable to make researches on these issues in different contexts. The results clearly indicate that the target of the efficiency of use of technical means in agriculture should be seen in the context of the growing area of agricultural land and also of the small farms increasing the production intensity.

Table 5. Gross replacement value of the machinery park

Specification		Farms							
		Małopolska Province				West Pomerania Province			
		including area [ha]:							
		Average	**0-5 ,0**	**5,1-15,0**	**15,1-30,0**	Average	**5,1-15,0**	**15,1-30,0**	**30,1- 50,0**
		[t PLN ·ha^{-1} of cropland]							
Total		22,97	27,86	28,42	14,37	5,46	15,36	12,92	2,70
in this:	vans	4,23	3,15	5,47	2,78	0,19	0,81	0,37	0,80
	tractors	7,72	10,71	9,28	4,82	1,44	4,14	3,36	0,76
	self-propelled	3,97	4,88	5,21	2,24	2,45	4,80	6,07	1,23
	other	7,05	9,13	8,47	4,52	1,38	5,61	3,11	0,63
		[t PLN·$farm^{-1}$]							
Total		261,74	107,14	304,55	341,42	281,12	230,45	285,24	322,24
in this:	vans	48,20	12,13	58,57	66,13	9,70	12,13	8,08	9,70
	tractors	87,94	41,16	99,46	114,55	74,39	62,14	74,26	90,79
	self-propelled	45,25	18,75	55,81	53,25	125,92	72,00	134,12	146,62
	other	80,36	35,10	90,71	107,50	71,11	84,18	68,79	75,13

[Source: own research]

REFERENCES:

1. **Auernhammer H. 2006.** Precision crop farming. Agricultural Engineering – Yearbook 2006, VDMA Landtechnik. VDI-MEG. KTBL. p. 35-42.
2. **Cupiał M. 2010.** Informacja a zarządzanie parkiem maszynowym w wybranych gospodarstwach Małopolski. Inżynieria Rolnicza. Nr 3 (121). p. 21-27.
3. **Durczak K. 2008.** Metoda wartościowania i oceny jakości maszyn rolniczych. Inżynieria Rolnicza. Nr 4 (102). p. 257-262.
4. **Hołownicki R. 2008.** Przed agroinżynierią stoją nowe zadania. Inżynieria Rolnicza. Nr 4 (102). p. 13-24.
5. **Kocira S. 2008.** Wpływ technicznego uzbrojenia procesu pracy na nadwyżkę bezpośrednią w gospodarstwach rodzinnych. Inżynieria Rolnicza. Nr 4 (102). p. 375.
6. **Kondo N. 2005.** Latest Agricultural Robots and Traceability Information Based on Robotic Agriculture. Resource. 9. p. 3-4.
7. **Kowalski J., Szeląg A. 2005.** Powierzchnia obszarowa gospodarstw, a wskaźniki eksploatacyjno-ekonomiczne parku maszynowego. Inżynieria Rolnicza. Nr 7 (67). p. 15-21.
8. **Kowalski J. i** inni. 2002. Postęp naukowo- techniczny, a racjonalna gospodarska energią w produkcji rolniczej. PTIR, Kraków. ISBN 83-905219-9-7.
9. **Kuboń M. 2007.** Miejsce i rola infrastruktury logistycznej w funkcjonowaniu przedsiębiorstw rolniczych. Inżynieria Rolnicza. Nr 9 (97). p. 87-93.
10. **Kuboń M. 2007a.** Wyposażenie i wykorzystanie środków transportowych w gospodarstwach o różnym typie produkcji rolniczej. Inżynieria Rolnicza 8(96). Kraków. p. 141-148.
11. **Marczuk A., Turski A. 2009.** Wpływ warunków gospodarstwa na dobór maszyn rolniczych do produkcji bydła. Inżynieria Rolnicza. Nr 6 (115). p. 191-197.
12. **Munack A. 2002.** Agriculture and the environment: New challenges for engineers". Paper presented at the Special Session on Agricultural Engineering and International Development in the Third Millennium. ASAE Annual International Meeting/CIGR World Congress, July 30, 2002, Chicago, IL. USA. Vol. IV. December, 2002.
13. **Muzalewski A. 2008.** Zasady doboru maszyn rolniczych. Kryteria oceny racjonalności doboru oraz wykorzystania wybranych maszyn i urządzeń rolniczych w ramach Programu Rozwoju Obszarów Wiejskich (PROW 2007-2013) pod katem działania „Modernizacja gospodarstw rolnych". IBMER, Warszawa, p. 7-8.
14. **Rybacki P., Rzeźnik Cz., Durczok K. 2010.** Wyniki badań dynamiki odnowy parku maszynowego w rolnictwie. Technika rolnicza - ogrodnicza - leśna 1/2011 PIMR Warszawa ISSN 1732-1719.
15. **Sikora J. 2009.** Analiza zmian potencjału technicznych środków produkcji gospodarstw rolnych w gminach Polski południowej. Infrastruktura i Ekologia Terenów Wiejskich. Nr 2009/ 09.
16. **Slaughter D.C., Giles D.K., Lamm R.D., Lee W.S. 2000.** Robotic weed control system for California row crops. Agricultural Engineering Conference, AgEng 2000-Warwick, Paper 00-PA-018.
17. **Szeląg-Sikora A. 2009.** Wykorzystanie funduszy unijnych w aspekcie zróżnicowania regionalnego. Problemy Inżynierii Rolniczej. Nr 2/2009. p. 39.
18. **Szeląg-Sikora A. 2008.** Zasoby użytków rolnych oraz wyposażenie w sprzęt rolniczy gospodarstw a poziom intensywności prowadzonej produkcji rolniczej. Inżynieria Rolnicza. Nr 9 (107). p. 283-290.
19. **Tabor S. 2006.** Postęp techniczny a efektywność substytucji pracy żywej pracą uprzedmiotowioną w rolnictwie. Inżynieria Rolnicza. Nr 10 (85).
20. **Waszkiewicz Cz., Krajewski M. 2011.** Zmiany w podaży narzędzi i maszyn rolniczych do uprawy gleby, siewu, sadzenia, nawożenia i ochrony roślin. Technika rolnicza - ogrodnicza - leśna 1/2011 PIMR Warszawa ISSN 1732-1719.
21. **Wójcicki Z. 2007.** Wpływ wyposażenia technicznego na efekty działalności gospodarstwa rodzinnego. Problemy Inżynierii Rolniczej nr 3/2007. IBEMR, Warszawa, p. 5-12.

REGIONALNE ZRÓŻNICOWANIE WYPOSAŻENIA PARKU MASZYNOWEGO W GOSPODARSTWACH ROLNYCH

Streszczenie. Celem pracy było dokonanie analizy poziomu wyposażenia parku maszynowego gospodarstw zróżnicowanych pod względem ich lokalizacji. W trakcie badań przeprowadzonych w formie wywiadu kierowanego, dobrano obiekty z woj. Małopolskiego i Zachodniopomorskiego. Uzyskane wyniki pozwalają wnioskować, iż w przypadku badanych gospodarstw istnieją różnice w poziomie wyposażenia parku maszynowego. Przykładem jest m.in. wartość mocy zainstalowanej w ciągnikach, gdzie w obiektach z woj. Małopolskiego jest to średnio 9,05 $kW \cdot ha^{-1}UR$, zaś w woj. Zachodniopomorskim tylko 1,99 $kW \cdot ha^{-1}UR$.

Słowa kluczowe: maszyny rolnicze, ciągniki, park maszynowy, gospodarstwo rolne.

TEKA. COMMISSION OF MOTORIZATION AND ENERGETICS IN AGRICULTURE – 2012, Vol. 12, No. 1, 289–292

Hardware configuration of the unitronics m90 controllers

Mariusz Szreder

Department of Mechanical Systems Engineering and Automatization; Institute of Mechanical Engineering
Faculty of Civil Engineering, Mechanics and Petrochemistry; Warsaw University of Technology
Address: ul. Jachowicza 2, 09 – 400 Płock, Polska; e-mail: szreder@pw.plock.pl

Summary. The paper presents selected issues related to designing of automation systems and hardware configuration of the Unitronics M90 controllers. The paper discusses several advantages of this series of controllers as devices of universal applications in non-complex control systems maintaining a simple configuration and programming tool.

Key words: PLC controller, automated control process, microchip system, programming.

INTRODUCTION

The Unitronics M90 controller is designed for automation of devices and processes in industry and home applications. The M90 controller is a useful tool in every location where a simple operator instrument panel is a basic requirement and the costs are limited. The controllers designed for industry applications are adapted for heavy-duty conditions [5, 7].

M90 is the smallest controller series by Unitronics fitted with extension ports. Thanks to such ports the controller can be extended by further inputs and outputs.

The most typical applications of this series of controllers are: control of assembly lines, packaging machinery, material conveyance systems, production machinery and building automatics.

Typical equipment of the M90 controllers [19, 21]:
– In/out: discrete (two-state), analog,
– Real time clock RTC,
– Fast counter up to 10 kHz,
– 15 programmable buttons,
– integrated operator instrument panel HMI,
– CANbus protocol support.

For the programming of the M90 controllers Unitronics developed a dedicated programming environment - U90 Ladder. This is complete software that enables hardware configuration of the controller, design of the control software in the ladder language, control of the operator instrument panel and communication with the controller [20].

DEVELOPING OF THE SYSTEM PROJECT

The description of the individual stages of the process of programming of the controller has been presented on the example of designing of an automated system of control of a package counter [1, 11].

In the presented example it was assumed that the machine counts the packages that are subsequently grouped in bulk packages. In the machine a photo-resistor is fitted that that sends a box sensing signal to the controller. The signal from the photo-resistor is also used to detect jamming of the conveyor or lack of packaging in the machine.

In order for the technician to operate the machine he has to log on to the system first. The technician can set the machine operating parameters through a keyboard:
– number of boxes in the bulk packaging,
– hours during which the machine will remain in standby.

During the operation of the machine on the display of the controller messages will appear regarding [6, 17, 21]:
– the number of counted boxes,
– completing of the bulk packaging,
– errors in machine operation.

Information related to the individual projects is saved in generated project files with the extension of **u90**. Hence, the project begins with the creation of a file through selecting the icon **New** or menu *Project*.

Fig. 1. Hardware configuration window of the M90 controller

During operation only one project can be open. Prior to opening of the project file a window will pop up in the system confirming the saved changes to the open project [8, 20].

When opening a new project file a controller configuration window will pop up– M90 Hardware Configuration (Fig. 1).

From the list of base models we choose the right model of the M90 controller. The mark of the model appears above the icon of the controller. Individual base models are different in terms of the number of available functions.

An example model M90-R2-CAN has 10 digital PNP inputs, 2 analogue 0÷10V inputs, 6 relay outputs and 1 input of the HSC fast impulse counter.

As we can see a low-cost controller has its limitations - the presented model supports only digital PNP inputs and analogue 0÷10V ones.

Let us assume that in our project we need to use the measurement sensors that require an NPN connection with a typical analogue 4÷20 mA input. We would have to replace the base model with a model that supports the required types of input signals i.e. M91 models (as long as the number of input/output signals is sufficient to service the project).

In the presented example we will continue with the base model M90 and will show the additional features resulting from the model being equipped with the extension ports. In the hardware configuration window of the controller we will extend the project by additional two mixed modules (digital and analogue): DI8-TO8/RO8 and IO-AI4-AO2 [3, 7, 10].

The digital module DI8-TO8/RO8 has 8 PNP/NPN inputs, 1 HSC counter and 8 PNP transistor outputs.

The analogue module IO-AI4-AO2 has 4 analogue inputs both voltage and current and 2 analogue outputs.

The system extended in such a way supports input and output signals in both positive and negative logic.

Below the screenshots of the selected configuration windows have been presented.

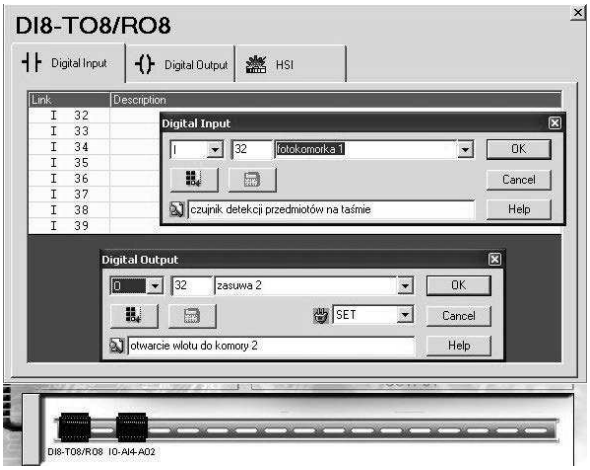

Fig. 2. DI8-TO8/RO8 module configuration window

As we can see in Fig. 2 the numbering of the IN/OUT signals for the first module of extensions starts from number 32 an for the subsequent modules 64 and so forth. Such a numbering system ensures clarity of the numbers in addressing of the IN/OUT signals.

Fig. 3. Defining of the output signal for the control of the valve

In the case of output signals there is a possibility of defining of the signal level after a possible system reset (in this case the flap is closed) [2, 12, 15].

In the example project the boxes need to be counted and subsequently sorted to appropriate collective chambers. For the counting of the boxes the function of additional module of the impulse counter was used that counts the impulses from the photo-resistor. The information on the number of counted boxes is saved in the MI2 record available under the variable name *Counter* (Fig. 4).

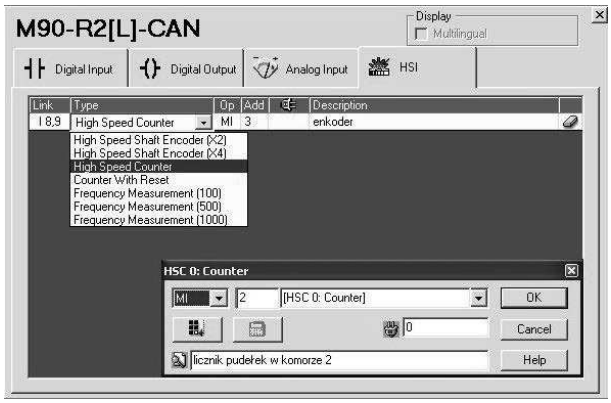

Fig. 4. HSC counter configuration

For the control of the speed of the conveyor a signal from the encoder is used from which the impulses are counted by the HSC counter available in the base model. The information on the number of counted impulses is saved in the MI3 record available under the variable name *encoder* [4, 16].

Regarding the analogue signals, also in the base model there is a limitation –only voltage signals are supported. Hence, to control the power of the heater the current output should be used, which is available in the additional module (Fig. 5).

Fig. 5. Configuration of the analogue signals

Some of the hardware devices need to be additionally software-initiated. The example could be the necessity of resetting of the counter.

Counter initiation [9, 18]

Before the counter starts operation, we need to set its initial value (assign it a zero value).

Fig. 6 shows a fragment of the software in a ladder language responsible for the initiation of the element counter:

– a connector sensing the growing slope associated with bit MB 5. Bit MB 5 assumes the value of 1 after confirming of the identification number of the operator.
– The variable recording function block (Store) that will enter "0" to the variable MI2.

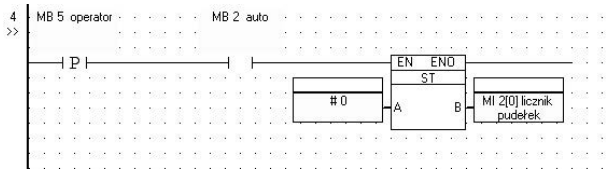

Fig. 6. Initiation of the box counter

- Configuration of the Modbus connection

In the discussed project of the control system, an additional possibility was assumed of the data transmission from the process to a master unit through a Modbus RTU protocol [13, 14].

To this end, in each controller participating in the combination, after a correct initiation of the communication port, the connection needs to be configured as Modbus Master and Slave.

Below a fragment of the software responsible for the configuration of the protocol as Modbus Master has been presented.

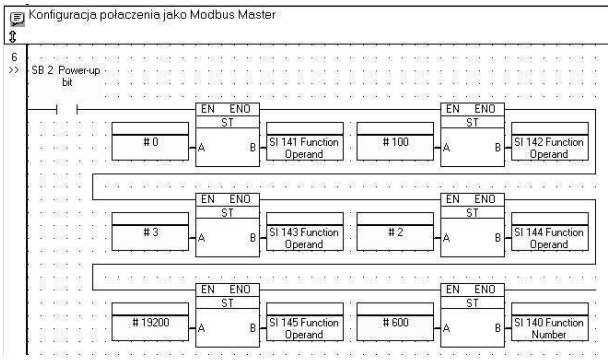

Fig. 7. Configuration of the Modbus RTU protocol as Master

CONCLUSIONS

In the paper the authors discussed selected fragments of the example system design with the M90 controller. The presented material shows some positive features of this series of controllers as universal devices for application in non-complex control systems maintaining a simple tool for configuration and programming.

REFERENCES

1. **Broel-Plater B. 2009:** Układy wykorzystujące sterowniki PLC. Wydawnictwo Naukowe PWN.
2. **Gutyrya S., Yaglinsky V. 2006:** System criteria analysis and function optimization of industrial robots. TEKA Kom. Mot. Energ. Roln. – OL PAN, 6A, p. 70-81.
3. ISO 11783: Tractors, Machinery for Agriculture and Forestry – Serial Control and Communication Network, p. 1-12.

4. **Jasiński B., Baryła M. 2004:** Engineering of microprocessor systems with CAN-bus. V International Scientific Conference on Microprocessor Systems in Agriculture. Płock, p. 42-49.
5. **Jasiński B., Krzywosiński S. 1999:** Zastosowanie sterowników PLC GE Fanuc w automatyzacji procesów w rolnictwie". PW, Płock, p. 46-52.
6. **Jasiński B., Szreder M. 2006:** Microprocessor systems PLC for agricultural machines investigation. X Międzynarodowe Sympozjum im. Prof. Cz. Kanafojskiego nt. „Problemy budowy oraz eksploatacji maszyn i urządzeń rolniczych". Płock, p. 75-76.
7. **Jasiński B., Szreder M. 2008:** Inżynieria mikroprocesorowych systemów monitorowania maszyn rolniczych. Wybrane zagadnienia mechaniki w budowie urządzeń technicznych. Płock, p. 153-194.
8. **Jasiński B., Szreder M. 1999:** Programowanie i testowanie rolniczych komputerów pokładowych. Zeszyty Naukowe „Mechanika". WPW, z. 176, p. 51-58.
9. **Kolesnikov A., Dyadichev V. 2010:** Industrial Enterprises Study of Automatic Control Systems. TEKA Kom. Mot. Energ. Roln. – OL PAN, 10A, p. 126-132.
10. **Kwaśniewski J. 2008:** Sterowniki PLC w praktyce inżynierskiej. Wydawnictwo BTC.
11. **Kwiatkowski W. 2010:** Wprowadzenie do automatyki. Wydawnictwo BEL Studio.
12. **Legierski T., i inni 2005:** Programowanie sterowników PLC. Wydawnictwa Pracowni Komputerowej J. Skamierskiego.
13. **Michalski R., Rychlik A. 2003:** Diagnozowanie maszyny roboczej z wykorzystaniem wnioskowania hybrydowego. Inżynieria Systemów Bioagrotechnicznych. Płock, p. 21-30.
14. **Sałat R., Korpysz K., Obstawski P. 2010:** Wstęp do programowania sterowników PLC. Wydawnictwo WKiŁ.
15. **Seta Z. 2002:** Wprowadzenie do zagadnień sterowania. Wydawnictwo Mikom.
16. **Szreder M., Krzywosiński S. 2004:** Implementation of PID controller in the GE FANUC PLC. V International Scientific Conference on „Microprocessor systems in agriculture". Płock, p. 201-205.
17. **Szreder M. 2006:** Mikroprocesorowy system nadzoru charakterystyk funkcjonowania kombajnu zbożowego. Wybrane Problemy Inżynierii Mechanicznej. Płock, p. 209-225.
18. **Szreder M. 2011:** Programowanie sterowników Unitronics. Inżynieria mechaniczna. WPW, Płock, p. 75-81.
19. Unitronics 2007: M90/M91 Podręcznik użytkownika. Warszawa.
20. Unitronics 2008: M90/M91 Instrukcja użytkownika (dane techniczne i montażowe). Warszawa.
21. **Wierzbicki S. 2006:** Diagnosing microprocessor-controlled systems. TEKA Kom. Mot. Energ. Roln. – OL PAN, 6, p. 182-188.

KONFIGURACJA SPRZĘTOWA STEROWNIKÓW UNITRONICS SERII M90

S t r e s z c z e n i e. W pracy zostały zaprezentowane wybrane zagadnienia dotyczące projektowania systemu automatyki i konfiguracji sprzętowej sterowników Unitronics z serii M90. W podanym materiale zaprezentowano atuty tej serii sterowników, jako urządzeń uniwersalnych do zastosowania w nierozbudowanych systemach sterowania, przy zachowaniu prostego w obsłudze narzędzia do konfiguracji i programowania systemu.

S ł o w a k l u c z o w e: sterownik PLC, proces automatycznej kontroli i sterowania, system mikroprocesorowy, programowanie.

TEKA. COMMISSION OF MOTORIZATION AND ENERGETICS IN AGRICULTURE – 2012, Vol. 12, No. 1, 293–300

Modeling of kinematics of movement on turn of a wheeled tractor with a hinge-operated drawbar on semitrailer

Georgij Tajanowskij, Wojciech Tanas**, Mariusz Szymanek***

* The Belarussian National Technical University,
** University of Life Sciences in Lublin, Poland

Summary. In the article the mathematical description and results of modeling of kinematics of turn of an agricultural tractor train with a hinge-operated drawbar on semitrailer is presented at various modes of turn. The developed technique allows for the solution of many practical research problems of shunting property of tractor trains with trailers of the new constructive scheme, for the purpose of a choice at a stage of working out of the trailer of the best parameters both of the trailer, of its connection with the tractor.

Key words: tractor train, semitrailer with hinge-operated drawbar, mathematical modeling of kinematics of unsteady turn.

INTRODUCTION

Development of tractor trains goes by the way of their specific increase, on units of constructive weight, load-carrying capacity, decrease in a body weight, increase of manoeuvrability and admissible speeds of movement with a tractor, and also indicators of other major properties [2, 5, 14, 17, 21]. In realization of the listed ways advantages of the semi-hook scheme of execution of a link of a tractor train bearing cargo before the scheme of the trailer with free hitch and the scheme of the semi-hinged trailer [3, 8, 10, 12, 16, 22] are accurately traced. Thus, the growth of load-carrying capacity of semitrailers is reached by an increase in the number of tandem-type wheel axes of the wheel cart, and increase of manoeuvrability of trailers with long-base ("breaking") operating hitch. However, many questions of dynamics of movement of such tractor trains demand further consideration [1, 5, 11, 18], for the purpose of the proved choice of rational design data of created new semitrailers, a control system of a forward rotary part drawbar and, if necessary, the turn of wheels or of the wheel cart as a whole with the semitrailer in the plane.

In the article methodical positions of modeling and an estimation of one of the major properties of tractor trains with a hinge-operated drawbar on semitrailer – the shunting property - are considered.

Growth of capacity and tonnage of agricultural tractor trains is accompanied by the increase of inertion and lengths. Thus they aim at an increase of speeds of movement at the expense of use of tractors with a gear change without rupture of a stream of capacity or transmissions with stepless change of the transfer relation, for example, the two-line. All it demands is the careful analysis of dynamics of movement of tractor trains with new constructive scheme and, in particular, their shunting property.

The purpose of the given article consists in working out of the mathematical description and reception of results of modeling of kinematics of turn of a tractor train with a hinge-operated drawbar on semitrailer at various modes of turn.

METHODICAL POSITIONS OF MODELING OF SHUNTING PROPERTY

At creation of the tractor transport technological unit on the basis of a wheel tractor obligatory section of design researches is the estimation of its shunting property. At such estimation for a case of movement of the machine tractor unit on a circular trajectory with the established speed radiuses of turn of characteristic points and corners of a relative positioning of links of the unit are defined. As the generalising estimated parametre of shunting property, the factor of manoeuvrability equal to the relation of dimensional width of the unit to dimensional width of its circular rotary strip is used, for example.

It is considered that the value of the factor of manoeuvrability is closer to unit, the best shunting properties the unit possesses. For an estimation of fitness of the tractor the unit to passage of turns of a surface of movement

the size of width of a dimensional lane is used at turn, and for an estimation of manoeuvrability of the unit at the maximum corners of turn of operated wheels of a tractor - the minimum dimensional radius of turn of the tractor unit [4, 6, 7, 9, 14, 19, 20].

To manoeuvrability estimations at static turn estimations of phases of trajectories of unsteady movement on turn are in case of need added: an input in turn and an exit from it, that is a phase which precedes the period of circular turn and which follows it [3, 8, 10].

Reception estimations of curvilinear movement of a tractor train is made on the basis of the general expressions for characteristics of curvilinear movement of wheel tractor units as a corner of turn of operated wheels at various values of regime parameter of turn which represent the system of the differential equations and allow to make a comparative estimation of units with one tractor and the same semitrailer, but with various laws of management of turn "breaking" on hinges operated trailer hitch the semitrailer [11, 13, 15, 20].

In the figures characteristic conditions of a relative positioning of links of the considered tractor unit are presented at circular turn.

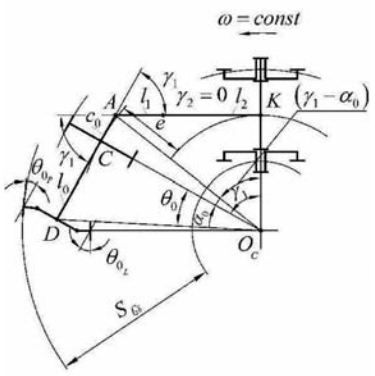

a)

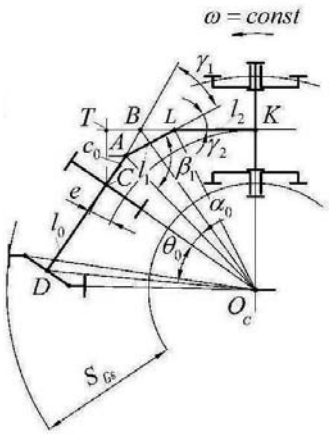

b)

Fig. 1. The scheme of the tractor unit on turn: a) corner $\gamma_2 = 0$; b) corner $\gamma_2 > 0$

Figure 1 presents the size *e* - displacement of trajectories of the middle of the back bridge of a tractor (point *C)* and the middle of the wheel dual cart of the semitrailer (point *K).* The corner size θ_o is equal to a half-sum of corresponding corners of turn of the right and left operated wheels of a tractor-tractor, other designations are clear from the figure.

At the analysis of the investigated tractor unit represents practical interest an estimation of influence on indicators of shunting property:

- base distance of the semitrailer;
- parities of base distances of a tractor and the semitrailer;
- relative length of a breaking-rotary part compound on hinges operated trailer hitch the semitrailer;
- a corner of turn of a rotary part compound on hinges operated trailer hitch the semitrailer;
- a start of a point of connection of links of the unit;
- a semitrailer track.

For definition of numerical values of indicators of manoeuvrability their analytical expressions have been received, lateral withdrawal of wheels was not considered. From geometrical parities on the basis of Figure 1a and Figure 1b, at introduction of a designation of radiuses of trajectories of characteristic *i*-th points of the settlement scheme of the tractor unit - R_i, it is received:

$$R_A = \overline{AO_c} = \sqrt{l_0^2 \cdot \operatorname{ctg}^2 \theta_0 + c_0^2}, \tag{1}$$

$$\angle\alpha_0 = \operatorname{arctg}\frac{c_0}{l_0 \cdot \operatorname{ctg}\theta_0}, \tag{2}$$

$$R_L = \sqrt{l_2^2 + R_K^2}, \tag{3}$$

$$R_K = l_0 \cdot \operatorname{ctg}\theta_0 \cdot \cos(\gamma_1 + \gamma_2) + c_0 \cdot \sin(\gamma_1 + \gamma_2) + l_1 \cdot \sin\gamma_2, \tag{4}$$

$$\overline{TK} = l_0 \cdot \operatorname{ctg}\theta_0 \cdot \sin(\gamma_1 + \gamma_2) = c_0 \cdot \cos(\gamma_1 + \gamma_2) + l_1 \cdot \cos\gamma_2 + l_2, \tag{5}$$

whence we will find the unknown corner γ_1.

It is known, that:

$$\sin(\gamma_1 + \gamma_2) = \sin\gamma_1 \cdot \cos\gamma_2 + \cos\gamma_1 \cdot \sin\gamma_2, \tag{6}$$

$$\cos(\gamma_1 + \gamma_2) = \cos\gamma_1 \cdot \cos\gamma_2 - \sin\gamma_1 \cdot \sin\gamma_2, \tag{7}$$

that we will transform last equality, having designated $l_0 \cdot \operatorname{ctg}\theta_0 = A_0$:

$$A_0 \cdot \sin\gamma_1 \cdot \cos\gamma_2 + A_0 \cdot \cos\gamma_1 \cdot \sin\gamma_2 = c_0 \cdot \cos\gamma_1 \cdot \cos\gamma_2 - c_0 \cdot \sin\gamma_1 \cdot \sin\gamma_2 + l_1 \cdot \cos\gamma_2 + l_2, \tag{8}$$

Let us group the similar:

$$\underbrace{\left(l_0 \cdot \operatorname{ctg}\theta_0 \cdot \cos\gamma_2 + c_0 \cdot \sin\gamma_2\right)}_{C_1} \cdot \sin\gamma_1 + \underbrace{\left(l_0 \cdot \operatorname{ctg}\theta_0 \cdot \sin\gamma_2 - c_0 \cdot \cos\gamma_2\right)}_{C_2} \cdot \cos\gamma_1 = \underbrace{l_1 \cdot \cos\gamma_2 + l_2}_{C_3}. \quad (9)$$

Taking into account the entered designations we will receive:

$$C_1 \cdot \sin\gamma_1 + C_2 \cdot \cos\gamma_1 = C_3. \quad (10)$$

Having solved last equation, we will receive size of a required corner γ_1.

The scheme a) (fig.1a):

$$\overline{O_c C} = R_C = l_0 \cdot \operatorname{ctg}\theta_0 \quad \overline{O_c A} = R_A = \sqrt{R_C^2 + c_0^2}, \quad (11)$$

$$\overline{O_c K} = R_K = \sqrt{R_A^2 + \left(l_1 + l_2\right)^2} = \sqrt{l_0^2 \cdot \operatorname{ctg}^2\theta_0 + c_0^2 + \left(l_1 + l_2\right)^2}, \quad (12)$$

$$\angle\alpha_0 = \operatorname{arctg}\frac{c_0}{l_0 \cdot \operatorname{ctg}\theta_0}, \quad (13)$$

$$\angle\left(\gamma_1 - \alpha_0\right) = \operatorname{arctg}\frac{l_1 + l_2}{\sqrt{l_0^2 \cdot \operatorname{ctg}^2\theta_0 + c_0^2 + \left(l_1 + l_2\right)^2}}, \quad (14)$$

$$\angle\gamma_1 = \operatorname{arctg}\frac{c_0}{l_0 \cdot \operatorname{ctg}\theta_0} + \operatorname{arctg}\frac{l_1 + l_2}{\sqrt{l_0^2 \cdot \operatorname{ctg}^2\theta_0 + c_0^2 + \left(l_1 + l_2\right)^2}}, \quad (15)$$

$$e = R_C - R_K = l_0 \cdot \operatorname{ctg}\theta_0 - \sqrt{l_0^2 \cdot \operatorname{ctg}^2\theta_0 + c_0^2 + \left(l_1 + l_2\right)^2}. \quad (16)$$

The scheme b) (fig. 1b):

$$\left.\begin{aligned} R_C &= l_0 \cdot \operatorname{ctg}\theta_0, \\ R_A &= \sqrt{R_C^2 + c_0^2} = \sqrt{l_0^2 \cdot \operatorname{ctg}^2\theta_0 + c_0^2} \\ \angle CAO_c &= \operatorname{arctg}\frac{R_C}{c_0} = \frac{l_0 \cdot \operatorname{ctg}\theta_0}{c_0}, \\ \angle\beta_1 &= 180^\circ - \gamma_1 - \angle CAO_c \\ \angle\alpha_0 &= \operatorname{arctg}\frac{c_0}{l_0 \cdot \operatorname{ctg}\theta_0}. \end{aligned}\right\} \quad (17)$$

The resulted expressions of the established turn allow for the investigation of influence on indicators of manoeuvrability of design data of a tractor and the semitrailer with a rotary part compound on hinge-operated trailer hitch. For studying of phases of unsteady turn of the tractor unit (Fig. 2) the differential equation concerning unknown size – a corner of folding γ_1 is received at change of a corner of turn of operated wheels θo with constant speed for cases of a constant corner of installation γ_2 rotary parts compound on hinges operated trailer hitch and its operated change by means of the crosswise communications shown in figure 2. The equation conclusion is not resulted because of bulkiness.

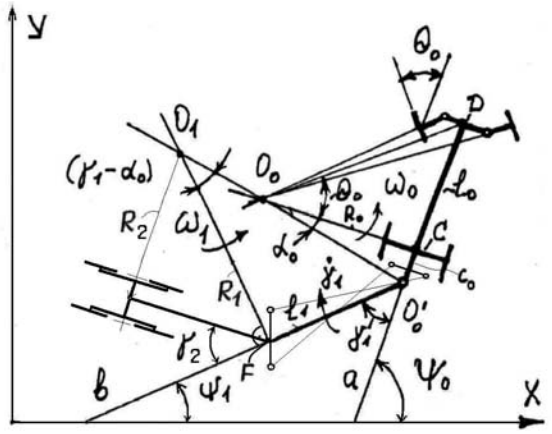

Fig. 2. Scheme of unsteady turn of a tractor with the semitrailer

Qualitative character of change estimations of shunting property at an input in turn and an exit from turn depending on a corner of turn of operated wheels of a tractor is shown in Figure 3.

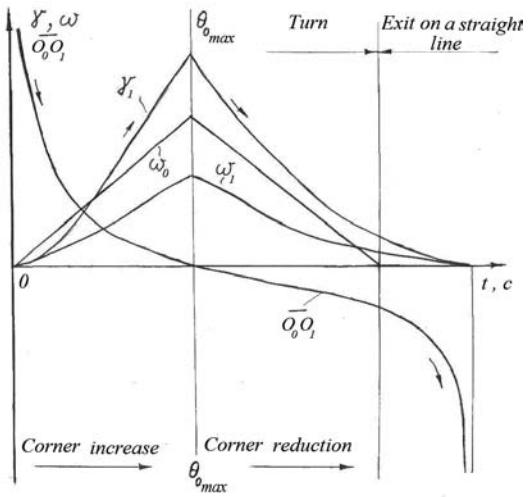

Fig. 3. Character of change of sizes of corners and angular speeds at turn of a tractor with the semitrailer

So, for example, the mentioned differential equation $\gamma_2 = 0$ looks like:

$$\left(\gamma_1\right)'_{\theta_o} = \frac{d\gamma_1}{d\theta_0} = \frac{1}{k_P \cdot R_o(\theta_o)} \cdot \left[1 - \frac{C_o}{\ell_1} \cdot \frac{\sin\left[\ \gamma_1 - \alpha_o(\theta_o)\ \right]}{\sin\left[\ \alpha_o(\theta_o)\ \right]}\right], \quad (18)$$

which allows for the choice of one of the known methods, for example, Euler's method to receive communication of corners θ_o and γ_1 during curvilinear movement of tractor units of the considered schemes. In equation $k_P = \frac{\dot{\theta}_o}{\upsilon_o}$ - regime parameter of turn,

where: υ_o - forward speed of the centre of a back axis of the tractor. For tractor units at small radiuses of turn in constrained conditions k_P lays in a range 0,05 … 0,15 it is rad·m^{-1}.

Initial values

$$\frac{d\gamma_1}{dt} = \frac{d\gamma_1}{d\theta_o} = 0; \quad \theta_o(t=0) = 0. \tag{19}$$

$\theta_{i(the\_final)}$ - its function from the accepted regime parameter and for range k_P, characteristic for universal wheeled tractors, it is possible to accept:

$\theta_{i(the\_final)} \le 0{,}58$ it is radian,

as limiting values of corners of turn of operated wheels or folding corners. As a rule, they do not exceed this value [3]. The step of integration of last equation can be accepted as equal to:

$\Delta\theta_o \approx 0{,}02$ *radian* or $\Delta\theta_o = 1$ degree.

As at turn of a tractor train, for example, on 90° the driver turns in the beginning wheels to some corner $\theta_{i\,max}$, and then turns them to zero in the opposite direction it is necessary for considering at integration of the differential equation.

The resulted expressions for a case of unsteady turn allow to receive a picture of change of characteristics of the maneuver made by the unit:

$\dot{\gamma}_1, \omega_o, \omega_1, \overline{O_oO_1}, \alpha_o, R_o, R_C, R_D, \overline{O_o'O_1}, R_F, \theta_o$

as time from the beginning of its fulfilment which have the following appearance (see fig. 3).

RESULTS OF MODELLING OF MANOEUVRABILITY OF THE UNIT

The analysis of the spent variants of calculations shows, that changes of the sizes characterising phases of unsteady turn, it is possible to present, as is shown in figure 3. On settlement data for the considered unit with the set sizes (l_0 = 2,75 m; l_1 = 1,2 m; l_2 = 2,5) the schedules resulted in figures 4, 5 are constructed. From schedules follows, that to a corner of turn of operated wheels of a tractor in 11 degrees growth of a corner of folding of the semitrailer concerning a tractor lags behind, and then advances corner growth θ_o, reaching value in 71,5 degrees at maximum on a technical characteristics of a tractor-tractor coal θ_o =37 degrees. And after return of operated wheels to a starting position the corner γ_1 is yet equal to zero and the exit on rectilinear movement occurs later in time, which confirms the generalized picture of process of turn of a tractor with the semitrailer (Fig. 3). However, at the maximum corners γ_1 and γ_2=0 the metal design of the semitrailer can adjoin to a tractor.

With increase in the corner γ_2, at installation of a rotary part under a corner to a longitudinal-vertical plane, possibility of not operational contact of metal designs of links of the unit will exist at smaller corners of turn of operated wheels θ_o.

In Figure 5 and 6 results of an estimation of influence of parameters of the unit on indicators of its manoeuvrability are resulted at circular turn. From the schedule in Figure 5 the corner of folding of the semitrailer concerning the tractor it follows that to values of a corner of turn of operated wheels of a tractor θo = 26 hailstones, at γ_2=0 changes practically linearly, and then there is its progressive growth, in comparison with the corner θ_o.

The resulted results of calculations on the received expressions have allowed for an establishment of the

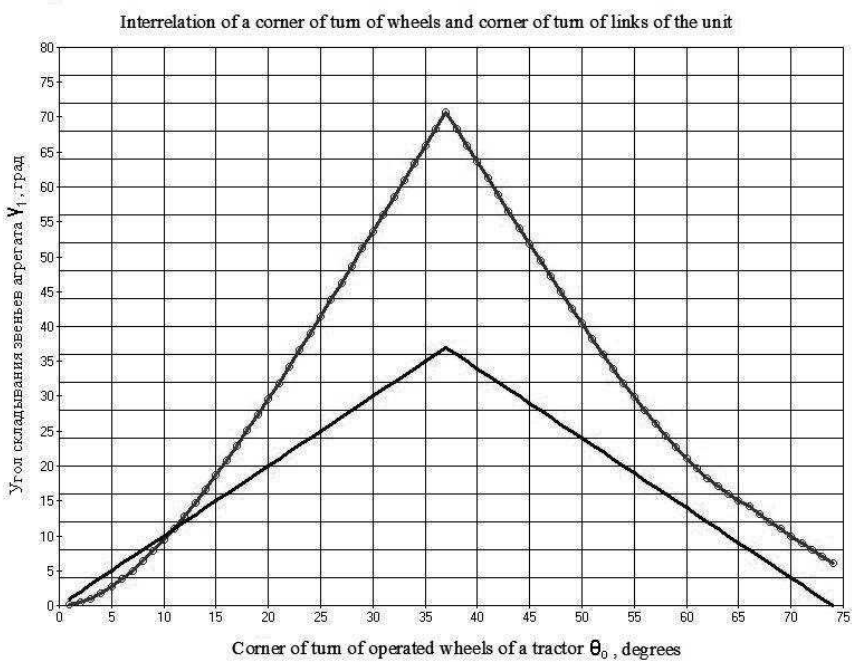

Fig. 4. Interrelation of the corner of turn of operated wheeled tractor and the corner of folding of the semitrailer

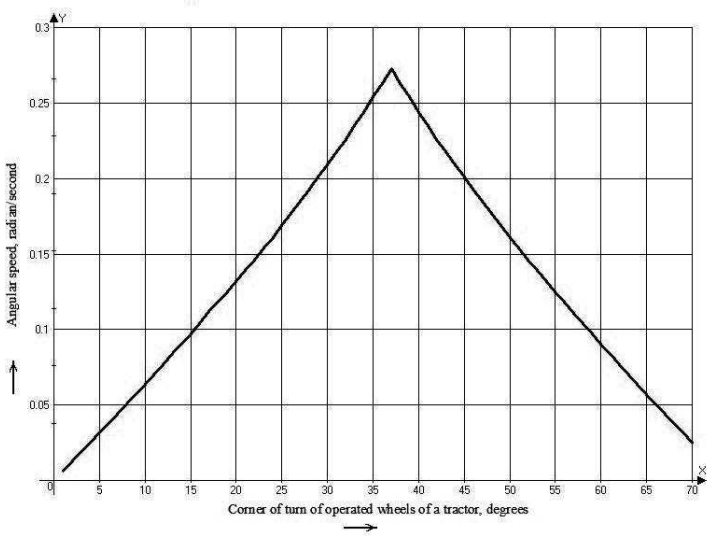

Fig. 5. Dependence of angular speed of turn of a tractor on the corner of turn of operated wheels

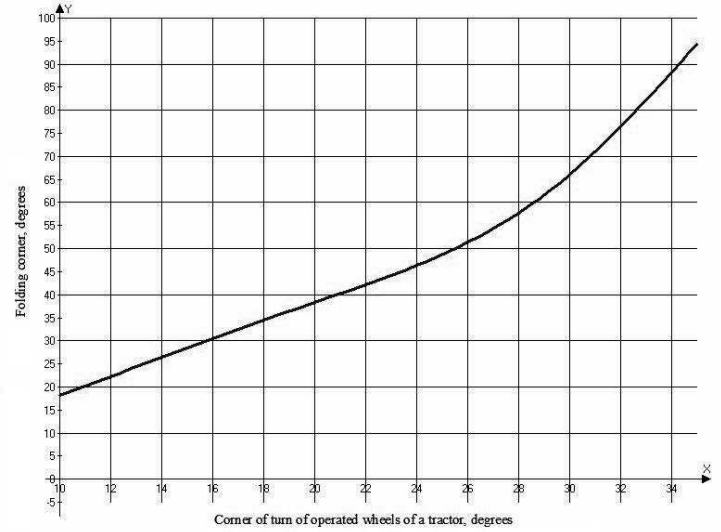

Fig. 6. Dependence $\gamma_1=f(\theta_o)$, at $\gamma_2=0$

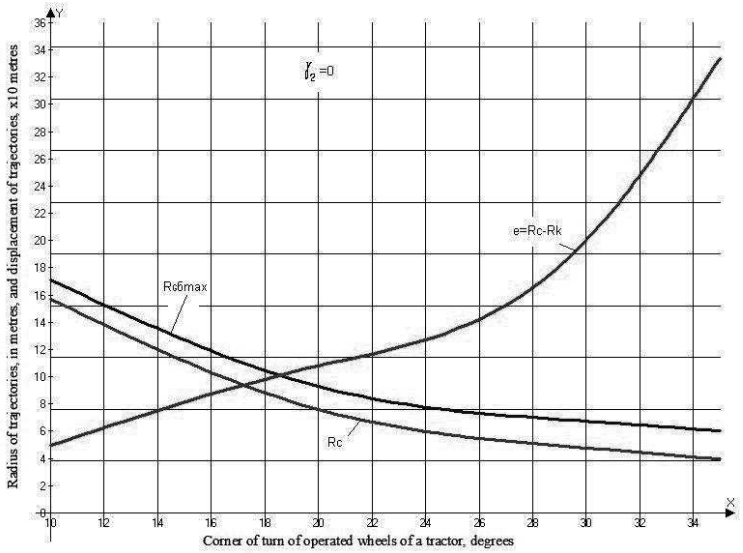

Fig. 7. Parameters of circular turn

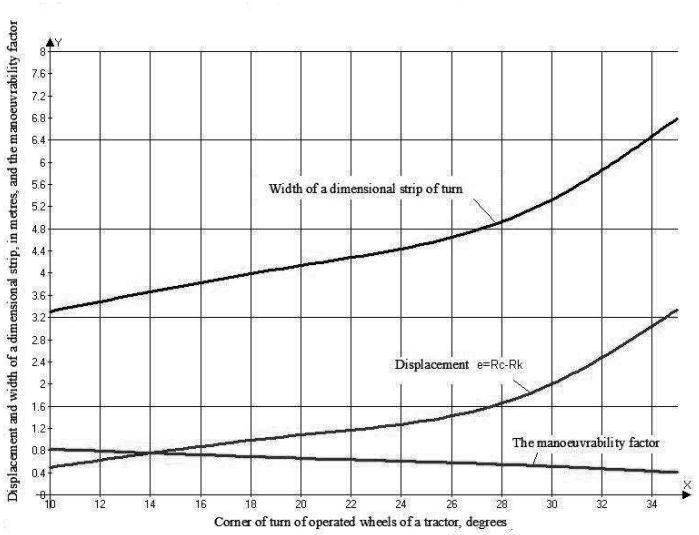

Fig. 8. Characteristics of turn of the tractor unit

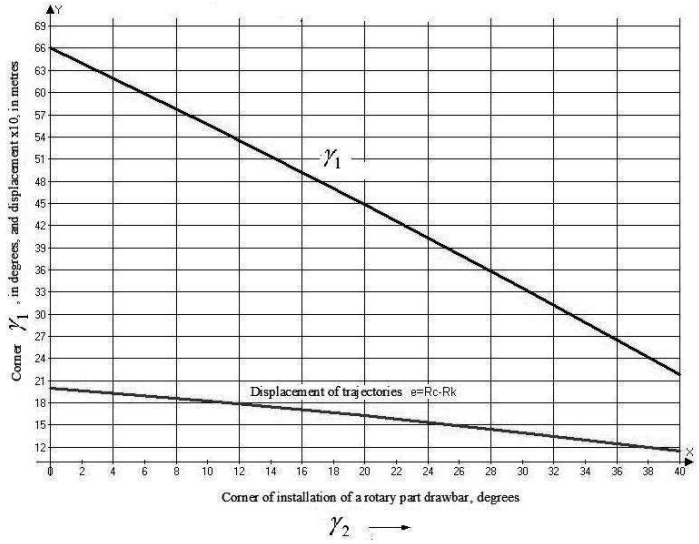

Fig. 9. Influence of the corner of installation of the rotary part of hinge-operated trailer hitch on manoeuvrability indicators

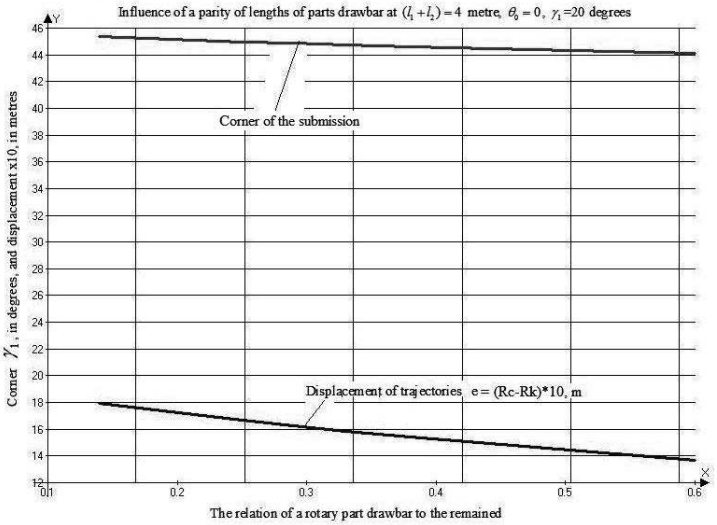

Fig. 10. Characteristics of manoeuvrability MTA at change of parities of lengths of rotary and non-rotary parts of a hitch on hinge -operated drawbar of semitrailer

character of influence of various installations and parameters on hinge-operated trailer hitch of the semitrailer, on shunting properties of a tractor train of the nonconventional construction scheme (Fig. 7, 8, 9, 10).

CONCLUSIONS

Thus, the technique of modeling and definition of indicators of shunting property of an agricultural tractor train with the hinge-operated trailer hitch is developed at various modes of turn.

The developed technique allows for the solution of many practical research problems of shunting property of tractor trains with trailers of the new constructive scheme, for the purpose of the choice at a stage of working-out of the trailer design of the best parameters both of the trailer and of its connection with the tractor. The stated method is applicable also at the decision of the return problem of kinematics of unsteady turn of returning automobile trains of big length, concerning development of operation drawbars for wheeled carts for maintenance of the set dimensional lane. The further development of the stated mathematical model consists in the establishment, at necessity, of corners of withdrawal of wheels and transition from purely kinematic model to dynamic model of the investigated unit.

REFERENCES

1. **Butenin N. V., Lunts Ya.L, Merkin D. R. 1985:** Course of Theoretical Mechanics, Vol.2 Dynamics, Nauka Moscow.
2. **Cieślikowski B. 2009:** Modelling of the vibration damping in an operator's seat system. // Teka commission of motorization and power industry in agriculture./Polish Academy of sciences branch in Lublin/ Volume IX, Lublin, p. 24-31.
3. **Dreszer K. A. and others 2005:** Napędy hydrostatyczne w maszynach rolniczych. PIMR Poznań.
4. **Guskov V. V., N. N. Velev, J. E. 1988:** Atamanov and other. Tractors: theory/ - M.: Engineering – p. 376.
5. Kinematyka i dynamika agregatow maszynowych. 2005: Dzialy wybrane. //Praca zbiorowa pod redakcja Eugeniusza Krasowskiego. Ropczyce – p. 127.
6. **Kuzmitski A. V., Tanas W. 2008:** Ground stress modeling. TEKA Komisji Motoryzacji i Energetyki Rolnictwo PAN, Lublin/ T. VIII, p. 135-140.
7. **Mielnikow S. W. 1980:** Experiment planning in research on process in agriculture (in Russian). Leningrad, Kolos.
8. **Nosko P., Vladimir B., Fihl P. 2009:** Multiparameter synthesis of non-contact machine drive. // Teka commission of motorization and power industry in agriculture./ Polish Academy of sciences branch in Lublin/ Volume IX, Lublin, p. 172-180.
9. **Osiecki A. 2004:** Hydrostatyczny napęd maszyn. WNT, Warszawa.
10. **Petrov V. A. 1988:** Hydrovolume transmissions of self-propelled machines. - M: Mechanical engineering – p. 248.
11. **Petrov L., Yakovenko A., Orobey V. 2008:** Theory of support application for higher gravitational quality indicators in wheel tractors. // Teka commission of motorization and power industry in agriculture./Polish Academy of sciences branch in Lublin/ Volume VIII, Lublin, p. 177-183.
12. **Sukach M.,Lisak S., Sosnowski S. 2010:** Kinematic analysis of the working process of trencher. // Teka commission of motorization and power industry in agriculture./Polish Academy of sciences branch in Lublin/ Volume X, Lublin, p. 425-431.
13. **Szydelski Z. 1993:** Napęd i sterowanie hydrauliczne w pojazdach i samojezdnych maszynach roboczych. WNT, Warszawa.
14. **Tajanowskij G.A. 2001:** The conception and tasks structure system of the analysis and approval of tractors transport units. News of Mogilev State Technical University, No. 1 – 198 p., p. 173-178.
15. **Tajanowskij G., Kalina A., Tanas W. 2008:** Mathematical model of harvest combine for Deception fuel chips from fast-growing plants// Teka commission of motorization and power industry in agriculture./ Polish Academy of sciences branch in Lublin/ Volume VIII, Lublin, p. 267-276.
16. **Tajanowskij G., Tanas W. 2010:** The analysis of regular wheel loadings distribution at a statically unstable running system of an agricultural machine on a rough surface. // Teka commission of motorization and power industry in agriculture./Polish Academy of sciences branch in Lublin/ Volume X, Lublin, p. 464-474.
17. **Tajanowskij G., Tanas W. 2007:** Distribution of loadings in transmission traction power means with all driving wheels and with system of pumping of trunks at work with hinged instruments // Teka commission of motorization and power industry in agriculture./ Polish Academy of sciences branch in Lublin/ Volume VII, Lublin, p. 217-224.
18. **Tajanowskij Georgij, Tanas Wojciech. 2006:** Stability of supersize tractor semi-trailers at uniloading. MOTROL-2006. Motoryzacja i energetyka rolnictwa. V. 8, Lublin, p. 220-229.
19. **Tajanowskij G. A., Tanas W., Romashko J. 2009:** Traction dynamics of the all-wheel drive machine tractor unit with hinged soil processing equipment. // Teka commission of motorization and power industry in agriculture./ Polish Academy of sciences branch in Lublin/ Volume IX, Lublin, p. 335-341.
20. **Tajanowskij G. A., Tanas W., Tajanowskij A. 2008:** Operating conditions of wheel drivers of active semi-trailers. // Teka commission of motorization and power industry in agriculture./Polish Academy of sciences branch in Lublin/ Volume VIII, Lublin, p. 257-265.
21. Tractors: theory/ V.V.Guskov , N.N. Velev, J.E. Atamanov and other.- M.: Engineering, 1988. – p. 376.
22. Under the editorship of Guskov V. V., 1987.: Hydropneumo automatic device and a hydrodrive of mobile cars. Minsk.: Higher School. – p. 310.

MODELOWANIE KINEMATYKI RUCHU CIĄGNIKA KOŁOWEGO Z NACZEPĄ ZE STEROWANIEM ZACZEPEM ZAWIASOWYM PODCZAS SKRĘCANIA

S t r e s z c z e n i e . W artykule przedstawiono matematyczny opis i wyniki modelowania skrętu ciągnikowego agregatu

z naczepą ze sterowanym zawiasowym zaczepem. Przedstawiono metodykę badań i określono wskaźniki manewrowości agregatu ciągnikowego. Opracowana metodyka pozwala rozwiązywać zadania badawcze w stadium opracowywania parametrów naczepy i agregatowania z wybranym ciągnikiem. Wykorzystanie wyników analizy pozwoli na przejście od modelu kinematycznego na dynamiczny model badanego agregatu.

S ł o w a k l u c z o w e: agregat ciągnikowy, naczepa, zawiasowy zaczep, sterowanie zaczepem, matematyczne modelowanie, kinematyka przy skręcaniu agregatu.

TEKA. COMMISSION OF MOTORIZATION AND ENERGETICS IN AGRICULTURE – 2012, Vol. 12, No. 1, 301–306

Quantitative time management methods in project management

Renata Walczak

Warsaw University of Technology, Faculty of Civil Engineering, Mechanics and Petrochemistry
Department of Mechanical Systems Engineering and Automation
Address: Al. Jachowicza 2/4, 09–402 Płock, Polska, e-mail: rpwalcza@pw.plock.pl

Summary. The paper presents an algorithm for the calculations of a network of relationships using the critical path method, the correlations for the total, free, conditional and independent slack time, the correlations for all kinds of relationships between the tasks: FS, SS, FF, SF. An example of a network with modifications has been presented.

Key words: project management, quantitative methods, critical path method.

INTRODUCTION

Quantitative methods of project management date back to the beginning of the XX century. Already before WWII a Pole, Karol Adamiecki, created the foundations of the quantitative time management in projects and rhythmical production [4, 8, 13, 16]. H. Gantt, F. Taylor, Ch. Babbage, the team of the professor P. Blacket, also contributed to the development of the quantitative method. Another step was the creation of the critical path method by Du Pont engineers and the simultaneous production of the Polaris ballistic missile along with the development of the PERT method [15, 18]. These methods could not advance due to a lack of calculation tools. Ever since personal computers advanced sufficiently the quantitative methods should have been sidetracked, yet this is not the case. Despite availability of sophisticated software for project management the software is not properly used. There is no knowledge on the mathematical quantitative methods used in the software [20]. On many occasions huge projects involving over 10 thousand tasks are planned manually and the project management software is merely there for printing purposes. The plans are prepared due to the requirements of public procurement or insurance companies but later they are sent directly to the archives and the project is managed by intuition. The aim of this paper is to acquaint the reader with the basics needed to employ the quantitative methods of managing time in project management and prepare the reader to use the software based on these methods.

WORK BREAKDOWN STRUCTURE

When organizing projects it is necessary to determine the aim of the task, the basic project checkpoints (milestones), the tasks that will be realized, duration of these tasks, used resources, expenses etc. After determining of the project aim a multilevel work breakdown structure is created (WBS) formed through a decomposition of the subsequent elements aiming at putting all the tasks together that will be realized during the project. In order o identify the individual tasks the structure is encoded [1, 2, 3, 5, 6, 7].

The work breakdown structure constitutes the basis for work planning, estimation of resources and expenses, determination of the scope of works, determination of the development path and the inspections, assignment of responsibility, risk identification and introduction of changes. The benefit resulting from the application of WBS is easy retrieval of information from previous projects with similar tasks, processes, assembly and components, the possibility of determining of the purchasing needs and specifications, the possibility of using joint integrated management system - joint databases, documentation, quotations, budgets, technical drawings, financial accounting systems as well as the possibility of performing of the cost analysis and other data.

The work breakdown structure is used on many managerial levels. Depending on the needs of the recipient it is possible to analyze information on different levels of the structure taking into account their different detail level. The highest level managers need consolidated information available at higher WBS levels while the lower level employees are interested in details characteristic of the lower levels.

The responsibility for the preparation of the work breakdown structure is on the side of the project manager. The WBS may be created through a top-down method (method dictated by the higher levels of authority), when the main scaffolding of the structure is created by the project manager and higher level managers and the detailed work is defined by the line managers. The bottom-up method consists in preparing of the structure from detail to general. This method is usually applied when the structure is created based on the already existing projects, the results to be achieved are known and the structure is composed of known elements. The structure is developed by employees of lower level and people responsible for the work realization and the adjustments and acceptance is done by the project manager. It is worth involving important interested parties such as clients in the WBS creation [17, 19].

An example of work breakdown structure has been presented below.

Level 1 Level 2 Level 3 Level 4

0. *Building a house*
- *0.**1.** Foundation*
  - *0.**1.1.** Digging the foundation*
  - *0.**1.2.** Shuttering*
  - *0.**1.3.** Pouring concrete*
- *0.**2.** Construction of a building*
  - *0.**2.1.** Construction of a basement ceiling*
  - *0.**2.2.** Building walls*
    - *0.**2.2.1.** Building partition walls*
    - *0.**2.2.2.** Building load bearing walls*
  - *0.**2.3.** Construction of a tie beam*
- *0.**3.** Construction of a roof*
  - *0.**3.1.** Fixing the ceiling*
  - *0.**3.2.** Construction of the roof elements*
  - *0.**3.3.** Roofing*
- *0.**4.** Installations*
  - *0.**4.1.** Water and sewage*
  - *0.**4.2.** Central heating*
- *0.**5.** Project management*
  - *0.**5.1.** Project organization*
  - *0.**5.2.** Planning*
  - *0.**5.3.** Project supervision*
  - *0.**5.4.** Documentation*

NETWORK METHODS OF PROJECT MODELLING

After the task has been identified a network model of a project is created. The tasks are set one after another in a technological order of performance. The basis of the network is digraphs i.e. ordered sets of vertices (nodes) and arches (edges) with one source and one exit:

$$G=\{\langle W(G),L(G)\rangle\} \tag{1}$$

The network is identified as a set of ordered threes:

$$S = [W, L, \varphi] \tag{2}$$

$$\varphi: W\times W \rightarrow L \tag{3}$$

where:
G digraph,
W set of graph vertices,
L set of graph branches,
S network,
φ relation.

In networks the arches are assigned weights. An ordered pair on the graph is presented with arrows connecting individual nodes oriented from the beginning of the arch to its end. The length of the graph arches does not represent the actual lengths between the edges but only represents the order of their occurrence. In the graphs showing the realization of the projects paths are determined i.e. such sets of vertices in which they occur only once and in which the arches are different. The longest path in the network is referred to as sensitive path, critical path or decisive sequence of tasks. The projects can be presented in the form of graphs where the vertices are assigned events and the arches are assigned tasks (tasks at the edges of the graph) or where the vertices of the graph are assigned tasks and the edges represent their technological order of performance (tasks in the graph nodes). The arches in these graphs are assigned weights denoting, for example, the duration of the task. The events (tasks) are assigned a date. In order to unequivocally determine the graph we only need to enter the set of ordered pairs and the values of the nodes or arches. The neighborhood matrices are determined too (for the edges or the vertices) or the incidence matrices (of the neighborhood of edges and arches). Additionally for identification of the network the weight matrix has to be specified. In this paper only simple network without multiple edges will be considered. One pair of nodes will always be assigned an arch. Cyclic networks (with loops) i.e. edges connecting the same vertices will not be considered [11, 12].

CRITICAL PATH METHOD

Critical Path Method (CPM) has been discussed in many publications, yet these publications present only the simplified form of calculation. Calculation methods are not presented for other relations than the finish of the predecessor task-beginning of the successor task. Not all the types of slack times (only total and free) are discussed. The principles of Project modeling through the Critical Path Method are thus worth revisiting.

The Critical Path Method is a fully deterministic method. It assumes both the deterministic value of duration of individual tasks and the deterministic construction of the network of relations.

The CPM was developed going on the assumption that there are no limited resources. Such networks can

obviously undergo optimizations in terms of resources availability upon construction of the network taking into account the logical sequence of tasks only.

The network calculations are performed in two stages. In the first stage (forward calculations) the earliest dates of the occurrence of all the events are set. In the second stage the latest dates of the occurrence are set [2, 5, 9, 10, 19]. Below the algorithm of the network calculation has been presented.

Network calculation algorithm

Stage I

1. Setting the start date of the project
2. Setting the earliest start dates of all tasks
3. Setting the earliest finish dates of all tasks
4. Setting the finish date of the project

Stage II

1. Setting the latest finish date of the project (most frequently this date is set as equal to the earliest finish date of the project)
2. Setting the latest finish dates of all tasks
3. Setting the latest start dates of all tasks
4. Setting the slack time
5. Setting the critical path

In the calculations the following symbols have been used:

WS	early start,
WK	early finish,
PS	late start,
PK	late finish,
ZC	total slack,
ZS	free slack
ZW	conditional slack,
ZN	independent slack,
t	duration of task,
p, poprz	predecessor task
n, nast.	successor task

Upon performing of the calculations for the assumed durations the optimization of the network is carried out taking into account the availability of resources and other adopted criteria.

In the first stage the start date of the project is set. In non-computer calculations the start date of the project is zero. Computer software assumes the start date of the project as a date given by the operator [2, 5, 9, 10, 19].

Another step in the calculation of the first stage is setting the earliest dates of all events. For each task the earliest start date needs to be set. Then the earliest finish date *WK* of this task is set, which is equal to the sum of the earliest start date *WS* and the duration of the task *t*. If, in the analyzed event, several tasks are finished we need to calculate the finish date of each of them and as the date of occurrence of the event we need to assume the greatest number because the successor task may start when the longest of the predecessor task is finished:

$$WK = max\ (WS + t). \tag{4}$$

Upon the completion of the calculations for all the tasks we obtain information on the earliest finish date of the project.

The second stage of the calculations begins with setting the latest admissible finish date of the project [2, 5, 9, 10, 19]. Most frequently, the earliest finish date of the project is assumed (the same as in the first stage of the calculations). This could also be a different date – a date set by a directive. The next step is setting the latest dates for the occurrence of all events. For each task first we need to set its latest finish date *PK*. Then the latest start dates *PS* of the tasks are set. The latest start date of a task *PS* equals the difference between the latest finish date of the task and the duration of the task *t.* If in an event several tasks are started we calculate the latest start dates of these tasks and as the latest date of the event occurrence we assume the least number. This ensures completion of the project in the assumed time:

$$PS = min\ (PK - t). \tag{5}$$

Upon completing the calculations for the tasks we can determine different types of slack times. The total slack time ZC is a minimum determined based on the calculations for the start and finish dates of the tasks. The total slack time can be determined as a difference between the latest finish date of a task and the earliest finish date of the same task. The total slack time can also be determined as a difference between the latest start date of a task and the earliest start date of the same task. The total slack time value is assumed as the least value of the two calculations:

$$ZC = min\ \{(PK - WK), (PS - PS)\}. \tag{6}$$

The total slack time is common for all tasks in one sequence. If it is used by the earlier tasks the later tasks will lose this slack time. It comprises all other slack times. If it is zero then the other slack times are also zero. The task under analysis is performed as early as possible. The subsequent task is performed as late as possible. The total slack time is also a difference between the latest start of the successor task (if there are several successor tasks we should choose the least value) and the earliest finish of the actual task.

Free slack time ZS is a difference between the earliest start date of the successor task (if subsequently there are several successor tasks we should choose the least value) and the earliest finish date of the actual task. The predecessor task is performed as early as possible. The actual task is performed as early as possible. The successor task is performed as early as possible:

$$ZS = min\ (WS_{nast}) - WK. \tag{7}$$

This slack time can be used and the successor tasks will not lose their slack time, yet the predecessor task must be performed in the earliest possible time.

Conditional slack time ZW is a difference between the minimum value of the latest start dates of the successor tasks and the sum of the maximum value of the latest finish dates of all predecessor tasks and the duration of the task for which the conditional slack time is calculated. The predecessor task is performed as late as possible. The actual task is performed right after the predecessor. The successor task is performed as late as possible:

$$ZW = min\ (PS_{nast}) - \{max\ (PK_{poprz}) + t\}. \quad (8)$$

The slack time allows performing the predecessor tasks at any time. The use of this slack time forces the performance of the successor task at the latest time i.e. all slack times of the successor tasks in this sequence will be used. The conditional slack time comprises independent slack time.

Independent slack ZN is a difference between the minimum value of the earliest start dates of all successor tasks and the sum of the maximum value of the latest finish dates of all predecessor tasks and the duration of the task for which the conditional slack time is calculated. The predecessor task is performed as late as possible. The actual task is performed right after the predecessor. The successor task is performed as early as possible:

$$ZN = min\ (WS_{nast}) - \{max\ (PK_{poprz}) + t\}.$$

This slack time provides information in what time the task can be performed without influencing the performance of the successor and predecessor tasks. They can be performed in times determined in the calculations and the independent slack time will remain intact. This slack time can assume negative values, which means that it is impossible to perform the actual task as late as possible and the successor task as early as possible. The negative value indicates how many units of time the successor task needs to shift to be after the actual task.

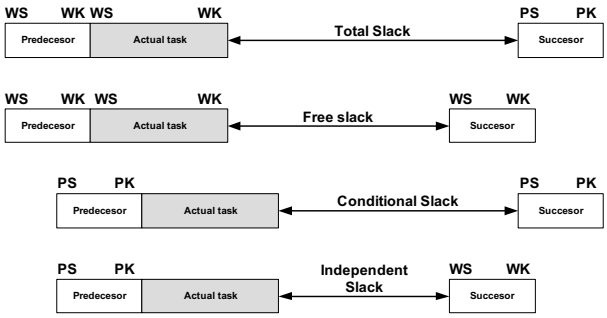

Fig. 2. Types of slacks for the same task presented in the time scale

The longest sequence of tasks in duration in the whole project is the critical path. This is at the same time a sequence that does not have slack times or has the least slack times of all sequences of tasks. The tasks on the critical path are subject to particular supervision on the side of the project manager. If any of the tasks on this path extends in time then the whole project will extend in time by the same amount of time. If the tasks on this path are shrunk in time the whole project may be finished earlier (but not always) by the time the critical path was shrunk. Upon shrinking of the critical path other paths may appear that may be longer than that being shrunk. In such a case the critical path becomes the longest path in the whole project. In a project there may be several critical paths. Then, completion of a project is dependent on the tasks on each of these paths.

In a project the tasks can be correlated in different ways. The basic and default relationship is the finish-start (FS) relationship. With this relationship when the predecessor task is finished we can start the successor task. The start-start (SS) relationship allows placing the start of the successor task after the start of the predecessor task. In the finish-finish relationship after finishing of the predecessor task finishing of the successor task takes place. The most controversial is the start-finish (SF) relationship. Here, after the start of the technologically predecessor task the finish of the technologically successor task is placed. Obviously, the first in time will be the task that finishes first, yet this finish depends on the start of the task that is placed as the successor in time. An example could be the change of the shifts of the security personnel. The employee can only end his shift if the next employee comes in to replace him.

Below complete relations have been presented for the determination of dates and slack times in the network.

Each successor task can be shifted against the predecessor by a relative or absolute period of time. Superimposing of rigid time schedules of the task realization is also possible.

DEPENDENCES OF THE CALCULATIONS FOR DIFFERENT RELATIONS IN THE NETWORK

- Stage I of the calculations

Calculating the earliest start for the successor task

For the relationship FS: $WS_n = WK_p + \Delta.$ (9)

For the relationship SS: $WS_n = WS_p + \Delta.$ (10)

For the relationship FF: $WS_n = (WK_p + \Delta) - t_n.$ (11)

For the relationship SF: $WS_n = (WS_p + \Delta) - t_n.$ (12)

Of all the WS_n value select the greatest value

Calculating the early finish of the successor task

$$WK_n = WS_n + t_n. \quad (13)$$

- II stage of the calculations

Calculating the latest finish of the predecessor task

For the relationship FS: $PK_p = PS - \Delta.$ (14)

For the relationship SS: $PK_p = (PS_n - \Delta) + t_p.$ (15)

For the relationship FF: $PK_p = PK_n - \Delta.$ (16)

For the relationship SF: $PK_p = PK_n - \Delta + t_p.$ (17)

Of all the PK_p values select the least value

Calculating the latest start of the predecessor task

$$PS_p = PK_p - t_p. \quad (18)$$

Total slack time

$$ZC = \min \{ (PS_p - WS_p), (PK_p - WK_p) \}. \quad (19)$$

Free slack time

For the relationship FS: $ZS = (WSn - WKp) - \Delta$. (20)

For the relationship SS: $ZS = (WSn - WSp) - \Delta$. (21)

For the relationship FF: $ZS = (WKn - WKp) - \Delta$. (22)

For the relationship SF: $ZS = (WKn - WSp) - D$. (23)

Of all the calculated free slack times select the least value

Example of the network of relations calculated with critical path method has been presented in figure 1.

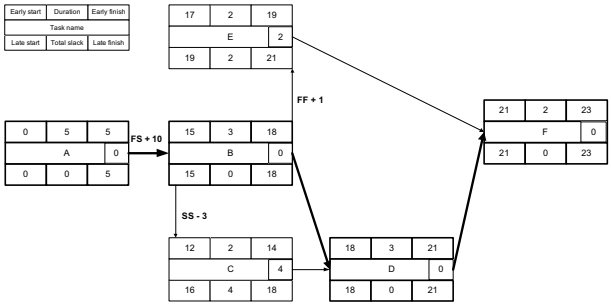

Fig. 1. Example of the network of relations drawn with the method activities on nodes

The calculations have been performed with the critical path method.

CONCLUSIONS

There are many methods of quantitative modeling of projects. Aside from the critical path method such methods were developed as the PERT method that takes into account the probabilistic characteristics of the task duration, the fully probabilistic GERT method, the method of critical chain taking into account only time and delay management or the earned value method whose purpose is to manage the realization of the project. A variety of methods optimizing the project have also been developed.

This paper aimed at consolidating the knowledge related to the basics in the network calculations with the use of the critical path method. It is the computer tools for project management that most frequently use this method. The exploration and full comprehension of the course of the calculations will enable a successful understanding of computer software for project management.

REFERENCES

1. A guide to The Project Management Body of Knowledge- PMBOK Guide. Third Edion. 2000. MT&DC.
2. **Badiru A. B. 1996:** Project management in manufacturing and technology operations. John Wiley & Sons Inc. New York.
3. **Cleland D.I. 1999:** Project management. Strategic design and implementation. McGraw-Hill, New York.
4. **Dibnis G. 2010:** The problems of administration for industrial enterprices. TEKA Kom. Mot. i Energ. Roln. – OL PAN, v. 10D, p. 101-106.
5. **Kerzner H. 2000:** Applied project management. Best practices on implementation. John Wiley & Sons Inc. New York.
6. **Kimmons R.L., Loweree J.H. 1989:** Project management. A reference for professionals. Marcel Dekker Inc., New York.
7. **Knutson J. 2001:** Project management for business professionals: a comprehensive guide. John Wiley and Sons, New York.
8. **Korobetsky Y., Sokolova Y., Doroshko V. 2010:** Imitation abstract models of production systems. TEKA Kom. Mot. i Energ. Roln. – OL PAN, v. 10A, p. 285-293.
9. **Lawrence J.A.Jr., Pasternack B.A. 1998:** Applied management science. A computer-integrated approach for decision making. John Wiley & Sons Inc. New York.
10. **Lientz B.P., Rea K.P. 1998:** Project management for the 21-st century. Academic Press, San Diego.
11. **Mantel S.J.Jr., Meredith J.R., Shafer S.M., Sutton M.M. 2001:** Project management in practice. John Wiley & Sons Inc. New York.
12. **Nicholas J.M. 2001:** Project management for business and technology. Principles and practice. Prentice Hall, Upper Saddle River, New Jersey.
13. **Riazantseva N., Tyulyenyev H. 2010:** Efficiency of decision making in the state institutions. TEKA Kom. Mot. i Energ. Roln. – OL PAN, v. 10D, p. 230-235.
14. **Samuelson F.W., Marks S.G. 1998:** Ekonomia menedżerska. PWE, Warszawa.
15. **Shapovalova A., Shapovalova S. 2010:** TEKA Kom. Mot. i Energ. Roln. – OL PAN, v. 10D, p. 249-256.
16. **Sharipova O. 2010:** Management of diversified entrepreneurial structures activity harmonization. TEKA Kom. Mot. i Energ. Roln. – OL PAN, v. 10D, p. 257-262.
17. **Shtub A., Bard J.F., Globerson S. 1994:** Project management, engineering, technology, and implementation. Prentice Hall, Englewood Cliffs, New Jersey.
18. **Slobodyanyuk M., Nechaev G. 2010:** TEKA Kom. Mot. i Energ. Roln. – OL PAN, v. 10B, p. 162-170.
19. **Stuckenbruck L.C. 1981:** The implementation of project management: the professional's handbook. Project Management Institute. Addison-Wesley Longman.
20. **Zhytna I., Yefremenko O. 2010:** Competitiveness of an enterprise and methods of its estimation.. TEKA Kom. Mot. i Energ. Roln. – OL PAN, v. 10D, p. 325-330.

METODY ILOŚCIOWE ORGANIZACJI CZASU W ZARZĄDZANIU PROJEKTAMI

S t r e s z c z e n i e. W pracy przedstawiono algorytm obliczeń sieci relacji używając metody ścieżki krytycznej, korelacji dla sumarycznego, wolnego, warunkowego i niezależnego

czasu lużnego, korelacji dla wszystkich rodzajów relacji między zadaniami: FS, SS, FF, SF. Zaprezentowano przykład sieci z modyfikacjami.

Słowa kluczowe: zarządzanie projektami, metody ilościowe, metoda ścieżki krytycznej.

TEKA. COMMISSION OF MOTORIZATION AND ENERGETICS IN AGRICULTURE – 2012, Vol. 12, No. 1, 307–313

Factors influencing the energy efficiency in dairy processing plants

Janusz Wojdalski, Agnieszka Kaleta, Bogdan Dróżdż, Aneta Chojnacka

Warsaw University of Life Sciences - SGGW; Faculty of Production Engineering
Nowoursynowska str. 166, 02–787 Warszawa

S u m m a r y. Panel heat exchangers (pasteurizers) are commonly used for the pasteurization of milk and dairy products. In the sterilization process sterilized tubes (sterilizers) are the most common solutions. Methods of increasing heat transfer efficiency were split into two groups. The first one includes methods used at the design stage (panels profiling, selection of the heat exchanger). The second group refers to methods that can be used during the use of heat exchangers (regulation of media flow intensity, control of the cleaning process frequency). The results of calculation of the impact of the deposits formation on the walls of the exchangers and the efficiency of energy conversion into the energy efficiency of four types of dairy plants were presented.

K e y w o r d s: heat exchangers, dairy industry, energy efficiency, intensity of media flow, heat transfer coefficient, steam boilers.

SYMBOLS AND ABBREVIATIONS

A_C – 24 hour total thermal energy consumption in a dairy plant, [GJ/24h];

A_4 –24 hour thermal energy consumption necessary to obtain final products (energy used before the modernization), [GJ/24];

$A_{C41;}$ A_{C42} – 24 hour thermal energy consumption necessary to obtain final products (energy used after the modernization) (where η_{41} and η_{42}), [GJ];

d_1 – inner diameter of tubes, [m];

d_2 – outer diameter of tubes, [m]; Index *os* –deposit, *s* –wall of a tube;

EE_C – energy efficiency before the modernization (EE_C=1/ W_C^{-1}), [dm^3/GJ];

EE_{C41} ; EE_{C42} – energy efficiency after the modernization (where η_{41} and η_{42}), [dm^3/GJ];

$\%EE_{C41}$;$\%EE_{C42}$ – energy efficiency increase after the modernization (where η_{41} and η_{42}), [%];

F – heat transfer surface, [m^2];

k – heat transfer coefficient, [W/(m^2·K)];

L – tube length, [m];

$\dot{Q}$ – current thermal power, [W];

$\dot{Q}_{max}$ – maximum thermal power possible, [W];

W_C – unit thermal energy consumption [GJ/1000 l];

W_{C41}; W_{C42} – unit energy consumption indicators after the modernization where η_{41} and η_{42} , ($W_{C41} = A_{C41}/Z$; $W_{C42} = A_{C42}/Z$), [GJ/1000l];

Z – 24 hour production volume, [m^3/24h];

α_1 – heat transfer to the inner surface coefficient, [W/(m^2·K)];

α_2 – heat transfer to the outer surface coefficient, [W/(m^2·K)];

η – heat exchanger thermal efficiency;

η_1 – partial efficiency of transformation at stage 1;

η_2;η_{21} – partial efficiency of transformation at stage 2 before and after the modernization;

η_3;η_{31} – partial efficiency of transformation at stage 3 before and after the modernization;

η_4;η_{41};η_{42} – overall efficiency of transformation in production plants;

λ – thermal conductivity of the tubes material, [W/(m·K)];

ΔB_{U41};ΔB_{U42} – energy savings expressed by coal equivalent where η_{41} and η_{42}($\Delta B_{U41} = \frac{300\Delta_{41}}{29,3076}$;$\Delta B_{U42} = \frac{300\Delta_{42}}{29,3076}$), [Mg/year];

Δt_m – average logarithmic temperature difference, [K] or [^{o}C];

$\Delta_{41;}$ Δ_{42} – decrease of thermal energy consumption where η_{41} ($\Delta_{41} = A_C - A_{C41}$) and where η_{42} ($\Delta_{42} = A_C - A_{C42}$), [GJ/24h];

SE_{41};SE_{42} – decrease of energy consumption during a year period 300Δ_{41} and 300Δ_{42} (where η_{41} and η_{42}), [GJ/year];

INTRODUCTION

Thermal processing of food is done to reduce the concentration of harmful substances such as bacteria or their spores. The product quality is affected by heat processes and sediments accumulated on the walls of the exchangers, formed by the reaction of milk components to the temperature. In dairy industry plate and pipe heat exchangers are commonly used. Efficiency is a concept with no clear empirical content. It may be regarded as a feature of efforts to achieve a positive outcome. Specific energy consumption (SEC-Specific Energy Consumption) varies depending on the type of dairy plant as well as on the efficiency of the thermal treatment of raw material. The possibilities of saving energy were presented by [5]. In the cited works a complete answer to the question what is the correlation between the state of surface contamination of heat exchangers and the conversion of energy efficiency and demand for energy carriers by the processing plant, was not found. Patterson (1996) made various attempts to organize concepts in this area. The aim of this study is to analyze the possibility of increasing the heat transfer efficiency especially in the heat exchangers and to analyze the efficiency of energy conversion and its impact on energy consumption of dairy plant. The scope of work includes discussion of the example of two types of heat exchangers (plate and pipe) and on two levels (methods used by heat exchangers users and methods used by the designers of these devices). The calculations take into account the thermal efficiency of steam boilers in four types of dairy plants.

PURPOSE AND METHODS

DEFINITION OF EFFICIENCY

Efficiency is commonly regarded as the result of economic activity, being this an indicator of the result obtained to the input made. Efficiency means positive outcome, effectiveness, process efficiency. The efficiency assessment is often associated with the relationship between the amount of manufactured products or outcomes (effects, results), and the quantity of factors used in the production process, i.e. inputs. Energy efficiency can also be defined as a reduction of energy consumption that occurs during processing, transmission, distribution or final use affecting the changes in technology, providing the same or higher level of production [22, 16]. Definition of energy consumption indicators (kWh/1000 liters of milk) and fuel consumption (GJ/1000 liters of milk), etc., allows for the control the energy efficiency of the plant. Nowadays the efficiency concept is often combined with eco-efficiency, aiming to achieve high environmental standards, and these translate into reduction of processing plant negative impacts on the environment.

According to Kostowski [10] thermal efficiency η of the exchanger is expressed as a relationship of two thermal powers:

$$\eta = \frac{\dot{Q}}{\dot{Q}_{\max}}, \tag{1}$$

where: the maximum possible value $\dot{Q}_{max}$ is limited in the heat exchanger by the factors temperature difference on their entrance to the exchanger. In the further analysis efficiency η will be regarded as efficiency defined by heat stream $\dot{Q}$ obtained from the equation:

$$\dot{Q} = kF\Delta t_m. \tag{2}$$

From an industrial point of view (i.e. the final product) in order to increase the efficiency of heat transfer in various heat exchangers, we should seek to maximize the value of $\dot{Q}$. In the present model $\dot{Q}_{max}$ assumes a constant value, so that the growth achieved in the heat flux will increase the overall efficiency η.

At the same time the production process requires $\dot{Q}$ value to be constant and it is regarded as the energy input. Under these conditions $\dot{Q}_{max}$ should be as large as possible, to achieve the greatest value of the thermal efficiency coefficient η. The energy efficiency of the processing plant is expressed as EE indicators, being these the inversion of specific energy consumption.

INCREASING THE EFFICIENCY OF HEAT TRANSFER IN HEAT EXCHANGERS

Methods for improving the efficiency of heat exchange are: choosing the right plate profile and the corresponding profile of the heat exchanger, appropriate control of flow rate and the proper cleaning of the heat exchanger.

Plate profile. Each plate consists of three basic elements A, B & C (Figure 1).

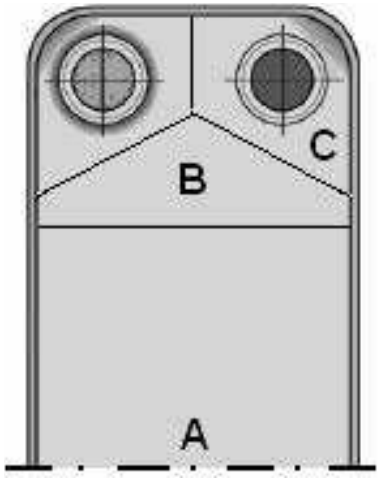

Fig. 1. Main parts of the plate in the heat exchanger: A - the main heat exchange zone at mid-plate, which is a critical area to produce a flow of high turbulence, according to the required pressure drop, B - the area of distribution at the top and bottom plates, corresponding to a uniform media distribution across the width of the plate and eliminating "dead "spaces, C - the main element of the corner of the plate - for a low inlet pressure and lower flow speed (connectors allow factors supplying / discharging to / from the heat exchanger).

The process of flow (exchange) begins where the holes are located (Figure 1-C). Plates with blind holes make it possible to change the direction of factor flow, thus creating a multi-circulation system (serial, parallel or mixed). Then the fluid flows through the area B to produce heat transfer in the center of the plate.

The size of the panel surface results in its shape, which is the way its profile is carved. The panel is strongly "wrinkled", which increases its surface area and provides greater stiffness [11]. Bansal et al. [1] have demonstrated a correlation between the shape of the panel and the tendency to the formation of sludge. It was found that the material of which the heat exchanger surface is made has an influence on the formation of impurities during the thermal processes to which the milk is subjected during its processing [18, 23].

Selection of heat exchanger. The selection of heat exchanger is supported by computer programs, prepared by the manufacturers. The parameters to be taken into consideration when choosing a heat exchanger are: the initial (input) and final (output) temperatures of factors between which the exchange of heat takes place, the flow rate of these factors, the heat transfer coefficient, the flow of heat exchanged and the heat transfer surface. When selecting the heat exchanger surface supply should be considered. The study Zander & Zander [26] describes the course of design processes when composing connection configuration in a panel heat exchanger. In the study [20] a mathematical model was formulated to predict accumulation of milk sediment (stone) in the heat exchanger as a function of time and place. [13, 14] developed a model that allows control of temperature and vapor pressure.

Liquids flow intensity. To obtain the objective intensity of the heat flow, it is necessary to ensure adequate temperature difference. In industrial practice, temperature process of milk heat processing is archived for a period of two years. [6] developed the concept of automatic process control system of milk pasteurization and visualization of this process enabling the control of the process. Reducing the milk flow intensity will increase the duration of heat exchange. In this case, the heat exchanger efficiency expressed in l / h is reduced, so that less quantity of product will be processed. It means that the heat exchanger lost its efficiency. It was found that there is a correlation between the rate of contamination accumulation and the Reynolds number. There is also a correlation between the air content in milk and air pollution. If the air content in milk is less, less sediment is produced [3, 9].

The washing process. The presence of contaminants is a transition state, as they are removed during the washing process. The cleanliness of machinery and equipment incorporated in the production line is of great importance in maintaining hygienic conditions during milk processing. So far a complete mechanism of milk stone formation in heat exchangers has not been presented. There are two types of milk sediments. The first is the relatively soft sediment, formed at 75-115°C temperature. Due to its high protein content (50-70% mass), this type of stone is called protein stone. The second type of sediment is formed at higher temperatures, above 110°C. It is hard, it has a granular structure with a high mineral content (up to 80% mas.) and therefore it is called mineral sediment. Studies have shown that

β-lactoglobulin plays a major role in the sedimentation process. The amount of sediment increases with time, i.e. with prolongation of heat exchanger work and depends on the heat exchanger section (regenerative, heating) [23]. The most common solution is the CIP cleaning method (cleaning in place). In the industry two types of CIP cleaning can be used: 1 – two-phase cleaning using alkali (usually sodium hydroxide) and then using acids (nitric or phosphoric acid), 2 – one phase cleaning using detergents containing wetting agents, surface agents or chelated compounds.

There are three solutions to minimize or reduce the formation of pollutants: 1 - modify the heat treatment process, to which a liquid is subjected, through changes in the temperature profile;

2 - modification in the design of the heat exchanger by changes in configuration or in the final surface of the heat exchanger;

3 - modifying the milk liquid processed, for example, by adding oxidizing agents to prevent the particles merging.

EFFECT OF SEDIMENT LAYERS ON HEAT TRANSFER DETERIORATION

This aspect will be shown using the example of milk cooling after pasteurization process. The calculations assumed that this process takes place in seven pipe heat exchanger. Temperature range of factors is respectively: for milk 75-30°C, for water 5-30°C, which means that the milk is cooled to a temperature of 30°C. Heat transfer coefficient k_1 for pipe compartments is determined by the formula (3):

$$\frac{1}{k_1} = \frac{1}{\alpha_1 d_1} + \frac{\ln \frac{d_2}{d_1}}{2\lambda_s} + \frac{\ln \frac{d_{2os}}{d_{1os}}}{2\lambda_{os}} + \frac{1}{\alpha_2 d_2} \tag{3}$$

The heat flow, including different sediment thicknesses is determined by the formula (4):

$$\dot{Q} = k_1 \pi L \Delta t_m \tag{4}$$

PLANTS CHARACTERISTICS, USE OF STEAM BOILERS AND ENERGY EFFICIENCY OF PRODUCTION PROCESS

There was used a methodology contained in the work of Wojdalski & Kaleta [7], in which three stages of energy efficiency partial conversion η_1, η_2 and η_3 were adopted. The study takes into account the working conditions of

steam boilers and relationships mentioned in the work of Szargut & Ziębik [2, 21], [8]. Next, the energy efficiency of four types of dairy plants (Table 1) were analysed, with different values of transformation efficiency at stages 2 and 3. Table 2 contains figures derived from the four types of individual dairy plants [7]. Partial conversion of energy efficiency η_1, η_2, η_3 and η_4 was presented.

Table 1. Types of analysed dairy plants

Types of plants	Processing characteristics
T1	Drinking milk, milk beverages, cream, curds, cheese, butter, casein, milk powder
T2	Processing structure similar to type T1 plants, but without milk powder production
T3	Processing structure similar to type T1 plants but without drinking milk, milk beverages, cream and curds production
T4	Exclusive production of drinking milk, milk beverages, cream and curds

Table 2. Input data for calculations, before the introduction of improvements

Item	Analysed plant			
	I (T1)	II(T2)	III(T3)	IV(T4)
A_C [GJ/24h]	432.60	119.00	148.10	59.30
W_C [GJ/m^3]	2.3207	1.3607	1.5542	1.0882
EE_C [dm^3/GJ]	430.9	734.9	643.4	918.9
Z [m^3/24h] (scope)	185 (180-188)	89 (84-91)	95 (90-116)	54 (50-62)
η_1	0.993	0.992	0.989	0.996
η_2	0.661	0.682	0.710	0.697
η_3	0.708	0.742	0.713	0.720
η_4	0.465	0.502	0.501	0.500
A_{41} [GJ/24h]	201.16	59.74	74.15	29.65

24 hour consumption of thermal energy (A_C), specific consumption of thermal energy (W_C), production energy efficiency (EE_C), the average production value (Z) and the ranges of its variation were taken into account. It was found that before modernization the partial performance changes for individual plants were: η_1 η_2 and η_3.

The overall record of changes for individual plants is described by formulas (5) and (6):

$$\eta_1 \cdot \eta_2 \cdot \eta_3 = \eta_4 \quad \text{whereas} \quad \eta_4 = \frac{A_4}{A_C}. \qquad (5),(6)$$

Thus:

$$A_4 = \eta_4 \cdot A_C$$

As a result of changes which improve heat transfer and increase thermal efficiency of a steam boiler two options were considered to increase energy efficiency of dairy plants.

Option I

The increased efficiency of transformation only at the stage 3 (devices for milk heat treatment) was considered, and the ratio η_3 increased to η_{31}. These coefficients took the intermediate values between the conditions of heat exchange for panels without sediment and the layers of milk and boilers sediment.

Thus, the overall record of change is expressed in the following form (formula 7):

$$\eta_{41} = \eta_1 \cdot \eta_2 \cdot \eta_{31}. \qquad (7)$$

It was assumed that input energy level A_{41} did not change (A_4=A_{41}). Thus:

$$\eta_{41} = \frac{A_{41}}{A_{C41}} \quad \text{and} \quad A_{C41=} A_{41}/\eta_{41}. \qquad (8)$$

24 hour reduction of energy consumption for individual plants is:

$$\Delta_{41} = A_C - A_{C41}. \qquad (9)$$

Thus year reduction of thermal energy consumption (300 24 hour periods/year) SE is:

$$SE_{41} = 300 \cdot \Delta_{41}. \qquad (10)$$

Option II

It was assumed that increased performance took place also at the stage 2, and that stem boiler thermal efficiency coefficient η_2 increased to η_{21}. Input energy volume A_{41}=A_{42}. The overall record of changes is expressed:

$$\eta_{42} = \eta_1 \cdot \eta_{21} \cdot \eta_{31}, \qquad (11)$$

$$\eta_{42} = \frac{A_{42}}{A_{C42}} \quad \text{and} \quad A_{C42=} A_{41}/\eta_{42}. \qquad (12)$$

24 hour and year reduction of energy consumption SE for individual plants is respectively:

$$\Delta_{42} = A_C - A_{C42} \quad \text{and} \quad SE_{42} = 300 \cdot \Delta_{42}. \qquad (13),(14)$$

Specific thermal energy consumption indicators W_{C41} and W_{C42} were calculated. Energy efficiency for individual plants is expressed:

$$EE_{41} = \frac{1}{W_{C41}} \quad \text{and} \quad EE_{42} = \frac{1}{W_{C42}}. \qquad (15),(16)$$

Energy efficiency increase for individual plants was expressed by means of indicators $\%EE_{41}$ and $\%EE_{42}$. Year savings of coal equivalent (ΔB) obtained as a result of

increased transformation performance for every option (with η_{41} and η_{42}) were expressed as ΔB_{U41} and ΔB_{U42}.

RESULTS AND DISCUSSION

Figure 2 shows the changes in heat stream $\dot{Q}_{os}$ caused by the formation of sediment in relation to the heat stream in the heat exchanger without sediment $\dot{Q}$ of milk and/or boiler stone of different thicknesses. In the case 5, 6 and 7 the situation of stone rising from the outer side of the tubes was shown. Heat exchangers are washed regularly from the side of food product flow. But there is also stone formation from the water side, especially if it is hot water. Dairy plants use treated water, which contributes to the slower formation of stone. So in the case of pasteurization both milk stone (the common one) and boiler stone (much less often) may appear. Case 8 describes the critical situation in which the sediment is formed on both sides of the tubes.

Fig. 2. Changes of heat stream $\dot{Q}_{os}$ caused by sediment formation in relation to heat stream in a heat exchanger with no sediment $\dot{Q}$: 1-no sediment; 2-milk stone of 0.12 mm thick;3-milk stone of 0.28 mm thick; 4-milk stone of 0.55 mm thick; 5- boiler stone of 0.14 mm thick; 6-boiler stone of 0.3 mm thick; 7-boiler stone of 0.6 mm thick; 8-milk stone of 0.55 mm thick inside the tube and boiler stone of 0.6 mm outside the tube.

Figure 2 shows that the sediment significantly reduces the value of heat stream exchanged. This stream decreases when increasing the sediment thickness, thus the milk stone affects more the heat transfer than boiler stone. Milk sediment of 0.12 mm thick (case 2) makes that heat stream is 0.67 of exchanged heat stream in the heat exchanger without sediment; the sediment of 0.28 mm thick (case 3), this value is 0.46 and for sediment of 0.55 mm thick (case 4) is only 0.30. In case of boiler stone the relationship of heat stream exchanged in an exchanger without sediment is respectively: for sediment of 0.14 mm thick (case 5) 0.70, for sediment of 0.30 mm thick (case 6) 0.53 and for sediment of 0.6 mm thick (case 7) 0.36. More adverse effect of milk stone on heat exchange is caused by lower value of its thermal conductivity coefficient compared to the same coefficient for boiler stone.

If both types of sediment occur simultaneously (case 8) this parameter is 0.19. It should be noted that the analyzed cases 5, 6 and 7 may also partially cover the inner surfaces of the steam boiler especially in the case of using water, which was not fully treated or residual deposits [12]. The calculation of the energy efficiency of the plant in the option I in accordance with the adopted methodology takes into account the partial efficiency indicators increasing from η_3 to η_{31}, that in cases 1-2 and 1-5 are respectively, above 0.67 and 0.70 (Figure 2). Option II also included increasing the thermal efficiency of steam boilers, which was affected by a number of additional factors cited in the work of [24]. The greatest savings were obtained for plants equipped with powdered milk processors. Using only option I led to annual savings of 3528 GJ and using it together with option II enabled to reduce energy demand by 7122 GJ (Table 3). Plants of this type are also the bigger energy consumers most energy intensive of the four types mentioned [4].

Prior to the introduction of improvements to process 1000 liters of milk 2.3207 GJ was consumed in the plant, it means more than double in the plant type IV (T4). At the same time energy efficiency of the plant type IV (T4) was highest among those listed in Table 4.

This was associated with the smallest range of thermal treatment and the least number of manufactured products (Table 1). Due to the smallest size of the daily processing Z, annual savings amounted to only 1317 GJ (Table 3). This represented about 5.4 times less in comparison with the biggest plant of type I (T1) equipped with powdered milk processor. The largest overall increase in energy efficiency occurred in plants of type II (T2) and III (T3), of respectively 13.1% and 12.9%. This increase resulted from the biggest improvement of transformation efficiency expressed as η_{21} and η_{31}. Increase of heat exchange efficiency in each plant (at stage 3) affected the energy efficiency improvement of entire plants from 2.01% in the plant type I (T1) to 7.72% in the plant type III (T3). At the same time, Table 4 shows that increasing the transformation efficiency at stage 2 led to increase of entire plants energy efficiency from 5.01% in the plant type I (T1) to 13.10% in the plant type II (T2). It should be highlighted that understanding the mechanism of thermal insulation failures and their elimination could also improve the energy efficiency of dairy plants (Perz 2009). To identify service failures of insulation systems thermography can be used [15, 17]. In studies on heat transfer the work of Kaljuzhnyj et al. (2010) can be useful.

Table 3. Plants characteristics after improvements

Item	Analysed plant			
	I(T1)	II(T2)	III(T3)	IV(T4)
η_1	0.993	0.992	0.989	0.996
η_{21}	0.681	0.721	0.744	0.708
η_{31}	0.728	0.781	0.770	0.766
$\eta_{41}=\eta_1\cdot\eta_2\cdot\eta_{31}$	0.478	0.528	0.541	0.532
$\eta_{42}=\eta_1\cdot\eta_{21}\cdot\eta_{31}$	0.492	0.558	0.567	0.540
A_{C41} [GJ/24h]	420.84	113.14	137.06	55.73
A_{C42} [GJ/24h]	408.86	107.06	130.78	54.91
$\Delta_{41} = A_C - A_{C41}$ [GJ/24h]	11.76	5.86	11.04	3.57
$\Delta_{42} = A_C - A_{C42}$ [GJ/24h]	23.74	11.94	17.32	4.39
$300\cdot\Delta_{41}$ [GJ/year]	3528	1758	3312	1071
$300\cdot\Delta_{42}$ [GJ/year]	7122	3582	5196	1317

Table 4. Increase of plants energy efficiency after improvements

Item	Analysed plant			
	I(T1)	II(T2)	III(T3)	IV(T4)
$W_{C41} = \frac{A_{C41}}{Z}$ [GJ/1000 l]	2.2748	1.2712	1.4427	1.0320
$W_{C42} = \frac{A_{C42}}{Z}$ [GJ/1000 l]	2.2100	1.2029	1.3766	1.0168
EE_{41} [dm^3/GJ]	439.3	786.9	693.1	969.0
$\%EE_{41} = \frac{EE_{41}}{EE_C}$ [%]	2.01	7.03	7.72	5.45
EE_{42} [dm^3/GJ]	452.5	831.3	726.4	983.5
$\%EE_{42} = \frac{EE_{42}}{EE_C}$ [%]	5.01	13.10	12.90	7.03
$\Delta B_{U41} = \frac{300\Delta_{41}}{29,3076}$ [Mg/year]	120.38	59.98	113.01	36.54
$\Delta B_{U42} = \frac{300\Delta_{42}}{29,3076}$ [Mg/year]	243.01	122.22	177.29	44.94

The results obtained refer to the study of Xu & Flapper (2011) relevant to energetic aspects of milk processing and the environmental impact of dairy production.

CONCLUSIONS

Based on the referred literature and own calculations we can say that heat transfer efficiency and energy efficiency of dairy plants may be affected by the following factors:

– Panel´s profile. More sculpted panels provide bigger heat exchange surface. There is a relationship between the plate pattern and a tendency to the sediment formation. Causing high turbulence profiles limit the accumulation of sediment which favors large values of the heat transfer coefficient.
– Selection of heat exchanger. Selection of heat exchanger is nowadays supported very often by computer programmes. Some of them take into account the formation of milk sediment.
– Flow intensity. Reducing milk flow intensity will increase the duration of heat exchange time and reduce the heat exchanger efficiency (l/ h). There is a relationship between the Reynolds number and the sediment accumulation speed.
– Washing process. If the heat exchange conditions are disturbed and the product leaving the heat exchanger does not reach the temperature required by the process technology, the installed devices should undergo a washing process in order to improve the working conditions of the pasteurizer / sterilizer.
– Washing removes the sediment of milk and boiler stone causing the decrease of heat transfer coefficient and therefore helps to increase heat exchange efficiency. Washing is a short-term process, but the effect persists over the entire cycle.
– For the adopted factors it was determined that the greatest amount of energy savings occur in plants with the highest daily milk processing and processing profile consisting of the largest number of manufactured products. The largest increase in energy efficiency was achieved in these types of plants in which the biggest improvement in total energy consumption of both individual changes of heat exchangers and steam boiler was reached.

REFERENCES

1. **Bansal B., Müller-Steinhagen H., Chen X. D. 2000:** Performance of panel heat exchangers during calcium sulphate fouling - investigation with an in-line filter, Chemical Engineering and Food Processing, 39, p. 507-519.
2. **Bhatt M. S. 2000:** Energy audit case studies I - steam systems, Applied Thermal Engineering, 20, p. 285-296.
3. **Changani S. D., Belmar-Beiny M. T., Fryer P. J. 1997:** Engineering and chemical factors associated with fouling and cleaning in milk processing, Experimental Thermal and Fluid Science, 14, p. 392-406.
4. **Figiel P. 2002:** Optymalizacja doboru płytowych wymienników ciepła, Chłodnictwo, 6, p. 22-23.
5. **Janzekovič M., Mursec B., Vindis P., Cus F. 2009:** Energy saving in milk processing, Journal of Achievements in Materials and Manufacturing Engineering, 33/2, p. 197-203.
6. **Juszka H., Tomasik M. 2005:** Wizualizacja procesu przepływowej pasteryzacji mleka, Acta Scientiarum Polonorum, Technica Agraria, 4(1), p. 77-83.
7. **Kaleta A., Wojdalski J. (red.) 2008:** Przetwórstwo rolno-spożywcze. Wybrane zagadnienia inżynieryjno-produkcyjne i energetyczne, Warszawa, Wyd. SGGW, p. 182-198.
8. **Kaczorek J. 2011.** Podstawy modernizacji gospodarki energią cieplną w polskim mleczarstwie. Materiały XXX Międzynarodowej Konferencji Naukowo-Technicznej pt. Problemy gospodarki energia i środowiskiem w mleczarstwie. Olsztyn, 7-10 września 2011, p. 173-179.
9. **Kaljuzhnyj G., Kovalenko A., Lyshtvan E. 2010:** Convective heat exchange in optopneumatic cell, TEKA Kom. Mot. i Energ. Roln.,10A, p. 218-222.
10. **Kostowski E. 2000.** Przepływ ciepła, Gliwice, Wydawnictwo Politechniki Śląskiej.
11. **Kukulka D. J., Devgun M. 2007:** Fluid temperature and velocity effect on fouling, Applied Thermal Engineering, 27, p. 2732-2744.
12. **Marjanowski J., Łasińska E., Ostrowski J. 2011:** Jakość wody oraz nowoczesne systemy uzdatniania wody przeznaczonej do spożycia, na potrzeby technologiczne, kotłowe i do układów chłodzenia w przemyśle mleczarskim, Materiały XXX Międzynarodowej Konferencji Naukowo-Technicznej pt. Problemy gospodarki energią i środowiskiem w mleczarstwie. Olsztyn, 7-10 września 2011, p. 20-46.
13. **Nema P. K., Datta A. K. 2005:** A computer based solution to check the drop in milk outlet temperature

due to fouling in a tubular heat exchanger, Journal of Food Engineering, 71, p. 133-142.
14. **Nema P. K., Datta A. K. 2006:** Improved milk fouling simulation in a helical triple tube heat exchanger, International Journal of Heat and Mass Transfer, 49, p. 3360-3370.
15. **Perz K. 2009.** Mechanizm powstawania uszkodzeń izolacji termicznych, MOTROL, 11c, p. 159-164.
16. **Patterson M.G. 1996:** What is energy efficiency? Concepts, indicators and methodological issues. Energy Policy, vol.24, 5, p. 377-390.
17. **Rochatka T..Bieńczak T. 2009.** Termowizja w identyfikacji eksploatacyjnych uszkodzeń układów termoizolacyjnych do transportu żywności, MOTROL, 11c, p. 170-175.
18. **Rosmaninho R., Santos O., Nylander T., Paulsson M., Beuf M., Benezech T., Yiantsios S., Andritsos N., Karabelas A., Rizzo G., Müller-Steinhagen H., Melo L. F. 2007:** Modified stainless steel surfaces targeted to reduce fouling – Evaluation of fouling by milk components, Journal of Food Engineering, 80, p. 1176–1187.
19. **Sahoo P. K., Ansari I. A., Datta A. K. 2002:** Computer-aided design and performance evaluation of an indirect type helical tube ultra-high temperature (UHT) milk sterilizer, Journal of Food Engineering, 51, p. 13-19.
20. **Sahoo P. K., Ansari I. A., Datta A. K. 2005:** Milk fouling simulation in helical triple tube heat exchanger, Journal of Food Engineering, 69, p. 235-244.
21. **Szargut J., Ziębik A. 1998:** Podstawy energetyki cieplnej. Wyd. PWN. Warszawa, p. 196-221, p. 411-440.
22. **Vidil R., Marvillet Ch. 2005:** The innovation process in the energy field, Energy, 30, p. 1233-1246.
23. **Visser J., Jeurnink Th. J. M. 1997:** Fouling of heat exchangers in the dairy, Experimental Thermal and Fluid Science, 14, p. 407-424.
24. **Wojdalski J. (red.) 2010:** Użytkowanie maszyn i aparatury w przetwórstwie rolno-spożywczym. Wyd. SGGW, Warszawa, p. 309-320.
25. **Xu T., Flapper J. 2011:** Reduce energy use and greenhouse gas emissions from global dairy processing facilities, Energy policy, 39, p. 234-247.
26. **Zander L., Zander Z. 2003:** Projektowanie płytowych wymienników ciepła, Instalacje Sanitarne, 2(7), p. 27-30.

CZYNNIKI WPŁYWAJĄCE NA ZWIĘKSZENIE EFEKTYWNOŚCI ENERGETYCZNEJ ZAKŁADÓW MLECZARSKICH

S t r e s z c z e n i e. Przedstawiono wpływ czynników technologicznych i technicznych na efektywność wymiany ciepła i efektywność energetyczną zakładów mleczarskich. Wyniki obliczeń uwzględniają wpływ profilu płyty, doboru wymienników ciepła, natężenia przepływu cieczy, procesu mycia i sprawności cieplnej kotłów parowych. Dla przyjętych czynników określono efektywność energetyczną czterech typów zakładów mleczarskich. Największe możliwości zaoszczędzenia energii występują w zakładach o największym dobowym przerobie mleka i profilu przerobu składającego się z największej liczby gotowych wyrobów. Największy wzrost efektywności energetycznej uzyskano w tych typach zakładów, w których łącznie wystąpiła największa poprawa efektywności energetycznej poszczególnych przemian energii zarówno wymienników ciepła jak i kotła parowego. Wykazano, że zwiększenie sprawności przemian energii wpłynęło na wzrost efektywności energetycznej badanych zakładów od 5,01 do 13,10%.

S ł o w a k l u c z o w e: wymienniki ciepła, przemysł mleczarski, efektywność energetyczna, natężenie przepływu, współczynnik przenikania ciepła, kotły parowe.

TEKA. COMMISSION OF MOTORIZATION AND ENERGETICS IN AGRICULTURE – 2012, Vol. 12, No. 1, 315–322

Influence of process conditions on selected texture properties of precooked buckwheat pasta

Agnieszka Wójtowicz

Department of Food Process Engineering, Faculty of Production Engineering,
University of Life Sciences, Doświadczalna 44, 20-280 Lublin, agnieszka.wojtowicz@up.lublin.pl

Summary. The paper presents the results of measurements of selected texture properties of gluten-free precooked pasta made from buckwheat flour using variable parameters of extrusion-cooking process. The different level of water addition to buckwheat flour was used due to the moisture content from 30 to 34%. Processing of buckwheat pasta products was performed at the barrel temperature ranged 90-110°C and cooling section temperature ranged 55-65°C on single-screw modified extrusion-cooker TS-45 with L/D = 18:1 using a varied screw speed: 60, 80, 100 and 120 rpm. Radial expansion ratio and selected texture properties of dry and hydrated products were tested depend on the screw speed and the dough moisture content applied. The cutting test was used for determination of cutting force of dry pasta and after 5-minutes hot water hydration for ready-to-eat products. Also OTMS tests with Ottawa equipment were performed for firmness, adhesiveness and chewiness by double-compression tests of hydrated precooked buckwheat pasta products. Highest screw speed increased cutting force of dry and hydrated buckwheat pasta, also affected by higher radial expansion ratio values for these products. Increased moisture content of raw materials lowered firmness of hydrated pasta and higher screw speed applied during processing improved chewiness of pasta products. Precooked buckwheat pasta processed at presented process conditions and raw materials moisture content characterized an acceptable texture and may be recommended as convenient food for consumers with celiac disease.

Key words: extrusion-cooking, buckwheat, precooked pasta, gluten-free pasta, texture.

INTRODUCTION

The extrusion-cooking process involves the mechanical and thermal treatment of the material under high pressure. It is a processing method which combines the respective sequences of both, the mixing, heating, flow, forming and shaping. The extruder-cooker is the reactor completed with the forming die. There are single- and twin-screw extruders, and their work space can be divided into three areas: dosing, mixing and compression. In the initial sections of the barrel material is mixed and moistened. Then, using a screw, material is moved to the kneading zone, which characterized a reduction in the space between the barrel and the screw, the compression ratio reaches 1:3 - 1:5 at the end of this zone and a significant increase in temperature and pressure occurs. Both, shearing and heating make the material plasticized, taking the form of precooked viscous dough [1, 5, 9, 17]. The residence time distribution of material in the extruder takes tens of seconds. The water contained in the material is overheated, and when it leaves the forming die, rapidly evaporates. This affects the expansion of the material, creating a porous structure and the consolidation of assigned shape of product [18].

In the case of instant or precooked pasta formation of this stage must be eliminated; if the final product should have the appropriate characteristics, the final part of the barrel must be cooled down, prevent the temperature exceeds 100°C, for example, by modifying the design of the extruders' barrel [12]. Precooked pasta products obtained in this way characterized by a high rate of starch gelatinization degree, compact internal structure, without the presence of empty spaces inside the pasta cross-section which can be caused by the presence of water vapor in the product [26, 28]. Extrusion-cooking used to produce precooked pasta brings several advantages, which include:

– the possibility of varying the raw materials composition, using not only wheat but also other cereal products, including gluten-free such as rice, corn and buckwheat,
– to obtain products with different structures,
– simplicity, since extrusion-cooked pasta doesn't require cooking or boiling in water, which reduces production costs and the finished product is ready for consumption after a short-time hot water hydration

– significantly reduced processing time and the drying of pasta compared with conventional press methods.

Gluten-free diet is used in the treatment and prevention of celiac disease or gluten intolerance. Celiac disease is a disorder consisting in the occurrence of digestive disturbance and intestinal absorption associated with intolerance of gluten in cereals [4].

The therapy requires the use of gluten-free diet, which consists in the total elimination of food products containing gluten: wheat, rye and barley [8, 19]. Even a minimal amount of gluten contained in products may cause a relapse. The long-term celiac disease left untreated can cause irreversible damage to the intestines that leads to impaired assimilation of nutritional components and malnutrition [10, 25].

For gluten-free pasta starchy raw materials include: corn flour, rice, oats, potato flour and flour from the seeds of leguminous plants [3, 4, 14]. The complicated method of gluten-free pasta production and functional additives (like guar gum, monoglycerides, carboxymethylcelluloze, alginates, modified starches) required to obtain a structure make products more expensive than conventional pasta [6, 7, 11, 16].

Common buckwheat (*Fagopyrum esculentum*) is characterized by interesting nutritional properties, such as the presence of proteins of a high biological value, natural antioxidants, minerals, vitamins (especially those of the B group) and dietary fiber [2, 22]. Presented in this paper a method for producing precooked buckwheat pasta not only allows to get gluten-free products without the use of any technological additives, but it gives an opportunity to create desired quality as well texture characteristics of pasta products which could be classified as convenience food.

The aim of this study was to determine some texture characteristics of extrusion-cooked buckwheat pasta processed with variable screw speed and different moisture levels of raw materials.

MATHERIALS AND METHODS

As the raw material buckwheat flour used (protein – 11.39%, fat - 1.06%, ash – 1.65%, fiber – 9.3%). Raw materials were moistened with appropriate amount of water and mixed to obtain a moisture content of the dough at 30, 32 and 34%. After mixing the raw materials were processed using a modified single-screw extrusion-cooker TS-45 (Metalchem, Gliwice, Poland) with L/D = 18:1, compression ratio 3:1, equipped with additional cooling section with glycol (chiller SW 8P MINI's Cool, Chotomów) at t he end of the barrel, in the temperature ranged from 90 to 110°C in the plasticizing zone and from 55 to 65°C in the cooling section of the extruder. Pasta products were shaped using a forming die with 12 openings with a diameter of 0.8 mm. Buckwheat pasta were processed at different screw speeds of 60, 80, 100 and 120 rpm. After drying, the samples were stored in closed bags.

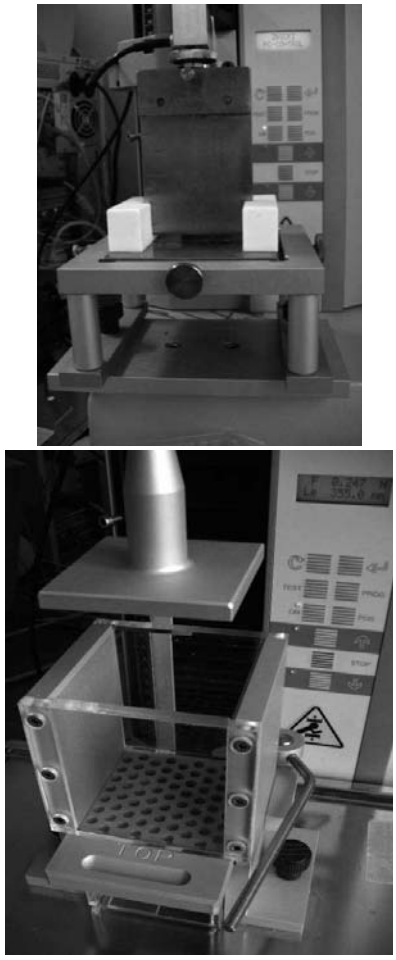

Fig. 1. Test adapters for texture measurements: a) Warner-Bratzler's knife, b) OTMS – Ottawa cell

Based on data collected during multiple measurements the radial expansion ratio of dry buckwheat pasta was tested as the ratio of the pasta single thread diameter to the die diameter (0.8 mm) [27]. Measurements of the diameter of pasta made with a digital caliper with accuracy of 0.01 mm. For selected texture properties of pasta it was used the universal testing machine Zwick BDO-FB0.5TH (Zwick GmbH & Co, Germany) equipped with Warner-Bratzler's knife, as shown on the Fig. 1a, for cutting tests of dry and hydrated pasta products, and with OTMS Ottawa cell for firmness tests of hydrated ready to eat buckwheat pasta (Fig. 1b). The evaluations of cutting force of dry pasta depend on processing conditions was tested as follow: single pasta thread was placed at testing adapter plate and cutting test was performed [24]. Value of cutting force was set at sample break.

Cutting force measurements of hydrated pasta was following after five minutes of hot water hydration, every 60 seconds single pasta thread was taken, rinsed with cold water and placed at 90° to the cutting knife, cutting force was reported at sample break. The distance between grips during the test was 210 mm, the threshold of force exclusion was set at 95% F_{max}, the threshold of damage control was set at 10% F_{nom}. The tests were performed with the head speed of 100 $mm \cdot min^{-1}$ in five replications.

The texture measurements of hydrated gluten-free pasta involved firmness, adhesiveness and chewiness evaluation with OTMS cell (Ottawa Texture Measuring System) with double compression test to 70% of sample layer thickness. Firmness was recorded as maximum force during compression, adhesiveness – as work required to overcoming an adhesion between sample and cell material surface, and chewiness was calculated as multiplication of firmness, cohesiveness and springiness registered during hydrated pasta products compression tests [21]. The tests were performed at 3 replications by placing 50 grams of hydrated and drained pasta and then double compressing with the head speed of 100 $mm \cdot min^{-1}$. The distance between testing grips was 210 mm, the threshold of force exclusion was set at 95% F_{max}, the threshold of damage control was set at 0.1% F_{nom}. *TestXpert®10.11* was applied for interpretation of measurements results of texture characteristics [25].

The results were processed statistically with Statistica 6.0 with response surface regression analysis [13] of influence of processing screw speed and moisture content applied on tested pasta characteristics. Correlation coefficients and Levene's univariate tests of significance were performed at p=0.05.

RESULTS

The moisture content of tested buckwheat pasta varied from 7.5 to 8.5% what is reasonable for storage stability of processed cereal products. The expansion ratio evaluated for precooked pasta reached values 1.35 to 1.60, dependencies of screw speed and initial moisture content of raw materials during processing on this parameter are illustrated on the Fig. 2.

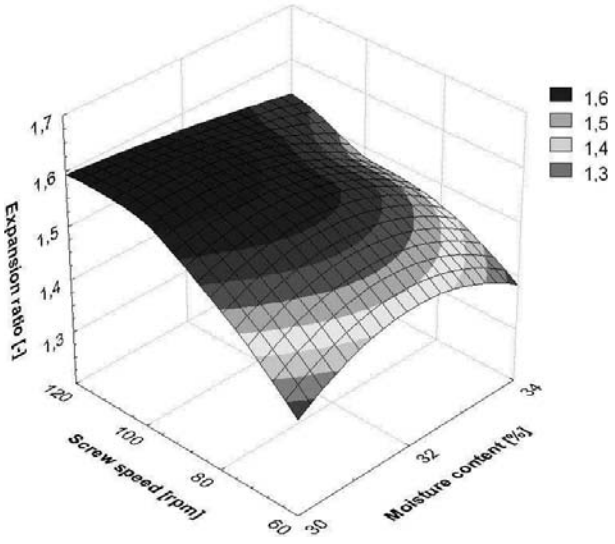

Fig. 2. Radial expansion ratio of gluten-free precooked pasta depend on processing conditions

Increasing of screw speed raised this parameter (correlation coefficient 0.80 at significance level p=0.002). It was found that the higher values of radial expansion index assessed in pasta products processed at lower moisture level and highest screw rpm.

Some texture characteristics of dry and ready to eat pasta are very often estimated as its quality aspects. The instrumental methods utilizing cutting tests, compression and extrusion tests allows to assignation a wide range of texture properties of food products [6, 7, 11, 20, 30]. For hardness measurements the cutting test may be useful with calculation of maximum cutting force necessary to break the sample [15, 24, 29].

Fig. 3 showed the results of cutting forces results of dry buckwheat pasta. The highest hardness of tested products was observed when extrusion-cooked pasta was processed at 100 and 120 rpm at buckwheat flour moisture content of 32% (16.94 N). Lowest values were evaluated for products extruded at 60 rpm at 34% initial moisture content of raw materials (8.15%). Hardness of gluten-free precooked pasta increased significantly with higher screw speed used (correlation coefficient 0.70 at significance level p=0.011). Growth of buckwheat flour water content influenced on rapid reduction of pasta hardness (even 50%) when up to 100 rpm was applied during processing, at highest screw speed unclear effect of increased moisture on cutting force was observed. Significant correlation of pasta cutting force and expansion ratio was evaluated (correlation coefficient 0.71 at significance level p=0.010).

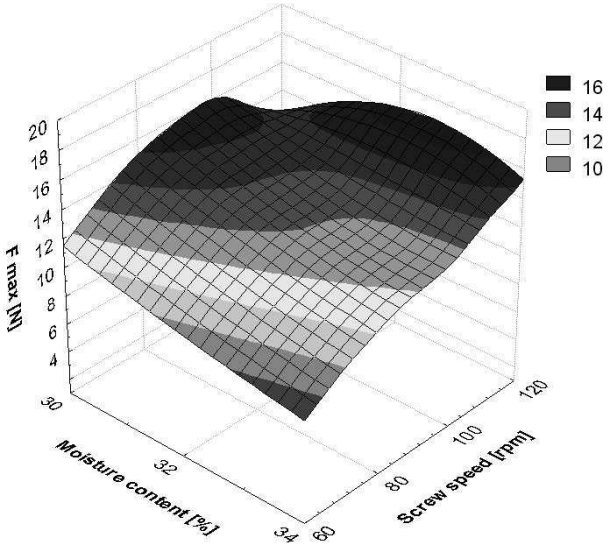

Fig. 3. Hardness of dry buckwheat precooked pasta in cutting test

Minimal preparation time for ready to eat consistency by hot water hydration varied from 4.0 to 6.5 minutes, being slightly longer for precooked pasta processed at higher screw rotational speed, which characterized the largest of the tested products expansion ratio values irrespectively the raw material moisture content applied. For textural properties tests the adequate preparation time was set, when they are at ready to consumption consistency.

A longer than required hydration time of buckwheat precooked pasta adversely affected its quality, the final

Table 1. Results of cutting force of precooked buckwheat pasta processed at different raw materials moisture content and screw speed at various hydration time (means ± standard deviation)

Moisture content [%]	Hydration time [min]	Cutting force of hydrated pasta [N]			
		60 rpm	80 rpm	100 rpm	120 rpm
30	1	12.57 ± 0.49	13.08 ± 1.95	15.46 ± 0.38	18.49 ± 0.59
	2	7.18 ± 0.95	6.16 ± 1.59	6.80 ± 0.64	13.89 ± 0.30
	3	3.43 ± 0.04	2.09 ± 1.13	4.92 ± 0.35	6.37 ± 0.45
	4	1.12 ± 0.07	1.67 ± 0.28	3.22 ± 0.80	4.09 ± 0.05
	5	0.80 ± 0.07	0.85 ± 0.17	1.45 ± 0.05	1.27 ± 0.15
32	1	11.29 ± 0.72	13.03 ± 2.87	14.83 ± 1.06	19.30 ± 0.29
	2	7.01 ± 1.56	7.06 ± 1.09	7.65 ± 1.58	11.22 ± 0.46
	3	3.43 ± 0.92	4.22 ± 0.48	3.46 ± 0.51	5.36 ± 0.19
	4	1.40 ± 0.06	1.42 ± 0.07	2.44 ± 0.43	3.82 ± 0.86
	5	0.86 ± 0.17	1.33 ± 0.04	1.56 ± 0.42	2.24 ± 0.95
34	1	6.30 ± 1.39	9.46 ± 0.87	12.57 ± 1.66	19.41 ± 0.37
	2	4.26 ± 0.24	5.69 ± 0.09	8.03 ± 0.21	8.36 ± 0.02
	3	2.01 ± 0.28	2.46 ± 0.21	5.71 ± 0.48	6.46 ± 0.65
	4	1.51 ± 0.41	1.51 ± 0.46	1.74 ± 0.20	3.04 ± 0.04
	5	0.86 ± 0.05	0.95 ± 0.02	0.87 ± 0.08	1.69 ± 0.29

product was too swollen and too soft in consistency. Good quality final products should be stable, shape-keeping and not disintegrated until will be fully hydrated and consumed.

Measurements of cutting forces of buckwheat hydrated pasta were analyzed according the moisture content of raw materials, screw rotational speed and changes occurred during the subsequent minutes of hot water hydration. The hydration time had the greatest influence on the hardness of pasta, lengthening the time of hydration resulted a significant reduction in cutting force values (correlation coefficient 0.88-0.94 at significance level $p \leq 0{,}05$). On the Fig. 4 diagrams of sample cutting tests of hydrated buckwheat pasta processed at different rpm at various moisture content of raw material are presented. The greatest differences between the tested products were observed during the first three minutes of hydration, then the cutting force decreased below 1-2 N irrespective of the processing parameters, products have become very soft and less flexible. Only pasta extruded at 100 and 120 rpm showed resistance during cutting in the final stage of hydration, which proves their greater hardness after preparation.

In Table 1 the results of cutting forces of tested pasta are showed after 5-minutes hot water hydration, depend on

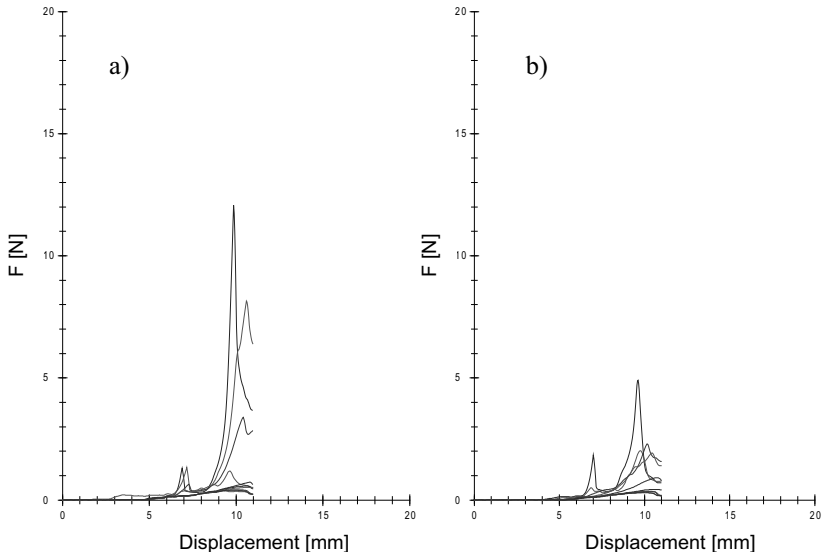

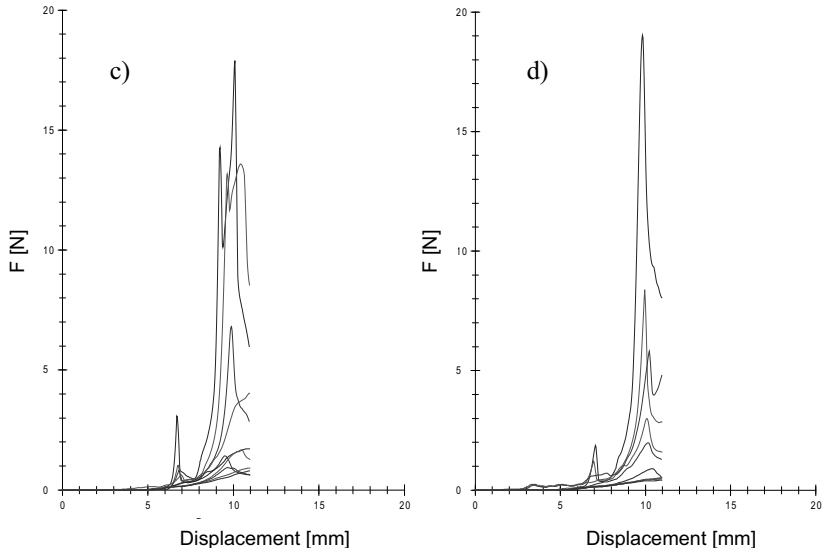

Fig. 4. Diagram of sample cutting test of hydrated buckwheat pasta processed at 60 rpm screw speed at various moisture content of raw material: a) 30%, 60 rpm, b) 34%, 60 rpm, c) 34%, 120 rpm, d) 34%, 120 rpm, after different hydration time

screw speed and moisture content during processing. The highest cutting forces for these products were recorded for pasta processed at 32 and 34% of buckwheat flour moisture content and a highest screw speed applied. When using a lower screw speed it was observed that cutting force of hydrated products decreased with increasing moisture content before processing.

At 120 rpm applied during processing of precooked pasta highest values of cutting forces have been noted and a slight increase in hardness with increasing moisture content of raw materials appeared. Also these products characterized the highest expansion ratio and the longest preparation time, what had impact on their greater hardness.

Schoenlechner et al. [22] examining buckwheat noodles obtained cutting force 1.57 N after 3 minutes of cooking, this value was close to the cutting force of wheat noodles (1.55 N). Buckwheat precooked pasta extrusion-cooked at 60 and 80 rpm demonstrated similar values of cutting force independent of raw materials moisture content. The texture properties of precooked buckwheat pasta evaluated with OTMS Ottawa cell were analyzed according to influence of screw speed applied during processing and initial moisture content of raw materials. The results of pasta firmness depend on processing conditions are presented on the Fig. 5.

The research has shown that the firmness of buckwheat pasta in a double compression test was dependent on the initial moisture content of flour. Firmness of hydrated pasta decreased with increasing of moistening level (correlation coefficient -0.82 at significance level

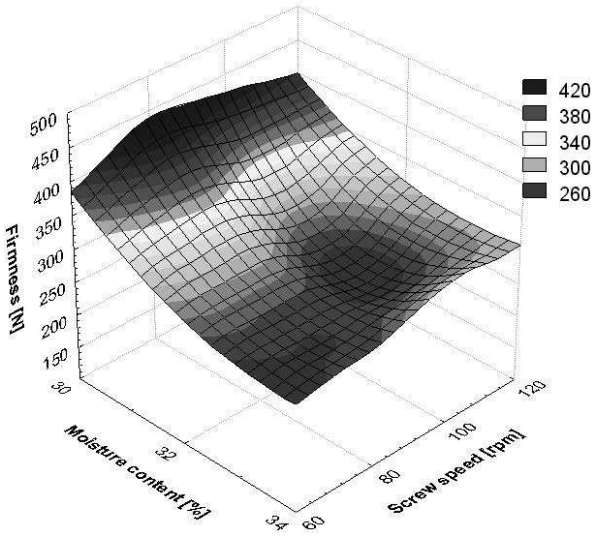

Fig. 5. Firmness of hydrated buckwheat precooked pasta in double-compression test

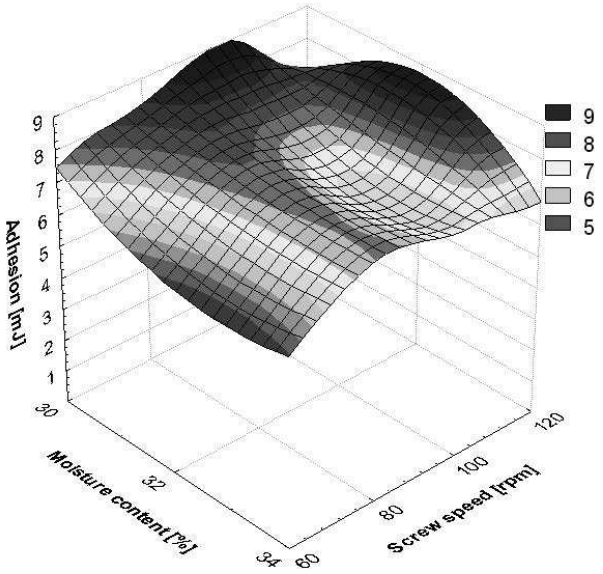

Fig. 6. Adhesiveness of hydrated buckwheat precooked pasta in double-compression test

Table 2. The results of Levene univariate tests of significance for tested parameters of precooked buckwheat pasta processed at various extrusion-cooking conditions

Parameter	Variable	SS	df	MS	F	p
Expansion ratio	Screw speed	0.039	3	0.013	6.05	0.001
	Moisture content	0.003	2	0.002	0.95	0.393
Cutting force	Screw speed	0.591	3	0.197	0.22	0.880
	Moisture content	0.044	2	0.022	0.01	0.990
Firmness	Screw speed	1838.468	3	612.823	0.69	0.583
	Moisture content	68.609	2	34.305	0.27	0.767
Adhesiveness	Screw speed	10.663	3	3.554	4.26	0.045
	Moisture content	3.979	2	1.990	1.83	0.216
Chewiness	Screw speed	1303.681	3	434.560	1.66	0.251
	Moisture content	1151.848	2	575.924	1.45	0.285

p=0,001). It was determined almost twice lower values of this parameter with increasing the moisture content from 30% to 34%. There was no significant effect of screw speed applied during processing on the firmness of buckwheat pasta after hydration.

Adhesiveness of precooked buckwheat pasta evaluated in a double compression test was low, the products were characterized by low stickiness, their surface was resilient and glossy after hydration at optimal hydration time for all the recipes used. Low values of pasta adhesion to the cell surface indicate the attractive texture of buckwheat precooked products. The results of pasta adhesiveness are presented on the Fig. 6. Slightly higher adhesiveness was observed for products processed at lowest moisture content of buckwheat flour, for these products lower hardness at cutting test and higher firmness were evaluated.

The results of Levene univariate tests of significance for tested properties of precooked buckwheat pasta processed at various extrusion-cooking screw speed and initial moisture content are presented in the table 2.

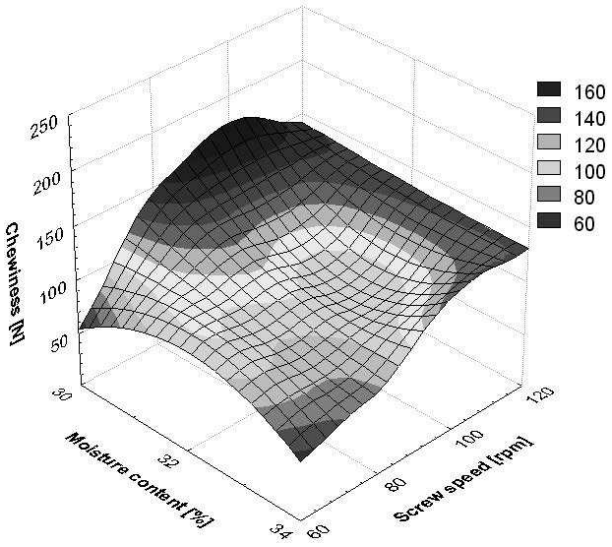

Fig. 7. Chewiness of hydrated buckwheat precooked pasta in double-compression test

Analysis of variance revealed significant differences at $p \leq 0.05$ in uniformity of the radial expansion ratio and adhesiveness of pasta analyzed for various screw rotational speed during extrusion-cooking of precooked pasta.

The results of chewiness of precooked buckwheat pasta are presented on the Fig. 7 depend on processing conditions. Higher values of chewiness were reported for products processed by extrusion-cooking at higher screw speed and at low moisture content of raw materials. Increasing the buckwheat flour moisture content resulted in the lower chewing ability of hydrated pasta products. Chewing ability was mostly affected by screw speed applied during processing, higher values were determined by increasing the screw speed (correlation coefficient 0.66 at significance level p=0,018). Greater chewiness was significantly correlated with a higher cutting force of dry pasta (0.77 at p=0.003), radial expansion ratio (0.73 at p= 0.006) and firmness of hydrated buckwheat pasta products (0.61 at p=0.010).

CONCLUSIONS

The evaluation of influence of processing parameters as screw speed and moisture content during the extrusion-cooking on selected properties of precooked buckwheat pasta showed a significant effect of screw speed applied on radial expansion ratio and cutting force of dry pasta and also for firmness and chewiness of hydrated products.

Application of proposed initial moisture content of raw materials and varied intensity of material mechanical treatment due to the screw speed during precooked pasta extrusion-cooking with single-screw TS-45 modified equipment allowed producing buckwheat pasta with acceptable texture properties without any technological additives. After hot water hydration gluten-free precooked pasta characterized stable consistency, low adhesiveness and proper firmness.

The best properties, confirmed by sensory analysis, were determined for buckwheat pasta processed at 80-100

rpm and 30-32% of flour moisture content. It could be an attractive precooked buckwheat pasta product ready for consumption after few minutes of hot water hydration, especially for consumers on a gluten-free diet.

REFERENCES

1. **Abecassis J., Abbou R., Chaurand M., Morel M. H., Vernoux P. 1994.** Influence of extrusion conditions on extrusion speed, temperature and pressure in the extruder and on pasta quality. Cereal Chemistry 71, 3, p. 247-253.
2. **Alamprese C., Casiraghi E., Pagani A.M. 2007.** Development of gluten-free fresh egg pasta analogues containing buckwheat. European Food Research Technology 225, p. 205-213.
3. **Alvarez-Jubete L., Arendt E., Gallagher E. 2010.** Nutritive value of pseudocereals and their increasing use as functional glutenfree ingredients. Trends in Food Science & Technology 21, p. 106-113.
4. **Bryant R.J., Kadan R.S., Champagne T.E., Vinyard B.T., Boykin D. 2001.** Functional and digestive characteristics of extruded rice flour. Cereal Chemistry 78, p. 131-137.
5. **Camire, M., Camire, A., Krumhar, K. 1990.** Chemical and nutritional changes in foods during extrusion. Food Science and Nutrition 29(1), p. 35-57.
6. **Charutigon C., Jitpupakdree J., Namsree P., Rungsardthong V. 2008.** Effects of processing conditions and the use of modified starch and monoglyceride on some properties of extruded rice vermicelli. LWT - Food Science and Technology 41, 4, p. 642-651.
7. **Chillo S., Laverse J., Falcone P.M., Del Nobile M.A. 2007.** Effect of carboxymethylcellulose and pregelatinized corn starch on the quality of amaranthus spaghetti. Journal of Food Engineering 83, p. 492-500.
8. **Counts D.R., Sierpina V.S. 2006.** Celiac Disease/Gluten Intolerance. EXPLORE 2, 1, p. 43-45.
9. **Ding Q.B., Ainsworth P., Tucker G., Marson H. 2005.** The effect of extrusion conditions on the physicochemical properties and sensory characteristics of rice-based expanded snacks. Journal of Food Engineering 66, p. 283-289.
10. **Hagenimana A., Ding X., Fang T. 2006.** Evaluation of rice flour modified by extrusion cooking. Journal of Cereal Science 43, p. 38-46.
11. **Hsi-Mei L. 2001.** Effects of rice properties and emulsifiers on the quality of rice pasta. Journal of the Science of Food and Agriculture 82, p. 203-216.
12. **Juśko S., Mościcki L., Wójtowicz A. 2009.** Sekcja chłodząco-formująca. Wzór użytkowy PL 64690 Y1, Biuletyn Urzędu Patentowego, 2(195), p. 25.
13. **Kuna-Broniowska I., Gładyszewska B., Ciupak A. 2011.** Storage temperature influence on Young modulus of tomato skin. TEKA Commission of Motorization and Power Industry in Agriculture 11, p. 218-228.
14. **Li J.H., Vasanthan T. 2003.** Hypochlorite oxidation of field pea starch and its suitability for noodle making using an extrusion cooker. Food Research International 36, p. 381-386.
15. **Martinez C., Ribotta P., León A., Añón C. 2007.** Physical, sensory and chemical evaluation of cooked spaghetti. Journal of Texture Studies 38, p. 666-683.
16. **Miedwiediew G.M. 1999.** Produkcja wyrobów makaronowych ze skrobiowych surowców bezglutenowych. Przegląd Zbożowo- Młynarski 2, p. 6-7.
17. **Mitrus M. 2006.** Investigations of thermoplastic starch extrusion cooking process stability. TEKA Commission of Motorization and Power Industry in Agriculture, 6A, p. 138-144.
18. **Moscicki L. (red.) 2011.** Extrusion-Cooking Technique, Wiley-VCH, Weinheim, Germany, ISBN 978-3-527-32888-8.
19. **Niewinski M. 2008:** Advances in celiac disease and gluten-free diet. Journal of the American Dietetic Association 108, 4, p. 661-672.
20. **Raina C. S., Singh S., Bawa A. S., Saxena D.C. 2005.** Effect of vital gluten and gum arabic on the textural properties of pasta made from pre-gelatinised broken rice flour. Food Science and Technology International 11, p. 433-442.
21. **Ross A. 2006.** Instrumental measurement of physical properties of cooked Asian wheat flour noodles. Cereal Chemistry 83(1), p. 42-51.
22. **Schoenlechner R., Drausinger J., Ottenschlaeger V., Jurackova K., Berghofer E. 2010.** Functional properties of gluten-free pasta produced from amaranth, quinoa and buckwheat. Plant Foods Human Nutrition 65, p. 339-349.
23. **Wójtowicz A. 2007.** Effect of monoglyceride and lecithin on cooking quality of precooked pasta. Polish Journal of Food and Nutrition Sciences 57, 3A, p. 157-162.
24. **Wójtowicz A. 2008.** Wpływ dodatku kwasu askorbinowego na teksturę ekstrudowanych makaronów podgotowanych, Acta Agrophysica 12(1), p. 245-254.
25. **Wójtowicz A. 2010.** Błyskawiczne makarony bezglutenowe – charakterystyka cech użytkowych i tekstury, in: Wpływ procesów technologicznych na właściwości materiałów i surowców roślinnych, ed. Witrowa-Rajchert D., Lenart A., Rybczyński R., Wydawnictwo Naukowe FRNA, Komitet Agrofizyki PAN, Lublin, 117-134, ISBN 978-83- 60489-17-8.
26. **Wójtowicz A. 2011.** Precooked pasta. in: Extrusion-Cooking Techniques. Applications, Theory and Sustainability (ed. Moscicki L.), Wiley-VCH, Weinheim, Germany, 99-117, ISBN 978-3-527-32888-8.
27. **Wójtowicz A., Mitrus M. 2010.** Effect of whole wheat flour moistening and extrusion-cooking screw speed on the SME process and expansion ratio of precooked pasta products. TEKA Commission of Motorization and Power Industry in Agriculture 10, p. 517-526.
28. **Wójtowicz A., Mościcki L. 2009.** Influence of extrusion-cooking parameters on some quality aspects of precooked pasta-like products. Journal of Food Science 74(5), p. 226-233.
29. **Yalla S., Manthey F. 2006.** Effect of semolina and absorption level on extrusion of spaghetti containing non-traditional ingredients. Journal of the Science of Food and Agriculture 86, p. 841-848.
30. **Yoenyongbuddhagal S., Noomhorm A. 2002.** Effect of raw material preparation on rice vermicelli quality. Starch/Starke 54, p. 534-539.

WPŁYW PARAMETRÓW PROCESU NA WYBRANE CECHY TEKSTURY PODGOTOWANYCH MAKARONÓW GRYCZANYCH

S t r e s z c z e n i e . W artykule przedstawiono wyniki pomiarów wybranych cech tekstury bezglutenowych makaronów błyskawicznych ekstrudowanych z mąki gryczanych przy zmiennych parametrach procesu. Podczas wytwarzania zastosowano zróżnicowany poziom dowilżenia mąki gryczanej do wilgotności od 30 do 34%. Ekstruzję podgotowanych makaronów gryczanych przeprowadzono z zastosowaniem temperatury cylindra w zakresie 90-110°C i temperaturą sekcji chłodzącej w zakresie 55-65°C z zastosowaniem zmodyfikowanego ekstrudera jednoślimakowego TS-45 z L / D = 18:1 przy użyciu zróżnicowanych prędkość ślimaka: 60, 80, 100 i 120 obr.min^{-1}. W zależności od obrotów ślimaka i wilgotności surowców przeprowadzono badanie wskaźnika ekspandowania promieniowego oraz ocenę wybranych cech tekstury suchych i uwodnionych podgotowanych makaronów gryczanych. Zastosowano test cięcia do wyznaczenia siły cięcia produktów suchych i poddanych 5-minutowej hydratacji wyrobów makaronowych gotowych do spożycia. Przeprowadzono także test podwójnego ściskania z zastosowaniem komory Ottawa (OTMS) do wyznaczenia jędrności, adhezyjności i żujności uwodnionych makaronów gryczanych. Zastosowanie wyższych prędkości ślimaka podczas ekstruzji wpłynęło na wyższą siłę cięcia zarówno suchych, jak i uwodnionych makaronów gryczanych, co również było spowodowane wyższym wskaźnikiem ekspandowania promieniowego. Zwiększanie wilgotności surowców wpłynęło na obniżenie jędrności makaronów uwodnionych, zaś wyższe obroty zwiększyły żujność wyrobów po hydratacji. Podgotowany makaron gryczany wytworzony w zaproponowanych warunkach procesu ekstruzji i przy przyjętej wilgotności surowców charakteryzował się akceptowalną teksturą i może być polecany jako żywność wygodna dla konsumentów chorych na celiakię.

S ł o w a k l u c z o w e : ekstruzja, gryka, makaron podgotowany, makaron bezglutenowy, tekstura.

TEKA. COMMISSION OF MOTORIZATION AND ENERGETICS IN AGRICULTURE – 2012, Vol. 12, No. 1, 323–329

Analysis of the significance of technological and organizational factors affecting the efficiency of agricultural tractors operation

*Waldemar Izdebski**, Jacek Skudlarski*, Stanislaw Zając****

*Warsaw University of Life Sciences,
**Warsaw University of Technology,
***State Higher Vocational School in Krosno

S u m m a r y. This paper presents a hierarchy of technological and organizational factors affecting the efficiency of agricultural tractors operation. Analysis of the impact of individual components of the tractor on the effectiveness of the tractor's work has shown that the engine has the greatest impact, after that the transmission, lift and external hydraulics follow. The system priorities of the 3rd order objectives showed that the following factors are the most significant for the efficiency of agricultural tractor: the use of electronic fuel delivery control systems and electronic control the operation of the engine auxiliary assemblies, the use of systems for controlling engine operation through on-board computer including the operating parameters of the other components as well as the use of devices that enable a temporary increase in engine power.

K e y w o r d s: tractor, efficiency, engine, components, efficiency.

INTRODUCTION

Performance of numerous agricultural practices requires the use of machines and tractors, which must fulfill the specified requirements. Compliance with selected expectations is assessed on the basis of the characteristics of quality and is sometimes referred to as efficiency [3]. According to Manteuffel [7], the efficiency is the ratio of any effect (benefit) to expenditure incurred on acquiring it.

To achieve high efficiency of the use of agricultural tractors on the farm, and thus lower production costs, is the primary objective of the farm managers (owners) or people managing the work of these machines [10]. The optimal farm equipment in farm tractors is extremely important [18]. Effectiveness of agricultural tractors depends on their technical level as well as the experience of the operator and the natural and productive conditions of farms [11].

Manufacturers of tractors offer more new models of tractors equipped with a number of additional technical equipment and electronics. These devices are improving the efficiency of agricultural tractor but also increase the price of the tractor, which is why it is important to study factors that influence the effectiveness of their work and determine which ones are the most important.

From a review of the literature can be said that many authors were engaged in examination of the efficiency of agricultural tractors, as well as factors that impact on it. [5, 11, 13, 6, 15, 17, 9, 4, 18]. However, there are no studies in which there are attempts to determine their hierarchy. This situation forces the need for research in this area and for utilitarian knowledge useful not only for farmers but also the manufacturer of agricultural tractors.

OBJECTIVE OF THE WORK

The aim of this study was to prioritize the most important technological and organizational factors affecting the efficiency of agricultural tractors. To conduct the study, primary and secondary sources of information were used. Domestic and foreign literature was used as a secondary source of information. In this paper, however, the fundamental importance was attributed to the primary sources of information obtained during field studies conducted using a questionnaire developed among experts, who were the owners of farms who have used tractors.

THE RESEARCH METHODOLOGY

In order to make a hierarchy of importance of technical and organizational factors affecting the efficiency of agricultural tractors the expert-mathematical method was used [1, 16]. Expert and mathematical method is an effective method that allows for the setting of the

hierarchy of importance of technical and organizational factors affecting the efficiency of agricultural tractors. The essence of this method is to use the data received as a result of a scientifically reasoned procedures for collecting, structuring and analysis of information from specialists in that field (experts). Expert and mathematical method allows us to analyze and evaluate very diverse factors, and the results obtained with its use are different from the results from other methods by 6-8%. Hence, this method was used for military, economic and scientific purposes [1, 8, 13].

Obtaining reliable results is associated with the conduct of research according to the established procedure in the method, which assumes the following stages:
– organization of the evaluation,
– selection of experts,
– carrying out research,
– processing test results.

Expert selection was based on the criteria discussed in detail in the literature [12, 13]. The expert group consisted of farmers who are competent users of tractors, with expertise and experience related to the use of farm tractors. The basic requirement for the selection of the farmer was work experience of not less than five years and a minimum of secondary education. A group of experts in accordance with the requirements of the method consisted of competent people with knowledge and experience in the field. The basic requirement was the work experience of not less than five years and a minimum of secondary education. The procedure of forming a group of experts assumed selection of individuals, who have achieved good economic results and production on the farm resulting, inter alia, from their knowledge. Other features that were taken into account, less relevant to the knowledge but also significant in the test procedure were kindness and willingness to participate in the survey.

The method of target selection of experts was used. Candidates for the experts were indicated by the experts from the industry of agricultural technology (such as journalists, agricultural magazines specializing in agricultural technology, local dealers for agricultural tractors and machinery, ODR workers). After the initial conversation and positive verification of the suitability of a person's expertise with regard to the aforementioned criteria, that person was included to the list of experts.

The expertise conducted in the expert and mathematical method is based on the evaluation by experts of many factors that determine the problem. It often happens that these factors are so numerous that it is difficult or impossible to compare and evaluate them by an expert. In this situation it is recommended to use the idea of the event tree (Isikawa tree), which is based on a combination of factors in groups and evaluating separate groups of factors and a separate assessment of factors in the group. This solution, used by the author and some researchers in their studies [inner room 2003, Masiuk 1998, Szpilko 1998] greatly facilitated the expert assessment of factors, and processing the information obtained by the authors. Literature studies, as well as personal experience helped to highlight a number of factors affecting the efficiency of agricultural tractors.

Because of their number, making it difficult to directly assess the validity of the idea, the event tree was used (Fig. 1), highlighting the six groups of factors, so-called second level targets (Table 1). In each group, the factors affecting the group were highlighted, and indirectly affecting the main objective, namely the factors determining the efficiency of agricultural tractors. They are the goals of the third level (Table 2). It is assumed that the impact of the six groups of factors (level II targets) on the amount of losses is 100%. It was assumed similarly, that the impact of factors in this group in total is also 100%.

Special interview questionnaire containing the tables, into which the examiner typed the desired information and evaluation, was developed. Putting goals in separate tables by subject allowed an expert to focus at the moment only on the group parameters, which helped him to assess their validity. Parameters shown in the tables were evaluated by an expert on a scale of 0 to 100, in order to distribute a total of 100 points (per cent) to individual parameters. Assessment equal to "0" assigned to the parameter by an expert meant that this parameter was irrelevant for the expert. The number of points greater than zero reflected the relative importance of the other parameters. The analysis of the research concerned the

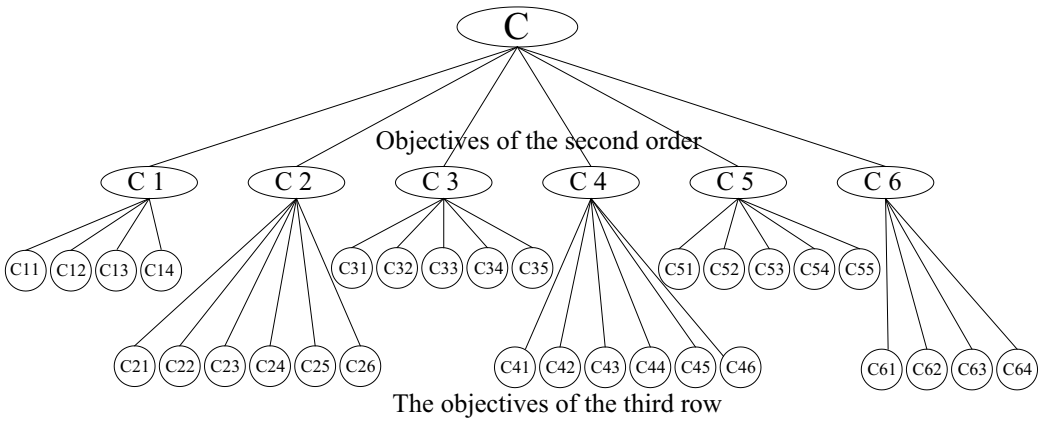

Fig. 1. Event Tree Diagram

importance of the technical solutions used in the different units of tractor in the impact on the efficiency of agricultural tractor. The objectives of the second level of the "Tree of events" highlights the different groups of tractor: engine, transmission, linkage and hydraulics, PTO, cab and steering. At the third level as an objective third row lists the various construction solutions currently used in agricultural tractors. Based on the data obtained from the experts local priorities and systems were calculated and hierarchy of factors made influencing the efficiency of agricultural tractors. Local priorities were evaluated in such a way that the sum of their points in the group was equal to one hundredth. This allowed for the obtainment of numerical values that represent the contribution of individual factors in the structure of the analyzed group.

The questionnaire contained information explaining to the expert how to evaluate the parameters, as well as phone number and email address needed to contact an expert with the author in a situation of having to provide additional guidance and clarification.

THE RESULTS

Based on the survey assessing the validity of 30 factors set out in the form of local priorities by 74 experts was conducted. Age of experts was in the range of 21-56 years, with an average age of 28. The average length of service in the holding of experts was 13 years with the fact that experts regarded the beginning of internship age when they had started independent work on the farm. In many cases, experts began to acquire their experience from the age of 15-16 years.

The experts represented the holdings of between 11 to 1,000 acres located in different Polish regions. Farms represented by experts followed different lines of production: only crop production, only livestock production and the multipurpose production. A vast group was represented by farms with only crop and multipurpose production.

Research analysis pertained to the importance of the technical solutions used in the different units of tractor with regard to impact on the efficiency of agricultural tractor. For this purpose, Isikawa tree was used distinguishing level II targets as individual components of a tractor: engine, transmission, lift and hydraulics, PTO, cab and steering. At the third level as an third level objective the various construction solutions currently used in agricultural tractors were listed. Based on data obtained from the experts local and system priorities were calculated, and hierarchy of factors influencing the efficiency of agricultural tractors was made. Local priorities were evaluated in such a way that the sum of their points in the group was equal to one hundred. This allowed for the obtainment of numerical values that represent the contribution of individual factors in the structure of the analyzed group.

The values of local priorities, which are the average of ratings of individual parameters, coefficients of concordance, rank sum, variance and χ-square test are shown in table 1 and 2. In order to realize that experts' compliance was not accidental χ-square test was used. If the calculated value of χ^2 is greater than the tabular χ^2tab, and the concordance coefficient is significantly different from zero, it can be argued that the compatibility of the experts' ratings is not random [2].

Compliance of expert judgments in local priorities rankings was determined by the coefficient of variance calculated according to the formula [8]. According to the literature it was considered that if Vj $\leq$ 0.25, the compliance of individual assessments appointed by experts is sufficient. If Vj 0.3, compliance were considered to be low.

As shown in Table 1 and 2 of the evaluation of experts who were involved in surveying were convergent, which is reflected in the size of the coefficient of concordance (average 0.36), and coefficient of variation in the range of 0,09-0,25. The average value of the χ-square criterion of the tested the third level factors was χ^2obl = 112.92. Array value for the χ-square = 15.10 was χ2tab. One can, therefore, say that in all cases, the following condition is satisfied: χ2obl> χ2tab. The resulting concordance coefficients are significant. This proves that the congruity of expert assessments is not a coincidence either within respondents 'groups' or between them. The determined values of the coefficients of variance also confirmed the compliance of experts' evaluation for both tested levels.

Table 1. Effect of tractor components (targets of the second order) on the economic efficiency of agricultural tractor.

Target label	Target name	Sum of ranks	Average	Variance coef.
C 1	Engine	77	29,7	0,09
C 2	Transmission (gearbox and drive units)	134	25,0	0,16
C 3	Lift and external hydraulics	208	15,2	0,18
C 4	PTO	275	10,7	0,19
C 5	cabin (control – operator's comfort)	281	10,3	0,22
C 6	Steering system	337	9,0	0,25
Concordance coefficient			0,509	
χ-square criterion			188,23	

Sources : own

Analysis of the impact of individual components on the effectiveness of the tractor's work has shown that the engine has the greatest impact, then the transmission, lift and hydraulics follow. Local priorities of design solutions (III level factors) affecting the efficiency of the tractor components are shown in Table 2.

Table 2. The significance of structural solutions to the efficiency of individual systems of tractor

Target label	Target name	Sum of ranks	Average	Variance coef.
Engine				
C 11	The use of mechanical control systems of fuel delivery, and auxiliary subassemblies (eg, turbocharger)	216	22,09	0,22
C 12	The use of electronic control systems fuel delivery and electronic control the operation of the engine auxiliary units (eg, adjusting of cooling fan to the working conditions, turbocharger operation, etc.)	83	28,45	0,12
C 13	The use of devices to allow a temporary increase in engine power	166	24,32	0,18
C 14	The use of systems for controlling engine operation through on-board computer including the operating parameters of other components such as drive system and lift	130	25,14	0,15
Concordance coefficient			0,353	
χ-square criterion			78,47	
Transmission (gearbox and drive units)				
C 21	Alpha The use of mechanical shift and mechanical reverse, front drive and differential lock switch	226	14,64	0,23
C 22	The use of electrohydraulic control and elimination of the need for a master clutch use to change the gears in the transmission, switching on the front drive, differential lock, reverse, etc.	150	21,29	0,17
C 23	The use of systems to maintain a constant speed (tempomat)	311	14,10	0,22
C 24	Using variable gearbox or gear box with a significant number of gears with automatic operation possibility with electro-hydraulic turning on of the reverse, front drive, differential lock (also in auto mode)	86	24,41	0,17
C 25	The use of gear enabling accessing higher transport speeds of the tractor	261	15,51	0,21
C 26	The use of systems for the tractor operation in ride back system (eg TwinTrac)	379	10,04	0,24
Concordance coefficient			0,540	
χ-square criterion			211,54	
Lift and external hydraulics				
C 31	The use of a mechanical system controlling the lift and the external hydraulics	315	12,95	0,25
C 32	The use of electrohydraulic lift and hydraulics control (eg, EHR)	155	22,67	0,19
C 33	Use of systems to enable lift and hydraulics to operate in the automatic mode on the headland, and while working in the field or on the road with the possibility of programming the order of execution steps by these devices and their operating parameters	100	25,24	0,15
C 34	The use in tractor hydraulic system of electronically controlled variable displacement pumps and devices for accessing the various expenses on different outputs of external hydraulics	185	22,88	0,19
C 35	The use of vibration compensation systems for tools mounted on the lift	257	16,26	0,23
Concordance coefficient			0,440	
χ-square criterion			143,30	
WOM				
C 41	The use of mechanical PTO drive switching	255	10,18	0,17
C 42	The use of electrohydraulic PTO drive switch	128	20,60	0,14
C 43	The use of the tractor so called economic speed of PTO	134	19,85	0,21

C 44	The use of automated solutions to switch off the PTO drive at the time of lifting the arm of hydraulic lift and on again on lowering the lift	80	22,52	0,16
C 45	The use of PTO drive circuit switches located on the fender	188	15,63	0,22
C 46	The use of the dependent speed in PTO system equipment	287	11,22	0,24
Concordance coefficient			0,410	
χ-square criterion			137,41	

Target label	**Target name**	**Sum of ranks**	**Average**	**Variance coef.**
Cabin (control – operator's comfort)				
C 51	Application of systems for parameters monitoring (eg wheel slip, engine load, etc.) and labor productivity of tractor in the form control panel with color display	136	19,1	0,15
C 52	Focusing the control functions in one place such as the armrest with adjustable position and multi-function levers	86	23,1	0,19
C 53	Shock absorbing system of the cab and / or application of the operator seat with automatic shock damping control	197	19,6	0,23
C 54	The use of air conditioning system with automatic temperature control	240	17,3	0,22
C 55	The use of electronic solutions that support the operator in driving such as GPS techniques systems or parallel driving	155	20,9	0,21
Concordance coefficient			0,290	
χ-square criterion			80,45	
Steering system				
C 61	Front axle suspension with the possibility of exclusion	95	25,6	0,19
C 62	Application of solutions to reduce the turning radius of the tractor (eg, turning axles)	162	25,3	0,21
C 63	Application solutions for getting better turning during the field work but with a smaller number of revolutions of the steering wheel	151	24,0	0,18
C 64	Application solutions for moving the tools hanging on the front lift with the tractor wheels turning	119	25,1	0,22
Concordance coefficient			0,130	
χ-square criterion			26,32	

Sources : own

System priorities of III order objectives are shown in Figure 2. As is apparent from the data , three factors C 12, C14 and C 13 stand for more than 23% of the goal accomplishment and eight main factors in the range of II and III for more than 39%. As the analysis shows, in the expert's opinion, three major factors affecting the efficiency of the tractor are: C12 - The use of electronic control systems fuel delivery and electronic control the operation

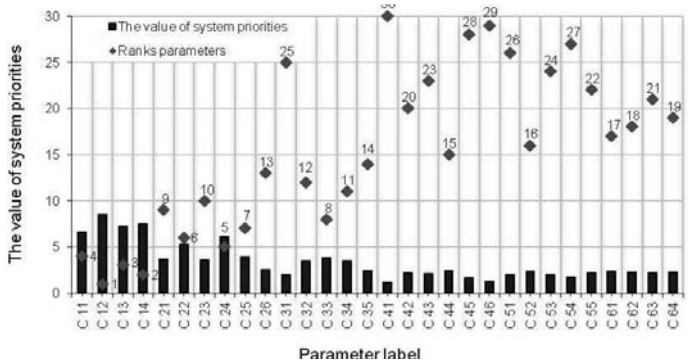

Fig. 2. Ranks and values of the third level system priorities

Source: Own

of the engine auxiliary units, C14 - The use of systems for controlling engine operation through on-board computer including the operating parameters of other components such as drive system and lift, and C13 - The use of devices to allow a temporary increase in engine power.

Subsequently, the priorities of the system were divided into four ranges: high (I), higher than the average (II), medium (III) and lower than the average (IV) by inserting in them the factors whose the priorities of the system are within the ranges of data. Also "the importance of priorities" of range was determined, which means the contribution of group of factors assigned to the range in order to achieve the main goal (Table 3).

CONCLUSIONS

1. Independent expert studies involving 74 experts showed that the three objectives, namely: C12 (The use of electronic control systems fuel delivery and electronic control the operation of the engine auxiliary units (eg, adjusting of cooling fan to the working conditions, turbocharger operation, etc.)), C14 (The use of systems for controlling engine operation through on-board computer including the operating parameters of other components such as drive system and lift), C13 (the use of devices to allow a temporary increase in engine power), for which the system parameters were 8.46, 7.48 ; 7.23, respectively, have the greatest impact on increasing the efficiency of agricultural tractors.
2. Also, the following parameters have a large impact: C11 (the use of mechanical control systems of fuel delivery, and auxiliary subassemblies (e.g. turbocharger)), C24 (using variable gearbox or gear box with a significant number of gears with automatic operation possibility with electro-hydraulic turning on of the reverse, front drive, differential lock (also in auto mode)), C22 (the use of electrohydraulic control and elimination of the need for a master clutch use to change the gears in the transmission, switching on the front drive, differential lock, reverse, etc.) for which the system parameters were 6.57, 6.11, 5.33, respectively.
3. Before the purchase, the prospective tractor buyer should make a detailed analysis of the significance of technical and operating parameters belonging to the first and second system priorities in the range offered on the market of agricultural tractors. Based on this analysis, he should ultimately choose the tractor, whose price and technical performance parameters included in the above-mentioned ranges are the most preferred.

The studies were conducted within the research project MNiSW N N 115 089639

REFERENCES

1. **Izdebski W., 2003:** Strategie wyposażenia gospodarstw rolnych w kombajny zbożowe. Rozprawa habilitacyjna. Wydawnictwo SGGW, Warszawa,
2. **Jevlanov Ł. G., 1981:** Osnowy tieorii prinatija reszenij. ANH ZSRR.
3. **Karepin P.A., 2000:** Ocenka efektywnosti sbornogo uzla selskohozjastvennyh maszin. Mechanizacja i Elektryfikacja Selkogo Chozjastva 9: p. 29-31.
4. **Koniuszy A., 2007:** Balancing of working indicators of agricultural tractor as the way to improve the efficiency of farming. TEKA Komisja Motoryzacji Energetyki. - OL PAN 7: p. 122-128.
5. **Kowalczuk J., 1994:** Metoda doboru sprzętu rolniczego do mechanizacji prac w procesach technologicznych realizowanych w produkcji roślinnej. Problemy Inżynierii Rolniczej 1: p. 81-87.
6. **Lorencowicz E., Kocira S. 2004:** Analiza wyposażenia technicznego gospodarstw rolnych z wykorzystaniem bazy danych. Problemy Inżynierii Rolniczej 4(46).
7. **Manteuffel R. 1981:** Ekonomika i organizacja gospodarstwa rolnego. PWRiL, Warszawa.
8. **Masiuk A. 1998:** Wpływ profilaktyki eksploatacyjnej na efektywność produkcji mleka. Rozprawa habilitacyjna. Fundacja „Rozwój SGGW", Warszawa.
9. **Olejnik K., 2005:** Agricultural tractor driver's s limitations of visual transmission in aspect of road safety in Poland. TEKA Komisji Motoryzacjii i Energetyki Rolnictwa 5: p. 158-167.
10. **Pawlak J. 1998:** Efektywność mechanizacji rolnictwa, Wyd. Instytut Budownictwa, Mechanizacji i Elektryfikacji Rolnictwa, Warszawa.
11. **Provotorov J., 1997:** Ocenka parametrow lesnych kolesnych traktorow. Lesnaja Promyslennost' 4: p. 21-22.
12. **Schobl R., Blobel R., Schlorf U. 1988:** Betriebswirtschaftliche Regelungen zur Verlangerung der Nutzungsdauer der technik. Kooperation 22 (5): p. 208-211.
13. **Skudlarski J., 2002:** Wpływ parametrów techniczno-ekploatacyjnych na efektywność pracy ciągników

Table 3. The ranges of system priorities

Range	Range values	Marking of targets included In the range	Range „priority weight" [%]	Average value of system priority In the range [%]
I	6,64-8,46	C 12, C 14, C 13	23,17	7,72
II	4,79-6,63	C 11, C 24, C 22	18,00	6,00
III	2,94-4,78	C 33, C 21, C 23, C 34, C 32	21,83	4,36
IV	1,09-2,93	C 26, C 35, C 44, C 52, C 61, C 62, C 64, C 42, C 43, C 63, C 55, C 53, C 31, C 51, C 54, C 45, C 46, C 41	37,00	2,05

Source: Own

rolniczych. Rozprawa doktorska. Wydział Inżynierii Produkcji, SGGW, Warszawa.

14. **Szpilko A.W. 1998:** Razwitie techniczeskoj bazy i inżyniernoj służby APK Rosji. Traktory i Selskochozjstwiennyje Masziny 8: p. 2-6.
15. **Yakovenko A., Doroshenko L., Plizga K., 2004:** Optimizacja rezimov raboty mashinno traktornyh agregatov. MOTROL Motoryzacja i Energetyka Rolnictwa 6: p. 317-323.
16. **Tinjakova V.I., 2006:** Matematicheskije metody ekspertnoj informacji. Voronezskij Gosudarstvennyj Universitet, Voronez.
17. **Zaharchuk V., Plizga K., 2004:** Matematicheskaja modiel dla issledovanija vlijanija rozlichnyh faktorov na ekonomicheskije i ekologicheskije pokazatieli kolesnogo traktora. MOTROL Motoryzacja i Energetyka Rolnictwa 6: p. 282-286.
18. **Zając S., Kusz D. 2010:** Optymalne wyposażenie gospodarstw rolnych w ciągniki rolnicze. Wyd. Roczniki Nauk Rolniczych, Seria G – Ekonomika Rolnictwa, tom 97, zeszyt 4, p. 247-257.

ANALIZA ZNACZENIA TECHNOLOGICZNYCH I ORGANIZACYJNYCH CZYNNIKÓW WPŁYWAJĄCYCH NA EFEKTYWNOŚĆ PRACY CIĄGNIKÓW ROLNICZYCH

S t r e s z c z e n i e . W pracy przedstawiono hierarchię technologicznych i organizacyjnych czynników wpływających na efektywność pracy ciągników rolniczych. Analiza wpływu poszczególnych elementów ciągnika na skuteczność ciągnika pracy wykazały, że silnik ma największy wpływ, po tym skrzynia biegów oraz pneumatyczna i zewnętrzna hydraulika. System priorytetów celów 3-go rzędu wykazał, że następujące czynniki są najbardziej znaczące dla efektywności ciągnika rolniczego: zastosowanie elektronicznych systemów podawania paliwa sterowania oraz elektroniczna kontrola pracy silnika zespołów pomocniczych, korzystanie z systemów kontroli silnika, praca przez komputer pokładowy, w tym parametrów operacyjnych innych składników, jak również zastosowanie urządzeń, które umożliwiają tymczasowe zwiększenie mocy silnika.

S ł o w a k l u c z o w e : ciągnik, wydajność, silnik, komponenty, wydajność.

TEKA. COMMISSION OF MOTORIZATION AND ENERGETICS IN AGRICULTURE – 2012, Vol. 12, No. 1, 331–336

Power demand in respect of environmentally friendly works carried out in motor transport facilities

*Edyta Zielińska**

* Rzeszow University of Technology, the Faculty of Mechanical Engineering and Aeronautics

Summary. The paper presents issues related to modelling an ecological strategy by taxonomic method for motor transport facilities. It describes the methodology and justifies the purpose of the application of the said method to assess environmental issues. Based on the example of the power demanded for the execution of environmentally friendly works in a company, the method, calculation results and their interpretation in respect of the selection of a technology suitable for the application were presented.

Key words: motor transport, ecological problems, taxonomic method.

INTRODUCTION

The development of motor transport stimulated by the increase in the number of vehicles used as well as by infrastructure investments has an adverse effect on the natural environment. The environment is adversely affected by combustion gases emitted by cars and by pollutants coming from motor transport facilities [5,15,18]. The pollution of the air by combustion gases and the excessive noise level are among the most important environmental risks occurring in motor transport facilities. The management and utilization of operating fluids, such as, for instance engine and gear oils, coolants from cooling or air-conditioning systems pose a big problem, too.

In order to remedy the adverse effect of motor transport on the natural environment any kind of environmentally conscious action should be undertaken. Appropriate country-specified governmental regulations on reducing the material consumption index, energy consumption as well as the costs of production, operation and recycling of worn-out vehicles are important in the easing of the adverse effect of motor transport on the environment, too [7,8,10]. The legal regulations regarding ecological safety should also apply to the functioning of motor transport facilities that are essential for normal use of vehicles.

The use of the taxonomic method allows dendrite ordering that is better to reproduce the positions of the examined factors in the multidimensional parameter space, as opposed to all kinds of optimization method that allow only linear ordering of selected indexes for problems arising in motor transport facilities [1,6,14].

A TAXONOMIC ANALYSIS OF POWER CONSUMPTION IN RESPECT OF ENVIRONMENTALLY CONSCIOUS ACTION

The application of the taxonomic method to analyse environmental problems in motor transport facilities results from the fact that describing technological issues involves parameters that are different physical quantities by nature and are measured using different units. The structure of taxonomic models allows linear ordering for the technologies under research [12,20].

For the purpose of this paper, the power demanded to conduct environmentally conscious action was chosen to be analysed by taxonomic method. Power consumption for environmental purposes is extremely essential in any company's economic balance, especially as there is an upward trend in the energy market [4,9,13]. Power consumption related data was received from 15 companies. The unit of measure adopted for the research was kWh/mth. The selected companies have different ownership and organisational structures and offer motor transport services. Some of the companies provided us with their documents and other materials related to the logistic action taken for environmental protection on condition that their business names and affiliations were not revealed; therefore, in this paper they are called "technologies".

Since the taxonomic method requires selection of the most favourable variant on account of the criteria adopted, three additional parameters (the so called model ones)

were singled out for comparison purposes. They refer to: emission of CO_2 to the environment (WP1), total amount of waste materials (WP2), overall "waste quality" in terms of toxicity (WP3). The fourth model parameter is power demand in respect of environmentally friendly works (WP4). Table 1 includes the model parameters selected for calculations and their corresponding units of measure [19].

Table 1. Parameters for pro-ecological assessment of a technical infrastructure of transport selected for analysis

No	Parameter symbol	Parameter type	Measurement unit
1.	P1	Emission of carbon dioxide (CO_2) to atmosphere	[kg/rok]
2.	P2	Total quantity of material waste	[kg/rok]
3.	P3	Overall „quality" of generated waste (toxicity)	[0-1]*
4.	P4	Energy demand with reference to pro-ecological projects	[kWh/m-c]

* 0 - lowest, 1 - highest

The collection of data related to those parameters involved sometimes considerable difficulties. The documents provided by some of the companies included insufficient data, their employees responsible for these issues were incompetent, and the like. So, the information regarding separate parameters is in many cases the result of additional analyses of the number of inspections, repairs, diagnostic testing and other services rendered within a specified time period. The data adopted for the parameters singled out were repeatedly consulted with the companies' technical inspectors and employees hired for specific jobs to ensure that credible results are obtained.

INTERPRETATION OF THE RESEARCH RESULTS

In this paper, the results obtained by taxonomic method have been additionally verified by Czekanowski's matrices. In the case of similarity of the results it can be concluded that the procedure adopted for the calculations was correct, which entitles us to explicitly interpret the results in the conclusions. The order of the connected points and the values of the mean differences between those points are of fundamental importance when analysing the results and drawing the conclusions. The closeness and the clustering of specified technologies show that the parameter concerned is similar, which allows selection of an optimal quantity [11,17].

The research results have been collated in tables and presented graphically in the form of dendrites and Czekanowski's matrices, namely:

- **Table 2** – collation of the analysed parameters for all the companies under research,
- **Table 3** – the parameter values determined by taxonomic method for the lowest power consumption for environmentally friendly works, in 5 of the companies under research,
- **Table 4** – mean differences between the technologies under research (according to Table 3),
- **Table 5** – Czekanowski's diagonal matrix (verification Fig. 2),
- **Table 6** – the parameter values determined by taxonomic method for the mean power consumption for environmentally friendly works, in 5 of the companies under research,
- **Table 7** – mean differences between the technologies under research (according to Table 6),
- **Table 8** – Czekanowski's diagonal matrix (verification Fig. 3),
- **Table 9** – the parameter values determined by taxonomic method for the higher power consumption for environmentally friendly works, in 5 of the companies under research,
- **Table 10** – mean differences between the technologies under research (according to Table 9),
- **Table 11** – Czekanowski's diagonal matrix (verification Fig. 4),
- **Fig. 1** – dendritic differentiation of technologies according to power consumption for the 5 lowest values,
- **Fig. 2** – dendritic differentiation of technologies according to power consumption for the 5 mean values,
- **Fig. 3** – dendritic differentiation of technologies according to power consumption for the 5 highest values.

Table 2. Analysed parameters for the 15 companies under research (including the model parameters)

Parameters / Technology	P1	P2	P3	P4
1	929	58 518	0,35	800
2	1 328	63 372	0,72	900
3	1 679	55 846	0,27	950
4	1 000	31 982	0,26	600
5	2 647	113 516	0,13	975
6	1 221	48 288	0,49	740
7	3 017	106 424	0,31	250
8	1 921	84 961	0,87	1000
9	1 395	62 282	0,59	430
10	896	55 423	0,70	740
11	1 093	63 230	0,18	800
12	4 329	161 326	0,19	940
13	2 247	57 013	0,64	800
14	1 444	65 510	0,25	850
15	2 309	124 893	0,13	900

WP1	672	41 568	1	555
WP2	750	23 987	1	450
WP3	1 441	63 721	1	750
WP4	2 262	79 818	1	187,5

Table 3. Parameters according to power consumption for the 5 lowest values from among 15 companies

Parameters / Technology	P1	P2	P3	P4
7	3 017	106 424	0,31	250
9	1 395	62 282	0,59	430
4	1 000	31 982	0,26	600
6	1 221	48 288	0,49	740
10	896	55 423	0,70	740
WP1	672	41 568	1,00	555
WP2	750	23 987	1,00	450
WP3	1 441	63 721	1,00	750
WP4	2 262	79 818	1,00	188

Table 4. Mean differences between the technologies under research (according to Table 3)

Technology	7	9	4	6	10	WP1	WP2	WP3	WP4
7		4301,99	7215,07	5704,15	5079,70	6315,27	7981,52	4214,46	2577,86
9	4301,99		2918,23	1812,08	1044,95	2121,03	3682,79	550,84	1883,30
4	7215,07	2918,23		1572,25	2252,50	1009,37	783,42	3058,33	4645,56
6	5704,15	1812,08	1572,25		1145,92	970,27	2352,95	1677,59	3221,37
10	5079,70	1044,95	2252,50	1145,92		1342,40	3019,58	893,54	2626,04
WP1	6315,27	2121,03	1009,37	970,27	1342,40		1689,32	2163,82	3809,71
WP2	7981,52	3682,79	783,42	2352,95	3019,58	1689,32		3837,11	5411,25
WP3	4214,46	550,84	3058,33	1677,59	893,54	2163,82	3837,11		2001,91
WP4	2577,86	1883,30	4645,56	3221,37	2626,04	3809,71	5411,25	2001,91	

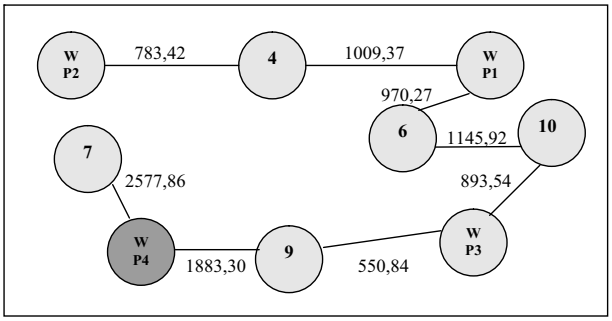

Fig. 1. Dendritic differentiation of technologies according to power consumption for the 5 lowest values

Table 5. Czekanowski's diagonal matrix (dendrite verification according to Fig. 1)

	Name	1	2	3	4	5	6	7	8	9
1	7	●	•						•	●
2	9	•	●	●	●	●	●	•	●	●
3	4		●	●	●	●	●	●	●	
4	6		●	●	●	●	●	●	●	•
5	10		●	●	●	●	●	•	●	●
6	WP1		●	●	●	●	●	●	●	•
7	WP2		•	●	●	•	●	●	•	
8	WP3	•	●	●	●	●	●	•	●	●
9	WP4	●	●		•	●	•		●	●

● 0 - 11845 ● 11846 - 24615 ● 24616 - 35742 • > 35742

Table 6. Parameters according to power consumption for the 5 mean values from among the companies under research

Parameters / Technology	P1	P2	P3	P4
13	2 247	57 013	0,64	800
1	929	58 518	0,35	800
11	1 093	63 230	0,18	800
14	1 444	65 510	0,25	850
2	1 328	63 372	0,72	900
WP1	672	41 568	1,00	555
WP2	750	23 987	1,00	450
WP3	1 441	63 721	1,00	750
WP4	2 262	79 818	1,00	188

Table 7. Mean differences between the technologies under research (according to Table 6)

Technology	13	1	11	14	2	WP1	WP2	WP3	WP4
13		839,54	1221,75	1207,25	931,81	1623,59	3238,84	802,90	2539,55
1	839,54		1567,27	966,97	886,19	1707,93	3320,58	1080,33	2371,91
11	1221,75	1567,27		1264,60	851,67	2251,43	3776,22	912,86	1757,25
14	1207,25	966,97	1264,60		479,62	2335,36	4011,45	745,66	1824,96
2	931,81	886,19	851,67	479,62		2127,11	3803,37	357,72	1812,33
WP1	1623,59	1707,93	2251,43	2335,36	2127,11		1689,32	2163,82	3809,71
WP2	3238,84	3320,58	3776,22	4011,45	3803,37	1689,32		3837,11	5411,25
WP3	802,90	1080,33	912,86	745,66	357,72	2163,82	3837,11		2001,91
WP4	2539,55	2371,91	1757,25	1824,96	1812,33	3809,71	5411,25	2001,91	

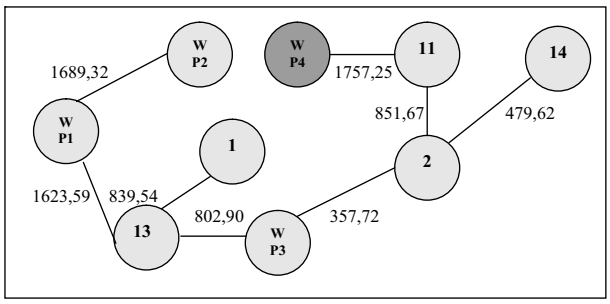

Fig. 2. Dendritic differentiation of technologies according to power consumption for the 5 mean values

Table 8. Czekanowski's diagonal matrix (dendrite verification according to Fig. 2)

	Name	1	2	3	4	5	6	7	8	9
1	13									
2	1									
3	11									
4	14									
5	2									
6	WP1									
7	WP2									
8	WP3									
9	WP4									

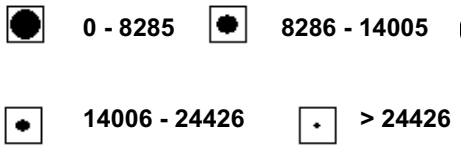

Table 9. Parameters according to power consumption for the 5 highest values from among 15 companies

Parameters / Technology	P1	P2	P3	P4
15	2 309	124 893	0,13	900
12	4 329	161 326	0,19	940
3	1 679	55 846	0,27	950
5	2 647	113 516	0,13	975
8	1 921	84 961	0,87	1000
WP1	672	41 568	1,00	555
WP2	750	23 987	1,00	450
WP3	1 441	63 721	1,00	750
WP4	2 262	79 818	1,00	188

Table 10. Mean differences between the technologies under research (according to Table 9)

Technology	15	12	3	5	8	WP1	WP2	WP3	WP4
15		3703,76	6617,01	2029,78	4225,07	8037,54	9714,72	5919,93	4383,47
12	3703,76		10182,73	4645,04	7466,31	11609,48	13285,65	9450,61	7901,15
3	6617,01	10182,73		5562,80	2813,09	1568,22	3105,89	989,99	2590,46
5	2029,78	4645,04	5562,80		3767,05	7041,35	8650,23	5360,95	3710,97
8	4225,07	7466,31	2813,09	3767,05		4220,54	5896,81	2060,95	1091,67
WP1	8037,54	11609,48	1568,22	7041,35	4220,54		1689,32	2163,82	3809,71
WP2	9714,72	13285,65	3105,89	8650,23	5896,81	1689,32		3837,11	5411,25
WP3	5919,93	9450,61	989,99	5360,95	2060,95	2163,82	3837,11		2001,91
WP4	4383,47	7901,15	2590,46	3710,97	1091,67	3809,71	5411,25	2001,91	

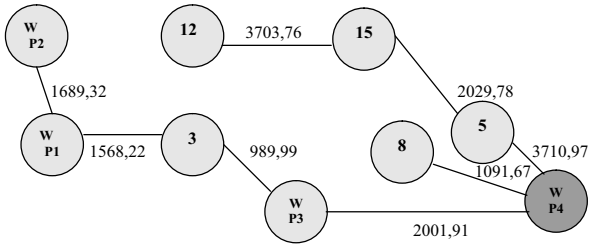

Fig. 3. Dendritic differentiation of technologies according to power consumption for the 5 highest values

Tabela 11. Czekanowski's diagonal matrix (dendrite verification according to Fig. 3)

	Name	1	2	3	4	5	6	7	8	9
1	15	●	●	·	●	●			·	●
2	12	●	●		●	·				·
3	3	·		●	·	●	●	●	●	●
4	5	●	●	·	●	●	·		·	●
5	8	●	·	●	●	●	●	●	●	●
6	WP1			●	·	●	●	●	●	●
7	WP2			●		●	●	●	●	●
8	WP3	·		●	·	●	●	●	●	●
9	WP4	●	·	●	●	●	●	●	●	●

● 0 - 24835 ● 24836 - 48398

● 48399 - 68685 · > 68685

CONCLUSIONS

Ordering environmentally friendly technologies in motor transport facilities with the use of the taxonomic method is an effective way to find the point determined using the defined criteria in the space of selected parameters. The taxonomic method can be used to effectively select logistic systems for environmental problems occurring in the motor transport sector [2,3,16]. It is also possible to verify the results of differentiation of environmentally friendly technologies with the use of Czekanowski's diagonal matrix.

The analysis of the results described in this paper allows their interpretation with respect to the usefulness of the technologies in question. Among the technologies with the lowest power consumed to carry out environmentally conscious action, the least energy-consuming is No. 7. It is close to the model technology WP4 but the gap between them is relatively wide. Within this group, technology No. 9 that is very close to the model technology WP3 and at the same time closer to the model technology WP4 than technology No. 7 is, looks best. It should be also emphasized that the dendritic differentiation made for the technologies of this group is linear, which makes it difficult to draw explicit conclusions.

Within the group of companies grouped according to the mean power consumption values, technologies 1, 11 and 13 are marked by the lowest values. However, the technology closest to the model one, WP4, is marked No. 11.

Within the group of companies with the highest power consumption for environmentally friendly works, among the 15 companies considered there is technology No. 8 that ranks closest to the model technology WP4. Attention should be also paid to technology No. 3 that is not the best in this company group but is close to the two model technologies WP1 and WP3 which may make one take it into consideration when designing motor transport facilities.

REFERENCES

1. **Abramek K., Uzdowski M. 2009:** Eksploatacja techniczna i naprawa. Wyd. Komunikacji i Łączności, Warszawa, p. 269.
2. **Bentkowska-Senator K., Kordel Z., Waśkiewicz J. 2009:** Transport samochodowy ładunków. Wyd. ITS, Warszawa, p. 217.
3. **Bentkowska-Senator K., Kordel Z., Balke I., Waśkiewicz J., Balke M., Dorosiewicz S. 2011:** Polski ciężarowy transport samochodowy u progu drugiej dekady nowego wieku. Zeszyty Naukowe ITS, z. nr 106, Warszawa, p. 134.
4. **Bentkowska-Senator K., Kordel Z., Waśkiewicz J. 2011:** Koszty w transporcie samochodowym. Wyd. ITS, Warszawa, p. 186.
5. **Biedrońska J. 2010:** Projektowanie obiektów motoryzacyjnych. Wyd. Politechniki Śląskiej, Gliwice, p. 415.
6. **Chaciński J., Jędrzejewski Z. 1982:** Zaplecze techniczne transportu samochodowego. Wyd. Komunikacji i Łączności, Warszawa, p. 423.
7. **Chamier-Gliszczyński N. 2010:** Life cycle of technical objects – environmental analysis. Polish Academy of Sciences – Branch in Lublin, TEKA, Vol. X, Lublin, pp. 19-25.
8. **Chamier-Gliszczyński N. 2010:** Model recycling system of end-of-life trabsport means. Polish Academy of Sciences – Branch in Lublin, TEKA, Vol. X, Lublin, pp. 26-32.
9. **Chojnacki A., Markow J. 2009:** Analiza kosztów przewozowych w transporcie samochodowym. Prace naukowe Politechniki Warszawskiej, z. 70, Warszawa, p. 33-44.
10. **Lejda K. 2003:** Selected problems in car recycling. Polish Academy of Sciences – Brench in Lublin, TEKA, Vol. IV, Lublin, pp. 113-118.
11. **Matusek M., Bartnicki M. 2003:** Metoda porównań międzyzakładowych z wykorzystaniem metod taksonomicznych. Zeszyty Nauk. PŚl, Nr 1597, Gliwice, pp. 45-53.
12. **Młodak A. 2006:** Analiza taksonomiczna w statystyce regionalnej. Wyd. DIFIN, Warszawa, p. 262.
13. **Rydzkowski W., Wojewódzka-Król K. 2009:** Transport. Wyd. Naukowe PWN, Warszawa, p. 550.

14. **Stolarski B. 1990:** Metody taksonomiczne w technologii samochodów. Wyd. Politechniki Krakowskiej, Kraków, p. 117.
15. **Uzdowski M., Abramek K., Garczyński K. 2003:** Eksploatacja techniczna i naprawa. Wyd. Komunikacji i Łączności, Warszawa, p. 295.
16. **Zielińska E. 2006:** Możliwość wykorzystania metody taksonomicznej do opracowania modelu zarządzania ekologicznego w zapleczu technicznych środków transportu. Materiały Międzynarodowej Konferencji Naukowej SAKON'06 nt. „Metody obliczeniowe i badawcze w rozwoju pojazdów samochodowych i maszyn roboczych samojezdnych; Zarządzanie i marketing w motoryzacji", Rzeszów-Przecław, p. 263-268.
17. **Zielińska E., Lejda K. 2009:** Wykorzystanie metody taksonomicznej do oceny problemów ekologicznych w zapleczu technicznym transportu. Czasopismo Logistyka Nº 1/ - wersja elektroniczna – CD.
18. **Zielińska E., Lejda K. 2010:** Ecological problems of transport vehicle. Polish Academy of Sciences – Branch in Lublin, TEKA, Vol. X, Lublin, pp. 548-556.
19. **Zielińska E., Lejda K. 2011:** The proposed methodology for analysis of ecological problems concering the technical infrastructure of motor transport. Polish Academy of Sciences – Branch in Lublin, TEKA, Vol. XI, Lublin, pp. 457-466.
20. **Zielińska E., Lejda K. 2011:** The taxonomic analysis of ecological threats caused by a technical infrastructure of motor transport based on the total quantity of material waste. Journal of Polish CIMAC (Energetic Aspects), Vol.6, Nº2, Gdańsk, p. 145-156.

ZAPOTRZEBOWANIE NA ENERGIĘ W ODNIESIENIU DO PRAC PROEKOLOGICZNYCH REALIZOWANYCH W ZAPLECZU TECHNICZNYM MOTORYZACJI

S t r e s z c z e n i e . W artykule przedstawiono zagadnienia dotyczące modelowania strategii ekologicznej w obiektach zaplecza transportu samochodowego metodą taksonomiczną. Opisano metodykę i uzasadniono cel wykorzystania tej metody do oceny zagadnień ekologicznych. Na przykładzie zapotrzebowania na zużycie energii potrzebnej do prowadzenia działań proekologicznych zaprezentowano metodę, wyniki obliczeń oraz ich interpretację odnośnie wyboru odpowiedniej technologii do aplikacji.

S ł o w a k l u c z o w e : transport samochodowy, problemy ekologiczne, metoda taksonomiczna.

Table of contents

List of the Reviewevs

1. Zbigniew Burski
2. Karol Cupiał
3. Kazimierz Dreszer
4. Dariusz Dziki
5. Mieczysław Dziubiński
6. Ł. Geczyk
7. Krzysztof Gołacki
8. Agnieszka Kaleta
9. Sławomir Kokoszka
10. Józef Kowalczuk
11. Sławomir Kurpaska
12. Elżbieta Kusińska
13. Andrzej Kusz
14. Kazimierz Lejda
15. Ryszard Lewkowicz
16. Andrzej Marciniak
17. Andrzej Marczuk
18. Jerzy Merkisz
19. Leszek Mościcki
20. Andrzej Mruk
21. Janusz Mysłowski
22. Halina Pawlak
23. Janusz Puchocki
24. Stanisław Sosnowski
25. Sławomir Stryczek
26. Mariusz Szymanek
27. G. A. Tajanowski
28. Wojciech Tanaś
29. Janusz Wojdalski
30. Tadeusz Złoto
31. Daniela Żuk

Editors of the „TEKA" journal of the Commission of Motorization and Energetics in Agriculture would like to inform both the authors and readers that the agreement was signed with the Interdisciplinary Centre for mathematical and Computational Modelling at the Warsaw University referred to as "ICM". Therefore, ICM is the owner and operator of the IT system needed to conduct and support a digital scientific library accessible to users via the Internet called the "ICM Internet Platform", which ensures the safety of development, storage and retrieval of published materials provided to users. ICM is obliged to pull all the articles printed in the "Teka" on the ICM Internet Platform. ICM develops metadata, which are then indexed in the "Agro" database.

Impact factor of the "TEKA" journal according to the Commission of Motorization and Energetics in Agriculture is 2.35 (August 2012).